

# **Synthesis of metal complexes of 5-nitroimidazoles to realize their biological potential**

**Thesis submitted for the degree of  
Doctor of Philosophy (Science) of  
Jadavpur University**

**Under the supervision of  
Dr. Saurabh Das**

**by  
PROMITA NANDY**



**Department of Chemistry  
Jadavpur University  
Kolkata – 700032  
India  
2022**





**JADAVPUR UNIVERSITY**  
KOLKATA-700 032  
MARK SHEET

NO. PHCW/1701/

(For Ph.D Course Work)

Results of the	PH.D. COURSE WORK EXAMINATION, 2016
In	SCIENCE held in NOVEMBER, 2016
Name	PROMITA NANDY
Examination Roll No.	PHDCHEM16235

Course Name / Subject	Credit Hr.(c)	Marks	Grade
COMPULSORY UNITS :: EX/CHEM/PHD/A & B RESEARCH METHODOLOGY & REVIEW OF RESEARCH WORK	4	80	A
ELECTIVE UNITS :: EX/CHEM/PHD/I-1 :: APPLICATION OF SPECTROSCOPIC STUDIES IN CHEMICAL RESEARCH EX/CHEM/PHD/I-2 :: MATERIALS, CATELYSES & ELECTROCHEMICAL STUDIES EX/CHEM/PHD/P-3 :: BIOPHYSICAL CHEMISTRY & SURFACE CHEMISTRY EX/CHEM/PHD/I-4 :: SINGLE CRYSTAL X-RAY STR. SUPRAMOLECULAR CHEM.& DFT COMPUTN.	4	83	A

Total Marks : 163 (out of 200 )

SGPA: 10.00

Remarks: P

Prepared by :

Checked by :

Date of issue : 07-02-2017

Controller of Examinations

## DECLARATION

I do, hereby declare, that the work embodied in the thesis entitled "**Synthesis of metal complexes of 5-nitroimidazoles to realize their biological potential**" submitted for the award of Doctorate of Philosophy (Ph.D.) in Science, is the completion of works carried out by me under the supervision of Dr. Saurabh Das at the Department of Chemistry, Jadavpur University. The work is original and has not been submitted in part or full for any equivalent degree or diploma or any other academic award elsewhere.

In keeping with the general practice of reporting scientific observations, due acknowledgements have been made wherever the work described was done taking an active assistance of a laboratory that expertises in that particular field of investigation.

*Promita Nandy*  
*20.12.2022*

**Promita Nandy**  
Research Fellow  
Department of Chemistry  
Jadavpur University  
Kolkata-700032  
India

*Dedicated to*  
*Maa and Baba*

## ACKNOWLEDGEMENT

First and foremost, praises to the Almighty for showering His blessings throughout my journey in this doctoral programme. This journey is truly a life-changing experience which would not have been possible without the continuous support, guidance and encouragement I received from many people.

I would like to express my heartfelt gratitude to my Ph.D supervisor Prof. Saurabh Das for his expert guidance, support and inspiration all through the period of my research. His knowledge and vision in the specific area of the research work inspired me during discussions that guided me to achieve my goal. He always created a homely atmosphere in the laboratory and helped us to work in a stress free environment. I am grateful to him because without his sincere interest and dynamic supervision, this would not have been possible.

I acknowledge the support of Department of Science & Technology, New Delhi for a DST-INSPIRE fellowship for conducting this research uninterruptedly.

I also wish to express my gratitude to the present Head, Department of Chemistry, Jadavpur University, Prof. Swapan Kumar Bhattacharyya and all former HoDs, during whose tenure I performed this work, for the continuous support I received from them, in times of need.

I convey my gratitude to Prof. Subenoy Chakraborty, Dean, Faculty Council of Science and all members of staff at the faculty office for the cooperation I received from them.

No words are enough to acknowledge the help received from Prof. Sanjay Kumar of the Department of Physics, Jadavpur University with regard to solving the structure of the complex prepared by me. I wish to sincerely thank his research scholar Dr. Soumen Singha for helping me evaluate the structures.

I am grateful to Dr. Arup Gayen and his research scholars for help in procuring the PXRD data of the complex at the departmental facility.

I wish to express my deepest gratitude to Dr. Partha Mahata of the Department of Chemistry and his scholars with regard to solving the structure of a complex prepared by me using single crystal XRD.

I would be failing in my duty if I do not convey my gratitude to Prof. Kasturi Mukhopadhyay of the School of Environmental Sciences, Jawaharlal Nehru University, New Delhi for her help regarding studies performed biological assay on amoeba strain. I am thankful to her research scholar Neha Banyal for her cooperation in this regard.

I acknowledge Dr. Moupriya Nag and Dibyajit Lahiri, Department of Biotechnology, University of Engineering and Management, Kolkata for the collaborative work on bacterial biofilm formation.

I am grateful to Prof. Shouvik Chattopadhyay of the Department of Chemistry for his constant support and encouragement during my research work. I received valuable suggestions from him and support with regard to instrumental facilities.

Special thanks are also due to Prof. Tapan Kumar Mondal and Prof. Mahammad Ali, all from the Department of Chemistry, Jadavpur University for the support received related to mass spectrometry analysis. I am grateful to their respective scholars also in this regard.

I express my gratitude and respect to all my teachers at the Department of Chemistry, Jadavpur University, who taught me during my graduation and post-graduation days and who directly or indirectly provided me inspiration, valuable suggestions during the course of this study.

I am grateful to lab seniors, Dr. Piyal Das, Dr. Ramesh Chandra Santra, Dr. Durba Ganguly, Dr. Bitapi Mandal, Dr. Mouli Saha for their encouraging and motivating guidance. Heartfelt thanks are due to Mr. Tanmay Saha, Mr. Tushar Kanti Mandal and all the M.Sc. project students with whom I worked in the laboratory and their helpful company will always be remembered.

I am grateful to all staff members of the “Research Section” and “Ph D cell” of our University, non-teaching staff members of the Department of Chemistry, Jadavpur University for the cooperation they extended to me.

Last but not least, I am grateful to my parents Mr. Probir Nandy and Mrs. Mitali Nandy for their unconditional loving support all along my academic career. Their moral and spiritual support enabled me to pursue this study. Whatever I have achieved in life is because of their love, sacrifice and blessings. I also express my thanks to my beloved Husband Mr. Ranadip Das for his constant support and encouragement.

*Promita Nandy*

Promita Nandy  
Research Fellow  
Department of Chemistry  
Jadavpur University  
Kolkata-700032  
India

Date: 20.12.2022

Place: Kolkata

## LIST OF ABBREVIATIONS USED

Onz	:	Ornidazole
Tnz	:	Tinidazole
Mnz	:	Metronidazole
PXRD	:	Powder X-ray Diffraction
ORTEP	:	Oak Ridge Thermal Ellipsoid Plot
CIF	:	Crystallographic Information File
UV-Vis	:	Ultraviolet-Visible
IR	:	Infrared
MS	:	Mass spectroscopy
EPR	:	Electron Paramagnetic Resonance
CV	:	Cyclic Voltammetry
DMF	:	<i>N, N</i> -dimethylformamide
DMSO	:	Dimethyl sulfoxide
TBAB	:	Tetrabutylammonium bromide
DNA	:	Deoxyribonucleic acid
RNA	:	Ribonucleic acid
c t DNA	:	Calf Thymus DNA
TRIS	:	2-amino-2-hydroxymethylpropane-1,3-diol
EtBr	:	Ethidium bromide
MIC	:	Minimum Inhibitory Concentration
MBC	:	Minimum Bactericidal Concentration
Gy	:	Gray
HPLC	:	High Performance Liquid Chromatography
ER	:	Enhancement Ratio
XOD	:	Xanthine Oxidase
PFOR	:	Pyruvate Ferredoxin Oxidoreductase
MCF-7	:	Michigan Cancer Foundation-7
EPS	:	Extracellular Polymeric Substances
QS	:	Quorum Sensing
AIP	:	Autoinducer Peptides

## ABSTRACT

5-nitroimidazoles are effective drugs for different parasites and pathogenic microbes. They are also potential radiosensitizers in the treatment of cancer. Efficacy of 5-nitroimidazoles depends mainly on the ease of formation of the nitro-radical anion ( $R\text{-NO}_2^{\cdot-}$ ). The compounds are reduced in the presence of the enzyme pyruvate ferredoxin oxidoreductase (PFOR); reduction of the nitro group helps them to enter cells by passive diffusion creating a favourable concentration gradient. Anti-microbial efficacy of 5-nitroimidazoles depends on the reduced species which following reduction (at the nitro group) bind to DNA disrupting or breaking strands that are able to cause cell death. As radiosensitizers, they interact with radicals formed on DNA, following the latter's interaction with the products of the radiolysis of water, forming  $R\text{-NO}_2^{\cdot-}$  that thereafter enhance strand unwinding or strand breaks.

However, like many known drugs, 5-nitroimidazoles also suffer from adverse drug reactions, neurotoxicity and drug resistance following their prolonged use. Too much generation of reactive intermediates like  $R\text{-NO}_2^{\cdot-}$  is responsible. In spite of all controversies, the positive impact of 5-nitroimidazoles tends to outweigh their negative aspects. However, for a safe use of this family of drugs, a more logical approach would be to generate the correct amount of reactive intermediates. Among several approaches, one is, to prepare metal complexes of such drugs that enhance their efficacy and address issues related to toxic side effects.

As a part of this work, Ornidazole [1-chloro-3-(2-methyl-5-nitro-1H-imidazole-1-yl)propan-2-ol], an important member of the family of 5-nitroimidazoles was chosen. Cu(II) and Zn(II) complexes of it were prepared and characterized through physicochemical experiments in solution and different spectroscopic methods of analysis in solid state. Structures of Cu(II) and Zn(II) complexes were determined from single crystal X-ray diffraction and powder X-ray diffraction respectively. DNA binding experiments were performed using calf thymus

DNA as the target. A comparison was made between Ornidazole and the prepared complexes by employing physicochemical and biological approaches.

Preparation of complexes decreases formation of  $R\text{-NO}_2^{\cdot-}$ . This was realized by performing an enzyme assay using xanthine oxidase, a model nitro-reductase. While neurotoxic side effects should decrease following complex formation owing to decreased  $R\text{-NO}_2^{\cdot-}$  generation, it would lead to a compromise on therapeutic efficacy in the free radical pathway. We tried to find out aspects related to biological activity of the prepared complexes to see if that is

affected in anyway, owing to decreased free radical ( $R-NO_2^-$ ) generation. For this purpose, several bacterial strains and *Entamoeba histolytica* (HM1:IMS Strain) were chosen as biological targets. Experiments reveal, not only complexes compete with ornidazole, in fact, under longer exposure times, complexes perform better than Ornidazole. Efficacy of complexes are probably due to their ability to bind to DNA better than Ornidazole which can be understood from DNA binding studies performed to evaluate interaction of Ornidazole and its complexes with calf-thymus DNA using cyclic voltammetry.

Attempts were made to look at aspects of interaction between  $R-NO_2^-$  and other reduction products of Ornidazole and its complexes with nucleic acid bases and calf thymus DNA to realize and correlate what might be happening when such molecules either on their own or complexed to metal ions are enzymatically reduced within a biological target cell. Reduction products of Ornidazole and its complexes were generated by reducing them electrochemically i.e. holding compounds at their respective reduction potentials, determined earlier with the help of cyclic voltammetry. Purine/pyrimidine bases and calf thymus DNA were maintained in the immediate vicinity of reduced species of each compound. Reactions of generated reduction products with purine or pyrimidine bases were followed using HPLC while the amount of calf thymus DNA not modified was determined by treating DNA with ethidium bromide and recording its fluorescence. The study revealed the damage and/or modification caused to different targets by reduced species that were formed either on Ornidazole or on its prepared complexes. The damage caused to purine and/or pyrimidine bases was subsequently correlated with that observed on calf thymus DNA. The study reveals complexes were better in causing modification to nucleic acid bases and DNA when compared to Ornidazole under identical experimental conditions. This supports the fact why there is better performance by complexes on *Entamoeba histolytica* or on several bacterial targets related to bio-film formation etc. as compared to Ornidazole alone.

Experiments were also carried out to compare performance of complexes as radiosensitizers and/ or hypoxic cytotoxins with that of Ornidazole. Nucleic acid bases (thymine, cytosine and adenine) or calf thymus DNA, considered as targets, were irradiated with  $^{60}Co$   $\gamma$  rays, either in the absence or in the presence of Ornidazole and its complexes. Radiation-induced damage of nucleic acid bases were followed by HPLC while modification of calf thymus DNA was followed by the ethidium bromide fluorescence technique. Studies indicate complexes have better radiosensitizing properties than Ornidazole on a chosen biological target.

Overall, the study indicates that the modified forms of 5-nitroimidazoles achieved through complex formation are better in biological activity than the molecules chosen in this research, be it on bacterial cells or on amoeba or as radiosensitizers on model biological targets. Results reveal an expectation, although not verified medically, that the complexes (modified forms of 5-nitroimidazoles) might be less neurotoxic.

## CONTENTS

	<b>Page No.</b>
Chapter 1: Introduction	1-6
Chapter 2: 5-Nitroimidazoles as anti-microbial agents	7-19
Chapter 3: Various stimuli induced damage of nucleic acid and DNA	20-30
Chapter 4: Metal complexes of Nitroimidazoles	31-44
Chapter 5: Genesis and Scope	45-54
Chapter 6: Experimental	55-77
Chapter 7: A Zn <sup>II</sup> complex of Ornidazole with decreased nitro radical anion formation is still active on Entamoeba histolytica	78-99
Chapter 8: A monomeric complex of Cu <sup>II</sup> with Ornidazole forms significantly less nitro radical anion but was still found active on Entamoeba histolytica like Ornidazole	100-118
Chapter 9: Electrochemical reduction of Ornidazole and its Cu <sup>II</sup> complex in aqueous and aqueous-dimethyl formamide mixed solvent: A cyclic voltammetric study	119-135
Chapter 10: Interaction of electrochemically generated reduction products of ornidazole with nucleic acid bases and calf thymus DNA	136-148
Chapter 11: In situ reactivity of electrochemically generated nitro radical anion on a monomeric Cu <sup>II</sup> complex of ornidazole; interaction with nucleic acid bases and calf thymus DNA	149-166
Chapter 12: In situ reactivity of electrochemically generated nitro radical anion on tinidazole, its monomeric and dimeric Cu <sup>II</sup> complexes on model biological targets with a relative manifestation of preventing bacterial biofilm formation	167-191
Chapter 13: Radiosensitizing attributes of Cu <sup>II</sup> & Zn <sup>II</sup> complexes of Ornidazole: Role of the nitro radical anion	192-215
Chapter 14: Summary and Conclusion	216-222

# **Chapter 1**

## **Introduction**

In the light of growing climatic and environmental changes that have created a hazardous condition for health, modern day civilization is in a dire need of a constant supply of antibiotics alongside several other medicinal requirements. 5-nitroimidazoles are a class of antibiotics important from a pharmaceutical point of view. These are present in a number of formulations and used to address a wide spectrum of medical issues ranging from infections caused by parasites to being used as radio-sensitizers during radiotherapy of cancer [1-10]. These drugs are extensively used for problems pertaining to anaerobic bacterial and parasitic infections, being its major application [3, 5-8]. Being cytotoxic to cells they are also effective as chemotherapeutic agents, as radiopharmaceuticals and radiosensitizers in the treatment of various forms of cancer and related medical applications [1, 9-11]. From a more chemical point of view, location of the nitro group on the imidazole moiety determines further classification of nitroimidazole antibiotics. The nitro group at position 5 on the imidazole ring (5-nitroimidazole) is the most common positional isomer being used as drugs [12-18]. Drugs of the 5-nitroimidazole moiety include metronidazole, tinidazole, nimorazole, dimetridazole, pretomanid, ornidazole, megalzol and azanidazole. Although major use is reported for metronidazole aspects like drug resistance, neurotoxicity etc. have prompted a search for other derivatives having comparable efficacy with less adverse effects [19-24]. Ornidazole [1-chloro-3-(2-methyl-5-nitro-1H-imidazole-1-yl)propan-2-ol], an important member of this family, is gradually gaining acceptability as a drug by being an essential component of many pharmaceutical formulations that are used to treat microbial infections. Through studies and various applications on patients, it is today established that reduction of the nitro group is crucial for their activity [7, 9, 25]. Their efficiency is mainly based on their ability to generate the cytotoxic nitro radical anion ( $NO_2^-$ ). Within the biological system, these drugs are reduced by enzymes like pyruvate ferredoxin oxidoreductase (PFOR) that prepares them for

entry into cells by passive diffusion, creating a favorable concentration gradient [8-10, 19]. After entering a target cell, antimicrobial activity of nitroimidazoles depend on the reduction of the nitro group to a nitro radical-anion and/or other potentially active compounds that includes nitroso and hydroxylamine derivatives [7, 25]. Reduction products of nitroimidazoles are damaging to various macromolecules including DNA, bringing about their degradation through modification of strands [7, 9].  $NO_2^-$  binds to DNA strands within cells thereby damaging them and causing cell death [26]. Nitroimidazoles acting as radiopharmaceuticals or radiosensitizers, the cause for their action is more or less the same, the only difference being in this form of application, the nitro-radical anion ( $R-NO_2^{\bullet-}$ ) probably has a larger role than other reduction products [1, 9-11]; “R” here signifying the portion of the nitroimidazole molecule other than the nitro group. However, as is true for all 5-nitroimidazoles, efficacy does not come without adverse effects [19, 22, 23]. The principal drawback of nitroimidazoles is that on prolonged use they tend to be neurotoxic that is a hindrance to their use; i.e.  $RNO_2^{\bullet-}$  is responsible both for efficacy and toxic side effects [27, 33]. Thus too much generation of reactive intermediates of this class of drugs often causes more harm than good [34-37]. Hence, generating the correct amount of nitro-radical anion or making it available through slow chemical release is becoming an important aspect of investigation these days [11, 21, 34-37]. Several modifications have been attempted to achieve this of which, formation of metal complexes is one [11, 21, 38].

Through several research it has been revealed that complex formation of 5-nitroimidazoles modulate the generation of  $RNO_2^{\bullet-}$  that might then be expected to decrease toxic side effects [11,21]. Again since  $RNO_2^{\bullet-}$  is important for drug efficacy, its decrease, following complex formation, should therefore affect drug action. However, experiments confirmed that

complex formation did not interfere with drug efficacy. In fact, most complexes were either similar in their performance on a chosen microbial target when compared to the 5-nitroimidazole from which the complex was prepared or the complex performed better [11, 20, 21, 38]. Since complexes result in a decrease in  $\text{RNO}_2^{\bullet-}$  and yet there is no loss in efficacy, this suggests they have some other attributes [11, 20, 21, 38] that enable them to overcome any deficiency that might occur in the free radical pathway. Since complexes are compromised on the aspect of the generation of the nitro radical anion, attempts were made to look at the electrochemical behavior of metal complexes of ornidazole with respect to ornidazole itself [11, 21, 38] so that the findings could explain why complexes are either better antimicrobial or anticancer agents.

## References

1. E. J. Hall, R. Miller, M. Astro, F. Rini, *Br. J. Cancer Suppl.*, **1978**, 3, 120-123.
2. J. S. Mahood, R. L. Willson, *Br. J. Cancer*, **1981**, 43, 350-354.
3. R. P. Mason, *Free Radicals in Biology*, Eds.: W. A. Pryor, Vol. V, Academic Press New York, **1982**, 161-222.
4. C. F. Chignell, *Environ. Health Persp.*, **1985**, 61, 133-137.
5. D. I. Edwards, *Comprehensive Medicinal Chemistry*, Eds.: C. Hansch, P. G. Sammes, J. B. Taylor, Pergamon Press Oxford **1990**, vol. 2, 725-751.
6. D. Petrin, K. Delgaty, R. Bhatt, G. Garber, *Clin Microbiol Rev.*, **1998**, 11, 300-317.
7. S. L. Cudmore, K. L. Delgaty, S. F. Hayward-McClelland, D. P. Petrin, G. E. Garber, *Clin. Microbiol. Rev.*, **2004**, 17, 783-793.
8. S. Sood, A. Kapil, *Ind. J. Sex Transm. Dis.*, **2008**, 29, 7-14.

9. M. Bonnet, C. R. Hong, W. W. Wong, L. P. Liew, A. Shome, J. Wang, Y. Gu, R. J. Stevenson, W. Qi, R. F. Anderson, F. B. Pruijn, W. R. Wilson, S. M. F. Jamieson, K. O. Hicks, M. P. Hay, *J. Med. Chem.*, **2018**, 3 (61), 1241-1254.
10. R. Sharma, *Current Radiopharmaceuticals*, **2011**, 4, 361-378; R. Sharma, *Current Radiopharmaceuticals*, **2011**, 4, 379-393.
11. R. C. Santra, D. Ganguly, D. Bhattacharya, P. Karmakar, A. Saha and S. Das, *New J. Chem.*, **2017**, 41, 11679-11685.
12. J. A. Upcroft, R. W. Campbell, K. Benakli, P. Upcroft, P. Vanelle, *Antimicrob Agents Chemother.*, **1999**, 43, 73-76. doi: 10.1128/AAC.43.1.73.
13. A. L. Crowell, K. A. Sanders-Lewis, W. E. Secor, *Antimicrob Agents Chemother.* **2003**; 47(4): 1407–1409; doi: 10.1128/AAC.47.4.1407-1409.2003.
14. W. Raether, H. Hänel, *Parasit. Res.*, **2003**; 90, S19-S39.
15. Y. Miyamoto, J. Kalisiak, K. Korthals, T. Lauwaet, D. C. Young, R. Lozano, E. R. Cobo, P. Upcroft, J. A. Upcroft, D. E. Berg, F. D. Gillin, V. V. Fokin, K. B. Sharpless, L. Eckmann, *Proc. Natl. Acad. Sci. USA.* **2013**; 110(43): 17564-17569, <https://doi.org/10.1073/pnas.1302664110>.
16. C. W. Ang, A. M. Jarrad, M. A. Cooper, M. A. T. Blaskovich, *J. Med. Chem.*, **2017**; 60 (18): 7636–7657.
17. K. C. Lamp, C. D. Freeman, N. E. Klutman, M. K. Lacy, *Clin. Pharmacokinet*, **1999**, 36, 353–373. <https://doi.org/10.2165/00003088-199936050-00004>.
18. M. D. Nair, K. Nagarajan, Nitroimidazoles as chemotherapeutic agents. In: Jucker E. (eds) *Progress in drug research/Fortschritte der Arzneimittelforschung/Progrès des recherches pharmaceutiques.*, **1983** Vol. 27, Birkhäuser Basel. [https://doi.org/10.1007/978-3-0348-7115-0\\_4](https://doi.org/10.1007/978-3-0348-7115-0_4).
19. J. Thulkar, A. Kriplani and N. Agarwal, *Ind. J. Pharmacol.*, **2012**, 44, 243-245.
20. R. C. Santra, K. Sengupta, R. Dey, T. Shireen, P. Das, P. S. Guin, K. Mukhopadhyay, S. Das, *J. Coord. Chem.*, **2014**, 67, 265-285.
21. R. C. Santra, D. Ganguly, J. Singh, K. Mukhopadhyay, S. Das, *Dalton Trans.*, **2015**, 44, 1992-2000.

22. O. Kurt, N. Girginkardeşler, I. C. Balcioglu, A. Ozbilgin, U. Z. Ok, *Clin. Microbiol. Infect.*, **2008**, 14, 601-604.
23. B. Oren, E. Schgurensky, M. Ephros, I. Tamir, R. Raz, *Eur. J. Clin. Microbiol. Infect. Dis.*, **1991**, 10, 963-965.
24. M. Castella, M. Malagolia, A. I. Ruberto, A. Baggio, C. Casolarib, C. Cermellib, M. R. Bossac, T. Rossid, F. Paoluccie, S. Roffia, *J. Antimicrob. Chemother.*, **1997**, 40, 19-25.
25. M. H. Wilcox, 147-Nitroimidazoles, Metronidazole, Ornidazole and Tinidazole; and Fidaxomicin In: *Infectious Diseases*, 4th Edition, Ed.: J. Cohen, W. G. Powderly and S. M. Opal, Volume 2, **2017**, 1261-1263.e1.
26. D. I. Edwards, *Br. J. Vener. Dis.*, **1980**, 56, 285.
27. J. S. Bakshi, J. M. Ghiara, A. S. Nanivadekar, *Drugs*, **1978**, 15, 33-42.
28. H. B. Fung, T. L. Doan, *Clin Ther.*, **2005**, 27, 1859-1884.
29. J. R. Schwebke, R. A. Desmond, *Am. J. Obstet. Gynecol.*, **2011**, 204, 211.e1-211.e6.
30. K. Ebel, H. Koehler, A. O. Gamer, R. Jäckh, "Imidazole and Derivatives." In *Ullmann's Encyclopedia of Industrial Chemistry*; **2002** Wiley-VCH, doi:10.1002/14356007.a13\_661.
31. G. Cammarota, O. Cannizzaro, R. Cianci, A. Armuzzi, A. Gasbarrini, A. Pastorelli, A. Papa, G. Gasbarrini, *Dig. Dis. Sci.*, **1999**, 44, 2386-2389.
32. E. L. Plummer, L. A. Vodstrcil, J. A. Danielewski, G. L. Murray, C. K. Fairley, S. M. Garland, J. S. Hocking, S. N. Tabrizi, C. S. Bradshaw, *PLoS ONE* **2018**, 13, e0190199; <https://doi.org/10.1371/journal.pone.0190199>.
33. D. I. Edwards, *J. Antimicrob. Chemother.* **1993**, 31, 9-20.
34. P. S. Guin, P. C. Mandal, S. Das, *ChemPlusChem*, **2012**, 77, 361-369; <https://doi.org/10.1002/cplu.201100046>.
35. P. S. Guin, P. C. Mandal, S. Das, *J. Coord. Chem.*, **2012**, 65, 705-721; [doi.org/10.1080/00958972.2012.659730](https://doi.org/10.1080/00958972.2012.659730).
36. B. Mandal, S. Singha, S. K. Dey, S. Mazumdar, T. K. Mondal, P. Karmakar, S. Kumar, S. Das, *RSC Adv.*, **2016**, 6, 51520-51532.

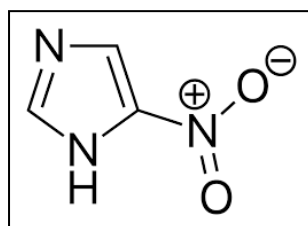
37. B. Mandal, S. Singha, S. K. Dey, S. Mazumdar, S. Kumar, P. Karmakar, S. Das, *RSC Adv.*, **2017**, 7, 41403-41418.

38. R. C. Santra, D. Ganguly, S. Jana, N. Banyal, J. Singh, A. Saha, S. Chattopadhyay, K. Mukhopadhyay, S. Das, *New J. Chem.*, **2017**, 41, 4879-4886. DOI: [10.1039/C7NJ00261K](https://doi.org/10.1039/C7NJ00261K).

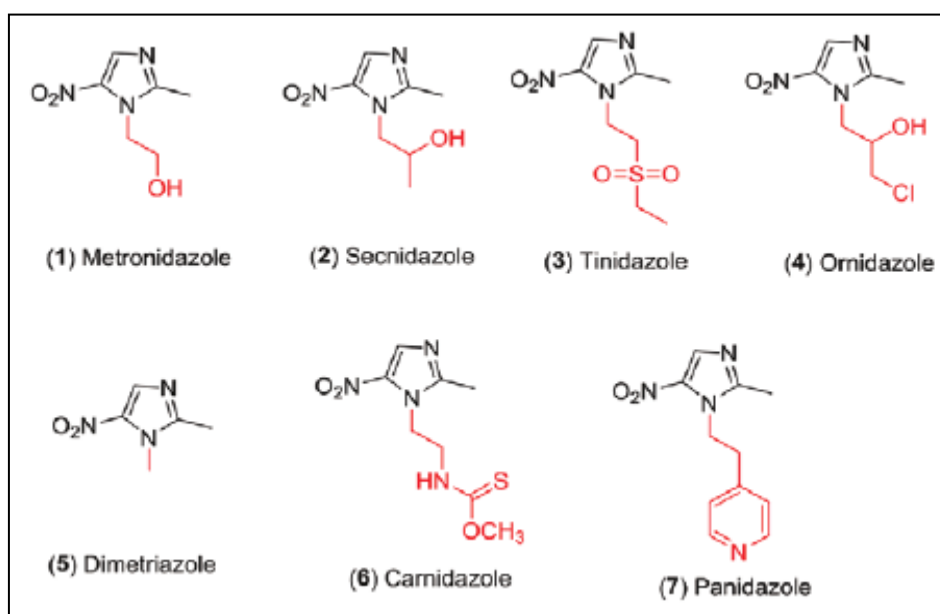
# **Chapter 2**

## **Nitroimidazoles as anti-microbial agents**

5-Nitroimidazole-based antibiotics are compounds extensively used for treating infections in human and animals that are caused by several important pathogens. Very few other groups of drugs display the kind of range of activity reported for nitroimidazoles in standard literature [1]. The mode of action of nitroimidazoles can help to explain why they have such a broad spectrum of activity.



5-Nitroimidazole



Some representative members of the 5-nitroimidazole family

This class of nitroimidazoles includes compounds that are important as antiparasitic agents having high biological activity. For instance, metronidazole (1), secnidazole (2), tinidazole (3), ornidazole (4), dimetridazole (5), carnidazole (6) and panidazole (7) are examples of drugs currently used to treat infections of anaerobic *Bacteroides sp.* and protozoans, such as

*Trichomonas sp.*, *Entamoeba sp.*, *Giardia sp.* and *Histomonas sp* [2]. Also, nitroimidazoles have other interesting properties, including antitubercular and antifungal activities, in the control of fertility, as radiosensitisers and acts against recombinant reverse transcriptase of the human immunodeficiency virus (HIV)-1 [2].

From a more chemistry perspective, nitroimidazole antibiotics can be classified according to the location of the nitro functional group on the imidazole ring. Among the three nitroimidazoles, 2-nitroimidazoles, 4-nitroimidazoles and 5-nitroimidazoles, nitro group at position 5 on the imidazole ring is the most appreciated positional isomer having a potential for drug action that have been extensively exploited in the field of anti-microbial activity.

Metronidazole has currently figured in the 22th edition of WHO's model lists of essential medicines [3]. It was discovered in mid 1950s at Rhône-Poulenc during a search for a cure for the sexually transmitted disease trichomoniasis caused by *Trichomonas vaginalis* [4]. Extracts from streptomycete 6670 were found to have potent activity against *T. vaginalis*. The purified active component was identified as azomycin (chemically known as 2-nitroimidazole) [4]. Consequently, Rhône-Poulenc developed an array of azomycin derivatives to explore this trichomonacidal activity and came up with metronidazole (1-( $\beta$ -hydroxyethyl)-2-methyl-5-nitroimidazole) which is still used today for treatment of trichomoniasis [4, 5]. The antiprotozoan activity of metronidazole was not restricted to *T. vaginalis*, since it was found to be effective against *Giardia lamblia*, the causative agent of giardiasis [6], and on *Trypanosoma cruzi*, which causes the Chagas disease (trypanosomiasis) [7]. 5 years after its discovery, metronidazole was clinically demonstrated to cure amoebic dysentery caused by *Entamoeba histolytica* [4, 8]. Since its discovery, metronidazole has been used successfully for the treatment of diseases caused by anaerobic bacteria, like in case of Gram-negative *Bacteroides fragilis*, causing peritoneal infections, the Gram-positive bacteria *Clostridium difficile* that causes pseudomembranous colitis [4] and *Helicobacter pylori*, which causes

stomach ulcers [4]. It is used extensively for the treatment of abscesses (e.g., brain, pelvis, pulmonary and tubo-ovarian), septicemias, pneumonia, endodermatitis and bacterial vaginosis, as well as anaerobic growth in the periodontal cavity [4, 9]. The drug is marketed all over the world by Pfizer and Sanofi under the trade name Flagyl. In India, it is the major component of the popular drug metrogyl. It is also sold under several other brand names in different countries. Metronidazole, which has been studied quite extensively began to be commercially used in the 1960s [10]. Metronidazole is indicated for treatment of bacterial vaginosis, commonly associated with overgrowth of gardnerella species and co-infective anaerobes (mobiluncus, bacteroides) in symptomatic patients [11]. It is also used for pelvic inflammatory disease in conjunction with other antibiotics such as ofloxacin, levofloxacin, or ceftriaxone [12]. It is prescribed for anaerobic infections like Fusobacterium spp, Peptostreptococcus spp, Prevotella spp, or other anaerobes in intra-abdominal abscess, peritonitis, diverticulitis, empyema, pneumonia, aspiration pneumonia, lung abscess, diabetic foot ulcer, meningitis and brain abscesses, bone and joint infections, septicemia, endometritis, or endocarditis [13-20]. Dental infections that are of bacterial origin like periapical abscess, periodontal abscess, acute pericoronitis of impacted or partially erupted teeth also uses metronidazole in conjunction with amoxicillin [21].

Metronidazole is not labeled as a veterinary medicine but is widely used to treat infections caused by giardia in dogs, cats and other companion animals. However, it does not reliably cure infection in these animals (dogs and cats) and therefore has to be supplemented by fenbendazole [22]. Metronidazole is also used for managing chronic inflammatory bowel disease in cats and dogs. Another common use is in the treatment of systemic and/or gastro intestinal clostridial infections in horses [23]. It is used in “aquarium hobby” to treat ornamental fish. It finds use as a wide spectrum treatment for bacterial and protozoan infections in reptiles and amphibians [24]. In general, it may be said that there is a substantial

use of metronidazole for the veterinary community to address many potentially susceptible anaerobic infections.

In spite of its wide range of use, metronidazole is associated with different forms of side effects that are a consequence of prolonged use which is today a matter of grave concern. Efforts are therefore being made to either modify metronidazole so that side effects are addressed or to use other analogues having comparable efficacy.

Tinidazole and ornidazole are two other 5-nitroimidazole drugs having comparatively less toxic side effects and sometimes a better cure rate than metronidazole [25, 26]. Of the nitroimidazoles, tinidazole and metronidazole have consistently demonstrated the greatest *in vitro* activity; tinidazole possessing a slight advantage. It is an anti-parasitic drug used against protozoan infections widely across Europe and the developing world; as a treatment for a variety of amoeba and parasitic infections. Developed in 1972, it was marketed by Mission Pharmacal under the brand name Tindamax, by Pfizer under the names Fasigyn and Simplotan, and in some Asian countries as Sporinex. There is a large body of clinical data that exists to support use of tinidazole for infections against amoebae, giardia, and trichomonas, just like metronidazole [27]. Tinidazole may be a therapeutic alternative in the setting of metronidazole tolerance and may also be used to treat vaginal infections (bacterial vaginosis, trichomoniasis) [28, 29]. It is also used to treat certain types of parasitic infections like giardiasis and amoebiasis [30]. Tinidazole is administered before gynaecological surgery or surgery of intestines to prevent post-operative infections from developing [31].

Another nitroimidazole derivative with fewer studies but excellent efficacy similar to that of tinidazole is ornidazole (Onz). It is a synthetic 5-nitroimidazole, commercially obtained from an acid-catalyzed reaction between 2-methyl-5-nitroimidazole and epichlorohydrin. It was first introduced for treating *trichomoniasis* before being recognized for its broad anti-

protozoan and anti-anaerobic-bacterial capacities. Onz is a drug that cures some protozoan infections. It is used by the poultry industry. It has also been investigated for use in Crohn's disease after bowel resection [32]. Ofloxacin with Onz, is a popular combination/formulation of antibiotics, prescribed for the treatment of peritonitis, diarrhoea, dysentery, gingivitis and pelvic inflammatory disease [33].

As already mentioned for metronidazole, this class of drugs has some common side effects. These are abdominal pain, nausea, bitter and metallic taste that prevails in the mouth, stomach upset, itchiness and headache [34]. Consumption of alcohol while taking these drugs causes an unpleasant disulfiram-like reaction causing nausea, vomiting, headache, increase of blood pressure, flushing, and shortness of breath [35]. It is advised that drugs of this group should not be prescribed during pregnancy and breastfeeding.

### **Mechanism of action**

Although there were some controversies in early literature concerning such molecules, mechanism of action of nitroimidazole drugs is reasonably well understood today. These molecules interact with several bio-chemical pathways of hosts and parasites. Several studies assumed that reductive bio-activation and generation of reactive intermediates are responsible for the overall effect. In general, nitroimidazole-based drugs are well defined as pro-drug, and the nitro functionality is responsible for their activity. Nitroimidazoles are activated by a bioreduction for which a low redox potential electron transfer system is a prerequisite and this activation is essential for their activity. Single-electron reduction of 5-nitroimidazoles produces a nitro radical anion which is unstable and can decompose to form the nitrite anion and an imidazole radical [46]. This pathway is particularly favored under anaerobic conditions. Alternatively, the nitro radical anion can be further reduced by a single electron to nitroso and hydroxylamine species and all such nitroimidazole species are capable of causing

DNA damage resulting in cell death [47] Hence the nitro group on the imidazole ring plays a major role in drug action. All drugs of this type require a reduction of the nitro group in order to kill susceptible cells. Hence, before reduction occurs the molecule must be able to enter cell. This is accomplished by a passive diffusion and is enhanced by intracellular reduction [36-38]. Reduction of the nitro group enables more drugs to enter the cell by a favourable concentration gradient as reduction proceeds intra-cellularly.

For a typical nitroaromatic compound, theoretically, six electrons would be involved in a complete reduction of the nitro group (R-NO<sub>2</sub>) to an amine (R-NH<sub>2</sub>). This classical pathway occurs by way of nitroso (R-NO) and hydroxylamino (R-NHOH) intermediates as shown in the following equation 1:



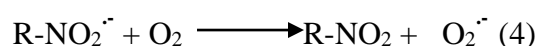
However for nitroimidazoles, the above sequence to R-NH<sub>2</sub> does not occur. The reason behind this is two-fold; first the energy required to reduce hydroxylamine to an amine is too high within a biological target cell. Secondly, reduction leads to a nitroradical anion (R-NO<sub>2</sub><sup>•-</sup>) which undergoes rapid decomposition forming a nitrite and an imidazole radical as shown in equation 2:



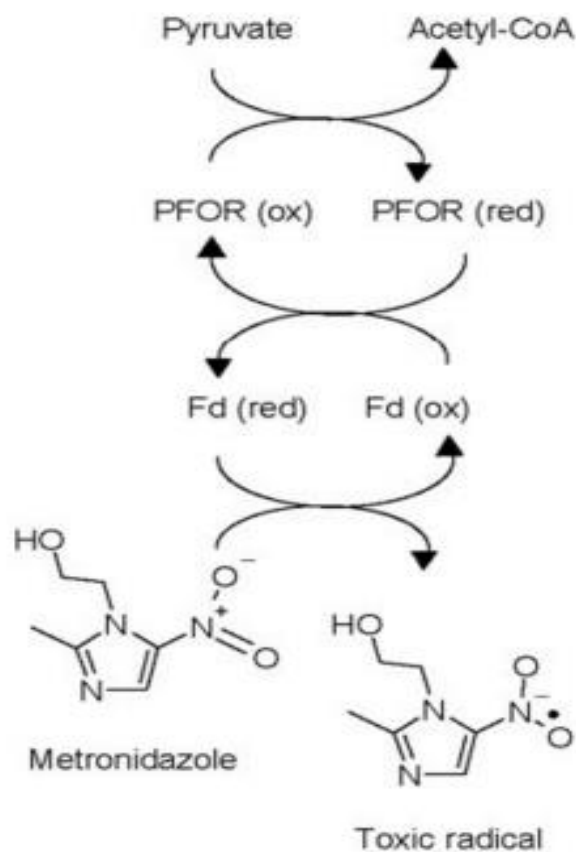
Tinidazole yields about 23% NO<sub>2</sub><sup>•-</sup> and metronidazole and ornidazole about 30% [39]. In general, therefore, 5-nitroimidazole participates in a reduction process that requires fewer than four electrons as shown in equation 1.

The activity of 5-nitroimidazoles is mainly limited to those organisms which have an anaerobic metabolism. The occurrence of reduction of the drugs will depend on the biological

redox system in the target cell. All anaerobes possess redox systems having reduction potential more negative (lower) than the drugs. Thus drugs become more efficient as electron acceptor and are subsequently reduced. The most negative redox potentials in aerobes are those of the NAD/NADH couple (-320 mV) and NADP/NADPH (-324 mV) which are more positive than nitroimidazoles. The later are therefore not reduced in aerobes and are consequently inactive. Even if reduction were to occur in presence of oxygen, damage would be limited or absent since oxygen is the naturally occurring best biological electron acceptor known and would rapidly remove the electron from the nitro radical anion, reforming the original drug and superoxide,  $O_2^{\bullet-}$  (equation 3 and 4), a process known as ‘futile cycling’ [40-43].



In a futile cycling, under aerobic conditions the nitro radical anion can reduce oxygen in micro-aerophilic organisms to form superoxide [55], which can be inactivated by superoxide dismutase and catalase enzymes. However, in presence of transition elements, such as iron or copper, which are present in the cell bound to a variety of proteins, superoxide reacts with hydrogen peroxide produced during oxidative metabolism to form hydroxyl radical by the Haber–Weiss reaction, which in turn is a potent agent of DNA damage causing DNA fragmentation thereby inhibiting DNA synthesis [55].

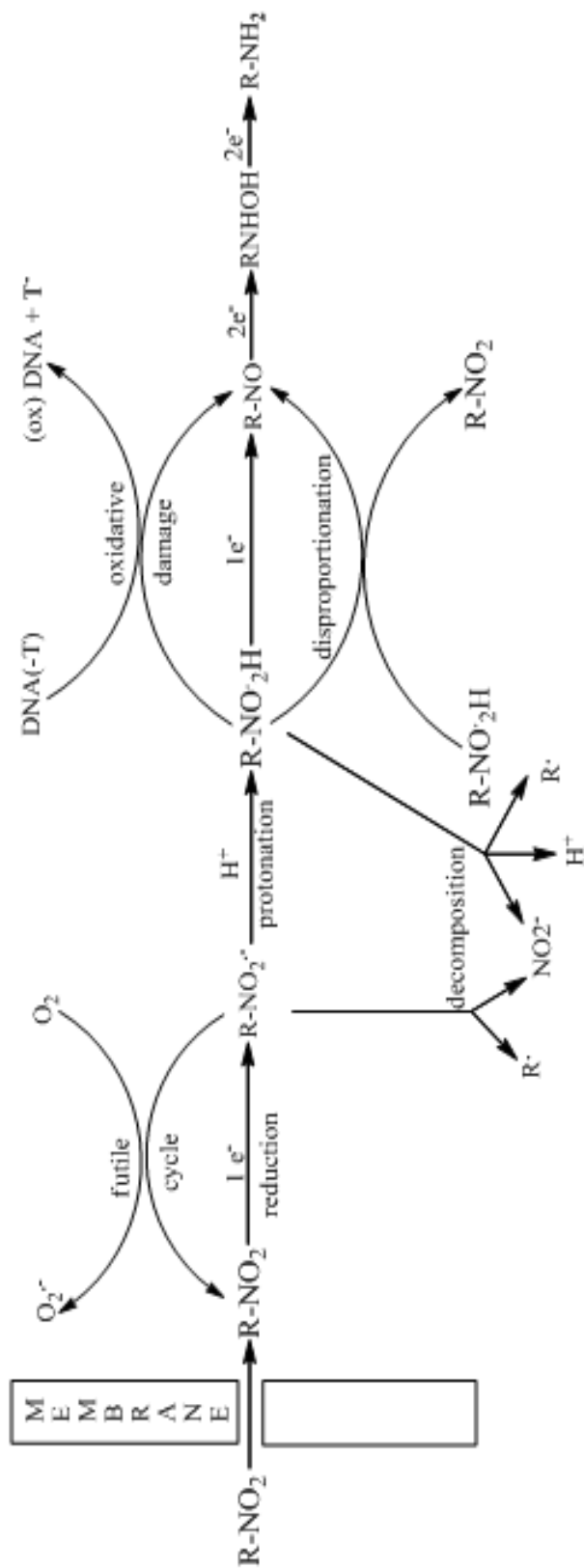


**A schematic activation mechanism of 5-nitroimidazole drugs in anaerobic bacteria, here illustrated with metronidazole**

Reduction occurs in typical anaerobes by the pyruvate ferredoxin oxidoreductase complex (formerly known as phosphoroclastic reaction), in which the nitroimidazole acts as an electron sink by capturing electrons from reduced ferredoxin which would normally be donated to hydrogen ions to form hydrogen gas in the hydrogenase reaction [44]. Pyruvate is oxidized into acetyl coenzyme A by pyruvate-ferredoxin oxidoreductase (PFOR) complex, and further, PFOR reduces ferredoxin (Fd), which finally reduces metronidazole in a single electron transfer into the toxic free radical. Thus cytotoxicity can be explained in terms of inhibition of gas production or interruption of electron flow in the cell. But these hypotheses were discarded as it was demonstrated later phosphoroclastic system recovers itself once the entire drug is reduced [45, 46]. This suggests that it is the reduction product of the drug which is responsible for cell death. The first evidence showing DNA as a target for nitroimidazoles

was from the study that demonstrated metronidazole inhibited the uptake of  $^{14}\text{C}$ -labelled thymidine in *T. vaginalis* [47]. Subsequently, it was shown that in *clostridia*, nitroimidazoles did not only inhibit DNA synthesis but degraded existing DNA strands [48]. Further, it was shown DNA degradation and strand breakage could be achieved by a chemical reduction [49]. The degree of damage caused to DNA, irrespective of how damage was measured, depended upon base composition of the DNA [50, 51]. Generally, nitroimidazoles damage DNA having a relatively high % A+T content; damage is maximal with artificial poly(d[AT]) polymers and absent with poly(d[GC]) polymers. This suggests the drug induce strand breakage specifically at adenine or thymine residues. Thymine is the more probable target because both 2- and 5-nitroimidazole release a mixture of thymine and thymidine phosphates from DNA but no other base [52].

Studies on hundreds of nitro-heterocycles indicate two important parameters; one is the reduction potential of the drug and another is the life time of the short lived reduction product. It was found that the more positive the reduction potential of the drug greater is the damage produced at the cellular level i.e. greater cytotoxicity. This relationship indicates that for each positive shift in the reduction potential by 100 mV, cytotoxicity of the compound gets doubled [53]. In addition, it is the lifetime of the damaging agent which is crucial to the action of drugs of this type. For example in a series of studies, it was shown that the lifetime of the 1-electron nitro-radical anion varied with the reduction potential and nature of the medium [54]. It was found that damage is enhanced at acidic pH indicating that the damaging agent is protonated [55]. All these studies enable one to construct a model for the mechanism of action of nitroimidazoles which is depicted below [56, 57].



Mechanism of action of nitroimidazoles

## References

1. D. I Edwards, *Biochemical Pharmacology*, **1986**, 35, 53-83.
2. N. Boechat, A. S Carvalho, K. Salomão, S. L de Castro, C. F Araujo-Lima, F. V. Mello, I. Felzenszwalb, C. A. Aiub, T. R. Conde, H. P. Zamith, R. Skupin, G. Haufe, *Mem Inst Oswaldo Cruz*, **2015**, 110(4), 492-499.
3. WHO/MHP/HPS/EML/2021.02.
4. T. Mukherjee, H. Boshoff, *Future Med. Chem.*, **2011**, 3(11), 1427–1454.
5. V A Roe, *J. Obstet. Gynecol. Neonatal Nurs.*, **1999**, 28 (6):639–648.
6. J.Schneider, *Bull. Soc. Pathol. Exot. Filiales.*, **1961**, 54, 84–95.
7. C. J Rodrigues, S L. De Castro, *Mem. Inst. Oswaldo Cruz.*, **2002**, 97(1), 3–24
8. F. J. Roe, *J. Antimicrob. Chemother.*, **1977**, 3(3):205–212.
9. C. E Barry, H. I Boshoff, C. S. Dowd, *Curr. Pharm. Des.*, **2004**, 10(26), 3239–3262.
10. D. I Edwards, *Antibiotics*, **1983**, Vol. VI, Springer Verlag, Berlin, 121-135.
11. D. A. Eschenbach, *Am. J. Obst. and Gyn.*, **1993**, 169, 441–445.
12. P. K. Heinonen, K. Teisala, R. Punnonen, R. Aine, M. Lehtinen, A. Miettinen, J. Paavonen, *Genitourinary Medicine*, **1986**, 62, 235–239.
13. J. S. Solomkin, J. E. Mazuski, J. S. Bradley, K. A. Rodvold, E. J.C. Goldstein, E. J. Baron, P. J. O'Neill, A. W. Chow, E. P. Dellinger, S. R. Eachempati, S. Gorbach, M. Hilfiker, A. K. May, A. B. Nathens, R. G. Sawyer, J. G. Bartlett, *Clin. Infect. Dis.*, **2010**, 50, 133-164.
14. J. S. Solomkin, H. H. Reinhart, E. P. Dellinger, J. M. Bohnen, O. D. Rotstein, S. B. Vogel, R.M. Echols, *Annals of Surgery*, **1996**, 223, 303–315.
15. B. Ohlin, A. Cederberg, H. Forssell, J. H. Solhaug, E. Tveit, *Eur. J. Surgery*, **1999**, 165, 875–884.
16. J. C. Monteiro, C. E. Levy, C. U. Reis, *Drug Investigation*, **1994**, 8, 1-9.
17. C. T. K. A. da Costa, C. Porter, K. Parry, A. Morris, A. H. Quoraishi, *Eur. J. Clin. Microb. and Infect. Dis.*, **1996**, 15, 75-77.
18. B. A. Lipsky, *Clin. Infect. Dis.*, **2004**, 39, S104-S114.
19. H. A. Miranda, S. M. Castellar-Leones, M. A. Elzain, L. R. Moscote-Salazar, *J. Neurosc. in Rural Practice*, **2013**, 4, S67–S81.
20. M. Gatter, *Obstetrics & Gynecology*, **2008**, 112, 1179-1180
21. R. E. Marx, Y. Sawatari, M. Fortin, V. Broumand, *J. Oral and Maxillofacial Surgery*, **63**, **2005**, 1567–1575.

22. Q. A. Mckellar, S. F. Sanchezbruni, D. G. Jones, *J Vet. Pharmaco. and Therap.*, **2004**, 27, 503–514.
23. K. G. Magdesian, M. Dujowich, J. E. Madigan, L. M. Hansen, D. C. Hirsh, DVM, S. S. Jang, *J. Am. Vet. Med. Ass.*, **2006**, 228, 751-755.
24. ‘Metronidazole’ in Wikipedia, link-<https://en.wikipedia.org/wiki/Metronidazole>.
25. J. Thulkar, A. Kriplani, N. Agarwal, *Ind. J. Pharmaco.*, **2012**, 44, 243–245.
26. S. L. Cudmore, K. L. Delgaty, S. F. Hayward-McClelland, D. P. Petrin, G. E. Garber, *Clin. Microb. Rev.*, **2004**, 17, 783–793.
27. ‘Tinidazole’ in Wikipedia, link-<https://en.wikipedia.org/wiki/Tinidazole>.
28. L. J Dickey, M. D Nailor, J. D Sobel, *Therapeutics and Clinical Risk Management*, **2009**, 5, 485–489.
29. R. C. R. Martinez, S. A. Franceschini, M. C. Patta, S. M. Quintana, B. C. Gomes, E. C. P. Martinis, Gregor Reid, *Can. J. Microb.*, **2009**, 55, 133-138.
30. H. B. Fung, T. L. Doan, *Clinical Therapeutics*, **2005**, 27, 1859–1884.
31. K. B. Fortner (editor), *The Johns Hopkins Manual of Gynecology and Obstetrics*, 3<sup>rd</sup> edition, **2007**, Baltimore, Maryland, USA, page 277.
32. P. Rutgeerts, G. Assche, S. Vermeire, G. D’Haens, F. Baert, M. Noman, I. Aerden, G. Hertogh, K. Geboes, M. Hiele, A. D’Hoore, F. Penninckx, *Gastroenterology*, **2005**, 128, 856–861.
33. [www.drugupdate.com](http://www.drugupdate.com), link-  
<http://www.drugupdate.com/generic/view/1256/Ofloxacin-+-Ornidazole>
34. W. Raether, H. Hänel, *Parasitology Research*, **2003**, 90, S19-S39.
35. S. J. Cina, R. A. Russell, S. E. Conradi, *The Am. J. Foren. Med. and Path.*, **1996**, 17, 343–346.
36. S. Sood, A Kapil, *Ind. J. Sex. Trans. Dis.*, **2008**, 29, 7-14.
37. D. Petrin, K. Delgaty, R. Bhatt, G. Garber, *Clin. Microb. Rev.*, **1998**, 11, 300-317.
38. D. I. Edwards, *The British J. Ven. Dis.*, **1980**, 56, 285–290.
39. R. J. Knox, D. I. Edwards, R. C. Knight, *Int. J. rad. Onc., Biology and Physics*, **1984**, 10, 1314-1318.
40. D. Leitsch, D. Kolarich, I. B. H. Wilson, F. Altmann, M. Duchêne, *PLoS Biology*, **2007**, 5, e211.
41. *Bioreduction in the Activation of Drugs*, Eds. P. Alexander, J. Gielen, A. C. Sartorelli, Pergamon Press, **2013**, page 56-57.

42. E. Perez-Reyes, B. Kalyanaraman, R. P. Mason, *Molecular Pharmacology*, **1980**, 17, 239-244.
43. R. C. Sealy, H. M. Swartz, P. L. Olive, *Bioph. and Biochem. Res. Comm.*, **1978**, 82, 680.
44. D. I. Edward, M. Dye, H. Carne, *J. Gen. Microb.*, **1973**, 76, 135-145.
45. R. W. O'Brien, J. G. Morris, *Archiv fur Mikrobiologie*, **1972**, 84, 225-233.
46. D. G. Lindmark, M. Muller, *J. Paratozoology*, **1974**, 21, 436.
47. R. M. J. Ings, J. A. McFadzean, W. E. Ormerod, *Biochem. Pharmacol.*, **1974**, 23, 1421-1429.
48. C. W. Plants, D. I. Edwards, *J. Antimicrob Chemother.*, **1976**, 2, 203-209.
49. D. I. Edwards, *J. Antimicrob Chemother.*, **1977**, 3, 43-48.
50. D. A. Roweley, R. C. Knight, I. M. Skolimowski, D. I. Edwards, *Biochem. Pharmacol.*, **1980**, 29, 2095-2099.
51. D. I. Edwards, R. J Knox, D. A. Roweley, I. M. Skolimowski, R. C. Knight, The biochemistry of nitroimidazole drug action. In *The Host-Invader Interplay*, Eds. H. V. den Bossche, **1980**, Elsevier/North Holland Biomedical Press, Amsterdam.
52. R. J Knox, R. C. Knight, D. I. Edwards, *Journal of medical science*, **1980**, 8, 190.
53. P. Wardman, Quantitative structure-activity relationship: principle and practice. In *Chemotherapeutic Strategy*, Eds. D. I. Edwards, D. H. Hiscock, **1983**, Macmillan, London, pp 173-192.
54. J. H. Tocher, D. I. Edwards, *Int. J. Rad. Bio.*, **1990**, 57, 45-53.
55. T. Mukherjee, H. Boshoff, C. E. Barry, *J Antimicrob. Chemother.*, **2012**, 67, 252-253
56. D. I. Edwards, R. C. Knight, A. Zahoor, *Int. J. Rad. Onco., Biology and Physics*, **1986**, 12, 1207-1209.
57. D. I. Edwards, *J Antimicrob. Chemother*, **1993**, 31, 9-20.

# **Chapter 3**

## **Various forms of stimuli induced damage of nucleic acid bases and DNA**

DNA lesion refers to a part of a DNA molecule having a primary damaged site i.e. a base alteration or a base deletion or a sugar alteration or a strand break [1]. If left unrepaired, such lesions can generate permanent mutations. The genomes in the cells of all organisms are under constant bombardment by genotoxic stress, both exogenous (e.g. ultraviolet and ionizing radiation, chemical combustion products) and endogenous (due to reactive oxygen species, nucleases etc.) [2]. These agents modify the chemical structure of DNA, alter the ability of regulatory elements to be recognized by DNA binding proteins and lead to cell death by interfering with such processes as replication and/or transcription. Lesions can occur in most parts of the DNA structure ranging from minor or major chemical modifications, single-strand breaks (SSBs) and gaps, to double-strand breaks (DSBs) [3]. Chemical modifications are the most common lesions while double-strand breaks are most lethal. Nucleic acid base lesions may be accompanied more rarely by sugar modifications and single-strand breaks. There are four major classes of base lesions: oxidation, deamination, alkylation and hydrolysis [2]. Reactive oxygen species (ROS) e.g. hydrogen peroxide, hydroxyl radical, superoxide radical anion are significant source of base damage. As a result, these chemical species have to be regulated very carefully; deliberately produced by oxidases and removed by scavengers. Hydroxyl radicals can be produced by ultraviolet (UV) radiation. Radiolysis of water caused by ionizing radiation also produces ROS in addition to reactive free protons and electrons which can produce similar sets of base lesions. Reactive oxygen and nitrogen compounds are also produced by macrophages and neutrophils at sites of inflammation and infections [4]. Such species attack DNA leading to adduct that impair base-pairing and/or block DNA replication and transcription, base loss, or DNA single-strand breaks. The most pervasive environmental DNA-damaging agent is ultraviolet light (UV). Ionizing radiation directly affects the DNA structure by inducing DNA breaks, particularly; DSBs [5]. Ionizing radiation can be divided into X-rays, gamma rays, alpha and beta particles

and neutrons. DNA damage of exposed tumour tissue leading to cell death is a detrimental effect of ionising radiation, however with a beneficial consequence in radiotherapy. Radiation therapy (RT) is widely used in cancer care strategies. Its effectiveness relies mainly on its ability to cause lethal damage to DNA of the cancer cells. However, radio-resistance of cancer cells is still a major limitation in radiotherapy. Efforts are continuously on to explore sensitizing targets for improving the outcome of radiotherapy.

One of the major problems in treating malignant cancer cells by radiotherapy is that cells become radio-resistant due to a lack of flow of blood to these cells that decreases oxygen concentration in them, making them hypoxic [6, 7]. Under such conditions, radiotherapy is unable to serve its desired purpose because molecular oxygen is an effective and a natural radiosensitizer. Hence, as an alternative to molecular oxygen in hypoxic cells, an agent is introduced that enhances radiation-induced damage of hypoxic cells using  $\gamma$  radiation used in a range of low dose so that normal cells are less affected. There has been an extensive search for such agents or compounds that are broadly classified as radiosensitizers. It is a chemical entity that is able to enhance radiation-induced damage of a tumor in a manner better than the effect obtained in its absence. The primary requirement for an efficient radiosensitizer is that it should have a good electron affinity and an ability to bind to DNA of target cells. Today a good number of radiosensitizers are known [8-13]. The effect of different types of radiosensitizers has been studied on model target molecules like nucleic acid bases, DNA and different tumor cells [14-21]. Such *in-vitro* model studies are important as they help to understand the actual mechanism of the functioning of various radiosensitizers.

Amongst radiosensitizers known, the most popular are electron affinic nitro compounds. These compounds possess different sensitizing ability depending on the position of the nitro group in the compound. Aliphatic nitro compounds like nitro alkanes have received very little

attention as radiosensitizers as they are weak oxidizing agents compared to their aromatic counterparts. As radiosensitizers, nitro-aromatic compounds include nitro-benzenes and such other compounds where the nitro group is substituted in a heterocyclic aromatic structure. These are nitrofurans, nitrothiophenes, nitrothiazoles, nitropyrazoles and nitroimidazoles [19-23]. Besides nitro derivatives, a few other classes of compounds like quinones, amino acids, amide derivatives, derivatives of uracil have also been reported as potential radiosensitizers [24-28]. Compounds containing the nitroso group have also been studied for radiosensitizing properties [30]. Besides typical organic radiosensitizers, many inorganic metal complexes have been reported to be effective radiosensitizers [29, 30]. Several studies suggest when an organic radiosensitizer is used as a ligand and metal complexes prepared, the latter turned out to be more efficient than the ligand itself. This clearly indicates the role of the metal centre during such processes [32-35].

Nitroimidazoles have also been studied extensively with regard to radiosensitization and a good number of its derivatives have made their way to clinics. The most popular being misonidazole (2-nitroimidazole derivative) and metronidazole (5-nitroimidazole derivative). Radiosensitizing properties of metronidazole were studied using bacteria, bean roots and on mammalian cells *in vitro* [39, 40]. Metronidazole has been shown to sensitize only anoxic cells in a manner that is concentration dependent. A maximum enhancement ratio of 1.9 was obtained for mammalian cells when metronidazole was used at a concentration of 8 mmol/L [36]. In another study, radiosensitization efficiencies of seven different 2-nitroimidazoles and two 5-nitroimidazoles that included metronidazole were determined using hypoxic Chinese Hamster cells as target [38]. All compounds turned out to be active hypoxic cell sensitizers. Enhancement ratio increased with increase in drug concentration. It was found that 2-nitroimidazole derivatives were more efficient than 5-nitroimidazoles. Sensitization efficiencies of compounds were correlated with their electron-affinities. Reports indicate

some quaternary salts of 5-nitroimidazole derivatives were tested for survival of mammalian TC-SV40 cells revealing that derivatives show no enhancement in aerobic condition but are quite effective under hypoxic conditions [39]. Metal complexes of nitroimidazoles have also been prepared and experiments designed to test their radiosensitizing efficiencies. One such study revealed  $\text{Cu}^{\text{II}}$  and  $\text{Ni}^{\text{II}}$  complexes of metronidazole significantly increased radiolytic degradation of thymine [40]. The compound as well as its complexes was found to promote the formation of thymine glycol with a significant increase observed for complexes. The higher radiosensitizing property observed for these complexes as compared to free metronidazole was said to be due to the higher rate of oxidation of transient thymine-OH radical adduct. In another study, four cis-platinum(II) complexes (analogues of *cis*-platin) were prepared taking 4- and 5-nitroimidazoles and their sensitizing properties examined to test the hypothesis that targeting nitroimidazoles to DNA through complexation with Pt(II) could enhance their radiosensitizing ability [38]. Structures of such nitroimidazole complexes being similar to *cis*-platin had actually enabled these researchers to have the idea to target DNA with nitroimidazoles. It was found in that same study that complexes were able to bind to DNA better than nitroimidazoles themselves.

It is often said “radiotherapy is free radical therapy” since it involves participation of products following the radiolysis of water, majority of which are free radicals. 70% of the cell being made up of water, 69% of the damage due to radiation is due to the interaction of free radicals derived from water with biological targets. Free radicals produced interact either with nucleic acid bases or with sugar moieties present on DNA initially leading to strand winding and subsequently to strand modification or strand break [44]. Hence, reason for cell death may be attributed to disruption of the double helical structure of DNA and to subsequent damage of intracellular DNA. The mechanism of DNA damage following irradiation is really very complex and there are a lot of studies on it [44]. The most accepted

pathway as understood so far seems to be due to formation of free radicals that are derived from radiolysis of water ( $\text{H}\cdot$ ,  $\text{OH}\cdot$ ,  $e_{\text{aq}}^-$ ) that react with purine or pyrimidine bases (Fig. 1) in intracellular DNA forming deoxyribonucleotide radicals [19]. These abstract hydrogen atoms from neighboring sugar moieties leading to strand breaks. There are many studies on the effect of ionizing radiation on pyrimidine bases, constituents of DNA [14-17, 43, 45]. These studies on pyrimidine bases with primary species obtained from the radiolysis of water are essential since they help us to realize what happens when radicals attack a macromolecule like DNA. The reactions and mechanistic pathways realized from such model studies that include the identification of intermediates along with an analysis of stable products formed help us to identify the damage caused to a structure like that of DNA. The products that have been characterized so far following radiolysis of pyrimidines include dimmers, pyrimidine glycols, hydroxyl dihydropyrimidines, isobarbituric acid, dialuric acid, 5-hydroxymethyluracil and some five member heterocyclic compounds [13, 14, 40].

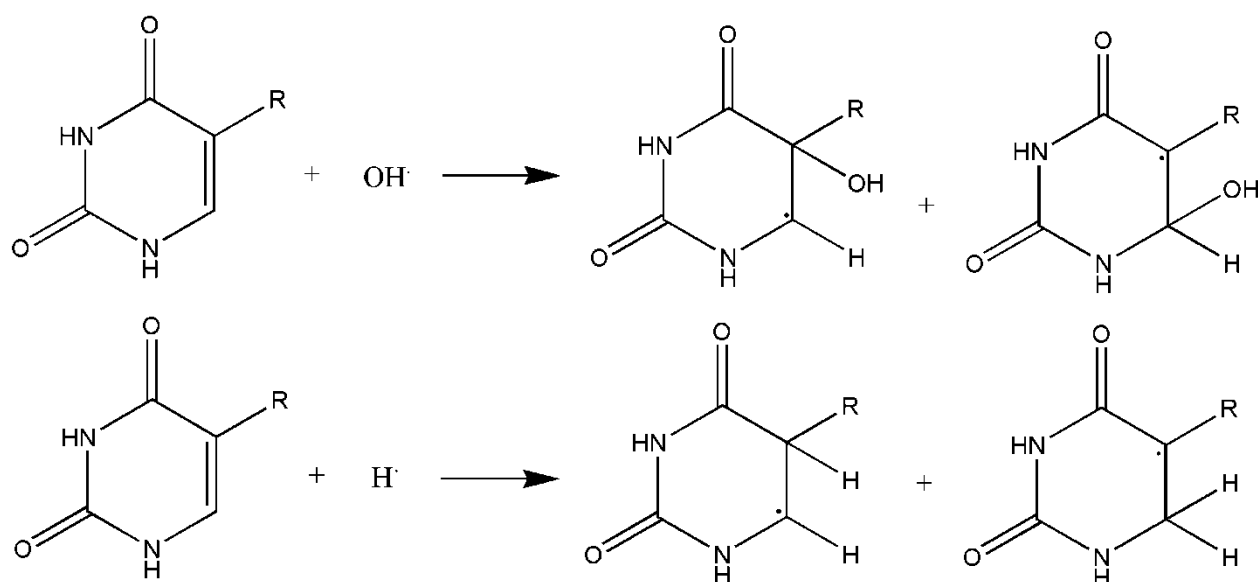


**Figure 1: Reactions of pyrimidines with  $\text{H}\cdot$  and  $\text{OH}\cdot$  (formed from the radiolysis of water)**

Mechanism of radiation induced damage in the presence of different radiosensitizers is different and depends on the structure of the sensitizer molecule. In general, there are two ways by which a radio sensitizer may enhance radiation induced damage on DNA [19, 42]. One is by directly interacting with radiolyzed products of water producing reactive intermediates that then interact with DNA causing damage. Another is when the radiolyzed products of water at first interacts with DNA at a site of a nucleic acid base forming reactive intermediates that are then acted upon by a sensitizer molecule using its electron affinic character which enhances DNA damage (Fig. 2). Oxygen and nitroimidazole derivatives are believed to follow the second mechanistic pathway. Radiolytic products of water such as  $\cdot\text{OH}/\cdot\text{H}$ . can add to the  $\text{C}_5\text{-C}_6$  double bond of pyrimidine bases to form a carbon centered radical (shown in the scheme ). Left to itself this radical on a carbon centre could either regenerate the double bond or proceed to modify the nucleic acid base permanently.

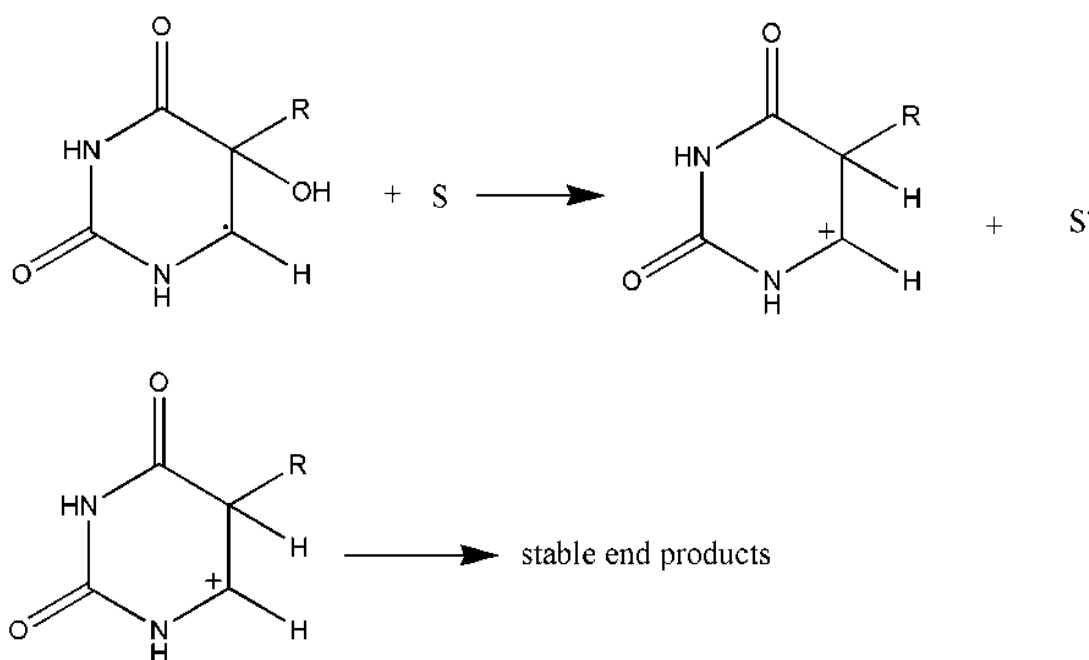


**Figure 2: One of the possible ways of sensitization: Sensitizer molecule (S) takes an electron from pyrimidine-OH adduct radical to form a carbocation which upon reaction with water molecule or other species forms different stable end products.**

In the presence of sensitizer molecules the first pathway is minimized as it quickly withdraws the electron on the carbon radical towards itself either through formation of an adduct or by simple intermolecular electron transfer not involving adduct formation i. e. generating a carbocation.

Once a carbocation is formed nucleic acid bases are modified immediately because water rushes in to convert the carbocation to an –OH linked carbon centre. Thus most often a glycol is the major product in the presence of a radiosensitizer. In case of a cell the situation is a lot more complicated since it involves DNA repair enzymes and various sensor molecules that detect radical formation on the DNA that could be damaging to the body. Hence compared to model studies use of a sensitizer for inducing DNA damage within cells is even more required [45-48]. One of the widely accepted mechanisms involving nitro-aromatic compounds, known as “electron affinic radiosensitizers” is that the electron is received at the nitro group with the sensitizer molecule forming an adduct with C5 or C6 of pyrimidine bases [19, 42]. The nitro radical anion of the adduct then abstracts hydrogen from a neighbouring sugar C-H that transfers the radical centre from the base to the sugar leading to strand breaks. So efficiency of the radiosensitizer in such a mechanism depends on its ability to accept electrons from a pyrimidine base by a nitro group. Electron affinity as well as DNA binding ability may significantly alter if metal complexes of this class of molecules are prepared. Studies of new transition metal complexes of nitroimidazoles in this regard would therefore be very interesting.

Another stimuli responsible for generation of nitro radical anion are electrons whereby such compounds are reduced by electrons of the electron transport present in mitochondria [49, 50]. Of the various range of potentials involved any one region or a group of regions could have the potential in which reduction of the nitro group in these drugs fall.

Hence we looked at the possibility as to what might happen if the compounds reach the mitochondria of cells. Once generated it would interact with biological targets. An attempt was therefore made to generate free radicals using a potentiostat maintaining glassy carbon electrode and monitor damage caused to a biological target. There are very few work in this regard and hence using a novel technique to mimic interaction of 5-nitroimidazoles and its complexes with the components of the electron transport chain (Fig. 3) is new and unique [51, 52]. 5-nitroimidazoles may be reduced by an electrochemical method using glassy carbon electrode, wherein, in the immediate vicinity of reduction products of the molecule four different nucleic acid bases (taken one at a time) or calf thymus DNA could be kept. The reduction products bring about a damage of the biological target which was followed with the help of suitable experimental techniques. Hence, to be able to do this work, it becomes necessary to identify the reduction potential of a 5-nitroimidazole that may be done in aqueous medium prior to start of such experiments.

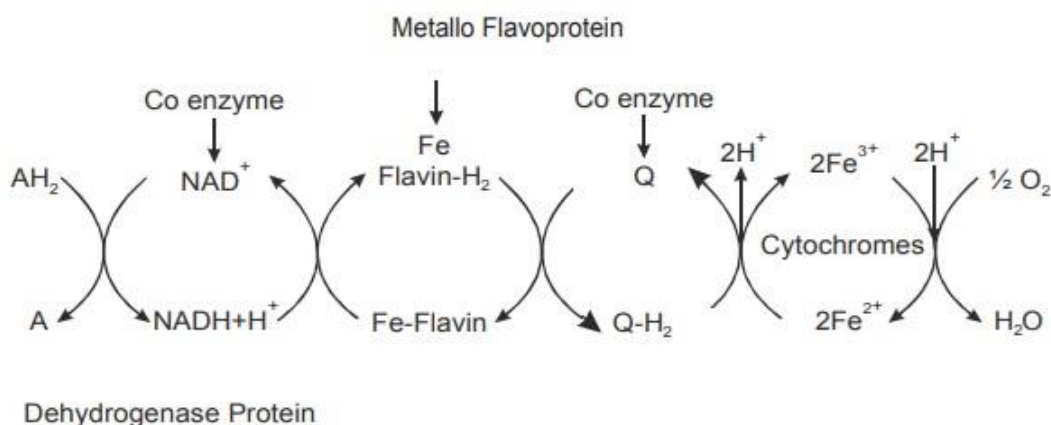


**Figure 3: Electron transport chain**

## References

1. DNA Lesion. In: Encyclopedic Reference of Genomics and Proteomics in Molecular Medicine. Springer, **2005**, [https://doi.org/10.1007/3-540-29623-9\\_6798](https://doi.org/10.1007/3-540-29623-9_6798)
2. N. C. Bauer, A. H. Corbett, P. W. Doetsch, *Nucleic Acids Res.*, **2015**, 43(21): 10083–10101.

3. W. J. Cannan, D. S. Pederson, *J Cell Physiol.*, **2016**, 231(1): 3–14.
4. S. P. Jackson, J. Bartek, *Nature*. **2009** , 461(7267), 1071–1078.
5. G. Borrego-Soto, R. Ortiz-López, A. Rojas-Martínez, *Genet Mol Biol.* **2015**, 38(4): 420–432.
6. W. E. Powers and L. J. Tolmach, *Nature (London)*, **1963**, 197, 710-711.
7. L. H. Gray, A. D. Conger, M. Ebert, S. Hornsey, O. C. H. Scott, *Br. J. Radiol.*, **1953**, 26, 638-648.
8. J. F. Fowler, *Int. J. Rad. Onco. Biology Physics*, **1985**, 11, 665-674.
9. J. F. Fowler, J. Denekamp, *Pharmacology & Therapeutics*, **1979**, 7, 413–444.
10. D. W. Siemann, *Int. J. Rad. Onco. Biology Physics*, **1982**, 8, 1029-1034.
11. J. Raviraj, V. K. Bokkasam, V. S. Kumar, U. S. Reddy, V. Suman, *Ind. J Dent. Res.*, **2014**, 25, 83-90.
12. A. G. Linkous, E. Yazlovitskaya, *Anticancer Res.*, **2012**, 32, 2487-2499.
13. H. B. Michaels, E. J. Rasburn, J. W. Hunt, *Rad. Res.*, **1976**, 65, 250-267.
14. J. R. Wagner, J- E. van Lier, L. J. Johnston, *Photochemistry and Photobiology*, **1990**, 52, 333–343.
15. R. B. Tishler, P. B. Schiff, C. R. Geard, E. J. Hall, *Int. J. Rad. Onco. Biology Physics*, **1992**, 22, 613-617.
16. B. A. Teicher, J. S. Lazo, A. C. Sartorelli, *Cancer Research*, **1981**, 41, 73-81.
17. T. S. Lawrence, J. E. Tepper, A. W. Blackstock, *Seminars in Radiation Oncology*, **1997**, 7, 260–266.
18. J. M. Brown, *Rad. Res.*, **1977**, 72, 469-486.
19. P. Wardman, *Clinical Oncology*, **2007**, 19, 397–417.
20. G. E. Adams, E. D. Clarke, I. R. Flockhart, R. S. Jacobs, D.S. Sehmi, I. J. Stratford, P. Wardman, M. E. Watts, J. Parrick, R. G. Wallace, C. E. Smithen, *Int. J. Rad. Bio. and Related Studies in Physics, Chemistry and Medicine*, **1979**, 35, 133-150.
21. M. E. Watts, *Int. J. Rad. Bio. and Related Studies in Physics, Chemistry and Medicine*, **1977**, 31, 237-50.
22. M. D. Threadgill, P. Webb, P. O'Neill, M. A. Naylor, M. A. Stephens, I. J. Stratford, S. Cole, G. E. Adams, E. M. Fielden, *J. Med. Chem.*, **1991**, 34, 2112–2120.

23. E. M. Fielden, G. E. Adams, S. Cole, M. A. Naylor, P. O'Neill, M. A. Stephens, I. T. Stratford, *Int. J. Rad. Onco. Biology Physics*, **1992**, 22, 707–711.
24. S. Das, A. Saha, P. C. Mandal, *J. Radioanal. and Nuclear Chem.*, **1995**, 196, 57-63.
25. P. S. Guin, P. C. Mandal, S. Das, *Rad. Phys. and Chem.*, **2013**, 89, 38–42.
26. S. Das, P. C. Mandal, *J. Radioanal. and Nuclear Chem*, **2014**, 299, 1665-1670.
27. S. Das, P. C. Mandal, *Rad. Phys. and Chem.*, **2009**, 78, 37–41.
28. L. Chomicz, M. Zdzrowowicz, F. Kasprzykowski, JanuszRak, A. Buonaugurio, Yi Wang, K. H. Bowen, *J. Phy. Chem. Let.*, **2013**, 4, 2853–2857.
29. Z.V. Kuropteva, T. T. Zhumabaeva, *Med Radiol (Mosk)*. **1986**, 31(12), 56-59.
30. D. M. L. Goodgame, C. J. Page, D. J. Williams, I. J. Stratford, *Polyhedron*, **1992**, 11, 2507–2515.
31. H. Ali, J. E. van Lier, *Chem. Rev.*, **1999**, 99, 2379-450.
32. P. K. L. Chan, K. A. Skov, B. R. James, N. P. Farrell, *Int. J. Rad. Onco. Biology Physics*, **1986**, 12, 1059–1062.
33. K. A. Skov, *Rad. Res.*, **1987**, 112, 217-242.
34. R. Chibber, I. J. Stratford, I. Ahmed, A. B. Robbins, D. Goodgame, B. Lee, *Int. J. Rad. Onco. Biology Physics*, **1984**, 10, 1213–1215.
35. K. A. Skov, N. P. Farrell, *Int. J. Rad. Bio.*, **1990**, 57, 947-958.
36. J. C. Asquith, J. L. Foster, R. L. Willson, *Br. J. Radiol.*, **1974**, 47, 474-81.
37. J. M. Brown, *Cancer Res.*, **1999**, 5863-5870.
38. G. E. Adams, I. R. Flockhart, C. E. Smithen, I. J. Stratford, P. Wardman, and M. E. Watts, *Rad. Res.*, **1976**, 67, 9-20.
39. L. Santos, M. C. L. Zumel, M. V. Alvarez, M. C. Izquierdo, *Int. J. Rad. Bio.*, **1989**, 55, 983-991.
40. M. B. Roy, P. C. Mandal, S. N. Bhattacharya, *Int. J. Rad. Bio.*, **1996**, 69, 471-480.
41. R. C. Santra, D. Ganguly, D. Bhattacharya, P. Karmakar, A. Saha, S. Das, *New J. Chem.*, **2017**, 41, 11679-11685.

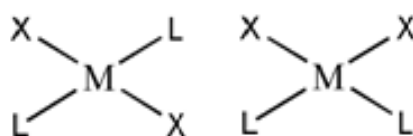
42. C. von Sonntag, *Free-radical-induced DNA damage and its repair. A chemical perspective*, **2006**, Berlin, Springer.
43. G. Iliakis, S. Kurtzman, G. Pantelias, R. Okayasu, *Rad. Res.*, **1989**, 119, 286-304.
44. A. Phaniendra, D. B. Jestadi, L. Periyasamy *Ind. J. Clin Biochem.* **2015**, 30(1): 11–26.
45. M. A. Morgan, L. A. Parsels, L. Zhao, J. D. Parsels, M. A. Davis, M. C. Hassan, S. Arumugarajah, L. Hylander-Gans, D. Morosini, D. M. Simeone, C. E. Canman, D. P. Normolle, S. D. Zabludoff, J. Maybaum, T. S. Lawrence, *Cancer Res.*, **2010**, 70, 4972-4981.
46. H. H. Kampinga, J. R. Dynlacht, E. Dikomey, *Int. J. Hypertherm.*, **2004**, 20, 131-139.
47. S. J. Veuger, N. J. Curtin, C. J. Richardson, G. C. M. Smith, B. W. Durkacz, *Cancer Res.*, **2003**, 63, 6008-6015.
48. A. Munshi, J. F. Kurland, T. Nishikawa, T. Tanaka, M. L. Hobbs, S. L. Tucker, S. Ismail, C. Stevens, R. E. Meyn, *Clin. Can. Res.*, **2005**, 11, 4912-4922.
49. Ru-Zhou Zhao, Shuai Jiang, Lin Zhang, Zhi-Bin Yu, *Int. J. Mol. Med.*, **2019**; 10.3892/ijmm.2019.4188
50. D. Nolfi-Donagan, A. Braganza, S. Shiva, *Redox Biology*, **2020**, 37, 101674
51. M. Saha, S. Das, *Heliyon*, **2021**, 7(8), e07746.
52. B. Mandal, H. K. Mondal, S. Das, *Biochim. Biophys Res Comm*, **2019**, 515, 505-509.

# **Chapter 4**

## **Metal complexes of Nitroimidazoles**

The importance of metal ions in the vital functioning of various constituents of living organisms, from mammals to bacteria has been widely recognized. Interaction of metal ions with drugs administered for therapeutic reasons is a subject of considerable interest. Development of bacterial resistance to existing drugs has encouraged a search for alternatives. Novel metal complexes and their derivatives represent an interesting approach for designing new antibacterial drugs. This is due to the dual role of both ligands (here drugs) and the metal ion involved interacting at different stages of the life cycle of bacteria. Transition metals in the form of different complexes are potentially used as drugs and/or diagnostic agents to treat a variety of diseases. Many inorganic complexes show antitumor, antibacterial, antifungal and antimicrobial activity. Literature survey reveals coordination of metal ions to biologically active compounds might enhance their activities. Imidazole derivatives have often been used as chelating ligands in the field of coordination chemistry and their metal complexes are of special interest for many years because of the variety of ways in which they are bonded to metal ions. It was found that complexes of transition metal salts with imidazole derivatives showed greater antimicrobial activity than the compound applied alone. From the perspective of coordination chemistry, mainly four types of metal complexes of 5-nitroimidazoles and their derivatives are reported in the literature. In most cases, 5-nitroimidazole acts as a ligand to coordinate the central metal ion using the 3 position (nitrogen) of the imidazole ring. There are a few exceptions where the nitro group is involved in bond formation with the metal center. Different types of complexes with various 5-nitroimidazole or its positional isomers have been prepared. Some of them are mentioned below.

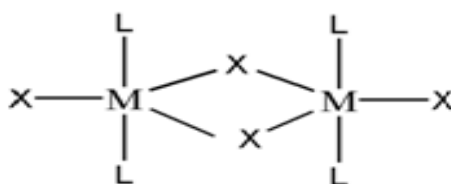
The **Type I** includes square planar complexes (mainly Pt(II) and Cu(II)) where the metal ion is bound to two 5-nitroimidazole moieties and two halide ions that are present as co-ligands.



**Type-I**

(M, X and L represent metal ion, halide and 5-nitroimidazole derivatives respectively)

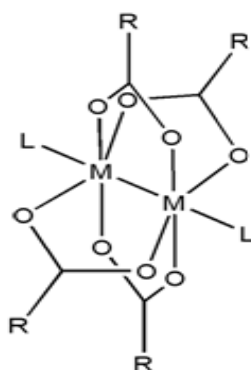
**Type II** has binuclear metal ion complexes with two metal centers, each bound to two nitroimidazoles and held together by bridging halide ions. These usually have a trigonal bipyramidal structure around each metal center with two 5-nitroimidazole ligands at the axial position and halide ions on the equatorial plane.



**Type-II**

(M, X and L represent metal ion, halide and 5-nitroimidazole derivatives respectively)

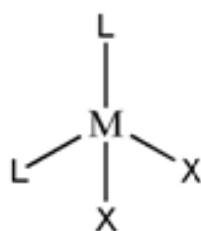
**Type III** includes complexes that are binuclear with a paddle wheel structure formed by carboxylate ions as bridging ligands. In these complexes, each metal center is connected to four oxygen atoms of the carboxylate while the fifth position is occupied by a 5-nitroimidazole forming a square pyramidal geometry.



**Type-III**

(M and L represent metal ion and 5-nitroimidazole derivatives respectively and R represents organic part of carboxylate ion).

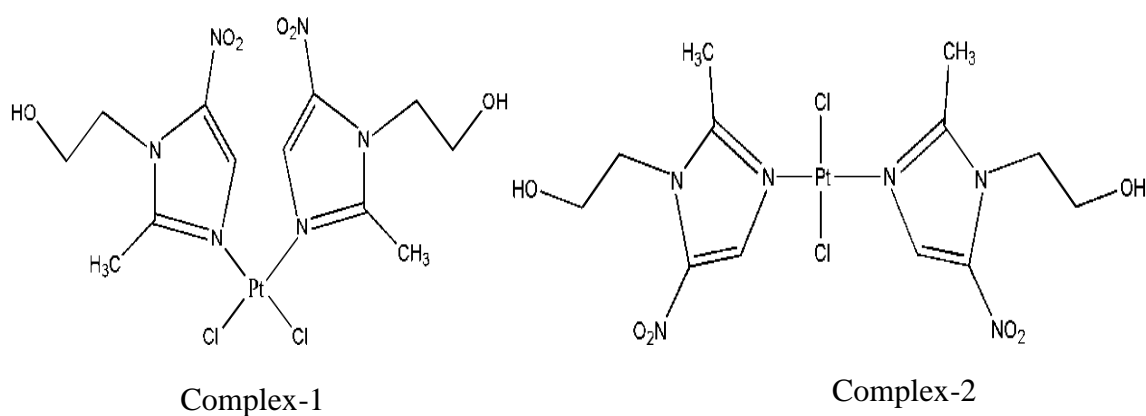
First row transition metal ions like Cu(II), Co(II), Zn(II)) form tetrahedral complexes (**Type IV**) with two 5-nitroimidazoles and two halide ions as co-ligands. Most reports centre around the synthesis, structural analysis, physical and/or spectral properties of the complexes. Apart from structural characterization, aspects related to spectroscopy, EPR and magnetic susceptibility measurements, majority of studies focus on the antimicrobial attributes of the compounds for which they are mostly known. 5-nitroimidazoles have also been studied extensively owing to their ability to act as radiosensitizers. Several reports indicate that derivatives of parent 5-nitroimidazoles that includes metal complexes were found to possess better radiosensitizing properties than the compounds from which the complexes were prepared. Hence, for different reasons there has been a growing interest in this area and a need for a thorough review for one to realize why researchers thought it necessary to prepare metal complexes of 5-nitroimidazoles.



**Type-IV**

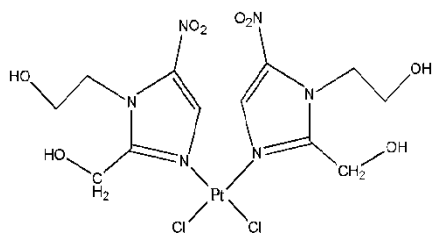
The first metal complex of the 5-nitroimidazole family was synthesized to arrive at an analogue of *cis*-platin and was reported in 1982 [1]. The complex was obtained by the addition of K<sub>2</sub>PtCl<sub>4</sub> to a suspension of metronidazole in water at 50<sup>0</sup> C. A yellow crystalline product was obtained. X-ray crystal structures of the *cis* complex (complex 1) was established the following year and it was found to be square planar around Pt(II) [2]. The complex was characterized by elemental analysis (C, H, N, Cl and Pt) and proton nuclear

magnetic resonance spectroscopy. The complex was found to be an efficient radiosensitizer with an enhancement ratio of 2.4 compared to what was found for metronidazole or other Pt(II) complexes on Chinese hamster ovary cells [1]. The structure of the *trans* isomer (complex 2) was also obtained when the *cis* form was melted and recrystallized. In both isomers, the imidazole rings are slightly tilted relative to the Pt(N)<sub>2</sub>Cl<sub>2</sub> square plane.

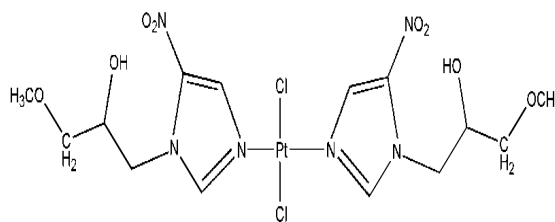


Many first row transition metals (Mn, Fe, Co, Ni, Cu) form complexes with 2-methyl-5-nitrobenzimidazole and metronidazole. These were synthesized and characterized and found to have the general formula M(nitroimidazole)<sub>2</sub>X<sub>2</sub> where X is Cl or Br or I [3]. A wide range of neutral platinum(II) complexes containing 5-nitroimidazoles, together with halides or dicarboxylates as ligands have also been reported [4]. In addition, 2- and 4-nitro-imidazole complexes of Pt(II) were prepared to compare their properties with those of 5-nitroimidazoles. Crystal structures of two square planar Pt<sup>II</sup>(nitroimidazole)<sub>2</sub>Cl<sub>2</sub> having two 5-nitroimidazole derivatives were obtained (complex-3 and complex-4) [4]. Synthesis, structural characterization and supramolecular interaction of many Co<sup>II</sup>, Cu<sup>II</sup> and Zn<sup>II</sup> complexes of metronidazole have also been reported. Coordination of the metal ion occurs through the imidazole nitrogen (N3) with hydroxyethyl and nitro groups acting as supramolecular synthons [5]. Co<sup>II</sup> and Zn<sup>II</sup> complexes (complex 5) have a structure shown earlier with the help of complex 3 or complex 4 having the general formula

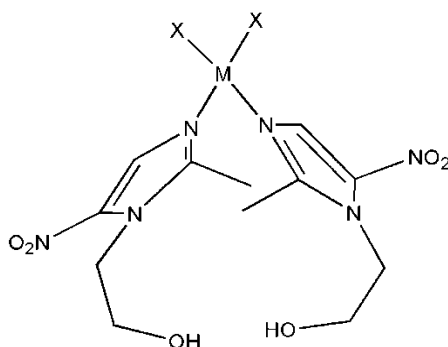
$M(\text{metronidazole})_2X_2$  where X is Cl and/or Br. In these complexes, metal ions were bound by two halide atoms and two nitrogen atoms of the two imidazole rings. Geometry of the complexes was nearly tetrahedral.



Complex-3

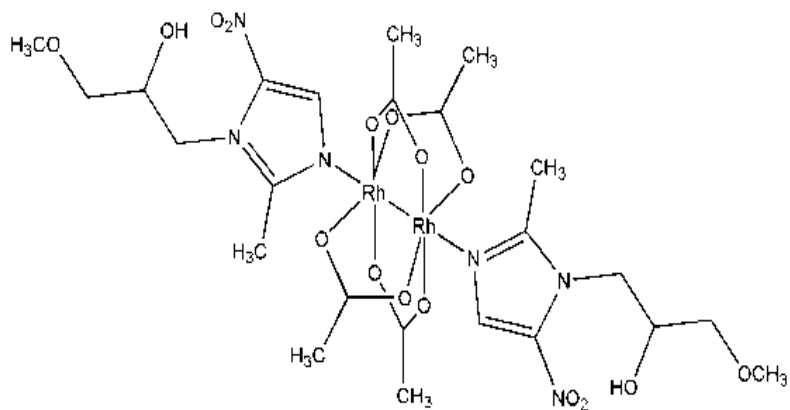


Complex-4



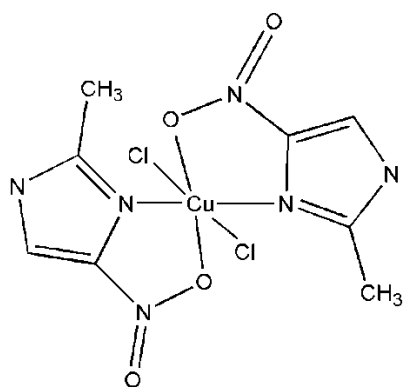
Complex-5

Some  $Rh^{II}$  bicarboxylate complexes of 2-nitroimidazole derivatives along with a 5-nitroimidazole derivative were synthesized and X-ray crystal structure (Complex-6) reported [6]. The complex possess a binuclear paddle wheel structure. Two Rh atoms were held by four acetate bridges and an N3 atom of the imidazole ring coordinated to Rh making a square pyramidal geometry around each Rh atom. The synthesized complexes were examined for their ability to act as radiosensitizers on Chinese hamster mammalian cells *in vitro*. The complexes were found to be more efficient than ligands (here the 5-nitroimidazoles).



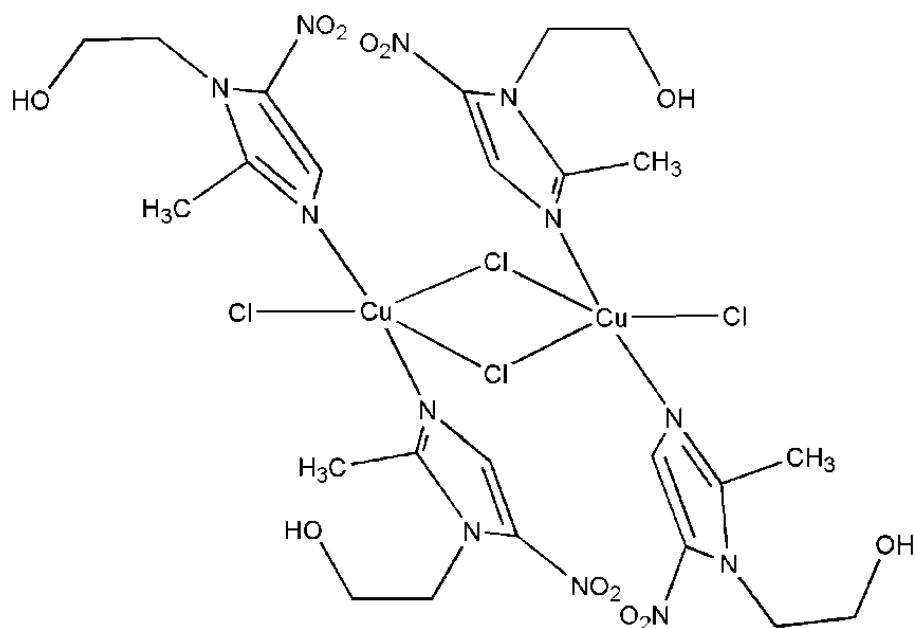
Complex-6

Different  $\text{Cu}^{\text{II}}$  and  $\text{Co}^{\text{II}}$  complexes having the general formula  $\text{ML}_2\text{X}_2$  but a completely different mode of coordination than that discussed using type (complex 3 and complex 4) were prepared;  $\text{L} = \text{metronidazole}$  and  $\text{X} = \text{Cl}/\text{Br}/\text{NO}_3/\text{OH}$ . These were characterized with the help of spectroscopy and single crystal X ray diffraction analysis [7]. Crystal structures of  $\text{Cu}(\text{2-methyl-5-nitroimidazole})_2\text{Cl}_2$  (Complex-7) and  $\text{Cu}(\text{metronidazole})_2\text{Cl}_2$  (Complex-8) reveals that in the type represented by complex 8, each 2-methyl-5-nitroimidazole ligand acts as a bidentate ligand, and more importantly, in these complexes the 5-nitro group is involved in coordinating the metal centre forming an octahedral species. The structure has a symmetry centre at the metal ion with a tetragonally distorted octahedral geometry and a *trans* diaxial coordination of one of the oxygen atoms of the nitro groups [7]. This is the first report of a nitroimidazole complex where the nitro group is coordinated to the metal centre.



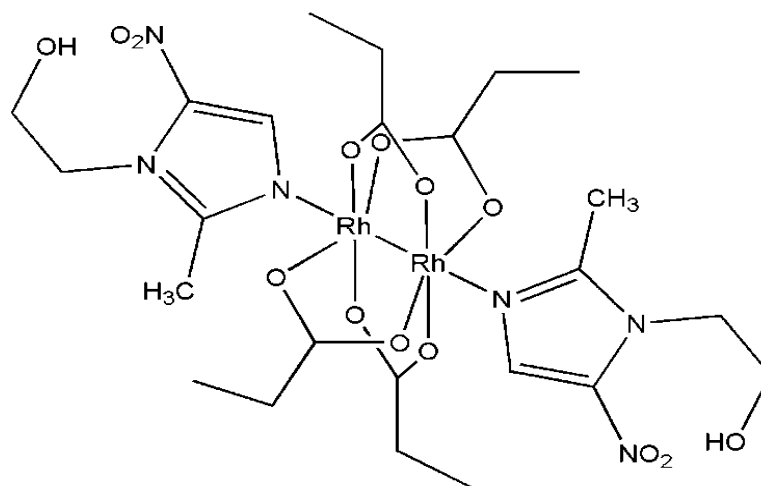
Complex-7

Complex-8 is a chloro-bridged dimer with coordination geometry around each copper centre being trigonal bipyramid. There are three equatorial chlorine atoms and two axial imidazole molecules coordinated by the N3 atom of the imidazole ring.



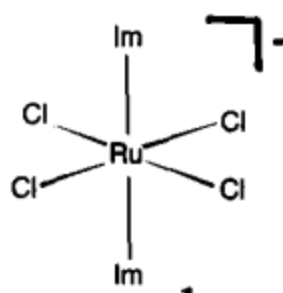
Complex-8

Synthesis and characterization of a  $[\text{Co}(2\text{-methyl-5-nitroimidazole})(\text{OAc})_2]^+$  and a  $[\text{Cu}(\text{metronidazole})(\text{OAc})_2]$  has also been reported [7]. A propionato-bridged dinuclear Rhodium complex (complex-9) with metronidazole was prepared and characterized by X-ray diffraction studies [8]. The structure was similar to that represented as complex-6. Antitumor activity as well as acute toxicity due to the complex has been studied. The complex showed its ability to inhibit DNA synthesis. Antimicrobial activity was studied by performing an MIC assay on bacterial strains (*Staphylococcus Aureus*, *Escherechia Coli*, *Klebsiella Pneumoiae*, *Pseudomona Aeruginosa*) and yeasts (*Candida Albicans*, *Cryptococcus Neofomans*). The complex was found to be more active on *Staphylococcus Aureus* and *Pseudomona Aeruginosa* than metronidazole.



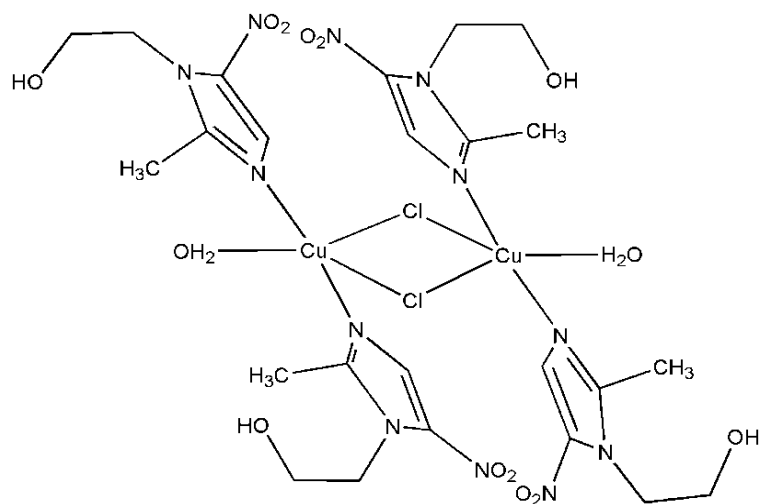
Complex-9

Tetrachlorobis(5-nitroimidazole) ruthenium(III) anion (Complex-10) was synthesized by reacting with 4-nitroimidazole (4-NO<sub>2</sub>Im) with activated RuCl<sub>3</sub> in aqueous solution containing HCl [9]. Crystallographic work on the corresponding compound revealed a *trans*-octahedral coordination about the metal centre and nitroimidazole binding as the 5-nitro tautomer. Solution chemistry was performed both in water and in methanol. [RuCl<sub>4</sub>(5-NO<sub>2</sub>Im)<sub>2</sub>]<sup>-</sup> was found to be less labile. After several days in D<sub>2</sub>O, most of the complex aquated to species like [RuCl<sub>3</sub>(D<sub>2</sub>O)(5-NO<sub>2</sub>Im)<sub>2</sub>] and [RuCl<sub>2</sub>(D<sub>2</sub>O)<sub>2</sub>(5-NO<sub>2</sub>Im)<sub>2</sub>]<sup>+</sup>. In methanol, only one solvolysis step was detected and the reaction was slow requiring several weeks. Although the presence of a nitro group on imidazole uncovers interesting effects on substitution reactions in the resulting complexes, lack of reactivity of [RuCl<sub>4</sub>(5-NO<sub>2</sub>Im)<sub>2</sub>]<sup>-</sup> with dimethyladenine in aqueous medium suggested that this complex may have limited biological implications.



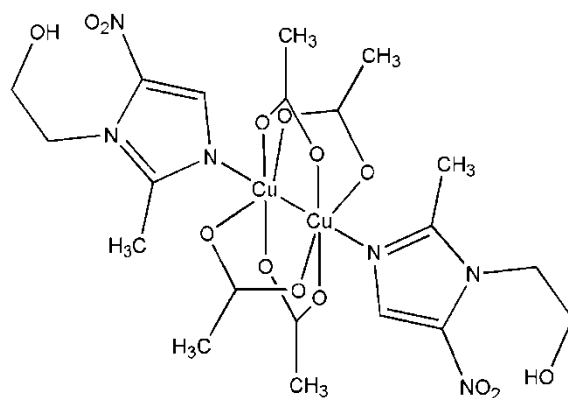
Complex-10

The structure of a chloro-bridged dimer (Complex-11) similar to complex-8 was reported with each copper atom present in a trigonal bipyramid geometry having two chloride atoms and a water molecule in equatorial position and two axial metronidazole coordinated by N3 of the imidazole ring. The complex being cationic, chloride was present outside the coordination sphere.



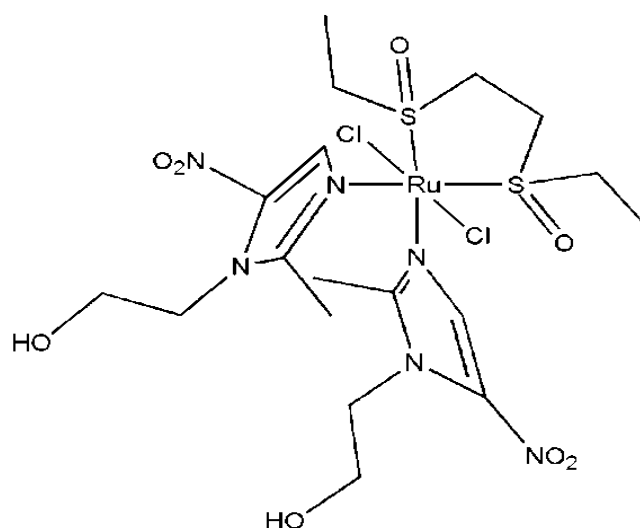
Complex-11

The crystal structure of a binuclear acetate bridged Cu(II) complex (Complex-12) similar to complex-6 was reported. The complex had a paddle wheel structure with penta-coordinated Cu<sup>II</sup> center in square pyramidal geometry. Each copper center was coordinated through four oxygen atoms of acetate bridges with the apical position being occupied by a nitrogen atom of the imidazole moiety.



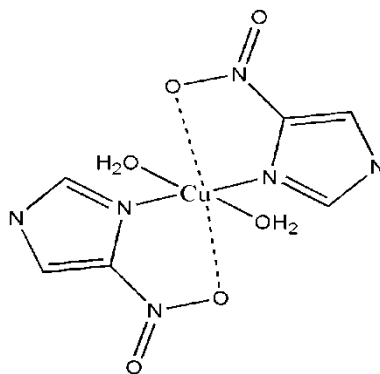
Complex-12

A Ru<sup>II</sup> bidentate sulfoxide-metronidazole complex [RuCl<sub>2</sub>(BESE)(metronidazole)<sub>2</sub>] (complex-13) was synthesized [BESE being 1,2-bis((ethylsulfinyl)ethane)] and characterized by <sup>1</sup>H NMR, UV-Vis, IR spectroscopy, elemental analysis, solution conductivity and cyclic voltammetry [10]. X-ray crystal structure revealed an octahedral geometry with S-bonded BESE *trans* to two metronidazole ligands coordinated by the imidazole ring having two Cl atoms at the fifth and sixth coordination sites. The complex was tested on human breast cancer cells (MDA-MB-435S) using an *in vitro* MTT assay. However, IC<sub>50</sub> obtained for this complex was much higher (860 μM) compared to *cis* platin (30 μM).



Complex-13

Crystal structure and antibacterial activities of some Cu(II) and Co(II) complexes of 5-nitroimidazoles along with other phenylimidazole derivatives have been reported [11]. The Cu(II) complex of 5-nitroimidazole (Complex-14) has a square plane around copper created by two N-bound 5-nitroimidazole groups and two water molecules. Two imidazole rings are bound almost perpendicular to the CuN<sub>2</sub>O<sub>2</sub> coordination plane so as to have one of the nitrate oxygens pointing towards the Cu centre at a semi-coordination distance. These played an apical role allowing the coordination polyhedra to be described as highly distorted octahedral. Charge balance was achieved by two nitrate counter ions as they were not involved in direct coordination with the Cu centre.



Complex-14

Three acetato-bridged dinuclear copper(II) complexes with 5-nitroimidazoles were prepared (having a structure similar to that of complex 12) by interaction of a dimeric copper(II)-acetate [ $\text{Cu}_2(\text{1-O}_2\text{CCH}_3)_4(\text{H}_2\text{O})_2$ ] with metronidazole and three other 5-nitroimidazole drugs, secnidazole [Secnim, 1-(2-methyl-5-nitro-1H-imidazol-1-yl)propan-2-ol], tinidazole [Tinim, 1-(2-ethylsulfonyl-ethyl)-2-methyl-5-nitro-imidazole] and nimorazole [Nimin, 4-[2-(5-nitroimidazol-1-yl)ethyl] morpholine]. These were characterized with the help of spectroscopy [12]. These complexes and their corresponding parent drugs showed radiosensitizing properties on Hep2 (human larynx cancer) cells *in vitro*. Maximum enhancement of radiosensitizing activity upon coordination of the drugs to copper(II) was found for nimorazole in that series of the complexes.

A binuclear paddle-wheel complex of Cu(II) with tnz was prepared and found to have a structure similar to that represented by complex 6 and complex 12, where each tnz was linked to a Cu(II) centre, the two Cu(II) ions being connected by four acetate bridges. The complex was characterized by single-crystal X-ray diffraction, IR, mass, EPR, elemental analysis, and cyclic voltammetry. Performance of  $[\text{Cu}_2(\text{OAc})_4(\text{tnz})_2]$  on two bacterial cells was better than tnz while in case of the fungal cell both had similar effect [13]. This suggests binding of Cu(II) to tnz brings about a change in the electronic environment that influenced biological function on bacterial cells showing improved activity. An attempt was also made to explain

the results of antimicrobial studies through DNA binding where the complex was clearly shown to be one order higher in its ability to bind to DNA than tinidazole. The binding of tinidazole and its Cu(II) complex with calf thymus DNA was followed in this case, using cyclic voltammetry which was also the first time for such compounds.

A novel series of Cd (II) complexes of 2-(1-substituted-5-nitro-1H-imidazol-2-yl)-1-substituted ethanone were synthesized by a direct reaction of the free ligand with cadmium chloride under refluxing conditions in good yield and *in-vitro* antibacterial activity were evaluated [14]. It is evident from antibacterial screening that some of the investigated compounds displayed moderate *in-vitro* antibacterial activity against Gram-positive bacteria only. In case of Gram-negative isolate, the complex did not exhibit any inhibitory activity.

A monomeric tetrahedral complex of Cu<sup>II</sup> with tinidazole (tnz) was prepared. In spite of a significant decrease in the generation of nitro radical anion for Cu(tnz)<sub>2</sub>Cl<sub>2</sub>, the study showed there was almost comparable biological activity for tnz and its monomeric Cu<sup>II</sup> complex on two chosen bacterial strains *Staphylococcus aureus* (ATCC 29213) and *Escherichia coli* (ATCC 25922) and also on *Entamoeba* cells (*E. histolytica*) [15].

Ruthenium compounds are known to be potential drug candidates since they offer the potential for reduced toxicity. Furthermore, in case of Ru in its various oxidation states, different mechanism of action and ligand substitution kinetics give them an advantage over platinum-based complexes, making them suitable for use in biological applications. Five new Ru complexes of nitroimidazoles were synthesized using [Ru(DMF)<sub>6</sub>]Tf<sub>3</sub> as the starting material. Another seven complexes were made from the commercially available RuCl<sub>3</sub>.3H<sub>2</sub>O as precursor. Nitroimidazoles used were 2- or 5-NO<sub>2</sub> derivatives including metronidazole, etanidazole of known biological value [16]. Another set of four different novel ruthenium (II) complexes with metronidazole as ligand were obtained [17].

[RuCl(MTNZ)(dppb)(4,4'-Mebipy)]PF<sub>6</sub> ; [RuCl(MTNZ)(dppb)(4,4'-Methoxybipy)]PF<sub>6</sub> ;  
[RuCl(MTNZ)(dppb)(bipy)]PF<sub>6</sub> ; [RuCl(MTNZ)(dppb)(phen)]PF<sub>6</sub>

(where, MTNZ = metronidazole, dppb = 1,4-bis(diphenylphosphino)butane, 4,4'-Mebipy = 4,4'-dimethyl-2,2'-bipyridine, 4,4'-Methoxybipy = 4,4'-dimethoxy-2,2'-bipyridine, bipy = 2,2'-bipyridine and phen = 1,10-phenanthroline.)

Each of the complexes were characterized by different techniques and their (1–4) interaction with DNA was evaluated. Their cytotoxicity profiles were determined on four different tumor cell lines derived from human cancer cells (SK-MEL-147, melanoma; HepG2, hepatocarcinoma; MCF-7, estrogen-positive breast cancer; A549, non-small cell lung cancer). From results obtained complexes 1 and 3 were found to be promising antitumor agents since they inhibited the proliferative behavior of MCF-7 cells and induced apoptosis [17].

These metal-nitroimidazole complexes have one or more reducible centres (i.e., nitroimidazole; transition metal core), each of which has a characteristic redox property and consequently unique interactions inside target (hypoxic) and normoxic tissues. In theory, complexes with reducible metal cores (i. e. transition metals) and reducible targeting vectors (i. e. nitroimidazole) potentially offer greater selectivity and sensitivity for hypoxic tissues than either reducible metal-complexes alone or the *nitroimidazole* without the reducible metal centre [18].

## References

1. J. R. Bales, P. J. Sadler, C. J. Coulson, M. Laverick and A. H. W. Nias, *Br. J. Cancer*, **1982**, 46, 701-705.
2. J. R. Bales, C. J. Coulson, D. W. Gilmore, M. A. Mazid, S. Neidle, R. Kuroda, B. J. Peart, C. A. Ramsden, P. J. Sadler, *J. Chem. Soc., Chem. Comm.*, **1983**, 432-433.
3. V. Callaghan, D. M. L. Goodgame and R. P. Tggze, *Inorg. Chim. Acta*, **1983**, 78, L1 - L4.

4. J. R. Bales, M. A. Mazid, P. J. Sadler, A. Aggarwal, R. Kuroda, and S. Neidle, D. W. Gilmour, B. J. Peart, C. A. Ramsden, *J. Chem. Soc. Dalton Trans.*, **1985**, 795-802.
5. N. Galvan-Tejada, S. Bernes, S. E. Castillo-Bluma, H. Noth, R. Vicente, N. Barba-Behrensa, *J. Inorg. Biochem.*, **2002**, 91, 339-348
6. D. M. L. Goodgame, A. S. Lawrence, A. M. Z. Slawin, D. J. Williams, *Inorg. Chim. Acta*, **1986**, 125, 143-149.
7. N. Barba-Behrens, A. M. Mutio-Rico, P. Joseph-Nathan and R. Contreras, *Polyhedron*, **1991**, 10, 1333-1341.
8. M. S. Nothenberg, S. B. Zyngier, A. M. Giesbrecht, M. T. P. Gambardella, R. H. A. Santaos, A. Kimura, R. Najjar, *J. Braz. Chem. Soc.*, **1994**, 5, 23-29.
9. C. Anderson, A. L. Beauchamp, *Inorg. Chim. Acta*, **1995**, 233, 33-41.
10. A. Wu, D. C. Kennedy, B. O. Patrick, and B. R. James, *Inorg. Chem.*, **2003**, 42, 7579-7586.
11. A. M. Atria, P. Cortés-Corté, M. T. Garland, R. Baggio, K. Morales, M. Soto and G. Corsini, *J. Chilian Chem. Soc.*, **2011**, 56, 786-792.
12. A. C. Valderrama-Negrón, W. A. Alves, Á. S. Cruz, S. O. Rogero, D. de O. Silva, *Inorg. Chim. Acta*, **2011**, 367, 85-92.
13. R. C. Santra, K. Sengupta, R. Dey, T. Shireen, P. Das, P. S. Guin, K. Mukhopadhyay, S. Das, *J. Coord. Chem.*, **2014**, 67(2), 265-285.
14. D. G. Desai, D. K. Sureja, B. R. Prajapati, A. K. Seth, K. I. Molvi, *J. Pharm. Res.*, **2016**, 10(11), 696-699.
15. R. C. Santra, D. Ganguly, S. Jana, N. Banyal, J. Singh, A. Saha, S. Chattopadhyay, K. Mukhopadhyay, S. Das, *New J. Chem.*, **2017**, 41, 4879-4886
16. I. R. Bairda, K. A. Skovb, B. R. James, *Inorg. Chim. Acta*, **2019**, 489, 100-107.
17. C. C. Candido, H. V. R. Silva, B. Zavan, M. Ionta, M. I. F. Barbosa, A. C. Doriguetto, *J. Inorg. Biochem.*, **2022**, 237, 112022.
18. C. L. Ricardo, P. Kumar, L. I. Wiebe, *J. Diag. Imag. in Ther.*, **2015**; 2(1) 103-158.

# **Chapter 5**

## **Genesis and Scope**

Nitroimidazoles are a class of antimicrobial drugs that shows broad spectrum of activity against anaerobic gram-positive and gram-negative bacteria, on parasites and mycobacteria [1-3]. They cure different microbial diseases occurring both in human beings and animals [4]. Nitroimidazoles represent one of the most essential and unique scaffolds in drug discovery since their identification in the 1950s [5]. They are usually classified based on the location of the nitro group in the molecule. The most widely used derivatives being metronidazole, tinidazole, ornidazole and secnidazole [6-8]. The mode of action of nitroimidazoles help to explain why they have a broad spectrum of activity [2]. The mechanism of action of this class of drugs mainly centres around the nitro group present on imidazole [12]. Nitroimidazoles are pro-drugs that require the reduction of the nitro group before they display any antimicrobial effect [12]. The mechanism is understood to have the following steps: (i) molecules enter cells through passive diffusion [4, 12-14], (ii) the nitro group is reduced to reactive radical species and (iii) radicals interact with the DNA causing destruction of the double helical structure leading to inhibition of protein synthesis; thus causing cell death [9, 12]. The main reason for cytotoxicity is the oxidative damage of intracellular DNA [12]. It is known that overuse of antibiotics results in antibiotic resistance. However, in case of nitroimidazoles drug resistance is comparatively less even after use for a long time [6, 7]. These days they are prescribed mainly in combination with other known antibiotics to increase efficacy [7, 10, 11]. Details of the mechanism of action during antimicrobial activity of the molecules on different micro-organisms have been discussed in *Chapter 2*.

Another important medicinal role of these drug molecules is being used as hypoxic cytotoxin, able to sensitize hypoxic tumor cells following irradiation on such cells [15-19]. Hypoxic cytotoxins that exclusively kill cells in a hypoxic environment form a group slightly different from radiosensitizers that help to improve radiotherapy under hypoxic conditions [20, 21]. Nitroimidazoles being "electron-affinic" react with DNA free radicals having the potential

for universal activity to combat hypoxia-associated radio-resistance [20, 22, 23]. As radiosensitizers, they interact with radical products generated on DNA following radiolysis of water, generating the nitro radical anion that either leads to strand unwinding or strand breaks [15]. Nitroimidazole derivatives have been studied as radiosensitizers for a long time and a lot of the early work suggested that the derivatives showed no activity under aerobic condition but were quite effective under hypoxic conditions. The fact makes them suitable radiosensitizers for treatment of cancer [24-27]. Hence there are a lot of studies done regarding the radiosensitization capability of these drugs [28-32]. Such studies revealed radiation induced damage mostly target the DNA within cells. Thus it was important to know how the radiation induced damage affect the constituents of DNA both in the absence and presence of sensitizer molecules. A huge literature is now available on the detailed facts about radiation induced damage of nucleic acid bases and sugar-phosphates that helps to know the basis of radiosensitization of tumor cells [33-42]. Also there were some focus on aspects like electron affinity and DNA binding capability of sensitizers to their actual performance on different biological cell lines which guide further research on the design of new derivatives as better radiosensitizers [43-46]. Metal complex formation of any existing sensitizer molecule is one such pathway. Majority of the metal complexes prepared are better sensitizers than the parent drug molecule [37, 47-53]. 5-nitroimidazole derivatives as radiosensitizers accept electrons from radical products of DNA forming the nitro radical anion enabling a permanent damage of DNA [15]. These aspects along with mechanism of radiosensitization by this class of molecules have been briefly reviewed in *Chapter 3*.

Binding to metal ions may control the association and conformation of biologically active molecules and so affect their chemical and biological properties. Nitroimidazole derivatives are of special interest due to their chemical and pharmacological properties [59]. Many transition metal complexes of 5-nitroimidazole derivatives are reported in the literature. In

most metal complexes, ligands to the metal center coordination occurs using the N3 nitrogen of the imidazole ring [54-61]. A few exceptions are known where the nitro group forms a bond with the metal center [57, 61]. The geometry of the monomeric complexes are either square planar or tetrahedral and penta-coordinated paddle wheel for binuclear species having either halide or carboxylate bridges [54-61]. Metal complexes of 5-nitro-imidazoles have also been studied to realize their antimicrobial and radiosensitizing property. These have been briefly summarized in *Chapter 4*.

Complex formation of 5-nitroimidazole derivatives with various transition metal ions is necessary to improve their efficiency either as an antimicrobial agent or as a radiosensitizing agent. Structural modification of an existing drug through complex formation also deals with the aspect as drug resistance. Another important factor is that toxicity is associated along with the tremendous efficacy of 5-nitroimidazoles on a number of fronts [62, 63]. When they are applied in therapeutic dosage, significant toxicity develops which makes them unsuitable clinically [64]. These molecules are neurotoxic upon prolonged use that is today established with the help of animal model studies and also understood from post application reports of patients administered with such drugs [65, 66]. Therefore, the same nitro radical anion necessary for cytotoxic action also has toxic side effects. Hence suitably modified forms that generate the correct amount of nitro radical anion necessary for cytotoxic action and leave no excess could control the toxic side effects of these molecules. Transition metal complexes of 5-nitroimidazoles could provide a solution to this problem.

Keeping all these in mind, attempt were made to synthesize copper (II) and zinc (II) complexes of ornidazole. Cu(II) was chosen since Cu(II) complexes are reasonably stable, possess good solubility and have excellent affinity towards DNA which is important for drug efficacy. In addition to its physiological role, zinc can have beneficial therapeutic and preventive effects on infectious diseases and, compared to other metal-based drugs, Zn(II)

complexes generally exert lower toxicity and have fewer side effects. In order to establish the structure of the complexes, single crystal X-ray diffraction as well as powder X-ray diffraction were used. Other spectroscopic characterizations, magnetic moment measurements and EPR of the complexes were attempted since they provide useful information addressing both structural issues as well as aspects related to biological activity. Redox properties and electrochemical behavior of 5-nitroimidazoles being crucial aspects pertaining to drug action electrochemistry of ornidazole was done. Changes in electrochemical properties upon complex formation were also attempted. Findings related to these aspects are discussed in *Chapters 7-12*.

As mentioned earlier, formation of the nitro radical anion is necessary for cytotoxic action but at the same time it is toxic to the central nervous system. It is expected that the amount of generation of the nitro radical anion would be different in case of the metal complexes but whether that would be sufficient for the desired biological activity while improving toxic side effects is worth knowing. This work attempts to find this aspect through the formation of Cu(II) and Zn(II) complexes of ornidazole. To realize the generation of the nitro radical anion in the drugs and its metal complexes, a model nitro reductase enzyme xanthine oxidase (XOD) was used in a reaction performed in deoxygenated medium where hypoxanthine acts as the electron source with the compounds (ornidazole and its metal complexes) being electron acceptors. Generation of the nitro radical anion and subsequent degradation of the compounds was identified with the help of a standard technique that was followed using UV-Vis spectroscopy. Details are available in *Chapter 6 (Experimental)*. *Chapters 7 and 8* have the details pertaining to the findings on enzyme assay in detail for all the compounds.

It is needless to mention interaction of the compounds with DNA is important and was therefore attempted to obtain better insights into the mechanism of action of these compounds. DNA interaction of all the compounds is discussed in *Chapters 7 and 8*.

Antiamoebic activity of the prepared complexes was done to compare the activity of the complexes with that of Onz. This was done to realize if the complexes were showing either similar or better activity as that of the drugs.

Although, there is some work in the literature on modification of DNA due to nitroimidazoles, there is lot of scope for further investigative work. Hence, we look into the aspect of *in situ* reactivity of electrochemically generated nitro radical anion on ornidazole and its metal complexes with nucleic acid bases and calf thymus DNA. The reduction potential was provided to our chosen nitroimidazoles by an electrochemical method where, in the immediate vicinity of reduction products of the molecule, four different nucleic acid bases and calf thymus DNA were kept. The reduction products cause a damage of the biological target which was followed with the help of suitable experimental techniques.

The radiosensitizing properties of the Cu(II) and Zn(II) complexes of Onz were also investigated alongside Onz. Studies related to damage of nucleic acid bases and modification of DNA using Onz and its metal complexes as radiosensitizers is discussed in *Chapter 13*. This was done with the purpose that if the complexes turned out to be better radiosensitizers then not only would this be an advantage but at the same time with complexes having less toxic side effects it would be more logical for use clinically.

## References

1. S.N. J. Moreno, R. Docampo, *Env. Health Pers.*, **1985**, 64, 199-208.
2. C. Thomas, C. D. Gwenin, *Biology*, **2021**, 10, 388-403.
3. J. G. Bartlett, *Clin. Infect. Dis.*, **1994**, 18, 265-272.
4. D. I. Edwards, *The Br. J. Ven. Dis.*, **1980**, 56, 285-290.
5. R. Gupta, S. Sharma, R. A. Vishwakarma, S. Mignani, P. Pal Singh, *Pharmaceuticals*, **2022**, 15, 561-654.
6. D. I Edwards, *Biochem. Pharma.*, **1986**, 35, 53-83.

7. D. I Edwards, *Antibiotics*, **1983**, Vol. VI, Springer Verlag, Berlin, 121-135.
8. L. Larina, V. Lopyrev, *Nitroazoles: Synthesis, Structure and Applications*, **2009**, Springer, New York, USA, 408-421.
9. Ang, Jarrad, A.M.; Cooper, M.; Blaskovich, *J. Med. Chem.* **2017**, 60, 7636–7657.
10. R. E. Marx, Y. Sawatari, M. Fortin, V. Broumand, *J. Oral and Maxillofacial Surg.*, **2005**, 63, 1567–1575.
11. www.drugupdate.com, link-http://www.drugupdate.com/generic/view/1256/Ofloxacin+-Ornidazole.
12. D. I. Edwards, *J. Antimicrob. Chemother.*, **1993**, 31, 9-20.
13. S. Sood, A. Kapil, *Ind. J. Sex. Trans. Dis.*, **2008**, 29, 7-14.
14. D. Petrin, K. Delgaty, R. Bhatt, G. Garber, *Clin. Microb. Rev.*, **1998**, 11, 300-317.
15. P. Wardman, *Clin. Onco.*, **2007**, 19, 397–417.
16. G. E. Adams, E. D. Clarke, I. R. Flockhart, R. S. Jacobs, D.S. Sehmi, I. J. Stratford, P. Wardman, M. E. Watts, J. Parrick, R. G. Wallace, C. E. Smithen, *Int. J. Rad. Bio. and Rel. Stud. in Phy., Chem. and Med.*, **1979**, 35, 133-150.
17. M. E. Watts, *Int. J. Rad. Bio. Rel. Stud. in Phy., Chem. and Med.*, **1977**, 31, 237-50.
18. M. D. Threadgill, P. Webb, P. O'Neill, M. A. Naylor, M. A. Stephens, I. J. Stratford, S. Cole, G. E. Adams, E. M. Fielden, *J. Med. Chem.*, **1991**, 34, 2112–2120.
19. E. M. Fielden, G. E. Adams, S. Cole, M. A. Naylor, P. O'Neill, M. A. Stephens, I. T. Stratford, *Int. J. Rad. Onco. Biology Physics*, **1992**, 22, 707-711.
20. (a) K. A. Skov, S. Macphail, *Int. J. Radiat. Oncol. Biol. Phys.* **1994**, 29, 87–93. (b) K. A. Skov, C. J. Koch, B. Marples, *Radiat. Oncol. Invest.* **1994**, 2, 164-170.
21. Van Belle, S. Do, *Chest*, **1996**, 109, 115S-118S.
22. P. Wardman, *Br. J. Radiol.* **2019**, 92, 20170915; doi:10.1259/bjr.20170915.
23. M. M. M Bamatraf, P. O'Neill, B. S. M. Rao, *J. Am. Chem. Soc.* **1998**, 120, 11852–11857; doi.org/10.1021/ja9823161
24. J. C. Asquith, J. L. Foster, R. L. Willson, *Br. J. Radiol.*, **1974**, 47, 474-81.
25. J. M. Brown, *Cancer Res.*, **1999**, 5863-5870.

26. G. E. Adams, I. R. Flockhart, C. E. Smithen, I. J. Stratford, P. Wardman, and M. E. Watts, *Rad. Res.*, **1976**, 67, 9-20.
27. L. Santos, M. C. L. Zumel, M. V. Alvarez, M. C. Izquierdo, *Int. J. Rad. Biol.*, **1989**, 55, 983-991.
28. G. Iliakis, S. Kurtzman, G. Pantelias, R. Okayasu, *Rad. Res.*, **1989**, 119, 286-304.
29. M. A. Morgan, L. A. Parsels, L. Zhao, J. D. Parsels, M. A. Davis, M. C. Hassan, S. Arumugarajah, L. Hylander-Gans, D. Morosini, D. M. Simeone, C. E. Canman, D. P. Normolle, S. D. Zabludoff, J. Maybaum, T. S. Lawrence, *Can. Res.*, **2010**, 70, 4972-4981.
30. H. H. Kampinga, J. R. Dynlacht, E. Dikomey, *Int. J. Hyperther.*, **2004**, 20, 131-139.
31. S. J. Veuger, N. J. Curtin, C. J. Richardson, G. C. M. Smith, B. W. Durkacz, *Can. Res.*, **2003**, 63, 6008-6015.
32. A. Munshi, J. F. Kurland, T. Nishikawa, T. Tanaka, M. L. Hobbs, S. L. Tucker, S. Ismail, C. Stevens, R. E. Meyn, *Clin. Can. Res.*, **2005**, 11, 4912-4922.
33. H. B. Michaels, E. J. Rasburn, J. W. Hunt, *Rad. Res.*, **1976**, 65 (2), 250-267.
34. T. Melvin, S. W. Botchway, A. W. Parker, P. O'Neill, *J. Am. Chem. Soc.*, **1996**, 118, 10031-10036.
35. P. O. Neill, E. M. Fielden, *Rad. Carcinogen. and DNA Alter.*, **1986**, 124, 425-438.
36. J. R. Wagner, J. E. van Lier, L. J. Johnston, *Photochem. and Photobiol.*, **1990**, 52, 333-343.
37. M. B. Roy, P. C. Mandal, S. N. Bhattacharya, *Int. J. of Rad. Biol.*, **1996**, 69, 471-480.
38. S. Das, A. Saha, P. C. Mandal, *J. Radioanal. and Nucl. Chem.*, **1995**, 196, 57-63.
39. S. Das, A. Saha, P. C. Mandal, *Env. Health Persp.*, **1997**, 105, 1459-1462.
40. S. Das, P. C. Mandal, *Rad. Phys. Chem.*, **2009**, 78, 37-41.
41. P. S. Guin, P. C. Mandal, S. Das, *Rad. Phys. Chem.*, **2013**, 89, 38-42.
42. S. Das, P. C. Mandal, *J. Radioanal. and Nucl. Chem.*, **2014**, 299, 1665-1670.
43. P. Wardman, In: *Chemotherapeutic Strategy*, **1983**, (Eds. D. I. Edwards, D. H. Hiscock), Macmillan, London, pp. 173-192.
44. P. Wardman, E. D. Clarke, In: *New Chemo and Radiosensitizing Drugs*, **1985**, (Eds. A. Breccia, J. F. Fowler), Lo Scarabeo, Italy, 21-38.
45. R. J. Knox, R. C. Knight, D. I. Edwards, *Br. J. Cancer*, **1981**, 44, 741-745.

46. D. I. Edwards, R. J. Knox, R. C. Knight, , *Int. J. Rad. Onco. Biology Physics*, **1982**, 8, 791-793.
47. K. A. Skov, *Rad. Res.*, **1987**, 112, 217-242.
48. K. A. Skov, N. P. Farrell, H. Adomat, *Rad. Res.*, **1987**, 112, 2, 273-282.
49. H. Ali, J. E. van Lier, *Chem. Rev.*, **1999**, 99, 2379–2450.
50. P.K. L. Chan, K. A. Skov, B. R. James, *Int. J. Rad. Biol.and Rel. Stud. in Phys., Chem. and Med.*, **1987**, **52**, 49-55.
51. K. A. Skov, N. P. Farrell, , *Int. J. Rad. Biol.*, **1990**, 57, 947-958.
52. R. Chibber, I. J. Stratford, I. Ahmed, A. B. Robbins, D. Goodgame, B. Lee, *Int. J. Rad. Onco. Biol. Phys.*, **1984**, 10, 1213-1215.
53. A. Cecilia Valderrama-Negrón, W. A. Alves, Á. S. Cruz, S. O. Rogero, D. de O. Silva, *Inorg. Chim. Acta*, **2011**, 367, 85-92.
54. J. R. Bales, C. J. Coulson, D. W. Gilmour, M. A. Mazid, S. Neidle, R. Kuroda, B. J. Peart, C. A. Ramsden, P. J. Sadler, *J. Chem. Soc., Chem. Comm.*, **1983**, 432-433.
55. J. R. Bales, M. A. Mazid, P. J. Sadler, A. Aggarwal, R. Kuroda, and S. Neidle, D. W. Gilmour, B. J. Peart, C. A. Ramsden, *J. Chem. Soc. Dalton Trans.*, **1985**, 759-802.
56. D. M. L. Goodgame, A. S. Lawrence, A. M. Z. Slawin, D. J. Williams, *Inorg. Chim. Acta*, **1986**, 125, 143-149.
57. N. Barba-Behrens, A. M. Mutio-Rico, P. Joseph-Nathan and R. Contreras, *Polyhedron*, **1991**, 10, 1333-1341.
58. M. S. Nothenberg, S. B. Zyngier, A. M. Giesbrect, M. T. P. Gambardella, R. H. A. Santaos, A. Kimura, R. Najjar, *J. Braz.. Chem. Soc.*, **1994**, 5, 23-29.
59. N. Galvan-Tejada, S. Bernes, S. E. Castillo-Bluma, H. Noth, R. Vicente, N. Barba-Behrensa , *J. Inorg. Biochem.*, **2002**, 91, 339-348.
60. A. Wu, D. C. Kennedy, B. O. Patrick, and B. R. James, *Inorg. Chem.*, **2003**, 42, 7579-7586.
61. A. M. Atria, P. Cortés-Corté, M. T. Garland, R. Baggio, K. Morales, M. Soto and G. Corsini, *J. Chilli. Chem. Soc.*, **2011**, 56, 786-792.
62. D. N. R. Rao, R. P. Mason, *The J. Biol. Chem.*, **1987**, 262, 11731-11736.

63. V. N. Coleman, J. Halsey, R. S. Cox, V. K. Hirst, T. Blaschke, A. E. Howes, T. H. Wasserman, R. C. Urtasun, T. Pajak, S. Hancock, T. L. Philips, L. Noll, *Can. Res.*, **1987**, 47, 319-322.
64. V. T. Kagiya, K. Sakano and S. Nishimoto, *Rad. Phys. Chem.*, **1987**, 29, 451.
65. C. K. Horlen, C. F. Seifert, C. S. Malouf, *The Annals of Pharmacother.*, **2000**, 34, 1273-1275.
66. E. J. Olson, S. C. Morales, A. S. McVey, D. W. Hayden, *Veter. Pathol.*, **2005**, **42**, 665-669.

# **Chapter 6**

## **Experimental**

## **Introduction:**

As mentioned in *Chapter 5 on Genesis and Scope* of this dissertation, work on metal complexes of some common 5-nitroimidazoles like tinidazole and ornidazole, that are extremely effective drugs against different parasites and pathogenic microbes, having the potential to act as radio-sensitizers in radiotherapy of cancer were prepared. The aim being to see, if owing to several attributes associated with complex formation, complexes are able to maintain the efficacy of 5-nitroimidazoles and take care of toxic side effects shown by them. Bio-friendly metal ions were chosen for this work. These were procured from reliable sources and the complexes were prepared using them. Complexes were characterized. All methods leading to the preparation of complexes are clearly outlined in this chapter. Various techniques that enable suitable characterization of the complexes are also mentioned.

Since a significant part of the study deals with an appropriate generation of radical anions, more specifically the nitro-radical anion ( $R\text{-NO}_2^{\cdot-}$ ) by prepared complexes, in reference to parent compounds like ornidazole and tinidazole, it was important to identify the amount of nitro-radical anion generated by the compounds. For this enzyme assay was carried out where formation of the nitro-radical anion ( $R\text{-NO}_2^{\cdot-}$ ) was realized using xanthine oxidase, a model nitro-reductase.

Since, with decrease in nitro-radical anion ( $R\text{-NO}_2^{\cdot-}$ ) formation, there is the possibility that complexes might be less effective in the free radical pathway, attempts were made to look at aspects of interaction between  $R\text{-NO}_2^{\cdot-}$  and other reduction products of Ornidazole and its complexes with nucleic acid bases and with calf thymus DNA to realize and correlate what might happen when such molecules either on their own or complexed to metal ions are reduced enzymatically within a biological target. Reduction products of Ornidazole and complexes were generated by reducing them electrochemically at their respective reduction

potential that was determined with the help of cyclic voltammetry. Reactions of such *in situ* generated reduction products with purine or pyrimidine based nucleic acid bases were followed by HPLC while calf thymus DNA not modified was determined by treatment with ethidium bromide and recording its fluorescence. Experiments were carried out to compare performance of complexes as radio-sensitizers and/or hypoxic cytotoxins with that of Ornidazole, following the same protocol as mentioned above for nucleic acid bases and calf thymus DNA.

In order to realize some of the other attributes of complex formation, studies on the binding of the compounds with DNA was undertaken. Binding of compounds with DNA was carried out using cyclic voltammetry. The data was fitted to standard equations and binding constant was evaluated. This was compared with that determined for the chosen 5-nitroimidazoles. .

Biological activity of prepared complexes, to see if that is affected in anyway, owing to decreased free radical ( $R\text{-NO}_2^{\cdot-}$ ) generation was also pursued. For this purpose, several bacterial strains were chosen as biological targets.

As a part of this work, Ornidazole [1-chloro-3-(2-methyl-5-nitro-1H-imidazole-1-yl)propan-2-ol], an important member of the family of 5-nitroimidazoles was chosen. Cu(II) and Zn(II) complexes were prepared and characterized through physicochemical experiments in solution and different spectroscopic methods of analysis in solid state. Structures of Cu(II) and Zn(II) complexes were determined from single crystal X-ray diffraction and powder X-ray diffraction respectively.

### **Materials used**

Ornidazole [purity (HPLC): >98.0%; melting point: 90.0 to 94.0 °C] and Tinidazole [purity (HPLC): >98.0%; melting point: 127.0 to 131.0 °C] were purchased from TCI, Japan and purified by recrystallization from hot methanol. Crystalline forms were obtained by slow

evaporation of the solvent. These were then isolated by filtration. Copper(II) chloride ( $\text{CuCl}_2 \cdot 2\text{H}_2\text{O}$ ) and Zinc(II) chloride ( $\text{ZnCl}_2$ ), obtained from E. Merck, India were used for the synthesis of complexes without any further purification.  $\text{NaCl}$ ,  $\text{NaNO}_3$ ,  $\text{KCl}$ ,  $\text{MgCl}_2$ , trichloro acetic acid (TCA), glacial acetic acid, sodium dihydrogen phosphate and disodium hydrogen phosphate (all AR grade) were obtained from E. Merck, India. While  $\text{NaCl}$  and/or  $\text{KCl}$  were either used as electrolyte for the dissolution of DNA and for electrolytic conduction in aqueous medium during electrochemical experiments,  $\text{MgCl}_2$  was used for dissolution of DNA.  $\text{NaNO}_3$  was used to maintain ionic strength of the medium either during any form of physico-chemical experiments or during DNA titration. Trichloro acetic acid (TCA), glacial acetic acid, sodium dihydrogen phosphate and disodium hydrogen phosphate were used to prepare different buffer solutions for various biochemical experiments. Triple distilled water was used for preparing all aqueous solutions. Calf thymus DNA and ethidium bromide were purchased from Sisco Research Laboratories, India. DNA was dissolved in phosphate buffer (pH  $\sim$  7.4) in the presence of 120 mM  $\text{NaCl}$ , 35 mM  $\text{KCl}$ , and 5 mM  $\text{MgCl}_2$  to maintain appropriate physiological conditions. Concentration of DNA in terms of nucleotide was determined using a molar extinction coefficient of  $6600\text{M}^{-1}\text{cm}^{-1}$  at 260 nm. Absorbance of the prepared DNA solutions were measured at 260 nm and 280 nm respectively.  $A_{260}/A_{280}$  was determined; the value being in the range 1.8–1.9, the DNA was considered ready for use without further purification. Quality of calf thymus DNA was also verified with the help of circular dichroism (CD) recording its response at 260 nm on a CD spectropolarimeter (J815, JASCO, Japan). For experiments related to cyclic voltammetry, tetrabutyl ammonium bromide (TBAB) (AR grade) from Spectrochem (India) Pvt. Ltd. was used as supporting electrolyte in non-aqueous medium (dimethyl formamide, DMF). DMF was obtained from E. Merck, India. Nucleic acid bases cytosine and thymine were purchased from Sisco Research Laboratories, India, while adenine and guanine were procured from

TCI, Japan. For experiments related to enzyme assay, Xanthine oxidase (XOD) isolated from cows' milk was obtained as a suspension in ammonium sulphate solution from Sigma Aldrich. Hypoxanthine, Crystal violet (CV), ethyl acetate, hydroxyl amine, NaOH, and ferric chloride were procured from Sisco Research Laboratories, India. Anthrone as reagent, Folin-Ciocalteu as reagent, congo red, cetyl trimethyl ammonium bromide (CTAB), chitin flakes, Tris-HCl,  $\beta$ -mercaptoethanol and phenylmethylsulfonyl fluoride (PMSF) (all AR grade) were purchased from E. Merck, India.

### **Instruments**

Absorption spectra of complexes were recorded on UV-630 spectrophotometer, JASCO, Japan. Fluorescence measurements were done on a RF-530 IPC Spectrofluorophotometer, Shimadzu, Japan.

A CD spectropolarimeter J815, JASCO, Japan was used to determine the quality of calf thymus DNA.

FTIR of solid samples as KBr pellets was obtained using a Perkin Elmer RX-I spectrophotometer.

Mass spectra were recorded on Micromass Q-Tofmicro<sup>TM</sup>, Waters Corporation.

Elemental analyses of complexes were done on a Perkin-Elmer 2400 Series-II CHN analyzer.

EPR spectrum of  $[\text{Cu}(\text{Onz})_2\text{Cl}_2]$  were recorded on JEOL JES-FA 200 ESR spectrophotometer.

Magnetic susceptibility measurements of powdered samples at a temperature of 303 K were recorded with the help of a Gouy method using Magway MSB MK1, Sherwood Scientific Ltd.

Voltammograms were recorded on a Metrohm-Autolab model PGSTAT 101 potentiostat.

Powder X-ray diffraction (PXRD) data was collected on Bruker D8 Advance diffractometer.

Single crystal X-ray diffraction data was collected on a Bruker D8 Advance diffractometer.

For radiation chemical experiments,  $^{60}\text{Co}$   $\gamma$ -rays were passed through solutions with the help of a GC-900 Gamma Chamber. Dose rate (1.618kGy/h) was measured using a Fricke dosimeter.

Nucleic acid base damage with or without additives under different forms of stimuli (*electrochemical* or *radiation*) in solution were analyzed using HPLC (Shimadzu Corporation, Japan) using a C-18 column and 5% methanol-95% water as mobile phase.

DNA damage with or without additives under different forms of stimuli (*electrochemical* or *radiation*) in solution were analyzed by Ethidium-bromide fluorescence method.

#### **Synthesis of $[\text{Cu}(\text{Onz})_2\text{Cl}_2]$**

A solution of ornidazole (0.439 g in 25 ml, 2.00 mmol) in methanol was gradually added with stirring to a solution of  $\text{CuCl}_2 \cdot 2\text{H}_2\text{O}$  (0.17 g in 25 ml, 1.00 mmol) in methanol [1-4]. The final mixture was warmed under reflux to a temperature of approximately 60 °C for 5 h. A green crystalline compound was obtained after ~10 days following slow evaporation of the solvent. The product was filtered, dried and stored carefully.

Analysis Calc. (%) for  $[\text{Cu}(\text{Onz})_2\text{Cl}_2]$  i.e.  $\text{C}_{14}\text{H}_{20}\text{Cl}_4\text{CuN}_6\text{O}_6$ : C, 29.29; H, 3.49; N, 14.65. Found: C, 29.85; H, 3.43; N, 14.79.

#### **Synthesis of $[\text{Zn}(\text{Onz})_2\text{Cl}_2]$**

A solution of ornidazole (0.8785 g in 25 mL, 4 mmol) in methanol was added to a solution of  $\text{ZnCl}_2$  (0.2725 g in 25 mL, 2 mmol) in methanol [1-4]. The mixture was warmed under reflux to a temperature of 60 °C for 6 hours. After almost a week, a white crystalline compound was obtained by very slow evaporation of the solvent. The solvent was filtered and the solid mass was collected. The filtered product was re-crystallized using a 1:1 aqueous-methanol and washed with chloroform, diethyl ether, ethanol, THF and acetonitrile separately depending on

solubility of ornidazole in these solvents, to wash away impurities. A pure complex was thus obtained.

Analysis: calc. (%) for  $C_{14}H_{20}Cl_4N_6O_6Zn$ , C: 29.21; H: 3.50; N: 14.61. Found: C:29.12; H: 3.26; N: 15.22.

### **Synthesis of $[Cu^{II}(tnz)_2Cl_2]$**

A solution of tinidazole (0.494 g in 25 ml, 2.00 mmol) in methanol was gradually added with constant stirring to a solution of  $CuCl_2 \cdot 2H_2O$  (0.17 g in 25 ml, 1.00 mmol) in methanol. The mixture was warmed under reflux to  $\sim 60^\circ C$  for 6 hours. A green crystalline monomeric compound was obtained after 10 days following slow evaporation of the solvent [4].

### **Synthesis of $[Cu^{II}_2(OAc)_4(tnz)_2]$**

A solution of tinidazole (0.494 g in 25 ml, 2.00 mmol) in methanol was gradually added with constant stirring to a solution of Cu(II) acetate (0.400 g in 25 ml, 2.00 mmol) in mildly warm methanol. The mixture was warmed under reflux to  $\sim 55^\circ C$  for 8 hours. A dimeric Cu(II) complex of tinidazole was obtained after a week's time following extremely slow evaporation of the solvent.

All complexes were purified and crystallized [5].

### **Solution of structures of complexes by refinement from X-ray powder diffraction data**

Powder X-ray diffraction (PXRD) data were collected at ambient temperature ( $25^\circ C$ ) on a Bruker D8 Advance diffractometer operating in reflection mode with  $Cu K\alpha_1$  radiation of wavelength  $1.540562 \text{ \AA}$ . The generator was set at 40 kV and 40 mA. The data was collected in  $2\theta$  range of  $4\text{--}60^\circ$  with  $0.02^\circ$  step size and 5s/step.

At first an initial molecular structure was generated using ACD/Chem Sketch and the geometry was optimized using MOPAC2016 to arrive at a reference structural model for the reflex powder solve module. This initial structure (model) consisting of two ornidazole

ligands, one Zn(II) ion and two Cl<sup>-</sup> ions was then imported into the new cell. After assigning motion groups to different fragments it was solved to represent an approximate structure of the complex.

Indexing and Pawley refinement of PXRD patterns for complexes were carried out using Reflex module of Material Studio [6, 7]. The PXRD pattern was indexed by means of TREOR 90 program [8] for the first 20 peaks. Peak profiles, zero-shift, background and unit-cell parameters were refined simultaneously. The background was refined using a 20th-order polynomial. Refinements yield  $R_p = 6.38\%$ ,  $R_{wp} = 4.52\%$ . Rietvelt refinement was done to arrive at the final structure by Reflex Powder Refinement module of Material Studio. To improve agreement between calculated and experimental powder diffraction patterns different parameters like Pseudo-Voigt profile parameters, background parameters, cell constants, zero point of diffraction pattern, position and orientation of motion groups, dihedral angles within moieties, the Berar-Baldinozzi asymmetry correction parameters and March-Dollase preferred orientation correction parameters were optimized step by step until a good agreement between calculated and experimental powder diffraction patterns emerged. Thermal parameters were set to be the global isotropic atom displacement parameters and refined thereafter.

### **Solution of the structure of [Cu(Onz)<sub>2</sub>Cl<sub>2</sub>] from single crystal X-ray diffraction data**

Single crystals of the complexes, having suitable dimensions, were used for data collection using a 'Bruker SMART APEX II' diffractometer equipped with graphite-monochromated Mo-K $\alpha$  radiation ( $\lambda = 0.71073 \text{ \AA}$ ) at 298 K. The molecular structures were solved using the SHELX-97 package [9]. Non-hydrogen atoms were refined with anisotropic thermal parameters. The hydrogen atom attached to oxygen was located by difference Fourier maps and was kept at fixed position. All other hydrogen atoms were placed in their geometrically idealized positions and constrained to ride on their parent atoms. Multi-scan empirical

absorption corrections were applied to the data using the program SADABS [10]. The figures were prepared using DIAMOND and ORTEP [11, 12].

### **Electrochemical measurement (Cyclic Voltammetry)**

Electrochemical behavior of ornidazole, tinidazole and their prepared complexes were studied by performing cyclic voltammetry using the conventional three-electrode system at 25°C. Temperature was maintained using a circulating water bath. A glassy carbon electrode of surface area 0.0314 cm<sup>2</sup> served as working electrode, a platinum wire acted as counter electrode while Ag/AgCl was used as reference electrode. Electrochemical experiments were performed in an air-tight 50 ml electrochemical cell using Autolab PGSTAT101 Potentiostat Galvanostat. Concentration of experimental solutions were 10<sup>-3</sup> M. 0.1 M Tetrabutyl ammonium bromide (AR grade) was used as supporting electrolyte in alcoholic and DMF media while 0.12 M KCl was used in case of aqueous medium. All experimental solutions were degassed for 30 minutes with high-purity argon gas.

Reduction of the nitro group on ornidazole, tinidazole and their complexes were followed [13-17] in aqueous, aqueous-dimethyl formamide (DMF) and pure DMF solvents using cyclic voltammetry. In DMF, there is initially one-electron reduction to -NO<sub>2</sub><sup>•-</sup> (Eq. 1) [18] that subsequently undergoes a three-electron reduction to -NHOH (Eq. 2) [13, 18].



As the percentage of water increases, clarity of the two reduction peaks is lost and in a purely aqueous solution a single step four electron reduction occurs (Eq. 3). Results were analyzed by plotting cathodic peak current (I<sub>pc</sub>) in amperes against square root of potential sweep rate

( $v^{1/2}$ ) using Randles-Sevcik equation (Eq. 4, Figure 1), to see if the process is under diffusion control [19-21].

$$i_{pc} = (2.69 \times 10^5) \cdot n^{3/2} \cdot D_0^{1/2} \cdot A \cdot C \cdot v^{1/2} \quad (4)$$

$i_{pc}$  refers to current in amperes at the cathodic peak potential,  $n$  denotes total number of electrons,  $D_0$ , diffusion coefficient of species,  $A$  refers to area of electrode in  $\text{cm}^2$ ;  $C$  refers to concentration of compounds in  $\text{moles}/\text{cm}^3$  and  $v$ , scan rate in  $\text{V s}^{-1}$ . Most of these parameters would have a role to play in the subsequent reduction of each compound performed in the presence of nucleic acid bases or calf thymus DNA for some of the model biochemical investigations.

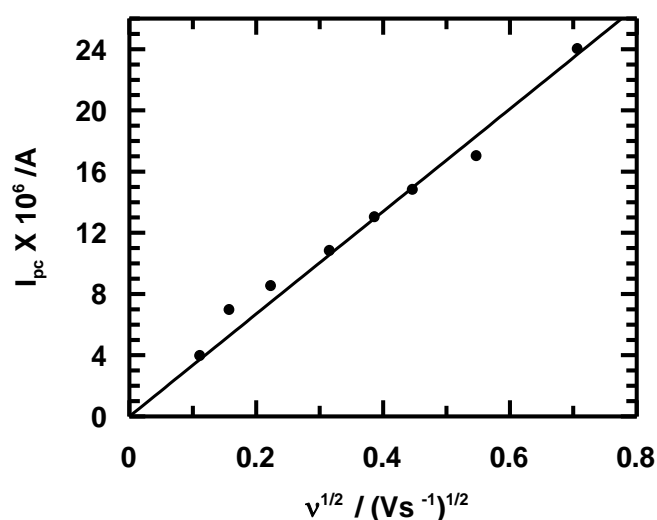


**Figure 1:** Plot of cathodic peak current ( $I_{pc}$ ) vs. square root of scan rate ( $v$ ) for the four-electron reduction of Ornidazole in aqueous solution at a potential of -0.827V and pH ~ 7.2. The values of current being in  $\mu\text{A}$  ( $10^{-6}$  A) the Y axis was labeled as  $I_{pc} \times 10^6/\text{A}$ .

Ratio of peak currents at different potential sweep rates was calculated using the Nicholson equation (Eq. 5) [22-24].

$$I_{pa}/I_{pc} = (I_{pa})_0 / I_{pc} + 0.485 \times (I_{sp})_0 / I_{pc} + 0.086 \quad (5)$$

$I_{pc0}$  denotes current at  $E_{\lambda}$ , the switching potential, and  $I_{pa0}$  refers to uncorrected anodic peak current with respect to zero current (baseline).

From voltammograms, reduction peak potential of different compounds were identified and subsequently used to reduce them at that potential in the presence of either nucleic acid bases or double stranded calf thymus DNA.

### **Enzyme assay**

The method uses xanthine oxidase (XOD), a model nitro-reductase [2, 4, 25]. Hypoxanthine serves as the reducing substrate while either tinidazole or ornidazole and its  $Cu^{II}$  and  $Zn^{II}$  complexes are electron acceptors. 225  $\mu$ L of XOD suspension was diluted to 1.5 mL with 0.025 M phosphate buffer (pH 7.4) in a quartz cuvette sealed with a rubber septum. Oxygen was purged out by passing argon through the solution. The enzyme (XOD) having a specific activity of 0.3 units/mg of protein contained  $\sim$ 10 units in 1.5 mL. In another quartz cuvette, 1.0 mL hypoxanthine (0.01M) in 0.1 M phosphate buffer ( $\sim$ pH 7.4) was taken along with 125  $\mu$ L of 1600  $\mu$ M either tinidazole or ornidazole and the complex was dissolved in DMF. The volume was made up to 2.0 mL using phosphate buffer (0.1M). The cuvette was sealed with a rubber septum and oxygen gas was purged out by passing argon gas through it. To initiate the reaction, 500  $\mu$ L of deoxygenated enzyme solution maintained in another cuvette was added with the help of a gas-tight syringe to the degassed solution containing hypoxanthine and test compounds. The final assay solution (2.5 mL) had 0.2 units/mL of XOD, 80  $\mu$ M of either tinidazole or ornidazole or its complexes and 4 mM of hypoxanthine. The cuvette was inverted to mix and monitored using UV-Vis spectroscopy against a buffer-DMF blank. A spectrum of the solution was taken every 5 minutes for 2 hours during assay. Change in absorbance at 320 nm was noted for either tinidazole or ornidazole and their complexes.

## Interaction of compounds with calf thymus DNA

Although complexes have an absorption at 320 nm, their interaction with DNA was not followed at that wavelength since DNA having a  $\lambda_{\max}$  at 260 nm, tailing of its absorbance extends up to 310 nm that interferes with the absorbance of the complexes. Hence, this could affect a correct determination of the actual change in absorbance, based on which a titration of complexes with calf thymus DNA leads to evaluation of binding constant values [2, 4, 5]. For this reason, cyclic voltammetry was used to study DNA interaction following reduction of the nitro group [2, 4, 5, 23, 26-28]. A 30 mL solution containing complexes (100  $\mu\text{M}$ ) were used. Calf thymus DNA was gradually added and cyclic voltammetry was performed. 20 mM Tris buffer and 120 mM NaCl was used to maintain pH and ionic strength of the medium during titration respectively. The change in current ( $\Delta I$ ) served as a measure of the extent to which complexes interact with calf thymus DNA. This change in current ( $\Delta I$ ) was subsequently fitted to standard equations (Eq. 6-9), yielding values for binding constant and site size of interaction [2, 4, 5, 23, 26-28].

## Equations for evaluating binding constants of complexes interacting with calf thymus DNA

$$\frac{1}{\Delta I} = \frac{1}{\Delta I_{\max}} + \frac{K_d}{\Delta I_{\max}(C_D - C_0)} \quad (6)$$

$$K_d = \frac{\left[ C_0 - \left( \frac{\Delta I}{\Delta I_{\max}} \right) C_0 \right] \left[ C_D - \left( \frac{\Delta I}{\Delta I_{\max}} \right) C_0 \right]}{\left( \frac{\Delta I}{\Delta I_{\max}} \right) C_0} \quad (7)$$

$$C_0 \left( \frac{\Delta I}{\Delta I_{\max}} \right)^2 - (C_0 + C_D + K_d) \left( \frac{\Delta I}{\Delta I_{\max}} \right) + C_D = 0 \quad (8)$$

$$\frac{r}{c_f} = K(n - r) \quad (9)$$

Glassy carbon was used as working electrode while a platinum wire and Ag/AgCl, satd. KCl were counter and reference electrodes respectively. The experimental solution was degassed for 15 min after addition of DNA using high-purity argon. Voltammograms were recorded at a scan rate of 100 mV/s.

In the medium used complexes and their parent compounds undergo reduction in the range from 750 to -950 mV. Upon increasing the concentration of calf thymus DNA, peak currents due to complexes gradually decreased. Based on the change in peak current ( $\Delta I$ ) binding constant values were evaluated considering the equilibrium shown by Eq. 10.

$$L + DNA = L - DNA; \quad K_d = \frac{[L][DNA]}{[L - DNA]} \quad (10)$$

For the complexes, a decrease in peak current during titration is a consequence of structural changes following binding of complexes with DNA, that gradually disables nitro groups from showing a response in cyclic voltammetry which was actually followed for evaluation of binding constants of the compounds [2, 4, 5, 23, 26-28].

### **Electrochemical generation of reduction products of 5-nitroimidazoles and complexes and interaction with biological targets**

To be able to do this work, it was necessary to identify reduction potentials of compounds in aqueous medium prior to start of actual experiments. The amount of reduced products formed depends on the time for which compounds are subjected to reduction at a constant potential. These reduced products cause a damage of the biological target which was investigated further with the help of suitable experimental techniques.

A glassy carbon electrode maintained at a previously determined reduction potential for each compound helped to electrochemically generate different reduction products in aqueous solution that includes  $RNO_2^{\bullet-}$  under de-aerated (Ar saturated) conditions. In the immediate vicinity of such *in situ* electrochemically generated reduction products, different nucleic acid

bases and calf thymus DNA were kept one at a time under de-aerated (Argon saturated) conditions [29]. The complex undergoes reduction at its ligand site in accordance with its electrochemical behaviour in aqueous solution generating different reduced species, that depend on the pH of the medium. In our case, pH was maintained at 7.4. The time allotted for *in situ* electrochemical generation of reduced species on each complex was strictly maintained constant for all forms of targets to be able to compare the results pertaining to creation of different species in solution, capable of bringing about a change on the target maintained in the immediate vicinity of such generation under identical conditions [30, 31].

### **Gamma irradiation experiments and aspects of radio-sensitization**

Stock solutions of nucleic acid bases were prepared in triple distilled water by weighing accurately each compound so that concentration of each nucleic acid base was  $1 \times 10^{-2}$  mol/L. Subsequently, utilizing these stock solutions, experimental solutions were prepared in which concentration of a nucleobase was  $1 \times 10^{-4}$  mole/L while ornidazole or its complexes were  $1 \times 10^{-5}$  mole/L. For experiments involving DNA, its concentration in the experimental solution was  $1 \times 10^{-4}$  mole/L while additives i.e. compounds had a concentration of  $1 \times 10^{-5}$  mol/L. Prior to irradiation, aqueous solutions of all samples were saturated with pure Ar by purging it through a 3 mL solution taken in a vial for at least 10 minutes. Solutions were irradiated with  $^{60}\text{Co}$  gamma rays at different time intervals. Dose rate (1.618 kGy/hr) was measured using a Fricke dosimeter.

### **Analysis of nucleobases using High Performance Liquid Chromatography**

The amount of each nucleic acid base remaining after experiment was determined using HPLC (a C-18 column as stationary phase and 5% aqueous methanol as mobile phase) for thymine, cytosine and adenine. In case of guanine, 40% aqueous methanol was used [30]. Here, also the concentrations of compounds used in the study were one-tenth of target

nucleic acid bases or calf thymus DNA. Control experiments were performed where aqueous solutions of nucleic acid bases or calf thymus DNA (without any compound) were subjected to a constant potential of -0.700 V (for tinidazole and its complexes) and -0.835 V (for ornidazole and its complexes) at pH 7.4, using the same glassy carbon electrode.

Following irradiation at different dose, solutions containing nucleobases with or without additives were analysed by HPLC using a C<sub>18</sub> column supported by a PDA detector. Components were eluted using 5% methanol in water as the mobile phase having flow rate of 1 ml min<sup>-1</sup>. From the area of peaks in each chromatogram, the concentration of a nucleobase remaining intact even after irradiation either in the absence or presence of additives could be ascertained and products identified. Determination of concentration was possible using standard plots prepared earlier for each nucleobase [32]. In this manner, radiation-induced damage of a nucleobase either in the absence or presence of a compound was obtained.

#### **Ethidium bromide fluorescence for monitoring the amount of DNA not modified**

Amount of calf thymus DNA remaining unaltered was determined by treating it with ethidium bromide (EtBr) and subsequently determining the fluorescence of the adduct on a RF-530 IPC Spectrofluorophotometer, Shimadzu, Japan [30, 33-35]. Interaction of EtBr with DNA leads to increase in fluorescence, a fact that was utilized to determine the amount of DNA that remained intact following interaction either with reduced species generated electrochemically or with species generated following radiolysis of water [33-35, 36, 37].

Information on radiation-induced damage caused to DNA, exposed to  $\gamma$ -radiation either when present alone or in the presence of sensitizers was obtained by treating all irradiated samples with ethidium bromide (EtBr). Subsequently fluorescence was recorded. Excitation was done at 510 nm and emission recorded over the range 590 nm to 610 nm. Fluorescence intensity of

the EtBr-DNA adduct was measured for each sample from where the amount of calf thymus DNA remaining could be determined (Eq. 11) [35-37].

$$\% \text{ DNA remaining} = (F_S - F_E) / (F_0 - F_E) \times 100 \quad (11)$$

Enhancement ratio indicates extent of damage caused to a target obtained from the ratio of slopes of linear plots (for solutions containing compounds to that obtained in the absence of any compound).

### **Biological assay on an amoeba strain**

Axenic *Entamoebahistolytica* strain HM1:IMSS was maintained and grown in TYIS-33 medium supplemented with 15% adult bovine serum, 1 × Diamond vitamin mix and antibiotics (0.3 units/ml penicillin and 0.25 mg/ml streptomycin) at 35.5°C. Cells were sub-cultured twice a week [38]. *Entamoeba* cells were taken from the log phase and an *in vitro* drug sensitivity assay was performed for 24 and 48 hours respectively [39].

The *in vitro* sensitivity assay was done on a 96 microtitre plate following a protocol described earlier [39]. In brief, stock solutions (10 mM) of different compounds were prepared in DMSO and further diluted in respective medium to arrive at a desired concentration. These were then added to the well of microtitre plate in triplicate. Strain HM1:IMSS was harvested at log phase and pelleted at 600 g for 5 min. Cells were counted using a Haemocytometer. Equal volumes of cell suspensions of Axenic strain HM1:IMSS ( $3 \times 10^5$ ) per well was added to wells containing different compounds. The final compound concentration in rows down the plate were 200, 100, 50, 25, 12.5, 6.25, 3.125  $\mu\text{M}$  respectively. Appropriate controls in triplicate were included in each plate having DMSO,  $\text{ZnCl}_2$  and non-treated media (allowing for 100% growth). Subsequently, the microtitre plate was placed in an incubation bag having an aerocult minisachet to maintain an anaerobic atmosphere. The incubation bag was sealed and placed in an incubator where the temperature was 35°C.

Cell growth was monitored on a daily basis at 24 and 48 hours respectively by comparing compounds containing wells with controls in same rows using an inverted microscope. Plates were properly examined and each well was scored according to well coverage, cell mobility, cell rounding. + was given to 30% well coverage area with rounded cells and ++++ for fully covered wells having pseudopodal movement. MIC is considered as the lowest concentration of a compound at which a score of + could be given.

*In vitro* compound susceptibility (Trypan blue) assay was done where  $3 \times 10^5$  Trophozoite was added in 3 replicate wells containing previously diluted different concentrations of compounds. A non-treated control (100% growth) was included in each plate. Culture plates were sealed and incubated for 24 and 48 hours respectively at 37°C. Trophozoite growth was determined after 24 hours and 48 hours by microscope counting using 0.4% trypan blue assay [40].

#### **Determination of minimum inhibitory and bactericidal concentration (MIC & MBC)**

MBC values of monomeric and dimeric complexes of  $\text{Cu}^{\text{II}}$  against *Pseudomonas aeruginosa* ATCC and *Staphylococcus aureus* ATCC were determined by micro-dilution techniques [40]. Bacterial cells were inoculated in microtitre plates at a concentration of  $10^6$  CFU/mL in a volume of 50 mL. Complexes of varying concentrations were added separately and incubated at 37°C for 24 hours. These were analyzed at 600 nm using a spectrophotometer. Antibacterial efficacy of monomeric and dimeric complexes was analyzed by determining the diameter of the zone of inhibition in millimeter. Sterilized discs of paper soaked in various concentrations of monomeric and dimeric complexes were placed on agar plates possessing *P. aeruginosa* and *S. aureus* followed by determination of clear zones of inhibition. Susceptibility of microbial strains to antimicrobial agents was determined by calculating zone of inhibition as per recommendations of National Committee for Clinical Laboratory Standards [41].

### **Formation of *P. aeruginosa* and *S. aureus* biofilm**

Formation of biofilm by *P. aeruginosa* and *S. aureus* was determined using 96 polystyrene well plates for a period of 72 hours at 37<sup>0</sup>C followed by washing with phosphate buffer and staining with 0.4% (v/v) crystal violet that was dissolved in glacial acetic acid 30% (v/v) for 10 minutes. It was then allowed to dry for 30-45 minutes followed by rinsing with phosphate buffer. Subsequently, it was allowed to dry at room temperature for approximately an hour. A 33% (v/v) acetic acid solution was added and optical density (OD) was measured at 540 nm using a spectrophotometer.

### **Assay of antibiofilm activity**

Rate of inhibition of biofilm formation achieved by the action of monomeric and dimericCu<sup>II</sup> complexes of tinidazole at MBC, incubated at 37<sup>0</sup>C for 72 hours were detected by the crystal violet assay [40, 42].

Percentage inhibition was measured with respect to untreated control using the formula mentioned below (Eq. 12).

$$\text{Percentage biofilm inhibition} = \frac{[(\text{OD of untreated control}) - (\text{OD of treated sample})]}{(\text{OD of untreated control})} \times 100 \quad (12)$$

### **Detection of Quorum sensing in test *P. aeruginosa* and *S. aureus***

The supernatant of bacterial culture broth was filtered using a membrane filter having pore size 0.2 μm. Ethyl acetate was added to the filtrate with gentle shaking for 10 minutes was done to allow for phase separation [40, 42]. The upper fraction of the mixture was mixed with 2M hydroxyl amine and 3.5 M NaOH (1:1) followed by 10 μl alcoholic ferric chloride

solution (Ferric chloride in 95% 1:1 ethanol). Colour of the solution was measured with a spectrophotometer at 520 nm [43].

### **Quantification of secondary metabolite pyocyanin produced by *P. aeruginosa* during biofilm formation**

Quantification of pyocyanin [44] produced by *P. aeruginosa* upon incubation with MBC concentrations of monomeric and dimeric Cu<sup>II</sup> complexes and amoxicillin (standard antibiotic) were done at 37°C for 48 hours. The culture supernatant (5ml) collected after centrifugation at 10,000 rpm for a period of 15 min [45] was added to 3 mL chloroform, followed by re-extraction with 1mL of 0.2N HCl, resulting in colour change from orange to pink that was detected at 520 nm using a spectrophotometer. This helped in determining percentage reduction of pyocyanin.

### **Determination of elastase activity**

Quantification of *las B* expression was done by determining elastase activity. An aliquot of culture supernatant (100 µl) was added to 900 µl of Elastin Congo Red (ECR) and incubated at 37°C for 3 hours. Insoluble ECR was removed by centrifugation and absorbance was measured at 495 nm [46].

### **Determination of Rhamnolipid production and Drop Collapse Assay**

The amount of rhamnolipid was estimated with cetyltrimethylammonium bromide (CTAB)-methylene blue plates in accordance with a method described earlier [47, 48]. Plates were supplemented with 0.2 % (w/v) cetyltrimethylammonium bromide (CTAB), 0.0005% (w/v) methylene blue and solidified with 1.5 % (w/v) agar. An overnight grown liquid culture of *P. aeruginosa* was used and a spot was applied at the middle of the plate for swarming assays. To all plates, except control, monomeric and dimeric Cu<sup>II</sup> complexes were added separately. Plates were incubated at 37°C for 24 hours followed by incubation at room temperature for

another 24 hours. Production of rhamnolipid was estimated by measuring the dark blue halo surrounding the colony and quantification was done following a protocol described earlier [49].

### **Detection of viability count of the sessile group of bacterial cells**

The working strain grown on 0.1% chitin flakes (w/v) for 72 hours was washed with 0.1% (w/v) normal saline to eliminate planktonic groups of cells. Following the treatment of sessile cells as control, or with monomeric and dimeric  $\text{Cu}^{\text{II}}$  complexes, bacterial growth was determined at 590 nm using a spectrophotometer at varying intervals of time [50].

### **Determination of EPS degradation on being challenged by monomeric and dimeric $\text{Cu}^{\text{II}}$ complexes**

Biofilms of the working strain were grown on chitin flakes 0.1 % (w/v) separately in 100 mL LB media, centrifuged at 12,000 rpm for 15mins at 4°C to break the biofilm. 5mL of PBS buffer was used to wash pellets collected after centrifugation and mixed with 2.5 mL 10 mM Tris-HCl (pH 7.8). After thorough cyclomixing, 20 mM  $\beta$ -mercaptoethanol and 1 mM PMSF were added. The cell suspension of bacterial culture was sonicated followed by centrifugation (12,000 rpm, 30 min) at 4°C followed by addition of 10% trichloroacetic acid (TCA) in acetone [51].

### **Estimation of carbohydrate and protein content in EPS when challenged by monomeric and dimeric complexes of $\text{Cu}^{\text{II}}$**

The carbohydrate present in EPS was quantified using Anthrone method [52]. Protein present in EPS was quantified by Lowry method [53].

### **Isolation and estimation of DNA from prokaryotic cells**

To have a check on adverse effects related to the use of monomeric and dimeric  $\text{Cu}^{\text{II}}$  complexes on genomic DNA of bacterial strains, they were isolated using CTAB, after

treatment with monomeric and dimeric complexes for 2 hours keeping the “control” untreated.

Concentration of DNA was measured spectrophotometrically at 260 nm and quantified as in Eq. 13.

$$\text{Units } (\times) \text{ mg ml}^{-1} = 50 \times \text{O D at 260nm} \times \text{dilution factor (13)}$$

## References

1. A. C. Valderrama-Negrón, W. A. Alves, Á. S. Cruz, S. O. Rogero, D. de Oliveira Silva, *Inorg. Chim. Acta*, **2011**, 367, 85-92.
2. R. C., Santra, D. Ganguly, J. Singh, K. Mukhopadhyay, S. Das, *Dalton Trans.* **2015**, 44, 1992-2000.
3. D. G. Desai, D. K. Sureja, B. R. Prajapati, A. K. Seth, K. I. Molvi, *J. Pharm. Res.*, **2016**, 10(11), 696-699.
4. R. C. Santra, D. Ganguly, S. Jana, N. Banyal, J. Singh, A. Saha, S. Chattopadhyay, K. Mukhopadhyay, S. Das, *New J. Chem.*, **2017**, 41, 4879-4886.
5. R. C. Santra, K. Sengupta, R. Dey, T. Shireen, P. Das, P. S. Guin, K. Mukhopadhyay, S. Das, *J. Coord. Chem.* **2014**, 67, 265-285.
6. Reflex Plus, Accelrys Material Studio 4.4, Accelrys Software Inc, **2008**.
7. G. S. Pawley, *J. Appl. Crystallogr.*, **1981**, 14, 357-361.
8. P. E. Werner, L. Eriksson, M. W. Treor, *J. Appl. Cryst.*, **1985**, 18, 367-370.
9. G. M. Sheldrick, SHELXS-97 and SHELXL-97, University of Göttingen, Germany, **1997**.
10. G. M. Sheldrick, SADABS: Software for Empirical Absorption Correction, University of Göttingen, Institute für Anorganische Chemie der Universität, Göttingen, Germany, **1999-2003**.
11. H. Putz, K. Brandenburg, Diamond-Crystal and Molecular Structure Visualization; Crystal Impact Kreuzherrenstr 102, 53227 Bonn, Germany. <http://www.crystalimpact.com/diamond>.

12. M. N. Burnett, C. K. Johnson, ORTEP-3: Oak Ridge Thermal Ellipsoid Plot Program for Crystal Structure Illustrations, Report ORNL-6895, Oak Ridge National Laboratory, Oak Ridge, TN, USA, **1996**.
13. J. A. Squella, P. Gonzalez, S. Bollo, *Pharm Res* **1999**, 16, 161-164.
14. P. Zanello, *Inorganic Electrochemistry: Theory, practice and application*, The Royal Society of Chemistry, **2003**.
15. J. A. Squella, S. Bollo, J. de la Fuente, L. J. Núñez-Vergara, *Bioelectrochem Bioenergetics*, **1994**, 34, 13–18.
16. J. A. Squella, M. Huerta, S. Bollo, H. Pessoa, L. J. Núñez-Vergara, *J. Electroanal. Chem.*, **1997**, 420, 63–70.
17. L. J. Núñez-Vergara, F. Garcia, M. Dominguez, J. de la Fuente, J. A. Squella, *J. Electroanal. Chem.*, **1995**, 381, 215–219.
18. P. C. Mandal, *J. Electroanal. Chem.* **2004**, 570, 55-61.
19. A. J. Bard, L. R. Faulkner, *Electrochemical methods Fundamental and application*, 2<sup>nd</sup> ed., John Wiley & Sons. Inc.: New York, **2001**, pp 236.
20. S. A. Ozkan, Z. Senturk, I. Biryol, *Int. J. Pharmaceutics*, **1997**, 157, 137–144.
21. R. S. Nicholson, *Anal. Chem.*, **1966**, 38, pp. 1406.
22. P. S. Guin, S. Das, *Int. J. Electrochem.*, Article ID 517371, **2014**, 8 pages.
23. B. Mandal, S. Das, *J. Indian Chem. Soc.*, **2020**, 97, 2633-2642.
24. H. Lund in *Cathodic Reduction of Nitro and Related Compounds*, in *Organic Electrochemistry*, Ed. Lund H and Baizer M M, p. 411, M. Dekker Inc. New York 3rd. Ed. (**1990**).
25. P. S. Guin, P. C. Mandal, S. Das, *ChemPlusChem*, **2012**, 77, 361-369.
26. X. Jiang, X. Lin, *Bioelectrochem.*, **2006**, 68, 206-212.
27. T. Deb, D. Choudhury, P. S. Guin, M. B. Saha, G. Chakrabarti, S. Das, *Chem-Biol. Inter.*, **2011**, 189, 206-214.
28. C. G. Clark, L. S. Diamond, *Clin. Microbiol. Rev.*, **2002**, 15, 329–341.
29. B. Mandal, H. K. Mondal, S. Das, *Biochem. Biophys. Res. Comm.*, **2019**, 515, 505-509.

30. A. R. Morgan, J. S. Lee, D. E. Pulleyblank, N. L. Murray and D. H. Evans, *Nucleic Acids Res.*, **1979**, 7, 547.
31. W. A. Prütz, *Radiat. Environ. Biophys.* **1984**, 23, 1-6.
32. D. L. Morris, Quantitative determination of carbohydrates with Dreywood's anthrone reagent. *Science*, **1948**, 107, 254-255.
33. H. C. Birnboim and J. J. Jevcak, *Can. Res.*, **1981**, 41, 1889-1892.
34. S. Das, A. Saha and P. C. Mandal, *Environ. Health Pers.*, **1997**, 105, 1459-1462.
35. M. Saha, S. Das, *Heliyon* **2021**, 7, e07746;
36. S. Das; P. C. Mandal, *J. Radioanal. Nucl. Chem.* **2014**, 299, 1665-1670.
37. R. C., Santra, D. Ganguly, D. Bhattacharya, P. Karmakar, A. Saha, S. Das., *New J. Chem.*, **2017**, 41, 11679-11685.
38. J A Upcroft and P Upcroft. ,*Chemother.*, **2001**, 45, 1810–1814.
39. E. Benere, R. A. I. Luz, M. Vermeersch, P. Cos and L. Maes, *J. Microbiol. Methods*, **2007**, 71, 101–106.
40. D. Lahiri, M. Nag, B. Dutta, I. Mukherjee, S. Ghosh, A. Dey, R. Banerjee, R. R. Ray, *Appl. Biochem. Biotechnol.* **2021**, 193, 1617-1630.
41. M. Balouiri, M. Sadiki, S. K Ibsouda, *J. Pharma. Anal.* **2016**, 6, 71-79.
42. D. Lahiri,; D. Nag, D.; D. Dutta, D.; S. Dash,; S. Ghosh,.; R. R. Ray, Ed.; Springer: Singapore, **2021**, 69-81.
43. R. Taghadosi,; M. R. Shakibaie, S., Masoumi, *Rep Biochem Mol Biol.* **2015**, 3, 56-61.
44. D. W. Essar,.; L. Eberly,; A. Hadero,.; I. P. Crawford, , *J Bacteriol.* **1990**, 172, 884.
45. J. H. Lee, J. H. Park,.; H. S. Cho,.; S. W. Joo,.; M. H., Cho, Lee, *J. Biofouling*, **2013**, 29, 491-499.
46. L. Rust,; C. R.; Messing, B. H. Iglewski, . *Methods Enzymol.* **1994**, 235, 554-562.
47. I. Siegmund,; F. Wagner, , *Biotechnol. Tech.* **1991**, 5, 265-268.
48. N. C. Caiazza,; R. M. Shanks,; G. A. O'Toole, , *J Bacteriol.* **2005**, 187, 7351.
49. T. S. Murray,.; B. I. Kazmierczak, *J Bacteriol* **2020**, 190, 2700.
50. R. Baishya,; A. Bhattacharya,; M. Mukherjee,; D. Lahiri,.; S. Banerjee, *Materials Today: Proceedings*, **2016**, 3, 3461-3466.
51. S. Pereira,; A. Zille,.; E. Micheletti,; P. Moradas-Ferreira,; R. De Philippis, P. Tamagnini, , *FEMS Microbiol Rev.* **2009**, 33, 917-941.

52. D. L. Morris,. Quantitative determination of carbohydrates with Dreywood'santhrone reagent. *Science*, **1948**, 107, 254-255.
53. O. H.; Lowry, N. J Rosebrough,.; A. L Farr,.; R. J. Randall, , *J Biol Chem.* **1951**, 193, 265-275.

## **Chapter 7**

**A Zn<sup>II</sup> complex of Ornidazole with decreased nitro radical anion formation is still active on *Entamoeba histolytica***

## Introduction

The passage of time and use of different compounds of the 5-nitroimidazole family revealed adverse drug reactions, neurotoxic side effects and drug resistance that pose challenges to the use of such drugs [1-4]. Metronidazole, tinidazole and ornidazole (Onz) are important molecules of the 5-nitroimidazole family that have made their way to clinics and are used in a number of pharmaceutical preparations [1-8]. Their efficacy is attributed to generation of nitro-radical anion ( $-\text{NO}_2^{\cdot-}$ ) [1-10]. To tackle infections caused by parasites the molecules are reduced by the enzyme pyruvate ferredoxinoxidoreductase (PFOR) acting as an electron sink [9, 10]. Reduction of the nitro group on 5-nitroimidazoles prepare them for entry in to cells by passive diffusion creating a favorable concentration gradient [9,10]. After entering target cells, the anti-microbial toxicity of 5-nitroimidazoles are dependent on the reduction of the nitro group to  $\text{NO}_2^{\cdot-}$  and other active species like nitroso and hydroxylamine derivatives. The nitro-radical anion ( $-\text{NO}_2^{\cdot-}$ ) binds to DNA disrupting or breaking strands which is a cause of cell death [9,10]. 5-nitroimidazoles are also potential radiosensitizers in the treatment of cancer [5-8]. As radiosensitizers they interact with the radicals formed on DNA following their interaction with the products of the radiolysis of water, forming  $-\text{NO}_2^{\cdot-}$  which thereafter enhance strand unwinding or strand breaks [6-8].

Unfortunately,  $-\text{NO}_2^{\cdot-}$  is associated with neurotoxic side effects, particularly when there is prolonged use of such molecules [9-11]. In a situation like this, aspects of neurotoxicity or other forms of side effects need to be checked to improve acceptability of such drugs. This would require a control on the generation of  $-\text{NO}_2^{\cdot-}$ . Too much generation of reactive intermediates either of this class of drugs or others often cause more harm than good [12-15]. Hence, generating the correct amount or making it available through slow chemical release is gradually becoming an important aspect of research in recent times [10-15]. This

chapter deals with the regulation of  $\text{-NO}_2^-$  for a specific cause, achieved here through complex

formation of Ornidazole with  $\text{Zn}^{\text{II}}$ , that probably generates the correct amount necessary for cytotoxicity of a biological target (Axenic *Entamoeba histolytica*) or it could be that, what it compromises in the free radical pathway by way of decreased generation of species like  $\text{-NO}_2^-$ , it makes it up through other attributes of complex formation. Earlier, a  $\text{Zn}^{\text{II}}$  complex of metronidazole, was shown to be active as an anticancer agent on a number of cancer cell lines [16]. Hence, complexes of the 5-nitroimidazole family containing a relatively non-toxic metal ion ( $\text{Zn}^{\text{II}}$ ) might be useful cytotoxic agents against a number of diseases.

## Results and Discussion

### Crystal structure of $[\text{Zn}(\text{Onz})_2\text{Cl}_2]$ from Powder X-ray Diffraction data

Structural analysis revealed the complex crystallizes in achiral  $Pna2_1$  space group belonging to the orthorhombic system having cell dimensions of  $a = 10.407(7) \text{ \AA}$ ,  $b = 7.756(5) \text{ \AA}$ ,  $c = 27.725(5) \text{ \AA}$ . The asymmetric unit of the complex consists of one  $\text{Zn}^{2+}$  ion, two Onz moieties and two  $\text{Cl}^-$ . The ORTEP diagram is shown in Figure 1. The metal center exhibits a four coordinated slightly distorted tetrahedral geometry. The two N atoms (N9, N29) of two different Onz moieties and two  $\text{Cl}^-$  ions (Cl2, Cl22) occupy the four corners of a tetrahedron surrounding  $\text{Zn}^{2+}$ . Zn-N bond distances are  $\sim 2.017 \text{ \AA}$  while Zn-Cl bond distances are  $\sim 2.239 \text{ \AA}$ . Two imidazole nitrogens of two different Ornidazole moieties bind the metal center in a syn-syn fashion. Some coordinated bond distances and bond angles are listed in Table 1.

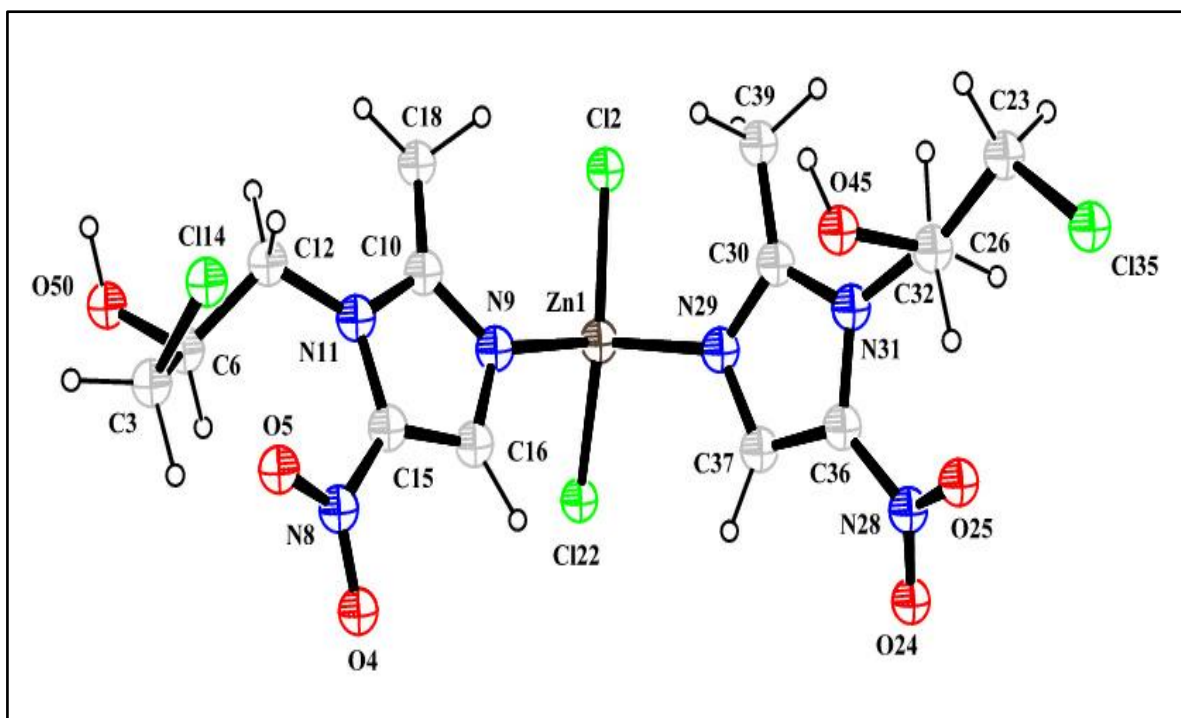


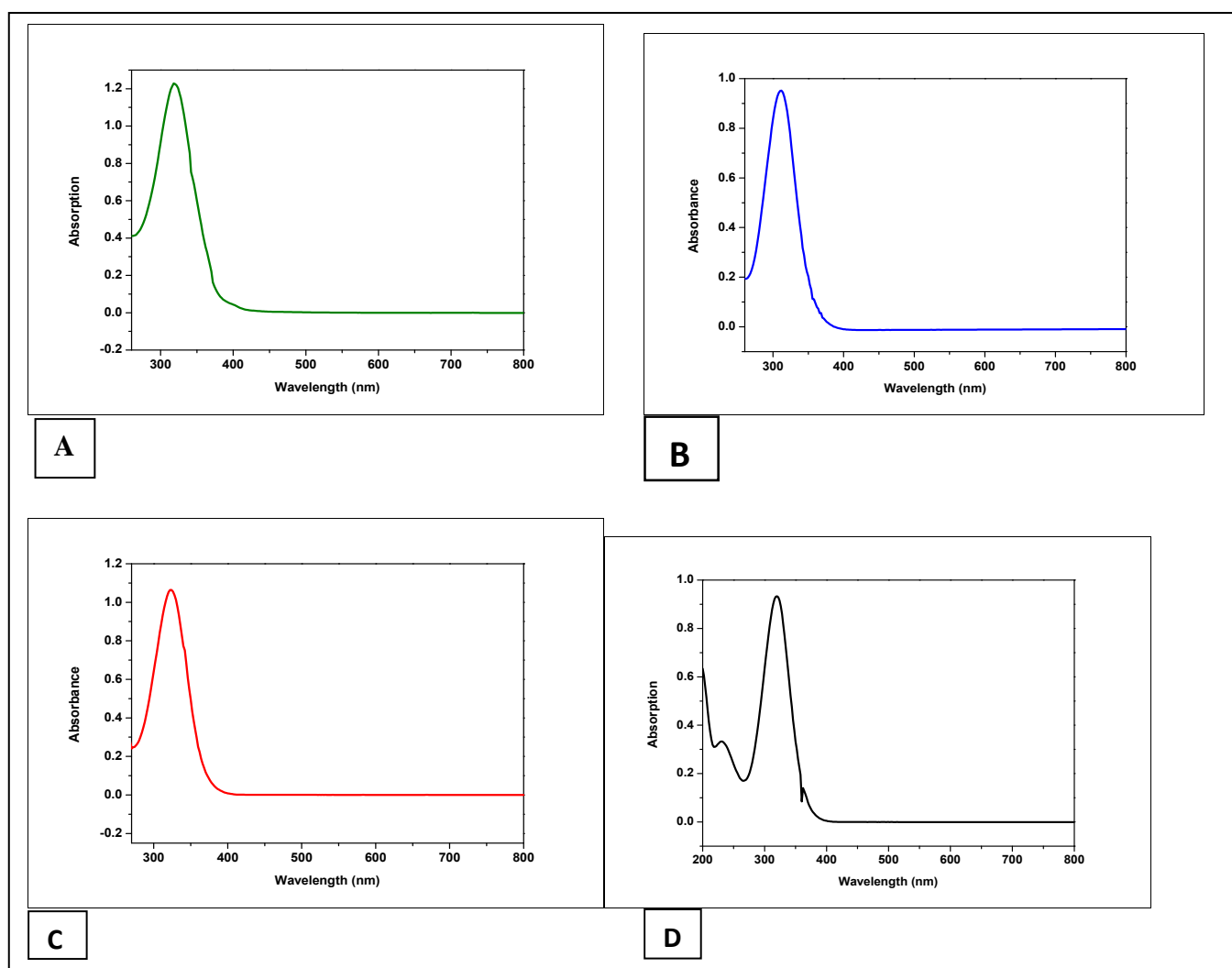
Figure1: A perspective view of the complex

Table 1: Some selected bond lengths (Å) and bond angles (°) of the complex

Bonds	Bond lengths (Å)	Bond angles	Amplitude (°)
Zn1—Cl2	2.238(7)	Cl2—Zn1—Cl22	134.95
Zn1—Cl22	2.238(5)	O50—C6—C3	108.88
Zn1—N9	2.017(2)	Cl2—Zn1—N9	106.13
Zn1—N29	2.017(3)	O50—C6—C12	111.68
Cl14—C3	1.779(7)	Cl2—Zn1—N29	98.84
Cl35—C23	1.779(9)	C3—C6—C12	110.57
C26—C32	1.549(3)	Cl22—Zn1—N9	98.90
C3—C6	1.533(9)	Cl22—Zn1—N29	106.16
C6—C12	1.549(4)	N9—Zn1—N29	111.32
C10—C18	1.470(7)	N11—C12—C6	111.25
C15—C16	1.408(9)	Cl35—C23—C26	108.88
C23—C26	1.533(9)	O45—C26—C23	108.89
O45—C26	1.417(4)	O45—C26—C32	111.68
O50—C6	1.417(5)	C23—C26—C32	110.56
N31—C32	1.470(6)	N31—C32—C26	111.25
		Cl14—C3—C6	108.89

## UV-Vis spectroscopy of Ornidazole and its Zn<sup>II</sup> complex in different solvents

Ornidazole and [Zn(Onz)<sub>2</sub>Cl<sub>2</sub>] were dissolved in different solvents (water, methanol, DMF, acetonitrile) having concentration 10<sup>-4</sup> M. UV-Vis spectrum of Onz and the complex showed a prominent response in the UV region from 260 to 320 nm (Figures 2 and 3 respectively). Absorption bands were similar (Table 2). Bands were attributed to intra-ligand charge transfer.



**Figure 2: UV-Vis spectra of Onz in A) water, B) methanol, C) DMF and D) acetonitrile**

**Table 2: Absorption (Abs.) of Ornidazole and Zn<sup>II</sup>-Ornidazole in different solvents**

Compound	Acetonitrile		DMF		Methanol		Water	
	$\lambda_{\max}$ (nm)	Abs. Intensity						
Onz	320	0.9335	324	1.0638	312	0.9519	318	1.2287
Zn(Onz) <sub>2</sub> (Cl) <sub>2</sub>	318	1.7287	324	1.2643	310	1.5615	320	1.1576

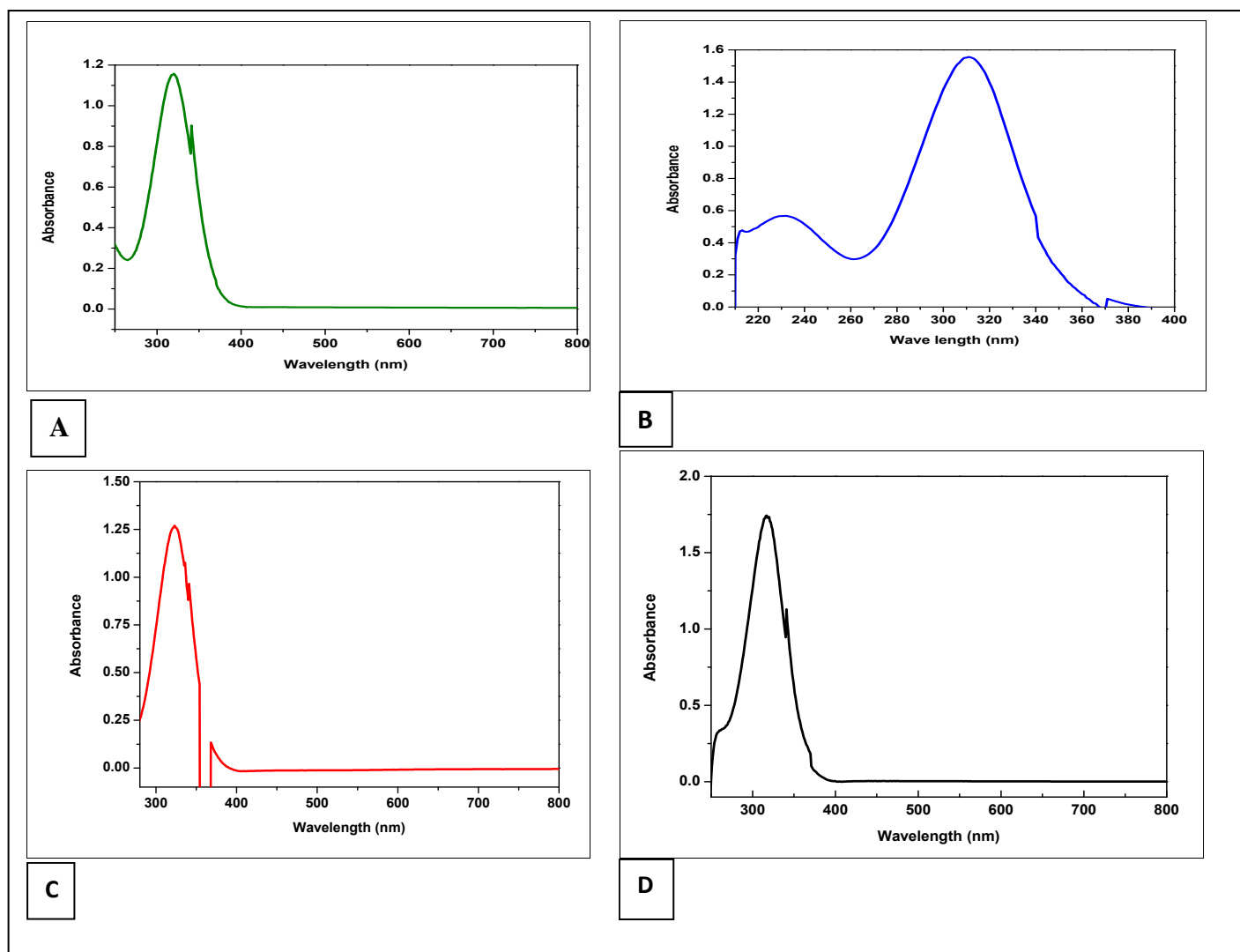


**Figure 3: UV-Vis spectra of [Zn(Onz)<sub>2</sub>Cl<sub>2</sub>] in A) water, B) methanol, C) DMF and D) acetonitrile**

### Analysis of IR spectra of Ornidazole and its monomeric Zn<sup>II</sup> complex

IR spectrum of Onz (Figure 4) shows a band at 1538.21 cm<sup>-1</sup>, assigned to  $\nu_{C=N}$  stretching of the imidazole ring that shifts to higher wave number (1565.80 cm<sup>-1</sup>) in Zn(Onz)<sub>2</sub>Cl<sub>2</sub> (Figure 5) suggesting coordination of Zn<sup>II</sup> by an imidazole nitrogen. Two NO<sub>2</sub> stretching vibrations,  $\nu_{as}$  1482cm<sup>-1</sup> and  $\nu_s$  1380cm<sup>-1</sup> in the complex are similar to that in Onz indicating -NO<sub>2</sub> does not participate in binding the metal ion (Table 3) [23].

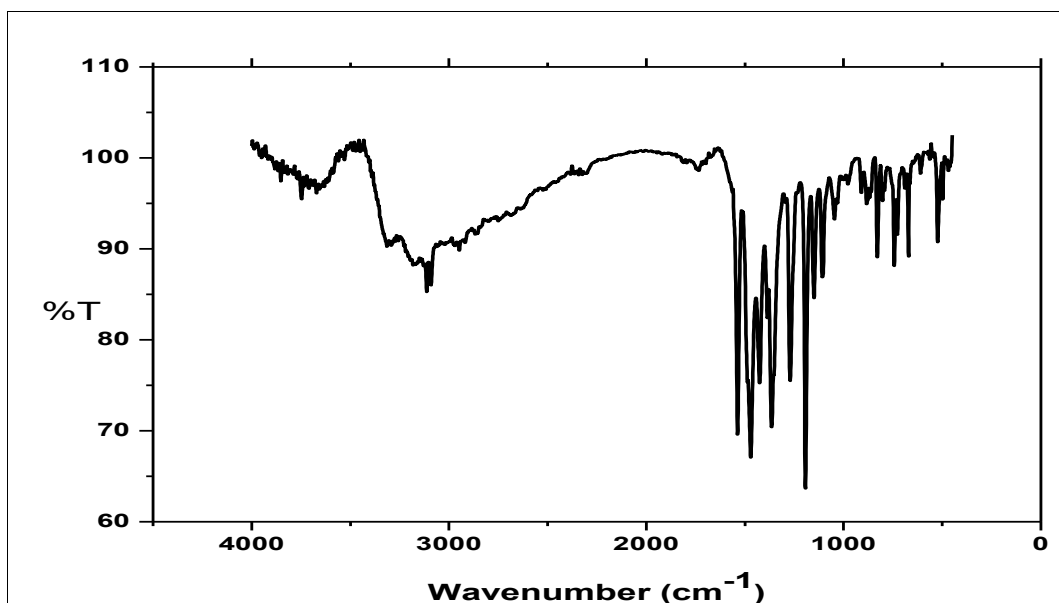


**Figure 4: IR spectrum of Onz**

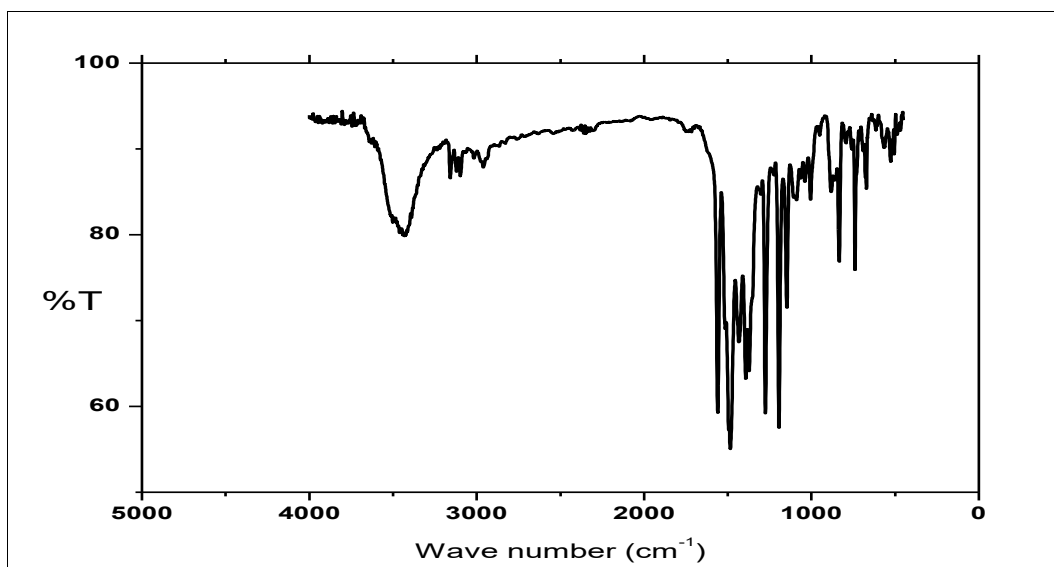


**Figure 5: IR spectrum of [Zn(Onz)<sub>2</sub>Cl<sub>2</sub>]**

**Table 3: IR stretching frequencies of Ornidazole and its monomeric Zn(II) complex**

Functional group	IR bands (values in $\text{cm}^{-1}$ )	
	Onz	$[\text{Zn}(\text{Onz})_2\text{Cl}_2]$
C=N	1538.21	1565.80
$\text{NO}_2$ ( $\nu_s$ )	1385.92	1380.48
$\text{NO}_2$ ( $\nu_{as}$ )	1471.60	1482.00

#### Mass spectrometry of the complex

Structure of the complex from the PXRD data suggests that its molecular formula should be  $\text{Zn}(\text{Onz})_2\text{Cl}_2$ . Hence, molecular ion peak in the mass spectrum should be found in the range  $m/z = 572$  to  $m/z = 582$  (considering isotope effects due to Cl in Ornidazole and also Cl present in the coordination zone surrounding the metal ion; isotope effects would be seen for Zn as well).

In the mass spectrum (Figure 6), the molecular ion peak, expected in the region mentioned above was not detected. However, a cluster of peaks (due to isotope effect) appeared having  $m/z$  values 536.8239, 538.8197, 540.8192 and 542.8129 that may be attributed to a species formed from the complex following loss of one Cl co-ordinated to Zn. Again, from the complex, besides a Cl (coordinated to Zn), if a  $-\text{CH}_3$  and  $-\text{NO}_2$  depart from each Onz unit, the species formed should have  $m/z$  values in the range from 419 to 423. Prominent experimental peaks with  $m/z$  between  $m/z = 420.0368$  and  $m/z = 422.0334$  were obtained. Besides, peaks

with  $m/z$  219.9733, 221.9697 and 223.0094 suggest presence of free Onz that got detached from the complex during mass spectrometry.

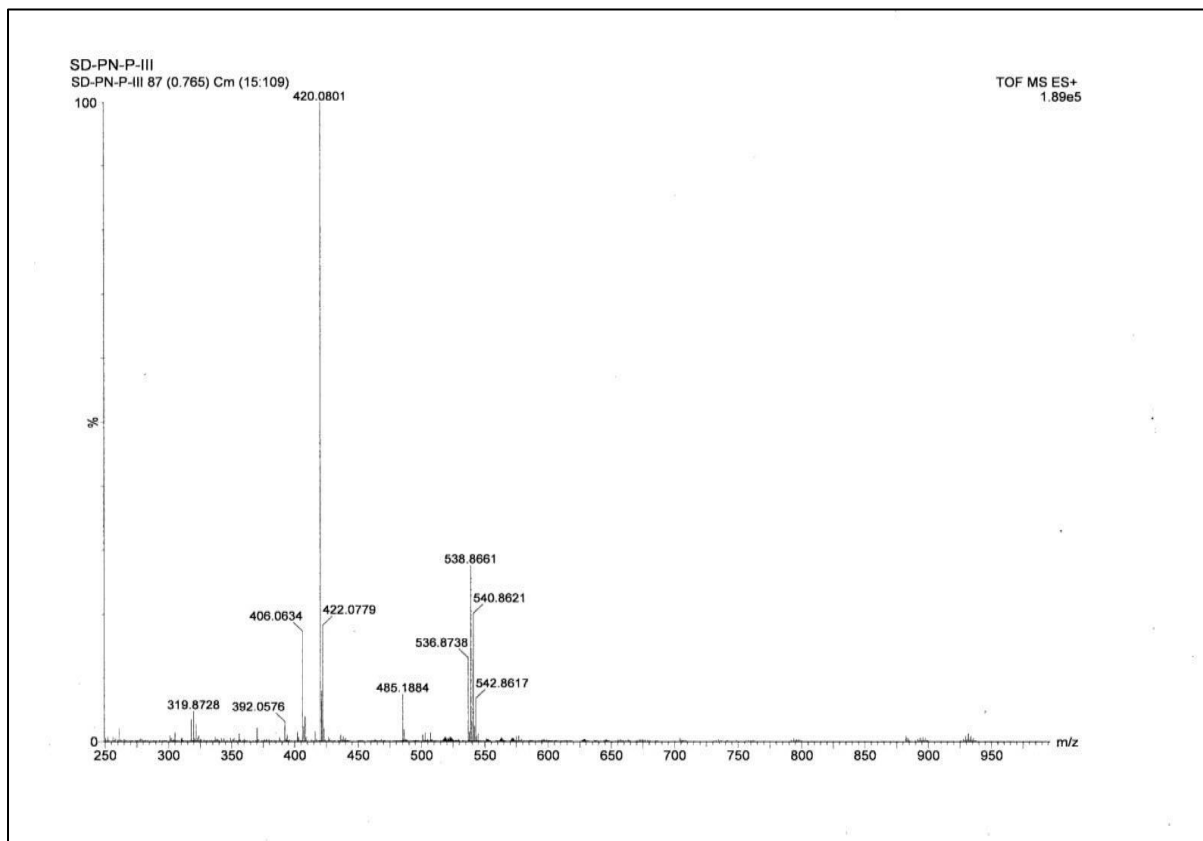
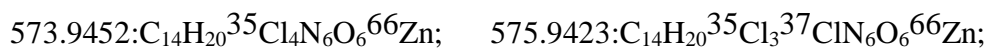
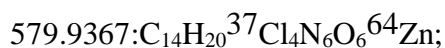


**Figure 6: Mass spectrum of the  $[Zn(Onz)_2Cl_2]$**

**Detailed analysis of peaks related to mass spectrum of  $C_{14}H_{20}Cl_4ZnN_6O_6$**

**Expected molecular ion peaks considering isotopic distribution due to Zn [isotopes  $^{64}Zn$  (49.2%),  $^{66}Zn$  (27.7%),  $^{67}Zn$  (4.0%) &  $^{68}Zn$  (18.5%)] and four Cl atoms (isotopes  $^{35}Cl$  &  $^{37}Cl$ ).**



581.9336:  $C_{14}H_{20}^{37}Cl_4N_6O_6^{66}Zn$ ;  
 574.9463:  $C_{14}H_{20}^{35}Cl_4N_6O_6^{67}Zn$ ;      576.9434:  $C_{14}H_{20}^{35}Cl_3^{37}ClN_6O_6^{67}Zn$ ;  
 578.9405:  $C_{14}H_{20}^{35}Cl_2^{37}Cl_2N_6O_6^{67}Zn$ ; 580.9376:  $C_{14}H_{20}^{35}Cl^{37}Cl_3N_6O_6^{67}Zn$ ;  
 582.9347:  $C_{14}H_{20}^{37}Cl_4N_6O_6^{67}Zn$ ;  
 575.9440:  $C_{14}H_{20}^{35}Cl_4N_6O_6^{68}Zn$ ;      577.9411:  $C_{14}H_{20}^{35}Cl_3^{37}ClN_6O_6^{68}Zn$   
 579.9382:  $C_{14}H_{20}^{35}Cl_2^{37}Cl_2N_6O_6^{68}Zn$ ; 581.9353:  $C_{14}H_{20}^{35}Cl^{37}Cl_3N_6O_6^{68}Zn$ ;  
 583.9324:  $C_{14}H_{20}^{37}Cl_4N_6O_6^{68}Zn$ ;

### **Explanation for peaks 536.8239, 538.8197, 540.8192 and 542.8129 in the mass spectrum**

**Possible masses for a fragment formed from the molecular ion due to loss of Cl coordinated to Zn, considering isotope distribution due to Zn [ $^{64}Zn$  (49.2%),  $^{66}Zn$  (27.7%),  $^{67}Zn$  (4.0%) &  $^{68}Zn$  (18.5%)] and the three Cl atoms [ $^{35}Cl$  (75%) &  $^{37}Cl$  (25%)].**

536.9795:  $C_{14}H_{20}^{35}Cl_3N_6O_6^{64}Zn$ ;      538.9766:  $C_{14}H_{20}^{35}Cl_2^{37}ClN_6O_6^{64}Zn$ ;  
 540.9737:  $C_{14}H_{20}^{35}Cl^{37}Cl_2N_6O_6^{64}Zn$ ; 542.9708:  $C_{14}H_{20}^{37}Cl_3N_6O_6^{64}Zn$ ;  
 538.9764:  $C_{14}H_{20}^{35}Cl_3N_6O_6^{66}Zn$ ;      540.9735:  $C_{14}H_{20}^{35}Cl_2^{37}ClN_6O_6^{66}Zn$ ;  
 542.9706:  $C_{14}H_{20}^{35}Cl^{37}Cl_2N_6O_6^{66}Zn$ ; 544.9677:  $C_{14}H_{20}^{37}Cl_3N_6O_6^{66}Zn$ ;  
 539.9795:  $C_{14}H_{20}^{35}Cl_3N_6O_6^{67}Zn$ ;      541.9746:  $C_{14}H_{20}^{35}Cl_2^{37}ClN_6O_6^{67}Zn$ ;  
 543.9717:  $C_{14}H_{20}^{35}Cl^{37}Cl_2N_6O_6^{67}Zn$ ; 545.9688:  $C_{14}H_{20}^{37}Cl_3N_6O_6^{67}Zn$ ;  
 540.9752:  $C_{14}H_{20}^{35}Cl_3N_6O_6^{68}Zn$ ;      542.9723:  $C_{14}H_{20}^{35}Cl_2^{37}ClN_6O_6^{68}Zn$ ;  
 544.9694:  $C_{14}H_{20}^{35}Cl^{37}Cl_2N_6O_6^{68}Zn$ ; 546.9665:  $C_{14}H_{20}^{37}Cl_3N_6O_6^{68}Zn$ ;

### **Explanation for the peak at m/z = 485.1884**

**Possible masses for a fragment formed from the molecular ion following the loss of two Cl coordinated to Zn and an -OH from any one Onz ligand, considering isotope distribution due to Zn [ $^{64}Zn$  (49.2%),  $^{66}Zn$  (27.7%),  $^{67}Zn$  (4.0%) &  $^{68}Zn$  (18.5%)] and the two Cl atoms [ $^{35}Cl$  (75%) &  $^{37}Cl$  (25%)].**

**The most probable ones based on relative abundance of Zn and Cl are shown below**

485.0080:  $C_{14}H_{20}^{35}Cl_2N_6O_5^{64}Zn$ ,      487.0049:  $C_{14}H_{20}^{35}Cl_2N_6O_5^{66}Zn$  and  
 489.0037:  $C_{14}H_{20}^{35}Cl_2N_6O_5^{68}Zn$

### Explanation for peaks with $m/z = 420.0801$ and $422.0779$

Possible masses for a fragment formed from a molecular ion following the loss of  $-CH_3$  and  $-NO_2$  from each Onz ligand along with loss of a  $-Cl$  from either Onz ligand on the complex, considering isotope distribution due to the Zn [ $^{64}Zn$  (49.2%),  $^{66}Zn$  (27.7%),  $^{67}Zn$  (4.0%) &  $^{68}Zn$  (18.5%)] and the Cl atom [ $^{35}Cl$  (75%) &  $^{37}Cl$  (25%)].

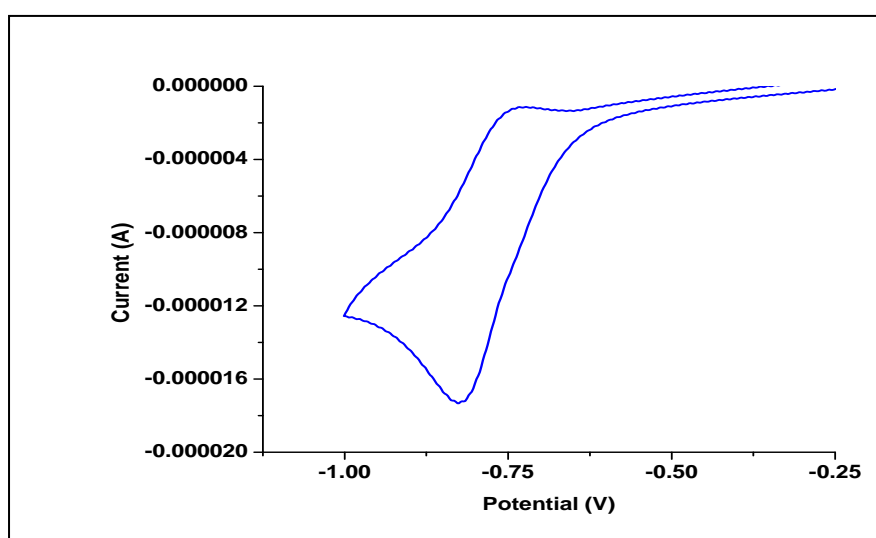
### The most probable ones based on relative abundance of Zn and Cl are shown below

419.9859:  $C_{12}H_{19}^{35}Cl_3N_4O_2^{64}Zn$ , 421.9828:  $C_{12}H_{19}^{35}Cl_3N_4O_2^{66}Zn$  and

423.9816:  $C_{12}H_{19}^{35}Cl_3N_4O_2^{68}Zn$

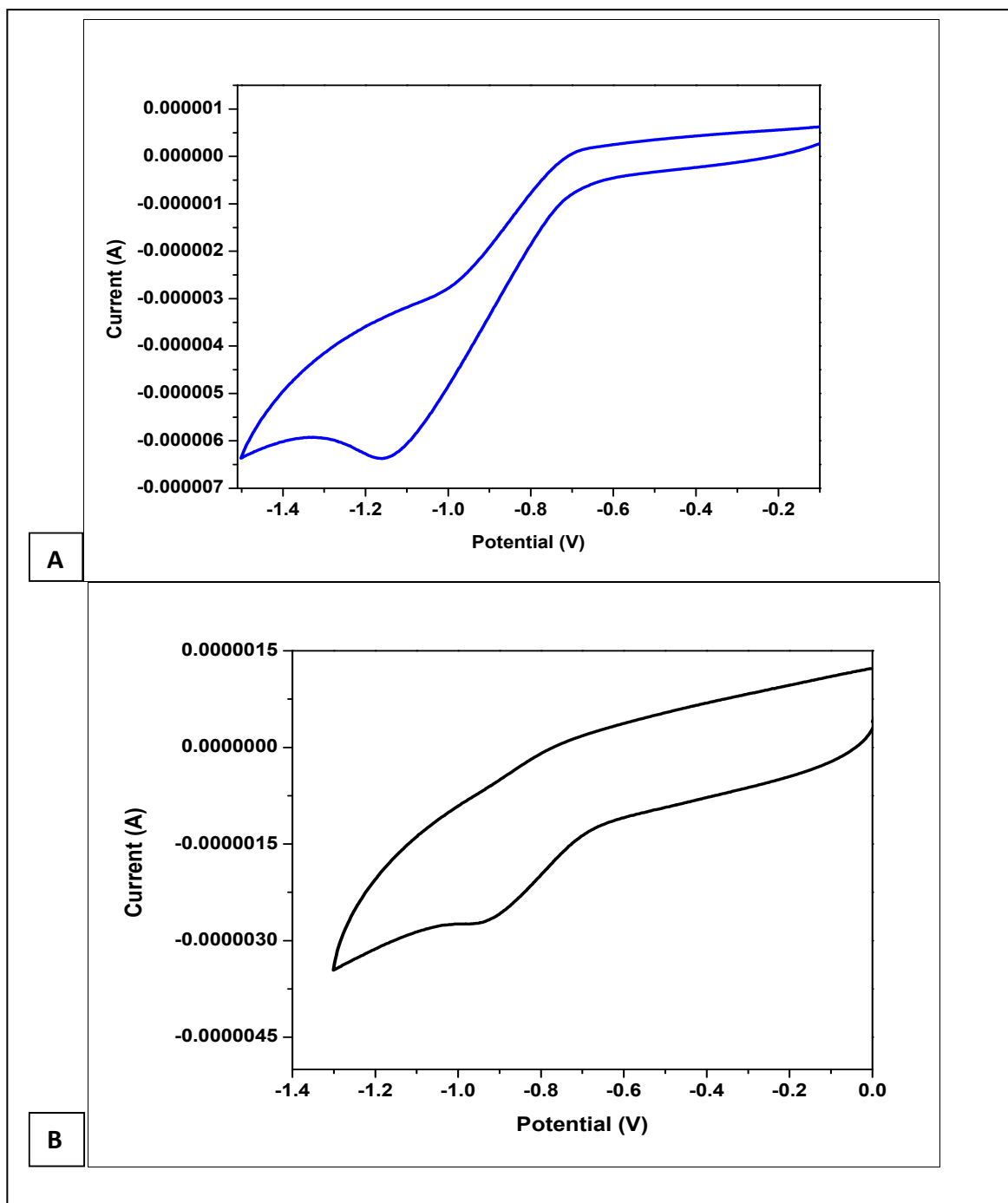
### Cyclic voltammetric studies

Cyclic voltammetry of Onz (Figure 7) and of  $Zn(Onz)_2Cl_2$  (Figure 8) were performed; the former in aqueous-20% methanol solution while the latter in pure methanol and pure aqueous solution at scan rate  $0.1 \text{ V s}^{-1}$ . The complex showed a peak at  $-0.925 \text{ V}$  against Ag/AgCl, satd. KCl (Figure 8) that was assigned to reduction of the  $-NO_2$  moiety in Onz. Cyclic voltammogram of Onz (Figure 7) showed a peak at  $-0.827 \text{ V}$  in aqueous - 20% methanol solution in presence of  $0.12 \text{ M}$  KCl on a glassy carbon electrode.

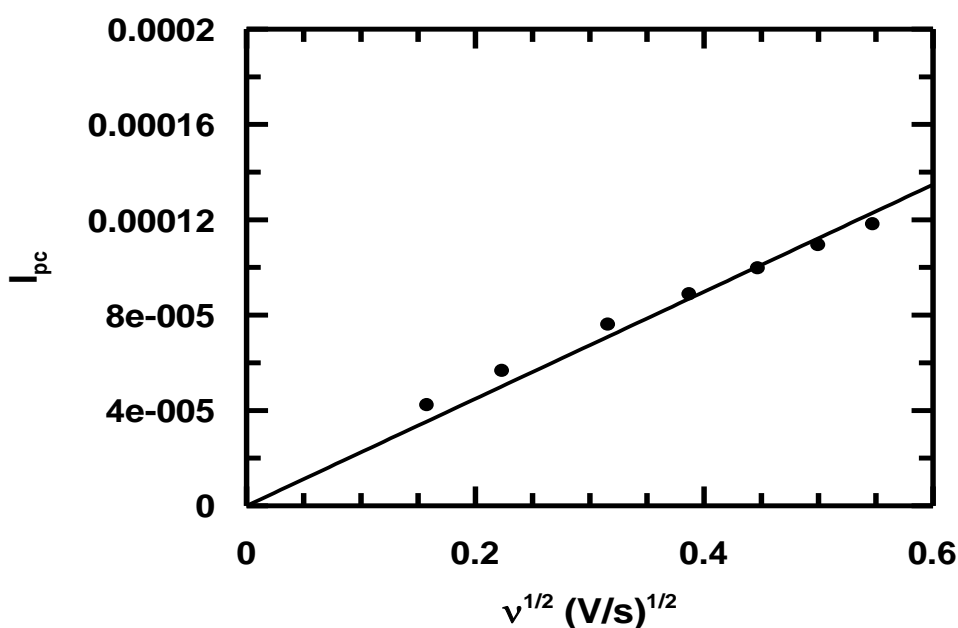


**Figure 7:** Cyclic voltammogram of 1 mM Onidazole showing a single step one electron reduction in aqueous - 20% methanol solution ( $0.12 \text{ M}$  KCl as electrolyte) on a glassy carbon electrode; Scan rate:  $100 \text{ mV/sec}$ .

Voltammograms for reduction of the nitro group in the complex was obtained at other scan rates as well.  $I_{pc}$  was plotted against square root of scan rate using Randles-Sevcik equation (Chapter: Experimental Eq. 4) [Figure 9]. A straight line passing through the origin suggests the complex undergoes reduction in a diffusion-controlled pathway and that there is no adsorption on the electrode surface.

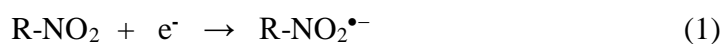


**Figure 8:** Cyclic voltammograms of 1 mM  $[Zn(Onz)_2Cl_2]$  in (A) 0.12 M tetrabutyl ammonium bromide in methanol and (B) in 0.12 M KCl in an aqueous solution on a glassy carbon electrode; Scan rate being 100mV/sec.



**Figure 9:** Dependence of cathodic peak current on square root of scan rate for the reduction of  $[\text{Zn}(\text{Onz})_2\text{Cl}_2]$  in aqueous solution.

In aprotic media, 5-nitroimidazoles undergo reversible one-electron reduction to form nitro radical anion ( $-\text{NO}_2^{\bullet-}$ ) (*Chapter: Experimental* Eq. 1). This is then followed by three-electron reduction to hydroxylamine derivatives (*Chapter: Experimental* Eq. 2). For most 5-nitroimidazoles the first step is reversible while the second is not, which is established with studies on metronidazole [17]. In aqueous solution, the two steps are not realized separately and a single step four electron reduction is observed (*Chapter: Experimental* Eq. 3) [17, 24].



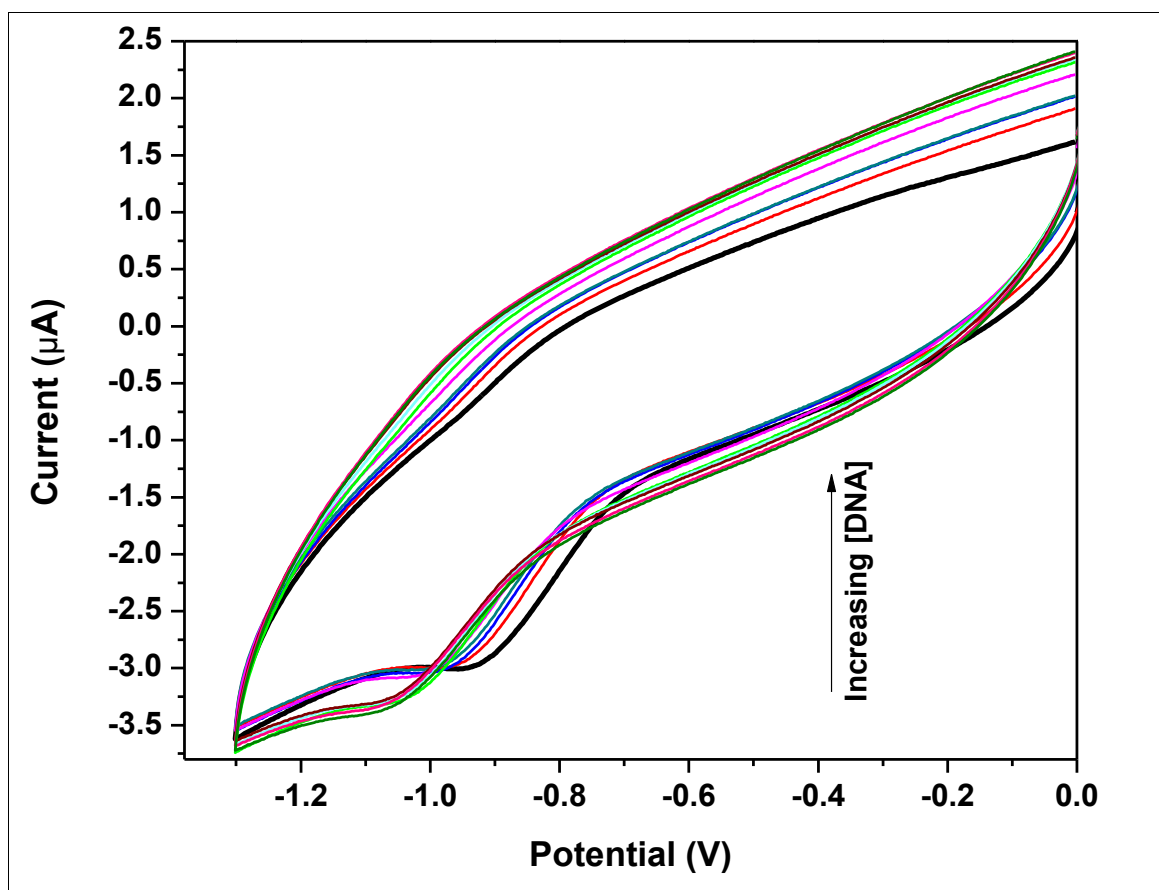


**Figure 10:** Cyclic voltammograms for  $\text{Zn}(\text{Onz})_2\text{Cl}_2$  in the absence (dark black line) and presence of different concentrations of calf thymus DNA,  $[\text{Zn}(\text{Onz})_2\text{Cl}_2] = 100 \mu\text{M}$ ;  $[\text{NaCl}] = 120 \text{ mM}$ ;  $\text{pH} = 7.4$ ;  $T = 301 \text{ K}$ .

### Binding of the complex to DNA

$\text{Zn}(\text{Onz})_2\text{Cl}_2$  was titrated with calf thymus DNA under physiological conditions using cyclic voltammetry. The reduction peak of the complex identified at  $-0.925 \text{ V}$  (against  $\text{Ag}/\text{AgCl}$ , satd.  $\text{KCl}$ ) was used to follow the titration. Upon addition of calf thymus DNA, the cathodic peak current ( $I_{pc}$ ) decreased gradually with shift to more negative potential (Figure 10). The shift to more negative potential is an indication of interaction between the complex and DNA and that as more and more DNA is added it becomes increasingly difficult for the complex to show a response in cyclic voltammetry as it progressively gets bound to DNA [18].

As already mentioned, binding of the complex to DNA results in redox active nitro groups on both Onz ligands to gradually lose their ability to show a response in cyclic voltammetry. Hence, gradual decrease in peak current maybe used as a measure of the extent of interaction between the complex and calf thymus DNA. Apparent binding constant values ( $K_{app}$ ) were evaluated from a double reciprocal linear plot (Chapter: Experimental Eq. 6) and also from non-linear square fit analysis (Chapter: Experimental Eq. 8) Results are shown in Figure 11 and Table 4 [10-12, 19-22].

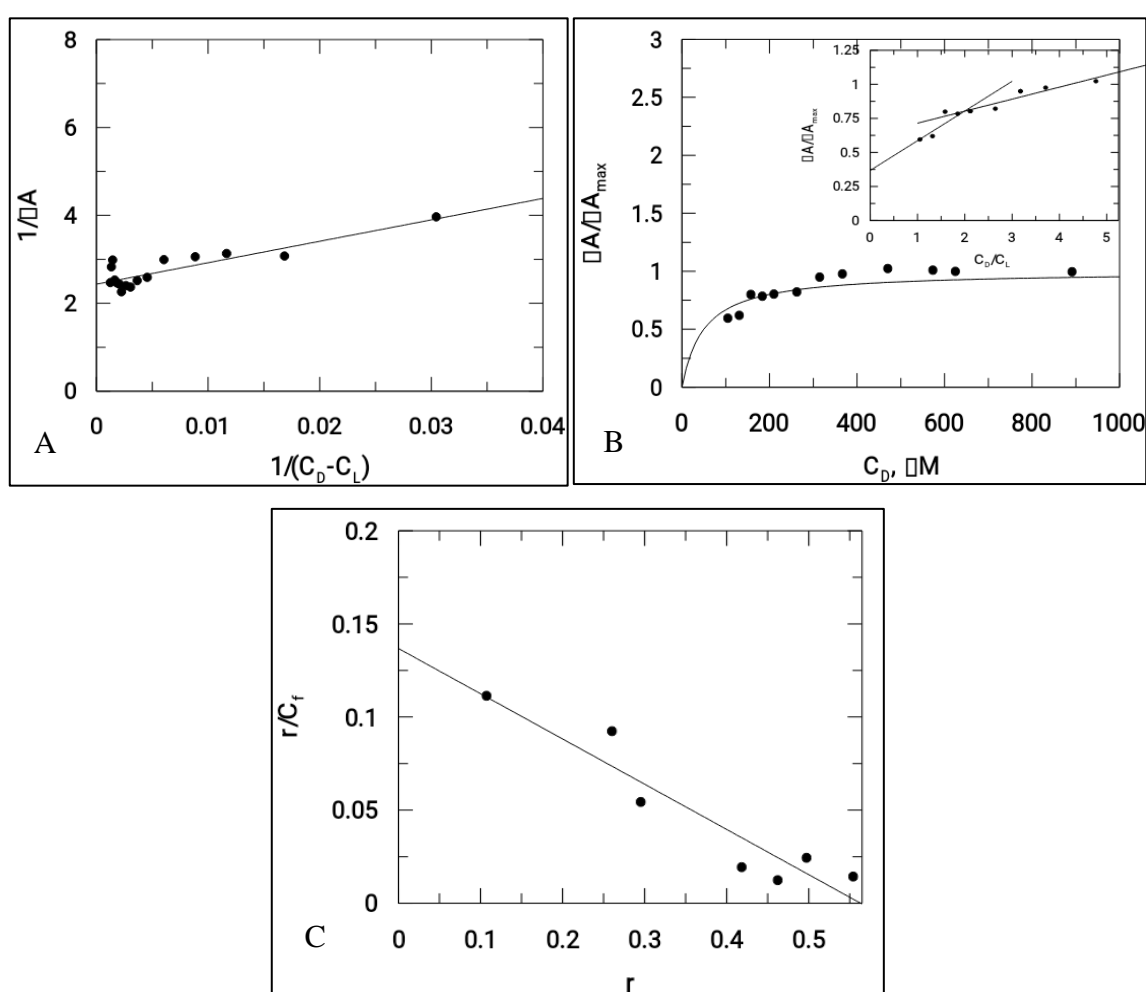


**Figure 11:** Interaction of calf thymus DNA with Zn(Onz)<sub>2</sub>Cl<sub>2</sub>; (A) double reciprocal plot, (B) non-linear plot, (C) Scatchard, [Zn(Onz)<sub>2</sub>Cl<sub>2</sub>]= 100  $\mu M$ ; [NaCl] = 120 mM; pH= 7.4; Temp. = 28°C.

An important parameter for binding to DNA is the site size of interaction ( $n_b$ ). It provides an estimate of the number of nucleotides bound to Zn(Onz)<sub>2</sub>Cl<sub>2</sub> during interaction with DNA. In

this case the value was 2 from the mole ratio plot (inset of Figure 11B). Since  $K_{app}$  provides the binding constant value of a substance binding to an isolated site, overall binding constant ( $K^*$ ) was obtained by multiplying  $K_{app}$  with site size of interaction ( $n_b$ ) [25]. These are provided in Table 4. Binding constant values for  $Zn(Onz)_2Cl_2$  were higher than Onz (determined earlier) [10], indicating this is an attribute of complex formation. Site size of interaction ( $n_b$ ) of Onz (reported earlier) [10] was in the range 1.39 to 1.5, while that of the monomeric  $Zn^{II}$  complex was found in the range from 1.85 to 2 (from two different methods of analysis) suggesting that the complex having two Onz ligands bound to  $Zn^{II}$  might be involved in two types of interactions with DNA. In one, it interacts in the same manner as Onz when present alone i.e. when one of the two Onz ligands bound to  $Zn^{II}$  in the complex interact with DNA. In the other mode, both Onz ligands bound to  $Zn^{II}$  interact with DNA. Hence, the value obtained for site size of interaction during experiment was intermediate between these two values. While inset of Figure 11B (mole ratio plot) provide a value of 2.0, Figure 11C (from modified Scatchard plot) provides a value of 1.85 This may be explained as that obtained between the values 1.5 (if one Onz interacts with DNA) and 3.0 (if both Onz interact), based on our earlier findings with Onz when present alone [10].

**Table 4: Binding constant values for the interaction of the complex with calf thymus DNA**

Compound	Apparent binding constants $K_{app} \times 10^{-4} (M^{-1})$			Site size ( $n_b$ ) from mole ratio plot	Overall binding constant ( $K' \times 10^{-4} (M^{-1})$ ) $K' = K_{app} \times n_b$			Overall binding constant $K' \times 10^{-4} (M^{-1})$ From Scatchard plot	Site size ( $n_b$ ) from Scatchard plot
	From double reciprocal plot	From non linear – fit	From double reciprocal plot with intercept = 1		Using $K_{app}$ from double reciprocal plot	Using $K_{app}$ from non linear – fit	Using $K_{app}$ from double reciprocal plot with y-intercept = 1		
Onz <sup>10</sup>	1.71	1.46	-	1.5	2.47	2.11	-	2.77	1.39
$Zn(Onz)_2Cl_2$	4.85	2.07	2.33	2.0	9.34	3.98	4.49	23.50	1.85

## Enzyme assay

Xanthine oxidase catalyzes the oxidation of hypoxanthine to xanthine and then to uric acid in the presence of oxygen. Under anaerobic conditions, there action does not occur since there is no substrate to accept the electrons. Therefore, under anaerobic conditions (i. e. when no oxygen is present) if an electron acceptor molecule is present in the system, the above oxidation of hypoxanthine to xanthine and to uric acid becomes possible. Nitroimidazoles being good electron acceptors participate in the above reaction forming nitro radical anions, thus enabling one to realize, using this enzyme assay the ability of 5-nitroimidazoles and their modified forms to get reduced and whether the nitro-radical anion that is generated is stable for some time to enable a change in absorbance of the original compound, recorded as a gradual decrease in absorbance. On the contrary, if the generated nitro-radical anion is not stable for long and can revert back to its original form by any pathway, it implies a decrease in its formation which could either be due to almost no decrease in absorbance of the original compound or that the decrease is considerably less than a compound where reduction leads to formation of a stable nitro-radical anion. Here, xanthine oxidase acts as a nitro-reductase that reduces the nitro group; hypoxanthine being the source of electron. In a previous study, we reported that formation of nitro radical anion by a  $\text{Cu}^{\text{II}}$  complex of ornidazole was significantly less than Onz followed by UV-Vis spectroscopy [11]. In this study, we tried to identify the amount of nitro radical anion formed by a  $\text{Zn}^{\text{II}}$  complex of Onz and how it compares with that of Onz. Since the enzyme assay reduces the nitro group, such reduction causes a change in absorption spectra. Continuous decrease in absorption of a compound during assay indicates that the nitro group is reduced which leads to the destruction of the chromophore. While a gradual decrease in absorbance was observed for Onz (Figure 12A), for the complex, there was no significant decrease (Figure 12B) indicating formation of the nitro radical anion on Onz is substantially controlled when bound to  $\text{Zn}^{\text{II}}$  in the complex.

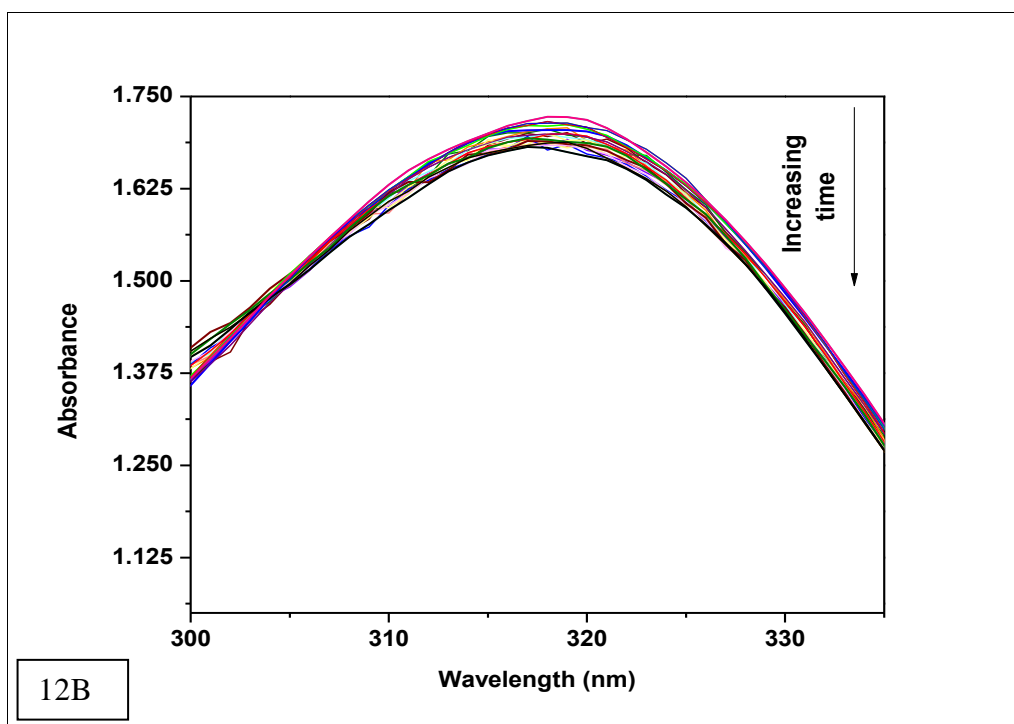
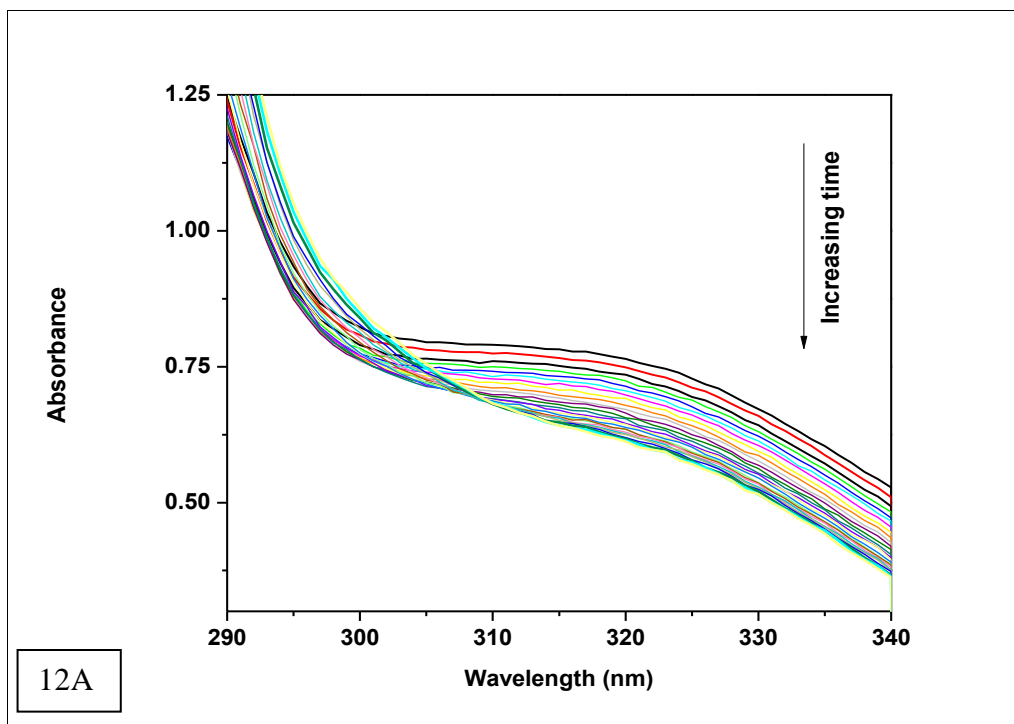


**Figure 12:** UV-Vis spectra of Onz (A) and  $Zn(Onz)_2Cl_2$  (B) in presence of hypoxanthine in 5% DMF and xanthine oxidase. Spectra of each compound were taken at an interval of 5 minutes for 2 hours. Enzyme activity = 0.2 units/mL in XOD and compound concentration = 80  $\mu$ M.

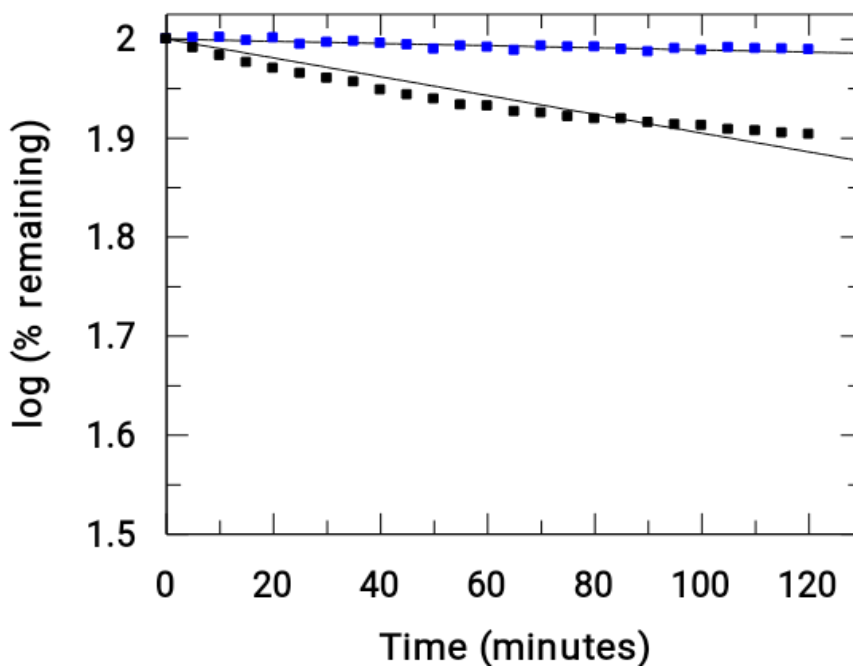


**Figure 13:** Comparison of the rate of reduction of Onz (■) and  $[\text{Zn}(\text{Onz})_2\text{Cl}_2]$  (■) under anaerobic conditions. (Initial concentrations =  $0.2 \text{ U mL}^{-1}$  in XOD,  $80 \text{ }\mu\text{M}$  in Onzor  $\text{Zn}(\text{Onz})_2\text{Cl}_2$  in the mixture,  $4 \text{ mM}$  in hypoxanthine and  $5\%$  in DMF).

Figure 13 denotes the amount of Onz and complex remaining upon a completion of the assay. Controlled formation of  $-\text{NO}_2^-$  following complex formation between Onz and  $\text{Zn}^{\text{II}}$  is important, for it prevents too much generation of  $-\text{NO}_2^-$ . While on the one hand, this is beneficial since it would make the complex less neurotoxic even on prolonged use, on the other, there is cause for concern, since formation of  $-\text{NO}_2^-$  is extremely important for drug action of the 5-nitroimidazole family and that its decrease might adversely affect efficacy by not being able to act on disease causing microbes with the efficiency shown by Onz, allowing pathogenic microbes to multiply faster than they are killed by a modified Onz like  $\text{Zn}(\text{Onz})_2\text{Cl}_2$ . Hence, it is essential to see the extent to which cytotoxicity is affected following complex formation of Onz with  $\text{Zn}^{\text{II}}$ . In order to check the performance of  $\text{Zn}(\text{Onz})_2\text{Cl}_2$  in comparison to Onz, both compounds were tried on *Entamoeba histolytica*.

### **Antiparasitic activity on *Entamoeba histolytica* (HM1: IMS Strain)**

Inhibition of cell viability of *Entamoeba histolytica* was followed by the trypan blue assay using different concentrations of Onz and  $\text{Zn}(\text{Onz})_2\text{Cl}_2$  for 24 hours and 48 hours respectively.<sup>35</sup> MIC values recorded after 24 hours for Onz and  $\text{Zn}(\text{Onz})_2\text{Cl}_2$  on *Entamoeba histolytica* were similar (12.5  $\mu\text{M}$ , Table 5). Upon increasing exposure time for each compound from 24 hours to 48 hours, the complex was found to be more cytotoxic with MIC value of 6.25  $\mu\text{M}$  while for Onz the value remained at 12.5  $\mu\text{M}$ . Therefore, the study clearly shows, that increasing exposure time has a positive effect for the complex that may be considered an advantage of complex formation. What is more important is that in spite of a decrease in formation of  $-\text{NO}_2^-$  following complex formation, efficacy is not affected as was thought earlier (speculating on the lines mechanism of action would suffer in the free radical pathway). So if we do not consider the data recorded at 48 hours and just compare that obtained after 24 hours, even then the complex seems to be better than Onz, having MIC values similar but with added benefits that it generates less  $-\text{NO}_2^-$ . This implies the complex is able to make up any compromise it has to make in the free radical pathway by other attributes of complex formation, one of which could be its strong binding to DNA that leads to cell death in disease causing microbes. Obviously, the other advantage of complex formation would be that it shows the complex to perform much better at longer exposure times (48 hours). This may be attributed to effective cellular uptake owing to the presence of a metal ion in the complex [26].

In an earlier study, we showed a  $\text{Cu}^{\text{II}}$  complex of an azo based ligand performed much better on a particular cell line than the ligand itself and that was essentially due to an effective cellular uptake of the complex (in that case of course the attributes required for a good performance of the complex were in fact similar to that of the compound (azo) forming the

metal complex suggesting an effective cellular uptake of the complex made the difference between them in their actions on the chosen cancer cell line) [26].

**Table 5: MIC values for Ornidazole and its monomeric Zn(II) complex when applied on**

*Entamoeba histolytica* (HM1:IMS strain)

Compound	MIC after 24 hrs	MIC after 48 hrs
Ornidazole	12.5 $\mu$ M	12.5 $\mu$ M
Zn(Onz) <sub>2</sub> Cl <sub>2</sub>	12.5 $\mu$ M	6.25 $\mu$ M
ZnCl <sub>2</sub>	>100 $\mu$ M	>100 $\mu$ M
DMSO	>100 $\mu$ M	>100 $\mu$ M

Likewise, for the Zn(Onz)<sub>2</sub>Cl<sub>2</sub> the fact that it performs better at longer exposure time (48 hours) could be that the complex enters cells of disease causing microbes better than Onz which allows it to be much more effective. The study also showed Onz and its Zn<sup>II</sup> complex diminished the viability of *Entamoeba Histolytica* in a concentration dependent manner.

Inspite of significant decrease in the formation of the nitro radical anion in the Zn(Onz)<sub>2</sub>Cl<sub>2</sub>, the study showed there was comparable biological activity of Onz and the monomeric Zn<sup>II</sup> complex on *Entamoeba histolytica* (HM1: IMS Strain) when incubated for 24 hours. At 48 hours incubation the complex performed better than Onz. This indicates either the nitro radical anion generated by the complex is sufficient for bringing about cytotoxic activity on the chosen biological target or if a compromise is made by the complex with regard to cytotoxic activity following a decrease in nitro-radical anion formation, the complex makes up such decrease in efficacy in the free radical pathway by other attributes of complex formation. As a consequence, the association of Zn<sup>II</sup> with Onz is useful for it not only maintains the efficacy of Onz but by decreasing nitro radical anion it helps to overcome the associated neurotoxic side effects of Onz upon prolonged use.

## References

1. Y. Miyamoto, J. Kalisiak , K. Korthals,T. Lauwaet, D Y Cheung, R Lozano, E. R. Cobo,P. Upcroft, J. A. Upcroft,D. E. Berg, F. D. Gillin, V. V. Fokin, K. B Sharpless, L. Eckmanna, *Proc. Natl. Acad. Sci. USA*, **2013**, 110, 17564-17569.
2. W Raether, H. Hänel, *Parasit. Res.*, **2003**, 90, S19-S39.
3. M. Van den Kerkhof, D Mabile, E Chatelain, C E Mowbray, S Braillard,S Hendrickx, L. Maes , G. Caljon, *Int J. Parasit: Drugs and Drug Resist.*, **2018**, 8 , 81-86.
4. E. F. F. da Cunha; T. C. Ramalho; D. T. Mancini; E. M. B. Fonseca; A. A. Oliveira, *J. Braz. Chem. Soc.*, **2010**, 21, <http://dx.doi.org/10.1590/S0103-50532010001000002>.
5. J. M. Brown , *Can. Res.*, **1999**, 59, 5863-5870.
6. P. Wardman , *Br J Radiol.*, **2019**, 92, 20170915, doi: 10.1259/bjr.20170915.
7. M. Bonnet, C. R. Hong ,W. W. Wong , L. P. Liew , A. Shome , J Wang, Y. Gu , R J Stevenson , W. Qi , R. F Anderson .,M. P. Hay , *J Med Chem.* **2018**, 61, 1241-1254. doi: 10.1021/acs.jmedchem.7b01678.
8. P. De, D. Bhattacharyya, K. Roy, *Struct. Chem.*, **2020**, doi:10.1007/s11224-019-01481-z
9. a) S. Sood , A. Kapil , *Ind. J Sex Transm Dis* **2008**, 29:7-14; b) V. Puri *Neurology India*, **2011**, 59:4-5.
10. R. C. Santra, D. Ganguly, J. Singh, K. Mukhopadhyay, S. Das , *Dalton Trans.*, **2015**, 44, 1992-2000.
11. R. C. Santra, D. Ganguly, S. Jana, N. Banyal, J. Singh, A. Saha, S. Chattopadhyay, K. Mukhopadhyay, S. Das , *New J. Chem.*, **2017**, 41, 4879-4886. DOI: 10.1039/C7NJ00261K.
12. P. S Guin, P. C. Mandal, S. Das, *ChemPlusChem*, **2012**, 77, 361-369; <https://doi.org/10.1002/cplu.201100046>.
13. P. S. Guin, P. C. Mandal, S. Das, *J. Coord. Chem.*, **2012**, 65, 705-721; [doi.org/10.1080/00958972.2012.659730](https://doi.org/10.1080/00958972.2012.659730).

14. B. Mandal, S. Singha, S K Dey, S. Mazumdar, T K Mondal, P, Karmakar, S. Kumar, S. Das, *RSC Adv.*, **2016**, 6, 51520-51532.
15. B. Mandal, S, Singha, S K, Dey, S. Mazumdar, S. Kumar, P. Karmakar, S. Das, , *RSC Adv.*, **2017**, 7, 41403-41418.
16. F. Ahmadi, N. Shabrandi, L. Hosseinzadeh, H. Azizian, *Nucleosides Nucleotides Nucleic Acids*. **2019**, 38, 449-480; doi: 10.1080/15257770.2018.1562073.
17. P. C. Mandal, *J. Electroanal. Chem.* **2004**, 570, 55-61.
18. A. J. Bard, L. R. Faulkner, *Electrochemical Methods Fundamental and Applications*, John Wiley & Sons, Inc. New York, **2001**.
19. R C Santra, K Sengupta, R Dey, T Shireen , P Das , P S Guin, K Mukhopadhyay, S Das S, *J. Coord. Chem.*, **2014**, 67, 265-285; DOI:10.1080/00958972.2013.879647.
20. P. S. Guin , S. Das, *Int. J. Electrochem.*, **2014**, Article ID 517371, 8 pages; <https://doi.org/10.1155/2014/517371>.
21. X. Jiang, X, Lin, *Bioelectrochem.* **2006**, 68, 206-212.
22. T. Deb, D. Choudhury, P. S. Guin, M. B. Saha ,G. Chakrabarti, S. Das, *Chem-Biol. Inter.*, **2011**, 189, 206-214.
  
23. K. Nakamoto, *Theory and Applications in Inorganic Chemistry*, 6th Edition Wiley-Interscience, New York, **2009**.
24. J. A. Squella, S. Bollo, L. J. Núñez-Vergara, *Curr. Org. Chem.*, **2005**, 9, 565-581.
25. F. Frezard, A. Garnier-Suillerot, *Biochim. Biophys. Acta*, **1990**, 1036, 121-127.
26. T. Deb, P.K Gopal, D. Ganguly, P. Das, M. Paul, M. B. Saha, S. Paul, S. Das, *RSC Adv.*, **2014**, 4, 18419-18430.

## **Chapter 8**

**A monomeric complex of  $\text{Cu}^{\text{II}}$  with Ornidazole forms significantly less nitro radical anion but was still found active on *Entamoebahistolytica* like Ornidazole**

## Introduction

Different 5-nitrimidazoles besides being effective anti-microbial agents and reasonably good radiosensitizers in cancer treatment, have associated adverse drug reactions like neurotoxic side effects and the aspect of drug resistance [1-8]. These two facts point at issues requiring immediate intervention [1-4]. Metronidazole (Mnz), tinidazole (Tnz) and ornidazole (Onz) are three important molecules of this family that have made their way to the clinics and are used in a good number of pharmaceutical preparations. Their efficacy is attributed to generation of  $\text{-NO}_2^-$  when they are reduced in presence of pyruvate ferredoxinoxidoreductase (PFOR), acting as an electron sink [1-10]. Reduction of the nitro group in such molecules prepares them for entry into cells by passive diffusion by creating a favorable concentration gradient [9, 10]. Once inside the cell, anti-microbial toxicity of 5-nitroimidazoles is dependent on the reduction of the nitro moiety to  $\text{NO}_2^-$  and other active species (nitroso and hydroxylamine derivatives). Besides, such radical formation, in order to tackle infections caused by parasites the  $\text{-NO}_2^-$  binds to DNA disrupting or breaking strands and is therefore a cause for cell death [9, 10]. As radiosensitizers these molecules, interact with various radicals that are formed on DNA following interaction of the latter with products of the radiolysis of water, forming  $\text{-NO}_2^-$  which thereafter enhance strand unwinding through disruption of hydrogen bonds or initiating strand breaks [6-8].

It is really unfortunate that the same  $\text{-NO}_2^-$  that is useful as an antimicrobial agent or as a radiosensitizer is associated with neurotoxic side effects, particularly upon prolonged use such molecules [7-10]. Such aspects of neurotoxicity or other forms of toxic side effects can however be checked if we are able to control the generation of  $\text{-NO}_2^-$ . Like many other known examples, too much generation of reactive intermediate besides doing good, does a lot of harm as well. Hence, either generating the correct amount or making it available at the site

of requirement through slow chemical release is the need of the hour forming an important aspect that can be pursued through research [7-10]. This study reports an effort aimed at regulating the formation of the nitro radical anion ( $-\text{NO}_2^{\cdot-}$ ) on Onz through complex formation with Cu(II). However, as mentioned earlier,  $-\text{NO}_2^{\cdot-}$  being important for antimicrobial action, following its decrease due to complex formation, there is the possibility that antimicrobial action might get affected. Whether that is really the case or that the complex is a better antimicrobial agent, was realized by conducting a study that seeks to find the action of Onz and its Cu(II) complex on Axenic *Entamoeba histolytica*.

## **Results and Discussions**

### **Crystal structure from single crystal X-ray diffraction data**

Single-crystal X-ray diffraction reveals that the complex of  $\text{Cu}^{\text{II}}$  with ornidazole got crystallized in an orthorhombic crystal system with *Pnma* space group. The asymmetric unit of the complex consists of one crystallographic independent  $\text{Cu}^{\text{II}}$  ion with half occupancy, ornidazole ligand, two coordinated chloride ions with half occupancy and a lattice water molecule (Figure 1). The  $\text{Cu}^{\text{II}}$  ion is four coordinated by two chloride ions and two nitrogen atoms of two different ornidazole ligands to adopt a distorted square planar geometry (Figure 2).

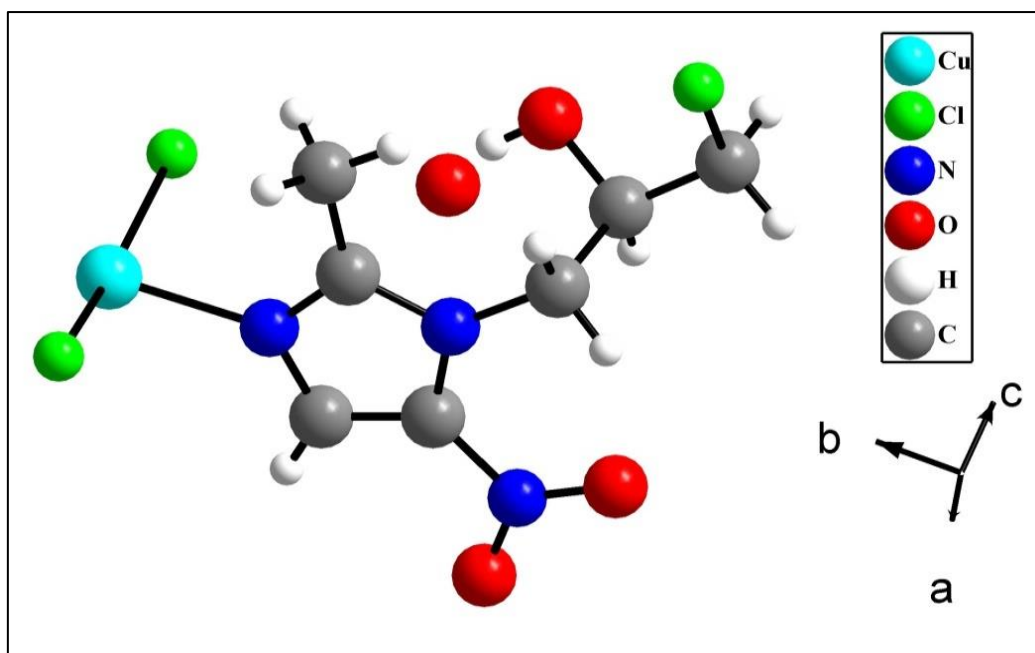


**Figure 1:**Figure shows the asymmetric unit of  $[\text{Cu}(\text{L})_2\text{Cl}_2]\cdot 2\text{H}_2\text{O}$  (L = ornidazole)

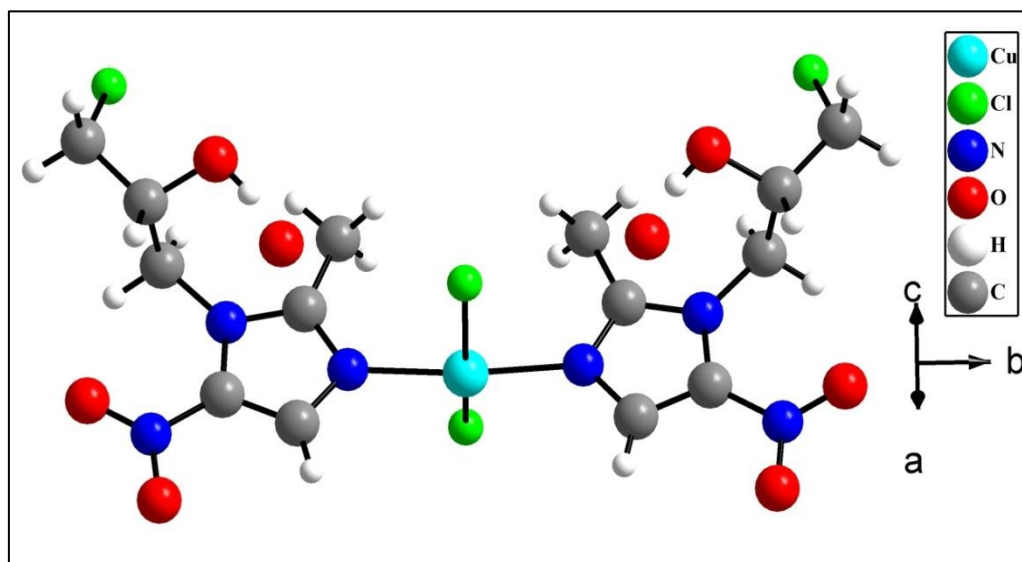


**Figure 2:** Figure shows the molecular structure of  $[\text{Cu}(\text{L})_2\text{Cl}_2]\cdot 2\text{H}_2\text{O}$  (L = ornidazole)

The details of the crystal and final refinement are given in Table 1.

**Table 1:** Crystal data and structure refinement parameters for [Cu(L)<sub>2</sub>Cl<sub>2</sub>].2H<sub>2</sub>O(L=ornidazole).

Empirical formula	C <sub>7</sub> H <sub>10</sub> Cl <sub>2</sub> Cu <sub>0.5</sub> N <sub>3</sub> O <sub>4</sub>
Formula weight	302.85
Crystal system	Orthorhombic
Space group	<i>Pnma</i>
a (Å)	7.200(6)
b (Å)	29.72(2)
c (Å)	11.962(10)
α (deg)	90
β (deg)	90
γ (deg)	90
Volume (Å <sup>3</sup> )	2560(4)
Z	8
T (K)	293(2)
ρ <sub>calc</sub> (mg m <sup>-3</sup> )	1.571
μ (mm <sup>-1</sup> )	1.319
θ range (deg)	2.669 to 27.106
λ (Mo Kα) (Å)	0.71073
R indices [I>2σ(I)], wR2	R <sub>1</sub> = 0.0534, wR <sub>2</sub> = 0.1286
R indices (all data), wR2	R <sub>1</sub> = 0.0762, wR <sub>2</sub> = 0.1443

$R_1 = \frac{\sum ||F_o| - |F_c||}{\sum |F_o|}$ ;  $wR_2 = \frac{\{\sum [w(F_o^2 - F_c^2)^2]\}}{\sum [w(F_o^2)^2]}^{1/2}$ .  $w = 1/[\sigma^2(F_o)^2 + (aP)^2 + bP]$ ,  
 $P = [\max.(F_o^2, 0) + 2(F_c^2)]/3$ , where  $a = 0.0576$  and  $b = 5.1877$

The Cu–N bonds have an average distance of 1.987 Å, and Cu–Cl bonds have an average length of 2.313 Å for the prepared complex. The Cl/N–Cu–N/Cl bond angles are in the range 89.49(11) –173.6°(2). The selected bond distances are given in Table 2 and selected bond angles are listed in Table 3.

**Table 2:** Selected bond distances (Å) observed in [Cu(L)<sub>2</sub>Cl<sub>2</sub>] $\cdot$ 2H<sub>2</sub>O (L = ornidazole).

Bond	Distances, Å
Cu(1)-N(1)	1.987(4)
Cu(1)-N(1)#1	1.987(4)
Cu(1)-Cl(2)	2.287(3)
Cu(1)-Cl(1)	2.339(2)

Symmetry transformations used to generate equivalent atoms: #1 x,-y+3/2,z

**Table 3:** Selected bond angles (°) observed in [Cu(L)<sub>2</sub>Cl<sub>2</sub>] $\cdot$ 2H<sub>2</sub>O (L = ornidazole)

Angle	Amplitude
N(1)-Cu(1)-N(1)#1	173.6(2)
N(1)-Cu(1)-Cl(2)	89.53(11)
N(1)#1-Cu(1)-Cl(2)	89.53(11)
N(1)-Cu(1)-Cl(1)	89.49(11)
N(1)#1-Cu(1)-Cl(1)	89.49(11)
Cl(2)-Cu(1)-Cl(1)	162.35(11)

## UV-Vis spectroscopy of Ornidazole and its Cu<sup>II</sup> complex in different solvents

Ornidazole and its monomeric Cu<sup>II</sup> complex were dissolved in different solvents like acetonitrile, methanol, DMF and water such that concentration of it in each solvent was 10<sup>-4</sup> M. Subsequently, their UV-Vis spectra were recorded. Ornidazole (Figure 3) and the complex (Figure 4) show their most prominent responses in the UV region from 310 nm to 324 nm (Table 4). Bands for the complex were similar to that of ornidazole and hence may be attributed to intra-ligand (IL) transitions of ligands. They are attributed to intra-ligand (IL) transitions.

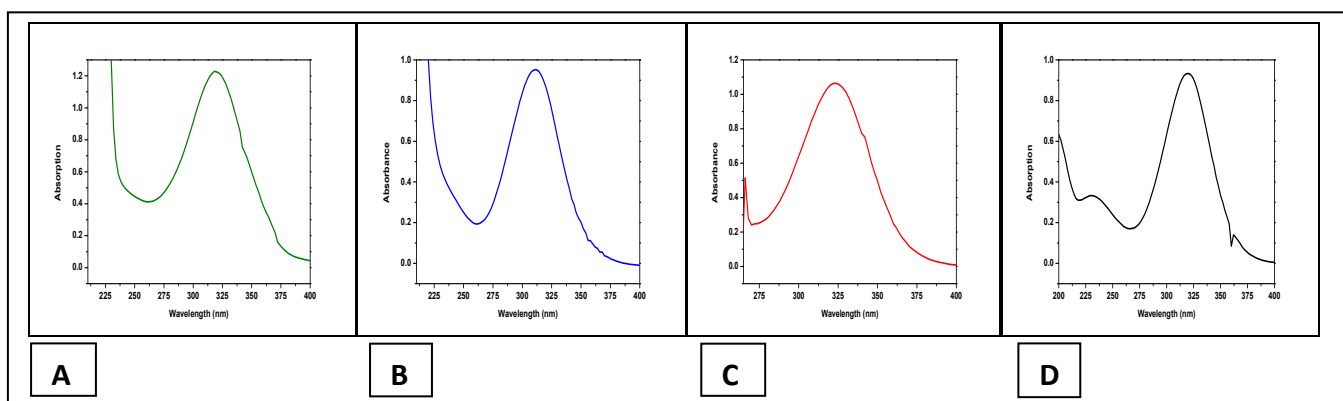


**Figure 3: UV-Vis spectra of Onz in A) water, B) methanol, C) DMF and D) acetonitrile**

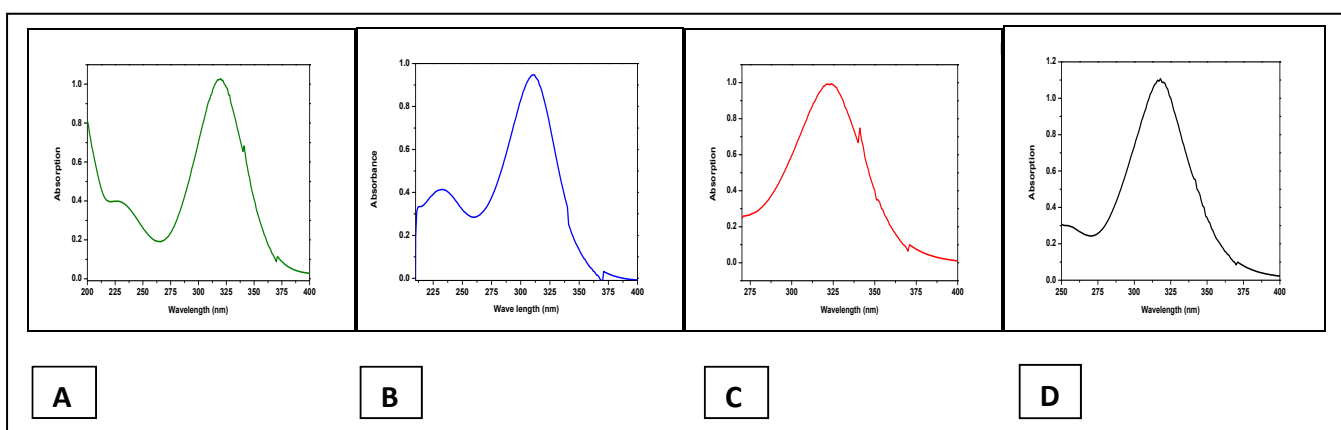


**Figure 4: UV-Vis spectra of [Cu(Onz)<sub>2</sub>Cl<sub>2</sub>] in A) water, B) methanol, C) DMF and D) acetonitrile**

**Table 4: Absorption of Ornidazole and Cu<sup>II</sup>-Ornidazole in different solvents**

Compound	Acetonitrile		DMF		Methanol		Water	
	$\lambda_{\max}$ (nm)	Absorption Intensity						
Onz	320	0.9335	324	1.0638	312	0.9519	318	1.2287
Cu(Onz) <sub>2</sub> (Cl) <sub>2</sub>	318	1.1080	324	0.9936	310	1.2231	320	1.0283

**Analysis of the IR spectra of Ornidazole and its monomeric Cu<sup>II</sup> complex**

IR spectrum of [Cu(Onz)<sub>2</sub>Cl<sub>2</sub>](Figure 5) showed slight shifts in all responses that were obtained earlier for Onz (Figure 4, Chapter 7) to higher frequencies [26]. For example, the peak at 1559.76 cm<sup>-1</sup> for  $\nu_{(C=N)}$  for the complex was obtained at 1538.21 cm<sup>-1</sup> for Onz indicating co-ordination with Cu<sup>II</sup> by an imidazole nitrogen [26]. NO<sub>2</sub> stretching frequencies  $\nu_{as} = 1478\text{cm}^{-1}$  and  $\nu_s = 1373\text{cm}^{-1}$  for [Cu(Onz)<sub>2</sub>Cl<sub>2</sub>] (Figure 5) were similar to  $\nu_{as} = 1471.57\text{cm}^{-1}$  and  $\nu_s = 1385.92\text{cm}^{-1}$  for Onz (Figure 4, Chapter 7). Splitting of NO<sub>2</sub> bands,  $\Delta\nu_{NO_2}$  was 105 cm<sup>-1</sup> for the complex while it was 86 cm<sup>-1</sup> for Onz clearly suggesting that the nitro group did not participate in a coordination of Cu<sup>II</sup>.

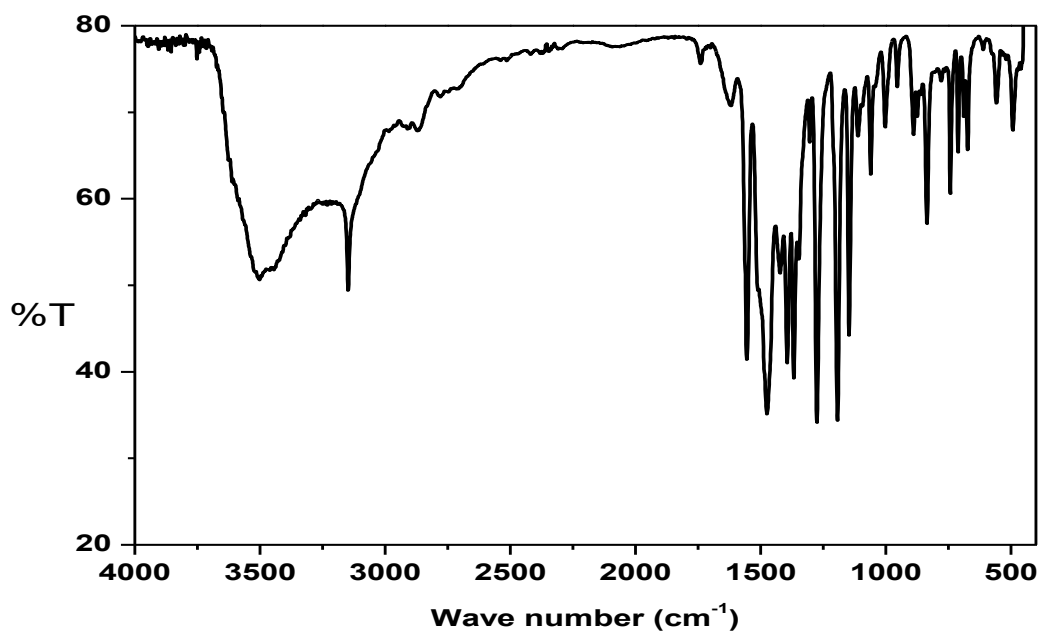


**Figure 5: IR spectrum of [Cu(Onz)<sub>2</sub>Cl<sub>2</sub>]**

---

### **Magnetic susceptibility measurement and EPR spectrum of [Cu(Onz)<sub>2</sub>Cl<sub>2</sub>]**

The effective magnetic moment was recorded at 273 K. It was found to be 1.32 BM, somewhat lower than the expected value for one unpaired electron in case of Cu(II)). Owing to close proximity of two coordination environments, there might be a case of spin pairing which got reflected in magnetic moment value of the Cu(II) centre, showing a significantly lower value than 1.73 BM.

EPR spectrum (Figure 6) recorded at room temperature showed X-band frequency of the powdered sample having a resonance signal at 318mT with a g value of 2.11.

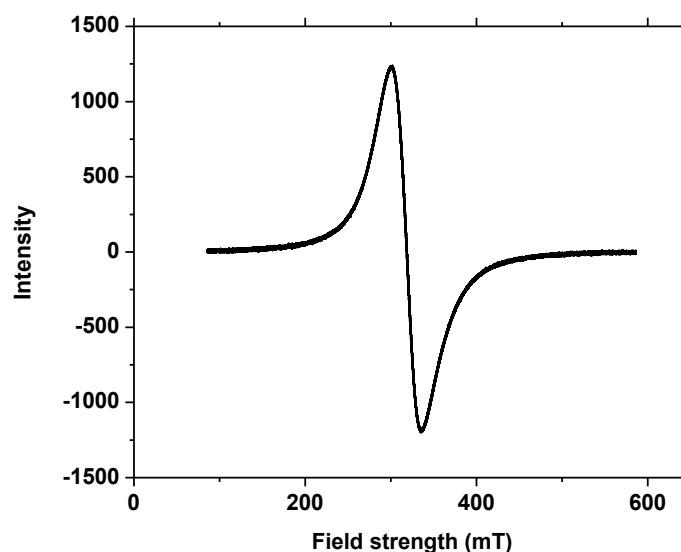


**Figure 6:** Room temperature EPR spectrum of  $[\text{Cu}(\text{Onz})_2\text{Cl}_2]$ ; resonance signal at 318mT, g value = 2.11

### Mass spectrum

Molecular ion peaks linked to an atom of sodium were detected in the vicinity of  $m/z = 600$ ; the two most prominent ones being at 600.88 and 602.88. Owing to the presence of Cu and Cl in the complex, isotope distributions were observed in different fragments recorded in the mass spectrum (Figure 7). Going by the molecular formula mentioned above and also determined from single crystal X ray diffraction data, molecular ion peaks (Na bound) were expected in the region of  $m/z$  from 594 to 604. From the molecular ion, if two Cl atoms (one from each ligand) departs then the species formed should have theoretical  $m/z$  values of 501.0 (both  $^{35}\text{Cl}$ ,  $^{63}\text{Cu}$ ) or 503.0 [(both  $^{35}\text{Cl}$ ,  $^{65}\text{Cu}$ ) or (one  $^{35}\text{Cl}$ , one  $^{37}\text{Cl}$ ,  $^{63}\text{Cu}$ )] or 505.0 [(one  $^{35}\text{Cl}$ , one  $^{37}\text{Cl}$ ,  $^{65}\text{Cu}$ ) or (both  $^{37}\text{Cl}$ ,  $^{63}\text{Cu}$ ) or 507.0 (both  $^{37}\text{Cl}$ ,  $^{65}\text{Cu}$ ). Experimental  $m/z$  values for this fragment were recorded at 500.98, 502.98, and 504.97 that explain isotope distributions mentioned above. Isotope distribution was also observed in the region  $m/z = 367.9662$  to  $m/z = 370.4658$  attributed to a fragment generated from the complex (i.e. molecular ion) following departure of two Cl atoms (one from each Onz), two -OH groups

(one from each Onz), two  $-\text{NO}_2$  groups (one from each Onz) and a  $-\text{CH}_3$  from any one Onz ligand.

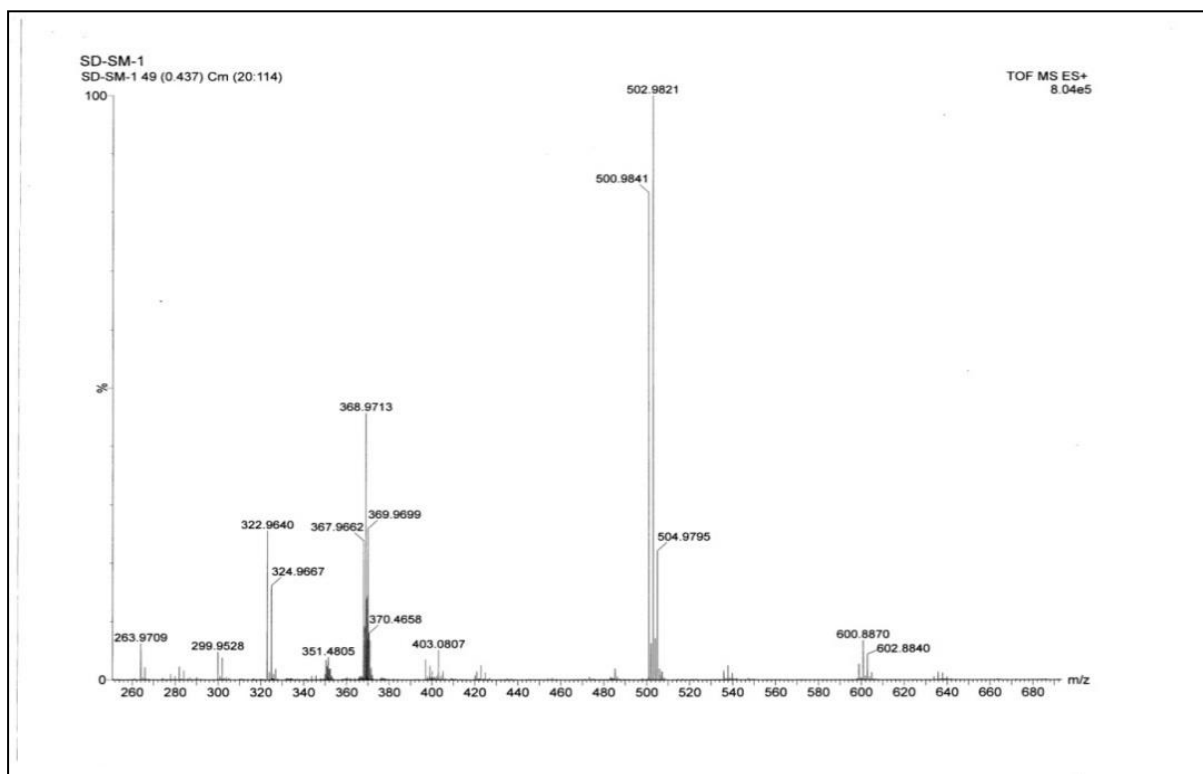
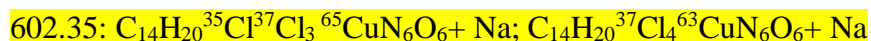
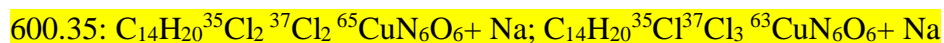
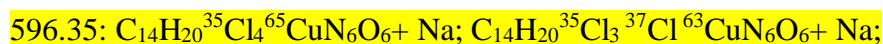
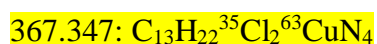


**Figure 7:** Mass spectrum of  $\text{Cu}(\text{Onz})_2\text{Cl}_2$

Expected molecular ion peaks bound to Na considering isotope distribution for Cu atom (isotopes of  $^{63}\text{Cu}$  &  $^{65}\text{Cu}$ ) and for four Cl atoms (isotopes of  $^{35}\text{Cl}$  &  $^{37}\text{Cl}$ ).



Isotope distribution for fragments detected in the region  $m/z = 367.9662$  to  $m/z = 370.4658$ .



369.347:  $C_{13}H_{22}^{35}Cl_2^{65}CuN_4$ ;  $C_{13}H_{22}^{35}Cl^{37}Cl^{63}CuN_4$

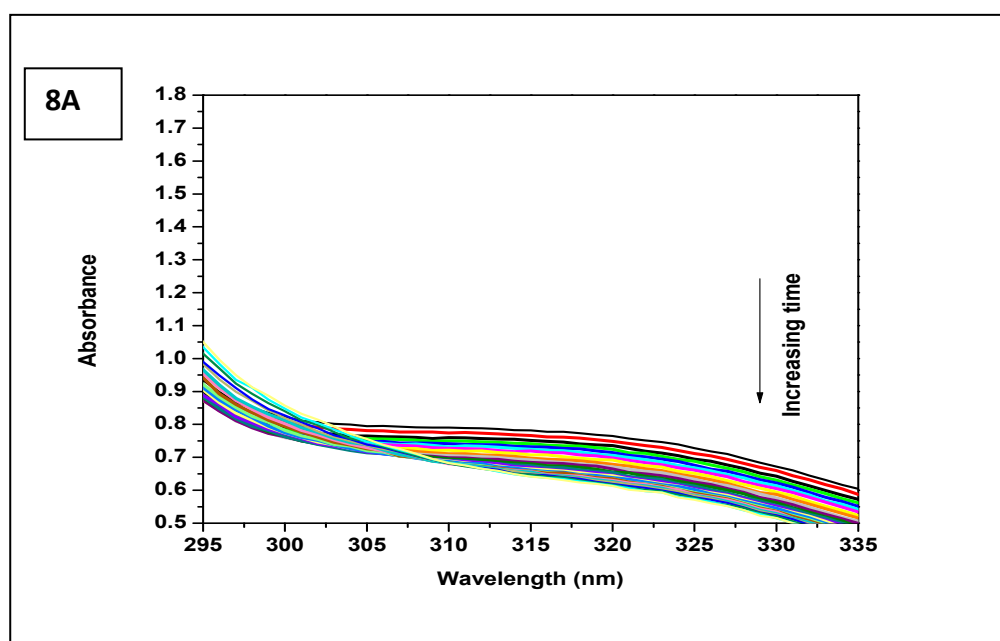
371.347:  $C_{13}H_{22}^{35}Cl^{37}Cl^{65}CuN_4$ ;  $C_{13}H_{22}^{37}Cl_2^{63}CuN_4$

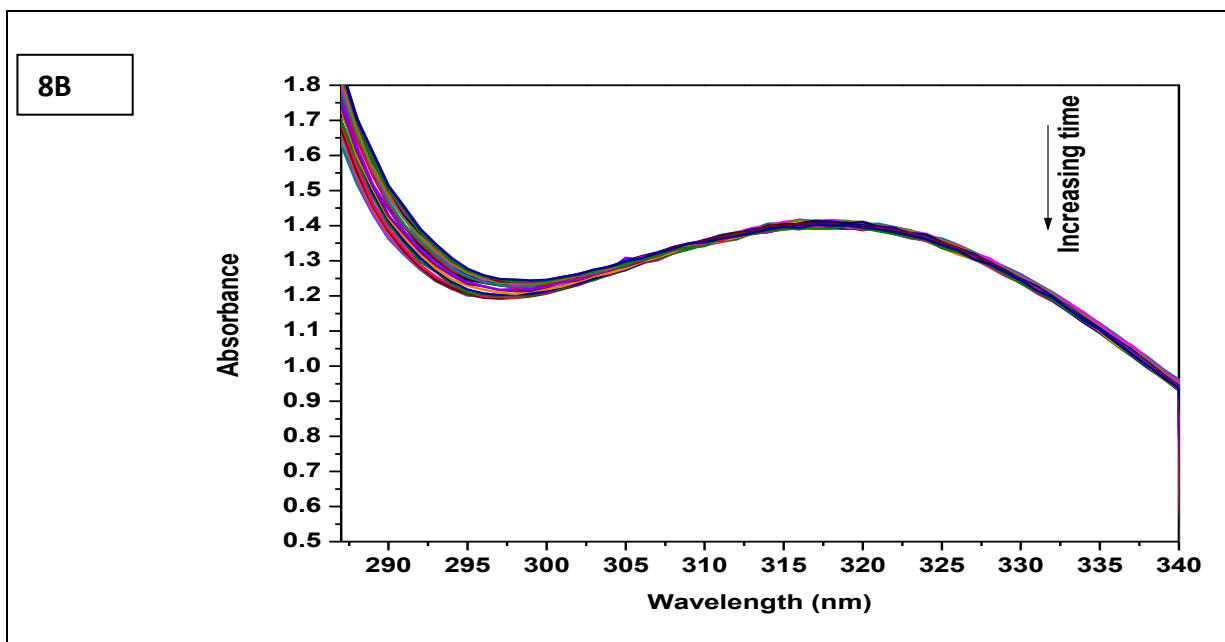
373.347:  $C_{13}H_{22}^{37}Cl_2^{65}CuN_4$

---

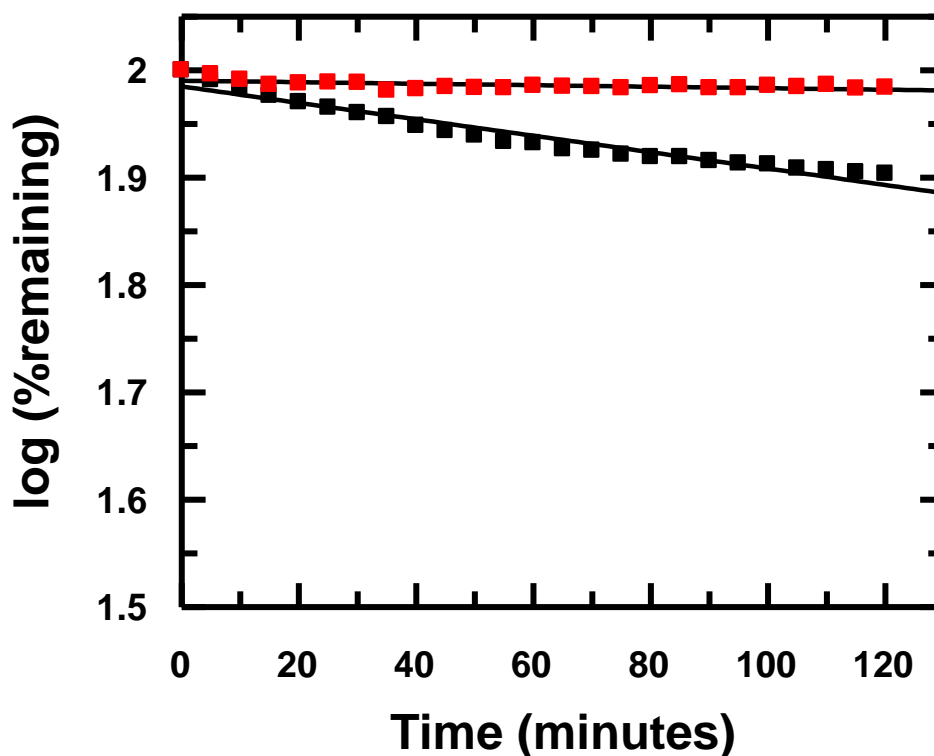
## Enzyme assay

Formation of nitro-radical anion due to ornidazole and its Cu(II) complex was determined following the procedure described in detail in *Chapter 6: Experimental, Section: Enzyme Assay*. In a previous study, it was reported that formation of nitro radical anion by Cu<sup>II</sup> complexes of 5-nitroimidazoles were significantly lower than the corresponding 5-nitroimidazole itself [10, 15]. Through this study, we tried to identify the amount of nitro radical anion formed by [Cu(Onz)<sub>2</sub>Cl<sub>2</sub>] and how it compares with that for Onz. Following reduction of the nitro group, there is a change in the absorption spectra. A continuous decrease in absorption during assay indicates that the nitro group is reduced leading to a destruction of the chromophore that gets manifested spectroscopically. While a gradual decrease in absorbance was observed for Onz (Fig. 8A), for the complex no significant decrease was recorded (Fig. 8B) indicating that formation of nitro radical anion on Onz is substantially controlled when it is bound to Cu<sup>II</sup> in the complex.





**Figure 8:** UV-Vis spectra of Onz (A) and  $[\text{Cu}(\text{Onz})_2\text{Cl}_2]$  (B) in the presence of xanthine oxidase and hypoxanthine in 5% DMF medium. Each spectrum was taken at 5 minutes interval for 2 hours. Enzyme activity = 0.2 units/mL in XOD and complex concentration = 80  $\mu\text{M}$ .



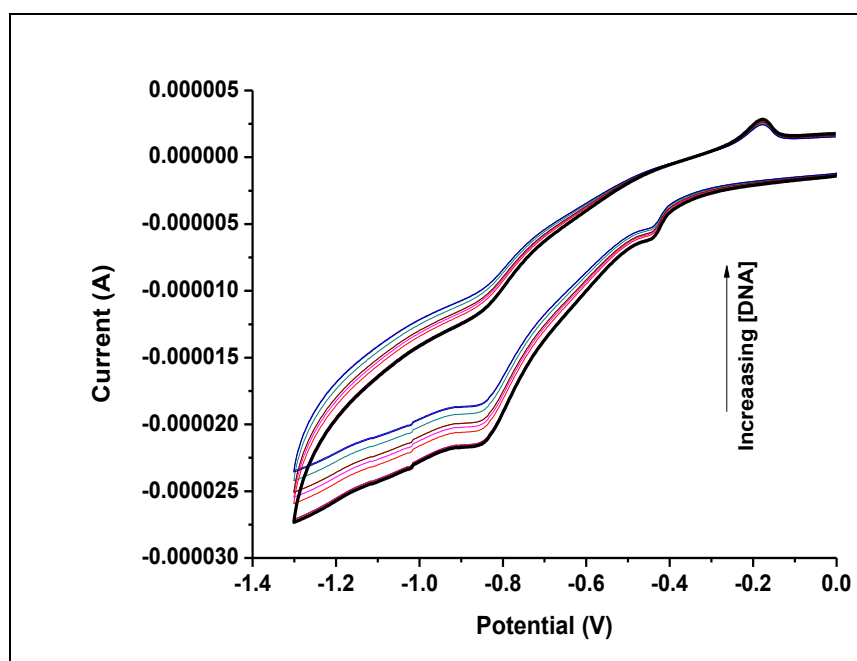
**Figure 9:** Comparison of the rate of reduction of Onz (■) with [Cu(Onz)<sub>2</sub>Cl<sub>2</sub>] (■) under anaerobic conditions. (Initial concentrations = 0.2 U mL<sup>-1</sup> in XOD, 80 μM in Onz or [Cu(Onz)<sub>2</sub>Cl<sub>2</sub>] in the mixture, 4 mM in hypoxanthine and 5% in DMF).

Figure 9 denotes the amount of Onz and complex remaining upon completion of the assay. Controlled formation of NO<sub>2</sub><sup>•-</sup> following complex formation is important for it prevents too much generation of NO<sub>2</sub><sup>•-</sup>. While on the one hand, this is beneficial since it would make the complex less neurotoxic even on prolonged use, on the other, there is some concern, since formation of -NO<sub>2</sub><sup>•-</sup> is important for drugs of the 5-nitroimidazole family to function properly; its decrease could adversely affect efficacy by not being able to act efficiently on disease causing microbes with the speed reported for Onz, allowing pathogenic microbes to multiply faster than the killing efficacy of a modified form of Onz [in this case Cu(Onz)<sub>2</sub>Cl<sub>2</sub>]. Hence, it is essential to see the extent to which cytotoxicity gets affected following complex

formation of Onz with  $\text{Cu}^{\text{II}}$ . To check the performance of  $\text{Cu}(\text{Onz})_2\text{Cl}_2$  in comparison to Onz, both compounds were tried on *Entamoeba histolytica* strain.

### Binding of the complex to DNA

$\text{Cu}(\text{Onz})_2\text{Cl}_2$  was titrated with calf thymus DNA under physiological conditions using cyclic voltammetry. A reduction peak for the complex was identified at  $-0.849\text{V}$  (against  $\text{Ag}/\text{AgCl}$ , satd.  $\text{KCl}$ ). This was subsequently used to follow the interaction of the complex with DNA. Upon addition of calf thymus DNA, cathodic peak current ( $I_{\text{pc}}$ ) gradually decreased (Figure 10) [22].



**Figure 10:** Cyclic voltammograms for  $\text{Cu}(\text{Onz})_2\text{Cl}_2$  in the absence (dark black line) and presence of different concentrations of calf thymus DNA,  $[\text{Cu}(\text{Onz})_2\text{Cl}_2] = 100 \mu\text{M}$ ;  $[\text{NaCl}] = 120 \text{ mM}$ ;  $\text{pH} = 7.4$ ;  $T = 27 \text{ K}$ .

Binding of the complex to DNA probably results in the redox active nitro group on both Onz ligands to gradually lose their ability to show a response in cyclic voltammetry which was actually used to monitor the interaction. Gradual decrease in peak current was used as a measure of the extent of interaction between the complex and calf thymus DNA. Apparent

binding constant values ( $K_{app}$ ) were evaluated from a double-reciprocal linear plot (Eq. 6, Chapter Experimental) and also from non-linear square fit analysis (Eq. 8, Chapter Experimental) [10, 15, 24-28]. Results are shown in Fig. 11, Table 5.

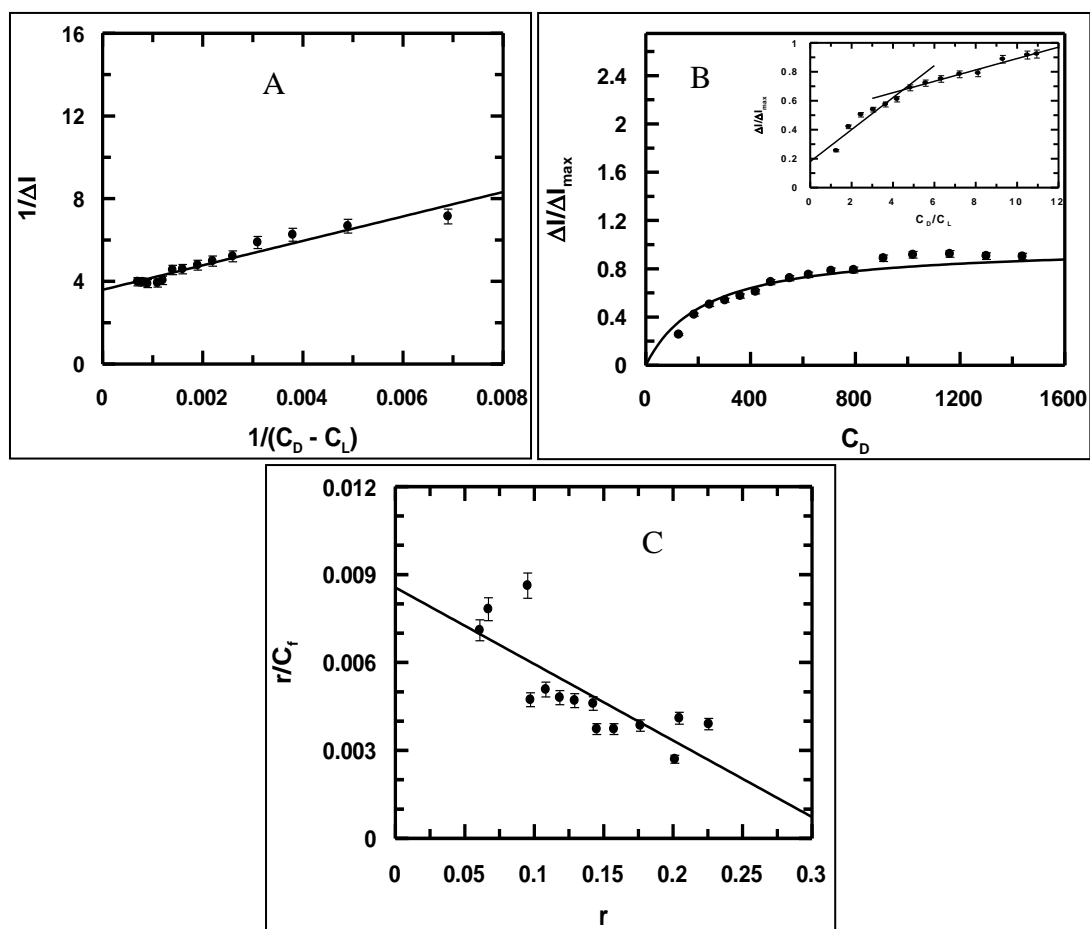


Figure 12: Interaction of calf thymus DNA with  $\text{Cu}(\text{Onz})_2\text{Cl}_2$ ; (A) double reciprocal plot, (B) non-linear square-fit analysis, (C) modified Scatchard plot;  $[\text{Cu}(\text{Onz})_2\text{Cl}_2] = 100 \mu\text{M}$ ;  $[\text{NaCl}] = 120 \text{ mM}$ ;  $\text{pH} = 7.4$ ;  $\text{Temp.} = 300\text{K}$ .

Another important parameter for such interactions is site size ( $n_b$ ) since it provides an estimate of the number of nucleotides bound to a binding agent during interaction with DNA. This value was 3.5 from the mole ratio plot (inset of Fig. 11B). Since  $K_{app}$  provides binding constant of a substance binding to an isolated site, overall binding constant ( $K^*$ ) was obtained by multiplying  $K_{app}$  with site size of interaction ( $n_b$ ) [32]. The values are provided in Table 5.

Binding constant values for Cu(Onz)<sub>2</sub>Cl<sub>2</sub> were comparable to that determined earlier for Onz. Site size of interaction (n<sub>b</sub>) of Onz (discussed in *Chapter 7* and now shown again as part of Table 5) was in the range 1.39 to 1.5, while that for the complex was found between 3 and 4 (from two different modes of analysis) suggesting both Onz ligands bound to Cu<sup>II</sup> are involved in binding DNA. While inset of Fig. 11B (mole ratio plot) is indicative of a value of 4.0, Fig. 11C (a modified Scatchard plot) provides a value of 3.0.

**Table 5: Binding constant values for interaction of the compounds with calf thymus DNA**

Compound	Apparent binding constants $K_{app} \times 10^{-4} (M^{-1})$		Site size (n <sub>b</sub> ) from mole ratio plot	Overall binding constant $(K' \times 10^{-4} (M^{-1}))$ $K' = K_{app} \times n_b$		Overall binding constant $K \times 10^{-4} (M^{-1})$ From Scatchard plot	Site size (n <sub>b</sub> ) from Scatchard plot
	From double reciprocal plot	From non linear – fit		Using K <sub>app</sub> from double reciprocal plot	Using K <sub>app</sub> from non linear – fit		
<b>Onz</b> ( <i>Chapter 7</i> )	<b>1.71</b>	<b>1.46</b>	<b>1.5</b>	<b>2.47</b>	<b>2.11</b>	<b>2.77</b>	<b>1.39</b>
<b>Cu(Onz)<sub>2</sub>Cl<sub>2</sub></b>	<b>0.66</b>	<b>0.44</b>	<b>4.0</b>	<b>2.64</b>	<b>1.78</b>	<b>2.61</b>	<b>3.0</b>

### Antiparasitic activity on *Entamoeba histolytica* (HM1: IMS Strain)

Inhibition of cell viability of *Entamoeba histolytica* was followed by trypan blue assay using different concentrations of Onz and Cu(Onz)<sub>2</sub>Cl<sub>2</sub> for 24 hours and 48 hours respectively [31]. MIC recorded after 24 hours for Onz and Cu(Onz)<sub>2</sub>Cl<sub>2</sub> on *Entamoeba histolytica* were 12.5 μM and 25.0 μM respectively (Table 6) suggesting by the end of 24 hours the Cu<sup>II</sup> complex is actually weaker than Onz in performance. However, upon increasing exposure time for each compound on the target, from 24 hrs to 48 hrs, the complex was found to be more cytotoxic with an MIC of 6.25 μM while for Onz the value remained at 12.5 μM (as that obtained at 24 hours). The study shows increasing exposure time has a positive impact

for the complex and may be considered an advantage of complex formation. What is more important is that in spite of a decrease in formation of  $\text{NO}_2^{\bullet-}$  due to the complex, efficacy is unaffected against a thought that prompts one to think that the complex might be less effective (speculating on the lines that the mechanism would suffer in the free radical pathway). This implies the complex is able to make up any compromise that it makes in the free radical pathway through other attributes of complex formation, one of which could be the presence of Cu(II) in the compound that apart from ensuring effective binding with DNA could lead to killing of cells of disease causing microbes either owing to an effective cellular uptake at longer exposure times (48 hours) or owing to the generation of  $\bullet\text{OH}$  because of the  $\text{Cu}^{\text{II}}/\text{Cu}^{\text{I}}$  couple [33].

**Table 6: MIC values for Ornidazole and its monomeric  $\text{Cu}^{\text{II}}$  complex when applied on *Entamoeba histolytica* (HM1:IMS strain)**

Compound	MIC after 24 hrs	MIC after 48 hrs
Ornidazole	12.5 $\mu\text{M}$	12.5 $\mu\text{M}$
$\text{Cu}(\text{Onz})_2\text{Cl}_2$	25.0 $\mu\text{M}$	6.25 $\mu\text{M}$
$\text{CuCl}_2$	>100 $\mu\text{M}$	>100 $\mu\text{M}$
DMSO	>100 $\mu\text{M}$	>100 $\mu\text{M}$

## References

1. Y. Miyamoto, J. Kalisiak, K. Korthals, T. Lauwaet, D. Y. Cheung, K. B. Sharpless, L. Eckmanna, *Proc. Natl. Acad. Sci. USA*, **2013**, 110, 17564-17569.
2. W. Raether, H. Hänel, *Parasit. Res.*, **2003**, 90, S19-S39.
3. M. Van den Kerkhof., D. Mabile, E. Chatelain, Caljon., *Int J. Parasit: Drugs and Drug Resist.*, **2018**, 8, 81-86.
4. E. F. F. da Cunha; T. C. Ramalho; D. T. Mancini; E. M. B. Fonseca; A. A. Oliveira, , *J. Braz. Chem. Soc.*, **2010**, 21, <http://dx.doi.org/10.1590/S0103-50532010001000002>.

5. J. M. Brown. , *Cancer Res.*, **1999**, 59, 5863-5870.
6. P. Wardman , *Br J Radiol.*, **2019**, 92, 20170915, doi: 10.1259/bjr.20170915
7. M. Bonnet ,C. R. Hong ,W. W. Wong ,M. P. Hay , *J Med Chem.* **2018**, 61, 1241-1254. doi: 10.1021/acs.jmedchem.7b01678.
8. P. De, D. Bhattacharyya, K. Roy, *Struct Chem.*, **2020**, doi:10.1007/s11224-019-01481-z
9. a)S. Sood , A. Kapil , *Ind. J Sex Transm Dis* **2008**, 29, 7-14; b) V. Puri, *Neurology India*, **2011**, 59, 4-5.
10. R. C. Santra, D. Ganguly, J. Singh, K. Mukhopadhyay, S. Das , *Dalton Trans.*, **2015**, 44, 1992-2000.
11. Reflex Plus, Accelrys Material Studio 4.4, Accelrys Software Inc, **2008**.
12. P. E. Werner, L. Eriksson, M. Westdahl,. *J. Appl. Cryst.* **1985**, 18, 367-370.
13. G. S. Pawley, *J. Appl. Crystallogr.*, **1981**, 14, 357-361.
14. K. E. Linder , Y. W. Chan , J. E. Cyr , M. F. Malley , D. P. Nowotnik , *J Med Chem.* **1994**, 37, 9-17.
15. R. C. Santra, D. Ganguly, S. Jana, N. Banyal, J. Singh, A. Saha, S. Chattopadhyay, K. Mukhopadhyay, S. Das, *New J. Chem.*, **2017**, 41, 4879-4886. DOI: 10.1039/C7NJ00261K.
16. J. A. Squella, S. Bollo , J. de. la. Fuente, L. J. Núñez-Vergara , *Bioelectrochem Bioenergetics* **1994**, 34:13–18.
17. J. A. Squella, M. Huerta, S. Bollo, H. Pessoa, L. J. Núñez-Vergara,. *J. Electroanal. Chem.* , **1997**, 420:63–70.
18. J. A. Squella, P. Gonzalez, S. Bollo *et al.* , *Pharm Res*, **1999**, 16, 161–164. <https://doi.org/10.1023/A:1011950218824>
19. L. J. Núñez-Vergara, F. Garcia, M. Dominguez, J. de la M Fuente, J. A. Squella, *J. Electroanal. Chem.* **1995**, 381, 215–219.
20. H. Lund in *Cathodic Reduction of Nitro and Related Compounds*, in *Organic Electrochemistry*, Ed. Lund H and BaizerMM, p. 411, M. Dekker Inc. New York 3rd. Ed. (**1990**).
21. P. C. Mandal, *J. Electroanal. Chem.* **2004**, 570, 55-61.

22. A. J. Bard , L R Faulkner, *Electrochemical Methods Fundamental and Applications*, John Wiley & Sons, Inc. New York, **2001**.
23. P. Zanello. *Inorg. Electrochem.: Theory, practice and application*, *The Royal Society of Chemistry*, **2003**.
24. R. C. Santra , K. Sengupta , R. Dey, T. Shireen, P. Das , P. S. Guin, K. Mukhopadhyay , S. Das, *J. Coord. Chem.*, **2014**, 67, 265-285; DOI:10.1080/00958972.2013.879647.
25. P. S. Guin, S. Das, *Int. J. Electrochem.*, **2014**, 2014, Article ID 517371, 8 pages; <https://doi.org/10.1155/2014/517371>.
26. P. S. Guin, P. C. Mandal, S. Das, *ChemPlusChem*, **2012**, 77, 361-369; <https://doi.org/10.1002/cplu.201100046>.
27. X. Jiang, X. Lin, *Bioelectrochem.*, **2006**, 68, 206-212.
28. T. Deb, D. Choudhury, P. S. Guin, M. B. Saha, G. Chakrabarti , S Das, *Chem-Biol. Inter.*, **2011**, 189, 206-214.
29. C. G. Clark , L. S. Diamond , *Clin. Microbiol. Rev.*, **2002**, 15, 329–341.
30. J. A. Upcroft, P. Upcroft ,*Agents Chemother.*, **2001**, 45, 1810–1814.
31. E. Benere, R. A. I. Luz, M. Vermeersch, P. Cos, L. Maes, *Microbiol. Methods*, **2007**, 71, 101–106.
32. F. Frezard, A. Garnier-Suillerot, *Biochim. Biophys. Acta*, **1990**, 1036, 121-127.
33. T. Deb, P. K. Gopal, D. Ganguly, P. Das, M. Paul, M. B. Saha, S. Paul, S. Das, *RSC Adv.*, **2014**, 4, 18419-18430.

# **Chapter 9**

**Electrochemical reduction of Ornidazole and its Cu<sup>II</sup>  
complex in aqueous and aqueous dimethyl  
formamide mixed solvent: A cyclic  
voltammetric study**

## Introduction

5-nitroimidazoles are well-known positional isomers of the nitroimidazole family [1-7]. Ornidazole [1-chloro-3-(2-methyl-5-nitro-1H-imidazole-1-yl)propan-2-ol], an important member of this family is gradually gaining acceptability as a drug, being an essential component of many pharmaceutical formulations used to treat microbial infections[8]. It has been investigated for use in Crohn's disease after bowel resection [9, 10]. Reduction of the nitro group to nitro radical anion equips it to enter cells creating a favorable concentration gradient with reduction proceeding intra-cellularly [1-7]. Inside the cell, the nitro radical anion interacts with DNA disrupting or breaking strands, being one of many mechanisms that lead to cell death [1-7, 11-15].

Formation of the nitro radical anion is crucial since on the one hand, it is an active component responsible for cytotoxic action (causing various forms of damage to cell organelles and DNA), and on the other on prolonged use is neurotoxic [11-15]. Neurotoxicity has been established from animal model studies and realized also from post application reports of patients administered with drugs having 5-nitroimidazole in them [9, 14-18]. Hence, for safe use of 5-nitroimidazoles, there is a need to control the formation of the nitro radical anion so that a correct amount, sufficient for cytotoxic action on target cells is present, not leaving too much in excess that may produce toxic side effects [14-18]. Chemotherapy-induced neurotoxicity is a matter of serious concern limiting the use of 5-nitroimidazoles [11-18].

Notwithstanding such controversies, 5-nitroimidazoles have remained in use because of high efficacy, not matched by another class of compounds [1-18]. Hence, although neurotoxic, positive attributes of 5-nitroimidazoles have actually outweighed their negative aspect [11-18]. Since neurotoxicity is a matter of concern and since such drugs cannot be done away with, a logical approach is to modify them. By doing so, one not only can address toxic side

effects but maintain drug efficacy [11-18]. Several modifications were attempted of which formation of metal complexes is one such [19-21].

Whatever the modification, monitoring of reactive intermediates on 5-nitroimidazoles is important. This *chapter* reports an investigation using electrochemical experiments on Ornidazole and its monomeric  $\text{Cu}^{\text{II}}$  complex. The amount of nitro radical anion generated under different solvent conditions (pure dimethyl formamide to aqueous-dimethyl formamide) on ornidazole and the complex was realized. This study made an attempt to correlate certain established facts, drawing examples from previous studies that show metal complexes of 5-nitroimidazoles were better or at least comparable in performance to 5-nitroimidazoles [19-21]. Since complexes compromise on generation of nitro radical anions, we made an attempt to look at electrochemical behavior of a metal complex of ornidazole with respect to ornidazole itself [19-21]. Findings help to explain the results discussed in previous chapters in the light of the free radical pathway, for one to conclude why complexes are either better antimicrobial or anticancer agents [19-22].

## **Results and Discussion**

### **Cyclic voltammetry of Onz and its monomeric $\text{Cu}^{\text{II}}$ complex in different media**

Using the conventional three-electrode system, experiments were performed with Onz and its monomeric  $\text{Cu}^{\text{II}}$  complex to realize their behavior in different solvent systems that were either aprotic (DMF) or protic polar (water) or intermediate between aprotic and protic polar (DMF-aqueous solutions). In a progressive manner, the aqueous part of aqueous-DMF mixtures were increased (Figure 1). It has long been established that in case of aprotic solvents, the nitro group of 5-nitroimidazoles undergo a reversible one-electron reduction to generate nitro radical anion followed by an irreversible three-electron reduction to hydroxylamine derivatives; formal potentials of reductions depending on polarity of solvent,

pH of the medium and also on supporting electrolyte that play an important role in deciding whether reduction takes place in two steps or a single step [28-31]. Electrochemical behavior is influenced by several other factors, one such is hydrogen bonding [32].



This electrochemical investigation performed on Onz and its monomeric Cu(II) complex looks at aspects related to the generation of nitro radical anion since it is considered important related to drug efficacy. Since activity of Onz and other such molecules depend on their ability to reduce to nitro radical anion, proper knowledge on its generation and existence under different environments become important. Studies reveal while on the one hand, their formation is important for cytotoxicity and helps to address issues related to microbial infections [1-5, 14, 15], or enables them to act as radio-sensitizers [32, 33]; too much generation make them neurotoxic [32].

Hence, suitable modifications that help to regulate the generation of nitro radical anion is welcome. In this chapter, there is an attempt to look at some behavioral changes between free Onz and when bound to a metal ion in a complex. When similar experiments were performed, findings revealed a few differences between these two forms of Onz that help to identify differences observed in drug action considering the electrochemical pathway, i. e. when such compounds are present inside the cells of a target organism [11, 13-15].

For Onz, cyclic voltammograms were recorded under changing solvent conditions starting with pure (100%) DMF and gradually increasing water content in aqueous-DMF mixtures. Figure 1 clearly demonstrates how voltammograms change as the percentage of water increased. In going from 100% DMF (Figure 1A) to 57% DMF (Figure 1F), the one-electron

and three-electron peaks gradually move closer to each other and eventually merge to form a single step-four-electron reduction at a composition of 54% DMF-46% water (Figure 1G).

One-electron and three-electron reduction peaks were observed at -784 mV ( $-\text{NO}_2^{\bullet-}$ ) and -1086 mV ( $-\text{NHOH}$ ) respectively in pure DMF where they were separated by  $\sim 300$  mV. This separation gradually decreased with an increase in percentage of water with peaks moving closer to each other. That the reduction is one electron followed by three electrons (Eqs. 1&2) is clearly evident from Figure 1A where  $I_{pc2}$  is almost thrice  $I_{pc1}$  (Table 1).

Unlike that observed earlier for metronidazole [30], in case of Onz we found the first step was almost completely irreversible while the second quasi-reversible. For pure DMF and for each successive aqueous-DMF compositions, when the scan was reversed at a potential immediately after the first reduction (voltammogram in black), peak current due to the anodic wave (i. e. oxidation of  $-\text{NO}_2^{\bullet-}$  to  $-\text{NO}_2$ ) was found to be somewhat less than when it was reversed after the second reduction i.e. after formation of  $-\text{NHOH}$  (voltammogram in red).

This indicates some  $-\text{NO}_2^{\bullet-}$  to have been generated through a chemical reaction besides being electro-generated, when the scan was allowed to proceed beyond the first step of one-electron reduction [19, 27, 34]. A logical conclusion to this observation is comproportionation occurring between an  $-\text{NHOH}$  containing moiety obtained from the reduction of Onz, with unreacted Onz in the medium, forming the nitro radical anion ( $-\text{NO}_2^{\bullet-}$ ) [19]. Therefore, it is important at this stage to realize  $-\text{NO}_2^{\bullet-}$  does not only form by a direct one step single electron reduction of nitroimidazoles but that it is also generated by comproportionation. This would be happening when nitroimidazoles act as drugs in the biological system. Hence, if a reducing agent is present in an environment and reduce nitroimidazoles by one electron, a nitro radical anion is generated, however, if the reducing agent is strong enough and converts it to an  $-\text{NHOH}$  derivative, then also  $-\text{NO}_2^{\bullet-}$  would result (by the interaction of an  $-\text{NHOH}$  containing moiety with unreacted nitroimidazoles).

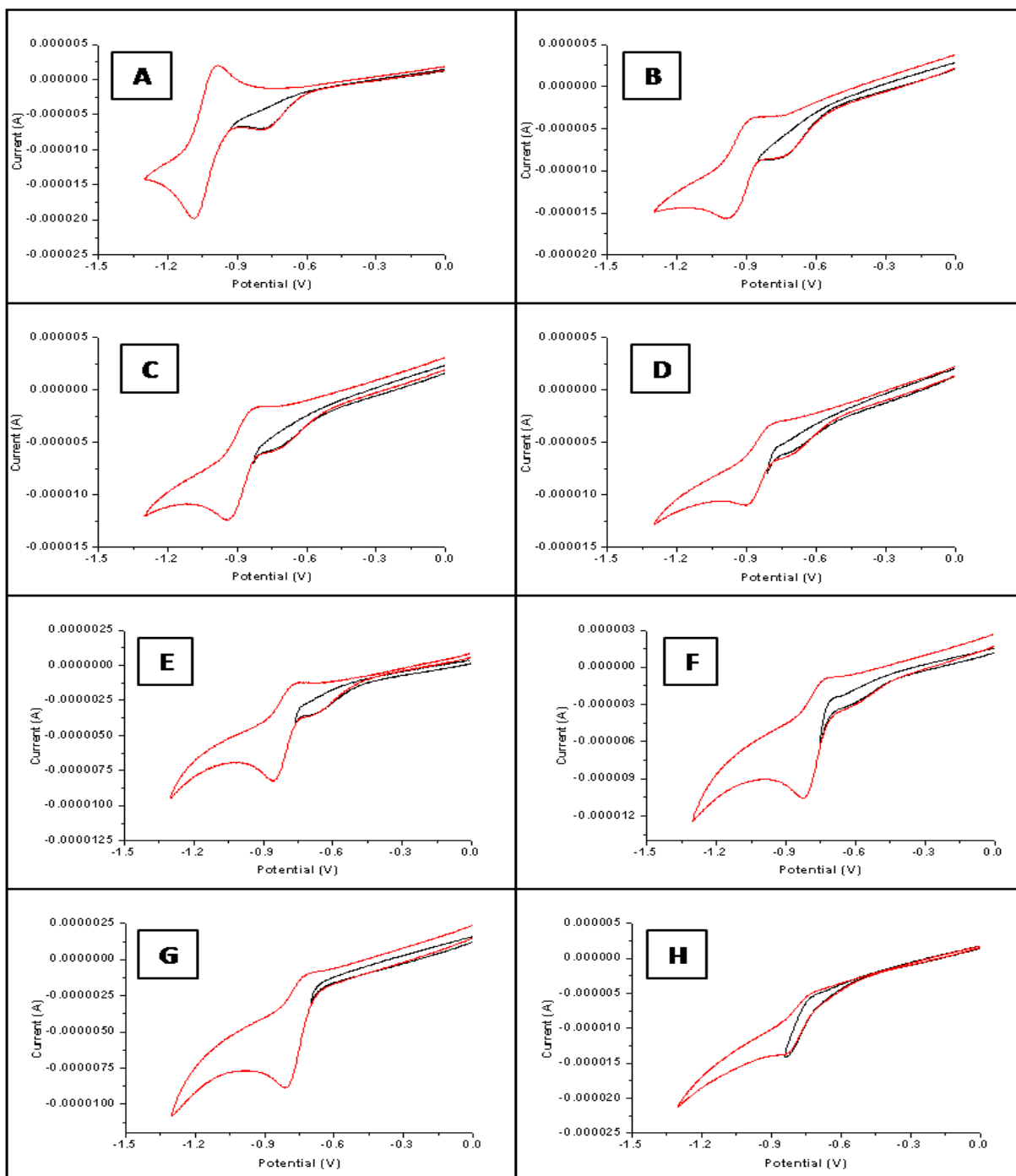


**Figure 1:** Cyclic voltammograms (red lines) of 1 mM ornidazole showing two successive one electron and three electron reduction in 0.1 mM TBAB in (A) pure DMF, (B) 90% aqueous DMF, (C) 80% aqueous DMF, (D) 70% aqueous DMF, (E) 60% aqueous DMF, (F) 57% aqueous DMF, (G) 54% aqueous DMF, (H) 50% aqueous DMF on glassy carbon electrode; scan rate 100mV/sec. Black lines show the voltammograms for the one electron reduction when the scan is reversed before the second reduction starts.

Nitro radical anions can react with molecular oxygen to form superoxide radical anion. However, it has been seen that biological manifestation of a nitro radical anion is far greater than the superoxide radical anion [35]. Rather, if  $-\text{NO}_2^{\cdot-}$  really generates  $\text{O}_2^{\cdot-}$ , then it has been seen that the efficacy of the 5-nitroimidazole under such circumstances are considerably less [35]. Hence, nitroimidazoles thrive and perform best under anaerobic conditions; their formation and presence being an important aspect having a lot of significance both with regard to electrochemistry and their application in biology [35].

Comproportionation constant,  $K_{\text{comp}}$  was obtained using the equation:

$$K_{\text{comp}} = \exp [-F (E_2 - E_1)] / RT \quad (5)$$

where  $F$  = Faraday (96500 C)

$R$  = Molar gas constant ( $8.314 \text{ JK}^{-1}\text{mol}^{-1}$ )

$T$  = Temperature (298K)

$E_{\text{pc1}}$  = Cathodic potential of the first reduction

$E_{\text{pc2}}$  = Cathodic potential of the second reduction

Table 1 indicates as the percentage of water increased in aqueous-DMF mixtures, potentials changed and nature of voltammograms were completely different suggesting electrochemical reduction of Onz was influenced by polarity of solvent (i. e. protic and aprotic solvents). Thus role of protic solvent could be realized through studies in aqueous-DMF solutions (mixed solvent). At 80 % DMF, two successive reduction waves were much closer to each other (-731 mV and -944 mV respectively) than they were for pure DMF. The gap between peaks progressively decreased up to 57% DMF when voltammogram showed a feeble first reduction but an intense second reduction peak (Figure 1).

**Table 1:** Reduction potentials ( $E_{pc1}$  and  $E_{pc2}$ ), comproportionation constant ( $K_{comp}$ ) and diffusion coefficients ( $D_0$ ) at different percentages of DMF;  $(D_0)_1$  = diffusion coefficient for cathodic peak of the one step one electron reduction,  $(D_0)_2$  = diffusion coefficient for cathodic peak of the subsequent one step three electron reduction.

% DMF	% H <sub>2</sub> O	$E_{pc1}$ (mV)	$I_{pc1}$ ( $\mu$ A)	$E_{pc2}$ (mV)	$I_{pc2}$ ( $\mu$ A)	$K_{comp}$	$D_0$ (cm <sup>2</sup> s <sup>-1</sup> )	
							$(D_0)_1$	$(D_0)_2$
100	0	-784	7.12	-1086	19.70	128.00 x 10 <sup>3</sup>	7.11 x 10 <sup>-6</sup>	2.04 x 10 <sup>-6</sup>
90	10	-750	8.15	-985	15.71	9.44 x 10 <sup>3</sup>	9.32 x 10 <sup>-6</sup>	1.28 x 10 <sup>-6</sup>
80	20	-731	5.73	-944	12.40	4.00 x 10 <sup>3</sup>	4.61 x 10 <sup>-6</sup>	0.79 x 10 <sup>-6</sup>
70	30	-715	6.19	-903	11.00	1.51 x 10 <sup>3</sup>	5.37 x 10 <sup>-6</sup>	0.63 x 10 <sup>-6</sup>
60	40	-680	3.48	-858	8.25	1.03 x 10 <sup>3</sup>	1.70 x 10 <sup>-6</sup>	0.35 x 10 <sup>-6</sup>
57	43	-633	3.26	-824	10.60	1.70 x 10 <sup>3</sup>	1.49 x 10 <sup>-6</sup>	0.58 x 10 <sup>-6</sup>
54	46	–	–	-812	8.88	-	-	-
50	50	–	–	-840	13.65	-	-	-

Change in formal reduction potentials for one electron ( $E_{pc1}$ ) and three electron ( $E_{pc2}$ ) reduction peaks of Onz in different aqueous-DMF compositions are shown in Table-1. It reveals as concentration of water increased, comproportionation constant ( $K_{comp}$ ) decreased.

Apparent comproportionation constants calculated for electrochemical processes in pure and aqueous-DMF mixtures indicate there is an influence of water on comproportionation rates.

Considering comproportionation to be  $-\text{NO}_2 + -\text{NHOH} \rightleftharpoons -\text{NO}_2^{\bullet-}$  [19], the comproportionation constant ( $K_{\text{comp}}$ ) could be determined for different solvent compositions (Table 1). Increase in concentration of water provides stability to  $-\text{NHOH}$  through hydrogen bonding [32]. Hence, the tendency of the  $-\text{NHOH}$  formed, following reduction of  $-\text{NO}_2$ , to interact with remaining  $-\text{NO}_2$  on Onz decreases. This is manifested by a gradually diminishing comproportionation constant that ultimately forms a plateau in the solvent composition range  $\sim 70\%$  DMF to  $\sim 57\%$  DMF (Table 1 and Figure 1).

An earlier report, where another 5-nitroimidazole (tinidazole) was studied in pure DMF, comproportionation was established by incorporating a homogeneous chemical reaction in an electrochemistry based simulation. The simulated data considering comproportionation was in good agreement with an actually performed experiment [19]. In the present study, Onz in varying compositions of aqueous-DMF mixtures were analyzed. Since a similar behavior was observed (i. e. excess nitro radical anion was generated each time when the scan was reversed after the second reduction) suggests that at all solvent compositions, comproportionation had occurred, although the ease of occurrence diminished with an increase in the concentration of water in these aqueous-DMF mixtures.

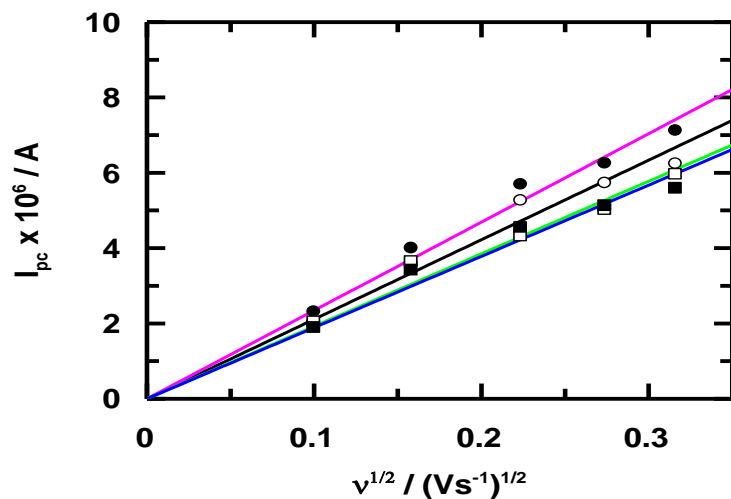


**Figure 2:** Dependence of cathodic peak currents for one electron reduction of Onz at different solvent composition (●= 100 % DMF, ○= 90% DMF, □= 80% DMF, ■ = 60% DMF) with square root of scan rate.

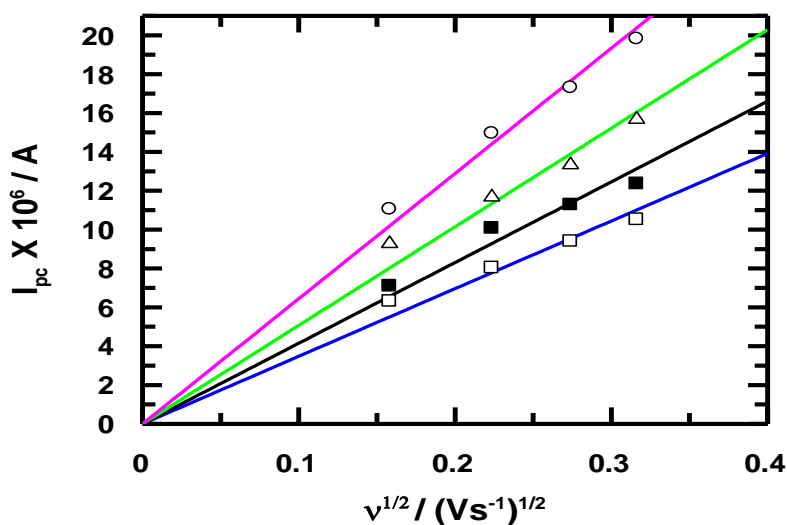


**Figure 3:** Dependence of cathodic peak current for the subsequent one step three electron reduction of Onz at different solvent composition (○ = 100 % DMF, Δ = 90% DMF, ■ = 80% DMF, □ = 57% DMF) with square root of the scan rate.

Figures 2 and 3 are plots of current ( $I_{pc}$ ) associated with the first and second reductions respectively plotted against square root of scan rate. A linear relationship, with lines passing

through the origin indicates that reduction was diffusion controlled with no adsorption on the electrode surface. The diffusion coefficient ( $D_0$ ) for Onz was determined using Eq. 1.

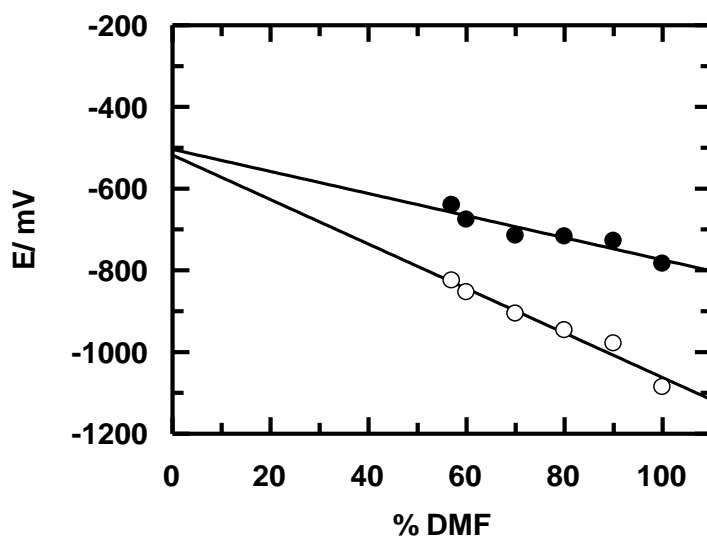


**Figure 4:** Change in cathodic potential with solvent composition: First one- electron reduction potential  $E_1(\bullet)$  and second three-electron reduction potential  $E_2(\circ)$

Formal electrode potentials determined for the first and second reduction steps were plotted against concentration of DMF. From an extrapolation of straight lines obtained (Figure4), successive reductions in pure water were read from the graph (i. e. at 0% DMF). Reduction potentials ( $E_{pc1}$  and  $E_{pc2}$ ) for Onz in pure aqueous medium were found to be  $-502$  mV and  $-530$  mV respectively, with only a small difference in peak potentials (of 28 mV). So Figure4 predicts that the two peaks would eventually merge in aqueous medium to a single wave four-electron reduction.

Changes in electrochemical behavior of Onz when bound to a metal ion were studied under similar experimental conditions. A monomeric  $Cu^{II}$  complex of Onz under different solvent compositions was investigated. In case of the complex two peaks were obtained for Onz but they appeared at much more negative potential than that for free Onz (Figure 5).

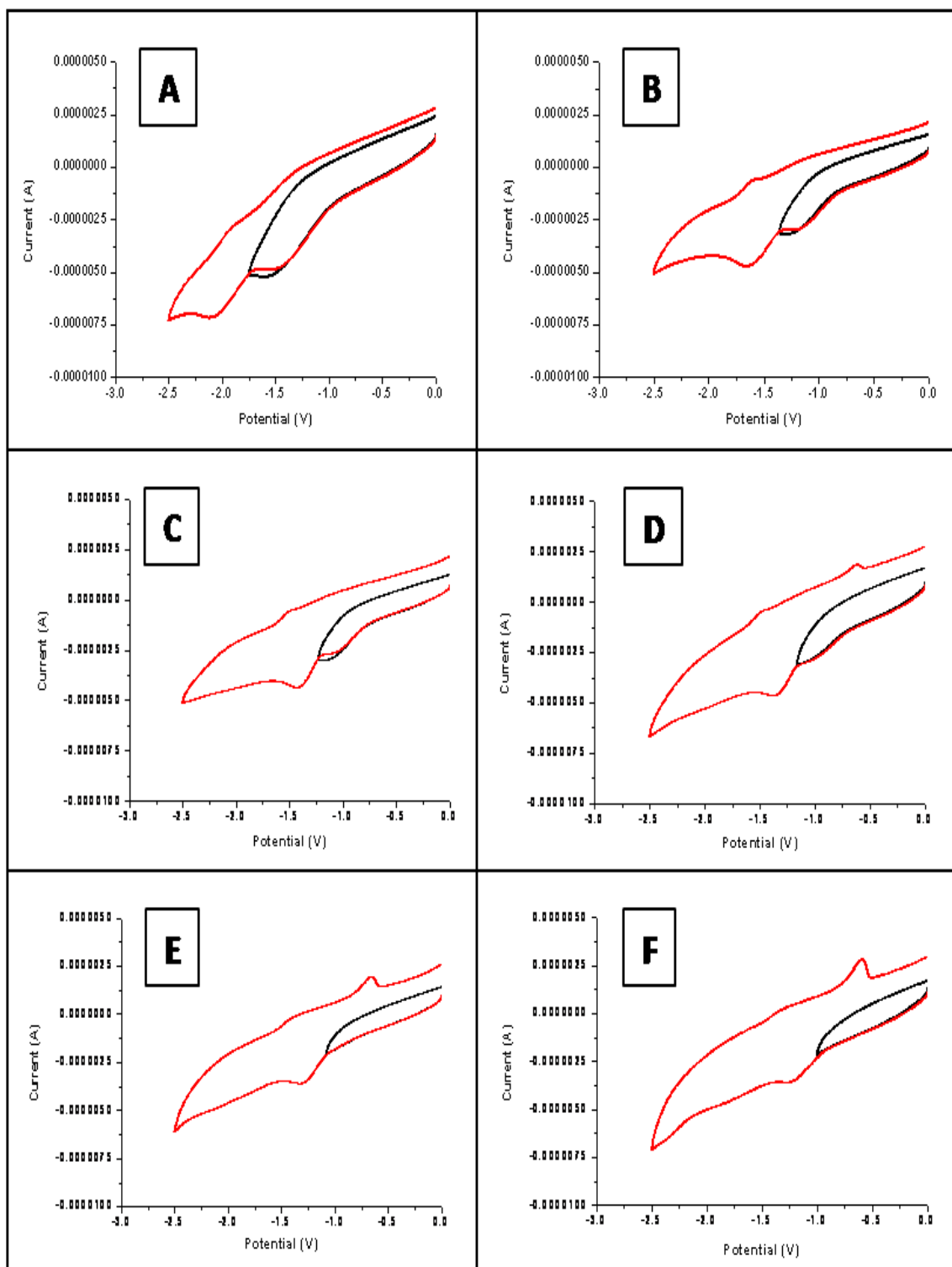


**Figure 5:** Cyclic voltammogram of 1 mM  $\text{Cu}^{\text{II}}$ -Ornidazole showing reduction in 0.1 M TBAB in pure (100%) DMF under different aqueous-DMF compositions on a glassy carbon electrode; scan rate 100 mV/sec.

In 100% DMF, for example, the first peak was found at -1480 mV while the second was at -2115 mV. This indicates complex formation made it difficult for the nitro group on Onz to be reduced. However, as observed for Onz, when water, in aqueous-DMF mixtures increased, the two peaks moved closer to each other. At 80% DMF, the two successive reduction waves were at -1032 mV and -1428 mV respectively while at 50% DMF they had merged (-1237 mV) to show a single step four electron reduction. As observed for Onz alone, in case of the complex also the first reduction gradually became less intense and that the second intensified. Like in case of Onz, for the complex also, two voltammograms were generated at each solvent composition. One, when the scan was reversed immediately after the first reduction and the other when it was reversed after the second reduction. Similar to observations for free Onz, for Onz bound to Cu(II) it was seen that the anodic wave for oxidation of nitro radical anion to nitro was greater for the voltammogram where the scan was reversed after the second reduction indicating that in case of the complex also there is a greater presence of  $\text{NO}_2^{\cdot-}$  in the medium compared to what was generated due to electrochemical reduction of the nitro group. Obviously then, it may be said that  $\text{NO}_2^{\cdot-}$  was being generated in a pathway other than electrochemical reduction (otherwise it would have been same for both voltammograms). The difference between Onz present alone in solution (Figure 1) and that present bound to Cu(II) in the complex (Figure 5) at each solvent composition may be realized from their respective voltammograms. difference in anodic current between scan reversed after the second reduction and that reversed after the first was greater for Onz present in the complex. This means that for Onz bound to Cu(II), electro-generation of  $\text{NO}_2^{\cdot-}$  by one-electron was substantially decreased, while that formed through chemical reaction (comproportionation), although less than that for free Onz appeared substantial. So in case of the complex, it is not only that Onz is reluctant to participate in electrochemical reduction

(Figur5) but that the amount of  $-\text{NO}_2^{\bullet-}$  formed was also low; however as mentioned above, difference between chemical and electrochemical processes appeared greater for the complex than for free Onz. This evidence obtained from electrochemical experiments performed on Onz and its monomeric  $\text{Cu}^{\text{II}}$  complex, supports earlier findings of similar metal complexes related to the generation of  $-\text{NO}_2^{\bullet-}$  as observed in xanthine-oxidase enzyme assay experiments showing less nitro radical anion formation by complexes [20, 21].

**Table 2:** Reduction potentials ( $E_{\text{pc1}}$  and  $E_{\text{pc2}}$ ),comproportionation constants ( $K_{\text{comp}}$ ) and diffusion coefficients ( $D_0$ ) at different percentage of DMF;  $(D_0)_1$  = diffusion coefficient for cathodic peak of a one step one electron reduction,  $(D_0)_2$  = diffusion coefficient for cathodic peak of the next one step three electron reduction for the monomeric  $\text{Cu}^{\text{II}}$  complex.

% DMF	% H <sub>2</sub> O	$E_{\text{pc1}}$ (mV)	$E_{\text{pc2}}$ (mV)	$K_{\text{comp}}$	$D_0$ (cm <sup>2</sup> s <sup>-1</sup> )	
					$(D_0)_1$	$(D_0)_2$
100	0	-1480	-2115	$5.51 \times 10^{10}$	$3.324 \times 10^{-6}$	$0.267 \times 10^{-6}$
90	10	-1185	-1660	$1.08 \times 10^8$	$1.246 \times 10^{-6}$	$0.116 \times 10^{-6}$
80	20	-1032	-1428	$4.99 \times 10^6$	$0.924 \times 10^{-6}$	$0.098 \times 10^{-6}$
70	30	-980	-1364	$3.13 \times 10^6$	$1.000 \times 10^{-6}$	$0.113 \times 10^{-6}$
60	40	-954	-1316	$1.33 \times 10^6$	$0.399 \times 10^{-6}$	$0.067 \times 10^{-6}$
50	50	-	-1237	-	-	$0.065 \times 10^{-6}$

The outcome of cyclic voltammetry studies performed on the complex in pure DMF and different aqueous-DMF compositions indicate

- i) that it is difficult to generate nitro radical anion on the complex,
- ii) even if generated, a certain portion of it is lost in some other pathway that could be a consequence of the presence of a metal ion and
- iii) generation of nitro radical anion by comproportionation was observed for the complex.

Hence, electrochemical experiments performed on the  $\text{Cu}^{\text{II}}$  complex of Onz, clearly suggest there is substantial decrease in the formation of the nitro radical anion. While this is beneficial and helps to check toxic side effects (neurotoxicity), on the other hand, it might affect efficacy on target micro-organisms. However, if in spite of decreased  $-\text{NO}_2^-$ , complexes are able to maintain their cytotoxic efficacy or sometimes even perform better, as shown in some previous studies, then such complexes would remain efficient with regard to drug action when compared with their respective 5-nitroimidazoles (from which they were prepared) [19-22]. Since performance of complexes are maintained or enhanced with respect to a 5-nitroimidazole, it may be said decrease in nitro radical anion formation by complexes does not interfere with cytotoxicity i. e. the action of drugs on disease causing microbes. Even if it does, then certain other attributes of complex formation would make up for any loss in efficacy in the free radical pathway.

## References

1. J. A. Upcroft, R. W. Campbell, K. Benakli, P. Upcroft, P. Vanelle. , *Antimicrob Agents Chemother.* **1999**, 43, 73-76. doi: 10.1128/AAC.43.1.73.
2. (a)A. L. Crowell, K. A. Sanders-Lewis, W. E. Secor , *Antimicrob Agents Chemother.* **2003**; 47(4), 1407–1409; doi: 10.1128/AAC.47.4.1407-1409.2003. (b)H. B. Fung,T. L Doan , *ClinTher.* **2005** 27(12), 1859-1884. (c)J. R. Schwebke , R. A. Desmond , *Am J Obstet Gynecol.* **2011**; 204(3): 211.e1–211.e6; doi: 10.1016/j.ajog.2010.10.898.
3. W. Raether , H. Hänel ,*Parasit. Res.* **2003**, 90, S19-S39.
4. Y. Miyamoto, J. Kalisiak, K. Korthals , T. Lauwaet , D. C. Young, R. Lozano ,E. R. Cobo ,P. Upcroft , J. A. Upcroft , D. E. Berg , F. D. Gillin, V. V. Fokin, K. B. Sharpless, L. Eckmann, *Proc. Natl. Acad. Sci. USA.* **2013**; 110(43), 17564-17569, <https://doi.org/10.1073/pnas.1302664110>.
5. C. W. Ang, A. M. Jarrad, M. A. Cooper, M. A. T. Blaskovich, *J. Med. Chem.*,**2017**; 60 (18), 7636–7657.
6. K. C. Lamp, C. D. Freeman, N.E. Klutman, M. K. Lacy, *ClinPharmacokinet*, **1999**, 36, 353–373. <https://doi.org/10.2165/00003088-199936050-00004>.
7. M. D. Nair, K. Nagarajan, Nitroimidazoles as chemotherapeutic agents. In: Jucker E. (eds) *Progress in drug research/Fortschritte der Arzneimittelforschung/Progrès des recherches pharmaceutiques.* Vol. 27, (1983) Birkhäuser Basel. [https://doi.org/10.1007/978-3-0348-7115-0\\_4](https://doi.org/10.1007/978-3-0348-7115-0_4).
8. H. Jinghui , L.R. McDougald., *Veterinary Parasitology*, **2004**, 121, 233-238.
9. J. K. Triantafillidis, D. Nicolakis, A. Emmanoullidis, A. Antoniou, K. Papatheodorou, P. Cheracakis, *Ital J Gastroenterol*, **1996**; 28, 10-14.
10. P. Rutgeerts, G. V. Assche, S. Vermiere, G. D’Haens, F. Baert, M. Noman, I. Aerden, G. dEHertogh, K. Geboes, M. Hiele, A. D’Hoore and F. Penninckx. *Gastroenterology*, **2005**; 128, 856 -861.
11. J. M. Brown , *Int J Radiat Oncol Biol Phys.*, **1982**, 8(3-4), 675-82. doi: 10.1016/0360-3016(82)90711-8.

12. D. Murray, R. E. Meyn, , *BiochemPharmacol.*, **1985**, 34(18), 3275-3279. doi: 10.1016/0006-2952(85)90345-4.
13. D. I. Edwards, R.C. Knight, A. Zahoor, Mutation Research/Reviews in *Genetic Toxicology*, **1981**, 86, 243-277.
14. a) S. Sood , A Kapil, *Ind. J Sex Transm Dis.* **2008**; 29, 7-14; b) V. Puri, *Neurology, India.* **2011**, 59, 4-5.
15. M. Rybczynska, L. Leclerc, E. Bursaux, M. Gentil, M. Hilly, C. Poyart, *Int J Clin. Pharmacol. Ther. Toxicol.*, **1986**, 24(9), 468-73.
16. H. Kato, H. Sosa, M. Mori, T. Kaneko, *Kansenshogaku Zasshi*, **2015**; 89(5), 559-566.
17. K. E. Andersson, *Scand J Infect Dis Suppl.*, **1981**; 26, 60-67.
18. R. C. Santra , K. Sengupta, R. Dey, T. Shireen, P. Das, P. S. Guin, K. Mukhopadhyay, S. Das, *J. Coord. Chem.*, **2014**, 67, 265-285; DOI:10.1080/00958972.2013.879647.
19. R. C. Santra, D. Ganguly, J. Singh, K. Mukhopadhyay, S. Das, *Dalton Trans.*, **2015**, 44, 1992-2000.
20. R. C. Santra, D. Ganguly, S. Jana, N. Banyal, J. Singh, A. Saha, S. Chattopadhyay, K. Mukhopadhyay, S. Das, *New Journal of Chemistry* **2017**, 41, 4879-4886. DOI: 10.1039/C7NJ00261K.
21. R. C. Santra, D. Ganguly, D. Bhattacharya, P. Karmakar, A. Saha, S. Das, *New J. Chem.*, **2017**, 41, 11679-11685.
22. J. E. B. Randles, *Trans. Faraday Soc.*, **1948**, 44, 327-338.
23. A.J. Bard, L. R. Faulkner, *Electrochemical methods Fundamental and application*, 2<sup>nd</sup> ed., John Wiley & Sons. Inc.: New York, **2001**, pp 236.
24. R. S. Nicholson, *Anal. Chem.* **1966**, 38, 1406.
25. P. S. Guin, S. Das, *Int. J. Electrochem.* Vol. **2014**, Article ID 517371, 8 pages. doi:10.1155/2014/517371.
26. B. Mandal, S. Das, *J. Ind. Chem. Soc.*, **2020**, 97, 2633-2642.
27. P. C. Mandal, *J. Electroanal. Chem.* **2004**, 570, 55-61.

28. J. A. Squella, P. Gonzalez, S. Bollo , *Pharm. Res*, **1999**, 16, 161–164.  
<https://doi.org/10.1023/A:1011950218824>.
29. P. S. Guin, S. Das, P. C. Mandal, *Int. Jour. of Electrochem.*, **2011**, ID 816202,  
22pages. <https://doi.org/10.4061/2011/816202>.
30. L. C. Deirdre , H. R. Rabin, E. J. Laishley, *J. Antimicro. Chemother.* **1990**, 25, 15–23.  
<https://doi.org/10.1093/jac/25.1.15>.
31. P. Wardman, *Br. J. Radiol.* **2019**, 92, 20170915, doi: 10.1259/bjr.20170915
32. P. De, D. Bhattacharyya, K. Roy, *Struct. Chem.*, **2020**, 31, 1043–1055.  
<https://doi.org/10.1007/s11224-019-01481-z>.
33. P. S. Guin, S. Das, P. C. Mandal, *Int. J. Electrochem. Sci.*, **3**, **2008**, 1016 – 1028.
34. P. Wardman, *Env. Health Pers.*, **1985**, 64, 309-320.

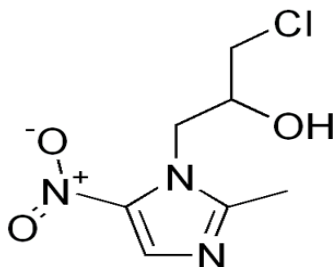
# **Chapter 10**

**Interaction of electrochemically generated  
reduction products of ornidazole with  
nucleic acid bases and calf thymus DNA**

## Introduction

Ornidazole [1-chloro-3-(2-methyl-5-nitro-1H-imidazole-1-yl)propan-2-ol], a 5-nitroimidazole, is under serious consideration these days for certain advantages it has over metronidazole, the most popular of the nitroimidazole family [1-13]. It is slowly becoming a major component of many important pharmaceutical formulations. Through various studies and application on patients, it has today emerged that reduction of the nitro group and subsequent formation of different reduction products are crucial for their activity [1, 7, 14]. As mentioned earlier after entering a target cell, antimicrobial activity of nitroimidazoles depend on the reduction of the nitro group to a nitro radical-anion ( $\text{NO}_2^{\bullet-}$ ) and/or other potentially active reduction products that includes nitroso and hydroxylamine derivatives [1, 14]. Reduction products of nitroimidazoles are damaging to various macromolecules including the DNA, bringing about their degradation through modification of strands [1, 7, 14]. Almost all nitroimidazoles are selectively toxic to different micro-organisms which provide them the required redox potential so that electron transport processes can occur; if cells of the micro-organism make the environment sufficiently negative, it can reduce the nitro group of the nitroimidazole inviting its own death. By and large, this has been the mechanism of activity of nitroimidazoles and pharmaceutical companies have exploited this to their advantage. For nitroimidazoles acting as radiopharmaceuticals or radiosensitizers, the cause for action is more or less the same. The only difference is that in this application,  $\text{R-NO}_2^{\bullet-}$  probably has a larger role than the other reduction products [6-9]; R signifying the portion of a nitroimidazole other than the nitro group. Although, there is some work in the literature on modification of DNA due to nitroimidazoles, there is lot of scope for further investigative work [15-16]. In this *chapter*, the aspect as to how the nitro radical anion or other reduction products generated within a cell equip molecules with to interact with nucleic acid bases or DNA was investigated with the help of model experiments. The reduction

potential was provided to Ornidazole by an electrochemical method using a glassy carbon electrode and four different nucleic acid bases (taken one at a time) or calf thymus DNA was maintained in the immediate vicinity of the generated reduction products.



**Ornidazole (Onz)**

## Results and Discussion

### Cyclic voltammetry studies

In aprotic media, the nitro group of 5-nitroimidazoles undergoes a reversible one-electron reduction to a nitro radical anion followed by a three-electron reduction to hydroxylamine derivatives. In aqueous solution, these two steps are not realized separately and a single step four electron reduction is observed [15, 16].



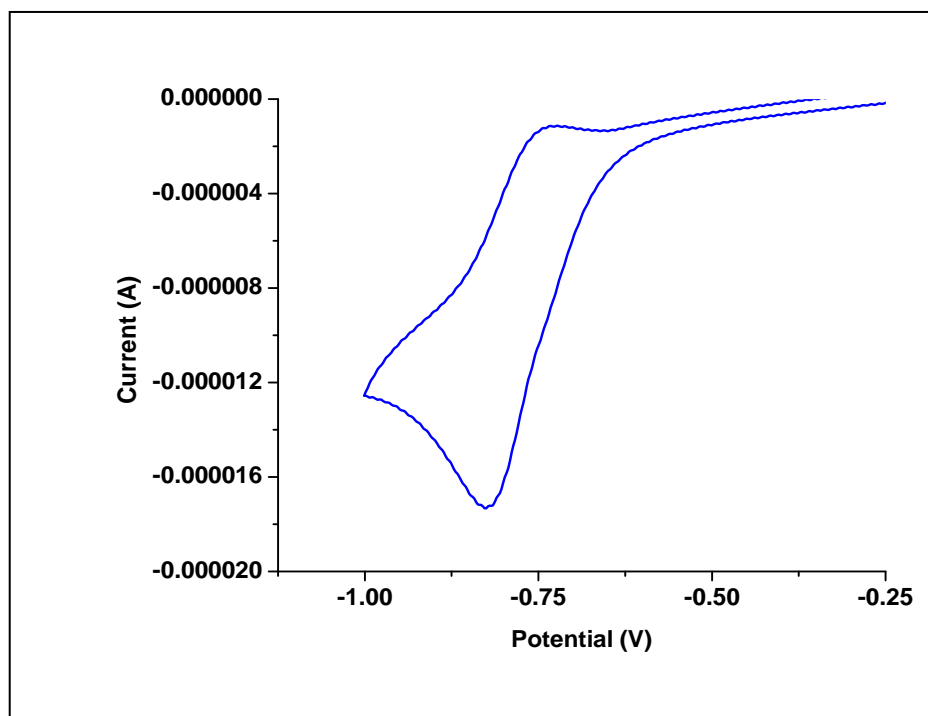


**Figure 1:** Cyclic voltammogram of 1 mM Ornidazole showing a single step one electron reduction in 0.12 M KCl in an aqueous - 20% methanol solution on a glassy carbon electrode; Scan rate being 100mV/sec.

Figure 1 shows a cyclic voltammogram of Onz in an aqueous - 20% methanol solution that was obtained at a scan rate of 100mV/sec. A reduction peak was obtained at -0.827 V against Ag/AgCl, satd. KCl ( $E_{1/2} = -0.835$  V). The peak was assigned to the reduction of  $-\text{NO}_2$  present on the imidazole ring of Ornidazole.

### **Interaction of reduction products of Ornidazole with biological targets**

As identified through previous studies [17], there is scope for interaction of various reduction products of nitroimidazoles, whereby RNHOH could participate in chemical reactions subsequent to its electrochemical generation. We made an attempt through this study to realize the scope of interaction of such reduced products of Ornidazole with different nucleic acid bases and DNA. This was done to investigate the interaction of the reduction products (here generated electrochemically) with DNA, i. e. after this category of drugs enter the cells

of a biological target that it eventually kills. Ornidazole, a molecule used in different pharmaceutical formulations [9-13] have significant medicinal applications and since drug activity essentially depends on its reduced products, it was chosen for investigation. As mentioned already, reduction of Ornidazole in aqueous solution was done by maintaining a glassy carbon electrode at its determined reduction potential identified prior to the start of the actual experiment (Figure 1). Nucleic acid bases or DNA with which reduction products generated on Ornidazole would interact were taken in an electrochemical cell along with Ornidazole. Reduction products of Ornidazole interact with a biological target kept in the immediate vicinity of its generation, taken one at a time during the experiments performed. There exists the possibility of the appearance of  $R\text{-NO}_2^{\bullet-}$  by comproportionation of  $R\text{NO}_2$  and  $R\text{NHOH}$  and subsequent disappearance by disproportionation [14, 16]. However, if there be a substrate, with which  $R\text{-NO}_2^{\bullet-}$  could interact then as normally expected, possibility of disproportionation decreases drastically unless the rate of disproportionation is significantly greater than the reaction of  $R\text{-NO}_2^{\bullet-}$  with a biological target. Usually this is not the case since concentration of the biological target in such experiments is a lot higher than the electrochemically reducible substance (here Ornidazole) [16].

### **HPLC Studies**

The amount of each nucleic acid base remaining after the experiment was determined with the help of HPLC using a C-18 column and 5% aqueous methanol as the mobile phase in case of thymine, cytosine and adenine and 40% aqueous methanol for guanine. HPLC profiles of pyrimidine base cytosine and purine base adenine following their damage after subjecting them to interaction with the reduction products of Ornidazole are obtained at 254nm shown in the Figures 2 & 3 respectively. Figures 4 & 5 are those for thymine and guanine respectively.

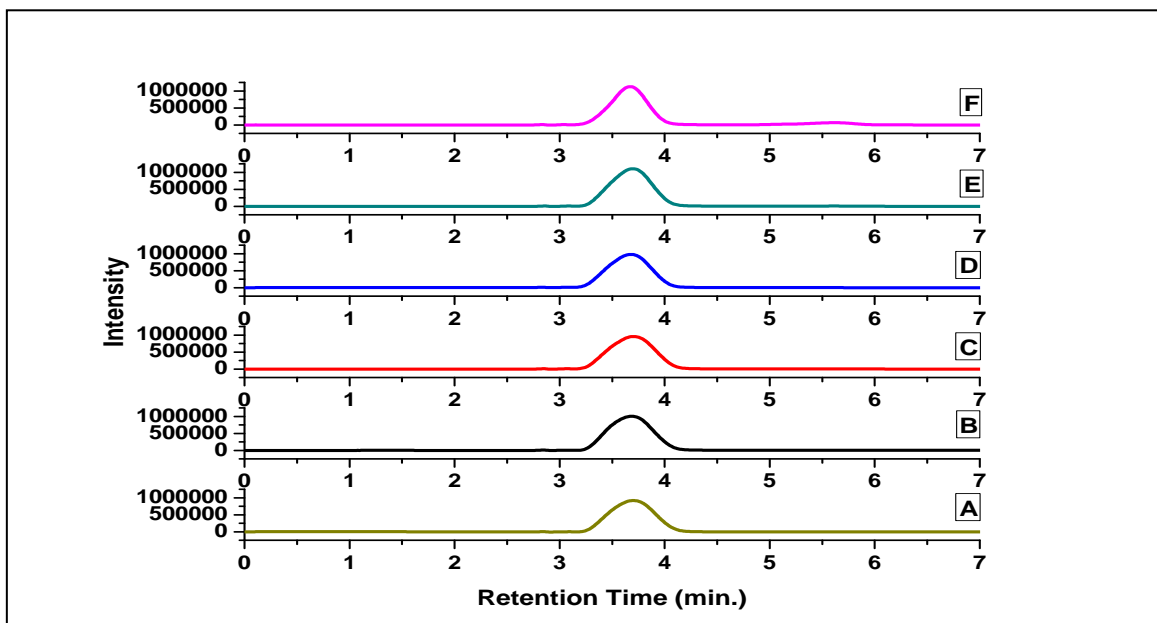


**Figure 2:** HPLC chromatograms recorded at 254 nm for  $1 \times 10^{-3} \text{ mol dm}^{-3}$  cytosine solution that was subjected to a potential of  $-0.827 \text{ V}$  in presence of  $1 \times 10^{-4} \text{ mol dm}^{-3}$  Ornidazole under Ar saturated conditions. A-F indicates the time in minutes that the potential was applied on the solution; A: 0 minutes, B: 2 minutes, C: 4 minutes, D: 6 minutes, E: 8 minutes, F: 10 minutes.

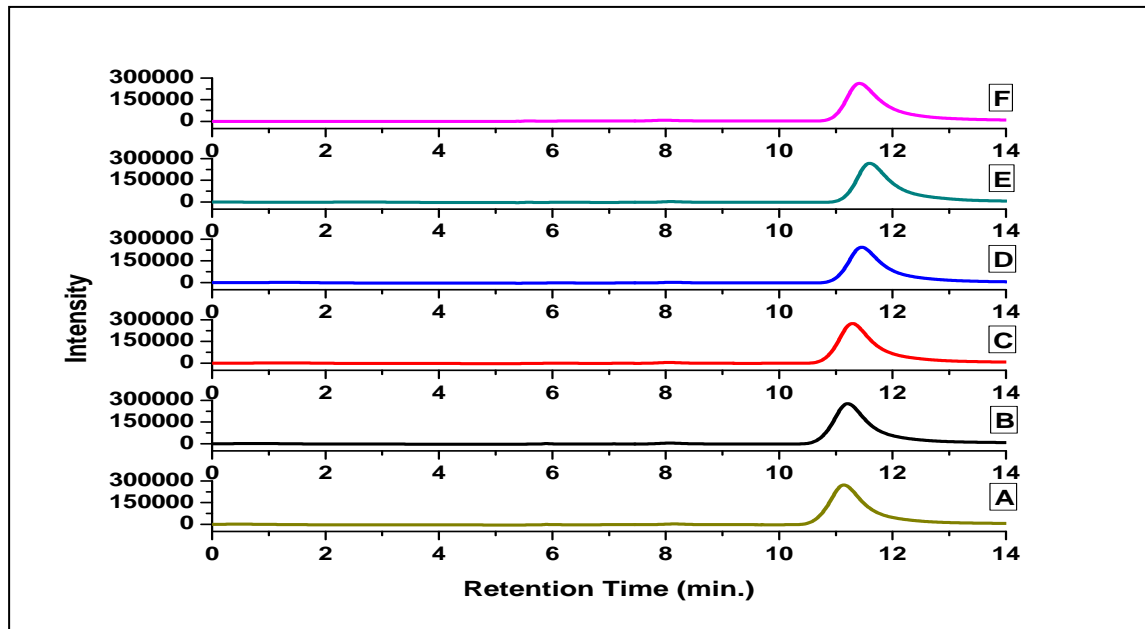


**Figure 3:** HPLC chromatograms recorded at 254 nm for  $1 \times 10^{-3} \text{ mol dm}^{-3}$  adenine solution that was subjected to a potential of  $-0.827 \text{ V}$  in presence of  $1 \times 10^{-4} \text{ mol dm}^{-3}$  Ornidazole under Ar saturated conditions. A-F indicates the time in minutes that the potential was applied on the solution; A: 0 minutes, B: 2 minutes, C: 4 minutes, D: 6 minutes, E: 8 minutes, F: 10 minutes.

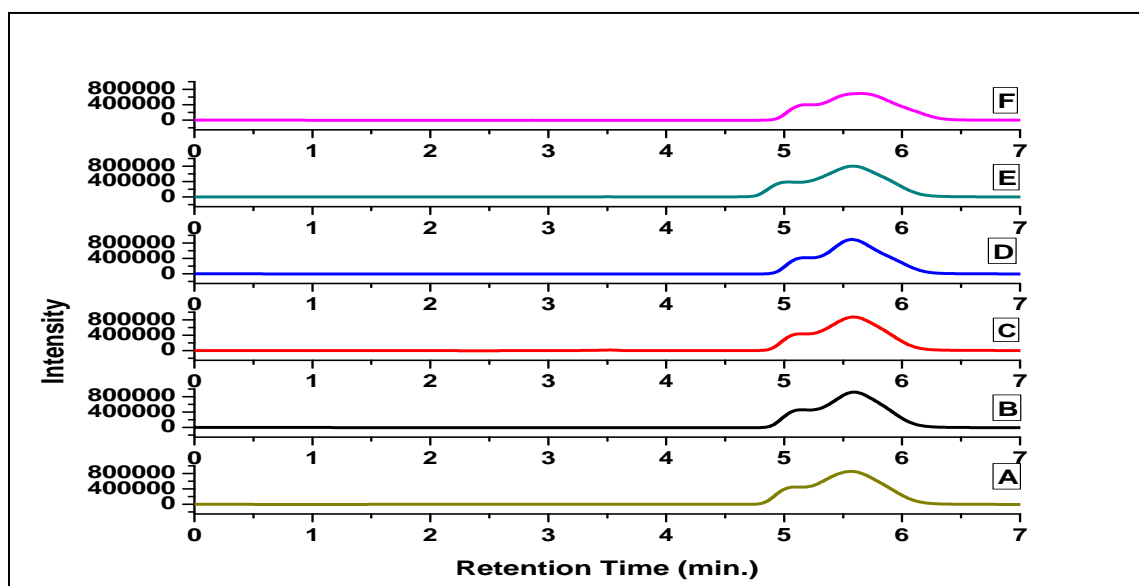


**Figure 4:** HPLC chromatograms recorded at 254 nm for  $1 \times 10^{-3} \text{ mol dm}^{-3}$  thymine solution that was subjected to a potential of  $-0.827 \text{ V}$  in presence of  $1 \times 10^{-4} \text{ mol dm}^{-3}$  Ornidazole under Ar saturated conditions. A-F indicates the time in minutes that the potential was applied on the solution; A: 0 minutes, B: 2 minutes, C: 4 minutes, D: 6 minutes, E: 8 minutes, F: 10 minutes.

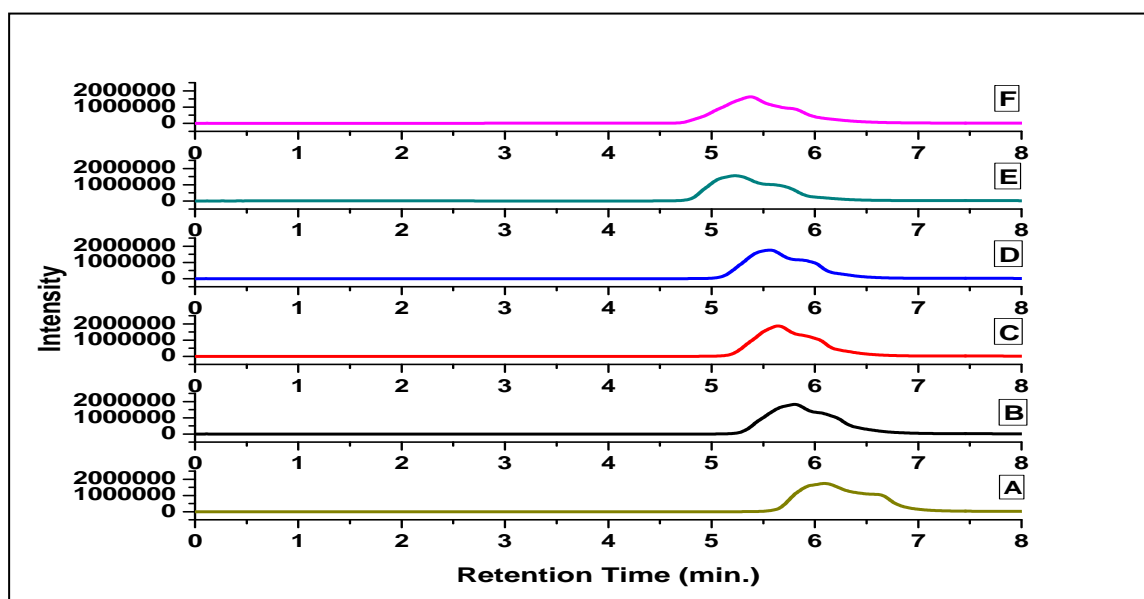


**Figure 5:** HPLC chromatograms recorded at 254 nm for  $1 \times 10^{-3} \text{ mol dm}^{-3}$  guanine solution that was subjected to a potential of  $-0.827 \text{ V}$  in presence of  $1 \times 10^{-4} \text{ mol dm}^{-3}$  Ornidazole under Ar saturated conditions. A-F indicates the time in minutes that the potential was applied on the solution; A: 0 minutes, B: 2 minutes, C: 4 minutes, D: 6 minutes, E: 8 minutes, F: 10 minutes.

Figures (2-5) indicate as time for the electrochemical reduction of Ornidazole increased gradually during experiment, a distinct change was observed in the area obtained for the eluting nucleic acid base. Base damage was subsequently identified by plotting percentage nucleic acid base remaining against the time provided to generate reduction products of Ornidazole using a glassy carbon electrode maintained at  $-0.827\text{ V}$  in aqueous solution at pH 7.2. Figure 6 shows this for cytosine and adenine while Figure 7 is for thymine and guanine.

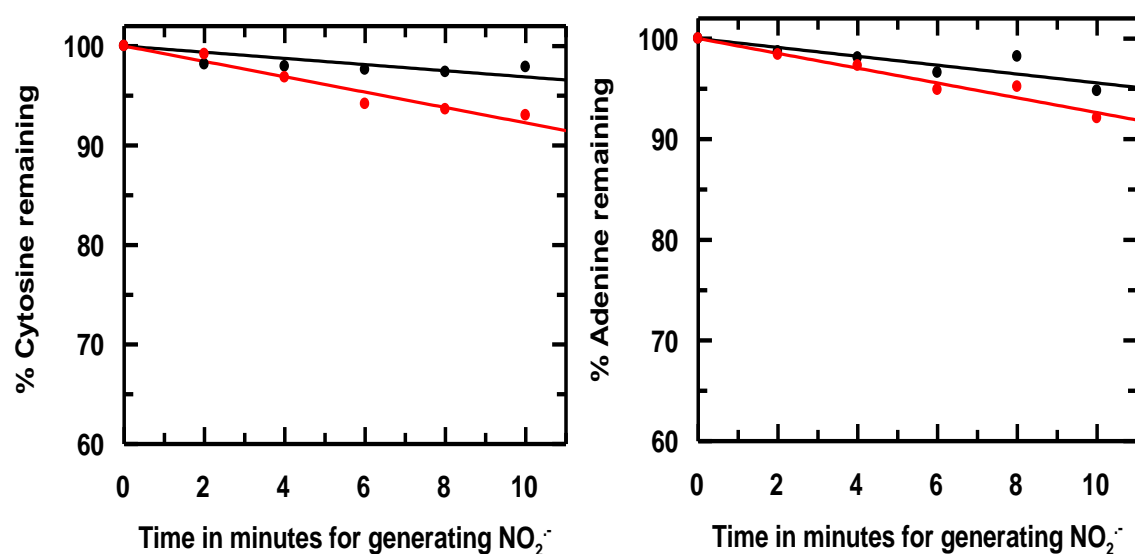


**Figure 6:** Nucleic acid base degradation plots for cytosine and adenine followed by HPLC at 254 nm after the compounds were subjected to a potential of  $-0.827\text{ V}$  under Ar saturated conditions in the absence and presence of a sensitizer molecule (Ornidazole);  $[\text{Ornidazole}] = 1 \times 10^{-4}\text{ mol dm}^{-3}$ . Black line indicates the absence of Ornidazole while the red line its presence.

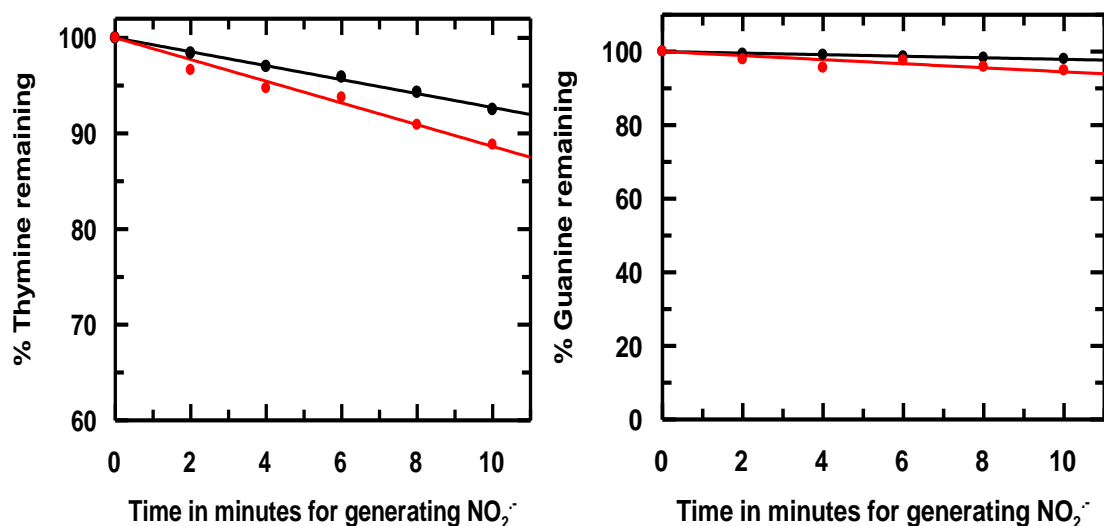


**Figure 7:** Nucleic acid base degradation plots for thymine and guanine followed by HPLC at 254 nm after the compounds were subjected to a potential of -0.827 V under Ar saturated conditions in the absence and presence of a sensitizer molecule (Ornidazole); [Ornidazole] =  $1 \times 10^{-4}$  mol dm<sup>-3</sup>. Black line indicates the absence of Ornidazole while the red line its presence.

### Fluorescence study

A similar study as described above was also performed keeping calf thymus DNA in the immediate vicinity of the generated reduction products of Ornidazole using a glassy carbon electrode maintained at -0.827 V in aqueous solution at pH 7.2. The only difference for the study with DNA was that slightly longer times were used in applying the reduction potential so that more reduction products of Ornidazole could be generated for enabling a visible recognition of the change i. e. modification caused to DNA upon its monitoring by the ethidium bromide-fluorescence technique [18-20]. Figure 8 shows a plot of the fluorescence following interaction of such treated calf thymus DNA with ethidium bromide that was subjected to an excitation at 510 nm using a fluorescence spectrophotometer.

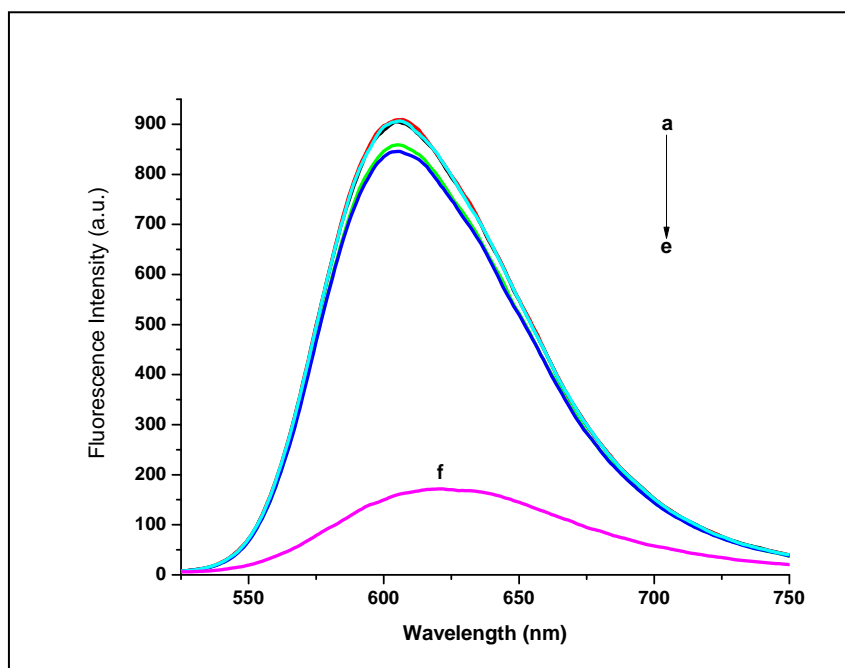


**Figure 8:** Fluorescence spectra of calf thymus DNA after treatment with ethidium bromide, following the DNA being subjected to a potential of  $-0.827$  V in the presence of  $1 \times 10^{-4} \text{ mol dm}^{-3}$  Ornidazole under Ar saturated conditions. (a-e) indicates the time in minutes for which the desired potential was applied to the solution; a: 0 minutes, b: 5 minutes, c: 10 minutes, d: 15 minutes, e: 20 minutes; f denotes the spectrum of ethidium bromide alone.

Modification caused to calf thymus DNA was realized by plotting the percentage of DNA remaining against the time provided to generate reduction products of Ornidazole using a glassy carbon electrode maintained at  $-0.827$  V in aqueous solution at pH 7.2 (Figure 9).

The outcome of the study is summarized in Table 1 (provided below), where we see that nucleic acid base damage inflicted on Cytosine and Guanine are much higher than that caused to thymine or adenine. It is also seen that enhancement ratio obtained for Cytosine and Guanine in presence of Ornidazole tallies appreciably with that obtained for calf thymus DNA. Since in calf thymus DNA percentage of Cytosine and Guanine is much higher than that of thymine and adenine it may be said that having some prior knowledge on the damage

inflicted by a certain molecule on a particular nucleic acid base, one can have an idea as to which type of DNA is more likely to be affected.

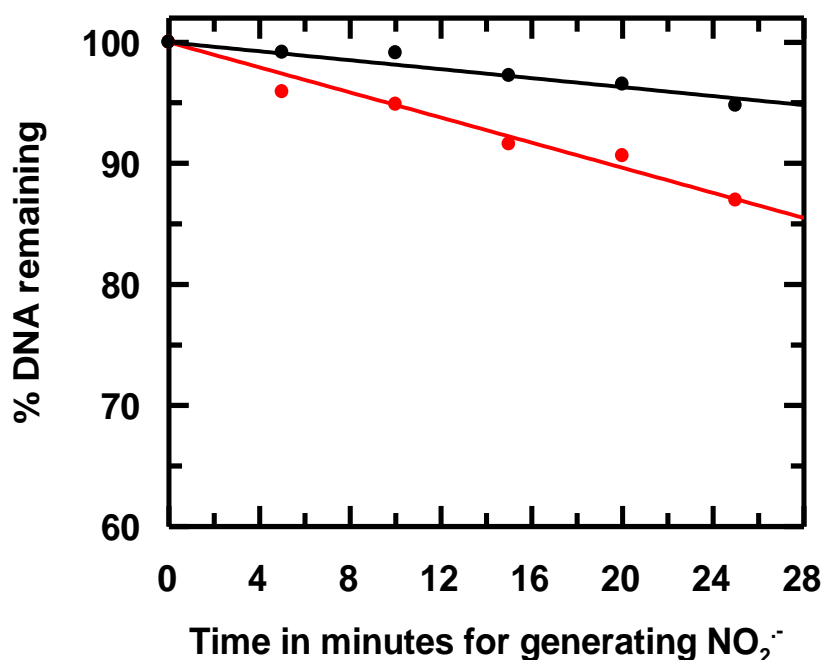


**Figure 9:** A plot for calf thymus DNA modification in the absence and presence of a sensitizer molecule (Ornidazole) after being subjected to a potential of -0.827 V under Ar saturated conditions; [Ornidazole] =  $1 \times 10^{-4}$  mol dm<sup>-3</sup>. Black line indicates the absence of Ornidazole while the red line its presence.

From this study it is evident that reduction products of Ornidazole modify nucleic acid bases as well as calf thymus DNA forming reactive intermediates that subsequently undergo reactions to give different compounds. As a result both purine and pyrimidine bases are degraded which was then correlated with that observed with calf thymus DNA. The nucleotide content of the DNA of a target organism is known, one can provide a good correlation between this study and any actual drug action reported (Table 2). The study provides a logical explanation as to why compounds containing ornidazole were either found to be active on GC rich DNA containing species or on species having a substantial presence of GC in their DNA [21-23].

**Table 1: Shows enhancement ratios for the damage caused to nucleic acid bases and calf thymus DNA in the presence of ornidazole for the study described above.**

Compound	T A R G E T									
	Adenine		Thymine		Cytosine		Guanine		Calf thymus DNA	
	Slope in Ar saturated medium	E R	Slope in Ar saturated medium	E R	Slope in Ar saturated medium	E R	Slope in Ar saturated medium	E R	Slope in Ar saturated medium	E R
–	-0.44	–	-0.73	–	-0.31	–	-0.21	–	-0.19	–
<b>Ornidazole</b>	-0.74	1.68	-1.14	1.56	-0.77	2.48	-0.55	2.62	-0.52	2.74

**Table 2: Aflox Oz, Alox-ON, Arrow–Ornidazole, Cefit –OZ, Oxit OZ, Fynal OZ (containing ornidazole as major constituent) is used for treatment of infections caused by:**

<u>Microbes</u>	<u>G-C content</u>
1. <i>Haemophilus influenza</i>	<b>38.0 %</b>
2. <i>Streptococcus pneumonia</i>	<b>39.7%</b>
3. <i>Staphylococcus aureus</i>	<b>33.0 %</b>
4. <i>Streptococcus pyogenes</i>	<b>38.5%</b>
5. <i>Proteus mirabilis</i>	<b>28.8%</b>
6. <i>Neisseria gonorrhoeae</i>	<b>52.4%</b>
7. <i>Chlamydia trachomatis</i>	<b>40.3%</b>
8. <i>Escherichia coli</i>	<b>50.9%</b>
9. <i>Moraxella catarrhalis</i>	<b>38.0 %</b>
10. <i>Citrobacterdiversus</i>	<b>51.0 %</b>
11. <i>Enterobacteraerogenes</i>	<b>64.0 %</b>
12. <i>Klebsiella pneumonia</i>	<b>57.4 %</b>
13. <i>Pseudomonas aeruginosa</i>	<b>65.0 %</b>
14. <i>Staphylococcus saprophyticus</i>	<b>33.0 %</b>
15. <i>Enterococcus faecalis</i>	<b>37.4 %</b>

16. <i>Enterobacter cloacae</i>	54.5 %-55.1%
17. <i>Serratiamarcescens</i>	58.0 %
18. <i>Haemophilusparainfluenzae</i>	38.0 %- 40.0 %
19. <i>Legionella pneumophila</i>	38.0 %
20. <i>Staphylococcus epidermidis</i>	32.0 %
21. <i>Bacillus anthracis</i>	35.4%
22. <i>Yersinia pestis</i>	47.5%

## References

1. S. L. Cudmore, K. L. Delgaty, S. F. Haywrad-McClelland, D. P. Petrin, G. E. Garber, *Clin. Microbiol. Rev.*, **2004**, 17, 783-793.
2. D. I. Edwards, Comprehensive Medicinal Chemistry, Eds.: C. Hansch, P. G Sammes, J. B. Taylor, Pergamon Press Oxford, **1990**, vol. 2, pp.725-751.
3. R. P. Mason, Free Radicals in Biology, Eds.: W. A. Pryor, Vol. V, Academic Press New York, **1982**, pp. 161-222.
4. S. Sood, A. Kapil, *Ind. J. Sex Transm. Dis.*, **2008**, 29, 7-14.
5. D. Petrin, K. Delgaty, R. Bhatt, G. Garber, *Clin. Microbio. Rev.*, **1998**, 11, 300-317.
6. E. J. Hall, R. Miller, M. Astro, F. Rini, *Br J Cancer Suppl.*, **1978**, 3, 120-128.
7. M. Bonnet, C. R. Hong, W. W. Wong, L. P. Liew, A. Shome, J. Wang, Y. Gu, R. J. Stevenson, W. Qi, R. F. Anderson, F. B. Pruijn, W. R. Wilson, S. M. F. Jamieson, K. O. Hicks, M. P. Hay, *J. Med. Chem.* , **2018**, 61(3), 1241-1254.
8. R. Sharma, *Current Radiopharmaceuticals*, **2011**, 4, 1-15.
9. R. C. Santra, D. Ganguly, D. Bhattacharya, P. Karmakar, A. Saha, S. Das, *New J. Chem.*, **2017**, 41, 11679-11685.
10. J. Thulkar, A. Kriplani, N. Agarwal, *Ind. J Pharmacol.* **2012**, 44, 243-245.
11. O. Kurt, N. Girginkardeşler, I. C. Balcioglu, A. Ozbilgin, U. Z. Ok, *Clin. Microbiol. Infect.* **2008**, 14, 601-604.
12. B. Oren, E. Schgurensky, M. Ephros, I. Tamir, R. Raz, *Eur J ClinMicrobiol InfectDis.* **1991**, 10, 963-965.

13. A. Khryanin, O. Reshetnikov, *Int. J. Antimicrob. Agents*, **2007**, 29, S220.
14. M. H. Wilcox, 147-Nitroimidazoles, Metronidazole, Ornidazole and Tinidazole; and Fidaxomicin In: *Infectious Diseases*, 4th Edition, Ed.: J. Cohen, W. G. Powderly, S. M. Opal, Volume 2, **2017**, Pages 1261-1263.e1.
15. J. A. Squella, S. Bollo, L.J. Núñez-Vergara, *Curr. Org. Chem.*, **2005**, 9, 565-581.
16. P. C. Mandal, *J. Electroanal. Chem.*, **2004**, 570, 55-61.
17. R. C. Santra, D. Ganguly, J. Singh, K. Mukhopadhyay, S. Das, *Dalton Trans.*, **2015**, 44, pp. 1992-2000.
18. A. R. Morgan, J. S. Lee, D. E. Pulleyblank, N. L. Murray, D. H. Evans, *NucleicAcids Res.* **1979**, 7, 547-569.
19. H. C. Birnboim, J. J. Jevcak, *Can. Res.*, **1981**, 41, 1889.
20. S. Das, A. Saha, P. C. Mandal, *Environ. Health Pers.* **1997**, 105,1459-1465.
21. F. S. Lehmann, J. Drewe, L. Terracciano, C. Beglinger, *Aliment Pharmacol. Ther.*, **2000**, 14, 305-309.
22. T. B. Gardner, D. R. Hill, *Clin. Microbiol. Rev.*, **2001**, 14, 114–128. DOI: 10.1128/CMR.14.1.114–128.2001.
23. L. Jokipii, A. M. M. Jokipii, *Gastroenterology*, **1982**, 83, 399-404.

## **Chapter 11**

***In situ* reactivity of electrochemically generated  
nitro radical anion on a monomeric Cu<sup>II</sup>  
complex of ornidazole; interaction with nucleic  
acid bases and calf thymus DNA**

## Introduction

Although a large body of literature identifies the fact that a reduced nitro group is crucial for activity of 5-nitroimidazoles [11, 13, 30], only few studies have investigated its role in detail [18, 19]. After entering the biological target cell, antimicrobial activity of nitroimidazoles depend upon the reduction of the nitro group to a nitro radical-anion ( $\text{NO}_2^{\bullet-}$ ) and/or other potentially active reduction products that includes nitroso and hydroxylamine derivatives [11, 30]. Reduced species of nitroimidazoles are damaging to various macromolecules including the DNA, bringing about their degradation through modification of strands [11, 13, 30]. It has been shown earlier that complex formation is able to modulate (decrease) the formation of  $\text{NO}_2^{\bullet-}$  which is expected to decrease toxic side effects [13, 14]. In this *chapter* we tried to look into aspects of cytotoxicity initiated by  $\text{NO}_2^{\bullet-}$  and other reduction products of a monomeric Cu(II) complex of Onz on nucleic acid bases and calf thymus DNA to correlate what really happens when similar molecules are enzymatically reduced within the biological system to different species [1, 6, 7, 12, 13]. Reduction products of the complex were generated electrochemically by maintaining a glassy carbon electrode at its determined cathodic potential. In the immediate vicinity of such electrochemically generated reduction products, nucleic acid bases and calf thymus DNA were maintained so that reduced products formed on the complex react with them. *In situ* reactivity of such generated reduction products with nucleic acid bases or DNA was subsequently followed to realize changes brought about on the target.

## Results and Discussions

### Cyclic voltammetry studies in different solvents

Electrochemical behavior of ornidazole and its  $\text{Cu}^{\text{II}}$  complex were studied with the help of cyclic voltammetry. Compounds were dissolved in methanol, DMF and water having concentration  $10^{-3}$  M. Cyclic voltammograms (Figure 1 and Figure 2) were obtained in

different solvents using a potentiostat/galvanostat. In aqueous medium, and in methanol, Onz and its  $\text{Cu}^{\text{II}}$  complex undergo a one step four electron reduction while in DMF the compounds underwent a one electron followed by three electron reduction.

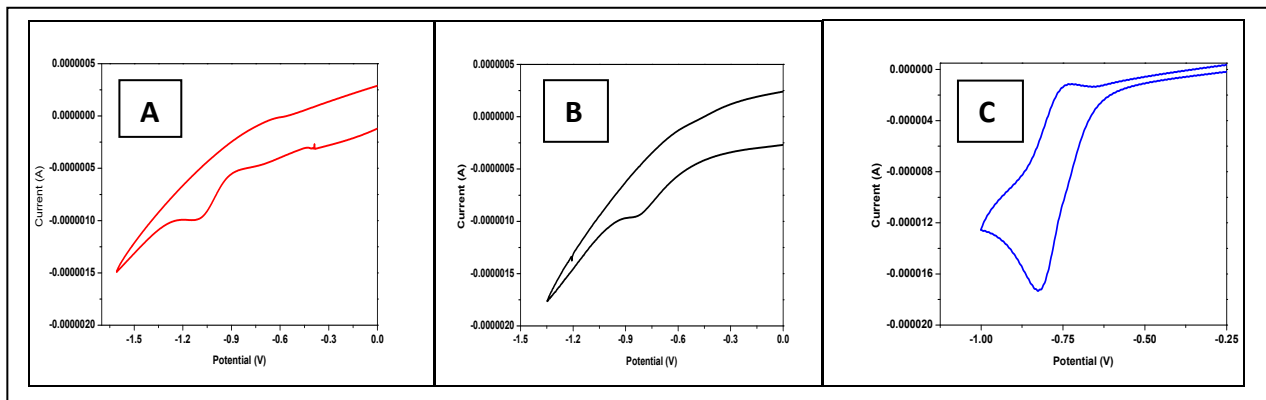


**Figure 1:** Cyclic voltammogram of 1 mM Onz in (A) DMF, (B) methanol and (C) water. In case of water, a single step four electron reduction of the nitro group is observed in 0.12 M KCl solution using a glassy carbon electrode; Scan rate 100mV/sec.

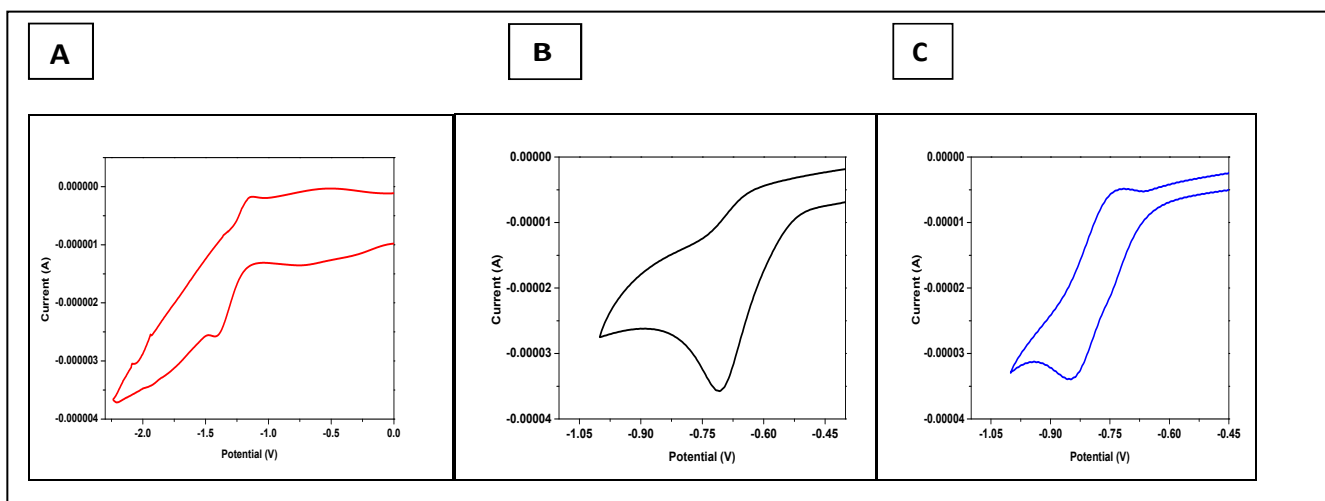
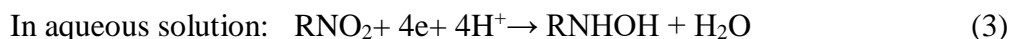


**Figure 2:** Cyclic voltammogram of 1 mM  $[\text{Cu}(\text{Onz})_2\text{Cl}_2]$  in (A) DMF, (B) methanol and (C) water. In case of water, a single step four electron reduction of the nitro group is observed in 0.12 M KCl solution using a glassy carbon electrode; Scan rate 100mV/sec.

### ***In situ* reactivity of electrochemically generated reduction products**

When the medium is aprotic, 5-nitroimidazoles participate in a reversible one-electron reduction initially forming a nitro radical anion, which then undergoes an irreversible three-electron reduction to  $\text{-NHOH}$  [18-20]. In aqueous solution, however, these two steps are not realized separately and a single step four electron reduction is observed [18-20]. The same is true for the monomeric  $\text{Cu}^{\text{II}}$  complex of Onz as well (Figure 4).



The cathodic peak current ( $I_{\text{pc}}$ ) in amperes at  $-0.827$  V was plotted against square root of potential sweep rate ( $v^{1/2}$ ) (Figure 3) to see if the process was diffusion controlled; the same being an essential criteria for the actual experiment to be performed.

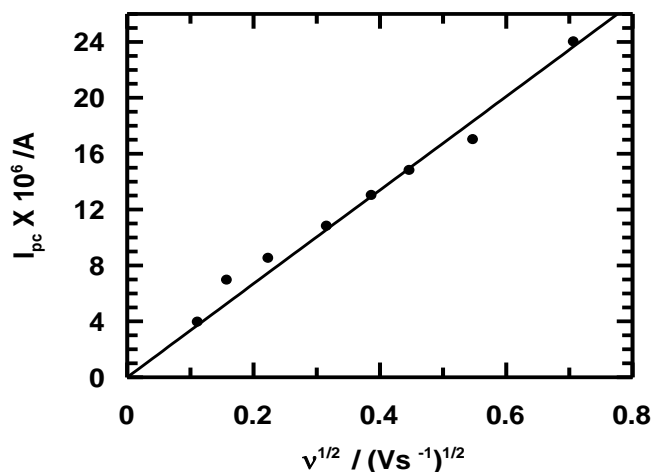


**Figure 3:** Plot of cathodic peak current ( $I_{\text{pc}}$ ) vs. square root of scan rate ( $v$ ) for a four-electron reduction of  $[\text{Cu}(\text{Onz})_2\text{Cl}_2]$  in aqueous solution at a potential of  $-0.849$  V,  $\text{pH} \sim 7.2$ .

Hence, in the immediate vicinity of the  $\text{Cu}^{\text{II}}$  complex subjected to electrochemical reduction at a previously determined potential of  $-0.849$  V (Figure 2C), if a target is maintained, there is

a possibility that reduction products from the complex would interact with the target. The outcome of such interactions (i. e. modifications caused) was ascertained for nucleic acid bases and calf thymus DNA. Since in aprotic media, the reversible one-electron reduction step forming  $\text{NO}_2^{\bullet-}$  can be identified separately, it is possible to assign interactions to it. However, in aqueous solution when a glassy carbon electrode is maintained at the cathodic potential of the complex i.e. at its “one step four electron reduction” potential, many species are generated. Therefore, the problem in aqueous solution is that a correct assignment of species (from amongst different reduction products) responsible for interaction with the target is not clearly possible.

More specifically, it should be said that it cannot be exclusively assigned to the formation of  $-\text{NO}_2^{\bullet-}$  because other reduction products are also formed in solution following an electrochemical reduction of the complex at  $-0.849\text{ V}$  (Eq. 1-3). At the same time, it is also true since formation of species containing  $-\text{NO}_2^{\bullet-}$  is the first step of the reduction process and since it is a radical, it should have a very high probability to interact with a target present in its immediate vicinity; in fact higher than successive reduction to other species (Eq. 2) [19]. Hence, although other reduction products of the complex could well be involved in modifying a target,  $-\text{NO}_2^{\bullet-}$  could have a substantial contribution to the damage caused to the target. The present study was performed to realize how different reduction products (generated electrochemically) on a 5-nitroimidazole or its complex might interact with nucleic acid bases or with DNA that might help to explain what happens when such drugs or their complexes enter the cells of a biological target. For a long time it is believed that drugs belonging to this class upon getting a favorable reduction potential must primarily be reduced to be active; established by several studies as the principle mechanism for the action of nitroimidazoles [4-9, 11]. It is also believed that these reduced products thereafter interact with DNA, however nothing very specific could be found for interactions at the cellular level

barring a few reports [1-17]. Previous reports suggest the ability of different Cu<sup>II</sup> complexes of 5-nitroimidazoles to significantly modulate the formation of NO<sub>2</sub><sup>•-</sup>, essential for curbing neuro-toxic side effects [13, 14]. In those reports, it was shown that in spite of decreased -NO<sub>2</sub><sup>•-</sup>, efficacy was not compromised due to the complexes; in fact complexes were mostly at par with the performance of 5-nitroimidazoles i. e. from which complexes were prepared. In some cases, complexes performed even better than the parent drug; tried on different biological targets [12-14]. Hence, the question that immediately comes up is, if generation of -NO<sub>2</sub><sup>•-</sup> is so essential for drug action, established by many studies, how then are Cu<sup>II</sup> complexes of 5-nitroimidazoles, with decreased -NO<sub>2</sub><sup>•-</sup> formation still so active, matching the efficacy of the respective drug molecule [12-14]. This prompted us to find out whether the mechanism of action of 5-nitroimidazoles and their Cu<sup>II</sup> complexes similar or different.

#### **Interaction of electrochemically generated reduction products on the complex with nucleic acid bases**

We reduced Onz using a glassy carbon electrode maintained at a constant potential of -0.827 V in aqueous solution, and showed that it modified nucleic acid bases and DNA (the target). Next modifications caused to similar targets by the Cu<sup>II</sup> complex of Onz were followed. Reduction products generated on the complex interact with the target kept in their immediate vicinity. Considering different reduction products formed there is a high possibility for the formation of a species containing -NO<sub>2</sub><sup>•-</sup> following comproportionation between a -NO<sub>2</sub> containing moiety on a complex and an -NHOH on another, either present on another Onz of the same complex or on an Onz of another complex. There is also the possibility of the disappearance of -NO<sub>2</sub><sup>•-</sup> by disproportionation [19, 26].

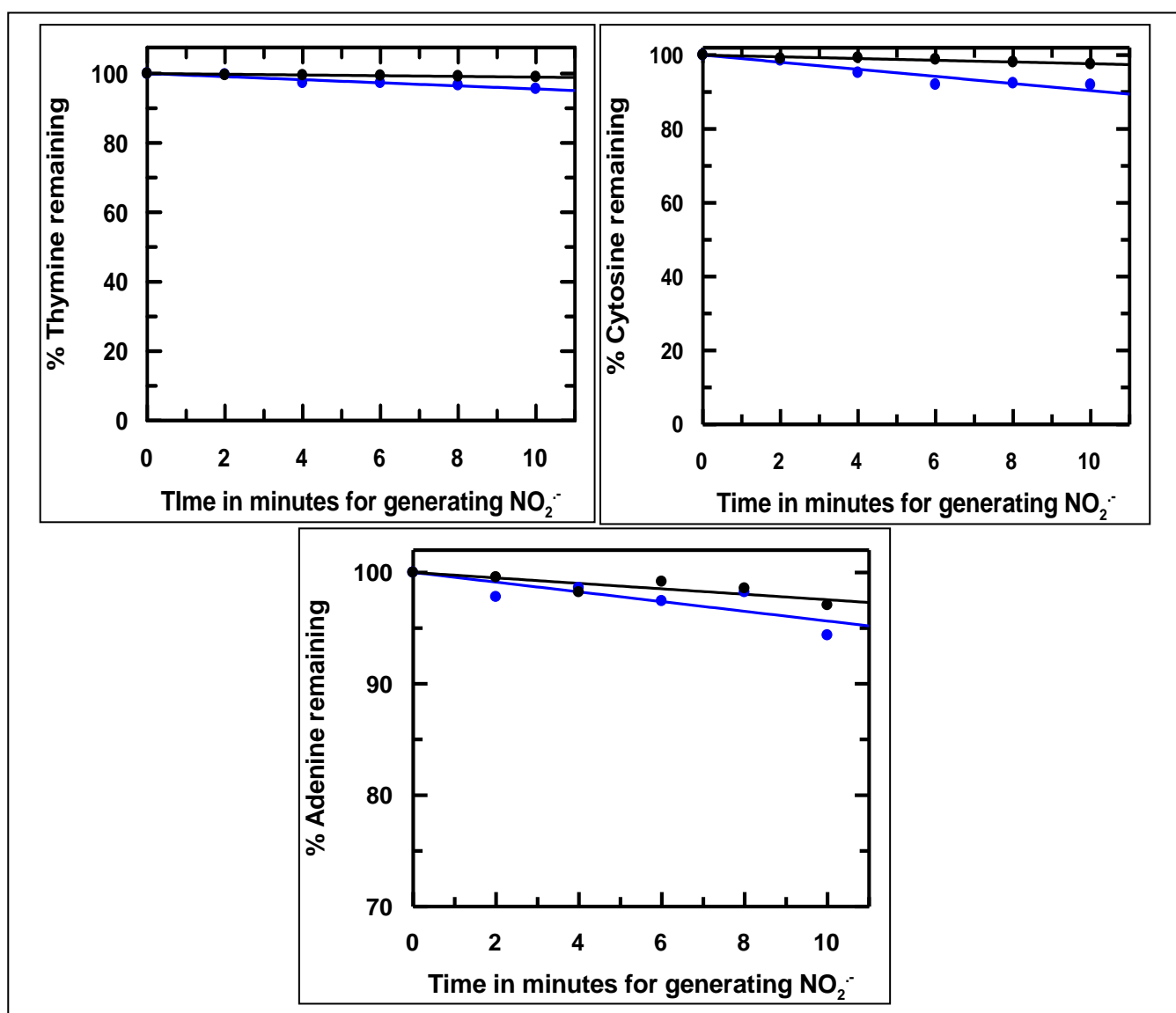


**Figure 4:** Degradation of thymine, cytosine and adenine followed by HPLC at 254 nm after being allowed to interact with nitro-radical anion that is generated from the monomeric complex of  $\text{Cu}^{\text{II}}$  with Ornidazole (blue line) following electrochemical reduction of the complex in aqueous DMF at a constant potential of  $-0.828\text{ V}$  (the first one-step reduction potential) under de-aerated ( $\text{Ar}$  saturated) conditions. The black lines indicate degradation of the respective nucleic acid base in the absence of the sensitizer in the same medium at the same potential.  $[\text{nucleic acid base}] = 1 \times 10^{-3}\text{ mol dm}^{-3}$ ;  $[\text{Cu(II)-Onz complex}] = 1 \times 10^{-4}\text{ mol dm}^{-3}$ .

However, since a substrate is present in solution with which  $-\text{NO}_2^{\bullet-}$  can interact there is a high possibility of it being consumed in that pathway. Hence,  $-\text{NO}_2^{\bullet-}$  depletion by disproportionation should be less unless the rate of disproportionation of species containing  $-\text{NO}_2^{\bullet-}$  (generated on the complex) is significantly higher than the rate of reaction between the generated  $-\text{NO}_2^{\bullet-}$  and a target (nucleic acid base or DNA). Besides, although disproportionation is a possibility, it cannot logically happen since the concentration of the target maintained in such experiments are almost ten times higher than the complex. Therefore, concentrations of electrochemically reduced species formed on the complex in solution in comparison to the target would be even less i. e.  $< 1:10$ , implying there would be very little scope for disproportionation. Consequently, although qualitatively explained, it can be realized that  $-\text{NO}_2^{\bullet-}$  could eventually be an important species amongst different reduced forms generated on the complex in solution that could interact with the target [19]. However, to be more sure, we performed another set of experiments (Figure 4), where we dissolved nucleic acid bases (thymine, cytosine and adenine) and the Cu(II) complex of Onz in DMF having the same concentrations as that for experiments in aqueous solution. Since when DMF is the solvent, the one electron reduction step of  $-\text{NO}_2$  containing moieties to  $-\text{NO}_2^{\bullet-}$  can be separately realized, this time the glassy carbon electrode was maintained at the first reduction potential ( $-0.828\text{V}$ ) of the complex. Hence,  $-\text{NO}_2^{\bullet-}$  was generated exclusively. Therefore, in DMF interaction with the target could be assigned to  $-\text{NO}_2^{\bullet-}$ .

HPLC chromatograms of pyrimidine and purine based nucleic acid bases were recorded following interaction with different reduced species of the complex in aqueous solution. Figure 5 shows HPLC chromatograms for thymine, adenine and cytosine, recorded following the performing of experiments in aqueous solution. Figure 6 indicates as time for electrochemical reduction of the complex at its determined reduction potential increased, a

distinct change was observed for area under the peaks in HPLC chromatograms of eluting nucleic acid bases. Hence, damage caused to a nucleic acid base could be ascertained.

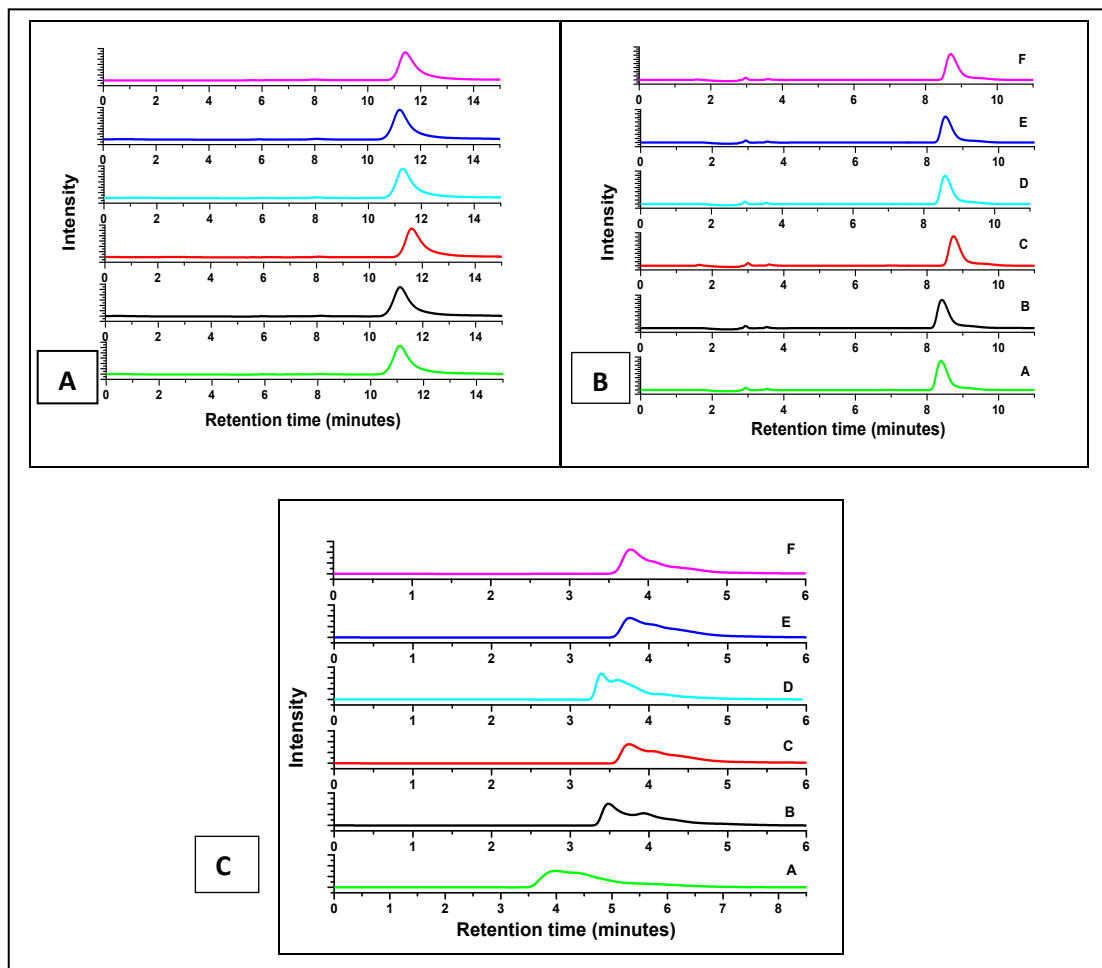


**Figure 5:** HPLC chromatograms recorded at 254 nm for  $1 \times 10^{-3} \text{ mol dm}^{-3}$  of (A) thymine, (B) adenine and (C) cytosine solutions subjected to a constant potential of  $-0.849 \text{ V}$  in presence of  $1 \times 10^{-4} \text{ mol dm}^{-3} \text{ Cu(II)-Onzunderdearated}$  (Argon saturated) conditions. A to F indicates the time in minutes for which such constant potential was applied to the solution; A: 0 minutes, B: 2 minutes, C: 4 minutes, D: 6 minutes, E: 8 minutes, F: 10 minutes.

This was done by plotting percentage of nucleic acid base remaining against time provided for electrochemical generation of reduction products on the complex, maintaining a glassy carbon electrode either at  $-0.849 \text{ V}$  in aqueous solution (pH 7.0) or at  $-0.828 \text{ V}$  in DMF.

Changes observed for each nucleic acid base following interaction with reduction products of the complex in aqueous solution is shown in Figure 6, Table 1 and that in DMF in Figure 4 and Table 2.

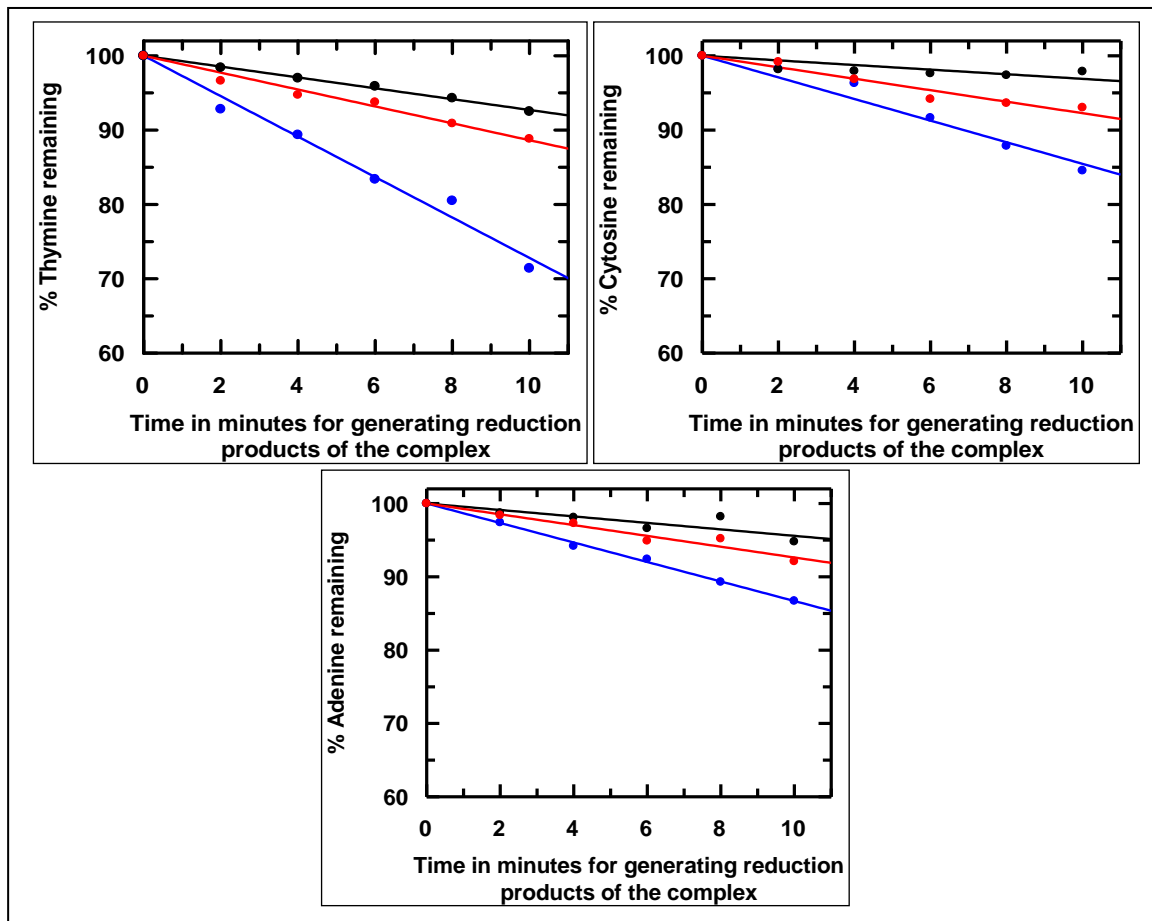


**Figure 6:** Degradation of thymine, cytosine and adenine followed by HPLC at 254 nm after being allowed to interact with reduction products generated from Ornidazole (red line) and the monomeric Cu(II)-Ornidazole complex (blue line) following electrochemical reduction of the compounds at constant potentials of -0.827 V and -0.849 V respectively under de-aerated (Argon saturated) conditions. The black line indicates degradation of the respective nucleic acid base in the absence of a sensitizer [Onz or Cu(II)-Onz] when subjected to a potential of -0.835 V. [nucleic acid base] =  $1 \times 10^{-3} \text{ mol dm}^{-3}$ ; [Ornidazole] = [Cu(II)-Onz complex] =  $1 \times 10^{-4} \text{ mol dm}^{-3}$ .

**Table 1: Enhancement ratio for damage of nucleic acid bases and calf thymus DNA following reduction of Ornidazole and its Cu<sup>II</sup> complex at their respective reduction potentials in aqueous solution generating different products that interact with the target.**

COMPOUND	TARGET									
	Adenine		Guanine		Thymine		Cytosine		Calf Thymus DNA	
	De-aerated medium (Ar saturated)	E R								
–	-0.44	–	-0.21	–	-0.73	–	-0.31	–	-0.19	–
Ornidazole	-0.74	1.68	-0.55	2.62	-1.14	1.56	-0.77	2.48	-0.52	2.74
[Cu(Onz) <sub>2</sub> Cl <sub>2</sub> ]	-1.33	3.02	-	-	-2.78	3.82	-1.45	4.66	-0.85	4.47

**Table 2: Enhancement ratio for damage of nucleic acid bases following reduction of monomeric Cu<sup>II</sup> complex of Onz at its first step one-electron reduction potential in DMF generating –NO<sub>2</sub><sup>•</sup> that interacts with targets.**

COMPOUND	T A R G E T S					
	Adenine		Thymine		Cytosine	
	De-aerated medium (Ar saturated)	E R	De-aerated medium (Ar saturated)	E R	De-aerated medium (Ar saturated)	E R
–	-0.245	–	-0.103	–	-0.233	–
[Cu(Onz) <sub>2</sub> Cl <sub>2</sub> ]	-0.436	1.78	-0.445	4.32	-0.963	4.13

A comparison of the damage inflicted on a target by the complex in DMF and that in aqueous solution helps in identification of the species responsible in each case in causing a change on the target. It was seen while damage (in terms of enhancement ratio) was significantly greater for adenine in aqueous solution than in DMF, in case of thymine it was only slightly higher in DMF and for cytosine it was slightly less in DMF than that observed in aqueous solution. Results indicate that for adenine other reduction products of the complex could be playing a

significant role besides species containing  $\text{NO}_2^{\bullet-}$ . However, in case of thymine and cytosine, the results for thymine suggest other reduction products probably do not have any major role in causing damage and that it is the  $\text{NO}_2^{\bullet-}$  species that plays the major part; for cytosine, other reduction products generated from the complex in aqueous solution (Eqs. 1-3) might be having some role in the nucleic acid's modification besides a species containing  $\text{NO}_2^{\bullet-}$ .

### **Interaction of electrochemically generated reduction products with calf thymus DNA**

A similar study as the one described above was performed by maintaining calf thymus DNA in aqueous solution at pH 7.4 in the immediate vicinity of the generated reduction products of the  $\text{Cu}^{\text{II}}$  complex of Onz using a glassy carbon electrode maintained at -0.849 V. The only difference when calf thymus DNA was the target was that slightly longer times were used for the electrochemical reduction of the complex. This was necessary to generate more reduction products on the complex so that an observable change could be detected in case of calf thymus DNA when monitored by fluorescence using EtBr, i.e. subsequent to its interaction with reduction products of the complex. Since interaction of EtBr and DNA lead to increase in fluorescence this was utilized to determine the amount of DNA remaining intact following interaction with reduced products of the complex [22, 23]. Figure 7 is a typical plot showing fluorescence of calf thymus DNA with EtBr either in the absence of any interaction with reduced products generated on the complex or having undergone an interaction with reduced products. In each case, adducts of DNA with EtBr were excited at 510 nm with the help of a fluorescence spectrophotometer (RF-530 IPC Spectrofluorophotometer, Shimadzu, Japan) [21-24] and emission was measured over the wavelength range 525 nm to 750 nm.

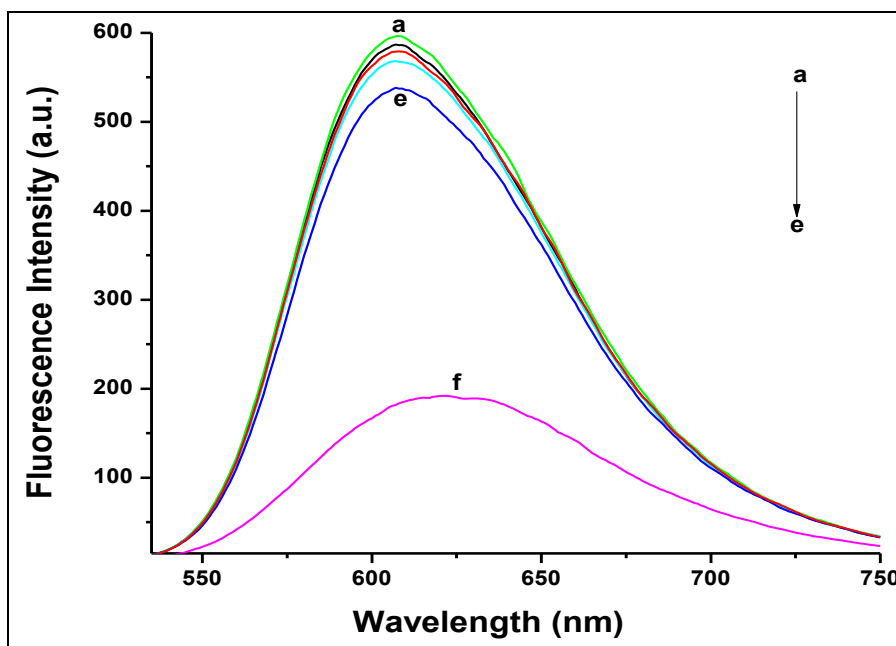


**Figure 7:** Fluorescence spectra of calf thymus DNA after treatment with EtBr following interaction of the DNA with reduction products generated from the monomeric Cu<sup>II</sup> complex of Ornidazole subjected to a constant potential at -0.849 V in de-aerated (Argon saturated) conditions. [Cu(II)-Ornidazole] =  $1 \times 10^{-4}$  mol dm<sup>-3</sup>. “a” to “e” indicates time in minutes for which such potential was applied to the solution; a: 0 minutes, b: 5 minutes, c: 10 minutes, d: 15 minutes, e: 20 minutes. “f” denotes the spectrum of EtBr when it was excited alone i. e. in the absence of DNA at 510 nm.

Modification caused to calf thymus DNA was established by plotting percentage of DNA remaining against time provided for generation of reduction products on the complex following maintenance of a glassy carbon electrode at -0.849 V in aqueous solution (pH 7.4; Figure 8).

The outcome of the study on the interaction of electrochemically generated reduced species of a Cu<sup>II</sup> complex of Onz with calf thymus DNA is summarized in Table 1. It is seen from the table, Onz affects guanine and cytosine to a much greater extent than adenine and thymine while the complex affects cytosine to a much greater extent than adenine or thymine.

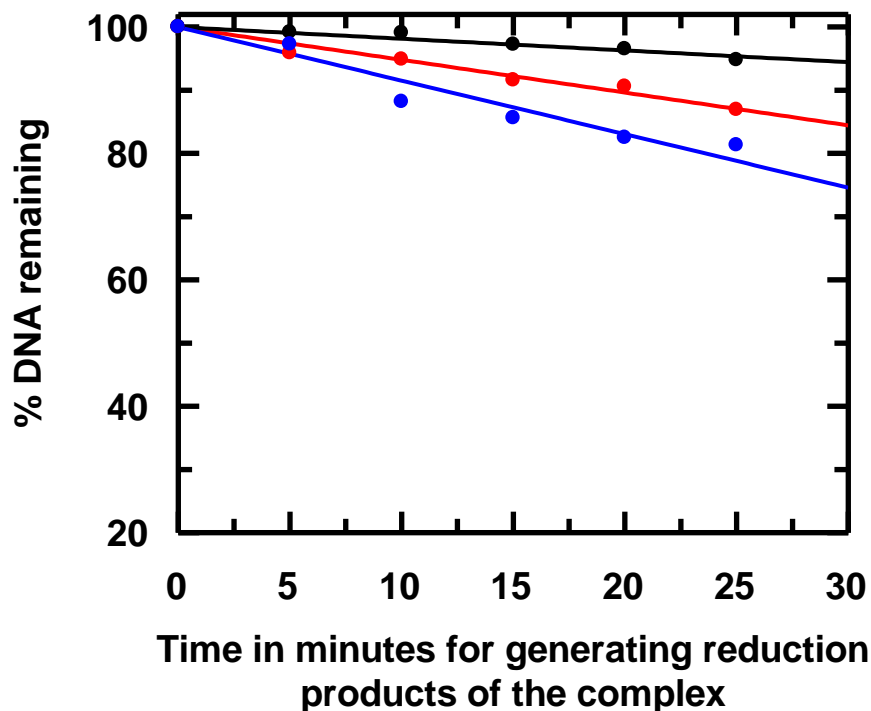


**Figure 8:** Plots showing modification of calf thymus DNA in the absence (black) and presence of sensitizer molecules, Ornidazole (red) and its monomeric  $\text{Cu}^{\text{II}}$  complex (blue) after each compound was subjected to reduction at a constant potential (-0.827 V for Onz) and (-0.849 V for  $\text{Cu}(\text{II})\text{-Onz}$ ) under de-aerated (Argon saturated) conditions;  $[\text{Onz}] = [\text{Cu}(\text{II})\text{-Onz}] = 1 \times 10^{-4} \text{ mol dm}^{-3}$ . The black line indicates modification of calf thymus DNA in the absence of any sensitizer but subjected to a constant potential of -0.835 V.

For the complex, experiments could not be performed using guanine since addition of the complex to an aqueous solution of guanine turned it faintly turbid suggesting an association between the two. This was checked several times to be sure that this was happening. We even performed HPLC of an aqueous solution of  $1 \times 10^{-4} \text{ M}$  guanine and an aqueous solution of guanine containing  $1 \times 10^{-5} \text{ M}$  complex. For the solution containing guanine with the complex, elution of guanine was completely different from that obtained when guanine was injected alone, indicating that there is an association of the two compounds (Figure 9). Such a thing did not happen for other nucleic acid bases with the complex. Since we detected an association of guanine with the complex, the actual experiment i. e. keeping guanine in the

immediate vicinity of electrochemically generated reduced species of the complex was not attempted.

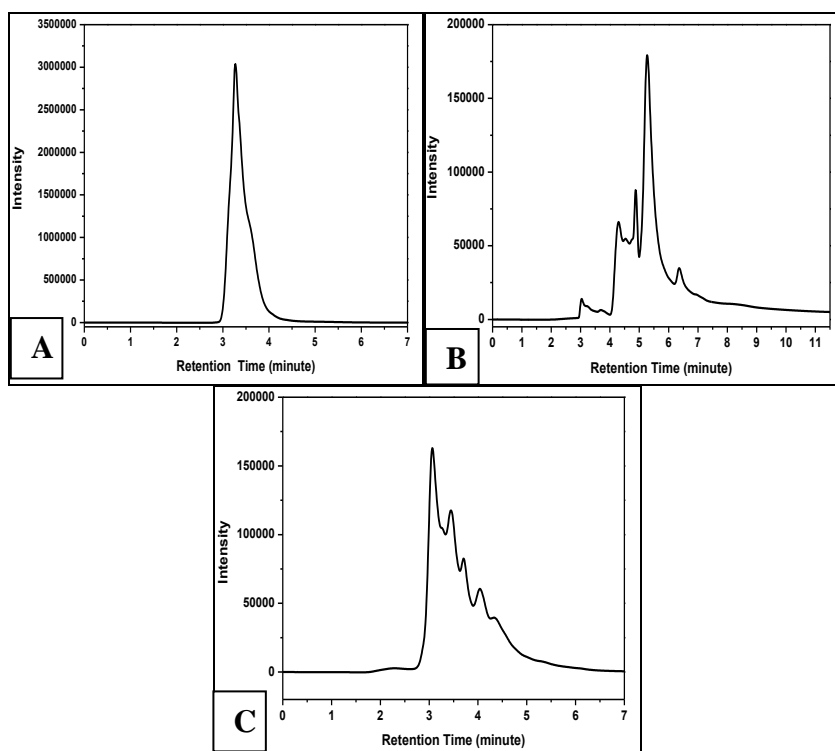


**Figure 9:** HPLC chromatograms recorded at 254 nm for (A)  $1 \times 10^{-3}$  mol  $\text{dm}^{-3}$  guanine solution and (B), (C) of  $1 \times 10^{-3}$  mol  $\text{dm}^{-3}$  guanine solution containing  $1 \times 10^{-4}$  mol  $\text{dm}^{-3}$  Cu(II)-Onz. In case of (B) the two compounds were allowed to interact for 45 minutes, following their mixing, after which HPLC was performed; in case of (C) they were allowed to interact for 24 hours, following their mixing, after which HPLC was performed.

The enhancement ratio for cytosine in presence of the complex (Table 1) tallies appreciably with that obtained for calf thymus DNA. Since in calf thymus DNA, percentage of guanine and cytosine is comparatively higher than adenine and thymine, it was concluded this could be one reason why calf thymus DNA showed substantial damage in presence of the Cu<sup>II</sup> complex of Onz under the experimental protocol used. The study also indicates that a prior knowledge on the “damage causing ability of compounds” on nucleic acid bases might help

to predict their activity on different types of DNA used as target based on their nucleic acid composition. If the target DNA is identified then the type of organism having such DNA composition should be most vulnerable to such compounds. In case of Ornidazole and its Cu<sup>II</sup> complex, the study provides a logical explanation as to why compounds chemically similar to the ones we studied were either found to be active on GC rich DNA containing species or on species having a substantial presence of GC in their DNA [26-29].

**Aflox Oz, Aloflox-ON, Arrow–Ornidazole, Cefit –OZ, Oxit OZ, Fynal OZ (containingornidazole as major constituent)** is used for treatment of infections caused by:

<b>Microbes</b>	<b>G-C content</b>
1. <i>Haemophilus influenza</i>	<b>38.0 %</b>
2. <i>Streptococcus pneumonia</i>	<b>39.7%</b>
3. <i>Staphylococcus aureus</i>	<b>33.0 %</b>
4. <i>Streptococcus pyogenes</i>	<b>38.5%</b>
5. <i>Proteus mirabilis</i>	<b>28.8%</b>
6. <i>Neisseria gonorrhoeae</i>	<b>52.4%</b>
7. <i>Chlamydia trachomatis</i>	<b>40.3%</b>
8. <i>Escherichia coli</i>	<b>50.9%</b>
9. <i>Moraxella catarrhalis</i>	<b>38.0 %</b>
10. <i>Citrobacterdiversus</i>	<b>51.0 %</b>
11. <i>Enterobacteraerogenes</i>	<b>64.0 %</b>
12. <i>Klebsiella pneumonia</i>	<b>57.4 %</b>
13. <i>Pseudomonas aeruginosa</i>	<b>65.0 %</b>
14. <i>Staphylococcus saprophyticus</i>	<b>33.0 %</b>
15. <i>Enterococcus faecalis</i>	<b>37.4 %</b>
16. <i>Enterobacter cloacae</i>	<b>54.5 %-55.1%</b>
17. <i>Serratiamarcescens</i>	<b>58.0 %</b>
18. <i>Haemophilusparainfluenzae</i>	<b>38.0 %- 40.0 %</b>
19. <i>Legionella pneumophila</i>	<b>38.0 %</b>
20. <i>Staphylococcus epidermidis</i>	<b>32.0 %</b>
21. <i>Bacillus anthracis</i>	<b>35.4%</b>
22. <i>Yersinia pestis</i>	<b>47.5%</b>

As mentioned earlier, inspite of decreased nitro-radical anion formation [12-14] the Cu<sup>II</sup> complex of Onz was found to be better than Onz itself. This could be an attribute of complex formation i.e. on an ability of the Cu<sup>II</sup> center in the complex to be active in a redox pathway generating radicals [30] capable of bringing about DNA double strand modification that would be detected by the methodology we had applied (i. e. identifying DNA double strand modification through decrease in DNA-EtBr fluorescence) [21-23]. There is also the possibility of a physical interaction of the complex with DNA or any other biomolecule, like that detected in this study for guanine, bringing about substantial changes on a target cell that eventually leads to cell death. Therefore, the outcome of experiments with calf thymus DNA are not due to free radical reactions alone, other factors could well be involved. Another aspect is that of binding of the complex with DNA [12, 13].

Therefore, from this study it is evident that reduction products of both compounds modify guanine and cytosine (G and C) much more than adenine and thymine (A and T). In fact the enhancement ratio for the damage of guanine-cytosine by ornidazole and the complex matches appreciably with the observed enhancement ratio for calf thymus DNA having a reasonably high G and C content. In all cases, the complex performed better than ornidazole, which may be attributed to the presence of Cu<sup>II</sup>. The study helped in correlating the fact why 5-nitroimidazole based antibiotics have been found to be very effective on organisms having either a high G-C content in their DNA or at least a substantial amount of it.

## References

1. E. J. Hall, R. Miller, M. Astro, F. Rini, *Br J Cancer Suppl.*, **1978**, 3, 120-123.
2. J. S. Mahood, R. L. Willson, *Br J Cancer*, **1981**, 43, 350-354.
3. R. P. Mason, *Free Radicals in Biology*, Eds.: W. A. Pryor, Vol. V, Academic Press New York, **1982**, 161-222.
4. C. F. Chignell, *Env. Health Persp.*, **1985**, 61, pp. 133-137.

5. D. I. Edwards, *Comprehensive Medicinal Chemistry*, Eds.: C. Hansch, P. G Sammes, J. B. Taylor, Pergamon Press Oxford **1990**, vol. 2, 725-751.
6. D. Petrin, K. Delgaty, R. Bhatt, G. Garber, *Clin. Microbiol. Rev.*, **1998**, 11, 300-317.
7. S. L. Cudmore, K. L. Delgaty, S. F. Hayward-McClelland, D. P. Petrin, G. E. Garber *ClinMicrobiol Rev.*, **2004**, 17, 783-793.
8. S. Sood, A. Kapil, *Ind. J. Sex Transm. Dis.*, **2008**, 29 , 7-14.
9. M. Bonnet, C. R. Hong, W. W. Wong, L. P. Liew, A. Shome, J. Wang, Y. Gu, R. J. Stevenson, W. Qi, R. F. Anderson, F. B. Pruijn, W. R. Wilson, S. M. F. Jamieson, K. O. Hicks, M. P. Hay, *J. Med. Chem.*, **2018**, 3 (61), 1241-1254.
10. R. Sharma, *Curr. Radiopharma.*, **2011**, 4, 361-393.
11. J. Thulkar, A. Kriplani, N. Agarwal, *Ind. J Pharmacol.*, **2012**, 44, 243-245.
12. R. C. Santra, K. Sengupta, R. Dey, T. Shireen, P. Das, P. S. Guin, K. Mukhopadhyay, S. Das, *J. Coordination Chem.*, **2014**, 67, 265-285.
13. R. C. Santra, D. Ganguly, J. Singh, K. Mukhopadhyay, S. Das, *Dalton Trans.*, **2015**, 44, 1992-2000.
14. R. C. Santra, D. Ganguly, D. Bhattacharya, P. Karmakar, A. Saha, S. Das, *New J. Chem.*, **2017**, 41, 11679-11685.
15. O. Kurt, N. Girginkardeşler, I. C. Balcioğlu, A. Ozbilgin, U. Z. Ok, *Clin. Microbiol. Infect.*, **2008**, 14, 601-604.
16. B. Oren, E. Schgurensky, M. Ephros, I. Tamir, R. Raz, *Eur J ClinMicrobiol Infect Dis.*, **1991**, 10, 963-965.
17. M. Castella, M. Malagolia, A. I. Rubertoa , A. Baggioa , C. Casolarib , C. Cermellib , M. R. Bossac , T. Rossid , F. Paoluccie, S. Roffiae, *J. Antimicrob. Chemother.*, **1997**, 40, 19-25.
18. J. A. Squella, S. Bollo, L. J. Núñez-Vergara, *Curr. Org. Chem.*, **2005**, 9, 565-581.
19. P. C. Mandal, *J. Electroanal. Chem.*, **2004**, 570, 55-61.
20. S. A. Ozkan, Z. Senturk, I. Biryol, *Int. J. Pharmaceutics*, **1997**, 157, 137-144.
21. B. Mandal, H. K. Mondal, S. Das, *Biochem. Biophys. Res. Comm.*, **2019**, 515 , 505-509.

22. A. R. Morgan, J. S. Lee, D. E. Pulleyblank, N. L. Murray and D. H. Evans, *NucleicAcids Res.* **1979**, *7*, 547.
23. H. C. Birnboim, J. J. Jevcak, *Cancer Research*, **1981**, *41*, 1889.
24. S. Das, A. Saha, P. C. Mandal, *Environ. Health Pers.* **1997**, *105*, 1459-1465.
25. K. Nakamoto, *Infrared and Raman spectra of inorganic and coordination compounds*. 3<sup>rd</sup> edn. Wiley-Interscience: New York, USA, **1978**.
26. Mark H. Wilcox, "147-Nitroimidazoles, Metronidazole, Ornidazole and Tinidazole; and Fidaxomicin in: Infectious Diseases", 4th ed., eds. J. Cohen, W. G. Powderly and S. M. Opal, **2017**, Vol. 2, 1261-1263.e1.
27. F. S. Lehmann, J. Drewe, L. Terracciano, C. Beglinger, *Aliment Pharmacol.Ther.*, **14** (2000), pp. 305-309.
28. T. B. Gardner, D. R. Hill, *Clin. MicrobioI. Rev.*, **14** (2001), pp. 114–128. DOI: 10.1128/CMR.14.1.114–128.2001.
29. L. Jokipii, A. M. M. Jokipii, *Gastroenterology*, **1982**, *83*, 399-404.
30. P. Wardman, *Environ. Health Persp.*, **1985**, *64*, 309-320.

## **Chapter 12**

***In situ* reactivity of electrochemically generated nitro radical anion on tinidazole, its monomeric and dimeric Cu<sup>II</sup> complexes on model biological targets with a relative manifestation of preventing bacterial biofilm formation**

## Introduction

5-nitroimidazoles are important molecules for pharmaceutical applications and are found in different formulations [1-5]. They address a wide spectrum of medical issues ranging from infections caused by different microbes to being used as anti-cancer agents in radiotherapy [1-8]. Although, metronidazole is mostly used, issues like drug resistance, neurotoxicity has resulted in a search for compounds having comparable efficacy but with significantly less adverse effects [1-3, 5-10]. Tinidazole (tnz) is a compound that nicely fits this requirement, although conflicting reports on its efficacy and adverse effects exist [11-14]. Since its anti-microbial activity was first reported, tinidazole showed a steady increase in acceptability as a drug [15-18]. However, as is true for all 5-nitroimidazoles, its efficacy is also accompanied by toxic side effects but that is quoted to be less than metronidazole [11-18]. The problem with this family of drugs is that, the nitro-radical anion,  $\text{RNO}_2^{\bullet-}$  (where R represents the portion other than the nitro group) is responsible both for efficacy and toxic side effects [11-18]. Hence, an approach that enables controlling the generation of  $\text{RNO}_2^{\bullet-}$  is an extremely relevant issue [19-21]. Within biological systems, 5-nitroimidazoles are first reduced by enzymes pyruvate ferredoxin oxidoreductase (PFOR) [9, 22, 23] that prepares them for entry into cells of the target organism. Thereafter, the nitro-radical anion imparts drug action.

Although, related literature mentions  $\text{RNO}_2^{\bullet-}$  to be responsible for drug action, very few studies have gone into details of such claims that would help us realize their contribution toward cytotoxic action. Research has revealed complex formation of 5-nitroimidazoles modulate the generation of  $\text{RNO}_2^{\bullet-}$  that might then be expected to decrease toxic side effects [20, 21]. Since  $\text{RNO}_2^{\bullet-}$  is important for drug efficacy, its decrease, following complex formation, should affect drug action. However, previous studies suggest complex formation did not interfere with drug efficacy. In fact, most complexes were either similar in performance on a chosen microbial target when compared to a 5-nitroimidazole, from which

the complex was prepared or that the complex performed better [20, 21, 24]. Since complexes result in a decrease in  $\text{RNO}_2^{\bullet-}$  and yet there is no loss in efficacy, this suggests they have other attributes [20, 21, 24] that enable them to overcome any deficiency that might occur in the free radical pathway.

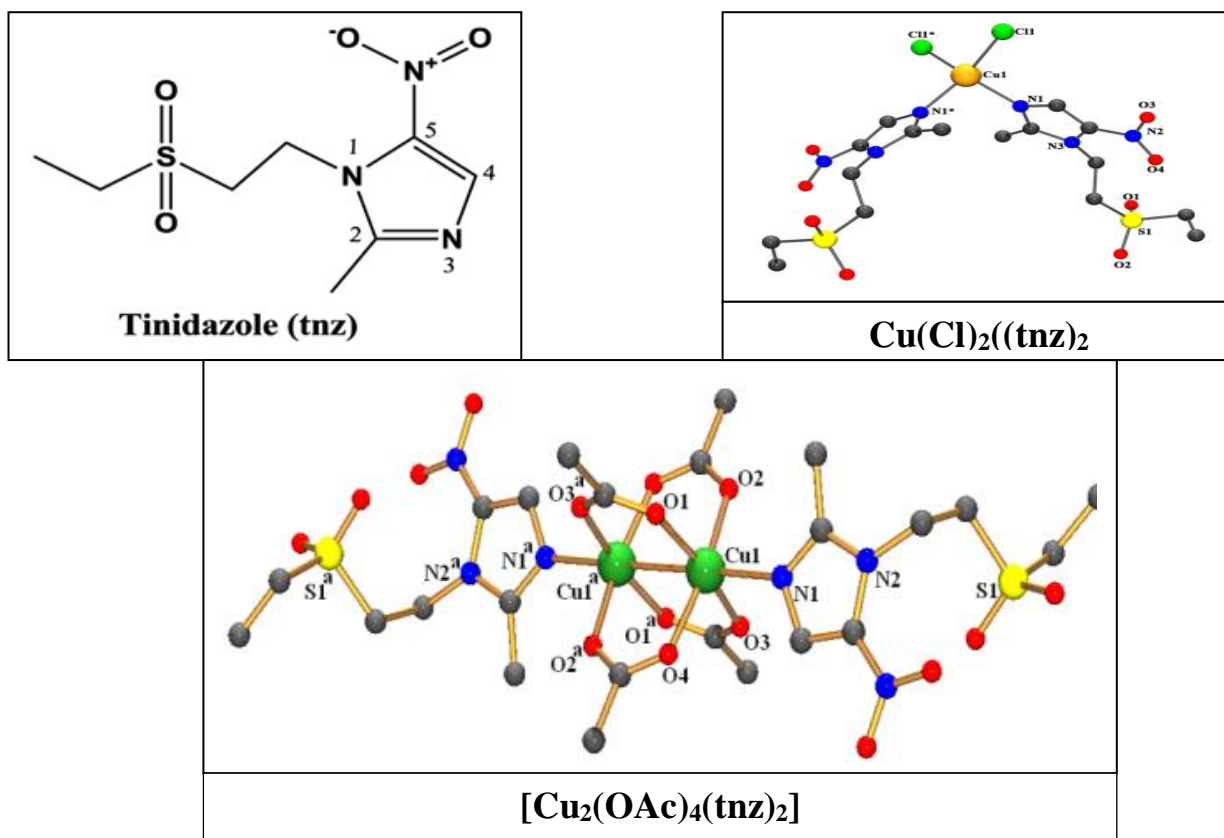


**Figure 1: Structure of tnz and its monomeric and dimeric  $\text{Cu}^{\text{II}}$  complexes**

In this chapter, we discuss aspects related to cytotoxicity that are either initiated by  $\text{RNO}_2^{\bullet-}$  or other reduction products formed on the monomeric and dimeric complexes of  $\text{Cu}^{\text{II}}$  with tinidazole (tnz) (Figure 1). Nucleic acid bases and calf thymus DNA were used as targets to correlate what might happen when such compounds are enzymatically reduced in biological systems, generating species that have the potential to kill disease causing microbes [9, 20-24]. Reduction products of each compound were generated electrochemically maintaining a glassy carbon electrode at its cathodic peak potential using a method described earlier [26, 27]. In

the immediate vicinity of electrochemically generated reduction products, nucleic acid bases or calf thymus DNA were maintained, one at a time so that reduced products react instantaneously. Although the reaction on a model target under laboratory conditions can never be identical with what happens inside cells, it can however throw some light on such processes, since similar species are generated enzymatically within cells following transfer of electron(s) to 5-nitroimidazoles by electron donating groups present within cells [9, 22, 23, 25]. *In situ* reactivity of reduction products with nucleic acid bases or calf thymus DNA were subsequently analyzed to understand changes that were brought about on a target. To check for a correlation between model studies and potency of monomeric and dimeric complexes to inhibit biofilm formation, detailed studies were performed on *P. aeruginosa* and *S. aureus*.

Most bacterial species possess an ability to live in complex sessile communities called biofilm, under environmentally stressed conditions. Such sessile micro-colonies remain embedded within self-secreted extracellular polymeric substances (EPS) and are responsible for the development of major types of nosocomial infections following biofilm formation [26, 27]. Biofilms are highly resistant both to specific (adaptive) and non-specific (innate) host defense mechanisms. The development of EPS and subsequent slower diffusion of antimicrobials through the biofilm matrix, reduced rate of metabolism etc. make bacterial cells less susceptible to phagocytic activities of macrophages and more resistant to antibiotics [28, 29]. Such enhancement of resistance resulted in a search for alternate therapies for treating biofilm associated chronic infections that are caused by *P. aeruginosa* and *S. aureus* [30, 31]. Through this work we had aimed to show the potent efficacy of monomeric and dimeric complexes of Cu(II) with tnz (Figure 1), in removing persistent microbial cells of *P. aeruginosa* and *S. aureus*.

## Results

### *In situ* reactivity of electrochemically generated reduction products

Figure 2 shows voltammograms for tnz, the monomeric  $[\text{Cu}(\text{tnz})_2\text{Cl}_2]$  and the dimeric  $[\text{Cu}^{\text{II}}_2(\text{OAc})_4(\text{tnz})_2]$  complexes when each was subjected to cyclic voltammetry in aqueous solution. From the voltammograms, the reduction peak potentials of tnz,  $[\text{Cu}(\text{tnz})_2\text{Cl}_2]$  and  $[\text{Cu}^{\text{II}}_2(\text{OAc})_4(\text{tnz})_2]$  were identified at -0.745 V, -0.700 V and -0.710 V respectively. It may be mentioned here, for 5-nitroimidazoles in aqueous solution, reduction to the nitro-radical anion is not identified separately; instead there is a single-step four electron reduction (Chapter: Experimental Eq. 3) [35, 36].

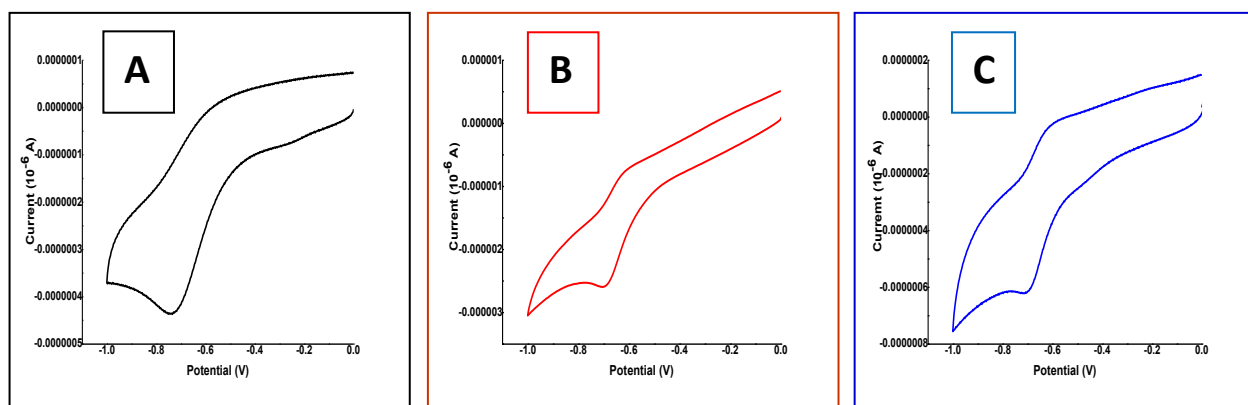


**Figure 2:** Cyclic voltammograms of 100  $\mu\text{M}$  of (A) tinidazole, (B) its monomeric Cu(II) complex and (C) its dimeric Cu(II) complex showing a single step four electron reduction of the nitro group in aqueous solution using a glassy carbon electrode;  $[\text{NaCl}] = 120 \text{ mM}$ ; Scan Rate = 0.025 V/s; Ag/AgCl, satd. KCl was used as the reference electrode; Temperature = 303 K.

Identification of the potential for reduction of each compound is important for the intended study where each compound would be reduced to generate suitable reduced species that might interact with a target. Hence, when in the immediate vicinity of any of the compounds, that were subjected to electrochemical reduction at a constant potential, nucleic acid bases or calf thymus DNA were maintained, reduced products would have a high probability to

interact with them. The outcome of such interactions was ascertained for nucleic acid bases using HPLC and for DNA by ethidium-bromide fluorescence technique [34].

### Interaction of electrochemically generated reduction products with nucleic acid bases

Various electrochemically reduced species generated in aqueous solution for a compound, following maintenance of a glassy carbon electrode at its cathodic peak potential, for different periods of time, indicate that it leads to a gradual degradation of nucleic acid bases (Figure 3). Response for nucleic acid bases shown in Figure 3 is based on their individual elution peaks under a specific solvent composition that elutes them, which was considered the standard HPLC chromatogram for that nucleic acid base (Figure 4).

Based on elution peaks of individual compounds, degradation plots were quantified (Figure 5). Such standard curves enabled the determination of the concentration of nucleic acid bases in the performed experiments.

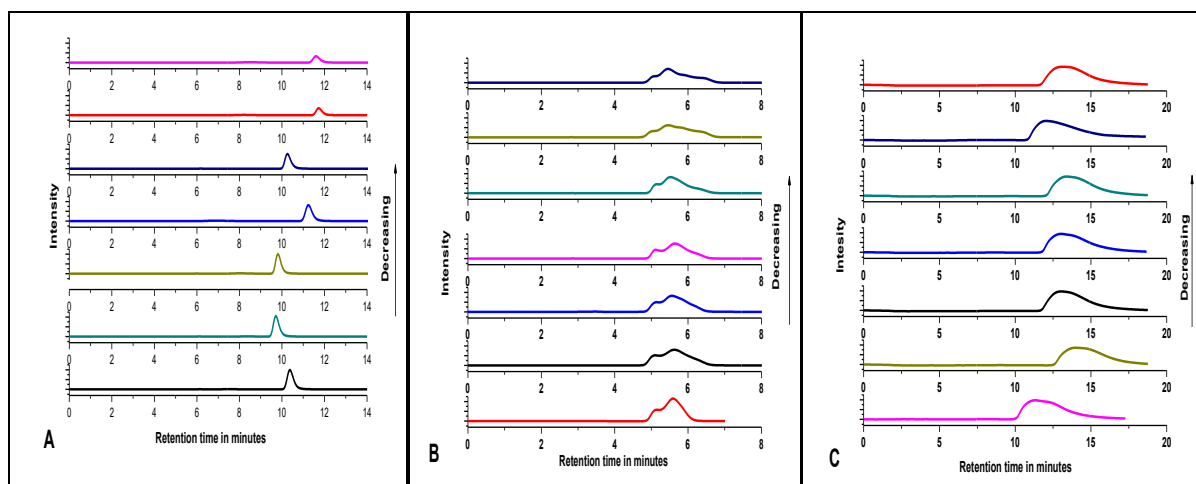


**Figure 3:** HPLC chromatograms of  $10^{-3}$  M A) thymine B) cytosine and C) adenine solutions recorded at 254 nm following their keeping in the immediate vicinity of electrochemically reduced  $10^{-4}$  M  $\text{Cu}^{\text{II}}_2(\text{OAc})_4(\text{tnz})_2$ .

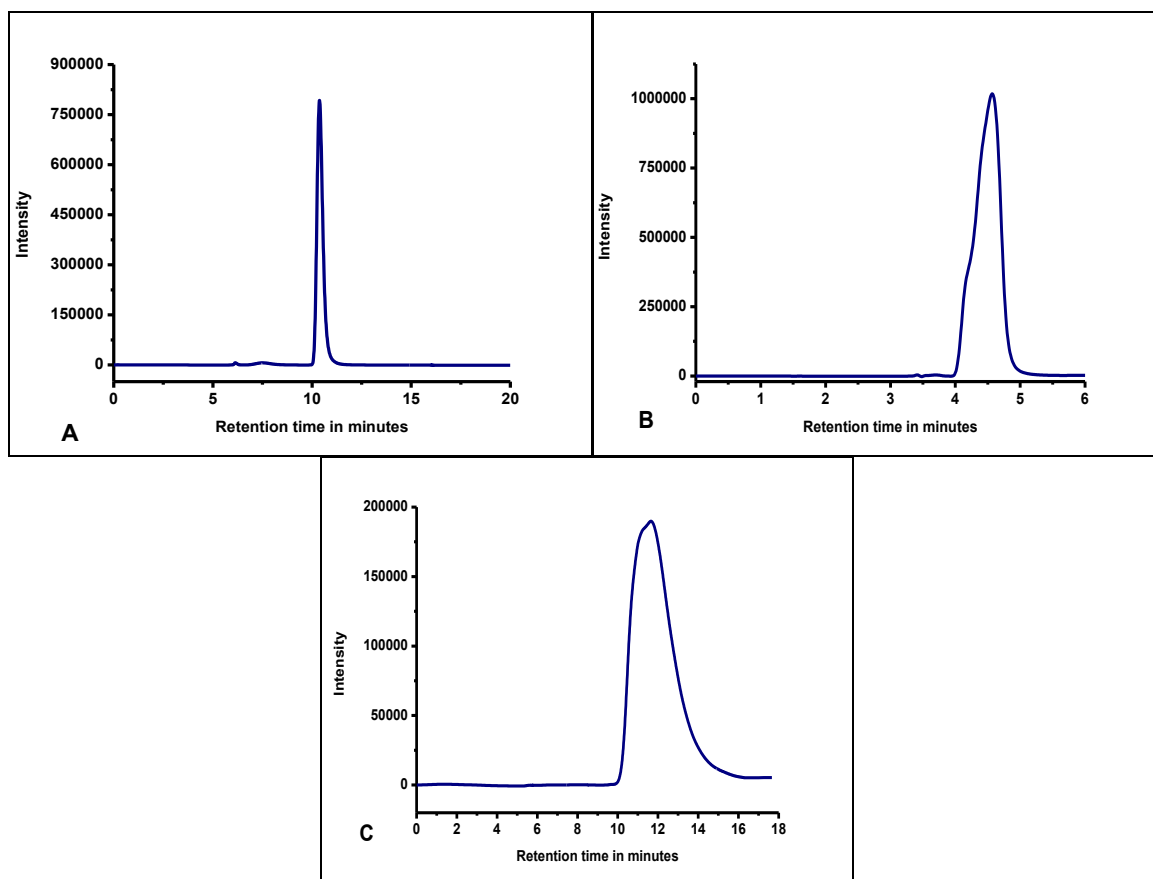


**Figure 4:** HPLC chromatograms for (A) thymine, (B) cytosine and (C) adenine recorded at 254 nm; [nucleic acid bases] =  $1 \times 10^{-3}$  mol dm<sup>-3</sup>.

The amount of a nucleic acid base remaining following interaction with reduced species was realized by collecting aliquots from the reaction vessel at different time intervals and evaluating them based on Figure 4. Figure 5 shows degradation of nucleic acid bases followed by HPLC at 254 nm after they were allowed to interact with reduced products obtained from tnz and its monomeric and dimeric complexes [34].

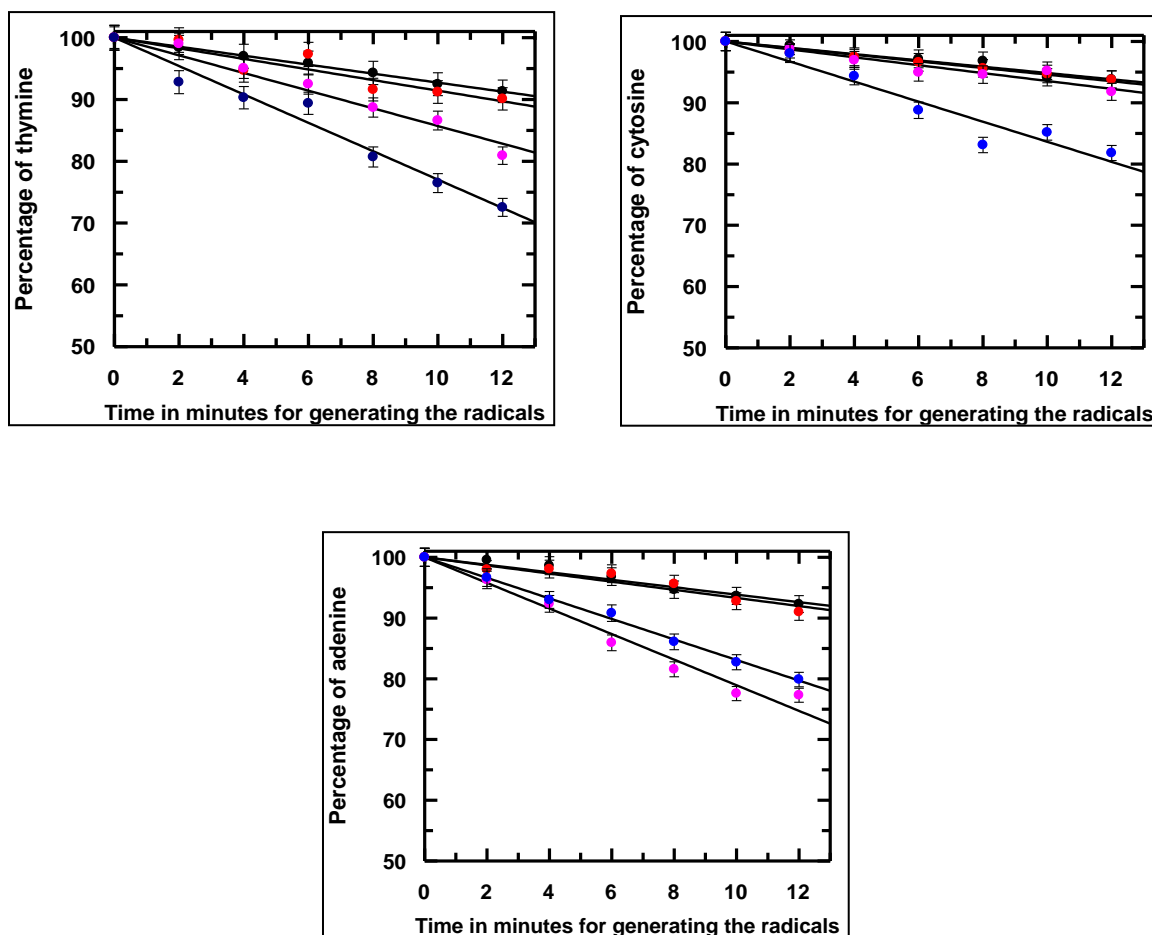


**Figure 5:** Damage of nucleic acid bases was monitored using HPLC at 254 nm following electrochemical reduction of compounds in whose immediate vicinity nucleic acid bases were maintained. Respective reduction potentials were -0.745 V for tnz, -0.700 V for the monomeric Cu(II) complex and -0.710 V for the dimeric Cu(II) complex. Electrochemical reduction was carried out under Argon saturated conditions. (●) indicates control experiments when a nucleic acid base was subjected to reduction in the absence of any compound; (●) in presence of tnz; (●) in presence of the monomeric complex and (●) in presence of the dimeric complex; [thymine] = [cytosine] = [adenine] =  $1 \times 10^{-3}$  mol dm<sup>-3</sup>; [tnz] = [monomeric Cu(II)-tnz] = [dimericCu(II)-tnz] =  $1 \times 10^{-4}$  mol dm<sup>-3</sup>.

**Table 1: Enhancement ratio for damage caused to thymine following reduction of tinidazole and its Cu(II) complexes at respective reduction potentials in aqueous solution.**

Sensitizer	Loss of thymine from slope of degradation plot	Enhancement ratio (forthymine)	Loss of cytosine from slope of degradation plot	Enhancement ratio (forcytosine)	Loss of adenine from slope of degradation plot	Enhancement ratio (foradenine)
-	0.73	–	0.51	–	0.61	–
Tinidazole	0.86	1.18	0.54	1.06	0.67	1.10
Cu-tnz monomer	1.43	1.96	0.65	1.27	2.11	3.46
Cu-tnz dimer	2.30	3.15	1.64	3.22	1.69	2.77

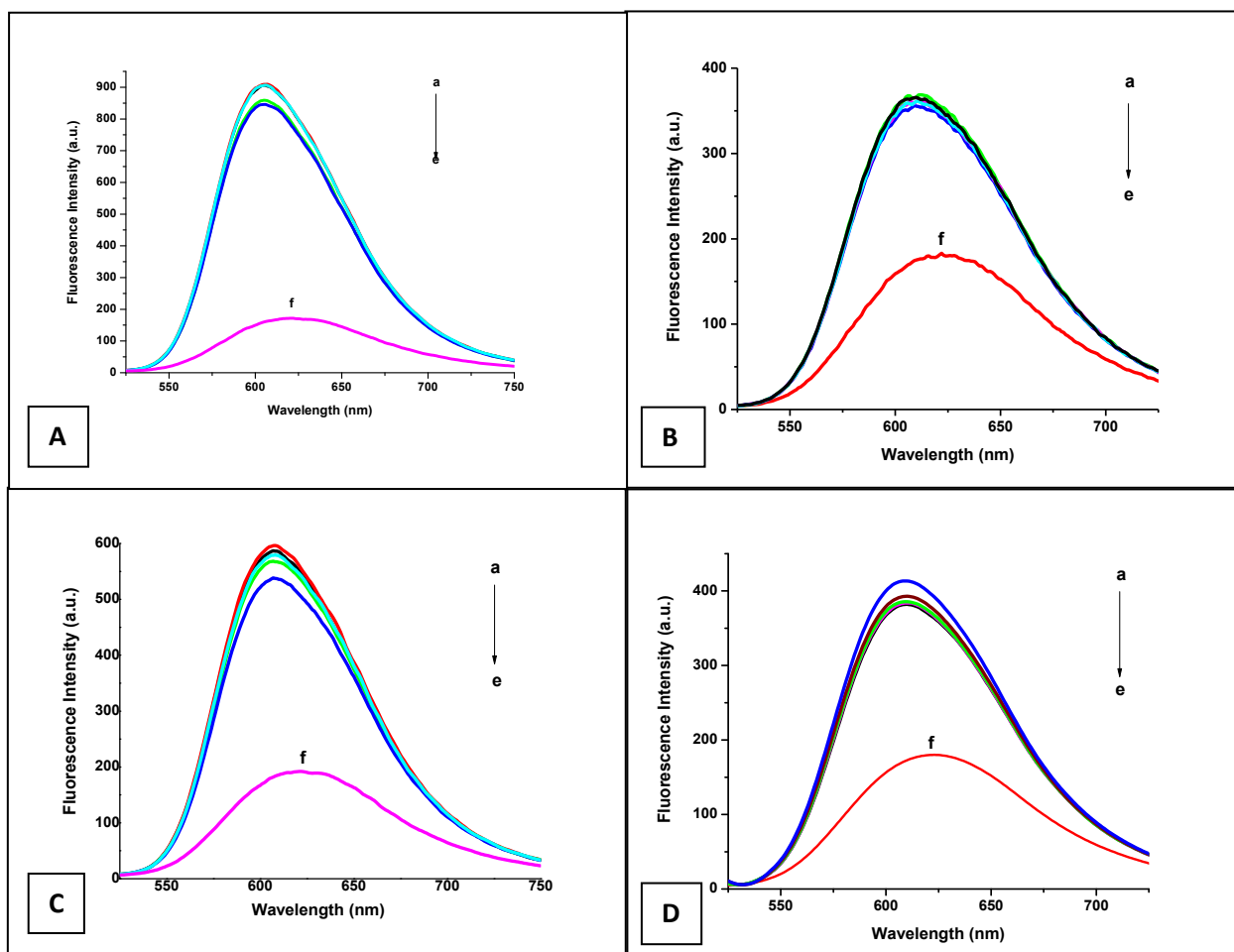
Generation of data for guanine was also attempted as it is easily damaged by various radical species. However, owing to issues concerning solubility in aqueous solution, inspite of best efforts I had to refrain from going ahead. Results obtained with guanine were erratic and inconsistent. Hence, it was decided to discuss the data obtained for thymine, cytosine and adenine only. However, if damage on guanine could be shown, things would have been explained better related to targeting of 5-nitroimidazoles and their metal complexes. Based on the nucleotide content of the DNA of a target organism onewould then have been in a better position to provide a good correlation between actual drug action reported and this study (Table 2). Although, without guanine it may still be realized, a data for guanine would have made it more convincing.

**Table 2:** Tindamax (containing tinidazole as major constituent) is used to treat

<b>Disease causing organism</b>	<b>Disease caused</b>	<b>A-T content ( % )</b>	<b>G-C content ( % )</b>
<i>Trichomonas vaginalis</i>	Trichomoniasis	64.0 %	36.0 %
<i>Giardia duodenalis</i>	Giardiasis	54.0 %	46.0 %
<i>Entamoebahistolytica</i>	Intestinal amebiasis&amebic liver abscess	77.6 %	22.4 %
<i>Haemophilus vaginalis or Gardnerellavaginalis</i>	Haemophilus vaginitis, Gardnerella vaginitis	58.6 %	41.4 %
<i>Vulvovaginitis pathogens like Trichomonas vaginalis</i>	Vulvovaginitis	59.7 %	40.3 %
<i>Neisseria gonorrhoeae (gonococcus)</i>	Gonorrhea	47.6 %	52.4 %
<i>Candida albicans</i>	fungal urinary tract infections	66.3 %	33.7 %

### **Interaction of electrochemically generated reduction products with calf thymus DNA**

A similar study as the one described above was performed maintaining calf thymus DNA in the immediate vicinity of electrochemically generated reduced species in aqueous solution at pH 7.4, using the same glassy carbon electrode maintained at an identified reduction potential of a compound. In experiments with calf thymus DNA, the system was subjected to slightly longer times than we used for electrochemical reduction of the compounds to reduced species in case of nucleic acid bases, so that the reduced products were produced in greater quantity and there was detectable change on DNA, monitored by fluorescence technique using EtBr [35-39].



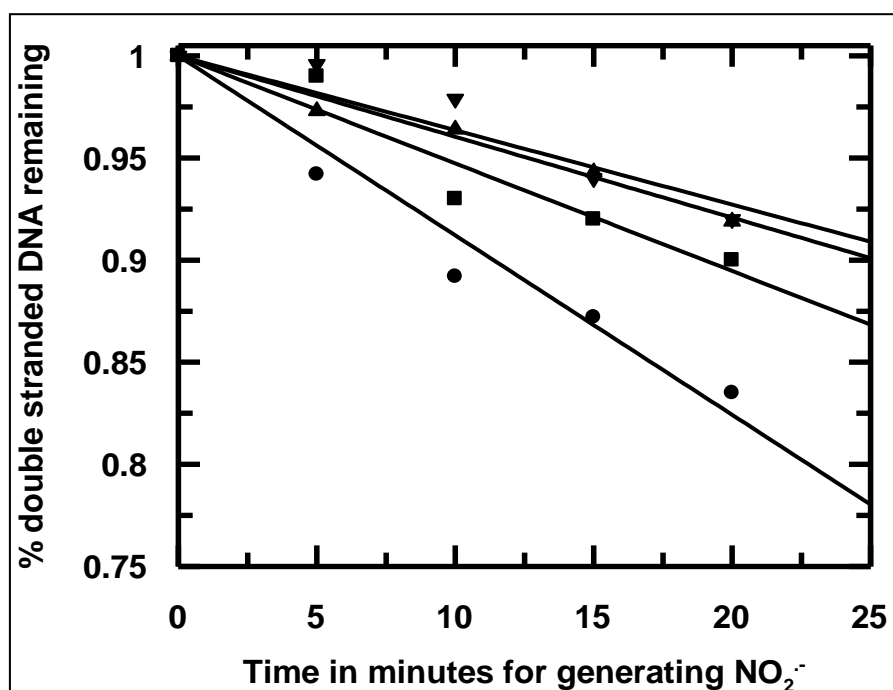
**Figure 6:** Decrease in fluorescence intensity of the DNA-EtBr adduct recorded at 600 nm ( $\lambda_{\text{ex}} = 510$  nm) following interaction with electrochemically generated reduced species in (A) absence of any compound; (B) presence of tnz, (c) presence of  $\text{Cu}(\text{tnz})_2\text{Cl}_2$  and (D) presence of  $\text{Cu}_2(\text{OAc})_4(\text{tnz})_2$  at different time intervals of (i) 0 min, (ii) 5 minutes, (iv) 10 minutes, (v) 15 minutes, (vi) 20 minutes. Spectrum (f) in each plot is that of free EtBr.

Figure 6 depicts plots showing fluorescence of calf thymus DNA with EtBr, after it was allowed to interact with reduced products generated electrochemically on each compound, in whose vicinity calf thymus DNA was maintained. In each experiment, mixtures of DNA and EtBr were excited at 510 nm and emission measured at 600 nm.

Modification of calf thymus DNA was realized by plotting percentage of DNA remaining intact against time provided for generation of electrochemically reduced species on each

compound following the maintenance of a glassy carbon electrode at the pre-determined reduction potential of a compound in aqueous solution at pH 7.4 (Figure 7). Both Figure 7 and Table 3 indicate damage caused to calf thymus DNA in the presence of the compounds used in the study. Considering  $I_0$  as the intensity of fluorescence of pure DNA treated with EtBr;  $I_{\text{EtBr}}$  as the intensity of fluorescence for EtBr itself and  $I_{\text{expt}}$  as the intensity of fluorescence of a DNA sample that was subjected to the conditions of the experiment and then treated with EtBr, the fraction of DNA remaining intact is obtained by

$$\text{Fraction of DNA remaining} = \frac{(I_{\text{expt}} - I_{\text{EtBr}})}{(I_0 - I_{\text{EtBr}})}$$



**Figure 7:** Degradation curves show modification of calf thymus DNA in the absence and presence of either tnz(▲)its monomeric(■), dimeric (●) Cu(II) complexes;[tnz] = [Cu(tnz)<sub>2</sub>Cl<sub>2</sub>] = [Cu<sub>2</sub>(OAc)<sub>4</sub>(tnz)<sub>2</sub>] = 1 × 10<sup>-4</sup> mol dm<sup>-3</sup>. (▼)indicates modification of calf thymus DNA in the absence of any compound when subjected to a constant potential of -0.700 V for the same duration of time.

**Table 3: Enhancement ratio for damage caused to calf thymus DNA following the reduction of tinidazole and its Cu(II) complexes at their respective reduction potentials in aqueous solution.**

<b>Sensitizer</b>	<b>DNA doublestrand modification from slopes of degradation plots</b>	<b>Enhancement ratio (for DNA)</b>
—	<b>0.0036</b>	-
<b>Tinidazole</b>	<b>0.0040</b>	<b>1.10</b>
<b>Cu-tnz monomer</b>	<b>0.0053</b>	<b>1.45</b>
<b>Cu-tnz dimer</b>	<b>0.0088</b>	<b>2.40</b>

### **Inhibitory action of complexes on biofilm formation**

#### **Determination of minimum bactericidal concentration (MBC)**

The monomeric Cu<sup>II</sup> complex showed inhibition of biofilm formation for *S. aureus* and *P. aeruginosa* at concentrations of 12.5 μM and 20.25 μM respectively while that for the dimeric complex was 40 μM and 45 μM respectively, suggesting that the monomeric complex showed better efficacy against biofilm formation by cells of *P. aeruginosa* and *S. aureus*. The minimum bactericidal concentrations of tnz for *S. aureus* and *P. aeruginosa* were 50 μM and 59.25 μM respectively. Although tnz is an established antibacterial drug [40, 41], very few literature show its anti-biofilm properties [42, 43].

#### **Inhibition of biofilm formed by *P. aeruginosa* and *S. aureus***

The monomeric complex of Cu<sup>II</sup> inhibited biofilm formation due to *P. aeruginosa* by 88.52 ± 3.45 % whereas the dimeric complex could decrease it by 76.95 ± 2.29 % (amoxicillin reduces biofilm formation by 62.12 ± 2.25 %). For *S. aureus*, decrease in biofilm formation due to the monomeric complex was by 92.16 ± 4.87 % while for the dimeric complex it was

81.25 ± 3.55 (amoxicillin decreases it by 72.56 ± 1.29) (monomer p<0.01, dimer p<0.05)(Figure 8).

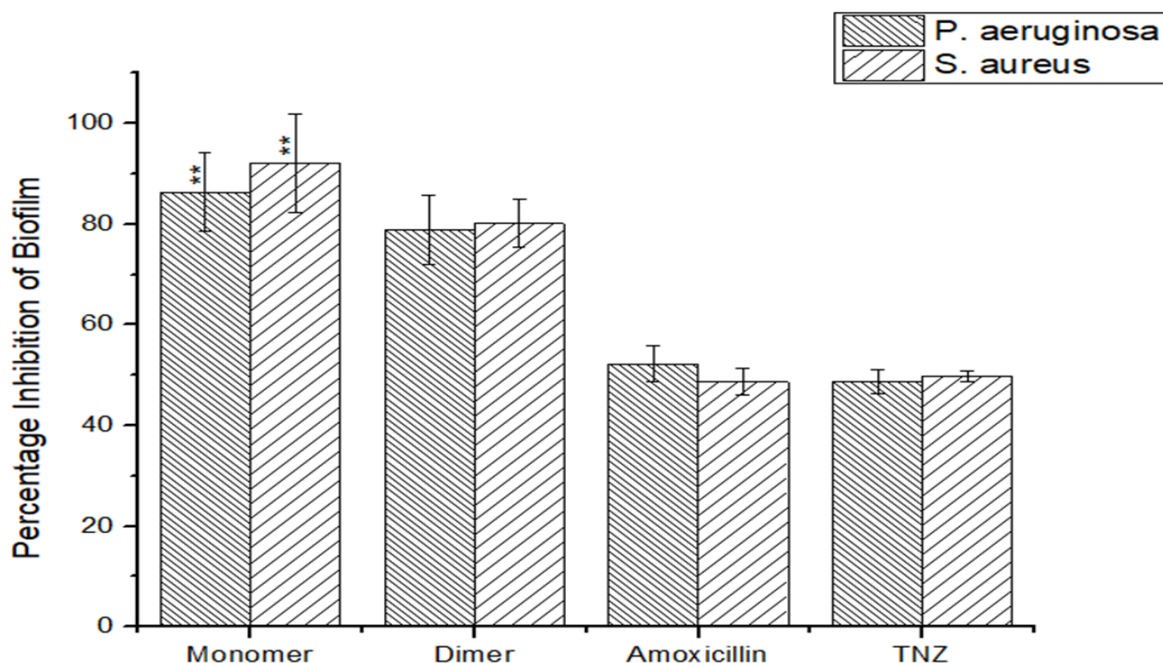


**Figure 8:** Maximum inhibition of biofilm formation due to *P. aeruginosa* and *S. aureus* was due to the monomeric complex (p<0.01).

### Disintegration of structural component of EPS

EPS matrix of a biofilm comprises of a rich supply of nutrients in addition to lipid molecules, nucleic acids, proteins, extracellular DNA, quorum sensing signaling molecules and water. Hence, removal of biofilm involves strategies that target the EPS matrix leading to its disintegration via a decrease in synthesis of biomolecules.

The monomeric complex inhibited carbohydrate content within the EPS of the biofilm formed due to *P. aeruginosa* by 75.26 ± 5.8 %, the dimeric complex by 71.23 ± 3.55 % and amoxicillin by 61.78 ± 2.47 %. In case of *S. aureus*, for the monomeric complex, the decrease was by 80.29 ± 5.8 %, for the dimeric complex, by 75.89 ± 4.7 % and for amoxicillin, by 69.56 ± 3.25 % (p<0.01). It was further observed that the monomeric complex was able to maximally reduce protein content of EPS of *P. aeruginosa* and *S. aureus* by 75.26 ± 5.8 %

and  $80.29 \pm 5.8$  % respectively ( $p < 0.01$ ) which was even higher than that achieved with the standard antibiotic amoxicillin (Figure 9).

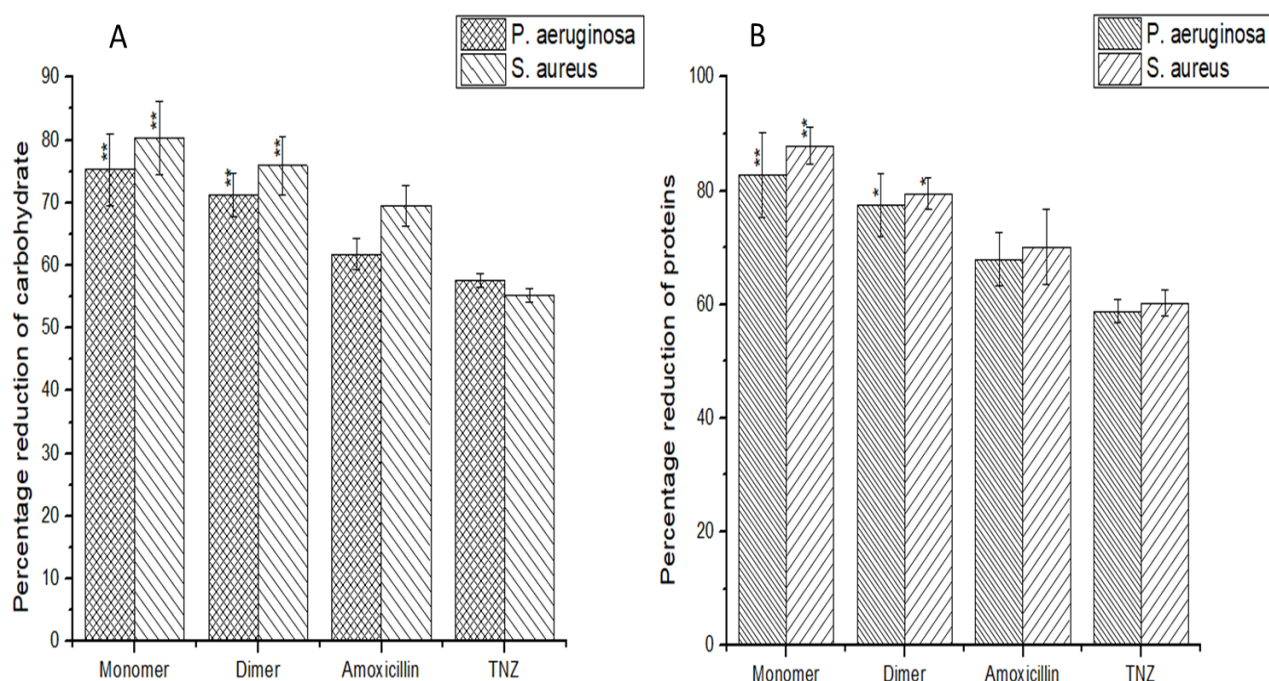


**Figure 9:** Reduction in carbohydrate (A) and protein (B) present within the EPS

### Down regulation of QS pathway during biofilm formation

Anti-microbial potential of monomeric and dimeric complexes of  $\text{Cu}^{\text{II}}$  with tnz identifies them as important therapeutic agents. It was earlier observed that the monomeric complex plays a key role in controlling infections caused by microbes [21]. *P. aeruginosa* is known to have many virulence genes viz *LasI / Rhl* that are activated during quorum sensing network leading to expression of virulence factors like elastase, rhamnolipid and pyocyanin [44]. The amount of las A protease and las B elastase were monitored with or without the  $\text{Cu}^{\text{II}}$  complexes (Figure 10). The *las*-regulated virulence genes *lasA* and *lasB* were significantly down regulated to  $82.4 \pm 4.25\%$  in the presence of the monomeric complex (Figures 8 A & B) as compared to the dimeric one or even in comparison to amoxicillin suggesting that the monomeric complex has the ability to block the synthesis of signaling molecules responsible for regulating biofilm formation by inhibiting LasI / Rhl I synthase [48]. A lack of production

of virulence factor pyocyanin after treatment of *P. aeruginosa* with both complexes was observed with a maximum reduction of  $86.34 \pm 7.25$  % in presence of the monomeric complex. Experimental results show the monomeric complex was able to bring about inhibition of QS maximally in *P. aeruginosa*.

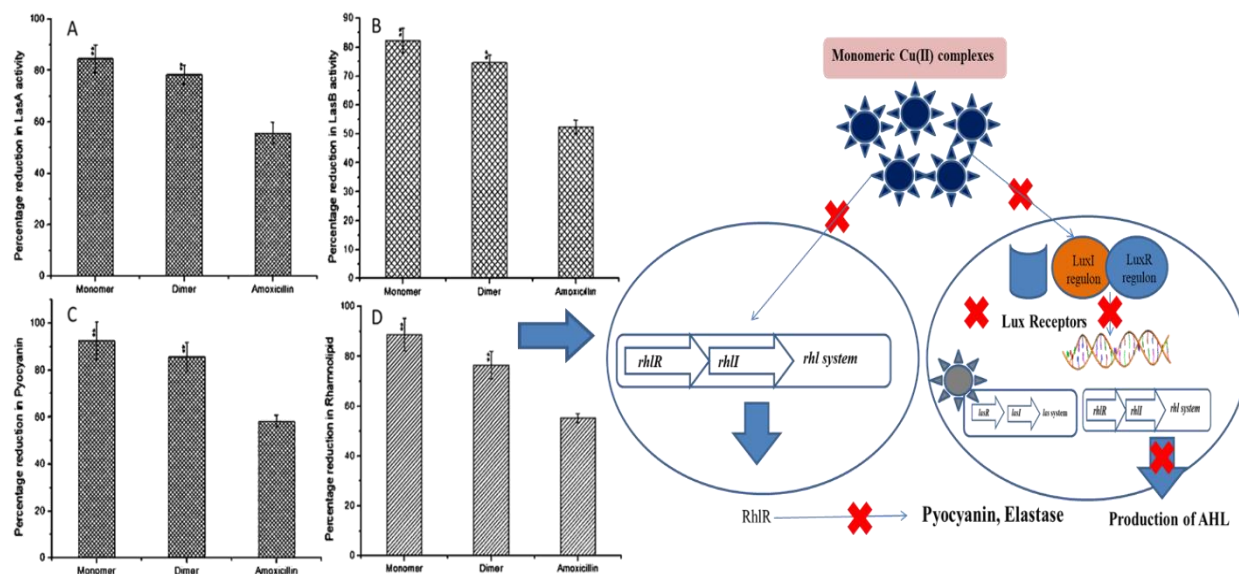
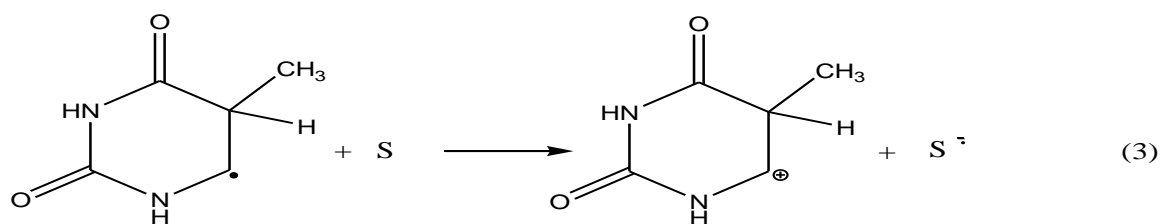
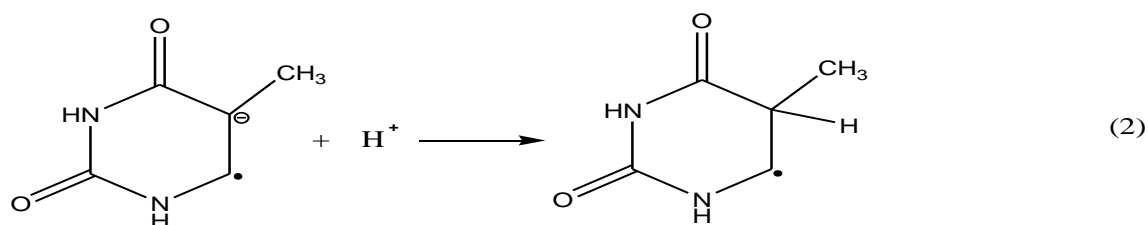
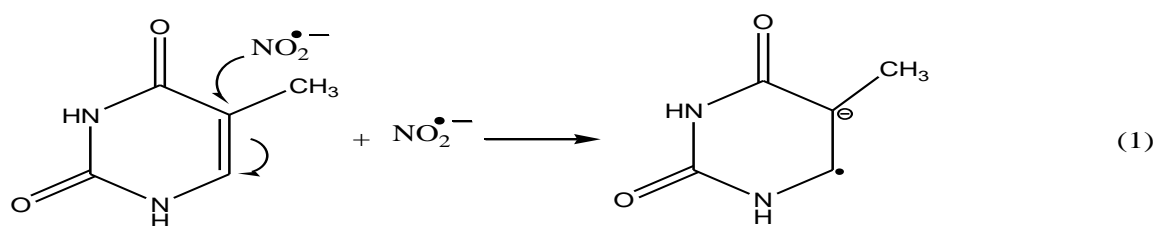


**Figure 10:** Inhibition of quorum sensing (QS) signaling mechanism during biofilm formation

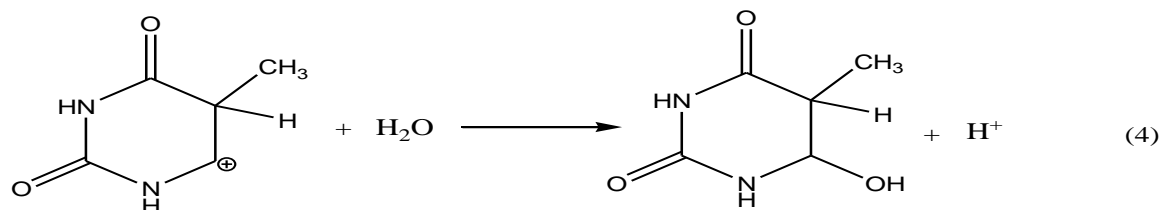
## Discussion

Maintenance of a glassy carbon electrode at cathodic peak potential of a compound, in aqueous solution, is evidenced to bring about “single step four electron reduction” of 5-nitroimidazoles. As a result, species are sequentially expected to be generated within a small time scale. Hence, the damage caused to a target, i.e. to nucleic acid bases or to calf thymus DNA, maintained in the immediate vicinity of such generation of reduced species may not be exclusively due to a particular species. While  $\text{RNO}_2^{\bullet-}$  could have a substantial role, other reduction products formed during the electrochemical reduction of the compounds would also generate species that could modify targets. Since formation of  $\text{RNO}_2^{\bullet-}$  is the first step of the reduction process and being a radical, it is likely to have a high probability to interact with a

target before being reduced to its next state. If the rate of interaction of  $\text{RNO}_2^{\bullet-}$  either with a nucleic acid base or with calf thymus DNA is higher than its tendency to be reduced further, interaction with  $\text{RNO}_2^{\bullet-}$  would be predominant. Hence, while other reduction products of a complex or of tnz could well be involved in a modification of the target,  $\text{RNO}_2^{\bullet-}$  might have a substantial contribution to the damage detected (Scheme I, shown with respect to thymine) [32]. This study was actually performed to realize how different reduction products generated electrochemically either on tnz or on its complexes with Cu(II) interact with nucleic acid bases and with DNA, to realize what would happen when they are present within cells and undergo enzymatic reduction. For several decades now, reduction of nitroimidazoles is considered very crucial for cytotoxic action for which they are much sought after [1-3, 5-14].



S = Potentially Favourable Electron Affinic Species



**Scheme I:** A probable mechanism for the interaction of the nitro-radical anion with thymine

Again, considering the variety of species that are formed in solution, there is a good possibility for the formation of  $\text{RNO}_2^{\bullet-}$  either directly or through comproportionation, when an  $-\text{NO}_2$  containing moiety (either on tnz or on the complex) interact with another molecule that contains say,  $-\text{NHOH}$  [19, 32, 33, 46, 47]. The possibility of disproportionation of  $\text{RNO}_2^{\bullet-}$ , known to depend on pH, on the solvent and also on the material of the electrode also exist [19, 32, 33, 46, 47]. Hence, depending on different reduction products that in turn depend on whether they were generated on tnz present alone or on tnz present as part of a complex, substrates (nucleic acid bases or calf thymus DNA) interacting with  $\text{RNO}_2^{\bullet-}$  becomes a high possibility. If the rate of depletion of  $\text{RNO}_2^{\bullet-}$  in solution either due to disproportionation or in some other pathway is less, there is a good possibility of it interacting with a target maintained in its immediate vicinity. If however it is otherwise, then interaction due to  $\text{RNO}_2^{\bullet-}$  would not be dominant i.e. it would not be the major cause of transformations either on nucleic acid bases or on calf thymus DNA. However, given the experimental design, although disproportionation is a possibility, it would only occur if the concentration of species formed in solution, are higher than that in our experiments. Under the conditions of the experiment, concentrations of electrochemically reduced species formed on tnz or its complexes would never be very high in solution; in fact immediately after their generation they would see more of the nucleic acid bases than one of its own kind (target : compound :: 10 : 1), hence scope of disproportionation of  $\text{RNO}_2^{\bullet-}$  would be small [19, 32, 33, 46, 47]. Although explained qualitatively,  $\text{RNO}_2^{\bullet-}$  could eventually become an important species amongst other reduced products generated either on free tnz or on tnz present as part of a  $\text{Cu}^{\text{II}}$  complex that might interact with a target.

A comparison of the damage caused to nucleic acid bases (Table 1) or to calf thymus DNA (Table 3) reveals that the dimeric complex is the most effective. As can be seen from the structures of the two complexes (Figure 1), both have two units of tnz in them. Moreover,

since it has been shown earlier that complex formation of tnz by  $\text{Cu}^{\text{II}}$  results in a decrease in nitro-radical anion formation [20, 21], hence greater efficacy due to the dimeric complex and its difference with the monomeric one may not be due to the presence of tnz in the complexes. Rather, the dimeric complex having two  $\text{Cu}^{\text{II}}$  centres, against one in the monomer, could serve as a possible reason for the difference in activity. A greater presence of  $\text{Cu}^{\text{II}}$  in the dimer could be responsible for more interaction of the dimeric complex with thymine or cytosine or with calf thymus DNA via  $\text{Cu}^{\text{II}}$  that could help in the modification of the target or simply enable the compound to engage more with the target. Either way, a certain amount of thymine or cytosine or a certain amount of calf thymus DNA would not be detected either by HPLC as free thymine or free cytosine (Table 1) or as free calf thymus DNA in fluorescence based EtBr experiments (Table 3). In case of adenine however, the monomeric complex performs much better which could be due to the larger size of the dimeric complex and that adenine, being a purine based nucleic acid base is also large.

Quite interestingly, trends observed in Table 1 and Table 3 are similar indicating DNA having a greater percentage of thymine, like that in calf thymus DNA (41.9 mole % G-C and 58.1 mole % A-T) should be susceptible to greater attack by  $\text{Cu}^{\text{II}}$  complexes of tnz. Hence, a prior knowledge on the damaging ability of a compound on nucleic acid bases is extremely important since it helps one to use the correct compound in targeting a disease causing microbe; at the same time such prior knowledge also enables one to know the extent to which the compound could be harmful to the host i.e. whether it could affect the DNA of the host as well. Therefore, findings of this study helps one to realize why tnz (tinidazole) has been so successful against disease causing microbes that have a high thymine content in their DNA (Table 2).

In spite of decreased nitro-radical anion formation [20, 21]  $\text{Cu}^{\text{II}}$  complexes of tnz were found to be better in performance on nucleic acid bases and calf thymus DNA than tnz. This is also

very interesting when for the 5-nitromidazole family of drugs, nitro-radical anion formation is considered important for drug action. Therefore, it seems the efficacy of the complexes are not due to free radical formation involving redox pathways that involve tnz; rather a better performance by complexes is due to certain attributes of complex formation, those that involve the Cu<sup>II</sup> centre [38, 39] or due to interaction between various constituents of DNA and the Cu<sup>II</sup> centre, that is able to cause double strand modification which is also detected by the technique used (i.e. the decrease in DNA-EtBr fluorescence) [35-39]. Therefore, results of experiments with calf thymus DNA indicate they are probably not a consequence of the free radical activity involving tnz, rather other factors, like presence of Cu<sup>II</sup> in the complex could well be involved.

To be sure about our model studies, an attempt was made to study the performance of the complexes, on their ability to prevent biofilm formation on *S. aureus* and *P. aeruginosa* that are responsible for causing nosocomial infections. Lower MBC values for the monomeric and dimeric Cu<sup>II</sup> complexes compared to tnz suggests better efficacy due to the complexes in removing biofilm cells. The indwelling bacterial cells within the biofilm matrix have a continuous and rich supply of nutrients and water molecules, much needed for their survival under stressed conditions due to the extremes of temperature, pH, salt concentration or the presence of antimicrobials. The biofilm matrix also consists of lipid molecules, nucleic acids, proteins, extracellular DNA, and quorum sensing signalling molecules needed for cell density dependent intercellular communications that are required for the growth of the biofilm and its sustenance. It was found that the Cu<sup>II</sup> complexes of tnz were able to bring about substantial changes in biofilm concentration both for *S. aureus* and *P. aeruginosa*; monomeric complex having better efficacy against sessile colonies.

Biofilm associated infections are found to occur via two mechanisms: 1) through biofilm formation by enhanced quorum sensing that occurs by production of small signaling

molecules capable of detecting the cell population density in the neighboring environment under stressed condition and 2) by the spreading of microbial cells from EPS matrix infecting newer places. From our study, we found that the monomeric complex has the ability to block the synthesis of signaling molecules responsible for regulating biofilm formation by inhibiting LasI / Rhl I synthase [48]. Thus the monomeric complex has the potential of inhibiting quorum sensing (QS) mechanism of *P. aeruginosa* by inhibiting QS-genes and blocking transcriptional regulatory proteins that inactivate LasR or RhlR systems.

While studying the interactions of tnz and its two complexes with nucleic acid bases and calf thymus DNA, it was revealed that the dimeric complex performs better, followed by the monomeric one and tnz. So, it was expected that efficacy in prevention of biofilm formation would also follow the same trend. However, in case of biofilm related experiments, we found the monomeric complex was most efficacious to the pathogenic target, followed by the dimeric complex and tnz. Such an anomaly isn't unexpected as nitro radical anions generated from tnz and its complexes vary widely. As observed in previous communications, complex formation is associated with quenching of nitro radical anion concentration [20, 21]. We expect the monomeric complex to quench radical anion concentration in a manner just sufficient to eliminate the excess that would be responsible for toxic side effects, keeping the efficacious concentration of radical anions intact. This combined with improved binding with DNA over tnz is expected to give it the much superior boost for maximum efficacy. The dimeric complex, on the other hand, is expected to quench radical anion concentration more extensively, due to the presence of two Cu<sup>II</sup> centres; hence more of the efficacious portion of the nitro radical anion concentration is eliminated. Moreover, owing to a larger size, efficacy of the dimeric complex through binding is probably compromised; reason why in our model studies also the dimeric complex performs better on pyrimidine based nucleic acid bases

cytosine and thymine but not on purine based adenine. The dimeric complex was however found to be more efficacious than tnz, owing to attributes of complex formation.

The concentrations of compounds varied from one another in biological studies on biofilm formation and the model studies since in case of prevention or eradication of bacterial biofilm formation and growth, emphasis was given to the obtained MIC and MBC values respectively. Hence, while anti-bacterial and anti-biofilm studies were performed keeping in mind MIC and MBC values on sessile *P. aeruginosa* (which for the monomeric Cu<sup>II</sup> complex was 20.25 µM and for the dimeric complex, 45.0 µM), for the model studies slightly higher concentrations were used since for the model studies, where the technique employed was electrochemical reduction, if sufficient material isn't present, the species generated might not be adequate for interaction with nucleic acid bases or with DNA.

The expression of biofilm forming bacterial genes is regulated by cell-population density dependent mechanism known as quorum sensing (QS). Both Gram-negative and Gram-positive bacteria perform QS by the mechanism of small signal molecules that varies from Gram-negative to Gram-positive bacteria. N-acyl homoserine lactone (AHL) molecules (autoinducer-1, AI-1) are widely detected in Gram-negative bacteria while for Gram-positive bacteria mainly peptides [autoinducer peptides (AIP) or quorum sensing peptides] are used [46]. We also checked the expression of virulence factors like pyocyanin production, elastase, las A protease and las B elastase in *P. aeruginosa* (Gram-negative) in the presence of monomeric form of the compound. This indicates modulation and prevention of biofilm forming signaling network in presence of antimicrobial agents. However, expression of virulence factors in Gram positive bacteria like *S. aureus* is directly linked to alterations in expression profiles of peptides/proteins like endotoxins, haemolysins, exotoxins, autoinducing peptide 2 (AIP2), proteases etc. that were not monitored as a part of this study [47].

Our main aim was to highlight anti-biofilm properties of copper(II) complexes by the formation of electrochemically generated nitro radical anion triggering bacteria mediated enzymatic reduction. For this purpose, we only showed alterations in QS mechanism in *P. aeruginosa*. Alteration in biofilm formation and growth is also effected in presence of copper(II) complexes in *S. aureus* as realized from Figure 9 that clearly depicts reduction of EPS components.

Tnz is reported to bind to DNA while inside a cell initiating cytotoxic action on a pathogen by forming nitro radical anion, considered responsible for its efficacy. Excess production of such nitro radical anion is responsible for idiosyncratic side effects which metal complexes with reduced formation might control. Hence, both from model studies and from prevention of biofilm formation, it may be said, what the complexes compromise in the free radical pathway, they make up through aspects like better interaction with a target or due to the redox active  $\text{Cu}^{\text{II}}/\text{Cu}^{\text{I}}$  couple. Hence,  $\text{Cu}^{\text{II}}$  complexes of tnz, on the one hand, by controlling generation of  $\text{RNO}_2^{\bullet-}$ , might control neurotoxic side effects, on the other, continue to be better cytotoxic agents than parent 5-nitroimidazoles (here, tinidazole) when one actually might expect them to have compromised on efficacy.

## References

1. J. P. Carlier, N. Sellier, M. N. Rager, G. Reysset, G. *Antimicrob Agents Chemother.* **1997**, 41, 1495-1499.
2. W. Raether, H. Hänel, *Parasit. Res.* **2003**, 90, S19-S39; doi: 10.1007/s00436-002-0754-9.
3. Y. Miyamoto, J. Kalisiak, K. Korthals, T. Lauwaet, D C Young, R Lozano, E R Cobo, P Upcroft, J A Upcroft, Berg, D. E.; Gillin, F. D.; Fokin, V. V.; Sharpless, K. B.; Eckmann, L. ., *Proc. Natl. Acad. Sci. USA* **2013**, 110, 17564-17569.
4. A. D. Verderosa, M Totsika, M.; *Front. Chem.* **2019**, 7, <https://doi.org/10.3389/fchem.2019.00824>.

5. C. W. Ang, A. M. Jarrad, M. A. Cooper, M. A. T. Blaskovich, *J. Med. Chem.* **2017**, 60, 7636-7657.
6. J. M. Brown, *Cancer Res.* **1999**, 59, 5863-5870.
7. M. Bonnet, C. R. Hong, W. W. Wong, L. P. Liew, A. Shome, J. Wang, Y. Gu, R. J. Stevenson, W. Qi, R. F. Anderson, F. B. Pruijn, W. R. Wilson, S. M. F. Jamieson, K. O. Hicks, M. P. Hay, *J Med Chem.* **2018**, 61, 1241-1254.
8. P. Wardman, *Br J Radiol.* **2019**, 92, 20170915; <https://doi.org/10.1259/bjr.20170915>
9. a) S. Sood, A. Kapil, *Ind. J Sex Transm Dis.* **2008**, 29, 7-14. b) V Puri, *Neurology, India.* **2011**, 59, 4-5.
10. H. Kato, H. Sosa, M. Mori, T. Kaneko, *KansenshogakuZasshi.* **2015**, 89, 559-566.
11. J. S. Bakshi, J. M. Ghiara, A. S. Nanivadekar, *Drugs* **1978**, 15, 33-42.
12. A. L. Crowell, K. A. Sanders-Lewis, W. E. Secor, *Antimicrob Agents Chemother.* **2003**, 47, 1407-1409.
13. H. B. Fung, T. L. Doan, *ClinTher.* **2005**, 27, 1859-1884.
14. J. R. Schwebke, R. A. Desmond, *Am J Obstet Gynecol.* **2011**, 204, 211.e1-211.e6.
15. K. Ebel, H. Koehler, A.O. Gamer, R. Jäckh, **2002** Wiley-VCH, doi:10.1002/14356007.a13\_661.
16. G. Cammarota, O. Cannizzaro, R. Cianci, A. Armuzzi, A. Gasbarrini, A. Pastorelli, Papa, G Gasbarrini, *Dig Dis Sci* **1999**, 44, 2386-2389.
17. E. L. Plummer, Vodstrcil, L. A.; Danielewski, J. A.; Murray, G. L.; Fairley, C. K.; Garland, S. M.; Hocking, J. S.; Tabrizi, S. N.; Bradshaw, C. S.. *PLoS ONE* **2018**, 13, e0190199; <https://doi.org/10.1371/journal.pone.0190199>.
18. D. I. Edwards, *J. Antimicrob. Chemother.* **1993**, 31, 9-20.
19. G. Armendariz-Vidales, L. S. Hernandez-Munoz, F. J. Gonzalez, A. A. de Souza, F. C. de Abreu, G. A. M. Jardim, E. N. da Silva, M. O. F. Goulart, C. Frontana, *J. Org. Chem.* **2014**, 79, 5201-5208.
20. R. C. Santra, D. Ganguly, J. Singh, K Mukhopadhyay, S. Das, *Dalton Trans.* **2015**, 44, 1992-2000.

21. R. C. Santra, D. Ganguly, S. Jana, N. Banyal, J. Singh, A. Saha, S. Chattopadhyay, K. Mukhopadhyay, S. Das, *New Journal of Chemistry* **2017**, 41, 4879-4886.
22. M. Dan, A. L Wang, C. C. Wang, *MolMicrobiol.* **2000**, 36, 447-456.
23. K. J Graves, J. Novak, W. E. Secor, P. J. Kissinger, J. R. Schwebke, C A Muzny, *Parasitology*, **2020**, 147, 1383-1391.
24. R. C. Santra, K. Sengupta, R. Dey, T. Shireen, P. Das, P. S. Guin, K. Mukhopadhyay, S Das, *J. Coord. Chem.* **2014**, 67, 265-285.
25. H. Lund, Cathodic reduction of nitro and related compounds. In *Organic Electrochemistry*, 3rd ed.; Lund, H.; Baizer, M. M., Ed.; M. Dekker Inc., New York, **1990**, 411.
26. J. W. Costerton, P. S. Stewart, E. P. Greenberg, *Science*, **1999**, 248, 1318-1322.
27. H. A. Khan, A. Ahmad, R. Mehboob, *As. Pac. J. Trop. Biomed.*, **2015**, 5, 509-514.
28. C. Potera, *Science*, **1999**, 283, 1837-1839. doi: 10.1126/science.283.5409.1837.
29. B. Amorena, Gracia, E.; Monzon, M.; Leiva, J.; Oteiza, C.; Pérez, M.; Alabart, J-L. J Hernández-Yago, *J. AntimicrobChemother.* **1999**, 44, 43-55; <https://doi.org/10.1093/jac/44.1.43>.
30. D. Lahiri, S. Dash, R. Dutta, M. Nag, *J Biosci.* **2019**, 44, 52(1-19).
31. P. S. Stewart, *Int. Jour. Med. Microbiol.* **2002**, 292, 107-113.
32. P. C. Mandal, *J. Electroanal. Chem.* **2004**, 570, 55-61.
33. J. A. Squella, P. Gonzalez, S. Bollo, *Pharm Res* **1999**, 16, 161-164.
34. S. Das, A. Saha, P. C. Mandal, *J. Radioanal. Nucl. Chem.* **1995**, 196, 57-63.
35. A. R. Morgan, J. S. Lee, D. E. Pulleyblank, N. L. Murray, D. H. Evans, *Nucleic Acids Res.* **1979**, 7, 547-565.
36. H. C. Birnboim, J. J. Jevcak, *Can. Res.*, **1981**, 41, 1889-1892.
37. W. A. Prütz, *Radiat. Environ. Biophys.* **1984**, 23, 1-6.
38. S. Das, A. Saha, P.C. Mandal, *Environ. Health Pers.* **1997**, 105, 1459-1462.
39. S. Das, P.C. Mandal, *J. Radioanal. Nucl. Chem.* **2014**, 299, 1665-1670.
40. C. E. Nord, *J. Antimicrob. Chemother.* **1982**, 10, 35-42.
41. C. E. Nord, L. Kager, *Infection* **1983**, 11, 54-60.
42. A. M. M. Jokipii, L. Jokipii, *Chemother.*, **1977**, 23, 25-31.

43. D. Machado, J. Castro, A. Palmeira-de-Oliveira, J Martinez-de-Oliveira, N. Cerca, *Front. Microbiol.* **2016**, 6, 1528; <https://doi.org/10.3389/fmicb.2015.01528>.
44. M. Kostylev, D. Y. Kim, N. E. Smalley, I. Salukhe, E. P. Greenberg, A. A. Dandekar, *P N A S, USA*, **2019**, 116, 7027-7032.
45. S. A. K .S. Ahmed, M. Rudden, T. J. Smyth, J. S. G. Dooley, R. Marchant, I. M Banat,. *Appl. Microbiol. Biotechnol.* **2019**, 103, 3521-3535.
46. F. Verbeke, S. De Craemer,; N. Debunne, Y. Janssens, E Wynendaele, E.; C.Van de Wiele, B. De Spiegeleer, *Front. Neurosci.* **2017**, 11, 183(1-18).
47. C. Kong, C. F. Chee, K. Richter, N. Thomas, N.A. Rahaman, S. Nathan, , UM-C162. *Sci Rep* **2018**, 8, 2758(1-16).

# **Chapter 13**

**Radiosensitizing attributes of Cu<sup>II</sup> & Zn<sup>II</sup> complexes  
of Ornidazole: Role of the nitro radical anion**

## Introduction

In the last few decades, spanning over half a century, work from different laboratories have established that solid tumors contain regions of mild to severe hypoxia that either alter the cellular metabolism of that region or increase its resistance to radiation and chemotherapy [1-4]. Detection of hypoxic cells in human tumors improved with discovery of new imaging techniques and use of predictive gene profiles [5-10]. Sufficient data is available on hypoxia in different human tumors, although considerable heterogeneity exists between individual types [1-4, 9, 10]. Clinical trials suggest effort was made to modify radiation resistance using either hypobaric hypoxia or normobaric/hyperbaric oxygen therapies that initially raised doubts because treatment of O<sub>2</sub> to cells was thought to support cell growth in cancer but later proved advantageous [11-14]. Not only did it help in radiotherapy but it influenced a tumor's micro-environment in a correct manner for treatment [11-14]. It was shown oxygen not only acts as a strong electron scavenger but by forming pyrimidine peroxy radical was able to further react within DNA affecting vicinal bases or 2-deoxyribose moieties [15, 16]. Such studies led to two important aspects i) importance of oxygen in radiotherapy and ii) identification of new chemical agents that might deliver results under hypoxic conditions [1, 2, 12, 14-19].

There is lot of attention on hypoxic cytotoxins [19-21], that selectively and preferably destroy cells in a hypoxic environment, a group slightly different from radiosensitizers that help to improve radiotherapy under hypoxic conditions [18, 22]. Hypoxic cytotoxins by killing cells in hypoxia not only overcome cellular resistance but exploit it, converting it into a therapeutic advantage [20, 21]. Nitroimidazoles are "electron-affinic" and hence they react with DNA free radicals to combat hypoxia-associated radio-resistance [18, 23, 24]. Several members were found clinically effective at tolerable dose [18, 23, 25]. However, most compounds had limited clinical success; their efficacy restricted by dose-limiting toxicity, attributed to

electron affinity; to the relative ease of reduction of  $-\text{NO}_2$  in nitroimidazoles to  $\text{RNO}_2^-$  [23]. Such reduction may be modulated by complex formation [26-28].

This chapter contains the performance of Ornidazole and its monomeric  $\text{Cu}^{\text{II}}$  and  $\text{Zn}^{\text{II}}$  complexes with regard to their radiosensitizing abilities [29-30]. The hypoxia-specific cytotoxin tirapazamine showed it was selective for hypoxic cells in solid tumors occurring as a consequence of DNA damage produced by free radicals during enzymatic reduction [21]. Studies on DNA damage and metabolism of tirapazamine in A549 human lung carcinoma cells and in isolated nuclei derived from cells showed although nuclei metabolizes it at a rate 20% compared to the whole cell, extent of DNA damage by nuclei was similar to that by cells [21]. The study observed tirapazamine radicals formed outside the nuclei do not contribute to intra-nuclear DNA damage and all DNA damage resulted from radicals generated within the nucleus. Hence, 80% of drug metabolism (occurring in the cytoplasm) is irrelevant with regard to killing of hypoxic cells [21]. This served as an inspiration towards using complexes of Ornidazole to investigate radiosensitizing and/or cytotoxic attributes that bring about substantial decrease in  $\text{RNO}_2^-$  formation; yet not compromising efficacy [26-28, 33]. Therefore, like in case of tirapazamine where 80% of drug metabolism is irrelevant in killing hypoxic cells, here also if we can show complexes of Onz are better radiosensitizers or hypoxic cytotoxins in spite of decreased  $\text{RNO}_2^-$  [26-28, 31], then the amount required for biological activity can be believed to be provided by the complexes. If the amount formed by Onz is much in excess of what is actually necessary then there is the risk of undesirable neurotoxic side effects [26-28, 31]. Hence, use of complexes could have the advantage that excess  $\text{RNO}_2^-$  would not be present leading to some clinical success regarding toxic side effects [26-28]. Worth mentioning is that complexes are either better DNA binding agents or DNA damaging agents or both, following interaction of *in situ* generated  $\text{RNO}_2^-$  with nucleobases and calf thymus DNA [24].

## Results and Discussion

### Radiation induced damage of adenine, thymine and cytosine by Onz and its monomeric Cu(II)/Zn(II) complexes

Aqueous solutions of nucleobases (thymine, cytosine and adenine) were irradiated with  $^{60}\text{Co}$  gamma rays in the range 2.8 Gy to 13.5 Gy, under Ar saturated conditions, in the absence or presence of Onz and its Cu(II)/Zn(II) complexes. They were subsequently followed by HPLC. Chromatograms of all nucleobases were recorded. While thymine eluted between 10.8 to 11.0 minutes, adenine eluted between 8.5 to 8.7 minutes and cytosine at 3.7 minutes. With gradual increase in radiation dose, concentrations of all nucleobases decreased. Such decrease in concentration with increase in radiation dose was different for each nucleobase and was found to depend on the compound in whose presence irradiation was administered.

For all three nucleobases, decrease was significant when irradiated in presence of  $\text{Cu}(\text{Onz})_2\text{Cl}_2$  followed by  $\text{Zn}(\text{Onz})_2\text{Cl}_2$  and Ornidazole. A linear dependence on dose was observed. Figure 1 shows HPLC profiles for the degradation of all three in the absence of a compound at different radiation dose. Figures 2, 3 and 4 show HPLC profiles for the degradation of nucleobases in the presence of 10  $\mu\text{M}$  Onz, 10  $\mu\text{M}$   $\text{Zn}(\text{Onz})_2\text{Cl}_2$  and  $\text{Cu}(\text{Onz})_2\text{Cl}_2$  respectively at different radiation dose.

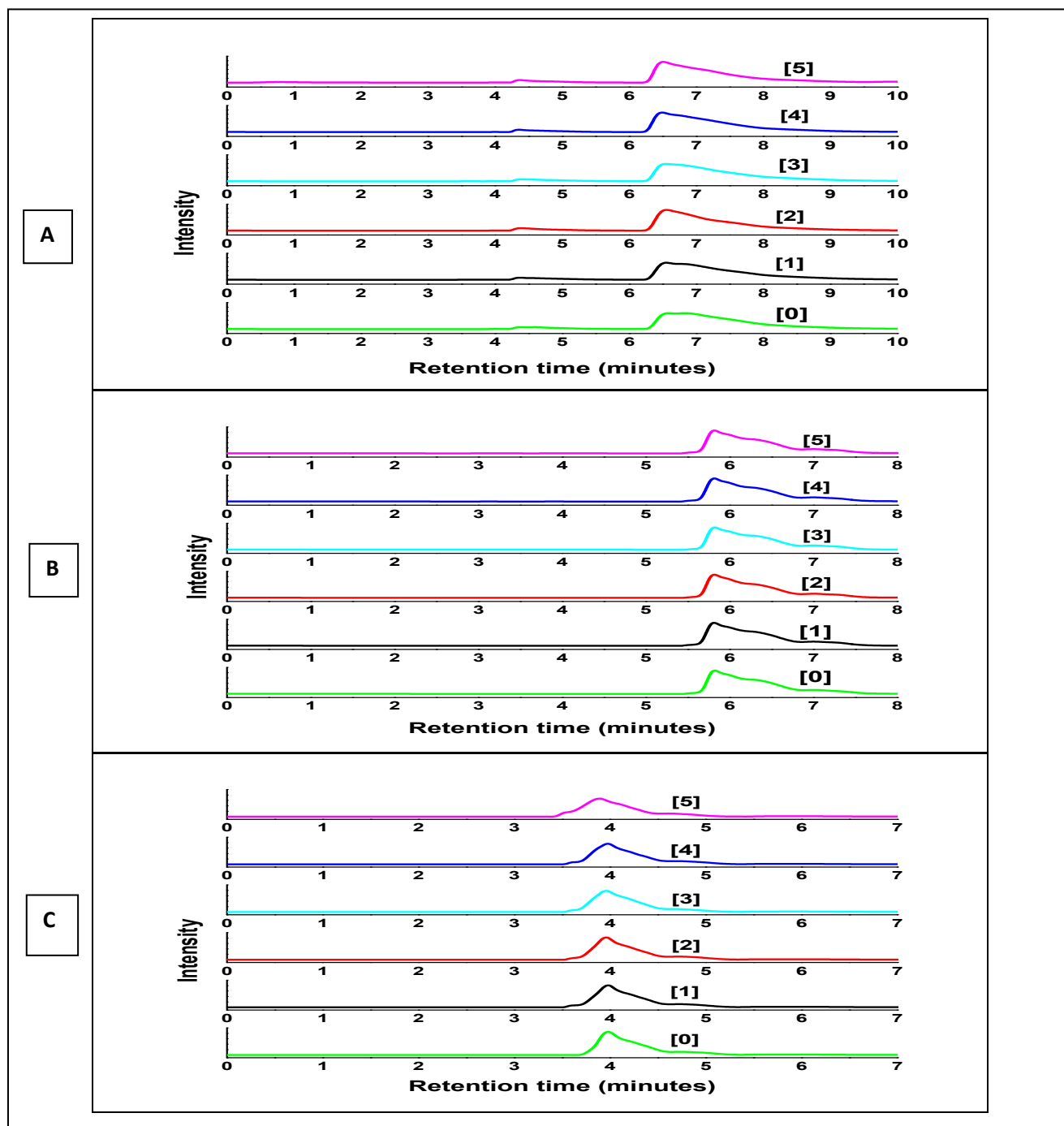


**Figure 1:** HPLC chromatograms monitored at 254 nm for  $10^{-4}$  M A) adenine, B) thymine and C) cytosine solutions irradiated at the mentioned dose. Zero indicates sample was not irradiated while 2.7 Gy (1), 5.4 Gy (2), 8.1Gy (3), 10.8 Gy (4) and 13.5 Gy (5) indicate irradiated dose in an Ar saturated medium in the absence of any compound.

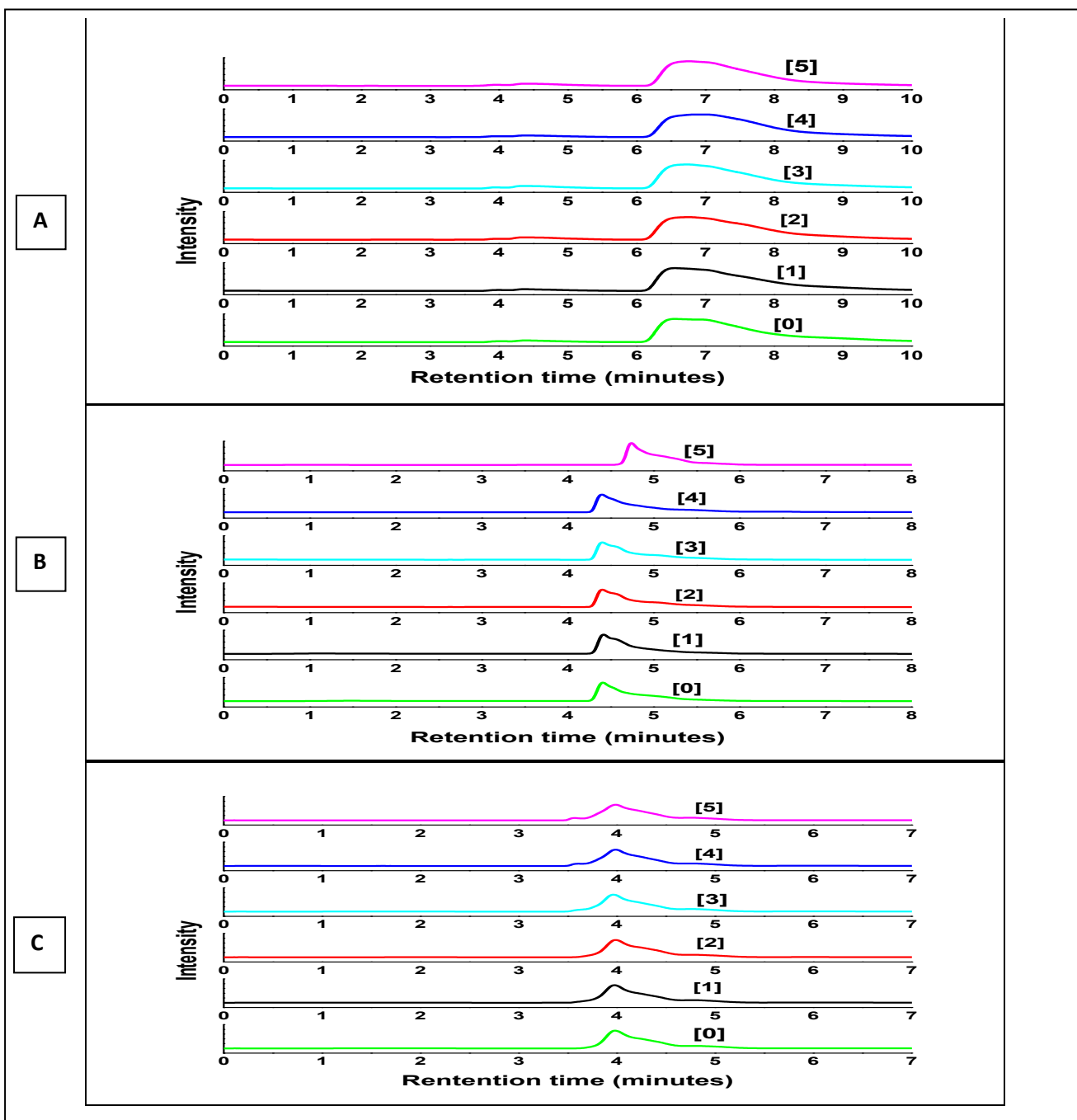


**Figure 2:** HPLC chromatograms monitored at 254 nm for  $10^{-4}$  M A) adenine, B) thymine and C) cytosine solutions irradiated at the mentioned dose. Zero indicates sample was not irradiated while 2.7 Gy (1), 5.4 Gy (2), 8.1Gy (3), 10.8 Gy (4) and 13.5 Gy (5) indicate irradiated dose in an Ar saturated medium in the presence of  $10^{-5}$ M Ornidazole.

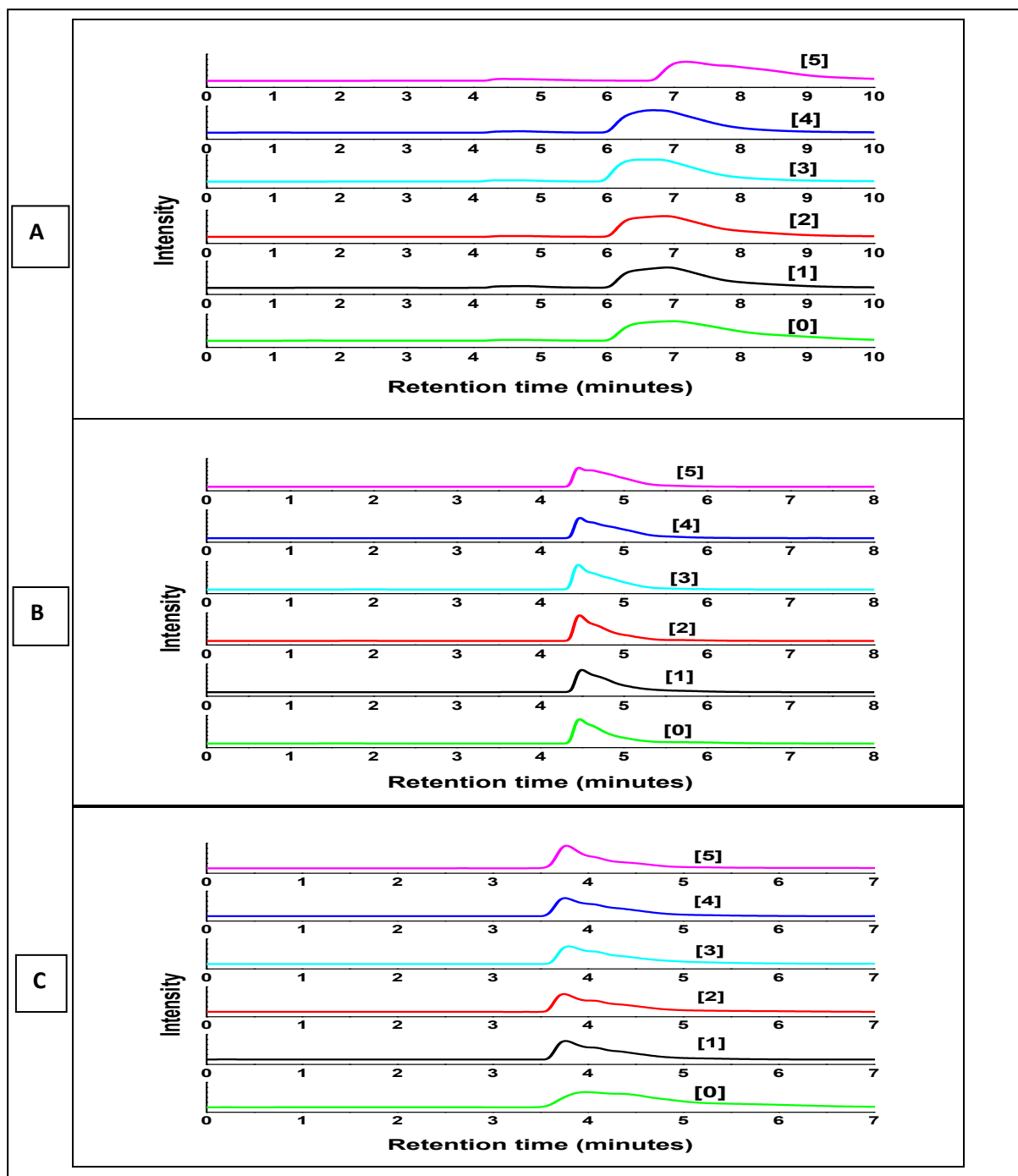


**Figure 3:** HPLC chromatograms monitored at 254 nm for  $10^{-4}$  M A) adenine, B) thymine and C) cytosine solutions irradiated at the mentioned dose. Zero indicates sample was not irradiated while 2.7 Gy (1), 5.4 Gy (2), 8.1Gy (3), 10.8 Gy (4) and 13.5 Gy (5) indicate irradiated dose in an Ar saturated medium in the presence of  $10^{-5}$ M  $Zn(Onz)_2(Cl)_2$ .

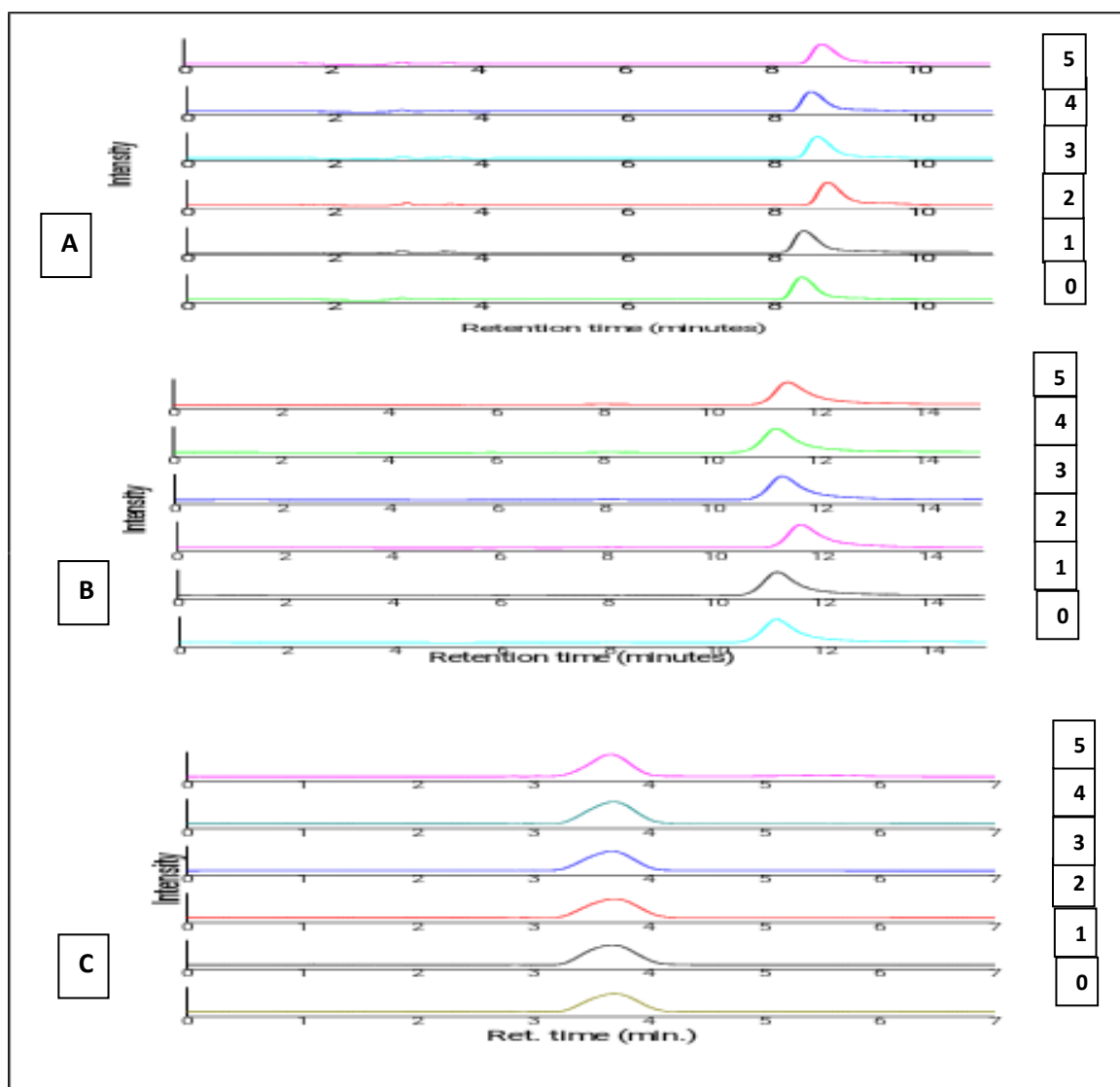


**Figure 4:** HPLC chromatograms at 254 nm for  $10^{-4}$  M A) adenine, B) thymine, C) cytosine solutions irradiated at the mentioned dose. Zero indicates sample was not irradiated. 2.7 Gy (1), 5.4 Gy (2), 8.1 Gy (3), 10.8 Gy (4) and 13.5 Gy (5) indicates irradiated dose in an Ar saturated medium in presence of  $10^{-5}$  M  $\text{Cu}(\text{Onz})_2\text{Cl}_2$ .

A previous study with dimeric Cu(II) complex of tinidazole, employing a much higher dose than one usually employs for physiological studies, characterized the products that were formed from degradation of thymine and uracil [31]. HPLC profiles for degraded products of thymine and uracil were generated by me as part of my HPLC studies and subsequently utilised to identify the products formed following degradation of thymine and cytosine when

irradiated in the absence and presence of compounds. Results for two relatively high doses (10.8 Gy and 13.5 Gy) indicate, irradiation provided in presence of  $\text{Cu}(\text{Onz})_2\text{Cl}_2$  results in the formation of 5,6-dihydroxy-5,6-dihydrothymine (thymine glycol) and 5-hydroxymethyl uracil. In case of  $\text{Cu}(\text{Onz})_2\text{Cl}_2$ , peaks were much more prominent than when Onz or  $\text{Zn}(\text{Onz})_2\text{Cl}_2$  were used as sensitizers. Peak for the formation of 5,6-dihydrothymine was however not detected even when thymine was irradiated in presence of  $\text{Cu}(\text{Onz})_2\text{Cl}_2$  in the dose range in which our experiments were performed. Since formation of 5,6-dihydrothymine depends on the formation of  $\bullet\text{H}$  and since G value of  $\bullet\text{H}$  at pH ~ 7.4 is extremely low [35], not much of it sufficient to be detected by HPLC was formed. For 5, 6-dihydrothymine to form, a much higher dose would be required at pH ~ 7.4, which was not used in this study. Products were identified from their respective retention times using authentic samples [31].

Another pyrimidine based nucleobase cytosine, differs from uracil at  $\text{C}_1$  of the molecule where an  $-\text{NH}_2$  group is present instead of  $-\text{OH}$  (in the enol form). Since 5,6-dihydroxy-5,6-dihydrocytosine (cytosine glycol) is unstable and known to convert to 5,6-dihydroxy-5,6-dihydrouracil (uracil glycol) by deamination, I developed method files on uracil to identify degradation products of cytosine [33, 38]. A peak in the chromatogram appearing at a retention time close to that of 5,6-dihydroxy-5,6-dihydrouracil as in the method file, could either be due to 5,6-dihydroxy-5,6-dihydrocytosine or 5,6-dihydroxy-5,6-dihydrouracil (i. e. if it had in the time between irradiation of cytosine and performing of HPLC converted either completely or partially from 5,6-dihydroxy-5,6-dihydrocytosine) [31,36]. It is known 5,6-dihydroxy-5,6-dihydrocytosine by dehydration converts to 5-hydroxycytosine or by deamination and dehydration to 5-hydroxyuracil [38]. Therefore, the uracil method file that was created for detecting uracil derivatives helped me to realize formation of 5,6-dihydroxy-5,6-dihydrocytosine that subsequently convert to several uracil derivatives as mentioned above [31]. These observations suggest pyrimidine based nucleobases experience an initial

free-radical attack by products of radiolysis of water ( $\text{H}^\bullet$ ,  $\text{OH}^\bullet$  and  $e_{\text{aq}}^-$ ) on the  $\text{C}_5\text{—C}_6$  double bond that subsequently yield different products [31, 35].

Figures 3 and 4 show degradation of nucleobases obtained in an Ar saturated medium, either in presence of Onz or  $\text{Zn}(\text{Onz})_2\text{Cl}_2$ . They suggest damage caused to nucleobases are not much in presence of Onz and that it increased only slightly when  $\text{Zn}(\text{Onz})_2\text{Cl}_2$  was used. Studies reveal it was maximum for  $\text{Cu}(\text{Onz})_2\text{Cl}_2$ . Under Ar saturated conditions,  $\bullet\text{OH}$  and  $e_{\text{aq}}^-$  are produced in almost equal amount unlike in  $\text{N}_2\text{O}$  saturated medium where  $e_{\text{aq}}^-$  converts to  $\bullet\text{OH}$  [35, 37]. Therefore, reactions responsible for damage of nucleobases are initiated both by  $\bullet\text{OH}$  and  $e_{\text{aq}}^-$ .

For a purine based nucleobase adenine, HPLC chromatograms did not show any new peak within a retention time of 15 minutes. Decrease in peak for adenine was significant for radiation provided in presence of  $\text{Cu}(\text{Onz})_2\text{Cl}_2$  in Ar saturated medium while it was almost the same in presence of Onz and  $\text{Zn}(\text{Onz})_2\text{Cl}_2$ . Concentrations of nucleobases remaining were plotted against radiation dose (Figure 5). Plots indicate radiation-induced damage of nucleobases was maximum when irradiated in presence of  $\text{Cu}(\text{Onz})_2\text{Cl}_2$ ; much greater than when irradiated either in presence of Onz or  $\text{Zn}(\text{Onz})_2\text{Cl}_2$ . While for adenine, radiation-induced damage was comparable when irradiated in presence of Onz and  $\text{Zn}(\text{Onz})_2\text{Cl}_2$ , for thymine, radiation-induced damage was better with Onz than  $\text{Zn}(\text{Onz})_2\text{Cl}_2$  (Figure 5, Table 1). For cytosine, no enhancement in radiation-induced damage was seen in presence of Onz (damage being similar to that with no additive). Radiation-induced damage in presence of  $\text{Zn}(\text{Onz})_2\text{Cl}_2$  was significantly less than that in presence of  $\text{Cu}(\text{Onz})_2\text{Cl}_2$ .

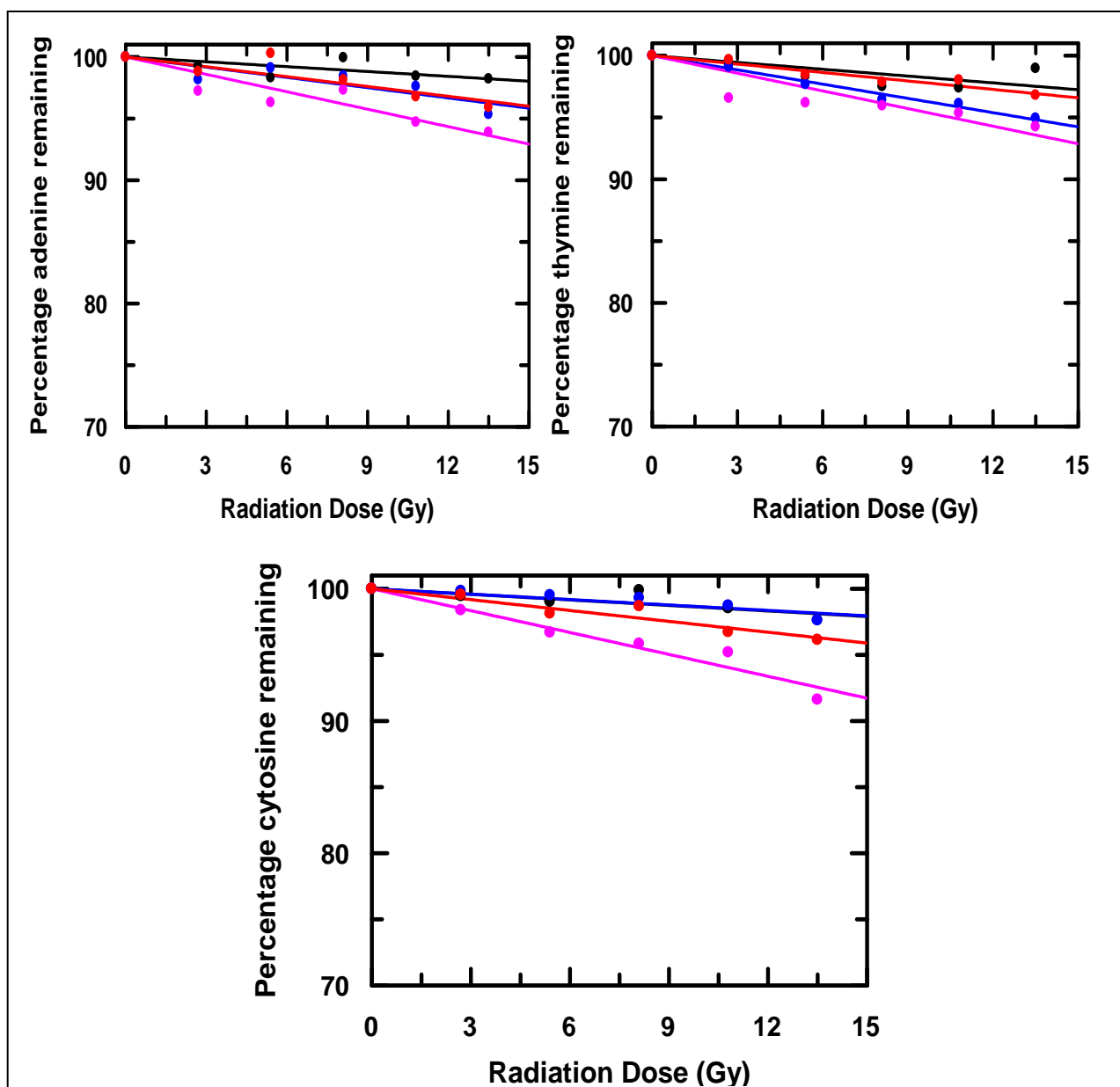


**Figure 5:** Amount of each nucleic acid base remaining on being subjected to  $\gamma$ -irradiation from a  $^{60}\text{Co}$  source in the absence (●) and presence of Onz (●),  $[\text{Cu}(\text{Onz})_2\text{Cl}_2]$  (●) and  $[\text{Zn}(\text{Onz})_2\text{Cl}_2]$  (●) under Ar saturated conditions against radiation dose.

The study suggests while  $\text{Cu}(\text{Onz})_2\text{Cl}_2$  was most effective in causing radiation-induced damage of a nucleobase, Onz and  $\text{Zn}(\text{Onz})_2\text{Cl}_2$  were either similar in performance (as in case of adenine) or one was better than the other and vice-versa (cytosine and thymine). A comparison and/or prediction of selectivity towards A—T or G—C due to compounds particularly  $\text{Cu}(\text{Onz})_2\text{Cl}_2$  could have been made as a part of the study had we been able to

perform experiments with guanine. However, this was not possible owing to poor solubility of guanine in aqueous solution (pH ~ 7.4) containing 120 mM NaCl, 35 mM KCl and 15 mM MgCl<sub>2</sub>. We tried performing experiments with guanine but as mentioned above owing to poor solubility results were erratic. Besides, we observed an interaction between guanine and Cu(Onz)<sub>2</sub>Cl<sub>2</sub> that prevented us from getting a clear picture of radiation-induced damage of guanine from HPLC chromatograms. Interaction was not evident to the naked eye when concentration of guanine was 10<sup>-4</sup> M and Cu(Onz)<sub>2</sub>Cl<sub>2</sub> 10<sup>-5</sup> M, but for slightly higher concentrations of guanine (10<sup>-3</sup> M) and Cu(Onz)<sub>2</sub>Cl<sub>2</sub> (10<sup>-4</sup> M), the solution became faintly turbid suggesting an association between them. This was checked several times and confirmed by HPLC of an aqueous solution of 1 × 10<sup>-3</sup> M guanine containing 1 × 10<sup>-4</sup> M Cu(II) complex. The solution containing guanine and Cu(II) complex showed an elution for guanine that was completely different from that obtained when guanine was present alone, indicating association of the two (Figure 6). This did not happen for any other nucleobase with Cu(Onz)<sub>2</sub>Cl<sub>2</sub>. Since such association of guanine with Cu(Onz)<sub>2</sub>Cl<sub>2</sub> was identified, it became clear to us that monitoring of guanine for radiation-induced damage by HPLC would not give us a correct picture. Hence, for reasons related to solubility and the fact that there was association or adduct formation of guanine and Cu(Onz)<sub>2</sub>Cl<sub>2</sub>, we refrained from making any statement on selectivity of compounds towards a particular nucleobase pair, realizing however, that this could have been an important outcome of the work. At the same time, the above discussion also makes it clear that Cu(Onz)<sub>2</sub>Cl<sub>2</sub> interacts with guanine. So, although we could not monitor a radiation-induced damage of it, Cu(Onz)<sub>2</sub>Cl<sub>2</sub> is likely to be effective on this nucleobase as well. Therefore, not only does Cu(Onz)<sub>2</sub>Cl<sub>2</sub> act as a radiosensitizer but it can also act as a hypoxic cytotoxin leading to modification of DNA at a site where guanine is present. Radiation chemical yields i. e. G (-values) of each nucleobase was determined from slopes of the corresponding linear plots (Figure 5) and these are shown in Table 1.

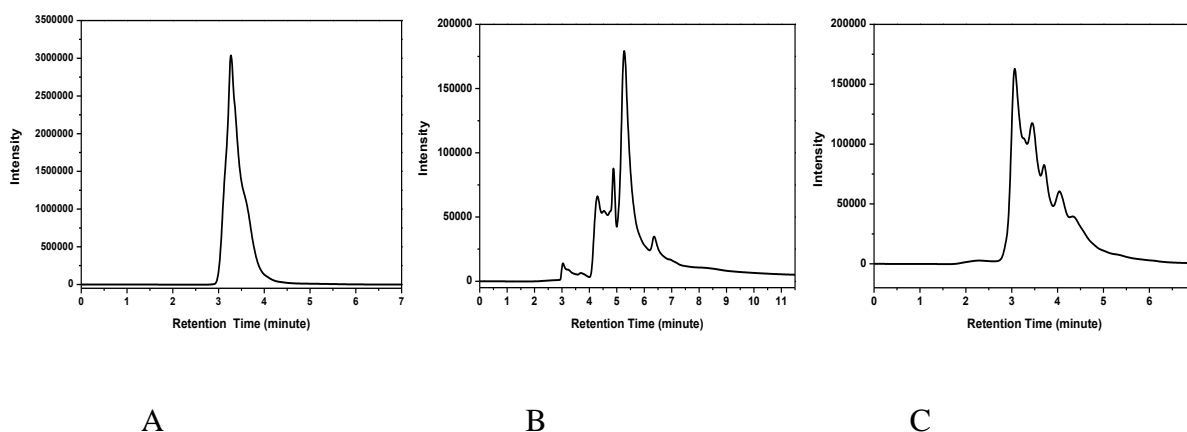


**Figure 6:** HPLC chromatograms recorded at 254 nm for (A) 2 ml  $1 \times 10^{-3}$  mol  $\text{dm}^{-3}$  solution of guanine through which Ar was purged for 10 minutes, (B) and (C) 2 ml of  $1 \times 10^{-3}$  mol  $\text{dm}^{-3}$  solution of guanine containing  $1 \times 10^{-4}$  mol  $\text{dm}^{-3}$   $\text{Cu}(\text{Onz})_2(\text{Cl})_2$ . For (B) guanine and Cu(II) complex were allowed to interact for 45 minutes, following mixing of the two and Ar gas was purged. Then HPLC was performed.; for (C) they were allowed to interact for 24 hours following their mixing and Ar gas was purged after which HPLC was performed.

**Table 1: G (-values) following damage of nucleic acid bases in units of molecules/100 eV and the corresponding enhancement ratio for base damage by compounds**

Compound	Target nucleic acid bases								
	Adenine			Thymine			Cytosine		
	% loss $\text{Gray}^{-1}$	G(-A)	E.R.	% loss $\text{Gray}^{-1}$	G(-T)	E.R.	% loss $\text{Gray}^{-1}$	G(-T)	E.R.
–	-0.131	1.26	–	-0.184	1.78	–	-0.139	1.34	–
Onz	-0.277	2.67	2.12	-0.384	3.71	2.08	-0.137	1.32	0.99
$[\text{Cu}(\text{Onz})_2\text{Cl}_2]$	-0.471	4.55	3.61	-0.476	4.59	2.58	-0.552	5.33	3.98
$[\text{Zn}(\text{Onz})_2\text{Cl}_2]$	-0.266	2.57	2.04	-0.228	2.20	1.24	-0.274	2.64	1.97

It is now known from previous reports that amongst different radicals formed during radiolysis of water,  $\bullet\text{OH}$  is highly effective in causing radiation-induced damage to nucleobases or to DNA [38-40]. Since in Ar saturated medium, G values for  $e_{\text{aq}}^-$  and  $\bullet\text{OH}$  are similar [37], they show equal probability for chemical reactions following their generation.  $\bullet\text{OH}$  reacts with a nucleobase (B) generating nucleobase radicals ( $\bullet\text{BOH}$ ) which upon interaction with a sensitizer (S) form  $+\text{BOH}$  (Figure 7 and Figure 8) [41]. Such nucleobase cations are then acted upon by molecules of water forming glycols (Figure 7 and Figure 8). Similar reactions occur with  $\bullet\text{H}$  (Figure 7 and Figure 8). When reactions are initiated by  $e_{\text{aq}}^-$ , it may either reduce a nucleobase (Figure 7 and Figure 8) or a sensitizer (S) present in the system [33, 34, 38-41]. Subsequently, the reduced sensitizer ( $\text{S}^-$ , in this case the nitro-radical anion) reacts with a nucleobase (B) to form a modified nucleobase shown in Figure 7 considering thymine and in Figure 8 considering cytosine [38-41].

In the dose range that was applied for this study, all products formed for radiation-induced damage of thymine, as reported by Cadet *et al* [42] were not obtained. In this study, since we wanted to be more close to a real life situation, smaller dose relevant to biological systems were used. As a result, we did not get all possible degradation products of a nucleic acid base or even if we got, some of them were formed in so small amounts that their detection was not possible.

For 5-nitroimidazoles, formation of  $\text{RNO}_2^-$  is crucial. Previous studies show upon complex formation with metal ions, 5-nitroimidazoles show decreased tendency to generate  $\text{RNO}_2^-$  [27, 28]. Given this fact, Onz should have been more effective in modifying nucleobases than complexes. However, this chapter showed clearly that  $\text{Cu}(\text{Onz})_2\text{Cl}_2$  was most effective.

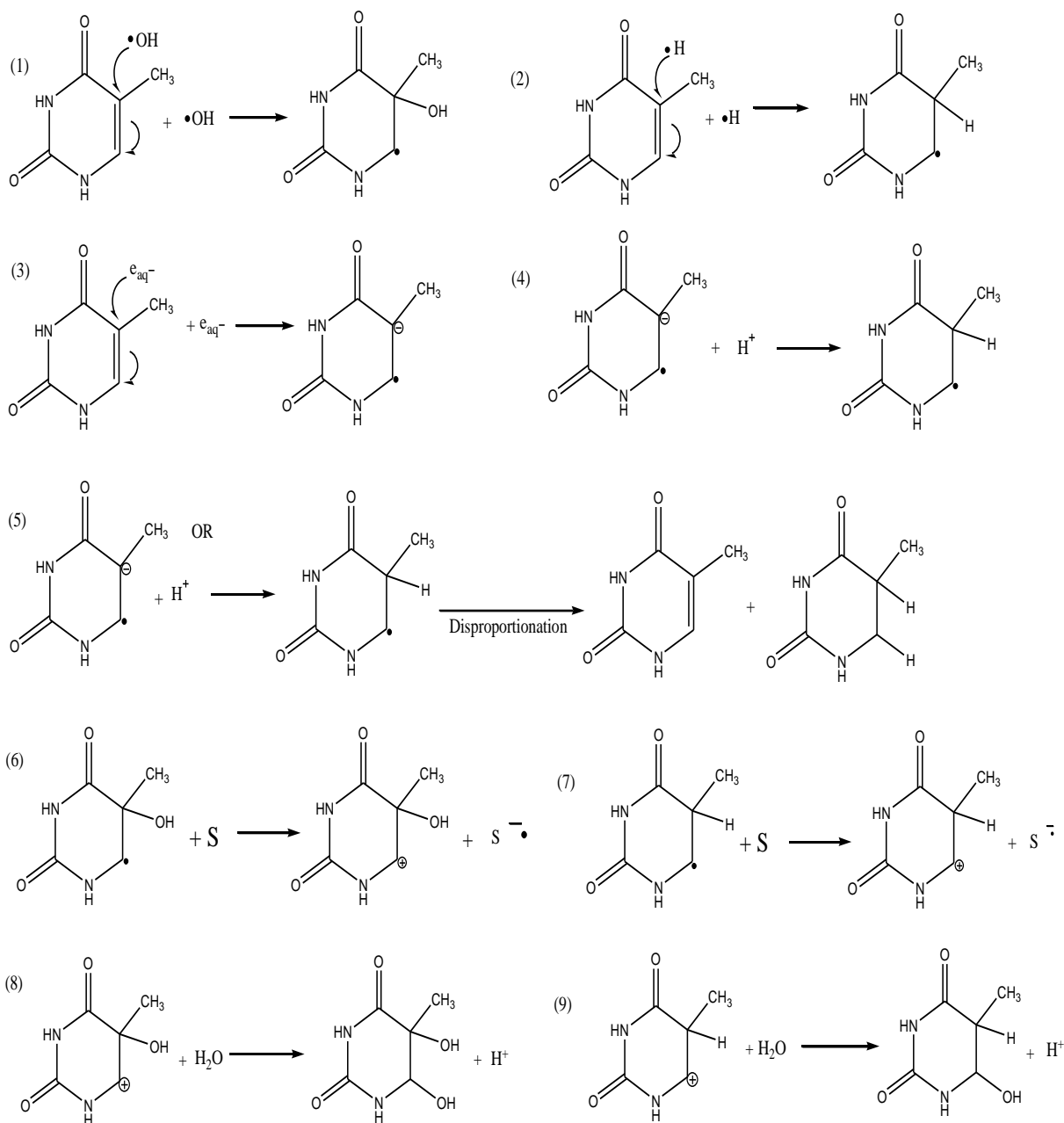


**Figure 7:** A schematic representation of the possible reactions that might occur during the radiation-induced damage of the nucleobase thymine. S indicates any sensitizer molecule and  $\text{S}^{\bullet-}$  the corresponding radical anion formed from S.

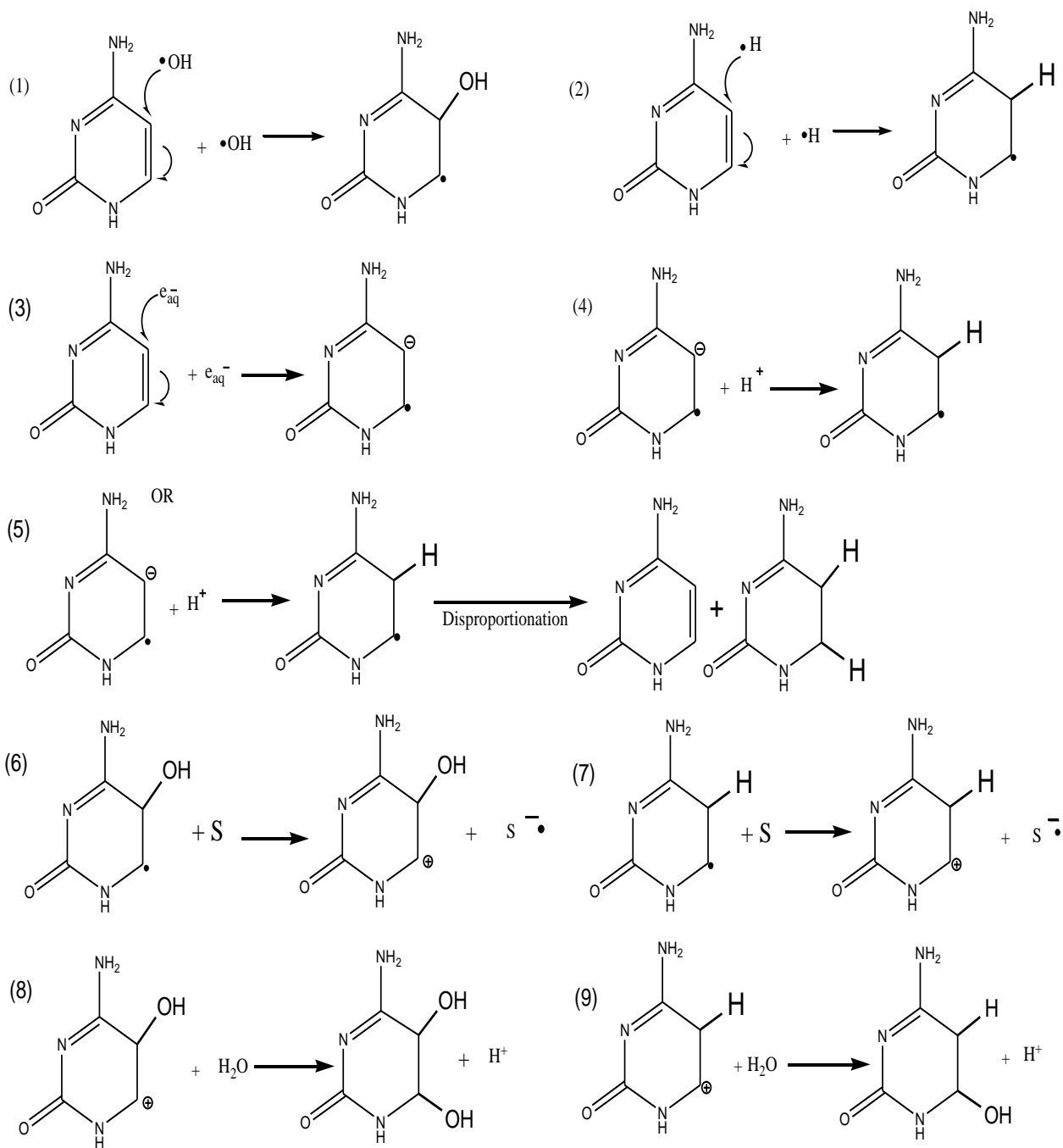


**Figure 8:** A schematic representation of the possible reactions that might occur during the radiation-induced damage of the nucleobase cytosine. S indicates any sensitizer molecule and  $\text{S}^{\cdot-}$  the corresponding radical anion formed from S.

Earlier studies demonstrate formation of  $\text{RNO}_2^-$  on Onz and  $\text{Cu}(\text{Onz})_2\text{Cl}_2$  in an electrochemical pathway was responsible for modification of nucleobases and calf thymus DNA under anaerobic (Ar saturated) conditions indicating the importance of  $\text{RNO}_2^-$  in causing nucleobase damage. Since radiation-induced chemical reactions also generate  $\text{RNO}_2^-$ , one can expect besides radiation-induced base damage by  $\bullet\text{OH}$  in solution, a substantial part of the damage could be due to  $\text{RNO}_2^-$  making such compounds effective hypoxic cytotoxins as well, and that it could be used on hypoxic tumors. Table 1 summarizes results of radiation-induced base damage on three nucleobases used as targets.

Our study using three nucleobases sets the stage for realizing the potential sites for base damage in DNA, suggesting all possible ways by which a nucleobase may be transformed following irradiation in the presence of our compounds (sensitizers) and the impact it might have on the destruction of a macromolecule like DNA.

### **Radiation induced damage of calf thymus DNA**

Ethidium bromide (EtBr) bound to double stranded DNA shows strong emission in the region 590 nm to 610 nm following excitation at 510 nm. Aqueous solutions of calf thymus DNA at physiological pH (~ 7.4) containing 120 mM NaCl, 35 mM KCl and 15 mM  $\text{MgCl}_2$  were exposed to gamma radiation from a  $^{60}\text{Co}$  source at different dose. Following irradiation, they were treated with a definite concentration of EtBr [32] and fluorescence was recorded (Figure 9). A gradual decrease in fluorescence intensity with increase in radiation dose indicates radiation-induced double strand modification in DNA. Percentage double stranded DNA remaining at each radiation dose was calculated using Eq. 11 (*Chapter 5; Experimental*).

$F_0$  and  $F_S$  are fluorescence intensities of the DNA-EtBr adduct with or without radiation respectively at a particular dose.  $F_E$  is the fluorescence intensity of EtBr alone.

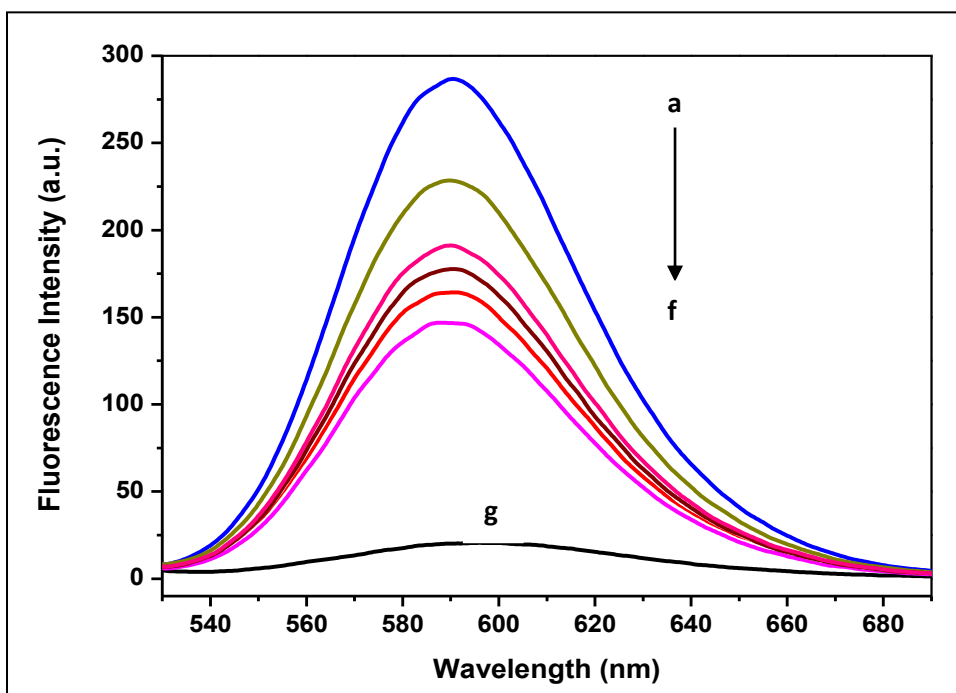


**Figure 9:** Decrease in fluorescence intensity of the DNA-EtBr adduct at 596 nm ( $\lambda_{\text{ex}} = 510$  nm) following irradiation of DNA in presence of  $\text{Cu}(\text{Onz})_2\text{Cl}_2$  at (a) no dose, (b) 4.05 Gy, (c) 6.74 Gy (d) 9.44 Gy, (e) 12.14 Gy and (f) 14.83 Gy. Spectrum (g) is that of free EtBr.

Percentage DNA remaining after irradiation showed linear dependence with radiation dose (Figure 10). Radiation-induced DNA damage was enhanced in presence of Onz and its complexes,  $\text{Cu}(\text{Onz})_2\text{Cl}_2$  and  $\text{Zn}(\text{Onz})_2\text{Cl}_2$  (Table 2). While enhancement ratio in presence of Onz was 1.67, it was substantially higher in presence of  $\text{Zn}(\text{Onz})_2\text{Cl}_2$  (ER = 2.72) and still higher for  $\text{Cu}(\text{Onz})_2\text{Cl}_2$  (ER = 3.76), indicating radiation-induced damage of calf thymus DNA clearly keeps  $\text{Cu}(\text{Onz})_2\text{Cl}_2$  ahead of other compounds (Table 2).

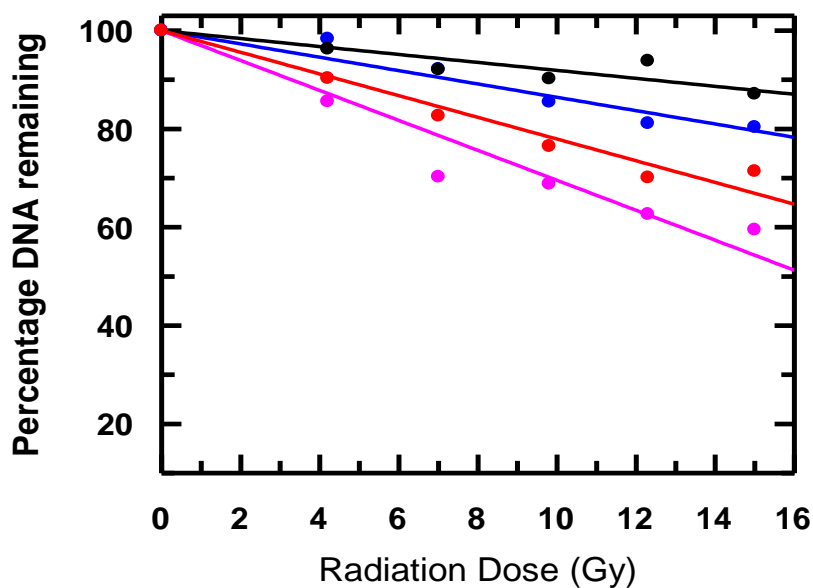


**Figure 10:** Degradation curves showing modification of calf thymus DNA in the absence (●) and presence of Onz (●), its Cu(II) complex (●) and its Zn(II) complex (●).

With  $\text{Cu}(\text{Onz})_2\text{Cl}_2$  being so much more effective in model studies on nucleobases and on calf thymus DNA it is highly likely that chances of it to show a reasonably good performance on cancer cell lines (hypoxic regions) should be high supported by an inherent affinity of Cu(II) for cancer cells that result in increased cellular uptake of Cu(II) complexes by such cells [43-47].

**Table 2:**  $\gamma$ -radiation induced modification of calf thymus DNA by compounds

Compound	Calf thymus DNA	
	% loss $\text{Gy}^{-1}$	E. R.
—	-0.810	—
Onz	-1.353	1.67
$\text{Zn}(\text{Onz})_2\text{Cl}_2$	-2.207	2.72
$\text{Cu}(\text{Onz})_2\text{Cl}_2$	-3.046	3.76

Another reason why a Cu(II) complex performs better is because of its ability to accept electrons either at the site of the nitro group in Onz in the complex or at the metal centre. Electron accepted from a radical is then effectively delocalized over Cu(Onz)<sub>2</sub>Cl<sub>2</sub>. Hence, base damage in presence of the Cu(II) complex is likely to increase according to Eq. 2 [33, 34].



Subsequently, Cu<sup>II</sup>(Onz)<sub>2</sub>Cl<sub>2</sub> reacts with H<sub>2</sub>O<sub>2</sub> present in the system (following radiolysis of water) [35, 36] to regenerate Cu<sup>II</sup>(Onz)<sub>2</sub>Cl<sub>2</sub> and release more •OH (Eq. 3) [35, 36, 51-53].



It was also reported that •OH is not the unique reactive species or the oxidative process that is induced by reaction of copper ions with H<sub>2</sub>O<sub>2</sub>. Evidence suggests the generation of singlet oxygen (<sup>1</sup>O<sub>2</sub>) by Cu(II)-H<sub>2</sub>O<sub>2</sub> while Cu(I)-H<sub>2</sub>O<sub>2</sub> is shown to degrade guanine by one-electron oxidation [51-53]. Since copper complexes show strong tendencies to bind to DNA [54], and are regenerated in solution as shown above with a simultaneous formation of •OH, this equips them to perform better than one would normally expect. Now if complexes are DNA bound, •OH in Eq. 3 would be present in the immediate vicinity of the binding site of DNA, capable of inflicting site-specific base damage (as described for guanine) [40-42]. While some researchers suggest formation of discrete •OH in the vicinity of a reaction site [48, 54], such formation is sometimes questioned by others who instead say a species closely resembling •OH co-ordinated to Cu<sup>I</sup> and/or Cu<sup>III</sup> co-ordinated to •OH is formed that react in a manner very similar to •OH [55]. Whether a discrete •OH, or a Cu<sup>II</sup> bound OH is formed, it eventually reacts with a base on either strand of DNA at the site of •OH generation. As a

consequence, it is only likely that radiation-induced damage of DNA due to  $\text{Cu}^{\text{II}}(\text{Onz})_2\text{Cl}_2$  would be enhanced by an extent that is not normal to the other compounds, being a reason why observed damage is higher than when Onz or  $\text{Zn}(\text{Onz})_2\text{Cl}_2$  is present. Hence, if  $\text{Cu}(\text{Onz})_2\text{Cl}_2$  is successful in getting inside a target cell, it should perform as predicted in this study [43-47]. Although this study does not include a performance by the compounds on a cancer cell line, in an earlier report for a dimeric Cu(II) complex of tinidazole we showed findings on model systems were actually holding good on MCF 7 breast cancer cells [31]. Therefore, logically the  $\text{Cu}(\text{Onz})_2\text{Cl}_2$  should be no different.

This study revealed efficacy of  $\text{Cu}(\text{Onz})_2\text{Cl}_2$  was much better than Onz and  $\text{Zn}(\text{Onz})_2\text{Cl}_2$ . When tried on three nucleobases (cytosine, thymine and adenine), radiation-induced enhancement was comparable for adenine and thymine in presence of Onz while on cytosine it was not effective.  $\text{Zn}(\text{Onz})_2\text{Cl}_2$  showed comparable activity on adenine and cytosine while it was less active on thymine. All three nucleobases underwent maximum radiation-induced modification in presence of  $\text{Cu}(\text{Onz})_2\text{Cl}_2$ ; adenine and cytosine being comparable.  $\text{Cu}(\text{Onz})_2\text{Cl}_2$  clearly showed its superiority in enhancing radiation-induced base damage for a number of reasons that were also seen in studies with calf thymus DNA. The study is important since complexes are likely to show less toxic side effects (neurotoxicity) owing to decreased formation of  $\text{RNO}_2^-$ . To conclude we say,  $\text{Cu}(\text{Onz})_2\text{Cl}_2$  in particular is able to strike a balance between efficacy and toxic side effects and that it would not be wrong to say with decreased  $\text{RNO}_2^-$  complexes are likely to be less neurotoxic as well, increasing its applicability as a drug.

## References

1. L. H. Gray, A. D. Conger, M. Ebert, S. Hornsey, O. C. H. Scott, *Br. J. Radiol.* **1953**, 26, 638–648.
2. E. A. Wright, P. Howard-Flanders, *Acta Radiol.*, **1957**, 48, 26–32.
3. M. R. Horsman, J. Overgaard, *J Radiat. Res.* **2016**, 57, i90–i98; doi: 10.1093/jrr/rrw007.
4. B. Muz, P. de la Puente, F. Azab, A. K. Azab, , *Hypoxia (Auckl)*. **2015**, 3, 83–92; doi: 10.2147/HP.S93413.
5. M. R. Horsman, *Int. J. Radiat. Oncol. Biol. Phys.* **1998**, 42, 701–704.
6. M. R. Horsman, L. S. Mortensen, J. B. Petersen, J. Busk, J. Overgaard, *Nat. Rev. Clin. Oncol.*, **2012**, 9, 674–687.
7. Chi, J.-T., Wang, Z., Nuyten, D. S. A., Rodriguez, E. H., Schaner, M. E., Salim, A., Wang, Y., Kristensen, G. B., Helland, Å., Børresen-Dale, A. -L., Giaccia, A., Longaker, M. T., Hastie, T., Yang, G. P., van de Vijver, M. J. and Brown, P. O., *PLoS Med*, **2006**, 3, e47; DOI: 10.1371/journal.pmed.0030047.
8. D. Marotta, J. Karar, W. T. Jenkins, M. Kumanova, K. W. Jenkins, J. W. Tobias, D. Baldwin, A. Hatzigeorgiou, P. Alexiou, S. M. Evans, R. Alarcon, A. Maity, C. Koch, C. Koumenis, **2011**, 71, 779-789; DOI: 10.1158/0008-5472.CAN-10-3061.
9. K. Toustrup, B. S. Sørensen, M. Nordmark, M. Busk, C. Wiuf, J. Alsner, J. Overgaard, *Cancer Research*, **2011**, 71, 5923-5931; DOI: 10.1158/0008-5472.CAN-11-1182.
10. A. El. Guerrab, A. Cayre, F. Kwiatkowski, M. Privat, J. M. Rossignol, F. Rossignol, F. Penault-Llorca, Y. J. Bignon, *PLoS One*, **2017**, 12 e0175960; doi: 10.1371/journal.pone.0175960.
11. Churchill-Davidson, I. *Oncologia*, **1966**, 20, 18–29; <https://doi.org/10.1159/000224392>
12. J. Daruwalla, C. Christophi, *World J Surg.* **2006**, 30, 2112-2131; DOI: 10.1007/s00268-006-0190-6.
13. J. A. Bertout, S. A. Patel, M. C. Simon, *Nat Rev Cancer.* **2008**, 8, 967–975;doi: 10.1038/nrc2540.

14. I. Moen, L. E .B. Stuhr, *Target Oncol.* **2012**, 7, 233–242; doi: 10.1007/s11523-012-0233-x.
15. A. G. Bourdat, T. Douki , S. Frelon ,D. Gasparutto, J. Cadet, *J Am. Chem. Soc.*, **2000**, 122, 4549–56.
16. G. Robert, J. R. Wagner, *Chem Res Toxicol* **2020**, 33, 566-575.
17. W. A. Tameemi, T. P. Dale, R. M. K. Al-Jumaily, N. R. Forsyth, *Front Cell Dev Biol.* **2019**, 7, 4; doi:10.3389/fcell.2019.00004.
18. (a) K. A. Skov, S. Macphail, *Int. J. Radiat. Oncol. Biol. Phys.* **1994**, 29, 87–93. (b) K. A. Skov, C. J. Koch, B. Marples, *Radiat. Oncol. Invest.* **1994**, 2, 164-170.
19. M. Weinmann, S. Welz, M. Bamberg, *Curr. Med. Chem. Anticanc. Agents.* **2003**, 3, 364-74.
20. J. M. Brown, *DrugResist. Updates*, **2000**, 3, 7-13.
21. J. W. Evans, K. Yudoh, Y. M. Delahoussaye, J. M. Brown, *Can. Res.*, **1998**, 58, 2098-2101.
22. S. Van Belle, *Chest*, **1996**, 109, 115S-118S.
23. P. Wardman, *Br J Radiol.* **2019**, 92, 20170915; doi:10.1259/bjr.20170915.
24. M. M. M. Bamatraf, P. O'Neill, B. S. M. Rao, *J. Am. Chem. Soc.* **1998**, 120, 11852–11857; doi.org/10.1021/ja9823161.
25. A. Valderrama-Negrón, W. Alves, A. Cruz, S. Rogero, D. De Oliveira Silva, *Inorg. Chim. Acta*, **2011**, 367, 85-92; DOI:10.1016/j.ica.2010.12.006.
26. R. C. Santra, K. Sengupta, R. Dey, T. Shireen, P. Das, P. S. Guin, K. Mukhopadhyay, S. Das, *J. Coord. Chem.* **2014**, 67, 265-285.
27. R. C. Santra, D. Ganguly, J. Singh, K. Mukhopadhyay, S. Das, *Dalton Trans.* **2015**, 44, 1992-2000.
28. R. C. Santra, D. Ganguly, S. Jana, N. Banyal, J. Singh, A. Saha, S. Chattopadhyay, K. Mukhopadhyay, S. Das, *New J. Chem.*, **2017**, 41, 4879-4886.
29. S. Okkan, R. Uzel, *Int J RadiatOncolBiol Phys.* **1982**, 8, 1735-1739.
30. S. Okkan, G. Atkovar, I. Sahinler, S. Turkan, R. Uzel, *Br J Cancer*, **1996**, 27, S282–S286.
31. R. C. Santra, D. Ganguly, D. Bhattacharya, P. Karmakar, A. Saha, S. Das, *New J. Chem.* **2017**, 41, 11679-11685.

32. W. A. Prütz, *Radiat. Environ. Biophys.* **1984**, 23, 1-6.
33. S. Das, A. Saha, P. C. Mandal, *Environ. Health Perspect.* **1997**, 105, 1459-1462.
34. S. Das, P.C. Mandal, *J. Radioanal. Nucl. Chem.*, **2014**, 299, 1665-1670.
35. Radiation Processing of Aqueous Systems from the “Lecture given at the IAEA's Interregional Training Course on Developments in the Application of Electron Beams in Industry and Environmental Protection”, Warsaw, Poland, 6-17 October 1997 by Peter Gehringer, SEIBERSDORF REPORT, **1997**, Page 2.
36. S. Tremblay, J. R. Wagner, *Nucleic Acids Res.* **2008**, 36, 284–293; doi:10.1093/nar/gkm1013.
37. R. Roots, A. Chatterjee, E. Blakely, P. Chang, K. Smith, C. Tobias, *Radiat. Res.* **1982**, 92, 245-254.
38. S. N. Bhattacharya, P. C. Mandal, *J. Chem. Soc., Faraday Trans.*, **1984**, 80, 1205-1215.
39. J. Cadet, T. Douki, J. L. Ravanat, *Acc. Chem. Res.*, **2008**, 41, 1075-1083.
40. J. Cadet, K. J. A. Davies, M. H. G. Medeiros, P. D. Mascio, J. R. Wagner, *Free Radic Biol Med.*, **2017**, 107, 13-34.
41. S. Steenken, V. Jagannadham, *J. Amer. Chem. Soc.*, **1985**, 107, 6818-6826.
42. (a) J. Cadet, M. Guttin-Lombard, R. Teoule, *Int J Radiat. Biol* **1976**, 30, 1-11; (b) J. Cadet, A. Balland, M. Berger, *Int J Radiat. Biol* **1981**, 39, 119-133.
43. S. Puig, D. J. Thiele, *Curr. Opin. Chem. Biol.* **2002**, 6, 171–180.
44. T. Deb, P. K. Gopal, D. Ganguly, P. Das, M. Paul, M. B. Saha, S. Paul, S. Das, *RSC Advances* **2014**, 4, 18419-18430.
45. P. Das, C. K. Jain, S. Roychoudhury, H. K. Majumder, S. Das, *Chem. Select* **2016**, 1, 6623–6631.
46. D. Ganguly, C. K. Jain, R. C. Santra, S. Roychoudhury, H. K. Majumder, T. K. Mondal, S. Das, *Chem. Select*, **2017**, 2, 2044–2054.
47. B. Mandal, S. Singha, S. K. Dey, S. Mazumdar, S. Kumar, P. Karmakar, S. Das, *RSC Adv.* **2017**, 7, 41403-41418.
48. S. Goldstein, G. Czapski, *J. Am. Chem. Soc.* **1986**, 108, 2244-2250.
49. B. G. Que, K. M. Downey, A. G. So, *Biochemistry*, **1980**, 19, 5987–5991.
50. L. E. Marshall, D. R. Graham, K. A. Reich, D. S. Sigman, *Biochemistry* **1981**, 20, 244–250.

51. K. Yamamoto, S. Kawanishi, *The J. Biol. Chem.*, **1989**, 264, 15435-15440.
52. S. Frelon, T. Douki, A. Favier, J. Cadet, *Chem. Res. Toxicol.* **2003**, 16, 191–197.
53. S. Oikawa, K. Murakami, S. Kawanishi, *Oncogene*, **2003**, 22, 3530–3538  
<https://doi.org/10.1038/sj.onc.1206440>
54. S. Prütz, W. A. Inhibition *Radiat. Environ. Biophys.* **1984**, 23, 7-18.
55. G. R. A. Johnson, N. B. Nazhat, *J. Am. Chem. Soc.*, **1987**, 109, 1990-1994.
-

# **Chapter 14**

## **Summary and Conclusion**

The study undertaken made an attempt to synthesize  $\text{Cu}^{\text{II}}$  and  $\text{Zn}^{\text{II}}$  complexes of ornidazole and tinidazole that were either monomeric or dimeric in nature with an aim to see the extent to which they compare with the performance of the 5-nitroimidazoles either as antimicrobial or anticancer agents. The intention behind selecting  $\text{Cu}^{\text{II}}$  and  $\text{Zn}^{\text{II}}$  as metal ions was to look for possible changes in the complexes owing to the nature of the metal ion involved; i. e.  $\text{Cu}^{\text{II}}$  having a stable lower oxidation state and  $\text{Zn}^{\text{II}}$  not having one. Complexes were characterized, their electrochemical, biophysical, antimicrobial and radiosensitizing attributes investigated. Since activity of 5-nitroimidazoles (here ornidazole and tinidazole) either as antimicrobial agent or radiosensitizer, centres around reduction of the nitro group leading to generation of nitro radical anion ( $\text{NO}_2^{\bullet-}$ ) and other products, a major emphasis of the work was to realize the formation of such reduced species. This was done with a purpose as the same nitro radical anion is responsible for toxic side effects, of which neurotoxicity is a matter of serious concern.

Monomeric complexes of  $\text{Cu}^{\text{II}}$  and  $\text{Zn}^{\text{II}}$  i.e.  $[\text{Cu}(\text{Onz})_2\text{Cl}_2]$  and  $[\text{Zn}(\text{Onz})_2\text{Cl}_2]$  were prepared while monomeric and dimeric complexes of  $\text{Cu}^{\text{II}}$  and tinidazole were prepared and characterized in our laboratory earlier.  $[\text{Cu}(\text{Onz})_2\text{Cl}_2]$  was characterized by single crystal X-ray diffraction analysis and found to crystallize in an orthorhombic crystal system with  $Pnma$  space group. On the other hand, for  $[\text{Zn}(\text{Onz})_2\text{Cl}_2]$  we did not get single crystals. Therefore, we took the help of powder X-ray diffraction data and Reitfeld analysis to arrive at a structure that was achiral,  $Pna2_1$  space group, also belonging to the orthorhombic system. Structures revealed  $\text{Cu}^{2+}$  was four coordinated to adopt a distorted square planar geometry while  $\text{Zn}^{2+}$  exhibits four coordinated slightly distorted tetrahedral geometry. The asymmetric unit of  $[\text{Cu}(\text{Onz})_2\text{Cl}_2]$  consists of one crystallographically independent  $\text{Cu}^{2+}$  ion with half occupancy, one ornidazole ligand, two coordinated  $\text{Cl}^-$  with half occupancy and a lattice water molecule. The asymmetric unit of  $[\text{Zn}(\text{Onz})_2\text{Cl}_2]$  consists of one  $\text{Zn}^{2+}$ , two Onz moieties and two  $\text{Cl}^-$ .

Both complexes were also characterized by different spectroscopic techniques and magnetic susceptibility measurements (wherever applicable). Bands in the IR spectra of the complexes shift to higher wave number for  $\nu_{(C=N)}$  stretching of the imidazole ring indicating coordination of the imidazole nitrogen to the metal centre. In the UV-Vis spectrum of  $[\text{Cu}(\text{Onz})_2\text{Cl}_2]$ , two bands were observed in different solvent media. The first one at about 320 nm for intra-ligand charge transfer and a weak d-d transition band near 700 nm. The UV-Vis spectra of  $[\text{Zn}(\text{Onz})_2\text{Cl}_2]$  in different solvents had only one band in the region 310-323 nm attributed to intra-ligand charge transfer. The  $\text{Cu}^{\text{II}}$  complex showed a characteristic EPR spectrum having a resonance signal at 318 mT with g value of 2.11. The effective magnetic moment for the copper complex was found to be 1.32 BM which is unexpected for one unpaired electron for  $d^9$  configuration of  $\text{Cu}^{\text{II}}$ . It could possibly be due to close proximity of two metal centres on two monomeric units that results in spin pairing leading to a lower than expected value for magnetic moment.

Cyclic voltammograms of each compound were recorded using glassy carbon as working electrode, Ag/AgCl-satd. KCl as the reference electrode and platinum as counter electrode, in different scan rates and different solvents. For each compound, there is a characteristic reduction peak assigned to the reduction of the nitro group on the imidazole ring.  $I_{\text{pc}}$  was plotted against square root of scan rate. A straight line was obtained passing through the origin demonstrating that compounds undergo reduction in a diffusion controlled pathway and that there is no adsorption on the electrode surface. The result of cyclic voltammetry studies performed on the  $\text{Cu}^{\text{II}}$  complex in pure DMF and different aqueous-DMF mixtures indicate it is difficult to generate the nitro radical anion on the complex, or even if generated, a certain portion of it is lost in some other pathway which could be a consequence of the presence of the metal ion. Generation of nitro radical anion by comproportionation was

observed for the complex. Hence, electrochemical experiments performed on  $[\text{Cu}(\text{Onz})_2\text{Cl}_2]$ , clearly suggest there is substantial decrease in the formation of nitro radical anion.

Enzyme assay experiments were performed on ornidazole and its complexes under anaerobic conditions using Xanthine Oxidase as a model nitro-reductase enzyme. Under similar experimental conditions, ornidazole undergoes reduction as a result of which it is degraded with time, which was detected spectro-photometrically. Complexes were seen to be reluctant to reduction of the nitro group on the imidazole ring, preventing formation of the nitro radical anion ( $\text{NO}_2^{\bullet-}$ ). Decrease in generation of  $\text{NO}_2^{\bullet-}$  through complex formation is important for its reported involvement in neurotoxicity. However, decrease in  $\text{NO}_2^{\bullet-}$  also implies complexes could be less cytotoxic considering the aspect of interaction of reduced products with DNA of disease causing microbes that lead to the destruction of their double helical structure.

Therefore, to understand the biological implications of complex formation, interaction of the complexes and the parent compounds with DNA was studied taking calf thymus DNA. This was done with the help of cyclic voltammetry. Results indicate overall binding constant ( $K^*$ ) of the  $\text{Zn}^{\text{II}}$  complex ( $2.35 \times 10^5 \text{M}^{-1}$ ) was  $\sim 8.5$  times greater than ornidazole ( $K^* = 2.77 \times 10^4 \text{M}^{-1}$ ). The  $\text{Cu}^{\text{II}}$  complex has comparable binding constant ( $K^* = 2.61 \times 10^4 \text{M}^{-1}$ ) with that of ornidazole. It implies complexes are either better in binding DNA or possess comparable binding ability as that of the parent drug (in this case, Ornidazole).

To see the manifestation of comparable or increased binding of complexes with DNA with respect to ornidazole, it was decided to test their performance on certain microbial strains. The effect of less generation of  $\text{NO}_2^{\bullet-}$  by complexes compared to Ornidazole, in the biology domain, of the parent compounds being used as medicines, may then be correlated. All compounds were treated to the amoebic strain *Entamoeba histolytica* (HM1: IMS Strain). Inhibition of cell viability of *Entamoeba histolytica* was followed by trypan blue assay using

different concentrations of ornidazole and  $\text{Cu}(\text{Onz})_2\text{Cl}_2$  for 24 hours and 48 hours respectively. MIC for ornidazole and  $[\text{Cu}(\text{Onz})_2\text{Cl}_2]$  after 24 hours were  $12.5\mu\text{M}$  and  $25.0\mu\text{M}$  respectively suggesting that by the end of 24 hours, the  $\text{Cu}^{\text{II}}$  complex was actually weaker than ornidazole in performance. However, upon increasing exposure time for each compound from 24 hrs to 48 hrs, the complex was found to be more cytotoxic with an MIC of  $6.25\mu\text{M}$  while for ornidazole the value remained at  $12.5\mu\text{M}$ . MIC values recorded after 24 hours for ornidazole and  $[\text{Zn}(\text{Onz})_2\text{Cl}_2]$  on *Entamoeba histolytica* were similar ( $12.5\mu\text{M}$ ). This indicates either that the nitro radical anion generated by the complex is sufficient for bringing about cytotoxic activity on a chosen biological target or if a compromise is made by the complex with regard to cytotoxic activity in the free radical pathway, following a decrease in nitro-radical anion formation, such decrease in efficacy is made up by the complex utilizing its other attributes.

Various studies have shown that metal complexes of bio-active ligands have performed much better on cell lines than the ligand itself, essentially owing to effective cellular uptake of the complex. Likewise, for  $[\text{Cu}(\text{Onz})_2\text{Cl}_2]$  the fact that it performs better at longer exposure time (48 hours) could be that with time, the complex is able to enter cells of disease causing microbes in a manner better than ornidazole, that allows it to be more effective. This study also showed ornidazole and its  $\text{Cu}^{\text{II}}$  complex diminished viability of *Entamoeba Histolytica* in a concentration dependent manner. In spite of a significant decrease in the formation of the nitro radical anion by  $[\text{Cu}(\text{Onz})_2\text{Cl}_2]$ , the study showed it had comparable biological activity as that of ornidazole on *Entamoeba histolytica* (HM1: IMS Strain) when incubated for 24 hours. Since in case of 48 hour incubation, the complex performed better than ornidazole it indicates either nitro radical anion generated by the complex is sufficient for bringing about cytotoxic activity on a biological target or if any compromise is made by the complex in the free radical pathway, it is made up by other attributes of complex formation, one of which

could be effective cellular uptake. As a consequence, association of  $\text{Cu}^{\text{II}}$  with Ornidazole is useful for it not only maintains the efficacy of ornidazole but by decreasing nitro radical anion it should help to control neurotoxic side effects associated with such drugs.

Tinidazole, like any 5-nitroimidazole, is reported to bind to DNA while inside a cell initiating cytotoxic action on a pathogen by forming nitro radical anions, considered responsible for efficacy. Excess production of nitro radical anion is responsible for idiosyncratic side effects which metal complexes with reduced formation might control. Hence, both from model studies and prevention of biofilm formation, it could be said, what complexes compromise in the free radical pathway, they make up through aspects like better interaction with a target or due to the presence of a redox active  $\text{Cu}^{\text{II}}/\text{Cu}^{\text{I}}$  couple.  $\text{Cu}^{\text{II}}$  complexes of tinidazole, on one hand, by controlling generation of  $\text{RNO}_2^{\bullet-}$ , might control neurotoxic side effects, and on the other, continue to be better cytotoxic agents than parent 5-nitroimidazoles, when one actually might expect them to have compromised on efficacy. This was clearly realized through model studies using thymine, cytosine, adenine, and calf thymus DNA as targets and through studies on prevention of biofilm formation. Electrochemically generated species on compounds under investigation mimics what happens when the compounds are actually reduced within cells, helping one to understand the mechanism by which compounds impart biological efficacy.

Aspects of cytotoxicity initiated by  $\text{NO}_2^{\bullet-}$  and other reduction products on a monomeric  $\text{Cu}^{\text{II}}$  complex of ornidazole was studied using nucleic acid bases and calf thymus DNA as target. These experiments were performed to correlate what actually happens when similar molecules are enzymatically reduced within biological systems in mitochondria. Electrochemical reduction of the complex at a constant potential (determined earlier) using a glassy carbon electrode in aqueous solution results in formation of various reduction products. All reduced species including  $\text{NO}_2^{\bullet-}$  instantly react with different nucleic acid bases

and calf thymus DNA maintained in the immediate vicinity of test solutions. Complexes performed better than ornidazole under similar conditions. From this experiment of *in situ* electrochemically generated nitro radical anion and other reduced species it was obtained that reduction products of both ornidazole and its  $\text{Cu}^{\text{II}}$  complex modify guanine and cytosine (G and C) much more than adenine and thymine (A and T). Since in calf thymus DNA, percentage of guanine and cytosine is comparatively higher than adenine and thymine, it was concluded to be a major reason why calf thymus DNA showed substantial damage in the presence of the  $\text{Cu}^{\text{II}}$  complex of ornidazole under similar experimental conditions. Thus this study helped in correlating why 5-nitroimidazole based antibiotics were found to be very effective on organisms having either a high G-C content in their DNA or at least a substantial amount of it. Hence, if a target DNA is identified then the type of organism (with high G-C content in its DNA) could be said to be most vulnerable to such drugs and their metal complexes. This might then be identified through correlation. In fact the study in a way indicates why various micro-organisms (bacteria or parasites) could be targeted effectively with 5-nitroimidazoles.

Radiosensitizing property of both  $\text{Cu}^{\text{II}}$  and  $\text{Zn}^{\text{II}}$  complexes was investigated against ornidazole to realize if complex formation is able to provide a better radiosensitizer. Systematic investigation were done starting with  $^{60}\text{Co}$  gamma radiation-induced damage of purine and pyrimidine based nucleic acid bases (adenine, thymine and cytosine). Studies on gamma radiation-induced damage of double stranded calf thymus DNA was performed. All experimental results were able to show that complexes were far better radiosensitizer compared to ornidazole but the more important thing about complexes is that with substantial decrease in nitro radical anion formation, side effects associated with ornidazole or for that matter 5-nitroimidazoles as radiosensitizers should be significantly suppressed and that complexes should be a lot safer material in radiation therapy of cancer.

Findings pertaining to antimicrobial activity and radiosensitizing attributes of complexes are very interesting. The complexes even with substantial decrease in  $\text{NO}_2^{\bullet-}$  are able to show better efficacy in reference to ornidazole. So the concern that complexes with decreased  $\text{NO}_2^{\bullet-}$  formation might have reduced cytotoxic activity i. e. is at a disadvantage with regard to radiosensitization is not true. At the same time, since generation of  $\text{NO}_2^{\bullet-}$  is known to affect the central nervous system adversely, this study suggests complexes of 5-nitroimidazoles could improve upon this aspect making them relatively safe. Thus complexes with lesser generated  $\text{NO}_2^{\bullet-}$  are able to balance between efficacy and adverse effect.

Hence, possibility that such complexes could be a viable alternative in near future exists.

# **APPENDIX- I**

## List of Publications

1. The importance of pKa in an analysis of the interaction of compounds with DNA, Mouli Saha, **Promita Nandy**, Mousumi Chakraborty, Piyal Das, Saurabh Das, *Biophysical Chemistry*, **2018**, 236, 15–21.
2. Interaction of electrochemically generated reduction products of Ornidazole with nucleic acid bases and calf thymus DNA, **Promita Nandy** and Saurabh Das, *J. Indian Chem. Soc.*, **2018**, 95, 1009-1014.
3. *In situ* reactivity of electrochemically generated nitro radical anion on Ornidazole and its monomeric Cu(II) complex with nucleic acid bases and calf thymus DNA, **Promita Nandy** and Saurabh Das, *Inorganica Chimica Acta*, **2020**, 501, 119267, 1-8.
4. A Zn<sup>II</sup> complex of ornidazole with decreased nitro radical anions that is still highly active on *Entamoeba histolytica*, **Promita Nandy**, Soumen Singha, Neha Banyal, Sanjay Kumar, Kasturi Mukhopadhyay and Saurabh Das, *RSC Adv.*, **2020**, 10, 23286-23296. (This was extremely well received and selected by Editors as a 2020 HOT RSC Advances article; RSC Advances HOT Article Collection).
5. Radio-Sensitizing effects of Cu<sup>II</sup> and Zn<sup>II</sup> complexes of Ornidazole: Role of nitro radical anion, **Promita Nandy**, Alivia Mukherjee, Chiranjit Pradhan, and Saurabh Das, *ACS Omega*, **2020**, 5, 25668–25676.
6. Utilization of Guanidine-Based ancillary ligands in arene–ruthenium complexes for selective cytotoxicity, Jit Karmakar, **Promita Nandy**, Saurabh Das, Debalina Bhattacharya, Parimal Karmakar and Samaresh Bhattacharya, *ACS Omega*, **2021**, 6, 8226-8238.
7. *In Situ* reactivity of electrochemically generated nitro radical anion on tinidazole and its monomeric and dimeric Cu<sup>II</sup> complexes on model biological targets with relative manifestation of preventing bacterial biofilm formation, **Promita Nandy**, Ramesh C. Santra, Dibyajit Lahiri, Moupriya Nag and Saurabh Das, *ACS Omega*, **2022**, 7, 8268–8280.

## **Manuscript to be communicated on the work included in the thesis**

1. Electrochemical reduction of Ornidazole and its Cu<sup>II</sup> complex in aqueous and aqueous dimethyl formamide mixed solvent: A cyclic voltammetric study, **Promita Nandy** and Saurabh Das, manuscript ready, would be communicated shortly.
2. A monomeric complex of Cu<sup>II</sup> with Ornidazole forms significantly less nitro radical anion but was found active on *Entamoeba histolytica* like Ornidazole, **Promita Nandy** and Saurabh Das, manuscript ready, would be communicated shortly.

# **APPENDIX-II**

## **List of Conference proceedings**

## **PUBLICATION OF ABSTRACT IN CONFERENCE PROCEEDINGS**

**2016 Poster:** Mouli Saha, **Promita Nandy**, Saurabh Das. “Influence of the pK values of purpurin on its interaction with calf thymus DNA helps to realize the contributions of the various forms of the molecule towards overall binding” at the Chemistry of Functional Materials of Current Interest, on March 16, 2016, organized by Department of Chemistry, Jadavpur University, Kolkata 700032.

**2017 Poster:** **Promita Nandy**, Ramesh Chandra Santra, Saurabh Das. “Electrochemically generated nitro radical anion induced damage of thymine and calf thymus DNA: a study with tinidazole, its monomeric and dimeric Cu(II) complexes” in the 5 th Symposium on Advanced Biological Inorganic Chemistry, organized by Tata Institute of Fundamental Research, Mumbai and Indian Association for the Cultivation of Science, Kolkata in Kolkata, January 7-11, 2017.

**2017 Poster:** **Promita Nandy**, Tanmoy Saha, Saurabh Das. “Electrochemically Generated Nitro Radical Anion Induced Damage of Nucleic Acid Bases and Calf Thymus DNA: A Study With Ornidazole and Its Monomeric Cu(II) Complex” in the Modern Trends in Inorganic Chemistry (MTIC)- XVII, Pune in December 2017.

**2018 Oral Presentation:** **Promita Nandy** and Saurabh Das. “A monomeric Zn(II) complex of Ornidazole shows better efficacy on Entamoeba histolytica (HM1:IMSS strain) in the International Conference on Synthetic Potent Molecule and Its Application (ICSPMIA-2018) in collaboration with Royal Society of Chemistry, Eastern India Section at Sikkim Manipal Institute of Technology (SMIT), Majitar, Sikkim during October 30-31, 2018.

**2019 Poster:** **Promita Nandy** and Saurabh Das. “Synthesis of Cu<sup>II</sup> and Zn<sup>II</sup> complexes of Ornidazole to determine efficacy towards  $\gamma$ -radiation induced modification of nucleic acid bases involving formation of nitro radical anion” in the Modern Trends in Inorganic Chemistry (MTIC)-XVIII, at Indian Institute of Technology Guwahati, Assam Organised by Department of Chemistry, IIT Guwahati in association with Gauhati University and Tezpur University, India in December 2019.

# **APPENDIX-III**

**Reprint of publications included  
in the thesis**

J. Indian Chem. Soc.,  
Vol. 95, August 2018, pp. 1-6

## Interaction of electrochemically generated reduction products of Ornidazole with nucleic acid bases and calf thymus DNA

Promita Nandy and Saurabh Das\*

Department of Chemistry, Inorganic Chemistry Section, Jadavpur University, Kolkata-700 032, India

E-mail: sdas@chemistry.jdvu.ac.in, dasrsv@yahoo.in

Manuscript received 27 July 2018, accepted 09 August 2018

5-Nitroimidazoles are important compounds used by the pharmaceutical industry with applications of combating infections caused by anaerobic bacteria, amoeba and other parasites. They are effective radiosensitizers also. Biological activity of 5-nitroimidazoles is attributed to reduction of the nitro group that equips them to enter cells of disease causing microbes by creating a concentration gradient. Several studies consider formation of the nitro radical anion ( $\text{NO}_2^{\bullet-}$ ) and other reduction products essential for their activity. While inside the cell, these reduction products interact with DNA, disrupting or breaking strands and causing cell death. To look into this aspect, Ornidazole [1-chloro-3-(2-methyl-5-nitro-1H-imidazole-1-yl)propan-2-ol], belonging to 5-nitroimidazoles was selected. Reduction products of Ornidazole was generated by an electrochemical reduction of it at constant potential (-0.827 V) determined using cyclic voltammetry. Purine and pyrimidine bases as well as calf thymus DNA were kept in the immediate vicinity of generated reduction products. The amount of reduction products generated depended upon the time for which Ornidazole was subjected to reduction at the constant potential. Reaction of the generated reduction products with purine or pyrimidine bases was followed using HPLC while the amount of calf thymus DNA that was not modified was determined by treating the DNA with ethidium bromide and recording its fluorescence following an excitation at 510 nm. The study revealed damage and/or modification caused to different targets by the generated reduction product of Ornidazole. The damage caused to purine and pyrimidine bases was then correlated with that observed on calf thymus DNA.

Keywords: Ornidazole, adenine, thymine, cytosine, guanine, calf thymus DNA.

### Introduction

Nitroimidazoles are a very useful class of drugs important for a number of reasons. They are extensively used for problems pertaining to anaerobic bacterial and parasitic infections; this being its major application<sup>1-5</sup>. These compounds being cytotoxic to cells are also effective as chemotherapeutic agents, as radiopharmaceuticals and radiosensitizers in various forms of cancer related medical applications<sup>6-9</sup>. Ornidazole [1-chloro-3-(2-methyl-5-nitro-1H-imidazole-1-yl) propan-2-ol], a 5-nitroimidazole, although less popular than metronidazole or tinidazole or even misonidazole is under serious consideration these days for certain advantages it has over metronidazole, the most popular of the 5-nitroimidazoles<sup>10-13</sup>, and is slowly becoming a major component of many important pharmaceutical formulations. Through studies and application on patients, it has emerged today that reduction of the nitro group and the subsequent formation of different reduction products are crucial for their

activity<sup>1,7,14</sup>. Having entered a target cell by diffusion, antimicrobial activity of nitroimidazoles depend upon the reduction of the nitro group to a nitro radical-anion and/or other potentially active compounds that includes the nitroso and the hydroxylamine derivatives<sup>1,14</sup>. Reduction products of nitroimidazoles are damaging to various macromolecules including DNA, bringing about their degradation through strand modification<sup>1,7,14</sup>. Almost all nitroimidazoles are selectively toxic to different micro-organisms who actually provide them the desired redox potential so that electron transport process can occur uninterrupted and if sufficiently negative, it is able to reduce the nitro group of the nitroimidazole moiety, in the process inviting its own death. By and large, this has been the mechanism of activity of the nitroimidazoles and pharmaceutical companies have exploited this aspect to their advantage. For nitroimidazoles acting as radio-pharmaceuticals or radiosensitizers, the cause for action is more or less the same, the only difference being

that in this form of application, the nitro-radical anion ( $R\text{-NO}_2^{\bullet-}$ ) probably has a larger role than other reduction products<sup>6-9</sup>; R signifying the portion of a nitroimidazole other than the nitro group. Although, there is some work in the literature on modification of DNA due to nitroimidazoles, there is lot of scope for further investigative work<sup>15,16</sup>. Here, in this communication, we look at the aspect as to how the nitro radical anion or other reduction products generated inside a cell that provide these molecules with the appropriate reduction potential, interact with nucleic acid bases or DNA. In our case, the reduction potential was provided to our chosen nitroimidazole (Ornidazole) by an electrochemical method using glassy carbon electrode, where, in the immediate vicinity of reduction products of the molecule four different nucleic acid bases (taken one at a time) or calf thymus DNA was kept. The reduction products bring about a damage of the biological target which was followed with the help of suitable experimental techniques. Hence, to be able to do this work, it was necessary to identify the reduction potential of Ornidazole which was done in aqueous medium prior to start of actual experiments.

## Experimental

### Materials used:

Ornidazole was purchased from Sigma Aldrich and purified by re-crystallization from alcohol. NaCl,  $\text{NaNO}_3$ , KCl (all AR grade) were purchased from E. Merck, India. Triple distilled water was used for preparing aqueous solutions. Calf thymus DNA was purchased from Sisco Research Laboratory, India and dissolved in triple distilled water. Concentration of DNA was determined in aqueous solution using a molar extinction coefficient of  $6600 \text{ M}^{-1} \text{ cm}^{-1}$  at 260 nm. Absorbance was also measured at 280 nm and  $A_{260}/A_{280}$  was found out. It being in the range of 1.8 to 1.9, the DNA was considered ready for use requiring no further purification. Quality of calf thymus DNA was also verified using circular dichroism (CD) recorded at 260 nm using a CD spectropolarimeter (J815, JASCO, Japan).

### Electrochemical behavior of Ornidazole:

Cyclic voltammetry was performed on Ornidazole to study its electrochemical behavior in aqueous solution using 0.12 M KCl as supporting electrolyte (Fig. 1). Before each electrochemical experiment, solutions were de-aerated with the help of Argon for 30 min. Electrochemical measurements were

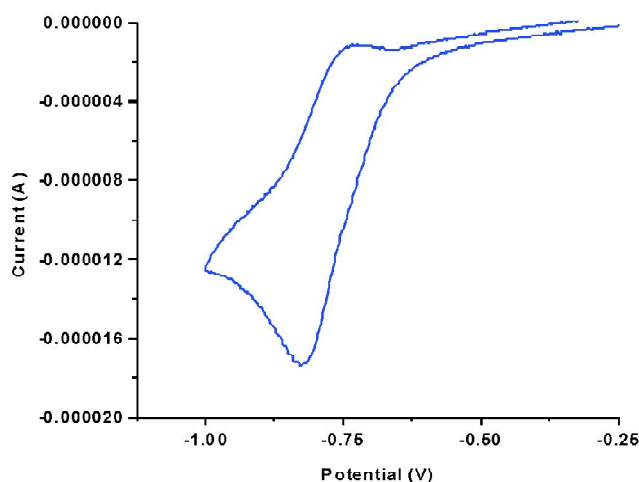


**Fig. 1.** Cyclic voltammogram of 1 mM Ornidazole showing a single step one electron reduction in 0.12 M KCl in an aqueous 20% methanol solution on a glassy carbon electrode; Scan rate being 100 mV/s.

made in a 50 ml electrochemical cell. The cathodic peak current ( $I_{pc}$ ) in amperes at  $-0.827 \text{ V}$  (Fig. 2) was plotted against square root of potential sweep rate ( $v^{1/2}$ ) to see if the process was diffusion controlled; the same being an essential criteria for the actual experiment to be performed.

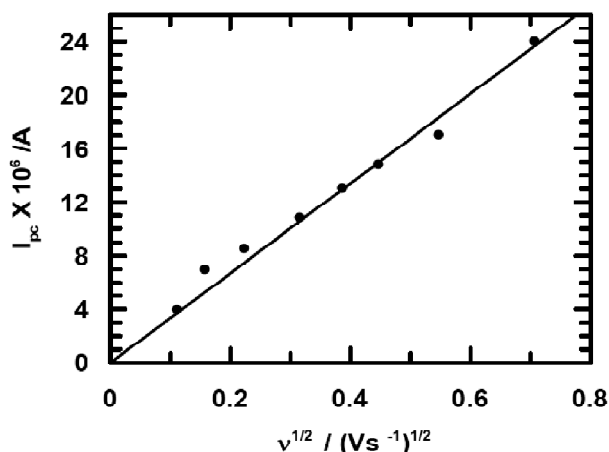


**Fig. 2.** Plot of cathodic peak current ( $I_{pc}$ ) vs square root of scan rate ( $v$ ) for the four-electron reduction of Ornidazole in aqueous solution at a potential of  $-0.827 \text{ V}$  and pH  $\sim 7.2$ .

### Interaction of reduction products of Ornidazole with biological targets:

Reduction of Ornidazole was achieved by maintaining a glassy carbon electrode at its previously determined reduction potential in aqueous medium. The generated reduction

products were allowed to react with nucleic acid bases or calf thymus DNA kept in its immediate vicinity. The amount of each nucleic acid base remaining after the experiment was determined with the help of HPLC (Shimadzu) using a C-18 column and 5% aqueous methanol as the mobile phase in case of thymine, cytosine and adenine and 40% aqueous methanol for guanine. The amount of calf thymus DNA not modified following interaction with the generated reduction products of Ornidazole was determined by treating such DNA with ethidium bromide, an established intercalator of DNA and reported to cause an increase in fluorescence upon interaction with DNA, by recording its fluorescence<sup>17-19</sup>. Fluorescence was recorded on a RF-530 IPC Spectrofluorophotometer, Shimadzu.

## Results and discussion

In aprotic media, the nitro group of 5-nitroimidazoles undergoes a reversible one-electron reduction to a nitro radical anion followed by a three-electron reduction to hydroxylamine derivatives. The first step is reversible, while the second involving three electrons is not, established through studies on metronidazole<sup>16</sup>. However, in aqueous solution these two steps are not realized separately and a single step four electron reduction is observed<sup>15,16</sup>.



As shown in Fig. 1, we too obtained a one-step four electron reduction of Ornidazole to hydroxylamine derivatives i.e. RNHOH. As identified through previous studies, there is scope for an interaction of the various reduction products of nitroimidazole, whereby RNHOH could participate in chemical reactions subsequent to its electrochemical generation. We made an attempt through this study to realize the interaction of such reduction products of Ornidazole formed in solution, with different nucleic acid bases and DNA. This was done to investigate the interaction of the reduction products (here generated electrochemically) with DNA, once this category of drugs enter the cells of a biological target that it ultimately kills. Ornidazole, a molecule used in different pharmaceutical formulations<sup>9-13</sup> have significant medicinal applications and since drug activity essentially depends on reduction products it was chosen with a purpose for this investigation. As mentioned already reduction of Ornidazole in

aqueous solution was done by maintaining a glassy carbon electrode at the determined reduction potential of it, as identified prior to start of the actual experiment (Fig. 1). Nucleic acid bases or DNA with which we wanted the reduction products generated from Ornidazole to interact were taken in an electrochemical cell along with Ornidazole and the previously determined reduction potential was applied. The reduction products of Ornidazole interact with a biological target kept in the immediate vicinity of its generation, taken one at a time in the experiments we performed. There exists the possibility of the appearance of  $\text{R-NO}_2^{\bullet-}$  by comproportionation of  $\text{RNO}_2$  and  $\text{RNHOH}$  and subsequent disappearance by disproportionation<sup>14,16</sup>. However, if there be a substrate, with which  $\text{R-NO}_2^{\bullet-}$  could interact then as normally expected, the possibility of disproportionation decreases drastically unless the rate of disproportionation is significantly greater than the reaction of  $\text{R-NO}_2^{\bullet-}$  with any biological target which is usually not the case since the concentration of a biological target taken in the experiment is a lot higher than the electrochemically reducible substance (here Ornidazole)<sup>16</sup>.

HPLC profiles of a pyrimidine base cytosine and purine base adenine following their damage after subjecting them to interaction with the reduction products of Ornidazole is shown in Figs. 3 and 4 respectively. Figures S1 and S2 (in Supplementary Information) are those for thymine and guanine respectively.

The figures indicate as time for electrochemical reduction of Ornidazole was gradually increased during experiment, a distinct change was observed in the area obtained for the eluting nucleic acid base. Base damage was subsequently identified by plotting percentage nucleic acid base remaining against the time provided to generate reduction products of Ornidazole using a glassy carbon electrode maintained at  $-0.827$  V in aqueous solution at pH 7.2. Fig. 5 shows this for cytosine and adenine while Fig. S3 (in Supplementary Information) is for thymine and guanine.

A similar study as described above was also performed keeping calf thymus DNA in the immediate vicinity of the generated reduction products of Ornidazole using glassy carbon electrode maintained at  $-0.827$  V in aqueous solution at pH 7.2. The only difference for the study with DNA was that slightly longer times were used in applying the reduction potential so that more reduction products of

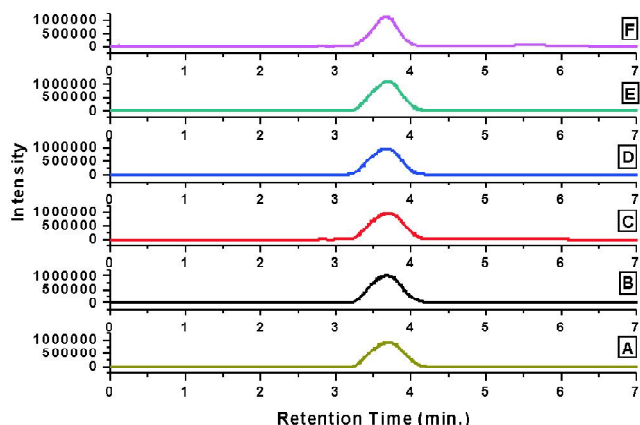


**Fig. 3.** HPLC chromatograms recorded at 254 nm for  $1 \times 10^{-3} \text{ mol dm}^{-3}$  cytosine solution that was subjected to a potential of  $-0.827 \text{ V}$  in presence of  $1 \times 10^{-4} \text{ mol dm}^{-3}$  Ornidazole under Ar saturated conditions. A-F indicates the time in minutes that the potential was applied on the solution; (A) 0 min, (B) 2 min, (C) 4 min, (D) 6 min, (E) 8 min, (F) 10 min.

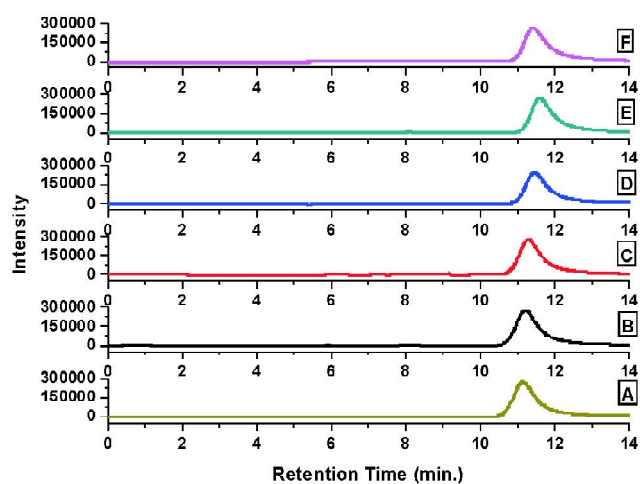


**Fig. 4.** HPLC chromatograms recorded at 254 nm for  $1 \times 10^{-3} \text{ mol dm}^{-3}$  adenine solution that was subjected to a potential of  $-0.827 \text{ V}$  in presence of  $1 \times 10^{-4} \text{ mol dm}^{-3}$  Ornidazole under Ar saturated conditions. A-F indicates the time in minutes that the potential was applied on the solution; (A) 0 min, (B) 2 min, (C) 4 min, (D) 6 min, (E) 8 min, (F) 10 min.

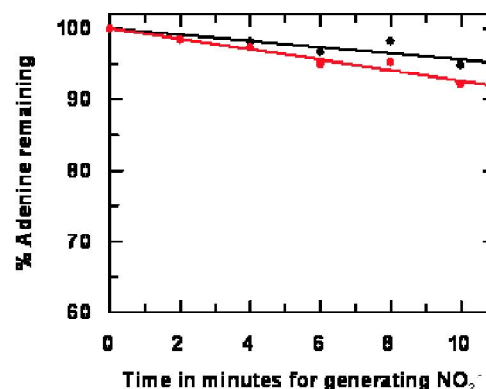
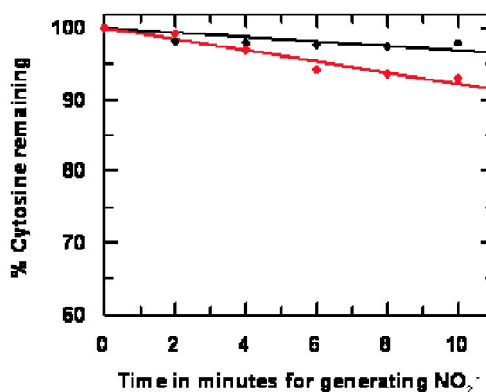


**Fig. 5.** Nucleic acid base degradation plots for cytosine and adenine followed by HPLC at 254 nm after the compounds were subjected to a potential of  $-0.827 \text{ V}$  under Ar saturated conditions in the absence and presence of a sensitizer (Ornidazole):  $[\text{Ornidazole}] = 1 \times 10^{-4} \text{ mol dm}^{-3}$ . Black line indicates the absence of Ornidazole while the red line its presence.

Ornidazole could be generated thus enabling a visible recognition of the change i.e. modification caused to DNA while monitoring by the ethidium bromide-fluorescence method. Fig. 6 shows a plot of the fluorescence following interaction of such treated calf thymus DNA with ethidium bromide that was subjected to an excitation at 510 nm using a fluorescence spectrophotometer.

**Table 1.** Shows enhancement ratios for the damage caused to nucleic acid bases and calf thymus DNA in the presence of Ornidazole for the study described above

Compound	Target									
	Adenine		Thymine		Cytosine		Guanine		Calf thymus DNA	
	Slope in Ar saturated medium	E R	Slope in Ar saturated medium	E R	Slope in Ar saturated medium	E R	Slope in Ar saturated medium	E R	Slope in Ar saturated medium	E R
-	-0.44	-	-0.73	-	-0.31	-	-0.21	-	-0.19	-
Ornidazole	-0.74	1.68	-1.14	1.56	-0.77	2.48	-0.55	2.62	-0.52	2.74

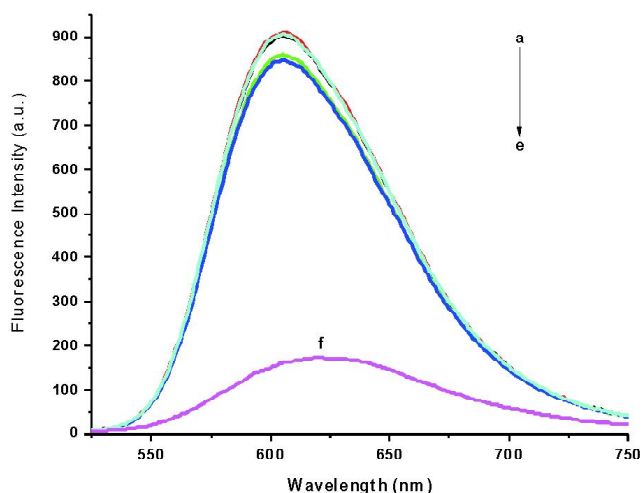


**Fig. 6.** Fluorescence spectra of calf thymus DNA after treatment with ethidium bromide, following the DNA being subjected to a potential of  $-0.827$  V in the presence of  $1 \times 10^{-4}$  mol  $\text{dm}^{-3}$  Ornidazole under Ar saturated conditions. a-e indicates the time in minutes for which the potential was applied to the solution: (a) 0 min, (b) 5 min, (c) 10 min, (d) 15 min, (e) 20 min, (f) denotes the spectrum of ethidium bromide alone.

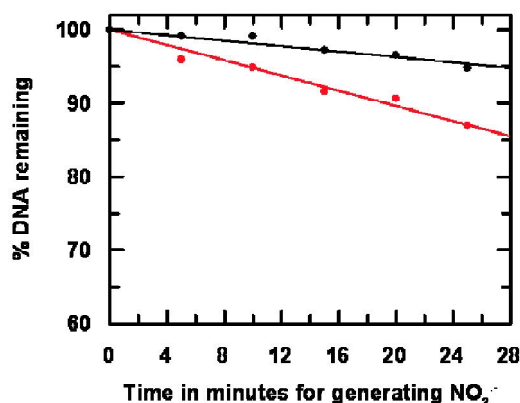


**Fig. 7.** A plot for calf thymus DNA modification in the absence and presence of a sensitizer (Ornidazole) after being subjected to a potential of  $-0.827$  V under Ar saturated conditions: [Ornidazole] =  $1 \times 10^{-4}$  mol  $\text{dm}^{-3}$ . Black line indicates the absence of Ornidazole while the red line its presence.

The modification caused to calf thymus DNA was realized by plotting the percentage of DNA remaining against the time provided to generate reduction products of Ornidazole using a glassy carbon electrode maintained at  $-0.827$  V in aqueous solution at pH 7.2 (Fig. 7).

The outcome of the study is summarized in Table 1 provided, where we see that nucleic acid base damage inflicted

on cytosine and guanine are much higher than that caused on thymine or adenine. It is also seen that enhancement ratio obtained for cytosine and guanine in presence of Ornidazole tallies appreciably with that obtained for calf thymus DNA. Since in calf thymus DNA percentage of cytosine and guanine are much higher than that of thymine and adenine it may be said that having a prior knowledge of the damage inflicted by a molecule on a particular nucleic acid base can be an advantage as one can then have an idea as to which type of DNA is more likely to be affected the most during the action of a drug that operates by the mechanism discussed.

## Conclusion

From this study it is evident that reduction products of Ornidazole modify nucleic acid bases as well as calf thymus DNA forming reactive intermediates that subsequently undergoes reactions to give different compounds as a result of which the base is eventually degraded.

## Acknowledgement

PN wish to thank the Department of Science and Technology, New Delhi for a DST-INSPIRE fellowship. SD is grateful to UGC, New Delhi for funds received as part of the research program on "Advanced Materials", a part of UPE II, operating at Jadavpur University. He is also grateful to the DST-PURSE program and the UGC-CAS program of the Government of India operating at the Department of Chemistry, Jadavpur University for financial support.

## References

1. S. L. Cudmore, K. L. Delgaty, S. F. Hayward-McClelland, D. P. Petrin and G. E. Garber, *Clin. Microbiol. Rev.*, 2004, **17**, 783.
2. D. I. Edwards, "Comprehensive Medicinal Chemistry", eds. C. Hansch, P. G. Sammes and J. B. Taylor, Pergamon Press, Oxford, 1990, Vol. 2, pp. 725-751.
3. R. P. Mason, "Free Radicals in Biology", ed. W. A. Pryor, Vol. V, Academic Press, New York, 1982, pp. 161-222.
4. S. Sood and A. Kapil, *Ind. J. Sex Transm. Dis.*, 2008, **29**, 7.
5. D. Petrin, K. Delgaty, R. Bhatt and G. Garber, *Clin. Microbiol. Rev.*, 1998, **11**, 300.
6. E. J. Hall, R. Miller, M. Astro and F. Rini, *Br. J. Cancer Suppl.*, 1978, **3**, 120.
7. M. Bonnet, C. R. Hong, W. W. Wong, L. P. Liew, A. Shome, J. Wang, Y. Gu, R. J. Stevenson, W. Qi, R. F. Anderson, F. B. Pruijn, W. R. Wilson, S. M. F. Jamieson, K. O. Hicks and M. P. Hay, *J. Med. Chem.*, 1961, **3**, 1241.

8. R. Sharma, *Current Radiopharmaceuticals*, 2011, **4**, 1.
9. R. C. Santra, D. Ganguly, D. Bhattacharya, P. Karmakar, A. Saha and S. Das, *New J. Chem.*, 2017, **41**, 11679.
10. J. Thulkar, Alka Kriplani and Nutan Agarwal, *Ind. J Pharmacol.*, 2012, **44**, 243.
11. O. Kurt, N. Girginkardeşler, I. C. Balcioğlu, A. Ozbilgin and U. Z. Ok, *Clin. Microbiol. Infect.*, 2008, **14**, 601.
12. B. Oren, E. Schgurensky, M. Ephros, I. Tamir and R. Raz, *Eur. J. Clin. Microbiol. Infect Dis.*, 1991, **10**, 963.
13. A. Khryanin and O. Reshetnikov, *Int. J. Antimicrob. Agents*, 2007, **29**, S220.
14. Mark H. Wilcox, "147-Nitroimidazoles, Metronidazole, Ornidazole and Tinidazole; and Fidaxomicin in: Infectious Diseases", 4th ed., eds. J. Cohen, W. G. Powderly and S. M. Opal, 2017, Vol. 2, pp. 1261-1263.e1.
15. J. A. Squella, S. Bollo and L. J. Núñez-Vergara, *Current Org. Chem.*, 2005, **9**, 565.
16. P. C. Mandal, *J. Electroanal. Chem.*, 2004, **570**, 55.
17. A. R. Morgan, J. S. Lee, D. E. Pulleyblank, N. L. Murray and D. H. Evans, *Nucleic Acids Res.*, 1979, **7**, 547.
18. H. C. Birnboim and J. J. Jevcak, *Cancer Research*, 1981, **41**, 1889.
19. S. Das, A. Saha and P. C. Mandal, *Environ. Health Pers.*, 1997, **105**, 1459.



ELSEVIER

Contents lists available at ScienceDirect

Inorganica Chimica Acta

journal homepage: [www.elsevier.com/locate/ica](http://www.elsevier.com/locate/ica)

Research paper

# *In situ* reactivity of electrochemically generated nitro radical anion on Ornidazole and its monomeric Cu(II) complex with nucleic acid bases and calf thymus DNA



Promita Nandy, Saurabh Das\*

Department of Chemistry, Inorganic Chemistry Section, Jadavpur University, Kolkata 700 032, India

## ARTICLE INFO

## Keywords:

Ornidazole  
Cu<sup>II</sup>(Onz)<sub>2</sub>Cl<sub>2</sub>  
Adenine  
Thymine  
Cytosine  
Guanine  
Calf thymus DNA

## ABSTRACT

A monomeric complex of Cu(II) with Ornidazole was synthesized and characterized. Electrochemical reduction of the complex, by maintaining a glassy carbon electrode in aqueous solution, at its cathodic potential, under de-aerated (Argon saturated) condition, generates different products. Such electrochemical reduction was carried out at different times in presence of either nucleic acid bases or calf thymus DNA. Since the nitro-radical anion (NO<sub>2</sub><sup>·-</sup>) and other reduction products of 5-nitroimidazoles or their complexes are crucial for biological activity, attempt was made to follow the interaction of electrochemically generated reduction products of the complex with nucleic acid bases or with DNA to realize what happens when these drugs enter the cells of a target organism, get reduced enzymatically and show activity that lead to cell death. The study reveals that the monomeric complex of Cu(II) with Ornidazole was better in causing modification of nucleic acid bases and to double strands of calf thymus DNA when compared with Ornidazole under identical experimental conditions. While Ornidazole was more effective on guanine and cytosine than thymine or adenine, the complex was found more effective on cytosine than thymine and adenine. For the complex, experiments with guanine could not be done because of a physical association between the two that turned the solution turbid, preventing the experimental protocol from being correctly implemented. In general, damage caused to nucleic acid bases or to calf thymus DNA was greater for the complex than for Ornidazole. This was correlated with results obtained for calf thymus DNA, providing a preliminary idea regarding the type of DNA (based on nucleic acid base composition) that is most likely to be affected by these compounds. The study also correlates the fact why organisms with a reasonably high GC content in their DNA have been reported to succumb to such compounds. It clearly indicates Ornidazole and its Cu(II) complex have a somewhat higher tendency to affect GC sites than AT. In brief, the study of *in situ* reactivity of electrochemically generated reduction products on Ornidazole and its Cu(II) complex with nucleic acid bases and calf thymus DNA reveal why literature shows Ornidazole to be active on GC rich DNA containing organisms.

## 1. Introduction

5-nitroimidazoles are an extremely important class of molecules from a pharmaceutical point of view, being present in a number of formulations used to address a wide spectrum of medical issues ranging from infections caused by parasites to being used as radiosensitizers in cancer treatment [1–10]. Although maximum use is reported for Metronidazole (Mnz), aspects like resistance to the drug and toxic side effects of which neurotoxicity is of a major concern have prompted the search for derivatives that have comparable efficacy but less adverse effects [4–17]. Ornidazole (Onz) is a compound that has made its way to clinics in a very short time since first being identified as a potential

drug. However, as is true for all 5-nitroimidazoles, efficacy does not come without adverse effects [11,15,16]. The most unfortunate part with 5-nitroimidazoles and with many other drugs is that the species responsible for efficacy is also responsible for adverse effects; for this class of drugs, it being the nitro radical anion (NO<sub>2</sub><sup>·-</sup>) [11,3–8,15–19]. Hence, controlling its generation has become very important [13]. Within the biological system, the drugs are reduced by enzymes like pyruvate ferredoxin oxidoreductase (PFOR) that prepare them for entry into cells by passive diffusion, creating a favorable concentration gradient [8–11]. Thereafter, NO<sub>2</sub><sup>·-</sup> imparts cytotoxicity within cells.

Although, a large body of literature identifies NO<sub>2</sub><sup>·-</sup> as responsible for drug efficacy, only few studies have investigated its role in detail

\* Corresponding author.

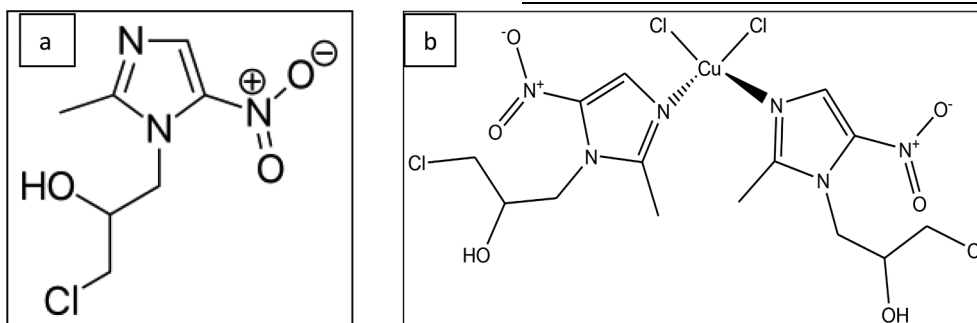
E-mail address: [darsrv@yahoo.in](mailto:darsrv@yahoo.in) (S. Das).<https://doi.org/10.1016/j.ica.2019.119267>

Received 31 July 2019; Received in revised form 4 October 2019; Accepted 4 November 2019

Available online 06 November 2019

0020-1693/ © 2019 Elsevier B.V. All rights reserved.

[18,19]. We earlier showed complex formation is able to modulate (decrease) the formation of  $\text{NO}_2^-$  – which is expected to decrease toxic side effects [13,14]. Although expected, decrease in  $\text{NO}_2^-$  – due to complex formation did not affect drug efficacy in spite of the fact that it is crucial for drug action [12–14]. This therefore implies that complexes might be having some attribute that makes up for decreased  $\text{NO}_2^-$  – [12–14]. Through this study we tried to look at aspects of cytotoxicity initiated by  $\text{NO}_2^-$  – and other reduction products of a monomeric complex of Cu(II) with Onz on nucleic acid bases and calf thymus DNA to correlate what could be happening when similar molecules are enzymatically reduced within the biological system of different species they eventually kill [1,6–7,12,13]. Reduction products of the complex were generated electrochemically by maintaining a glassy carbon electrode at the cathodic potential of the complex [20]. In the immediate vicinity of such electrochemically generated reduction products, nucleic acid bases and calf thymus DNA were kept so that reduced products of the complex could react with them. Although never identical as to what happens within cells, it can throw some light on what could be happening when similar species are biologically (i.e. enzymatically) generated within cells following the transfer of electron (s) to a 5-nitroimidazole moiety by an electron donating group present within the cell. *In situ* reactivity of such generated reduction products of the complex with nucleic acid bases or DNA were subsequently followed to realize changes brought about on a target that was maintained in the immediate vicinity of the reduction products. The Cu(II) complex of Onz was reduced at its pre-determined reduction potential using an electrochemical method that maintains a glassy carbon electrode at that potential in de-aerated (Ar saturated) environment for different periods of time [20].



Structure of (a) Ornidazole and (b) its monomeric Cu(II) complex

## 2. Experimental

### 2.1. Materials used

Ornidazole was purchased from TCI, Japan and purified by recrystallization from methanol. Copper(II) chloride ( $\text{CuCl}_2 \cdot 2\text{H}_2\text{O}$ ), NaCl,  $\text{NaNO}_3$  and KCl, (all AR grade) were purchased from E. Merck, India. Four different nucleic acid bases namely adenine, guanine, cytosine and thymine were purchased from TCI, Japan. Calf thymus DNA was purchased from Sisco Research Laboratories, India. It was dissolved in triple distilled water in the presence of suitable electrolytes. Its concentration in aqueous solution was determined using a molar extinction coefficient of  $6600 \text{ M}^{-1} \text{ cm}^{-1}$  at 260 nm. Absorbance of the prepared DNA solution was also measured at 260 nm and 280 nm.  $A_{260}/A_{280}$  was determined; the value being in the range 1.8–1.9, the DNA was considered ready for use without any further purification. Quality of calf thymus DNA was also verified with the help of circular dichroism (CD) recording its response at 260 nm on a CD spectropolarimeter (J815 - JASCO, Japan). Aqueous solutions of all other substances were prepared in triple distilled water.

### 2.2. Synthesis of $[\text{Cu}(\text{Onz})_2\text{Cl}_2]$

A solution of Onz (0.439 g in 25 ml, 2.00 mmol) in methanol was gradually added with stirring to a solution of  $\text{CuCl}_2 \cdot 2\text{H}_2\text{O}$  (0.17 g in 25 ml, 1.00 mmol) in methanol. [13,21] The final mixture was warmed under reflux to a temperature of approximately  $60^\circ\text{C}$  for 5 h. A green crystalline compound was obtained after  $\sim 10$  days following a slow evaporation of the solvent. The product was filtered, dried and stored very carefully.

Anal. Calc. (%) for  $[\text{Cu}(\text{Onz})_2\text{Cl}_2]$  i.e.  $\text{C}_{14}\text{H}_{20}\text{Cl}_4\text{CuN}_6\text{O}_6$ : C, 29.29; H, 3.49; N, 14.65. Found: C, 29.85; H, 3.43; N, 14.79.

### 2.3. Physical measurements

Absorption spectra of the complex were recorded on JASCO V-630 spectrophotometer, JASCO, Japan. FTIR of solid samples in the form of KBr pellets was obtained using a Perkin Elmer RX-I spectrophotometer. Elemental analysis was done on Perkin-Elmer 2400 Series-II CHN analyzer. EPR spectrum was recorded on JEOL JES-FA 200 ESR spectrophotometer.

### 2.4. Electrochemical measurements

Electrochemical experiments were performed using an air-tight 50 ml electrochemical cell. Voltammograms were recorded on a Metrohm–Autolab model PGSTAT 101 potentiostat. Data analysis was done using NOVA 1.10.1.9 program. A conventional three-electrode system, glassy carbon as working electrode, a platinum wire as counter electrode and Ag/AgCl, satd. KCl as reference electrode were used.

Before any electrochemical experiment, the solution was degassed for  $\sim 30$  min using a highly pure argon source. Reduction of the nitro group in the monomeric Cu(II) complex of Onz was followed in aqueous, aqueous-dimethyl formamide (DMF) and pure DMF as solvent. As already reported, in DMF, there is initially a one-electron reduction to nitro-radical anion [19]. Subsequent to this, there is a three-electron reduction that converts  $\text{NO}_2^-$  – to  $-\text{NHOH}$  [19]. As the percentage of water increases, clarity of the two reduction peaks is lost and in a purely aqueous solution a one-step four electron reduction is observed. Results were analyzed according to the Randles-Sevcik equation (Eq. 1) [22,23].

$$i_{pc} = (2.69 \times 10^5) \cdot n^{3/2} D_0^{1/2} \cdot A \cdot C \cdot \nu^{1/2} \quad (1)$$

where  $i_{pc}$  refers to current in amperes at the cathodic peak potential,  $n$  denotes total number of electrons involved,  $D_0$ , diffusion coefficient of the species,  $A$ , the area of the electrode in  $\text{cm}^2$ ,  $C$ , concentration of the substance in moles/ $\text{cm}^3$  and  $\nu$ , scan rate in  $\text{V s}^{-1}$ . Fig. 1 is a typical voltammogram of  $[\text{Cu}(\text{Onz})_2\text{Cl}_2]$  subjected to cyclic voltammetry in aqueous solution. From the voltammogram, the reduction peak potential ( $-0.849 \text{ V}$ ) of the complex was identified and subsequently used to reduce the complex at that potential in presence of either nucleic acid

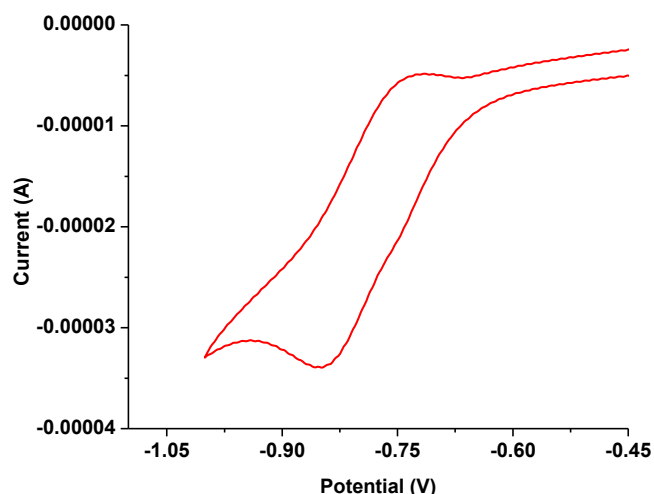


Fig. 1. Cyclic voltammogram of 1 mM  $[\text{Cu}(\text{Onz})_2\text{Cl}_2]$  showing a single step four electron reduction of the nitro group in an aqueous 0.12 M KCl solution using a glassy carbon electrode; Scan rate 100 mV/s.

bases or double stranded calf thymus DNA. The cathodic peak current ( $I_{pc}$ ) in amperes at  $-0.849$  V was plotted against square root of potential sweep rate ( $\nu^{1/2}$ ) (Fig. S1, S I) to verify that the process is diffusion controlled, an essential criterion for experiments to follow.

## 2.5. Interaction of reduction products formed on $[\text{Cu}(\text{Onz})_2\text{Cl}_2]$ with the target:

A glassy carbon electrode was maintained at the previously determined reduction potential of the complex ( $-0.849$  V) in aqueous solution. In the immediate vicinity of such *in situ* electrochemically generated reduction products (like  $-\text{NO}_2^-$  etc.), different nucleic acid bases and calf thymus DNA were kept one at a time under de-aerated (Argon saturated) conditions.<sup>20</sup> The complex undergoes reduction at its ligand site in accordance with electrochemical behavior in aqueous solution generating different reduced species depending on the pH of the medium; in our case 7.0. The time allotted for *in situ* electrochemical generation of reduced species on the monomeric Cu(II) complex of Onz was strictly maintained same for all targets to be able to compare results pertaining to the creation of species in solution, capable of bringing about a change on the target maintained in the immediate vicinity of such generation under identical conditions. In an earlier study, using an exactly similar experimental setup, a glassy carbon electrode was used to reduce Onz at  $-0.827$  V in aqueous solution (pH 7.2) and interaction of its various reduction products with nucleic acid bases and calf thymus DNA was investigated [20]. In that study also, in the immediate vicinity of *in situ* electrochemically generated reduction products ( $-\text{NO}_2^-$  and others), different nucleic acid bases and calf thymus DNA were maintained one at a time under de-aerated (Argon saturated) conditions [20]. Concentration of the complex was one-tenth of the chosen biological target. Control experiments were performed where an aqueous solution of a nucleic acid base or calf thymus DNA (without complex) was subjected to a constant potential of  $-0.835$  V (approximately midway between  $-0.827$  V for Onz [20] and  $-0.849$  V for complex) with the help of a glassy carbon electrode.

Amount of each nucleic acid base remaining unaltered was determined by HPLC using C-18 column as the stationary phase and 5% aqueous-methanol as mobile phase [20,24]. The amount of calf thymus DNA not modified following an interaction with *in situ* generated reduction products was determined by treating such DNA with ethidium bromide (EtBr, an established DNA intercalator) and subsequently recording its fluorescence on a RF-530 IPC Spectrofluorophotometer, Shimadzu, Japan [20,24–27].

## 3. Results and discussions

### 3.1. Characterization of the complex

#### 3.1.1. UV-VIS spectra

Electronic spectrum of  $\text{Cu}(\text{Onz})_2\text{Cl}_2$  in methanol (Fig. S2) was recorded on a JASCO V-630 spectrophotometer, Japan and compared with that of Onz (Fig. S3). An intense band located at an almost similar maximum wavelength (311 nm) for non-coordinated Onz is ascribed to intra-ligand (IL)  $\pi-\pi^*$  transition ( $\epsilon = 18950 \text{ M}^{-1}\text{cm}^{-1}$ ) [28–30].

#### 3.1.2. IR spectra

IR spectrum of  $\text{Cu}(\text{Onz})_2\text{Cl}_2$  (Fig. 2a) showed slight shifts in almost all responses recorded for Onz (Fig. 2b) to higher frequencies [31]. The peak at  $1559.76 \text{ cm}^{-1}$  for  $\nu_{(\text{C}=\text{N})}$  for example, in case of the complex was at  $1538.21 \text{ cm}^{-1}$  for Onz indicating coordination of the metal centre by the imidazole nitrogen [31].  $\text{NO}_2$  stretching frequencies  $\nu_{\text{as}} = 1478 \text{ cm}^{-1}$  and  $\nu_{\text{s}} = 1373 \text{ cm}^{-1}$  for  $[\text{Cu}(\text{Onz})_2\text{Cl}_2]$  (Fig. 2a) were however similar to  $\nu_{\text{as}} = 1471.57 \text{ cm}^{-1}$  and  $\nu_{\text{s}} = 1385.92 \text{ cm}^{-1}$  for Onz (Fig. 2b). Splitting of  $\text{NO}_2$  bands,  $\Delta\nu_{\text{NO}_2}$  was  $105 \text{ cm}^{-1}$  in case of the complex while it was  $86 \text{ cm}^{-1}$  for Onz suggesting that the nitro group does not participate in coordinating Cu(II).

#### 3.1.3. EPR spectrum of $\text{Cu}(\text{Onz})_2\text{Cl}_2$

EPR spectrum (Fig. 3) recorded at room temperature showed the X-band frequency of the powdered sample having resonance signal at 318 mT with a g value of 2.11.

#### 3.1.4. Mass spectra

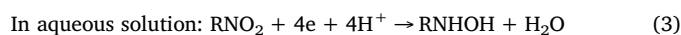
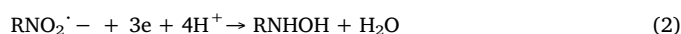
Molecular ion peaks bound to an atom of sodium were detected in the vicinity of  $m/z = 600$ ; the two most prominent ones were at 600.88 and 602.88. Owing to the presence of Cu and Cl in the complex, isotope distributions were observed in different fragments recorded in the mass spectrum (Fig. 4). Going by the molecular formula mentioned earlier, molecular ion peaks (Na bound) were expected in the  $m/z$  range 594 to 604 (details in SI). However, experimentally only those peaks that involved the relatively heavier isotopes of Cu and Cl were obtained. From the molecular ion, if two Cl atoms (one from each ligand) departs, then the species formed should have a theoretical  $m/z$  value of 501.0 (both  $^{35}\text{Cl}$ ,  $^{63}\text{Cu}$ ) or 503.0 [(both  $^{35}\text{Cl}$ ,  $^{65}\text{Cu}$ ) or (one  $^{35}\text{Cl}$ , one  $^{37}\text{Cl}$ ,  $^{63}\text{Cu}$ )] or 505.0 [(one  $^{35}\text{Cl}$ , one  $^{37}\text{Cl}$ ,  $^{65}\text{Cu}$ ) or (both  $^{37}\text{Cl}$ ,  $^{63}\text{Cu}$ ) or 507.0 (both  $^{37}\text{Cl}$ ,  $^{65}\text{Cu}$ ). Experimental  $m/z$  values for this fragment were recorded at 500.98, 502.98, 504.97 that explain isotope distributions mentioned above. Isotope distribution was also observed in the region of  $m/z = 367.9662$  to  $m/z = 370.4658$  attributed to a fragment generated from the complex (i.e. molecular ion) following the departure of two Cl atoms (one from each Onz), two  $-\text{OH}$  groups (one from each Onz), two  $-\text{NO}_2$  groups (one from each Onz) and a  $-\text{CH}_3$  from any one of the two Onz ligands (details in SI).

### 3.2. *In situ* reactivity of electrochemically generated reduction products

When the medium is aprotic, 5-nitroimidazoles participate in a reversible one-electron reduction initially forming a nitro radical anion that then undergoes an irreversible three-electron reduction to  $-\text{NHOH}$  (Eqs. 1 and 2) [18,19,23]. In aqueous solution, these two steps are not realized separately and a single step four electron reduction is observed (Eq. 3) [18,19,23]. The same is true for the monomeric Cu(II) complex of Onz (Fig. 1).



In aprotic media:



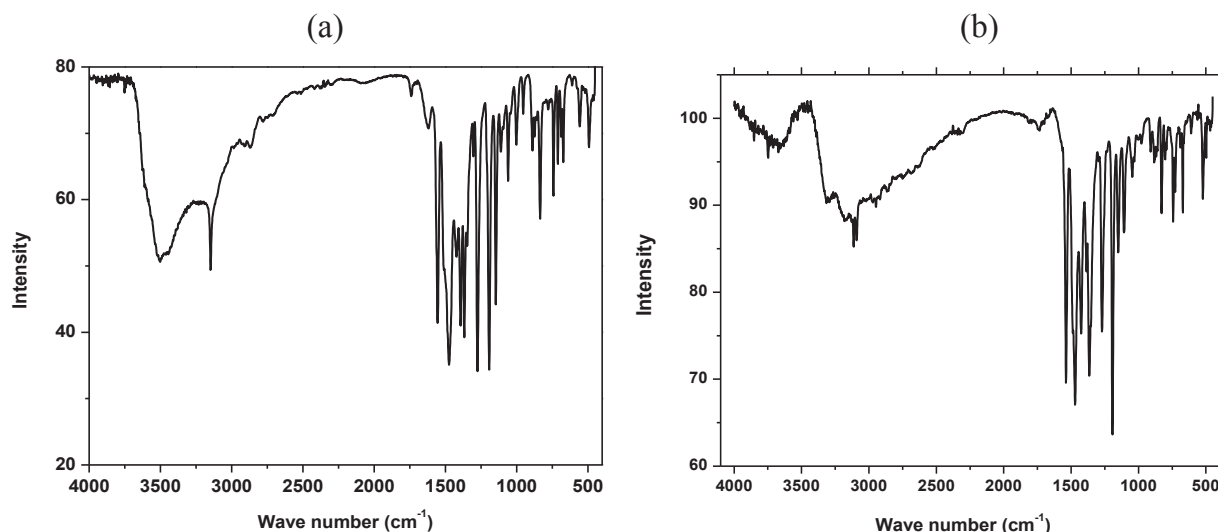


Fig. 2. IR spectra of (a)  $[\text{Cu}(\text{Onz})_2\text{Cl}_2]$  and (b) Ornidazole.

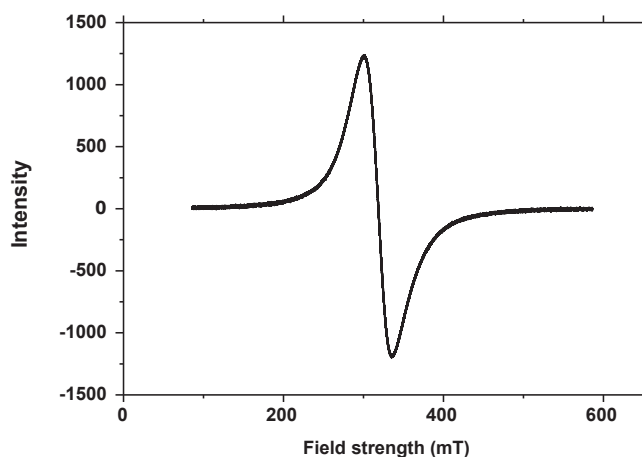


Fig. 3. Room temperature EPR spectrum of  $[\text{Cu}(\text{Onz})_2\text{Cl}_2]$ .

Hence, in the immediate vicinity of a Cu(II) complex subjected to electrochemical reduction at a constant potential ( $-0.849\text{ V}$ ) as previously determined (Fig. 1), if a target is maintained, there is the possibility that reduction products of the complex would interact with the target. The outcome of such interactions (modifications) for nucleic acid bases and calf thymus DNA was ascertained. Since in aprotic media, the reversible one-electron reduction step forming  $\text{NO}_2^{\cdot-}$  is identified separately, it is possible to assign the interactions to it. However, in case of aqueous solutions when a glassy carbon electrode is maintained at the cathodic potential of the complex i.e. at its “one step four electron reduction” potential, many species are generated. Hence, in aqueous solution a correct assignment of species (from different reduction products) responsible for interaction with the target is not possible without an error. More specifically said it means that the interaction cannot be exclusively assigned to the formation of  $\text{NO}_2^{\cdot-}$  since other reduction products are also formed in solution following the electrochemical reduction of the complex at  $-0.849\text{ V}$  (Eqs. 1–3). At the same time, it is also true, since formation of species containing  $\text{NO}_2^{\cdot-}$  is the first step of the reduction process and being a radical it should have high probability to interact with a target present in its vicinity; in fact higher than successive reduction to other species (Eq. 2) [19]. Hence, although other reduction products of the complex could well be involved in modifying the target,  $\text{NO}_2^{\cdot-}$  could have a substantial contribution to the damage caused to a target. The present study was performed to realize how different reduction products (generated electrochemically) on a 5-nitroimidazole and its complex might

interact with nucleic acid bases or DNA that might help to explain what happens when such drugs or their complexes enter the cells of a biological target. For a long time it is believed that drugs belonging to this class at a favourable reduction potential must primarily get reduced in order to be active; mentioned by several studies as the principle mechanism of action for nitroimidazoles [5–9]. It is also believed these reduced products thereafter interact with DNA, however nothing very specific is reported for interactions at the cellular level barring a few reports [1–17]. We, in previous reports mentioned the ability of different Cu(II) complexes of 5-nitroimidazoles to significantly modulate the formation of  $\text{NO}_2^{\cdot-}$ , essential for curbing neuro-toxic side effects [13,14]. In these reports, we showed in spite of decreased  $\text{NO}_2^{\cdot-}$ , efficacy was not compromised due to complex formation; in fact complexes were mostly at par with the performance of drugs from which they were prepared [12–14]. In some cases, complexes performed even better than the parent drug when tried on different biological targets [12–14]. Hence, the question that immediately comes up is, if generation of  $\text{NO}_2^{\cdot-}$  is so essential for drug action, as established by several studies, how then are Cu(II) complexes of 5-nitroimidazoles, having decreased  $\text{NO}_2^{\cdot-}$  formation still so active that it matches the efficacy of the respective drug molecules from which they were prepared [12–14]. This prompted us to find out whether mechanism of action of 5-nitroimidazoles and their Cu(II) complexes were similar or different.

### 3.2.1. Interaction of electrochemically generated reduction products with nucleic acid bases:

In a previous report we mentioned about Onz being reduced using a glassy carbon electrode maintained at a constant potential ( $-0.827\text{ V}$ ) in aqueous solution [20]. When nucleic acid bases and calf thymus DNA were maintained in the immediate vicinity of the reduced products of Onz their modification was observed [20]. Herein, we report modifications caused to similar targets by a monomeric complex of Cu(II) with Onz. Reduction products generated from the complex interact with the target kept in the immediate vicinity of their formation. Considering different reduction products formed in solution there is a possibility for the formation of species having  $\text{NO}_2^{\cdot-}$  following comproportionation between  $\text{NO}_2$  containing species and  $\text{NHOH}$  containing species, present either on different Onz of the same complex or on different Onz of different complexes. There is also the possibility of disappearance of  $\text{NO}_2^{\cdot-}$  by disproportionation. [19,32] However, since a substrate is present in solution with which  $\text{NO}_2^{\cdot-}$  can interact there is a high possibility of it being consumed in that pathway. Hence,  $\text{NO}_2^{\cdot-}$  depleting by disproportionation should be less unless the rate of disproportionation of species containing  $\text{NO}_2^{\cdot-}$  (generated on a complex) is significantly higher than the rate of reaction between a generated  $\text{NO}_2^{\cdot-}$  and a target (either a nucleic acid base or DNA).

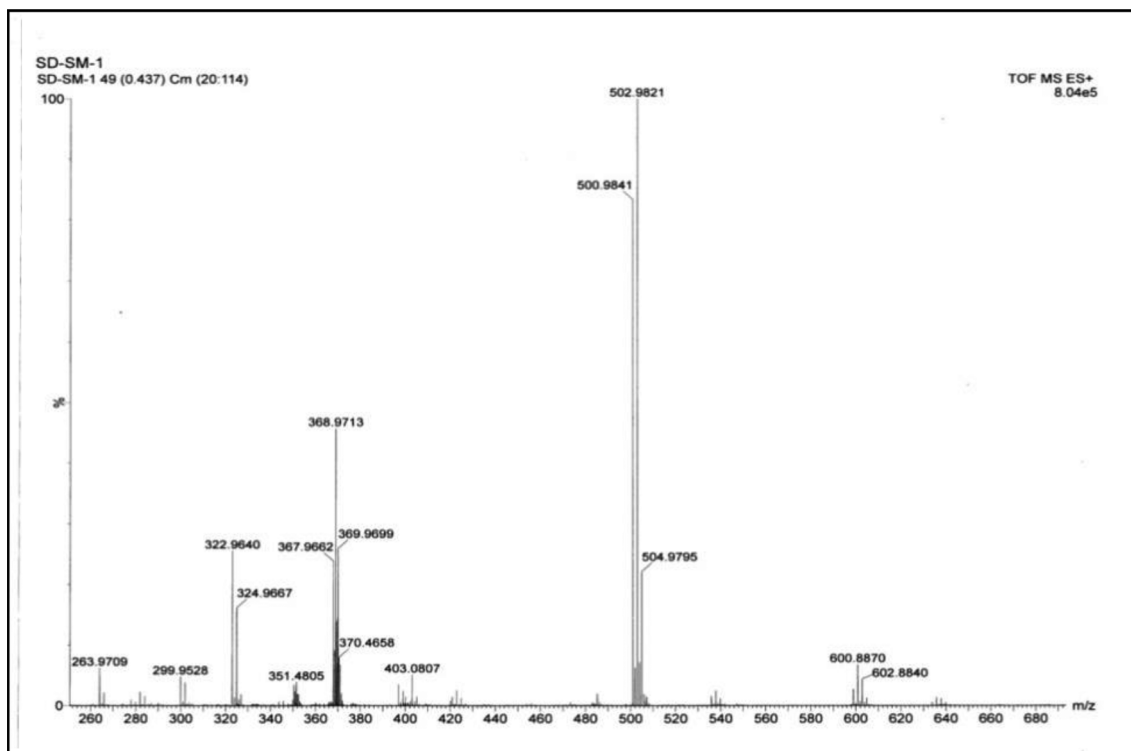


Fig. 4. Mass spectrum of  $\text{Cu}(\text{Onz})_2\text{Cl}_2$ .

Besides, although disproportionation is a possibility, it cannot logically occur since the concentration of the target maintained during experiments is almost ten times higher than the complex. Therefore, concentrations of electrochemically reduced species formed from the complex in solution in comparison to the target would be even less 1:10, implying little scope for disproportionation. Hence, although qualitatively explained, it can be realized that  $-\text{NO}_2^-$  could eventually become an important species amongst the different reduced forms generated from the complex that interact with the target [19]. However, to be more sure, we performed another set of experiments (Figs. S4, SI), where we dissolved each nucleic acid base (thymine, cytosine and adenine) separately along with the  $\text{Cu}(\text{II})$  complex of Onz in DMF having the same concentration as that for experiments performed in aqueous solution. When DMF is the solvent, since the one electron reduction step of  $-\text{NO}_2^-$  converting to  $-\text{NO}_2^{\cdot-}$  is realized separately, a glassy carbon electrode was maintained at the first reduction potential ( $-0.828\text{ V}$ ) of the complex and  $-\text{NO}_2^{\cdot-}$  generated exclusively. Therefore, with DMF as solvent,

interaction with the target may be assigned to  $-\text{NO}_2^{\cdot-}$ . (Table S1, SI).

HPLC chromatograms of pyrimidine and purine based nucleic acid bases were recorded following interaction of different reduced species of the complex in aqueous solution. Fig. 5 shows HPLC chromatograms for thymine and adenine recorded after these two nucleic acid bases were allowed to interact with the electrochemically reduced products of the complex in aqueous solution. Figs. S5, SI is an HPLC chromatogram of cytosine recorded following an electrochemical reduction of the complex in aqueous solution in its vicinity. Fig. 5 and Fig. S5 indicate as time for electrochemical reduction of the complex at its pre-determined reduction potential was increased, a distinct change was observed for area under the peaks in the respective HPLC chromatograms of the eluting nucleic acid bases from where the damage caused to the nucleic acid base could be ascertained. This was done by plotting percentage of a nucleic acid base remaining against time provided for the electrochemical generation of reduction products on the complex by maintaining a glassy carbon electrode either at  $-0.849\text{ V}$  in aqueous

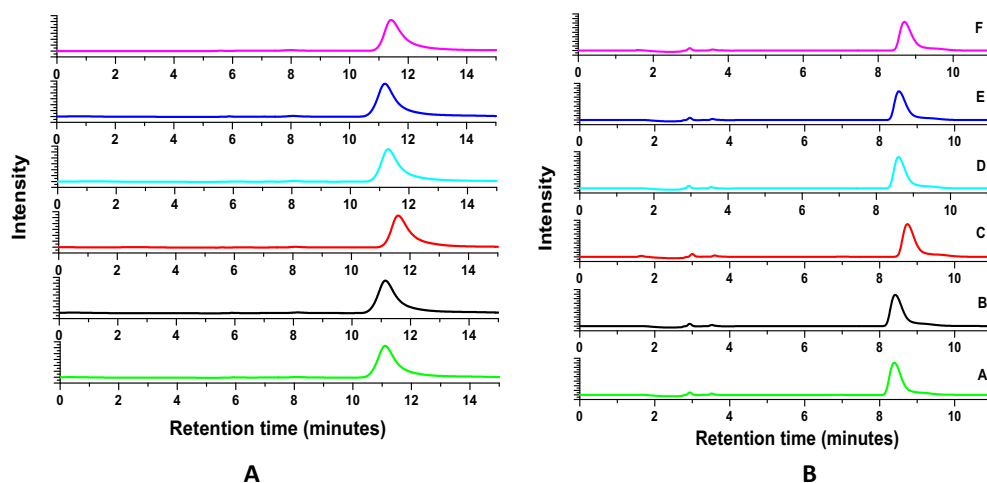


Fig. 5. HPLC chromatograms were recorded at  $254\text{ nm}$  for  $1 \times 10^{-3}\text{ mol dm}^{-3}$  of (A) thymine and (B) adenine after each solution was subjected to a constant potential of  $-0.849\text{ V}$  in the presence of  $1 \times 10^{-4}\text{ mol dm}^{-3}$   $\text{Cu}(\text{II})$ -Onz under deaerated (Argon saturated) conditions. A to F indicates time in minutes for which the constant potential was applied to each solution; A: 0 min, B: 2 min, C: 4 min, D: 6 min, E: 8 min, F: 10 min.

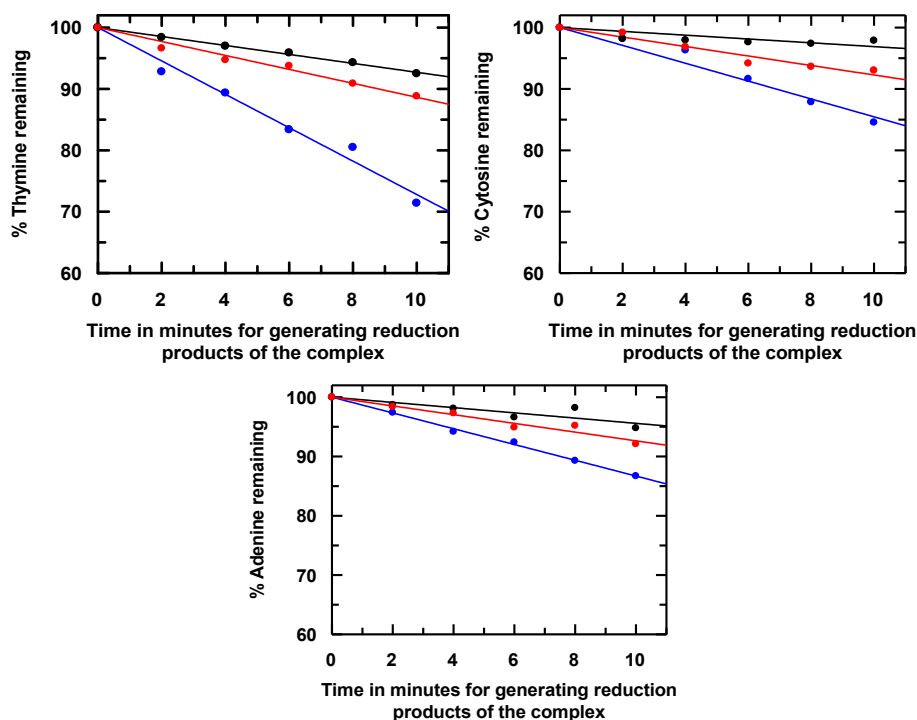


Fig. 6. Degradation of thymine, cytosine and adenine followed by HPLC at 254 nm after being allowed to interact with the reduction products generated from Ornidazole (red line) and the Cu(II)-Ornidazole complex (blue line) following electrochemical reduction of the compounds at constant potentials of  $-0.827$  V and  $-0.849$  V respectively under de-aerated (Argon saturated) conditions. The black line indicates degradation of the respective nucleic acid base in the absence of a sensitizer [Onz or Cu(II)-Onz], when it was subjected to a potential of  $-0.835$  V. [nucleic acid base] =  $1 \times 10^{-3}$  mol dm $^{-3}$ ; [Ornidazole] = [Cu(II)-Onz complex] =  $1 \times 10^{-4}$  mol dm $^{-3}$ . (For interpretation of the references to colour in this figure legend, the reader is referred to the web version of this article.)

solution (pH 7.0) or at  $-0.828$  V in DMF. Changes observed for each nucleic acid base following interaction with the reduction products of the complex in aqueous solution is shown in Fig. 6, Table 1 and that in DMF in Fig. S4, Table S1.

Comparison of the damage inflicted on a target by the complex in DMF and in aqueous solution helps to identify the species responsible in each case that causes a change on the target. It was seen while damage (reported in terms of E R) was significantly greater for adenine in aqueous solution than in DMF, for thymine it was only slightly higher in DMF and for cytosine it was slightly less in DMF than in aqueous solution. Results indicate in case of adenine other reduction products formed on the complex could be playing a significant role besides species containing  $\text{NO}_2^-$ . However, the results for thymine suggest other reduction products probably do not have a major role in causing damage to it and that it is  $\text{NO}_2^-$  containing species that has a major contribution; for cytosine, other reduction products generated from the complex in aqueous solution (Eqs. 1–3) might have a role in nucleic acid base modification besides species containing  $\text{NO}_2^-$ .

### 3.2.2. Interaction of electrochemically generated reduction products with calf thymus DNA

A similar study as the one described above was performed by maintaining calf thymus DNA in aqueous solution at pH 7.4 in the immediate vicinity of the generated reduction products of the Cu(II) complex of Onz using a glassy carbon electrode maintained at

$-0.849$  V. For calf thymus DNA as the target, slightly longer times were used for electrochemical reduction of the complex. This was necessary to generate more reduction products so that an observable change was obtained when the modified calf thymus DNA was monitored by fluorescence using EtBr, i.e. subsequent to its interaction with reduction products of the complex. Since interaction of EtBr with DNA leads to increase in fluorescence, this was utilized to determine the amount of calf thymus DNA remaining intact following its interaction with reduced products formed by the complex [25,26]. Fig. 7 is a typical plot showing fluorescence of calf thymus DNA with EtBr either in the absence of any interaction or having undergone an interaction with reduced products formed from the complex. In each case, the adducts of DNA with EtBr were excited at 510 nm using a fluorescence spectrophotometer (RF-530 IPC Spectrofluorophotometer, Shimadzu, Japan) and emission was measured over the wavelength range 525 nm–750 nm

Modification caused to calf thymus DNA was established by plotting percentage DNA remaining against the time provided for the generation of reduction products on the complex following maintaining of a glassy carbon electrode at  $-0.849$  V in aqueous solution (pH 7.4; Fig. 8).

The outcome of the study on interaction of electrochemically generated reduced species of the Cu(II) complex of Onz with calf thymus DNA is summarized in Table 1. It is seen from the table, Onz affects guanine and cytosine to a much greater extent than adenine and thymine while the complex affects cytosine to a much greater extent than adenine or thymine. In case of the complex, experiments could not be

Table 1

Enhancement ratio for the damage of nucleic acid bases and calf thymus DNA following reduction of Ornidazole and its Cu(II) complex at their respective reduction potentials in aqueous solution generating different products that interact with the target.

COMPOUND	Target									
	Adenine		Guanine		Thymine		Cytosine		Calf Thymus DNA	
	De-aerated medium (Ar saturated)	E R								
–	–0.44	–	–0.21	–	–0.73	–	–0.31	–	–0.19	–
Ornidazole <sup>20</sup>	–0.74	1.68	–0.55	2.62	–1.14	1.56	–0.77	2.48	–0.52	2.74
[Cu(Onz) <sub>2</sub> Cl <sub>2</sub> ]	–1.33	3.02	–	–	–2.78	3.82	–1.45	4.66	–0.85	4.47

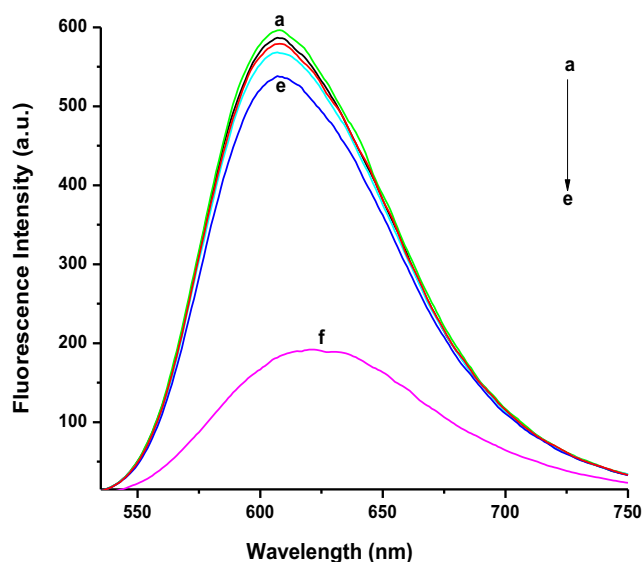


Fig. 7. Fluorescence spectra of calf thymus DNA after treatment with EtBr following an interaction of the DNA with the reduction products generated from the monomeric Cu(II) complex of Ornidazole subjected to constant potential at  $-0.849$  V in de-aerated (Argon saturated) conditions.  $[\text{Cu(II)-Ornidazole}] = 1 \times 10^{-4} \text{ mol dm}^{-3}$ . "a" to "e" indicates the time in minutes for which such potential was applied to the solution; a: 0 min, b: 5 min, c: 10 min, d: 15 min, e: 20 min. "f" denotes the spectrum of EtBr when it was excited alone i.e. in the absence of DNA at 510 nm.

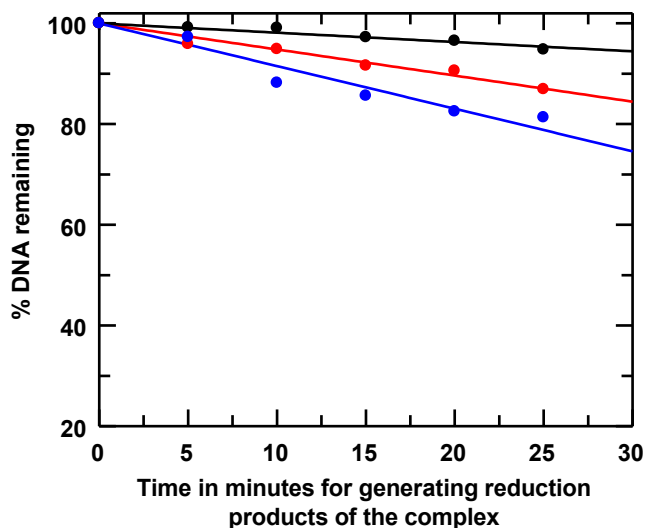


Fig. 8. Plots showing modification of calf thymus DNA in the absence (black) and presence of sensitizer molecules, Ornidazole (red)[20] and its monomeric Cu(II) complex (blue) after each compound was subjected to reduction at constant potentials of  $-0.827$  V (Onz) and  $-0.849$  V  $[\text{Cu(II)-Onz}]$  under de-aerated (Argon saturated) conditions;  $[\text{Onz}] = [\text{Cu(II)-Onz}] = 1 \times 10^{-4} \text{ mol dm}^{-3}$ . The black line indicates modification of calf thymus DNA in the absence of any sensitizer but subjected to a constant potential of  $-0.835$  V. (For interpretation of the references to colour in this figure legend, the reader is referred to the web version of this article.)

performed using guanine since addition of the complex to an aqueous solution of guanine turned it very faintly turbid suggesting an association of the two. We checked it several times to be sure this was happening. We even performed HPLC of an aqueous solution of  $1 \times 10^{-4}$  M guanine in the absence and presence of  $1 \times 10^{-5}$  M complex. For the solution that contained guanine and the complex, elution of guanine on a C-18 column was completely different from that obtained when guanine was alone, indicating an association of the two

compounds (Fig. S6, S I). Such a thing did not happen for the three other nucleic acid bases and the complex. Owing to this, the actual experiment keeping guanine in the immediate vicinity of electrochemically generated reduced species of the complex was not done.

Enhancement ratio (E R) for cytosine in presence of the complex (Table 1) tallies appreciably with that obtained for calf thymus DNA. Since in calf thymus DNA, percentage of guanine and cytosine is comparatively higher than adenine and thymine, it was concluded that this could be a reason why calf thymus DNA showed substantial damage in the presence of the complex in the experimental protocol used. The study also indicates that a prior knowledge on "damage causing ability of compounds" on nucleic acid bases help to predict their activity on different types of DNA used as target (based on their respective nucleic acid composition). If the target DNA is identified, then the type of organism having a certain DNA composition based on nucleic acid bases, that should be most vulnerable to such compounds may be realized. This study on Ornidazole and its Cu(II) complex provides a logical explanation as to why compounds chemically similar to the ones we studied in this work were found active on species having a substantial presence of guanine and cytosine (G C) in their DNA (details in S I) [32–35].

As mentioned earlier, inspite of decreased nitro-radical anion formation, Cu(II) complex of Onz was found to be better than Onz itself. This could be an attribute of complex formation i.e. an ability of Cu(II) in the complex to be active in redox pathway that generate radicals [36] capable of bringing about DNA double strand modification that could be detected by the methodology we followed (i. e. identifying DNA double strand modification by decrease in DNA-EtBr fluorescence) [24–26]. There is also the possibility of a physical interaction of the complex either with DNA or any other biomolecule, like the one we detected in this study for the nucleic acid base guanine, bringing about substantial changes on the target cell that eventually lead to cell death. Therefore, the outcome of the experiments performed with calf thymus DNA are not due to free radical reactions alone, other factors could very well be involved. Another aspect is the binding of the complex to DNA. Although we are yet to perform binding studies of this complex with DNA, similar complexes of Cu(II) with tinidazole were shown to possess strong binding affinity [12,13].

#### 4. Conclusion

A monomeric complex of Cu(II) with ornidazole was prepared and characterized. Electrochemical reduction of the complex at a constant potential using a glassy carbon electrode in aqueous solution results in formation of different reduction products that react with different nucleic acid bases and calf thymus DNA maintained in the solution. Degradation of nucleic acid bases following interaction with reduction products of the complex was monitored using HPLC while calf thymus DNA was determined by fluorescence using ethidium bromide. Results were then compared with a similar study performed earlier using ornidazole. This study as well as the one where ornidazole was used, indicate reduction products of both compounds [Ornidazole and its monomeric Cu(II) complex] modify guanine and cytosine (G and C) to a greater extent than adenine and thymine (A and T). In fact enhancement ratio for damage of guanine-cytosine by ornidazole and the complex matches appreciably with the observed enhancement ratio for calf thymus DNA (having a reasonably high G C content). In all cases, the complex performed better than ornidazole, attributed to the presence of Cu(II). This study helped us correlate the fact why 5-nitroimidazole based antibiotics were found effective on organisms having a high G C content in their DNA.

#### Declaration of Competing Interest

The authors declare that they have no known competing financial interests or personal relationships that could have appeared to influence the work reported in this paper.

## Acknowledgements

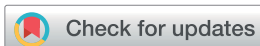
P N wishes to thank the Department of Science & Technology, New Delhi for a DST-INSPIRE Senior Research Fellowship. S D is grateful to the RUSA 2.0 programme of the Government of India operating at Jadavpur University for a project under the scheme "Research Support to Faculty Members" in the Research Thrust Area: Research in Sustainable Development having reference no. R-11/438/19 dated 30.05.2019. S D is grateful to UGC, New Delhi for funds received as part of research on "Advanced Materials", a part of UPE II, operating at Jadavpur University. SD is also grateful to the DST-PURSE program and the UGC-CAS program of the Government of India, operating at the Department of Chemistry, Jadavpur University for substantial financial support.

## Appendix A. Supplementary data

Supplementary data to this article can be found online at <https://doi.org/10.1016/j.ica.2019.119267>.

## References

- [1] E.J. Hall, R. Miller, M. Astro, F. Rini, *Br. J. Cancer Suppl.* 3 (1978) 120–123.
- [2] J.S. Mahood, R.L. Willson, *Br. J. Cancer* 43 (1981) 350–354.
- [3] R.P. Mason, *Free Radicals in Biology*, Academic Press, New York, 1982, pp. 161–222.
- [4] C.F. Chignell, *Environ. Health Persp.* 61 (1985) 133–137.
- [5] D.I. Edwards, *Comprehensive Medicinal Chemistry*, Pergamon Press Oxford, 1990, pp. 725–751.
- [6] D. Petrin, K. Delgaty, R. Bhatt, G. Garber, *Clin. Microbiol. Rev.* 11 (1998) 300–317.
- [7] S.L. Cudmore, K.L. Delgaty, S.F. Hayward-McClelland, D.P. Petrin, G.E. Garber, *Clin. Microbiol. Rev.* 17 (2004) 783–793.
- [8] S. Sood, A. Kapil, *Ind. J. Sex. Transm. Dis.* 29 (2008) 7–14.
- [9] M. Bonnet, C. R. Hong, W. W. Wong, L. P. Liew, A. Shome, J. Wang, Y. Gu, R. J. Stevenson, W. Qi, R. F. Anderson, F. B. Pruijn, W. R. Wilson, S. M. F. Jamieson, K. O. Hicks, M. P. Hay, *J. Med. Chem.*, 3 (61) pp. 1241–1254.
- [10] R. Sharma, *Current Radiopharmaceuticals* 4 (2011) 361–378; R. Sharma, *Current Radiopharmaceuticals* 4 (2011) 379–393.
- [11] J. Thulkar, A. Kriplani, N. Agarwal, *Ind. J. Pharmacol.* 44 (2012) 243–245.
- [12] R.C. Santra, K. Sengupta, R. Dey, T. Shireen, P. Das, P.S. Guin, K. Mukhopadhyay, S. Das, *J. Coordinat. Chem.* 67 (2014) 265–285.
- [13] R.C. Santra, D. Ganguly, J. Singh, K. Mukhopadhyay, S. Das, *Dalton Trans.* 44 (2015) 1992–2000.
- [14] R.C. Santra, D. Ganguly, D. Bhattacharya, P. Karmakar, A. Saha, S. Das, *New J. Chem.* 41 (2017) 11679–11685.
- [15] O. Kurt, N. Girginkardeşler, I.C. Balcioğlu, A. Ozbilgin, *U.Z. Ok, ClinMicrobiolInfect.* 14 (2008) 601–604.
- [16] B. Oren, E. Schgurensky, M. Ephros, I. Tamir, R. Raz, *Eur J. ClinMicrobiol. Infect. Dis.* 10 (1991) 963–965.
- [17] M. Castella, M. Malagolia, A.I. Ruberto, A. Baggio, C. Casolarib, C. Cermellib, M.R. Bossac, T. Rossid, F. Paoluccie, S. Roffiae, *J. Antimicrob. Chemother.* 40 (1997) 19–25.
- [18] J.A. Squella, S. Bollo, L.J. Núñez-Vergara, *Curr. Organ. Chem.* 9 (2005) 565–581.
- [19] P.C. Mandal, *J. Electroanal. Chem.* 570 (2004) 55–61.
- [20] P. Nandy, S. Das, *J. Ind. Chem. Soc.* 95 (2018) 1009–1014.
- [21] Mishra Gupta, et al., *J. Ind. Chem. Soc.* 90 (2013) 867.
- [22] A.J. Bard, L.R. Faulkner, *Electrochemical Methods: Fundamentals and Applications*, John Wiley & Sons Inc., New York, 2001.
- [23] S.A. Ozkan, Z. Senturk, I. Biryol, *Int. J. Pharmaceut.* 157 (1997) 137–144.
- [24] B. Mandal, H.K. Mondal, S. Das, *Biochem. Biophys. Res. Comm.* 515 (2019) 505–509.
- [25] A.R. Morgan, J.S. Lee, D.E. Pulleyblank, N.L. Murray, D.H. Evans, *Nucl. Acids Res.* 7 (1979) 547.
- [26] H.C. Birnboim, J.J. Jevcak, *Cancer Res.* 1981 (1889) 41.
- [27] S. Das, A. Saha, P.C. Mandal, *Environ. Health Persp.* 105 (1997) 1459.
- [28] A.C. Valderrama-Negrón, W.A. Alves, Á.S. Cruz, S.O. Rogero, D.O. Silva, *Inorg. Chim. Acta* 367 (2011) 85.
- [29] Z. Yu, E.R. Bernstein, *Jour. Chem. Phys.* 137 (2012) 114303.
- [30] I.R. Bairda, B.O. Patrick, K.A. Skov, B.R. James, *Canadian J. Chem.* 96 (2018) 299.
- [31] K. Nakamoto, *Infrared and Raman spectra of inorganic and coordination compounds*, 3rd ed., Wiley-Interscience, New York, USA, 1978.
- [32] Mark H. Wilcox, 147-Nitroimidazoles, Metronidazole, Ornidazole and Tinidazole; and Fidaxomicin, in: J. Cohen, W.G. Powderly, S.M. Opal (Eds.), *Infectious Diseases*, 4th, 2017 1261–1263.e1.
- [33] F.S. Lehmann, J. Drewe, L. Terracciano, C. Beglinger, *Aliment, Pharmacol. Ther.* 14 (2000) 305.
- [34] T.B. Gardner, D.R. Hill, *Clin. Microbiol. Rev.* 14 (2001) 114–128, <https://doi.org/10.1128/CMR.14.1.114-128.2001>.
- [35] L. Jokipii, A.M.M. Jokipii, *Gastroenterology* 83 (1982) 399.
- [36] Peter Wardman, *Environ. Health Persp.* 64 (1985) 309.


 Cite this: *RSC Adv.*, 2020, **10**, 23286

# A Zn<sup>II</sup> complex of ornidazole with decreased nitro radical anions that is still highly active on *Entamoeba histolytica*†

 Promita Nandy,<sup>a</sup> Soumen Singha,<sup>b</sup> Neha Banyal,<sup>c</sup> Sanjay Kumar,<sup>b</sup> Kasturi Mukhopadhyay <sup>c</sup> and Saurabh Das <sup>\*a</sup>

A monomeric complex of Zn<sup>II</sup> with ornidazole [Zn(Onz)<sub>2</sub>Cl<sub>2</sub>] decreases formation of the nitro-radical anion (R-NO<sub>2</sub><sup>•-</sup>), and this is realized by recording it in an enzyme assay using xanthine oxidase, which is a model nitro-reductase. Although the formation of R-NO<sub>2</sub><sup>•-</sup> is essential for drug action, as it is also associated with neurotoxic side effects, it is imperative to control its generation in order to avoid excess presence. With a decrease in R-NO<sub>2</sub><sup>•-</sup>, while the neurotoxic side effects should decrease, it can be expected that a compromise with regard to therapeutic efficacy will be seen since the complex will be less active in the free radical pathway. Since R-NO<sub>2</sub><sup>•-</sup> is crucial for the functioning of 5-nitroimidazoles, we attempted to find out if its biological activity is affected in any way in our effort to control its formation. For this purpose, *Entamoeba histolytica* (HM1:IMS Strain) was chosen as a biological target to realize the performance of the complex with respect to ornidazole (R-NO<sub>2</sub>). The experiments revealed that the complex not only compares well with ornidazole, but in fact, under longer exposure times, it also performs better than it. This efficacy of the complex was seen despite a decrease in R-NO<sub>2</sub><sup>•-</sup>, as identified by an enzyme assay, and this was probably due to certain attributes of the complex formation that are not known for ornidazole. These attributes outweigh any loss in efficacy in the free radical pathway following complex formation. This is certainly an advantage of complex formation and helps to improve the therapeutic index. This study has attempted to look at some of the possible reasons why the complex performs better than ornidazole. One reason is its ability to bind to DNA better than ornidazole does, and this can be understood by following the interaction of ornidazole and its Zn(II) complex with calf-thymus DNA using cyclic voltammetry. Therefore, this study showed that despite a decrease in R-NO<sub>2</sub><sup>•-</sup>, the complex does not compromise its efficacy, and this was examined using a biological target. In addition, the complex is likely to have less toxic side effects on the host of the disease-causing microbes.

 Received 20th March 2020  
 Accepted 27th May 2020

DOI: 10.1039/d0ra02597f

[rsc.li/rsc-advances](http://rsc.li/rsc-advances)

## 1. Introduction

5-Nitroimidazoles are important molecules with established efficacy and have been used to combat pathogenic microbes such as anaerobic bacterial and parasitic infections.<sup>1-4</sup> They are reductively activated in hypoxic cells, after which they undergo redox recycling or decompose to form products that are cytotoxic.<sup>1-4</sup> Over time, as more and more compounds in this family have been used, it was revealed that adverse drug reactions, neurotoxic side effects and drug resistance were some of the

challenges associated with these drugs that require attention.<sup>1-4</sup> 5-Nitroimidazoles are also potential radiosensitizers used in radiotherapy for cancers.<sup>5-8</sup> Metronidazole, tinidazole and ornidazole (Onz) are the three most important molecules of this family that have made their way to the clinics and are being used in a number of pharmaceutical preparations for different reasons.<sup>1-8</sup> Their efficacy is attributed to the generation of the nitro-radical anion (R-NO<sub>2</sub><sup>•-</sup>).<sup>1-10</sup> In order to tackle infections caused by parasites, these molecules are first reduced by the enzyme pyruvate ferredoxin oxidoreductase (PFOR) that acts as an electron sink.<sup>9,10</sup> Reduction of the nitro group prepares them for entry into cells by passive diffusion, creating a favorable concentration gradient.<sup>9,10</sup> After entering the target cells, the anti-microbial toxicity of 5-nitroimidazoles depends on the reduction of the nitro moiety to R-NO<sub>2</sub><sup>•-</sup> and other active species such as nitroso and hydroxylamine derivatives. R-NO<sub>2</sub><sup>•-</sup> binds to DNA, disrupting or breaking strands, leading to cell death.<sup>9,10</sup> As radiosensitizers, they interact with the radicals formed on DNA following the interaction of the latter with the

<sup>a</sup>Department of Chemistry (Inorganic Section), Jadavpur University, Kolkata – 700 032, India. E-mail: [dasrsv@yahoo.in](mailto:dasrsv@yahoo.in); Fax: +91 33 24146223; Tel: +91 8902087756

<sup>b</sup>Department of Physics, Jadavpur University, Kolkata – 700 032, India

<sup>c</sup>School of Environmental Sciences, Jawaharlal Nehru University, New Delhi – 110 067, India

† Electronic supplementary information (ESI) available. CCDC 1987809. For ESI and crystallographic data in CIF or other electronic format see DOI: 10.1039/d0ra02597f

products of the radiolysis of water, forming  $R\text{-NO}_2^{\cdot-}$ , which thereafter enhances strand unwinding or strand breaks.<sup>6–8</sup>

Unfortunately, the same  $R\text{-NO}_2^{\cdot-}$  ion is associated with the neurotoxic side effects, particularly when there is prolonged use of such molecules.<sup>9–11</sup> In such a situation, the aspects of neurotoxicity, or other forms of side effects, become a matter of concern, creating a need to control the generation of  $R\text{-NO}_2^{\cdot-}$ . Too much generation of these reactive intermediates for this class of drugs and others can often cause more harm than good.<sup>12–15</sup> Hence, generating the correct amount or making it available through slow chemical release is becoming an important aspect of research.<sup>10–15</sup> This study reports the regulation of  $R\text{-NO}_2^{\cdot-}$  for a specific cause, and this is achieved through the complex formation of one of the members of the 5-nitroimidazole family (ornidazole) with  $\text{Zn}^{\text{II}}$ , which can likely generate the correct amount necessary for cytotoxicity of a biological target (axenic *Entamoeba histolytica*). In addition, what the drug compromises for by forming less free radical species, ( $R\text{-NO}_2^{\cdot-}$ ), it makes up for by other attributes of complex formation. Previously, a  $\text{Zn}^{\text{II}}$  complex of metronidazole was also shown to be very active as an anticancer agent on a number of cancer cell lines.<sup>16</sup> Hence, such complexes of the 5-nitroimidazole family containing a relatively non-toxic metal ion ( $\text{Zn}^{\text{II}}$ ) might be useful cytotoxic agents against a number of diseases.

## 2. Experimental section

### 2.1 Materials and methods

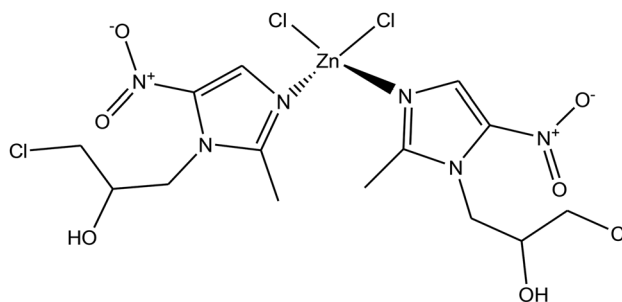
Ornidazole [purity (HPLC): >98.0%; melting point: 90.0 to 94.0 °C] was purchased from TCI, Japan. Zinc(II) chloride ( $\text{ZnCl}_2$ , assay (complexometric) 98.0–100.0%, melting point: 293 °C) was purchased from E. Merck, India. Xanthine oxidase (XOD) isolated from cows' milk was obtained as a suspension in ammonium sulphate solution from Sigma Aldrich. Hypoxanthine and calf-thymus DNA were purchased from Sisco Research Laboratories, India. Calf-thymus DNA was dissolved in triple-distilled water using proper electrolytes. Its concentration was determined in terms of nucleotides, taking  $\epsilon_{260} = 6600 \text{ mol}^{-1} \text{ dm}^3 \text{ cm}^{-1}$ . Tris buffer solution (Spectrochem Pvt. Ltd., India) and NaCl (AR, Merck, Germany) were used to maintain physiological conditions.

**2.1.1 Synthesis of a monomeric complex of ornidazole with  $\text{Zn}^{\text{II}}$ .** A solution of ornidazole (0.8785 g in 25 mL, 4 mmol) in methanol was added to a solution of  $\text{ZnCl}_2$  (0.2725 g in 25 mL, 2 mmol) in methanol. The mixture was warmed under reflux to a temperature of 60 °C for 6 hours. After a week, a white crystalline compound was obtained by very slow evaporation of the solvent. The solvent was filtered and the solid mass was collected. The filtered product was re-crystallized using a 1 : 1 aqueous-methanol mixture. This was done three times. A pure complex was obtained. Elemental analysis was performed on a PerkinElmer 2400 Series-II CHN analyzer. Analysis: calc. (%) for  $\text{C}_{14}\text{H}_{20}\text{Cl}_4\text{N}_6\text{O}_6\text{Zn}$ , C: 29.21; H: 3.50; N: 14.61. Found: C: 29.12; H: 3.26; N: 15.22.

**2.1.2 Solution of the structure of the complex by refinement from X-ray powder diffraction data.** Powder X-ray diffraction (PXRD) data were collected at ambient temperature

(25 °C) on a Bruker D8 Advance diffractometer operating in reflection mode with  $\text{Cu K}\alpha_1$  radiation of wavelength 1.540562 Å. The generator was set at 40 kV and 40 mA. The data was collected in the  $2\theta$  range of 4–60° with a 0.02° step size and a 5 s per step.

Indexing and Pawley refinement of the PXRD pattern of the complex was carried out using the Reflex module of Material Studio.<sup>17</sup> The PXRD pattern was indexed by the TREOR 90 program<sup>18</sup> for the first 20 peaks. Indexing revealed that the complex crystallizes in an orthorhombic system with  $a = 10.411(2)$  Å,  $b = 7.759(2)$  Å and  $c = 27.730(1)$  Å. Pawley refinements<sup>19</sup> were performed in the  $2\theta$  range of 5–60° on the unit cell. Peak profiles, zero-shift, background and unit-cell parameters were refined simultaneously. Peak profiles were refined by the pseudo-Voigt function with Berar–Baldinozzi asymmetry correction parameters. The background was refined using a 20th-order polynomial. Refinement yields of  $R_p = 6.38\%$  and  $R_{wp} = 4.52\%$  were determined. Statistical analysis gave  $Pna2_1$  (33) as the most likely space group.



**An initial probable structure of the prepared complex.**

Firstly, an initial molecular structure was drawn using ACD/ChemSketch (shown above) and its geometry was optimized with the help of MOPAC2016 to obtain a reference structural model for the reflex powder solve module. This initial structure (model), consisting of two Onz complexes as ligands, one  $\text{Zn}^{\text{II}}$  ion and two  $\text{Cl}^-$  ions, was then imported into the new cell. After assigning motion groups to different fragments, the structure was solved to represent an approximate structure of the complex.

Next, a Rietveld refinement was carried out in order to obtain the final structure using the Reflex Powder Refinement module of Material Studio. To improve the agreement between the calculated and experimental powder diffraction patterns, different parameters such as pseudo-Voigt profile parameters, background parameters, cell constants, zero point of diffraction pattern, position and orientation of motion groups, dihedral angles within the Onz moieties, Berar–Baldinozzi asymmetry correction parameters and March–Dollase preferred orientation correction parameters were optimized step-by-step until the best agreement between the calculated and experimental powder diffraction patterns emerged (Fig. 1).

Thermal parameters were set as the global isotropic atom displacement parameters and were refined thereafter. The final  $R$ -factors of  $R_p = 6.58\%$  and  $R_{wp} = 8.99\%$  were obtained using the following unit cell parameters: space group =  $Pna2_1$ ,

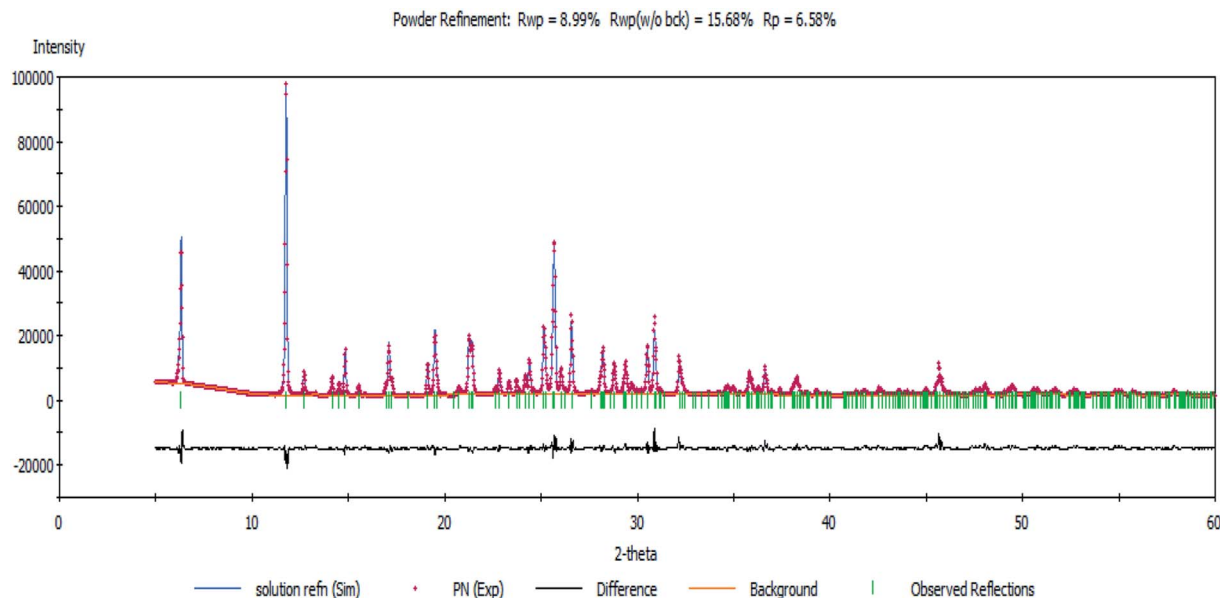


Fig. 1 The Rietveld refinement plot showing an agreement between the calculated and measured X-ray powder diffractograms of the complex.

$a = 10.407(7)$  Å,  $b = 7.756(5)$  Å,  $c = 27.725(5)$  Å and  $V = 2238.20(5)$  Å<sup>3</sup>. The crystal data is summarized in Table 1. The CSD number of our inorganic structure is 1987809.

## 2.2 Physical measurements

The UV-vis spectrum of  $Zn(Onz)_2Cl_2$  was recorded on a JASCO V-630 spectrophotometer, JASCO, Japan. FTIR of the solid sample on a KBr pellet was recorded on a PerkinElmer RX-I spectrophotometer. Elemental analysis of the complex was carried out on a PerkinElmer 2400 Series-II CHN analyzer.

## 2.3 Enzyme assay

The method used xanthine oxidase (XOD) as a model nitroreductase.<sup>10,11,20</sup> Hypoxanthine was the reducing substrate,

while Onz and the  $Zn^{II}$  complex were electron acceptors. 225  $\mu$ L of an XOD suspension was diluted to 1.5 mL with 0.025 M phosphate buffer (pH 7.4) in a quartz cuvette that was sealed with a rubber septum. Oxygen was purged out by passing argon gas through the solution. The enzyme (XOD), with a specific activity of 0.3 units per mg of protein, contained  $\sim$ 10 units in 1.5 mL. In another quartz cuvette, 1.0 mL hypoxanthine (0.01 M) in 0.1 M phosphate buffer ( $\sim$ pH 7.4) was taken, along with 125  $\mu$ L of 1600  $\mu$ M Onz, and the complex was dissolved in DMF. The volume was made up to 2.0 mL with the help of phosphate buffer (0.1 M). The cuvette was sealed with a rubber septum and oxygen was purged out by passing argon gas through the solution. To initiate the reaction, 500  $\mu$ L of deoxygenated enzyme solution that was kept in another cuvette was added with the help of a gas-tight syringe to the degassed solution containing hypoxanthine and the test compounds. The final assay solution (2.5 mL) had 0.2 units per mL of XOD, 80  $\mu$ M of Onz or its complex and 4 mM of hypoxanthine. The cuvette was inverted to mix and was monitored using UV-vis spectroscopy against a buffer-DMF blank. A spectrum of the solution was taken every 5 minutes for 2 hours during the assay. A change in absorbance at 320 nm was noted for Onz and for the complex.

Table 1 Summary of the crystal data structural refinement results of the complex<sup>a</sup>

Formula	$C_{14}H_{20}Cl_4N_6O_6Zn$
Molecular weight (g)	575.55
Absorption coefficient ( $\mu$ ) ( $mm^{-1}$ )	1.619
Crystal system	Orthorhombic
Space group, $Z$	$Pna2_1, 4$
$a$ (Å)	10.407(7)
$b$ (Å)	7.756(5)
$c$ (Å)	27.725(5)
$V$ (Å <sup>3</sup> )	2238.20(5)
$T$ (K)	298
Wavelength (Å)	1.540562
$\theta$ range used for refinement ( $^\circ$ )	5–60
Reliability factors	$R_p = 0.0658$ $R_{wp} = 0.0899$

$$^a R_p = \frac{\sum |cY^{sim}(2\theta_i) - I^{exp}(2\theta_i) + Y^{back}(2\theta_i)|}{\sum |I^{exp}(2\theta_i)|}, R_{wp} = \left\{ \frac{\sum [cY^{sim}(2\theta_i) - I^{exp}(2\theta_i) + Y^{back}(2\theta_i)]^2 / \sum w_p [I^{exp}(2\theta_i)]^2}{\sum w_p [I^{exp}(2\theta_i)]^2} \right\}^{1/2}, \text{ and } w_p = 1 / I^{exp}(2\theta_i), R_1 = \frac{\sum |F_o| - |F_c|}{\sum |F_o|}, wR_2 = \left[ \frac{\sum w(F_o^2 - F_c^2)^2}{\sum w(F_o^2)^2} \right]^{1/2}.$$

## 2.4 Cyclic voltammetry

Cyclic voltammetry (CV) experiments were carried out on a Metrohm Autolab electrochemical analyzer. A conventional three-electrode system was used, consisting of glassy carbon as the working electrode, a platinum wire as the counter electrode and Ag/AgCl in satd KCl as the reference electrode. Reduction of the nitro group in Onz and its  $Zn^{II}$  complex was followed.<sup>21–26</sup> Before performing cyclic voltammetry on an experimental solution, it was very carefully degassed for 30 min using high-purity Ar. The results were analyzed according to the Randles-Sevcik equation [eqn (1)].<sup>27,28</sup>

$$i_{pc} = (2.69 \times 10^5) n^{3/2} D_0^{1/2} A C \nu^{1/2} \quad (1)$$

$i_{pc}$  refers to the current in amperes at the cathodic peak potential,  $n$  denotes the total number of electrons involved in the electrochemical reduction,  $D_0$  is the diffusion coefficient of the species,  $A$  denotes the area of the electrode in  $\text{cm}^2$ ,  $C$  is the concentration of the substance in  $\text{moles cm}^{-3}$  and  $\nu$  is the scan rate in  $\text{V s}^{-1}$ .

## 2.5 DNA binding

Although the complex has absorption at 320 nm, its interaction with DNA was not tracked at that wavelength since DNA has a  $\lambda_{\text{max}}$  at 260 nm, and the tail of its absorbance peak extends up to 310 nm, which would therefore interfere with the absorbance of the complex. This, in turn, could affect the correct determination of the change in absorbance, upon which a titration of the complex with calf-thymus DNA, leading to the evaluation of a binding constant, is based.<sup>10,11,29</sup> Hence, cyclic voltammetry was used to study DNA interaction following a reduction of the nitro group of Onz that is present as a ligand in the complex.<sup>10,11,29–32</sup> A 30 mL solution containing the complex (100  $\mu\text{M}$ ) was used. Calf-thymus DNA was gradually added to the solution and cyclic voltammetry was performed. 20 mM Tris buffer and 120 mM NaCl were used to maintain the pH and ionic strength of the medium, respectively, during the titration. The change in current ( $\Delta I$ ) served as a measure of the extent to which the complex interacts with the calf-thymus DNA. The change in current ( $\Delta I$ ) was subsequently used in standard equations (ESI<sup>†</sup>), yielding values for the binding constant and the site size of interaction.<sup>10,11,29–32</sup> Glassy carbon was used as the working electrode while a platinum wire and Ag/AgCl, satd KCl were used as the counter and reference electrodes, respectively. The experimental solution was degassed for 15 minutes after every addition of DNA, using high-purity Ar. Voltammograms were recorded at a scan rate of 100  $\text{mV s}^{-1}$ .

In the medium used,  $\text{Zn}(\text{Onz})_2\text{Cl}_2$  undergoes reduction at  $-945$  mV. As the concentration of the calf-thymus DNA was gradually increased, the peak current due to the complex gradually decreased. Based on the change in peak current ( $\Delta I$ ), binding constant values were evaluated considering the equilibrium in eqn (2) where  $K_d$  denotes the dissociation constant related to the process.

$$\text{L} + \text{DNA} = \text{L} - \text{DNA}; K_d = \frac{[\text{L}][\text{DNA}]}{[\text{L} - \text{DNA}]} \quad (2)$$

For the complex,  $[\text{Zn}(\text{Onz})_2\text{Cl}_2]$ , a decrease in peak current during the titration is a consequence of structural changes following the binding of the complex to DNA that gradually disables nitro groups from showing a response in cyclic voltammetry results, and this was therefore followed for the evaluation of the binding constant.<sup>10,11,29–32</sup>

## 2.6 Biological assay on an amoeba strain

Axenic *Entamoeba histolytica* strain HM1:IMSS was maintained and grown in TYIS-33 medium supplemented with 15% adult

bovine serum, 1 $\times$  diamond vitamin mix and antibiotics (0.3 units per mL penicillin and 0.25  $\text{mg mL}^{-1}$  streptomycin) at 35.5 °C. The cells were sub-cultured twice a week.<sup>33</sup> *Entamoeba* cells were taken from the log phase and an *in vitro* drug sensitivity assay was carried out for 24 hours and 48 hours, respectively.<sup>34</sup>

An *in vitro* sensitivity assay was carried out on a 96 micro-titre plate following a protocol described previously.<sup>34</sup> Briefly, stock solutions (10 mM) of different compounds were prepared in DMSO and further diluted with their respective media to obtain the desired concentration. These were added to the well of a micro-titre plate, in triplicate. Strain HM1:IMSS was harvested at the log phase and pelleted at 600 g for 5 min and then a cell suspension was made. Cells were counted using a haemocytometer. Equal volumes of the cell suspension of the axenic strain HM1:IMSS were added to wells containing different compounds so that the total number of trophozoites per well was  $3 \times 10^5$ . Final compound concentrations in the rows down the plate were 200, 100, 50, 25, 12.5, 6.25, and 3.125  $\mu\text{M}$ , respectively. Appropriate controls in triplicate were included in each plate with DMSO,  $\text{ZnCl}_2$  and non-treated media (allowing for 100% growth). Subsequently, the micro-titre plate was placed in an incubation bag with an aerocult mini sachet to maintain an anaerobic atmosphere. The incubation bag was sealed and placed in an incubator where the temperature was 35 °C.

Cell growth was monitored on a daily basis at 24 hours and 48 hours by comparing the compound contained in the wells with the controls in same rows using an inverted microscope. Plates were properly examined and each well was scored according to its well coverage, cell mobility, and cell rounding. + was given to 30% well coverage area with rounded cells and ++++ for fully covered wells with pseudopodal movement. MIC was considered as the lowest concentration of a compound where a score of + could be given.

An *in vitro* compound susceptibility (Trypan blue) assay was carried out where  $3 \times 10^5$  trophozoite was added in 3 replicate wells containing previously diluted different concentrations of compounds. A non-treated control (100% growth) was included in each plate. Culture plates were sealed and incubated for 24 hours and 48 hours, respectively, at 37 °C. Trophozoite growth was determined after 24 hours and 48 hours by counting with a microscope using a 0.4% trypan blue assay.<sup>35</sup>

## 3. Results and discussions

### 3.1 Characterization of the complex

**3.1.1 Crystal structure from powder X-ray diffraction data.** Structural analysis revealed that the complex crystallizes in an achiral  $Pna2_1$  space group belonging to the orthorhombic system and that it has cell dimensions of  $a = 10.407(7)$  Å,  $b = 7.756(5)$  Å, and  $c = 27.725(5)$  Å. The asymmetric unit of the complex consists of one  $\text{Zn}^{2+}$  ion, two Onz moieties and two  $\text{Cl}^-$  ions. An ORTEP diagram is shown in Fig. 2. The metal center exhibits a four-coordinated slightly distorted tetrahedral geometry. The two N atoms (N9 and N29) of two different Onz moieties and two  $\text{Cl}^-$  ions (Cl2 and Cl22) occupy the four

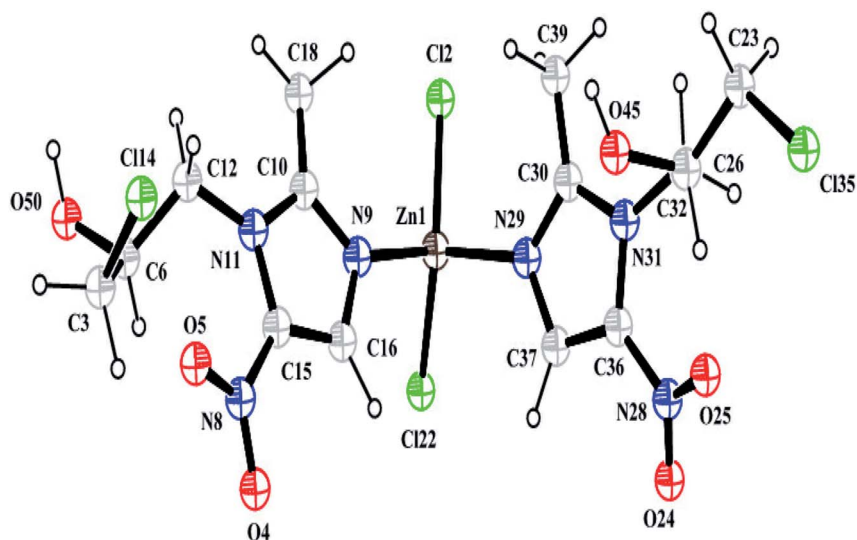


Fig. 2 A perspective view of the complex.

corners of a tetrahedron surrounding the  $\text{Zn}^{2+}$  ion. Zn–N bond distances were  $\sim 2.017$  Å, while Zn–Cl bond distances were  $\sim 2.239$  Å. Two imidazole nitrogen atoms of two different Onz moieties bind to the metal center in a syn–syn fashion. Some of the coordinated bond distances and bond angles are listed in Table 2.

**3.1.2 UV-vis spectroscopy of ornidazole and its  $\text{Zn}^{\text{II}}$  complex in different solvents.** Ornidazole and  $\text{Zn}(\text{Onz})_2\text{Cl}_2$  were dissolved in different solvents (acetonitrile, DMF, methanol and water) with concentrations of  $10^{-4}$  M. The absorption spectra of Onz and of the complex showed a strong response in the UV region from 260 nm to 320 nm (Fig. S1 and S2 in the ESI†, respectively). Absorption bands were similar (Table 3) and can be assigned to the intra-ligand charge transfer.

**3.1.3 Analysis of the IR spectra of ornidazole and its monomeric  $\text{Zn}^{\text{II}}$  complex.** The IR spectrum of Onz (Fig. S3 in the ESI†) shows a band at  $1538.21$   $\text{cm}^{-1}$ , which can be assigned to the  $\nu_{\text{C}=\text{N}}$  stretching vibration of the imidazole ring that shifts to

a higher wavenumber ( $1565.80$   $\text{cm}^{-1}$ ) in  $\text{Zn}(\text{Onz})_2\text{Cl}_2$  (Fig. S4 in the ESI†), suggesting coordination of  $\text{Zn}^{\text{II}}$  by the imidazole nitrogen. Two  $\text{NO}_2$  stretching vibrations,  $\nu_{\text{as}}$   $1482$   $\text{cm}^{-1}$  and  $\nu_{\text{s}}$   $1380$   $\text{cm}^{-1}$ , in the complex were similar to those in Onz, indicating that  $-\text{NO}_2$  does not participate in coordination of the metal center (Table S1 in the ESI†).<sup>36</sup>

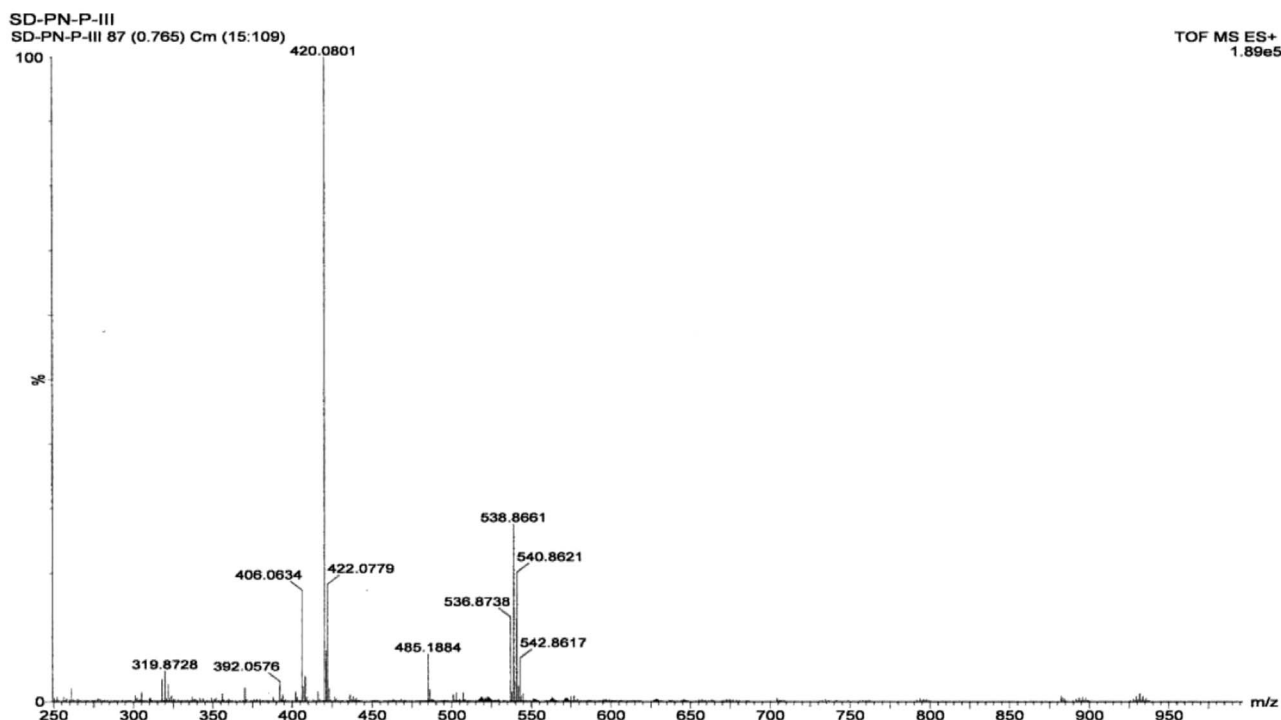
**3.1.4 Mass spectrometry of the complex.** PXRD data, showing the structure of the complex, suggest that its molecular formula is  $\text{Zn}(\text{Onz})_2\text{Cl}_2$ . Hence, a molecular ion peak in the mass spectrum should be found in the range from  $m/z = 572$  to  $m/z = 584$  (considering isotope effects due to Cl present in ornidazole, Cl present in the coordination zone around the metal ion and due to isotope effects for Zn; details in the ESI†). However, the molecular ion peak, which was expected in the above mentioned region, was not seen in Fig. 3, although indications that were not very prominent were seen in the region, suggesting that the molecular ion was not very stable to the electrospray stimuli. A cluster of peaks were obtained at  $m/z$  values of 536.8239, 538.8197, 540.8192 and 542.8129 that may be attributed to a species formed from the complex following the loss of a Cl atom coordinated to Zn (likely peaks are shown in the ESI† based on isotopic distribution). Only those peaks for which the relative abundance of isotopes is high were actually found, and not all possibilities are indicated in the ESI†. The peak at  $m/z = 485.1884$  can be attributed to the formation of a fragment from the loss of two Cl atoms from the coordination sphere and an  $-\text{OH}$  group from an ornidazole moiety present as a ligand in the complex (details in the ESI†). Prominent experimental peaks with  $m/z$  values of 420.0368 and 422.0334 were also detected in the mass spectrum and were assigned to a fragment formed from the molecular ion where  $-\text{CH}_3$  and  $-\text{NO}_2$  depart from each Onz moiety, along with the loss of a Cl atom from either of the two Onz moieties in the complex ( $m/z_{\text{theo}}$  ranges from 420 to 424; possibilities for such a fragment are shown in the ESI†).

Table 2 Some selected bond lengths (Å) and bond angles ( $^\circ$ ) of the complex

Zn1–Cl2	2.238(7)	Zn1–Cl22	2.238(5)	Zn1–N9	2.017(2)
Zn1–N29	2.017(3)	Cl14–C3	1.779(7)	Cl35–C23	1.779(9)
C26–C32	1.549(3)	C3–C6	1.533(9)	C6–C12	1.549(4)
C10–C18	1.470(7)	C15–C16	1.408(9)	C23–C26	1.533(9)
O45–C26	1.417(4)	O50–C6	1.417(5)	N31–C32	1.470(6)
Cl2–Zn1–Cl22	134.95	O50–C6–C3	108.88		
Cl2–Zn1–N9	106.13	O50–C6–C12	111.68		
Cl2–Zn1–N29	98.84	C3–C6–C12	110.57		
Cl22–Zn1–N9	98.90	Cl22–Zn1–N29	106.16		
N9–Zn1–N29	111.32	N11–C12–C6	111.25		
Cl35–C23–C26	108.88	O45–C26–C23	108.89		
O45–C26–C32	11.68	C23–C26–C32	110.56		
N31–C32–C26	111.25	Cl14–C3–C6	108.89		

Table 3 Absorption of ornidazole and Zn<sup>II</sup>-ornidazole in different solvents

Compound	Acetonitrile		DMF		Methanol		Water	
	$\lambda_{\max}$ (nm)	Absorption intensity						
Onz	320	0.9335	324	1.0638	312	0.9519	318	1.2287
Zn(Onz) <sub>2</sub> Cl <sub>2</sub>	318	1.7287	324	1.2643	310	1.5615	320	1.1576

Fig. 3 Mass spectrum of the Zn(Onz)<sub>2</sub>Cl<sub>2</sub> complex.

**3.1.5 Cyclic voltammetry studies.** Cyclic voltammetry of Zn(Onz)<sub>2</sub>Cl<sub>2</sub> (Fig. S5†) and of Onz (Fig. S6†) were performed; the former in aqueous-methanol and in pure aqueous solution, while the latter was carried out in aqueous solution at a scan rate of 0.1 V s<sup>-1</sup>. The complex showing a peak at -0.925 V against Ag/AgCl, satd KCl [Fig. S5†] was assigned to the reduction of the -NO<sub>2</sub> moiety in Onz. A cyclic voltammogram of Onz alone (Fig. S6†) showed a peak at -0.827 V. Voltammograms for the reduction of the nitro group in the complex were obtained at other scan rates as well. *i*<sub>pc</sub> was plotted against the square root of the scan rate using the Randles-Sevcik equation [Fig. S7†]. A straight line passing through the origin suggested that the complex undergoes reduction in a diffusion-controlled pathway and that there is no adsorption on the electrode surface.

In aprotic media, 5-nitroimidazoles undergo reversible one-electron reduction to form the nitro radical anion (R-NO<sub>2</sub><sup>•-</sup>). This is then followed by a three-electron reduction to hydroxylamine derivatives. For most 5-nitroimidazoles, the first step is reversible whilst the second step is not reversible, and this can be seen from studies on metronidazole (eqn (3) and (4)).<sup>26</sup> In aqueous solution, the two steps cannot be carried out separately

and a single-step four-electron reduction is observed (eqn (5)).<sup>26,37</sup>



### 3.2 Binding of the complex to DNA

Zn(Onz)<sub>2</sub>Cl<sub>2</sub> was titrated with calf-thymus DNA under physiological conditions using cyclic voltammetry. The reduction peak of the complex, identified at -0.925 V (against Ag/AgCl, satd KCl), was used to follow the titration. Upon addition of the calf-thymus DNA, the cathodic peak current (*i*<sub>pc</sub>) gradually decreased with a shift to a more negative potential (Fig. 4). This shift to a more negative potential indicated that there is an interaction between the complex and the DNA. As more DNA is added, it becomes increasingly difficult for the complex to show a response in cyclic voltammetry (indicated by a shift to more

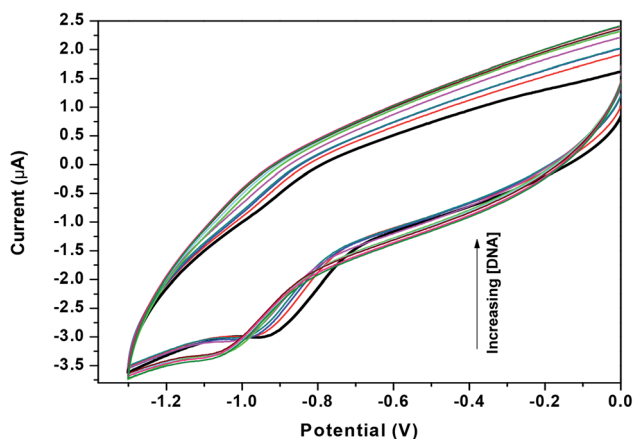


Fig. 4 Cyclic voltammograms for  $\text{Zn}(\text{Onz})_2\text{Cl}_2$  in the absence (dark black line) and presence of different concentrations of calf-thymus DNA.  $[\text{Zn}(\text{Onz})_2\text{Cl}_2] = 100 \mu\text{M}$ ;  $[\text{NaCl}] = 120 \text{ mM}$ ;  $\text{pH} = 7.4$ ;  $T = 301 \text{ K}$ .

negative potential), as the complex becomes progressively bound to the DNA.<sup>27</sup>

As previously mentioned, binding of the complex to DNA results in the redox active nitro groups on both Onz ligands to gradually lose their ability to show a response in the cyclic voltammetry tests. Therefore, this gradual decrease in peak current could be used as a measure of the extent of interaction between the complex and calf-thymus DNA. Apparent binding constant ( $K_{\text{app}}$ ) values were evaluated from a linear plot (eqn (S3) in the ESI<sup>†</sup>) and also from non-linear square fit analysis results (eqn (S5) in the ESI<sup>†</sup>). The results are shown in Fig. 5 and Table 4.<sup>10–12,29–32</sup>

Another important parameter for binding to DNA is the site size of interaction ( $n_b$ ). This provides an estimate of the number of nucleotides that are bound to the material during the interaction. This value was 2 for  $\text{Zn}(\text{Onz})_2\text{Cl}_2$  binding to DNA, and this could be calculated from the molar ratio plot (inset of Fig. 5B). Since  $K_{\text{app}}$  provides the binding constant value of a substance binding to an isolated site, an overall binding constant ( $K^*$ ) can be obtained by multiplying  $K_{\text{app}}$  with the site size of interaction ( $n_b$ ).<sup>38</sup> These values are provided in Table 4. The binding constant values for  $\text{Zn}(\text{Onz})_2\text{Cl}_2$  were higher than

for Onz (determined earlier),<sup>10</sup> indicating that this is an attribute of complex formation. The site size of interaction ( $n_b$ ) of Onz (reported earlier)<sup>10</sup> was in the range of 1.39 to 1.5, while that of the monomeric  $\text{Zn}^{\text{II}}$  complex was found in the range from 1.85 to 2 (from two different methods of analysis), suggesting that the complex with two Onz ligands bound to  $\text{Zn}^{\text{II}}$  might be involved in two types of interaction with the DNA. In one interaction, the complex interacts in the same manner as free Onz does, *i.e.* one of the two Onz ligands bound to  $\text{Zn}^{\text{II}}$  in the complex interacts with the DNA while the other does not. In the other mode, both Onz ligands bound to  $\text{Zn}^{\text{II}}$  interact with the DNA. Hence, the values obtained for the site size of interaction during the experiments were intermediate between the two values obtained. While the inset of Fig. 5B (the molar ratio plot) provides a value of 2.0, Fig. 5C (the modified Scatchard plot) provides a value of 1.85. This may be explained by the obtained values between 1.5 (if one Onz ligand interacts with DNA) and 3.0 (if both Onz ligands interact), based on our earlier findings with Onz itself interacting with calf-thymus DNA.<sup>10</sup>

### 3.3 Enzyme assay

Xanthine oxidase catalyzes the oxidation of hypoxanthine to xanthine and then to uric acid in the presence of oxygen. Under anaerobic conditions, this action does not occur as there is no substrate to accept the electrons. Therefore, under anaerobic conditions (*i.e.* in the absence of oxygen) if an electron acceptor molecule is present in the system, the above oxidation of hypoxanthine to xanthine and to uric acid becomes possible. Nitroimidazoles are good electron acceptors and so can participate in the above reaction, forming the nitro radical anion ( $\text{RNO}_2^{\cdot-}$ ). Therefore, it can be seen that, using an enzyme assay, the ability of 5-nitroimidazoles and their modified forms to reduce and to know whether the nitro-radical anion generated is stable for enough time to cause a change in absorbance of the compound on which it is formed, can be recorded as a gradual decrease in absorbance. In contrast, if  $\text{RNO}_2^{\cdot-}$  does not form or if its generation is not stable for long, *i.e.* it can revert back to its original form (the nitro group) by any pathway, it can be inferred that there is a decrease in the formation of  $\text{RNO}_2^{\cdot-}$ , leading to either almost no decrease in absorbance of the original

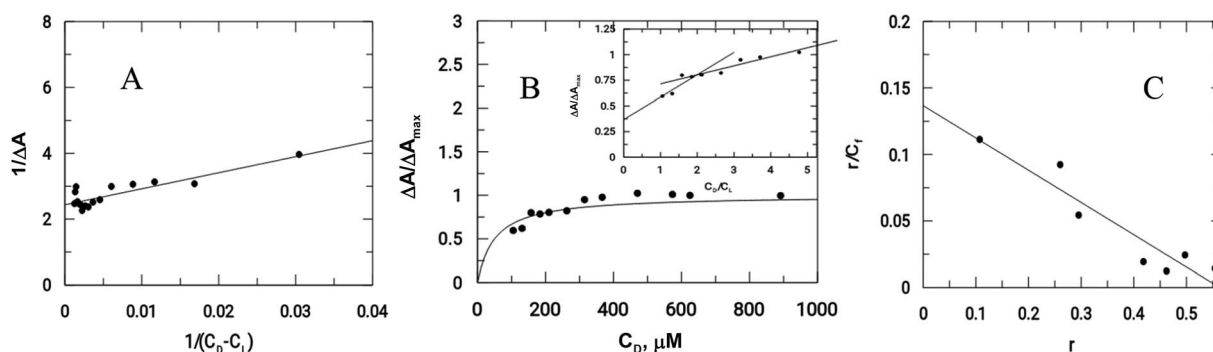


Fig. 5 Interaction of calf-thymus DNA with  $\text{Zn}(\text{Onz})_2\text{Cl}_2$ . (A) Double reciprocal plot, (B) non-linear plot, (C) Scatchard plot;  $[\text{Zn}(\text{Onz})_2\text{Cl}_2] = 100 \mu\text{M}$ ;  $[\text{NaCl}] = 120 \text{ mM}$ ;  $\text{pH} = 7.4$ ;  $\text{Temp.} = 28 \text{ }^\circ\text{C}$ .



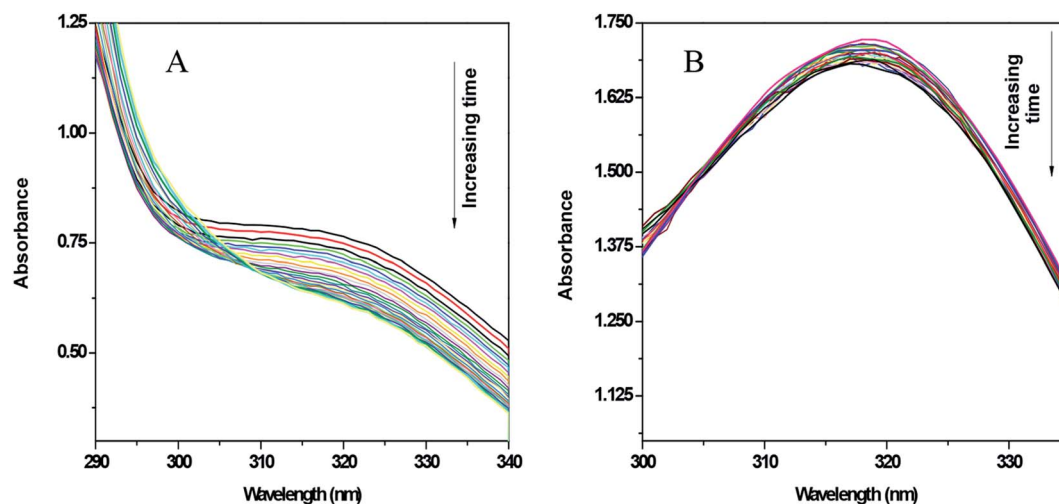


Fig. 6 UV-vis spectra of Onz (A) and  $\text{Zn}(\text{Onz})_2\text{Cl}_2$  (B) in the presence of hypoxanthine in 5% DMF and xanthine oxidase. Spectra of each compound were taken at intervals of 5 minutes for 2 hours. Enzyme activity = 0.2 units per mL in XOD and compound concentration = 80  $\mu\text{M}$ .

in the free radical pathway). Even if we do not consider the data recorded at 48 hours, which is clearly beneficial, and just compare the data recorded at 24 hours, we see the complex is better than Onz, as it has a similar MIC value but added benefits with regard to the toxic side effects, since it generates less  $\text{R-NO}_2^-$ . The complex therefore makes up for any compromise it

makes in the free radical pathway by other attributes of complex formation, one of which could be its strong binding affinity for DNA, leading to cell death in disease-causing microbes. The other advantage of complex formation, enabling it to perform much better at longer exposure times (48 hours), could be its effective cellular uptake due to the presence of a metal ion in the complex.<sup>39</sup>

In an earlier study, we showed that a  $\text{Cu}^{\text{II}}$  complex of an azo-based ligand performed much better on a particular cell line than the ligand itself, and that this was essentially due to effective cellular uptake of the complex (in that case all attributes required for good performance were in fact similar for the complex and the azo compound forming the complex), suggesting that effective cellular uptake is an essential criteria and can make a difference in performance.<sup>39</sup> Likewise, in this study of  $\text{Zn}(\text{Onz})_2\text{Cl}_2$ , the fact that it performs better at longer exposure times (48 hours) could mean that it enters cells of disease-causing microbes much better than Onz alone. The study also showed that both Onz and its  $\text{Zn}^{\text{II}}$  complex diminished the viability of *Entamoeba histolytica* in a concentration dependent manner.

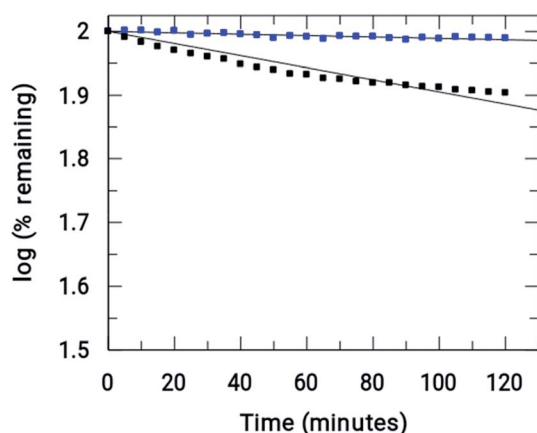


Fig. 7 Comparison of the rate of reductions of Onz (■) and  $[\text{Zn}(\text{Onz})_2\text{Cl}_2]$  (■) under anaerobic conditions. (initial concentrations = 0.2  $\text{U mL}^{-1}$  in XOD, 80  $\mu\text{M}$  in Onz or  $\text{Zn}(\text{Onz})_2\text{Cl}_2$  in the mixture, 4 mM in hypoxanthine and 5% in DMF).

Table 5 MIC values for ornidazole and  $\text{Zn}(\text{Onz})_2\text{Cl}_2$  when applied to *Entamoeba histolytica* (HM1:IMS Strain)

Compound	MIC after 24 h	MIC after 48 h
Ornidazole	12.5 $\mu\text{M}$	12.5 $\mu\text{M}$
$\text{Zn}(\text{Onz})_2\text{Cl}_2$	12.5 $\mu\text{M}$	6.25 $\mu\text{M}$
$\text{ZnCl}_2$	>100 $\mu\text{M}$	>100 $\mu\text{M}$
DMSO	>100 $\mu\text{M}$	>100 $\mu\text{M}$

## 4. Conclusions

Despite a significant decrease in the formation of the nitro radical anion in  $\text{Zn}(\text{Onz})_2\text{Cl}_2$ , this study showed that there was comparable biological activity of Onz and the monomeric  $\text{Zn}^{\text{II}}$  complex on *Entamoeba histolytica* (HM1:IMS Strain) when incubated for 24 hours. After 48 hours of incubation, the complex performed better than Onz. This indicates that either the nitro radical anion generated by the complex is sufficient for cytotoxic activity on the chosen biological target or, if a compromise is made by the complex in the free radical pathway following a decrease in nitro-radical anion formation, that the cytotoxic activity is unaffected, implying that the complex makes up for the loss in efficacy in the free radical pathway by other attributes of complex formation. Consequently, association of  $\text{Zn}^{\text{II}}$  with Onz is useful as it not only

maintains the efficacy of Onz but, by decreasing  $R-NO_2^{\cdot-}$ , it also helps to overcome the associated neurotoxic side effects of Onz. The study also suggests avoiding too much generation of  $R-NO_2^{\cdot-}$ , since the amount is probably in excess of what is required for cytotoxicity and, if left unattended in the system, it results in toxic side effects. Therefore, if a complex like  $Zn(Onz)_2Cl_2$  is used instead of Onz, there will be no compromise in cytotoxic activity, but there could be a significant decrease in toxic side effects associated with Onz. This could be a tremendous benefit in the use of 5-nitroimidazoles and their derivatives.

## Conflicts of interest

There are no conflicts to declare.

## Abbreviations

Onz or R-	Ornidazole
$NO_2^{\cdot-}$	
CV	Cyclic voltammetry
MIC	Minimum inhibitory concentration
$R-NO_2^{\cdot-}$	Denotes the nitro radical anion formed either on an ornidazole moiety or on an ornidazole bound to $Zn(II)$ in the complex

## Acknowledgements

PN and SS wish to thank the Department of Science & Technology, New Delhi for DST-INSPIRE Senior Research Fellowships. NB acknowledges UGC for her non-NET fellowship. SD wishes to thank the "RUSA 2.0" program of the Government of India operating at Jadavpur University, in which he received "Research Support to Faculty Members" in the thrust area "Research in Sustainable Development" (Sanction Ref. no. R-11/438/19 dated 30.05.2019). SD is grateful to the DST-FIST program of the Government of India for providing funds for the purchase of the powder X-ray diffractometer in the Department of Chemistry, Jadavpur University. He is also grateful to Dr Arup Gayen and his research scholars for their help in procuring PXRD data of the complex at the departmental facility. SD gratefully acknowledges support received from UGC, New Delhi, through funding of the research program on "Advanced Materials" as part of UPE II to Jadavpur University, from where funds were used for this study. He wishes to thank the "UGC-CAS-II" program operating at the Department of Chemistry, Jadavpur University, for financial support under the heading: Chemicals/Consumable/Glassware. KM is grateful for receiving funds from DST-PURSE (Phase-II) and UGC (UPE-II: ID 59) which came to Jawaharlal Nehru University.

## References

- 1 Y. Miyamoto, J. Kalisiak, K. Korthals, T. Lauwaet, D. Y. Cheung, R. Lozano, E. R. Cobo, P. Uproft, J. A. Uproft, D. E. Berg, F. D. Gillin, V. V. Fokin, K. B. Sharpless and L. Eckmanna, *Proc. Natl. Acad. Sci. U. S. A.*, 2013, **110**, 17564–17569.
- 2 W. Raether and H. Hänel, *Parasitol. Res.*, 2003, **90**, S19–S39.
- 3 M. Van den Kerkhof, D. Mabile, E. Chatelain, C. E. Mowbray, S. Braillard, S. Hendrickx, L. Maes and G. Caljon, *Int. J. Parasitol.: Drugs Drug Resist.*, 2018, **8**, 81–86.
- 4 E. F. F. da Cunha, T. C. Ramalho, D. T. Mancini, E. M. B. Fonseca and A. A. Oliveira, *J. Braz. Chem. Soc.*, 2010, **21**, 1787–1806, DOI: 10.1590/S0103-50532010001000002.
- 5 J. M. Brown, *Cancer Res.*, 1999, **59**, 5863–5870.
- 6 P. Wardman, *Br. J. Radiol.*, 2019, **92**, 20170915, DOI: 10.1259/bjr.20170915.
- 7 M. Bonnet, C. R. Hong, W. W. Wong, L. P. Liew, A. Shome, J. Wang, Y. R. J. Stevenson, W. Qi, R. F. Anderson, F. B. Pruijn, W. R. Wilson, S. M. F. Jamieson, K. O. Hicks and M. P. Hay, *J. Med. Chem.*, 2018, **61**, 1241–1254, DOI: 10.1021/acs.jmedchem.7b01678.
- 8 P. De, D. Bhattacharyya and K. Roy, *Struct. Chem.*, 2020, **31**, 1043–1055, DOI: 10.1007/s11224-019-01481-z.
- 9 (a) S. Sood and A. Kapil, *Indian J. Sex. Transm. Dis.*, 2008, **29**, 7–14; (b) V. Puri, *Neurol. India*, 2011, **59**, 4–5.
- 10 R. C. Santra, D. Ganguly, J. Singh, K. Mukhopadhyay and S. Das, *Dalton Trans.*, 2015, **44**, 1992–2000.
- 11 R. C. Santra, D. Ganguly, S. Jana, N. Banyal, J. Singh, A. Saha, S. Chattopadhyay, K. Mukhopadhyay and S. Das, *New J. Chem.*, 2017, **41**, 4879–4886, DOI: 10.1039/c7nj00261k.
- 12 P. S. Guin, P. C. Mandal and S. Das, *ChemPlusChem*, 2012, **77**, 361–369, DOI: 10.1002/cplu.201100046.
- 13 P. S. Guin, P. C. Mandal and S. Das, *J. Coord. Chem.*, 2012, **65**, 705–721, DOI: 10.1080/00958972.2012.659730.
- 14 B. Mandal, S. Singha, S. K. Dey, S. Mazumdar, T. K. Mondal, P. Karmakar, S. Kumar and S. Das, *RSC Adv.*, 2016, **6**, 51520–51532.
- 15 B. Mandal, S. Singha, S. K. Dey, S. Mazumdar, S. Kumar, P. Karmakar and S. Das, *RSC Adv.*, 2017, **7**, 41403–41418.
- 16 F. Ahmadi, N. Shabrandi, L. Hosseinzadeh and H. Azizian, *Nucleosides, Nucleotides Nucleic Acids*, 2019, **38**, 449–480, DOI: 10.1080/15257770.2018.1562073.
- 17 Reflex Plus, *Accelrys Material Studio 4.4*, Accelrys Software Inc, 2008.
- 18 P. E. Werner, L. Eriksson and M. Westdahl, *J. Appl. Crystallogr.*, 1985, **18**, 367–370.
- 19 G. S. Pawley, *J. Appl. Crystallogr.*, 1981, **14**, 357–361.
- 20 K. E. Linder, Y. W. Chan, J. E. Cyr, M. F. Malley, D. P. Nowotnik and A. D. Nunn, *J. Med. Chem.*, 1994, **37**, 9–17.
- 21 J. A. Squella, S. Bollo, J. de la Fuente and L. J. Núñez-Vergara, *Bioelectrochem. Bioenerg.*, 1994, **34**, 13–18.
- 22 J. A. Squella, M. Huerta, S. Bollo, H. Pessoa and L. J. Núñez-Vergara, *J. Electroanal. Chem.*, 1997, **420**, 63–70.
- 23 J. A. Squella, P. Gonzalez, S. Bollo and L. J. Núñez-Vergara, *Pharm. Res.*, 1999, **16**, 161–164, DOI: 10.1023/A:1011950218824.
- 24 L. J. Núñez-Vergara, F. Garcia, M. M. Dominguez, J. de la Fuente and J. A. Squella, *J. Electroanal. Chem.*, 1995, **381**, 215–219.

- 25 H. Lund, Cathodic reduction of nitro and related compounds, in *Organic Electrochemistry*, ed. H. Lund and M. M. Baizer, M. Dekker Inc., New York, 3rd edn, 1990, p. 411.
- 26 P. C. Mandal, *J. Electroanal. Chem.*, 2004, **570**, 55–61.
- 27 A. J. Bard and L. R. Faulkner, *Electrochemical Methods Fundamental and Applications*, John Wiley & Sons, Inc., New York, 2001.
- 28 P. Zanello, *Inorganic Electrochemistry: Theory, practice and application*, The Royal Society of Chemistry, 2003.
- 29 R. C. Santra, K. Sengupta, R. Dey, T. Shireen, P. Das, P. S. Guin, K. Mukhopadhyay and S. Das, *J. Coord. Chem.*, 2014, **67**, 265–285, DOI: 10.1080/00958972.2013.879647.
- 30 P. S. Guin and S. Das, *Int. J. Electrochem.*, 2014, **2014**, 517371, DOI: 10.1155/2014/517371.
- 31 X. Jiang and X. Lin, *Bioelectrochemistry*, 2006, **68**, 206–212.
- 32 T. Deb, D. Choudhury, P. S. Guin, M. B. Saha, G. Chakrabarti and S. Das, *Chem.-Biol. Interact.*, 2011, **189**, 206–214.
- 33 C. G. Clark and L. S. Diamond, *Clin. Microbiol. Rev.*, 2002, **15**, 329–341.
- 34 J. A. Upcroft and P. Upcroft, *Antimicrob. Agents Chemother.*, 2001, **45**, 1810–1814.
- 35 E. Benere, R. A. I. Luz, M. Vermeersch, P. Cos and L. Maes, *J. Microbiol. Methods*, 2007, **71**, 101–106.
- 36 K. Nakamoto, *Infrared and Raman spectra of inorganic and coordination compounds, Part A: Theory and Applications in Inorganic Chemistry*, Wiley-Interscience, New York, 6th edn, 2009.
- 37 J. A. Squella, S. Bollo and L. J. Núñez-Vergara, *Curr. Org. Chem.*, 2005, **9**, 565–581.
- 38 F. Frezard and A. Garnier-Suillerot, *Biochim. Biophys. Acta*, 1990, **1036**, 121–127.
- 39 T. Deb, P. K. Gopal, D. Ganguly, P. Das, M. Paul, M. B. Saha, S. Paul and S. Das, *RSC Adv.*, 2014, **4**, 18419–18430.



# Radio-Sensitizing Effects of Cu<sup>II</sup> and Zn<sup>II</sup> Complexes of Ornidazole: Role of Nitro Radical Anion

Promita Nandy, Alivia Mukherjee, Chiranjit Pradhan, and Saurabh Das\*



Cite This: *ACS Omega* 2020, 5, 25668–25676



Read Online

ACCESS |



Metrics & More

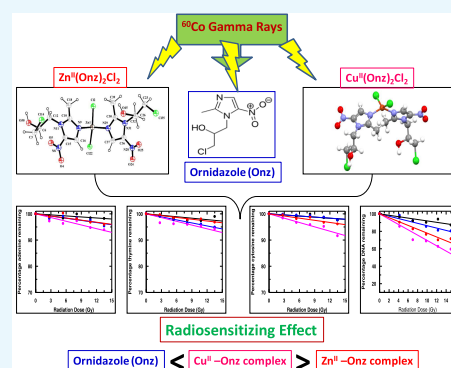


Article Recommendations



Supporting Information

**ABSTRACT:** The treatment of malignant cells that are deficient in oxygen due to the insufficient flow of blood is often seen as a major hindrance in radiotherapy. Such cells become radio-resistant because molecular oxygen, the natural and best radio-sensitizer, is depleted. Hence, to compensate this deficiency in oxygen, there is a need for agents that enhance radiation-induced damage of cells (radio-sensitizers) in a manner that normal cells are least affected. Simultaneously, agents capable of showing activity under hypoxic conditions are known as hypoxic cytotoxins that selectively and preferably destroy cells under hypoxic environments. 5-Nitroimidazoles fit both definitions. Their efficiency is based on their ability to generate the nitro radical anion that interacts with the strands of DNA within cells, either damaging or modifying them, leading to cell death. 5-Nitroimidazoles are important radio-pharmaceuticals (radio-sensitizers) in cancer-related treatments where the nitro radical anion has an important role. Since its generation leads to neurotoxic side effects that may be controlled through metal complex formation, this study looks at the possibility of two monomeric complexes of Ornidazole [1-chloro-3-(2-methyl-5-nitro-1*H*-imidazole-1-yl)propan-2-ol] with Cu<sup>II</sup> and Zn<sup>II</sup> to be better radio-sensitizers and/or hypoxic cytotoxins than Ornidazole. The study reveals that although there is a decrease in nitro radical anion formation by complexes, such a decrease does not hamper their radio-sensitizing ability. Nucleic acid bases (thymine, cytosine, and adenine) or calf thymus DNA used as targets were irradiated with <sup>60</sup>Co  $\gamma$  rays either in the absence or presence of Ornidazole and its monomeric complexes. Radiation-induced damage of nucleic acid bases was followed by high-performance liquid chromatography (HPLC), and modification of calf thymus DNA was followed by ethidium bromide fluorescence. Studies indicate that the complexes were better in performance than Ornidazole. Cu<sup>II</sup>-ornidazole was significantly better than either Ornidazole or Zn<sup>II</sup>-ornidazole, which is attributed to certain special features of the Cu<sup>II</sup> complex; aspects like having a stable lower oxidation state enable it to participate in Fenton reactions that actively influence radio-sensitization and the ability of the complex to bind effectively to DNA.



## 1. INTRODUCTION

In the last few decades spanning over half a century, work from different laboratories have established that solid tumors contain regions of mild to severe hypoxia that either alter cellular metabolism of that region or increase its resistance to radiation and chemotherapy.<sup>1–4</sup> Detection of hypoxic cells in human tumors improved with the discovery of new imaging techniques and with the use of predictive gene profiles.<sup>5–10</sup> Sufficient data is now available on hypoxia in different human tumors, although considerable heterogeneity exists between individual types.<sup>1–4,9,10</sup> Clinical trials suggest that efforts were made to modify radiation resistance using either hypobaric hypoxia or normobaric/hyperbaric oxygen therapies that initially raised doubts, because treatment of O<sub>2</sub> to cells was thought to support cell growth in cancer; however, later proved advantageous.<sup>11–14</sup> Not only did it help in radiotherapy but also it influenced a tumor's microenvironment in a correct manner for treatment.<sup>11–14</sup> It was shown that oxygen not only acts as a strong electron scavenger but, by forming pyrimidine peroxy radical, is able to further react within DNA affecting vicinal bases or 2-deoxyribose moieties.<sup>15,16</sup> Such studies led to

two important aspects (i) importance of oxygen in radiotherapy and (ii) identification of new chemical agents that might deliver results under hypoxic conditions.<sup>1,2,12,14–19</sup>

There is a lot of attention on hypoxic cytotoxins<sup>19–21</sup> that selectively and preferably destroy cells in a hypoxic environment, a group slightly different from radio-sensitizers that help to improve radiotherapy under hypoxic conditions.<sup>18,22</sup> Hypoxic cytotoxins by killing cells in hypoxia not only overcome cellular resistance but actually exploit it converting it into a therapeutic advantage.<sup>20,21</sup> Nitroimidazoles being “electron-affinic” react with DNA free radicals having the potential for universal activity to combat hypoxia-associated radio-resistance.<sup>18,23,24</sup> Several members were found clinically

Received: June 13, 2020

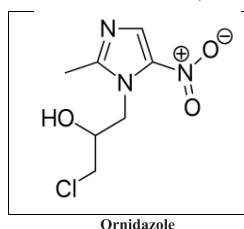
Accepted: September 17, 2020

Published: October 1, 2020



effective at a tolerable dose.<sup>18,23,25</sup> However, most compounds had limited clinical success; their efficacy is restricted by dose-limiting toxicity, attributed to electron affinity, i.e., to the relative ease of reduction of  $-\text{NO}_2$  in nitroimidazoles to nitroimidazole radical anion ( $\text{RNO}_2^{\bullet-}$ ).<sup>23</sup> Such a reduction may be modulated by complex formation.<sup>26–28</sup>

Here, we report a study performed on Ornidazole (Onz, a 5-nitroimidazole) with regard to its radio-sensitizing capabilities.<sup>29,30</sup> Its monomeric  $\text{Cu}^{\text{II}}$  and  $\text{Zn}^{\text{II}}$  complexes<sup>31,32</sup> were tried. A report on the hypoxia-specific cytotoxin tirapazamine showed that it was selective for hypoxic cells in solid tumors occurring through DNA damage produced by free radicals generated in enzymatic reduction.<sup>21</sup> Studies on the DNA damage and metabolism of tirapazamine in A549 human lung carcinoma cells and in isolated nuclei derived from cells showed although that nuclei metabolize it at a rate 20% compared to the whole cell, extent of DNA damage by nuclei was similar to that by cells.<sup>21</sup> The study showed that tirapazamine radicals formed outside the nuclei do not contribute to intranuclear DNA damage and that all forms of DNA damage resulted from radicals generated within the nucleus. Hence, 80% of drug metabolism (occurring in the cytoplasm) is really irrelevant with regard to killing of hypoxic cells.<sup>21</sup> This was an inspiration toward using complexes of Ornidazole to investigate their radio-sensitizing and/or cytotoxic attributes by bringing about a substantial decrease in  $\text{RNO}_2^{\bullet-}$  formation and yet not compromising on efficacy.<sup>26–28,33</sup> Therefore, like in tirapazamine where 80% of drug metabolism is irrelevant in killing hypoxic cells, here also if we could show that complexes of Onz are better radio-sensitizers or hypoxic cytotoxins in spite of decreased  $\text{RNO}_2^{\bullet-}$ ,<sup>26–28,33</sup> the amount required for biological activity can be believed to be provided by the complexes. If the amount formed by Onz is much in excess of what is actually necessary, then there is the risk of undesirable neurotoxic side effects.<sup>26–28,33</sup> Hence, use of complexes could have the advantage that excess  $\text{RNO}_2^{\bullet-}$  would not be present in the system, leading to some clinical success with regard to toxic side effects.<sup>26–28</sup> Worth mentioning here is that the complexes are either better DNA-binding agents or DNA-damaging agents or both, following interaction of in situ generated  $\text{RNO}_2^{\bullet-}$  with nucleobases and calf thymus DNA.<sup>24,31,32</sup>



## 2. EXPERIMENTAL SECTION

**2.1. Materials.** Onz was purchased from TCI, Japan. Copper(II) chloride ( $\text{CuCl}_2 \cdot 2\text{H}_2\text{O}$ ), zinc(II) chloride ( $\text{ZnCl}_2$ ),  $\text{NaCl}$ ,  $\text{NaNO}_3$ , and  $\text{MgCl}_2$  (AR grade) were purchased from E. Merck, India. Nucleic acid bases cytosine and thymine were purchased from Sisco Research Laboratories, India, while adenine was procured from TCI, Japan. Calf thymus DNA and ethidium bromide were purchased from Sisco Research Laboratories, India. DNA was dissolved in phosphate buffer (pH  $\sim 7.4$ ) containing  $\text{NaCl}$ ,  $\text{KCl}$ , and  $\text{MgCl}_2$  as electrolytes. Concentration of DNA in terms of nucleotide was determined

considering  $\epsilon_{260} = 6600 \text{ mol}^{-1} \text{ dm}^3 \text{ cm}^{-1}$ . Phosphate buffer (pH  $\sim 7.4$ ) was prepared using sodium dihydrogen phosphate and disodium hydrogen phosphate (AR, Merck, Germany) in triple-distilled water.

**2.2. Methods.** **2.2.1. Synthesis of Monomeric  $\text{Cu}(\text{II})$  and  $\text{Zn}(\text{II})$  Complexes of Ornidazole.** Solutions of Onz in methanol (0.439 g in 25 mL, 2.00 mmol) were gradually added with stirring once to a solution of  $\text{CuCl}_2 \cdot 2\text{H}_2\text{O}$  (0.17 g in 25 mL, 1.00 mmol) in methanol and in another to a solution of  $\text{ZnCl}_2$  (0.1363 g in 25 mL, 2 mmol) in methanol.<sup>27,28,31,32</sup> Both mixtures were warmed under reflux to a temperature  $\sim 60^\circ \text{C}$  for 4–5 h. A green crystalline compound was obtained after  $\sim 10$  days following slow evaporation of the solvent for the  $\text{Cu}(\text{II})$  complex, while for the  $\text{Zn}(\text{II})$  complex, a white crystalline compound was obtained by slow evaporation of the solvent in a week's time. In both cases, products were filtered, dried, and stored carefully. They were characterized and used.<sup>31,32</sup>

**2.2.2. Preparation of Solutions of Nucleic Acid Bases and Calf Thymus DNA for Gamma Irradiation Experiments.** Stock solutions of nucleic acid bases were prepared in triple-distilled water by accurately weighing each compound so that the concentration of each was  $1 \times 10^{-2} \text{ mol/L}$ . Subsequently, utilizing stock solutions, experimental solutions were prepared, in which the concentration of a nucleobase was  $1 \times 10^{-4} \text{ mol/L}$  while that of Onz or its complexes was  $1 \times 10^{-5} \text{ mol/L}$ . For experiments with DNA, its concentration in experimental solution was  $1 \times 10^{-4} \text{ mol/L}$ , while that of the additives was  $1 \times 10^{-5} \text{ mol/L}$ . Prior to irradiation, aqueous solutions of all samples were saturated with pure Ar by purging a 3 mL solution in a vial for at least 10 min. Solutions were irradiated with  $^{60}\text{Co}$   $\gamma$  rays at different time intervals. Dose rate (1.618 kGy/h) was measured using a Fricke dosimeter.

**2.2.3. High-Performance Liquid Chromatography: Used for Analyzing Nucleobases.** Following irradiation at different doses, all solutions containing nucleobases with or without additives were analyzed by high-performance liquid chromatography (HPLC) using a  $\text{C}_{18}$  column supported by a PDA detector. Components were eluted using 5% methanol in water as the mobile phase having flow rate  $1 \text{ mL min}^{-1}$ . From the area of peaks in each chromatogram, the concentration of a nucleobase remaining after irradiation either in the absence or in presence of additives could be ascertained and products identified. Determination of concentration was possible using standard plots prepared earlier for each nucleobase.<sup>33</sup> In this manner, radiation-induced damage of each nucleobase either in the absence or presence of a compound was obtained.

**2.2.4. Ethidium Bromide Fluorescence for Monitoring the Amount of DNA Not Modified.** Information on radiation-induced damage caused to DNA exposed to  $\gamma$ -radiation either when present alone or with sensitizers (S) was obtained by treating all irradiated samples with ethidium bromide (EtBr). Subsequently, fluorescence was recorded. Excitation was done at 510 nm and emission was recorded over 590–610 nm. The fluorescence intensity of EtBr-DNA adduct was measured for each sample from where the amount of calf thymus DNA remaining was determined.<sup>34–36</sup> Enhancement ratio indicates the extent of damage caused to a target obtained from the ratio of slopes of linear plots (for solutions containing compounds to that obtained in the absence of a compound).

### 3. RESULTS AND DISCUSSION

**3.1. Radiation-Induced Damage of Adenine, Thymine, and Cytosine by Onz and Its Monomeric Cu(II)/Zn(II) Complexes.** Aqueous solutions of nucleobases (thymine, cytosine, and adenine) that were irradiated with  $^{60}\text{Co}$   $\gamma$  rays in the range 2.8–13.5 Gy, under Ar-saturated conditions, in the absence or presence of Onz and its Cu(II)/Zn(II) complexes were subsequently followed by HPLC. Chromatograms of all nucleobases were recorded. While thymine eluted between 10.8 and 11.0 min, adenine eluted between 8.5 and 8.7 min and cytosine at 3.7 min. With a gradual increase in radiation dose, concentrations of all nucleobases detected by HPLC decreased. Such a decrease in concentration with an increase in radiation dose was different for each nucleobase and was found to depend on the compound in whose presence irradiation was administered.

For all three nucleobases, decrease was significant when irradiated in the presence of  $\text{Cu}(\text{Onz})_2\text{Cl}_2$  followed by  $\text{Zn}(\text{Onz})_2\text{Cl}_2$  and Ornidazole, where a linear dependence on dose was observed. Figure 1 shows the HPLC profiles for

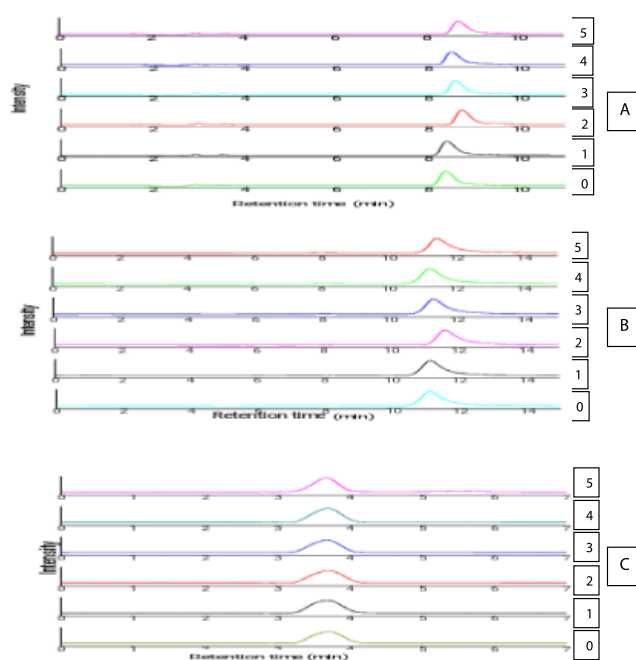


**Figure 1.** HPLC chromatograms at 254 nm for  $10^{-4}$  M (A) adenine, (B) thymine, and (C) cytosine solutions irradiated at the mentioned dose; 0 indicates the sample was not irradiated; 2.7 Gy (1), 5.4 Gy (2), 8.1 Gy (3), 10.8 Gy (4), and 13.5 Gy (5) indicate irradiated dose in an Ar-saturated medium in the presence of  $10^{-5}$  M  $\text{Cu}(\text{Onz})_2\text{Cl}_2$ .

degradation of all three nucleobases in the presence of  $10 \mu\text{M}$   $\text{Cu}(\text{Onz})_2\text{Cl}_2$  at different radiation doses. Figures S1–S3 (Supporting Information) show the HPLC profiles for the degradation of nucleobases either in the absence of any compound or in the presence of  $10 \mu\text{M}$  Onz or  $\text{Zn}(\text{Onz})_2\text{Cl}_2$ , respectively, at different radiation doses.

In a previous study, with a dimeric Cu(II) complex of tinidazole, employing a much higher dose than the one usually employed for such physiological studies, we characterized the products that were formed from the degradation of thymine and uracil.<sup>33</sup> Since HPLC profiles for the degraded products of thymine and uracil were saved as method files in our HPLC program, these were utilized in this study to identify the

products formed following degradation of thymine and cytosine when irradiated in the absence and presence of compounds that were used in this study. Results for two relatively high doses (10.8 and 13.5 Gy) indicate that when irradiation was provided in the presence of  $\text{Cu}(\text{Onz})_2\text{Cl}_2$ , 5,6-dihydroxy-5,6-dihydrothymine (thymine glycol) and 5-hydroxymethyl uracil were identified. In the case of  $\text{Cu}(\text{Onz})_2\text{Cl}_2$ , peaks were much more prominent than when Onz or  $\text{Zn}(\text{Onz})_2\text{Cl}_2$  were used as the sensitizers. Peak for the formation of 5,6-dihydrothymine was however not detected even when thymine was irradiated in the presence of  $\text{Cu}(\text{Onz})_2\text{Cl}_2$  in the dose range in which our experiments were performed. Since formation of 5,6-dihydrothymine depends on the formation of  $\cdot\text{H}$  and since the G value of  $\cdot\text{H}$  at pH  $\sim 7.4$  is extremely low,<sup>37</sup> not much of it, i.e., sufficient to be detected by HPLC, was formed. For 5,6-dihydrothymine to form, a much higher dose would be required at pH  $\sim 7.4$ , which was not used in this study (but reported in one of our previous studies where the effort was to detect all possible degradation products of these nucleobases).<sup>33,37</sup> Products were identified from their respective retention times using authentic samples.<sup>33</sup>

The pyrimidine-based nucleobase cytosine differs from uracil at the  $\text{C}_1$  position of the molecule where an  $-\text{NH}_2$  group is present instead of  $-\text{OH}$  (in enol form). Since 5,6-dihydroxy-5,6-dihydrocytosine (cytosine glycol) is unstable and known to convert to 5,6-dihydroxy-5,6-dihydrouracil (uracil glycol) by deamination, we used our existing HPLC method files on uracil to identify the degradation products of cytosine.<sup>33,38</sup> A peak in the chromatogram appearing at a retention time close to that of 5,6-dihydroxy-5,6-dihydrouracil as saved in our earlier method file could be due to either 5,6-dihydroxy-5,6-dihydrocytosine or 5,6-dihydroxy-5,6-dihydrouracil (i.e., if it had in the time frame between irradiation of cytosine and performance of HPLC, converted either completely or partially from 5,6-dihydroxy-5,6-dihydrocytosine).<sup>33,38</sup> It is known that 5,6-dihydroxy-5,6-dihydrocytosine by dehydration converts to 5-hydroxycytosine or by deamination and dehydration to 5-hydroxyuracil.<sup>38</sup> Therefore, our uracil method file, created for detecting uracil derivatives, helped us realize an initial formation of 5,6-dihydroxy-5,6-dihydrocytosine that subsequently converts into several uracil derivatives, as mentioned above.<sup>33</sup> These observations suggest that pyrimidine-based nucleobases experience an initial free-radical attack by the products of radiolysis of water ( $\text{H}\cdot$ ,  $\text{OH}\cdot$ , and  $e_{\text{aq}}^-$ ) on the  $\text{C}_5$ – $\text{C}_6$  double bond that subsequently yield different products.<sup>33,37</sup>

Figures S2 and S3 (Supporting Information) show degradation of nucleobases obtained in an Ar-saturated medium, in the presence of either Onz or  $\text{Zn}(\text{Onz})_2\text{Cl}_2$ . They suggest that damage caused to nucleobases is not much in the presence of Onz and that it increased only slightly when  $\text{Zn}(\text{Onz})_2\text{Cl}_2$  was used. Studies clearly reveal that it is maximum for  $\text{Cu}(\text{Onz})_2\text{Cl}_2$ . Under Ar-saturated conditions,  $\cdot\text{OH}$  and  $e_{\text{aq}}^-$  are produced in almost equal amounts unlike in  $\text{N}_2\text{O}$ -saturated medium where  $e_{\text{aq}}^-$  converts into  $\cdot\text{OH}$ .<sup>37,39</sup> Therefore, reactions responsible for the damage of nucleobases are initiated by both  $\cdot\text{OH}$  and  $e_{\text{aq}}^-$ .

For a purine-based nucleobase adenine, HPLC chromatograms did not show any new peak within the retention time of 15 min. A decrease in the peak for adenine was significant for radiation provided in the presence of  $\text{Cu}(\text{Onz})_2\text{Cl}_2$  in Ar-saturated medium, while it was almost the same in the

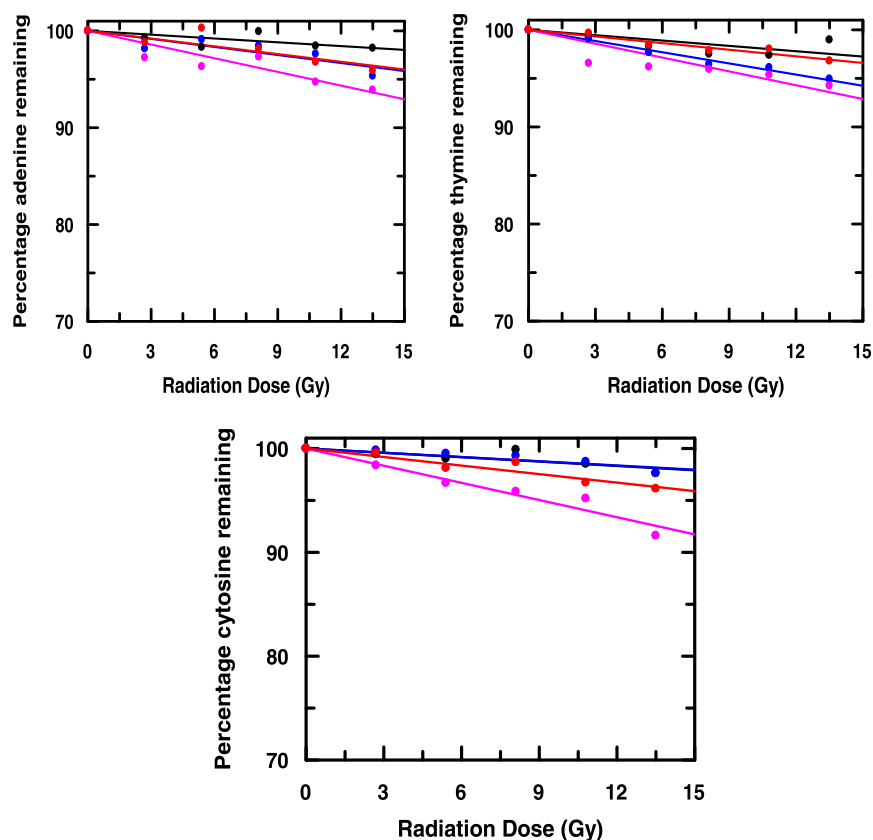


**Figure 2.** Amount of each nucleic acid base remaining on being subjected to  $\gamma$ -irradiation from a  $^{60}\text{Co}$  source in the absence ( $\bullet$ ) and presence of Onz (blue circle solid),  $[\text{Cu}(\text{Onz})_2\text{Cl}_2]$  (pink circle solid), and  $[\text{Zn}(\text{Onz})_2\text{Cl}_2]$  (red circle solid) under Ar-saturated conditions against radiation dose.

**Table 1.**  $G$  (values) Following Damage of Nucleic Acid Bases in Units of Molecules/100 eV and the Corresponding Enhancement Ratio for Base Damage by the Compounds

compound	target nucleic acid bases								
	adenine			thymine			cytosine		
	(% loss $\text{Gy}^{-1}$ )	$G$ ( $-\text{A}$ )	ER	(% loss $\text{Gy}^{-1}$ )	$G$ ( $-\text{T}$ )	ER	(% loss $\text{Gy}^{-1}$ )	$G$ ( $-\text{T}$ )	ER
Onz	-0.131	1.26		-0.184	1.78		-0.139	1.34	
$[\text{Cu}(\text{Onz})_2\text{Cl}_2]$	-0.277	2.67	2.12	-0.384	3.71	2.08	-0.137	1.32	0.99
$[\text{Zn}(\text{Onz})_2\text{Cl}_2]$	-0.471	4.55	3.61	-0.476	4.59	2.58	-0.552	5.33	3.98
	-0.266	2.57	2.04	-0.228	2.20	1.24	-0.274	2.64	1.97

presence of Onz and  $\text{Zn}(\text{Onz})_2\text{Cl}_2$ . Concentrations of nucleobases remaining were plotted against radiation dose (Figure 2). Plots indicate that radiation-induced damage of nucleobases was maximum when irradiated in the presence of  $\text{Cu}(\text{Onz})_2\text{Cl}_2$ ; much greater than when irradiated in the presence of either Onz or  $\text{Zn}(\text{Onz})_2\text{Cl}_2$ . While for adenine, radiation-induced damage was comparable when irradiated in presence of Onz and  $\text{Zn}(\text{Onz})_2\text{Cl}_2$ , in case of thymine, radiation-induced damage was better with Onz than with  $\text{Zn}(\text{Onz})_2\text{Cl}_2$  (Figure 2, Table 1).

For cytosine, no enhancement in radiation-induced damage was seen in the presence of Onz (damage being similar to that with no additive). Radiation-induced damage in the presence of  $\text{Zn}(\text{Onz})_2\text{Cl}_2$  was significantly less than that obtained in the presence of  $\text{Cu}(\text{Onz})_2\text{Cl}_2$ . The study suggests while  $\text{Cu}(\text{Onz})_2\text{Cl}_2$  was most effective in causing radiation-induced damage of a nucleobase, Onz and  $\text{Zn}(\text{Onz})_2\text{Cl}_2$  were either similar in performance (as in the case of adenine) or one was

slightly better than the other and vice versa (cytosine and thymine).

A comparison and/or prediction of selectivity toward A–T or G–C due to the compounds particularly for that due to  $\text{Cu}(\text{Onz})_2\text{Cl}_2$  could have been made as a part of this study had we been able to perform experiments with guanine. However, this was not possible owing to the poor solubility of guanine in aqueous solution (pH  $\sim$  7.4) containing 120 mM NaCl, 35 mM KCl, and 15 mM  $\text{MgCl}_2$ . We tried performing experiments with guanine, but as mentioned above, owing to poor solubility, the results were erratic. Besides, we observed an interaction between guanine and  $\text{Cu}(\text{Onz})_2\text{Cl}_2$  that prevented us from getting a clear idea of the radiation-induced damage of guanine from HPLC chromatograms. Although such interaction was not evident to the naked eye when the concentration of guanine was  $10^{-4}$  M and that of  $\text{Cu}(\text{Onz})_2\text{Cl}_2$   $10^{-5}$  M but for slightly higher concentrations of guanine ( $10^{-3}$  M) and  $\text{Cu}(\text{Onz})_2\text{Cl}_2$  ( $10^{-4}$  M), the solution became faintly

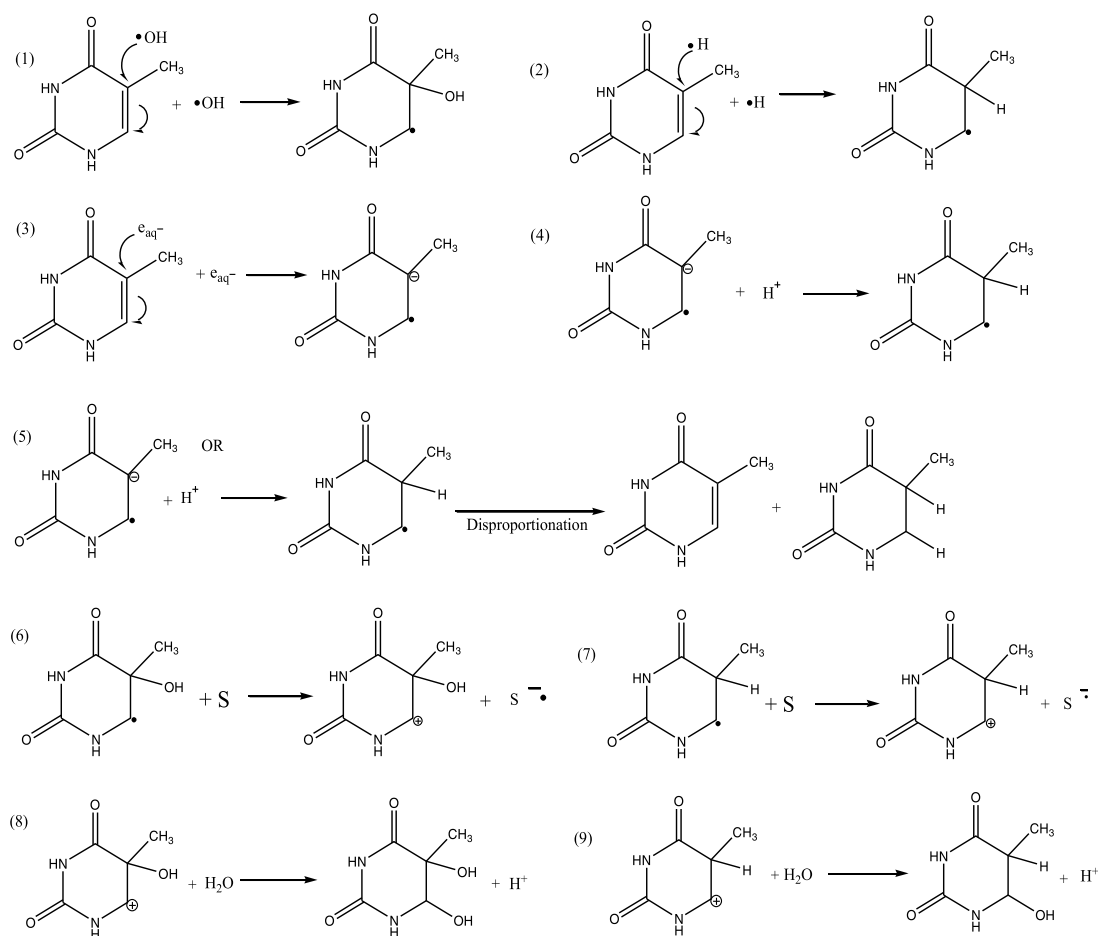


**Figure 3.** Schematic representation of the possible reactions that might occur during the radiation-induced damage of thymine. S indicates any sensitizer molecule, and  $S^{\bullet-}$  indicates the corresponding radical anion formed from S.

turbid, suggesting an association between the two. This was checked several times and confirmed by HPLC of an aqueous solution of  $1 \times 10^{-3}$  M guanine containing  $1 \times 10^{-4}$  M  $\text{Cu}(\text{Onz})_2\text{Cl}_2$ . The solution containing guanine and  $\text{Cu}(\text{Onz})_2\text{Cl}_2$  showed an elution for guanine that was completely different from that obtained when guanine was present alone, indicating an association between the two (Figure S4, Supporting Information). This did not happen for any other nucleobase and  $\text{Cu}(\text{Onz})_2\text{Cl}_2$ . Since such an association of guanine with  $\text{Cu}(\text{Onz})_2\text{Cl}_2$  was identified, it became clear to us that the monitoring of guanine for radiation-induced damage by HPLC would not give us a correct picture. Therefore, for reasons related to solubility and the fact that there is an association or adduct formation between guanine and  $\text{Cu}(\text{Onz})_2\text{Cl}_2$ , we refrained from making any statement on the selectivity of the compounds toward a particular nucleobase pair, realizing, however, this could have been an important outcome of the work. At the same time, the above discussion also makes it very clear that  $\text{Cu}(\text{Onz})_2\text{Cl}_2$  might target guanine as it is seen to interact with it. So, although we could not monitor a radiation-induced damage of guanine,  $\text{Cu}(\text{Onz})_2\text{Cl}_2$  is likely to be very effective on this nucleobase as well. Therefore, not only does  $\text{Cu}(\text{Onz})_2\text{Cl}_2$  act as an effective radio-sensitizer, but it can also act as a hypoxic cytotoxin, leading to the modification of DNA at a site where guanine is present. Radiation chemical yield, i.e.,  $G$  (value) of each nucleobase, was determined from the slopes of the

corresponding linear plots (Figure 2), and these are shown in Table 1.

It is now known from previous reports among different radicals formed during the radiolysis of water,  $\bullet\text{OH}$  is highly effective in causing radiation-induced damage to the nucleobases or to DNA.<sup>40–42</sup> Since in Ar-saturated medium,  $G$  values for  $e_{\text{aq}}^-$  and  $\bullet\text{OH}$  are similar,<sup>39</sup> they show equal probability for chemical reactions following their generation.  $\bullet\text{OH}$  reacts with a nucleobase (B) generating nucleobase radicals ( $\bullet\text{BOH}$ ), which upon interaction with a sensitizer (S) form  $\text{+BOH}$  (Figures 3 and S5, Supporting Information).<sup>43</sup> Such nucleobase cations are then acted upon by molecules of water-forming glycols (Figures 3 and S5, Supporting Information). Similar reactions occur with  $\bullet\text{H}$  (Figures 3 and S5, Supporting Information). When reactions are initiated by  $e_{\text{aq}}^-$ , there could either be a reduction at a nucleobase (Figures 3 and S5, Supporting Information) or a sensitizer (S) present in the system could be reduced.<sup>35,36,40–43</sup> Subsequently, the reduced sensitizer ( $S^{\bullet-}$ , in this case, the nitro radical anion) reacts with a nucleobase (B) to form a modified nucleobase that is shown in Figure 3 considering thymine and in Figure S5, Supporting Information, considering cytosine.<sup>40–43</sup>

In the dose range applied for this study, all products that are supposed to form for the radiation-induced damage of thymine, as reported by Cadet et al.,<sup>44</sup> were not obtained. In fact, we also, in a previous work,<sup>33</sup> reported more products than we identified here. However, in that work, we had

intentionally used very high dose radiation to identify all possible products that may be formed to have a clear idea of the mechanistic pathway.<sup>24,44</sup> In this study, since we wanted to be more close to a real-life situation, a much smaller dose relevant to biological systems was used. As a result, we did not get all possible degradation products of a nucleic acid base, or even if we got, they were formed in such small amounts that their detection was not possible.

For 5-nitroimidazoles, the formation of  $\text{RNO}_2^{\bullet-}$  is extremely crucial. Previous studies show that upon complex formation with metal ions, 5-nitroimidazoles show a decreased tendency to generate  $\text{RNO}_2^{\bullet-}$ .<sup>27,28,32</sup> Given this fact, Onz should have been more effective in modifying the nucleobases used than the complexes. However, this study clearly showed that  $\text{Cu}(\text{Onz})_2\text{Cl}_2$  was the most effective. Earlier, we demonstrated that formation of  $\text{RNO}_2^{\bullet-}$  on Onz and  $\text{Cu}(\text{Onz})_2\text{Cl}_2$  in an electrochemical pathway was responsible for modification of nucleobases and calf thymus DNA under anaerobic (Ar-saturated) conditions, indicating the importance of  $\text{RNO}_2^{\bullet-}$  in causing damage to a nucleobase.<sup>31,45</sup> Since radiation-induced chemical reactions also generate  $\text{RNO}_2^{\bullet-}$ , one can expect that besides radiation-induced base damage by  $^{\bullet}\text{OH}$  in solution, a substantial part of the damage could be due to  $\text{RNO}_2^{\bullet-}$ , making such compounds effective hypoxic cytotoxins as well, and that it could be used on hypoxic tumors. Table 1 summarizes the results of radiation-induced base damage on the three nucleobases used as targets.

Our study using the three nucleobases sets the stage for a realization of the potential sites for base damage in DNA, suggesting all possible ways by which a nucleobase may be transformed following irradiation in the presence of our compounds (sensitizers) and the impact it might have on the destruction of a macromolecule like DNA.

### 3.2. Radiation-Induced Damage of Calf Thymus DNA.

Ethidium bromide (EtBr) bound to double-stranded DNA shows strong emission in the region from 590 to 610 nm following an excitation at 510 nm. Aqueous solutions of calf thymus DNA at physiological pH (~7.4) containing 120 mM NaCl, 35 mM KCl, and 15 mM  $\text{MgCl}_2$  were exposed to gamma radiation from a  $^{60}\text{Co}$  source at different doses. Following irradiation, they were treated with a definite concentration of EtBr and fluorescence was recorded (Figure 4). A gradual decrease in fluorescence intensity with an increase in radiation dose indicates radiation-induced double-strand modification in DNA. Percentage double-stranded DNA remaining at each radiation dose was calculated using eq 1.

$$\% \text{DNA} = (F_S - F_E) / (F_0 - F_E) \times 100 \quad (1)$$

where  $F_0$  and  $F_S$  are fluorescence intensities of the DNA-EtBr adduct with and without radiation, respectively, at a particular dose.  $F_E$  is the fluorescence intensity of EtBr alone.

Percentage DNA remaining after irradiation showed a linear dependence with radiation dose (Figure 5). Radiation-induced DNA damage was enhanced in the presence of Onz and its complexes,  $\text{Cu}(\text{Onz})_2\text{Cl}_2$  and  $\text{Zn}(\text{Onz})_2\text{Cl}_2$  (Table 2). While enhancement ratio in the presence of Onz was 1.67, it was substantially higher in the presence of  $\text{Zn}(\text{Onz})_2\text{Cl}_2$  (ER = 2.72) and still higher for  $\text{Cu}(\text{Onz})_2\text{Cl}_2$  (ER = 3.76), indicating that radiation-induced damage of calf thymus DNA clearly keeps  $\text{Cu}(\text{Onz})_2\text{Cl}_2$  ahead of other compounds (Table 2).

With  $\text{Cu}(\text{Onz})_2\text{Cl}_2$  being so much more effective in model studies on nucleobases and on calf thymus DNA, it is highly likely that its chances to show a reasonably good performance

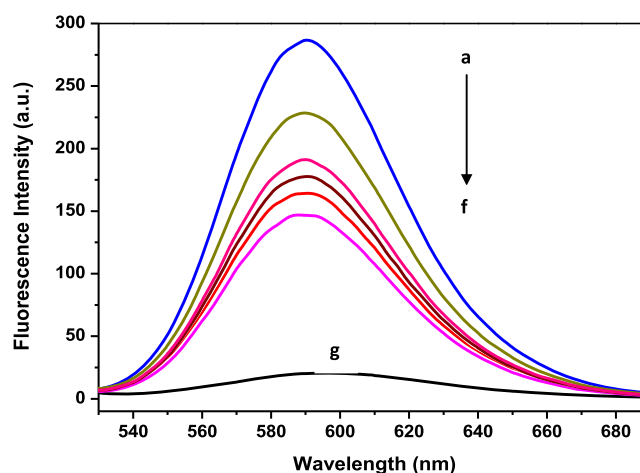


**Figure 4.** Decrease in fluorescence intensity of the DNA-EtBr adduct at 596 nm ( $\lambda_{\text{ex}} = 510$  nm) following irradiation of DNA in the presence of  $\text{Cu}(\text{Onz})_2\text{Cl}_2$  at (a) no dose, (b) 4.05 Gy, (c) 6.74 Gy, (d) 9.44 Gy, (e) 12.14 Gy, and (f) 14.83 Gy. Spectrum (g) is that of free EtBr.

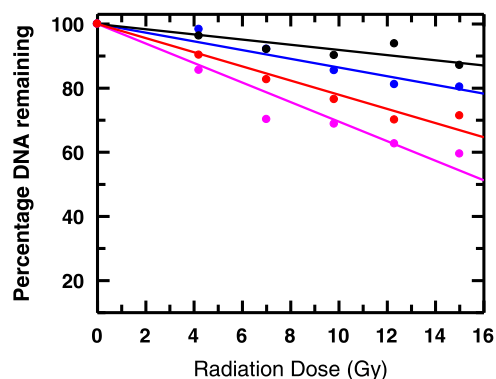


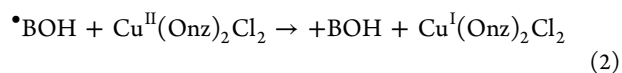
**Figure 5.** Degradation curves showing modification of calf thymus DNA in the absence (●) and presence of Onz (blue circle solid), its  $\text{Cu}(\text{II})$  complex (pink circle solid), and its  $\text{Zn}(\text{II})$  complex (red circle solid).

**Table 2.**  $\gamma$ -Radiation-Induced Modification of Calf Thymus DNA by Compounds

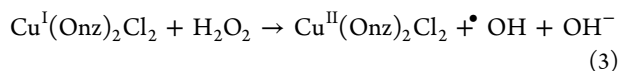
compound	calf thymus DNA	
	% loss $\text{Gy}^{-1}$	ER
	-0.810	
Onz	-1.353	1.67
$\text{Zn}(\text{Onz})_2\text{Cl}_2$	-2.207	2.72
$\text{Cu}(\text{Onz})_2\text{Cl}_2$	-3.046	3.76

on cancer cell lines (hypoxic regions) should be high supported by an inherent affinity of  $\text{Cu}(\text{II})$  for cancer cells that result in increased cellular uptake of  $\text{Cu}(\text{II})$  complexes by such cells.<sup>46–50</sup>

Another reason why a  $\text{Cu}(\text{II})$  complex performs better is its ability to accept electrons either at the nitro group of Onz in the complex or at the metal center. Electron accepted from a radical is then effectively delocalized over  $\text{Cu}(\text{Onz})_2\text{Cl}_2$ . Hence, base damage in presence of the  $\text{Cu}(\text{II})$  complex is likely to increase according to eq 2.<sup>35,36</sup>



Subsequently,  $\text{Cu}^{\text{I}}(\text{Onz})_2\text{Cl}_2$  reacts with  $\text{H}_2\text{O}_2$  present in the system (following radiolysis of water)<sup>35,36</sup> to regenerate  $\text{Cu}^{\text{II}}(\text{Onz})_2\text{Cl}_2$  and release more  $\cdot\text{OH}$  (eq 3).<sup>35,36,51–53</sup>



It has also been reported that  $\cdot\text{OH}$  is not the unique reactive species or the oxidative process that is induced by reaction of copper ions with  $\text{H}_2\text{O}_2$ . Evidence suggests the generation of singlet oxygen ( $^1\text{O}_2$ ) by  $\text{Cu}(\text{II})\text{-H}_2\text{O}_2$  while  $\text{Cu}(\text{I})\text{-H}_2\text{O}_2$  is shown to degrade guanine by one-electron oxidation.<sup>54–56</sup> Since copper complexes also show strong tendencies to bind to DNA,<sup>57</sup> and are regenerated in solution as shown above with a simultaneous formation of  $\cdot\text{OH}$ , this equips them to perform better than one would normally expect. Now if complexes are DNA-bound,  $\cdot\text{OH}$  in eq 3 would be present in the immediate vicinity of the binding site of DNA, capable of inflicting site-specific base damage (as described for guanine).<sup>42–44</sup> While some researchers suggest the formation of discrete  $\cdot\text{OH}$  in the vicinity of a reaction site,<sup>51,57</sup> such formation is sometimes questioned by others who instead say a species closely resembling  $\cdot\text{OH}$  coordinated to  $\text{Cu}^{\text{II}}$  and/or  $\text{Cu}^{\text{III}}$  coordinated to  $\cdot\text{OH}$  is formed that react in a manner similar to  $\cdot\text{OH}$ .<sup>58</sup> Whether a discrete  $\cdot\text{OH}$  or a  $\text{Cu}^{\text{II}}$ -bound  $\text{OH}$  is formed in solution, it eventually reacts with a base on either strand of DNA at the site of  $\cdot\text{OH}$  generation. As a consequence, it is only likely that radiation-induced damage of DNA due to  $\text{Cu}^{\text{II}}(\text{Onz})_2\text{Cl}_2$  would be enhanced by an extent not normal for other compounds, being a reason why the observed damage is higher than when  $\text{Onz}$  or  $\text{Zn}(\text{Onz})_2\text{Cl}_2$  is used. Hence, if  $\text{Cu}(\text{Onz})_2\text{Cl}_2$  is successful in getting inside a target cell, it should perform as predicted in this study.<sup>47–50</sup> Although this study does not include a performance by the compounds on a cancer cell line, in an earlier report for a dimeric  $\text{Cu}(\text{II})$  complex of tinidazole, we showed that findings on model systems were actually holding good on MCF 7 breast cancer cells.<sup>33</sup> Therefore, logically,  $\text{Cu}(\text{Onz})_2\text{Cl}_2$  should be no different.

#### 4. CONCLUSIONS

Through this study, an attempt was made to see if monomeric complexes of  $\text{Cu}(\text{II})$  and  $\text{Zn}(\text{II})$  with Ornidazole show properties of effective radio-sensitizers over and above that reported for Ornidazole and other 5-nitroimidazoles. The study revealed that efficacy of  $\text{Cu}(\text{Onz})_2\text{Cl}_2$  was much better than  $\text{Onz}$  and  $\text{Zn}(\text{Onz})_2\text{Cl}_2$ . When tried on the three nucleobases (cytosine, thymine, and adenine), radiation-induced enhancement was comparable for adenine and thymine in the presence of  $\text{Onz}$  while that on cytosine was not effective.  $\text{Zn}(\text{Onz})_2\text{Cl}_2$  showed comparable activity on adenine and cytosine while it was less active on thymine. All three nucleobases underwent maximum radiation-induced modification in the presence of  $\text{Cu}(\text{Onz})_2\text{Cl}_2$ , adenine and cytosine being comparable.  $\text{Cu}(\text{Onz})_2\text{Cl}_2$  clearly showed its superiority in enhancing radiation-induced base damage for a number of reasons that were also seen in studies with calf thymus DNA. This study is important since complexes are likely to show less toxic side effects (neurotoxicity) owing to decreased formation of  $\text{RNO}_2^{\bullet-}$ .  $\text{RNO}_2^{\bullet-}$  that is essential for radio-sensitization of such compounds may also act as an efficient hypoxic cytotoxin. To conclude, we can say,  $\text{Cu}(\text{Onz})_2\text{Cl}_2$  in particular is able to strike a balance between efficacy and toxic side effects and that it would not be wrong to

say that with decreased  $\text{RNO}_2^{\bullet-}$ , complexes are likely to be less neurotoxic, therefore increasing its application as a drug.

#### ■ ASSOCIATED CONTENT

##### Supporting Information

The Supporting Information is available free of charge at <https://pubs.acs.org/doi/10.1021/acsomega.0c02811>.

HPLC chromatograms of  $10^{-4}$  M adenine, thymine, and cytosine solutions irradiated at the mentioned dose in Ar-saturated medium either in the absence of any compound or in the presence of  $\text{Onz}$  and its  $\text{Zn}^{\text{II}}$  complex; HPLC chromatograms for a solution of guanine and a solution of guanine containing  $\text{Cu}(\text{Onz})_2(\text{Cl})_2$  to realize possible interactions between guanine and the complex that prevents an analysis using HPLC; and schematic representation of possible reactions that might occur during radiation-induced damage of the nucleobase cytosine (PDF)

#### ■ AUTHOR INFORMATION

##### Corresponding Author

Saurabh Das – Department of Chemistry, Inorganic Chemistry Section, Jadavpur University, Kolkata 700032, India; [orcid.org/0000-0002-0455-8760](https://orcid.org/0000-0002-0455-8760); Phone: +91 33 2457 2148; Email: [dasrsv@yahoo.in](mailto:dasrsv@yahoo.in), [saurabh.das@jadavpuruniversity.in](mailto:saurabh.das@jadavpuruniversity.in); Fax: +91 33 2414 6223

##### Authors

Promita Nandy – Department of Chemistry, Inorganic Chemistry Section, Jadavpur University, Kolkata 700032, India  
†Alivia Mukherjee – Department of Chemistry, Inorganic Chemistry Section, Jadavpur University, Kolkata 700032, India  
‡Chiranjit Pradhan – Department of Chemistry, Inorganic Chemistry Section, Jadavpur University, Kolkata 700032, India

Complete contact information is available at: <https://pubs.acs.org/10.1021/acsomega.0c02811>

##### Notes

The authors declare no competing financial interest.

†Worked as an M.Sc. project student on the topic.

‡Worked as a project student on the topic immediately after his M.Sc. examination.

#### ■ ACKNOWLEDGMENTS

PN thanks Department of Science & Technology, New Delhi, for a DST-INSPIRE Senior Research Fellowship. S.D. thanks the “RUSA 2.0” program of the Government of India operating at Jadavpur University under which a “Research Support to Faculty Members” in the thrust area “Research in Sustainable Development” (Sanction Ref No. R-11/438/19 dated 30.05.2019) was received. He gratefully acknowledges the support received from UGC, New Delhi, through funding of research on “Advanced Materials”, part of UPE II to Jadavpur University, from which funds were utilized for this work. He thanks the UGC-CAS-II program that had just finished its tenure of 5 years at the Department of Chemistry, Jadavpur University, for financial support.

#### ■ REFERENCES

(1) Gray, L. H.; Conger, A. D.; Ebert, M.; Hornsey, S.; Scott, O. C. A. The concentration of oxygen dissolved in tissues at the time of

- irradiation as a factor in radiotherapy. *Br. J. Radiol.* **1953**, *26*, 638–648.
- (2) Wright, E. A.; Howard-Flanders, P. The influence of oxygen on the radiosensitivity of mammalian tissues. *Acta Radiol.* **1957**, *48*, 26–32.
- (3) Horsman, M. R.; Overgaard, J. The impact of hypoxia and its modification of the outcome of radiotherapy. *J. Radiat. Res.* **2016**, *57*, i90–i98.
- (4) Muz, B.; de la Puente, P.; Azab, F.; Azab, A. K. The role of hypoxia in cancer progression, angiogenesis, metastasis, and resistance to therapy. *Hypoxia* **2015**, *3*, 83–92.
- (5) Horsman, M. R. Measurement of tumor oxygenation. *Int. J. Radiat. Oncol. Biol. Phys.* **1998**, *42*, 701–704.
- (6) Horsman, M. R.; Mortensen, L. S.; Petersen, J. B.; Busk, M.; Overgaard, J. Imaging hypoxia to improve radiotherapy outcome. *Nat. Rev. Clin. Oncol.* **2012**, *9*, 674–687.
- (7) Chi, J.-T.; Wang, Z.; Nuyten, D. S. A.; Rodriguez, E. H.; Schaner, M. E.; Salim, A.; Wang, Y.; Kristensen, G. B.; Helland, Å.; Børresen-Dale, A.-L.; Giaccia, A.; Longaker, M. T.; Hastie, T.; Yang, G. P.; van de Vijver, M. J.; Brown, P. O. Gene expression programs in response to hypoxia: Cell type specificity and prognostic significance in human cancers. *PLoS Med.* **2006**, *3*, No. e47.
- (8) Marotta, D.; Karar, J.; Jenkins, W. T.; Kumanova, M.; Jenkins, K. W.; Tobias, J. W.; Baldwin, D.; Hatzigeorgiou, A.; Alexiou, P.; Evans, S. M.; Alarcon, R.; Maity, A.; Koch, C.; Koumenis, C. In vivo profiling of hypoxic gene expression in gliomas using the hypoxia marker EF5 and laser-capture microdissection. *Cancer Res.* **2011**, *71*, 779–789.
- (9) Toustrup, K.; Sørensen, B. S.; Nordmark, M.; Busk, M.; Wiuf, C.; Alsner, J.; Overgaard, J. Development of a hypoxia gene expression classifier with predictive impact for hypoxic modification of radiotherapy in head and neck cancer. *Cancer Res.* **2011**, *71*, 5923–5931.
- (10) El Guerrab, A.; Cayre, A.; Kwiatkowski, F.; Privat, M.; Rossignol, J.-M.; Rossignol, F.; Penault-Llorca, F.; Bignon, Y.-J. Quantification of hypoxia-related gene expression as a potential approach for clinical outcome prediction in breast cancer. *PLoS One* **2017**, *12*, No. e0175960.
- (11) Churchill-Davidson, I. The oxygen effect in radiotherapy. *Oncology* **1966**, *20*, 18–29.
- (12) Daruwalla, J.; Christophi, C. Hyperbaric oxygen therapy for malignancy: a review. *World J. Surg.* **2006**, *30*, 2112–2131.
- (13) Bertout, J. A.; Patel, S. A.; Simon, M. C. The impact of O<sub>2</sub> availability on human cancer. *Nat. Rev. Cancer.* **2008**, *8*, 967–975.
- (14) Moen, I.; Stuhr, L. E. B. Hyperbaric oxygen therapy and cancer—a review. *Targeted Oncol.* **2012**, *7*, 233–242.
- (15) Bourdat, A.-G.; Douki, T.; Frelon, S.; Gasparutto, D.; Cadet, J. Tandem base lesions are generated by hydroxyl radical within isolated DNA in aerated aqueous solution. *J. Am. Chem. Soc.* **2000**, *122*, 4549–56.
- (16) Robert, G.; Wagner, J. R. Tandem lesions arising from 5-(Uracilyl)methyl peroxy radical addition to guanine: Product analysis and mechanistic studies. *Chem. Res. Toxicol.* **2020**, *33*, 566–575.
- (17) Al Tameemi, W.; Dale, T. P.; Al-Jumaily, R. M. K.; Forsyth, N. R. Hypoxia-modified cancer cell metabolism. *Front. Cell Dev. Biol.* **2019**, *7*, 4.
- (18) (a) Skov, K. A.; Macphail, S. Low concentrations of nitroimidazoles: effective radiosensitizers at low doses. *Int. J. Radiat. Oncol. Biol. Phys.* **1994**, *29*, 87–93. (b) Skov, K. A.; Koch, C. J.; Marples, B. Effect of etanidazole on absolute sensitivity and increased radioresistance in hypoxic cells at low doses. *Radiat. Oncol. Invest.* **1994**, *2*, 164–170.
- (19) Weinmann, M.; Welz, S.; Bamberg, M. Hypoxic radiosensitizers and hypoxic cytotoxins in radiation oncology. *Curr. Med. Chem.: Anti-Cancer Agents* **2003**, *3*, 364–374.
- (20) Brown, J. M. Hypoxic cytotoxic agents: a new approach to cancer chemotherapy. *Drug Resist. Updates* **2000**, *3*, 7–13.
- (21) Evans, J. W.; Yudoh, K.; Delahoussaye, Y. M.; Brown, J. M. Advances in brief Tirapazamine is metabolized to its DNA-damaging radical by intranuclear enzymes. *Cancer Res.* **1998**, *58*, 2098–2101.
- (22) Van Belle, S. Do radiosensitizers enhance the treatment of patients with NSCLC? The need for better models and alternative methods of treatment. *Chest* **1996**, *109*, 1155–1185.
- (23) Wardman, P. Nitroimidazoles as hypoxic cell radiosensitizers and hypoxia probes: misonidazole, myths and mistakes. *Br. J. Radiol.* **2019**, *92*, No. 20170915.
- (24) Bamtraf, M. M. M.; O'Neill, P.; Rao, B. S. M. Redox dependence of the rate of interaction of hydroxyl radical adducts of DNA nucleobases with oxidants: Consequences for DNA strand breakage. *J. Am. Chem. Soc.* **1998**, *120*, 11852–11857.
- (25) Valderrama-Negrón, A. C.; et al. Synthesis, spectroscopic characterization and radiosensitizing properties of acetato-bridged copper(II) complexes with 5-nitroimidazole drugs. *Inorg. Chim. Acta* **2011**, *367*, 85–92.
- (26) Santra, R. C.; Sengupta, K.; Dey, R.; Shireen, T.; Das, P.; Guin, P. S.; Mukhopadhyay, K.; Das, S. X-ray crystal structure of a Cu(II) complex with the antiparasitic drug tinidazole, interaction with calf thymus DNA and evidence for antibacterial activity. *J. Coord. Chem.* **2014**, *67*, 265–285.
- (27) Santra, R. C.; Ganguly, D.; Singh, J.; Mukhopadhyay, K.; Das, S. A study on the formation of the nitro radical anion by ornidazole and its significant decrease in a structurally characterized binuclear Cu<sup>(II)</sup>-complex: impact in biology. *Dalton Trans.* **2015**, *44*, 1992–2000.
- (28) Santra, R. C.; Ganguly, D.; Jana, S.; Banyal, N.; Singh, J.; Saha, A.; Chattopadhyay, S.; Mukhopadhyay, K.; Das, S. Synthesizing a CuII complex of tinidazole to tune the generation of the nitro radical anion in order to strike a balance between efficacy and toxic side effects. *New J. Chem.* **2017**, *41*, 4879–4886.
- (29) Okkan, S.; Uzel, R. The radiosensitizing effect of ornidazole in hypoxic mammalian tissue: An in vivo study. *Int. J. Radiat. Oncol. Biol. Phys.* **1982**, *8*, 1735–1739.
- (30) Okkan, S.; Atkovar, G.; Sahinler, I.; Turkan, S.; Uzel, R. A randomised study of ornidazole as a radiosensitiser in carcinoma of the cervix: long term results. *Br. J. Cancer* **1996**, *27*, S282–S286.
- (31) Nandy, P.; Das, S. In situ reactivity of electrochemically generated nitro radical anion on Ornidazole and its monomeric Cu(II) complex with nucleic acid bases and calf thymus DNA. *Inorg. Chim. Acta* **2020**, *501*, No. 119267.
- (32) Nandy, P.; Singha, S.; Banyal, N.; Kumar, S.; Mukhopadhyay, K.; Das, S. A Zn<sup>II</sup> complex of Ornidazole with decreased nitro radical anion is still very active on *Entamoeba histolytica*. *RSC Adv.* **2020**, *10*, 23286–23296.
- (33) Santra, R. C.; Ganguly, D.; Bhattacharya, D.; Karmakar, P.; Saha, A.; Das, S.  $\gamma$  radiation-induced damage of nucleic acid bases, calf thymus DNA and DNA within MCF-7 breast cancer cells by [Cu<sub>2</sub>(OAc)<sub>4</sub>(tnz)<sub>2</sub>]: a potential radiosensitizer. *New J. Chem.* **2017**, *41*, 11679–11685.
- (34) Prütz, W. A. Inhibition of DNA-ethidium bromide intercalation due to free radical attack upon DNA, I. Comparison of the effects of various radicals. *Radiat. Environ. Biophys.* **1984**, *23*, 1–6.
- (35) Das, S.; Saha, A.; Mandal, P. C. Radiation-induced double-strand modification in calf thymus DNA in the presence of 1, 2-dihydroxy-9,10-anthraquinone and its Cu(II) complex. *Environ. Health Perspect.* **1997**, *105*, 1459–1462.
- (36) Das, S.; Mandal, P. C. Anthracyclines as radiosensitizers: A Cu(II) complex of a simpler analogue modifies DNA in Chinese Hamster V79 cells under low-dose  $\gamma$  radiation. *J. Radioanal. Nucl. Chem.* **2014**, *299*, 1665–1670.
- (37) Radiation Processing of Aqueous Systems from the "Lecture given at the IAEA's Interregional Training Course on Developments in the Application of Electron Beams in Industry and Environmental Protection", Warsaw, Poland, 6–17 October 1997 by Peter Gehringer, SEIBERSDORF REPORT, 1997; p 2.
- (38) Tremblay, S.; Wagner, J. R. Dehydration, deamination and enzymatic repair of cytosine glycols from oxidized poly(dG-dC) and poly(dI-dC). *Nucleic Acids Res.* **2008**, *36*, 284–293.

- (39) Roots, R.; Chatterjee, A.; Blakely, E.; Chang, P.; Smith, K.; Tobias, C. Radiation responses in air, nitrous oxide, and nitrogen-saturated mammalian cells. *Radiat. Res.* **1982**, *92*, 245–254.
- (40) (a) Bhattacharyya, S. N.; Mandal, P. C. Effect of Cu(II) ions on the  $\gamma$ -radiolysis of uracil. *J. Chem. Soc., Faraday Trans. 1* **1983**, *79*, 2613–2629. (b) Bhattacharyya, S. N.; Mandal, P. C. Reactions of some free radicals derived from uracil with nickel(II) compounds. *J. Chem. Soc., Faraday Trans. 1* **1984**, *80*, 1205–1215.
- (41) Cadet, J.; Douki, T.; Ravanat, J.-L. Oxidatively generated damage to the guanine moiety of DNA: mechanistic aspects and formation in cells. *Acc. Chem. Res.* **2008**, *41*, 1075–1083.
- (42) Cadet, J.; Davies, K. J. A.; Medeiros, M. H. G.; Mascio, P. D.; Wagner, J. R. Formation and repair of oxidatively generated damage in cellular DNA. *Free Radical Biol. Med.* **2017**, *107*, 13–34.
- (43) Steenken, S.; Jagannadham, V. Reaction of 6-yl radicals of uracil, thymine, and cytosine and their nucleosides and nucleotides with nitrobenzenes via addition to give nitroxide radicals. Hydroxide ion-catalyzed nitroxide heterolysis. *J. Am. Chem. Soc.* **1985**, *107*, 6818–6826.
- (44) (a) Cadet, J.; Guttin-Lombard, M.; Teoule, R. Gamma radiolysis of thymine in oxygen-free aqueous solution in the presence of electron affinic radiosensitizers: identification of stable products. *Int. J. Radiat. Biol.* **1976**, *30*, 1–11. (b) Cadet, J.; Balland, A.; Berger, M. Radio-induced Degradation of Thymidine in Deaerated Aqueous Solution. *Int. J. Radiat. Biol.* **1981**, *39*, 119–133.
- (45) Nandy, P.; Das, S. Interaction of electrochemically generated reduction products of Ornidazole with nucleic acid bases and calf thymus DNA. *J. Indian Chem. Soc.* **2018**, *95*, 1009–1014.
- (46) Puig, S.; Thiele, D. J. Molecular mechanisms of copper uptake and distribution. *Curr. Opin. Chem. Biol.* **2002**, *6*, 171–180.
- (47) Deb, T.; Gopal, P. K.; Ganguly, D.; Das, P.; Paul, M.; Saha, M. B.; Paul, S.; Das, S. Enhancement of anti-leukemic potential of 2-hydroxyphenyl-azo-2'-naphthol (HPAN) on MOLT-4 cells through conjugation with Cu(II). *RSC Adv.* **2014**, *4*, 18419–18430.
- (48) Das, P.; Jain, C. K.; Roychoudhury, S.; Majumder, H. K.; Das, S. Design, synthesis and in vitro anticancer activity of a Cu(II) complex of carminic acid: a novel small molecule inhibitor of human DNA topoisomerase I and topoisomerase II. *ChemistrySelect* **2016**, *1*, 6623–6631.
- (49) Ganguly, D.; Jain, C. K.; Santra, R. C.; Roychoudhury, S.; Majumder, H. K.; Mondal, T. K.; Das, S. Anticancer activity of a complex of Cu<sup>II</sup> with 2-(2-hydroxyphenylazo)-indole-3'-acetic acid on three different cancer cell lines: a novel feature, for azocomplexes. *ChemistrySelect* **2017**, *2*, 2044–2054.
- (50) Mandal, B.; Singha, S.; Dey, S. K.; Mazumdar, S.; Kumar, S.; Karmakar, P.; Das, S. Cu<sup>II</sup> complex of emodin with improved anticancer activity as demonstrated by its performance on HeLa and Hep G2 cells. *RSC Adv.* **2017**, *7*, 41403–41418.
- (51) Goldstein, S.; Czapski, G. Mechanisms of the reactions of some copper complexes in the presence of DNA with superoxide, hydrogen peroxide, and molecular oxygen. *J. Am. Chem. Soc.* **1986**, *108*, 2244–2250.
- (52) Que, B. G.; Downey, K. M.; So, A. G. Degradation of DNA by a 1, 10-phenanthroline copper complex. The role of hydroxyl radicals. *Biochemistry* **1980**, *19*, 5987–5991.
- (53) Marshall, L. E.; Graham, D. R.; Reich, K. A.; Sigman, D. S. Cleavage of deoxyribonucleic acid by the 1,10-phenanthroline-cuprous complex. Hydrogen peroxide requirement and primary and secondary structure specificity. *Biochemistry* **1981**, *20*, 244–250.
- (54) Yamamoto, K.; Kawanishi, S. Hydroxyl free radical is not the main active species in site-specific DNA damage induced by copper(II) ion and hydrogen peroxide. *J. Biol. Chem.* **1989**, *264*, 15435–15440.
- (55) Frelon, S.; Douki, T.; Favier, A.; Cadet, J. Hydroxyl radical is not the main reactive species involved in the degradation of DNA bases by copper in the presence of hydrogen peroxide. *Chem. Res. Toxicol.* **2003**, *16*, 191–197.
- (56) Oikawa, S.; Murakami, K.; Kawanishi, S. Oxidative damage to cellular and isolated DNA by homocysteine: implications for carcinogenesis. *Oncogene* **2003**, *22*, 3530–3538.
- (57) Prütz, W. A. Inhibition of DNA-ethidium bromide intercalation due to free radical attack upon DNA, II. Copper(II)-catalysed DNA damage by O<sub>2</sub><sup>•-</sup>. *Radiat. Environ. Biophys.* **1984**, *23*, 7–18.
- (58) Johnson, G. R. A.; Nazhat, N. B. Kinetics and mechanism of the reaction of the bis(1,10-phenanthroline) copper(I) ion with hydrogen peroxide in aqueous solution. *J. Am. Chem. Soc.* **1987**, *109*, 1990–1994.



# In Situ Reactivity of Electrochemically Generated Nitro Radical Anion on Tinidazole and Its Monomeric and Dimeric Cu<sup>II</sup> Complexes on Model Biological Targets with Relative Manifestation of Preventing Bacterial Biofilm Formation

Promita Nandy, Ramesh C. Santra, Dibyajit Lahiri, Moupriya Nag, and Saurabh Das\*



Cite This: *ACS Omega* 2022, 7, 8268–8280



Read Online

ACCESS |



Metrics & More

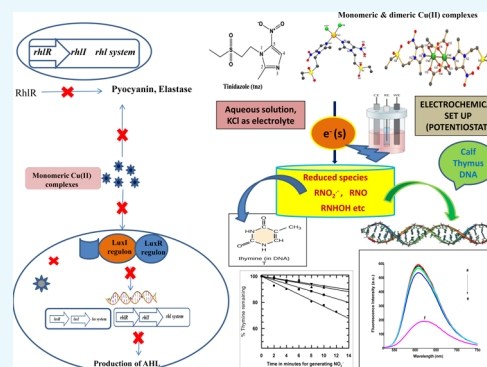


Article Recommendations



Supporting Information

**ABSTRACT:** Formation of nitro radical anion ( $-\text{NO}_2^{\bullet-}$ ) and other reduction products of 5-nitroimidazoles, although important for antimicrobial activity, makes the drugs neurotoxic. Hence, an appropriate generation and their role in the free radical pathway needs proper realization. This was attempted by studying the action of tinidazole and its Cu<sup>II</sup> complexes on model targets (nucleic acid bases and calf thymus DNA). Results obtained were correlated with studies on biological species where prevention of biofilm formation on *Staphylococcus aureus* and *Pseudomonas aeruginosa* was followed. Tinidazole and its Cu<sup>II</sup> complexes subjected to electrochemical reduction in aqueous solution, under de-aerated conditions, interact with model nucleic acid bases and calf thymus DNA. These model targets were followed to realize what happens when such compounds undergo enzymatic reduction within cells of microorganisms that they eventually kill. Studies reveal that Cu<sup>II</sup> complexes were better in modifying nucleic acid bases and calf thymus DNA than tinidazole; damage caused to nucleic acid bases was correlated with that caused to DNA, indicating that compounds affect DNA rich in thymine and adenine. Minimum bactericidal concentrations on sessile *S. aureus* and *P. aeruginosa* for the monomeric Cu<sup>II</sup> complex were 12.5 and 20.25  $\mu\text{M}$  respectively, while those for the dimeric complex were 40.0 and 45.0  $\mu\text{M}$ , respectively. Biofilm formation by *P. aeruginosa* and *S. aureus* and viability count of sessile cells were also determined. Cu<sup>II</sup> complexes of tinidazole brought about substantial reduction in carbohydrate and protein content in *S. aureus* and *P. aeruginosa*. Downregulation of quorum sensing signaling mechanism viz. reduced production of pyocyanin and elastase during biofilm formation was also detected. Cu<sup>II</sup> complexes showed much higher tendency to prevent biofilm formation than tinidazole, almost comparable to amoxicillin, an established drug in this regard.



## INTRODUCTION

5-Nitroimidazoles are important molecules for pharmaceutical applications and are found in different formulations.<sup>1–5</sup> They address a wide spectrum of medical issues ranging from infections caused by different microbes to being used as anticancer agents in radiotherapy.<sup>1–8</sup> Although metronidazole is the most used, issues like drug resistance and neurotoxicity have resulted in a search for compounds having comparable efficacy but with significantly less adverse effects.<sup>1–3,5–10</sup> Tinidazole (tnz) is a compound that nicely fits this requirement, although conflicting reports on its efficacy and adverse effects do exist.<sup>11–14</sup> Since its antimicrobial activity was first reported, tnz showed a steady increase in acceptability as a drug.<sup>15–18</sup> However, as is true for all 5-nitroimidazoles, its efficacy is accompanied by toxic side effects, which although quoted to be less than metronidazole, do exist.<sup>11–18</sup> The problem with this family of drugs is that, the nitro-radical anion,  $\text{RNO}_2^{\bullet-}$  (where R represents the portion other than the nitro group) is responsible both for efficacy and toxic side

effects.<sup>11–18</sup> Hence, an approach that enables controlling the generation of  $\text{RNO}_2^{\bullet-}$  is an extremely relevant issue.<sup>19–21</sup> Within biological systems, 5-nitroimidazoles are first reduced by enzymes pyruvate ferredoxin oxidoreductase<sup>9,22,23</sup> that prepares them for entry into the cells of the target organism. Thereafter, the nitro-radical anion imparts its drug action.

Although related literature mentions  $\text{RNO}_2^{\bullet-}$  to be responsible for drug action, very few studies have gone into details of such claims that would help us realize their contribution toward cytotoxic action. Research has revealed that complex formation of 5-nitroimidazoles modulate the generation of  $\text{RNO}_2^{\bullet-}$  that might then be expected to decrease

Received: September 10, 2021

Accepted: February 10, 2022

Published: March 1, 2022



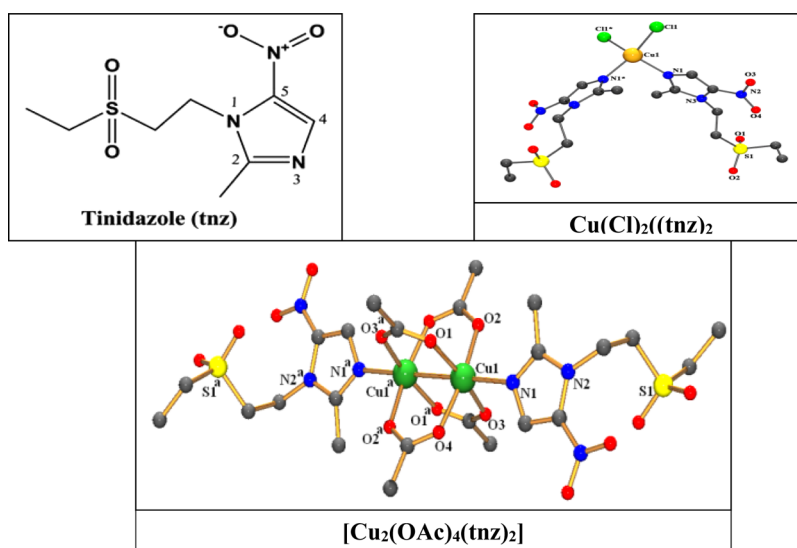


**Figure 1.** Structure of tnz and its monomeric and dimeric Cu<sup>II</sup> complexes.

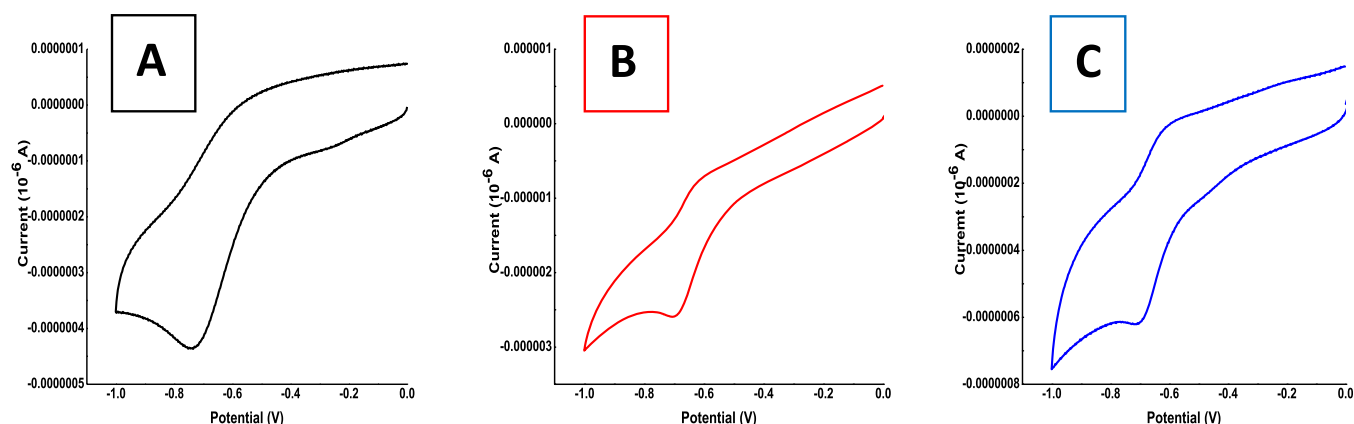


**Figure 2.** Cyclic voltammograms of 100  $\mu\text{M}$  (A) tnz, (B) its monomeric Cu(II) complex, and (C) its dimeric Cu(II) complex showing a single-step four electron reduction of the nitro group in aqueous solution using a glassy carbon electrode;  $[\text{NaCl}] = 120 \text{ mM}$ ; scan rate = 0.025 V/s; Ag/AgCl, satd. KCl was used as the reference electrode; and temperature = 303 K.

toxic side effects.<sup>20,21</sup> Because  $\text{RNO}_2^{\bullet-}$  is important for drug efficacy, its decrease, following complex formation, should logically affect drug action. However, we found from several previous studies that complex formation did not interfere with drug efficacy. In fact, most complexes were either similar in performance on a chosen microbial target when compared with 5-nitroimidazole, from which the complex was prepared, or that the complex performs better.<sup>20,21,24,25</sup> Because complexes result in a decrease in  $\text{RNO}_2^{\bullet-}$  and yet there is no loss in efficacy, this suggests they have other attributes<sup>20,21,24,25</sup> that enable them to overcome any deficiency that might occur in the free radical pathway.

Through this study, we tried to look at aspects related to cytotoxicity that are either initiated by  $\text{RNO}_2^{\bullet-}$  or other reduction products formed on the monomeric and dimeric complexes of Cu<sup>II</sup> with tnz (Figure 1) on nucleic acid bases and calf thymus DNA to correlate what might happen when such compounds are enzymatically reduced in biological systems, generating species having the potential to kill disease-causing microbes.<sup>9,20–25</sup>

Reduction products of each compound were generated electrochemically maintaining a glassy carbon electrode at its cathodic peak potential using a method described earlier.<sup>26,27</sup>

In the immediate vicinity of electrochemically generated reduction products, nucleic acid bases or calf thymus DNA were maintained, one at a time so that reduced products react instantaneously. Although the reaction on a model target under laboratory conditions can never be identical with what happens inside cells, it can however shed some light on such processes because similar species were generated enzymatically within cells following the transfer of electron(s) to 5-nitroimidazoles by electron-donating groups present within cells.<sup>9,22,23,28</sup> In situ reactivity of reduction products with nucleic acid bases or calf thymus DNA were subsequently analyzed to realize changes brought about on a target maintained in the immediate vicinity of such generation. To check for a correlation between model studies and the potency of the monomeric and dimeric complexes to inhibit biofilm formation, detailed studies were performed on *Pseudomonas aeruginosa* and *Staphylococcus aureus*.

Most bacterial species possess an ability to live in complex sessile communities called biofilm under environmentally stressed conditions. Such sessile micro-colonies remain embedded within self-secreted extracellular polymeric substances (EPSs) and are responsible for the development of major types of nosocomial infections following biofilm

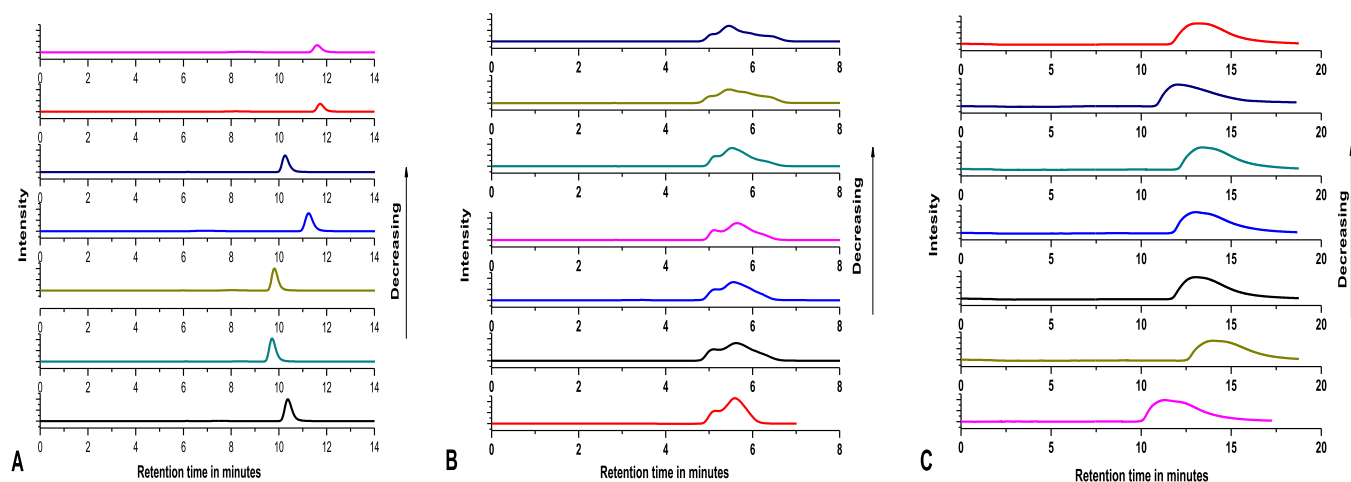


**Figure 3.** HPLC chromatograms of  $10^{-3}$  M (A) thymine, (B) cytosine, and (C) adenine solutions recorded at 254 nm following them being kept in the immediate vicinity of electrochemically reduced  $10^{-4}$  M  $\text{Cu}_2^{\text{II}}(\text{OAc})_4(\text{tnz})_2$ .

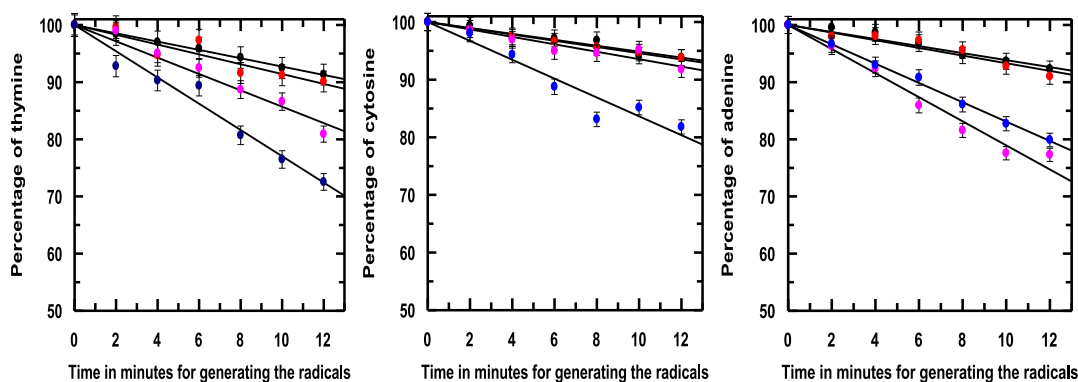


**Figure 4.** Damage of nucleic acid bases was monitored using HPLC at 254 nm following an electrochemical reduction of compounds in whose immediate vicinity nucleic acid bases were maintained. Respective reduction potentials were  $-0.745$  V for tnz,  $-0.700$  V for the monomeric Cu(II) complex, and  $-0.710$  V for the dimeric Cu(II) complex. Electrochemical reduction was carried out under argon saturated conditions. (Black ●) indicates control experiments when a nucleic acid base was subjected to reduction in the absence of any compound; (red ●) in presence of tnz; (brown ●) in presence of the monomeric complex; and (green ●) in presence of the dimeric complex. [thymine] = [cytosine] = [adenine] =  $1 \times 10^{-3}$  mol  $\text{dm}^{-3}$ ; [tnz] = [monomeric Cu(II)–tnz] = [dimeric Cu(II)–tnz] =  $1 \times 10^{-4}$  mol  $\text{dm}^{-3}$ .

formation.<sup>29,30</sup> Biofilms are highly resistant both to specific (adaptive) and nonspecific (innate) host defense mechanisms. The development of EPS and subsequent slower diffusion of antimicrobials through the biofilm matrix reduced the rate of metabolism, and so forth, and make bacterial cells less susceptible to phagocytic activities of macrophages and more resistant to antibiotics.<sup>31,32</sup> Such enhancement of resistance resulted in a search for alternate therapies for treating biofilm-associated chronic infections caused by *P. aeruginosa* and *S. aureus*.<sup>33,34</sup> Through this work, we aim to show the potent efficacy of monomeric and dimeric complexes of Cu(II) with tnz (Figure 1) in removing persistent microbial cells of *P. aeruginosa* and *S. aureus*.

## RESULTS

**In Situ Reactivity of Electrochemically Generated Reduction Products.** Figure 2 shows voltammograms for tnz, monomeric  $[\text{Cu}(\text{tnz})_2\text{Cl}_2]$ , and dimeric  $[\text{Cu}_2^{\text{II}}(\text{OAc})_4(\text{tnz})_2]$  complexes when each was subjected to cyclic voltammetry in an aqueous solution. From the voltammograms, reduction peak potentials of tnz,  $[\text{Cu}(\text{tnz})_2\text{Cl}_2]$ , and  $[\text{Cu}_2^{\text{II}}(\text{OAc})_4(\text{tnz})_2]$  were identified at  $-0.745$ ,  $-0.700$ , and  $-0.710$  V, respectively. It may be mentioned here that for 5-nitroimidazoles in

aqueous solution, reduction to the nitro-radical anion is not identified separately; instead, there is a single-step four electron reduction (eq 1).<sup>35,36</sup>



Identification of the potential for the reduction of each compound is important for the study to be undertaken because each compound would have to be reduced to generate suitable reduced species that might interact with a target. Therefore, when in the immediate vicinity of any of the compounds, subjected to electrochemical reduction at a constant potential, nucleic acid bases or calf thymus DNA were maintained, and reduced products would have a high probability to interact with them. Outcome of such interactions was ascertained for nucleic acid bases using HPLC (high-performance liquid chromatography) and for DNA using the ethidium bromide fluorescence technique.<sup>26,27,37</sup>

**Interaction of Electrochemically Generated Reduction Products with Nucleic Acid Bases.** Various electrochemically reduced species generated in aqueous solution for a compound, following maintenance of a glassy carbon electrode at its cathodic peak potential, for different periods of time,

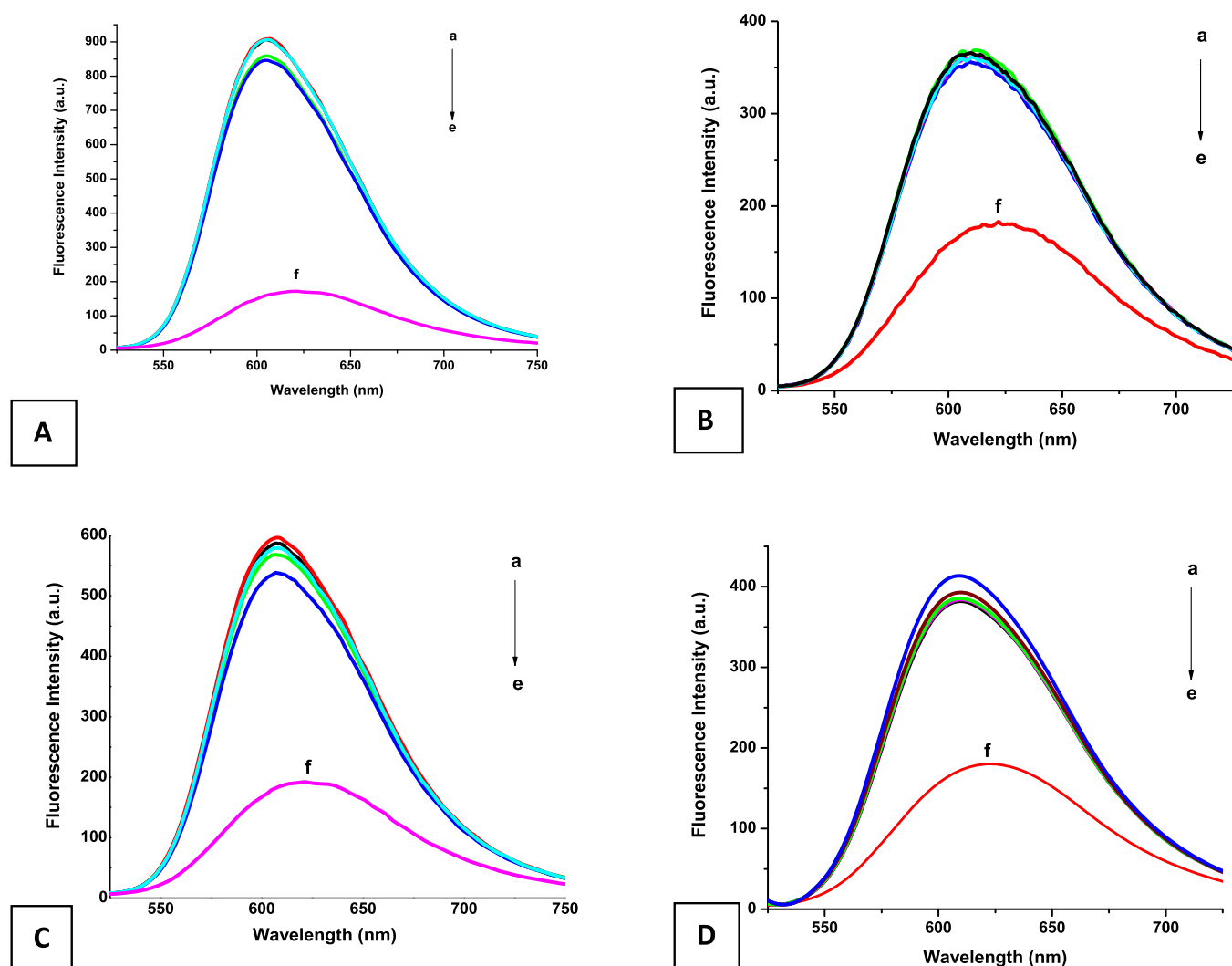


**Figure 5.** Decrease in fluorescence intensity of the DNA-EtBr adduct recorded at 600 nm ( $\lambda_{\text{ex}} = 510$  nm) following the interaction with electrochemically generated reduced species in (A) absence of any compound, (B) presence of tnz, (C) presence of  $\text{Cu}(\text{tnz})_2\text{Cl}_2$ , and (D) presence of  $\text{Cu}_2(\text{OAc})_4(\text{tnz})_2$  at different time intervals of (i) 0 min, (ii) 5 min, (iv) 10 min, (v) 15 min, and (vi) 20 min. Spectrum (f) in each plot is that of free EtBr.

indicate that it leads to a gradual degradation of nucleic acid bases (Figure 3).

Responses for nucleic acid bases shown in Figure 3 is based on their individual elution peaks under a specific solvent composition eluting them, which was considered as the standard HPLC chromatogram for that nucleic acid base (Figure S1, Supporting Information). Based on elution peaks of individual compounds, degradation plots were quantified (Figure 4). Such standard curves enabled determination of the concentration of nucleic acid bases in the performed experiments. The amount of a nucleic acid base remaining following interaction with reduced species was realized by collecting aliquots from the reaction vessel at different time intervals and evaluating them based on Figure S1, Supporting Information. Figure 4 shows the degradation of nucleic acid bases followed by HPLC at 254 nm after they were allowed to interact with reduced products obtained from tnz and its monomeric and dimeric complexes.<sup>37</sup>

We wanted to generate the data for guanine also because guanine is easily damaged by various radical species. However, owing to issues concerning its solubility in aqueous solution

which despite our best efforts, we had to refrain from going ahead with it. The results we got with guanine were erratic and inconsistent. Hence, we decided to discuss the data obtained for thymine, cytosine, and adenine only. However, if the damage on guanine could be shown, we would have been in a better position to explain the targeting of 5-nitroimidazoles and their metal complexes based on nucleotide content of DNA of the target organism which could then provide a good correlation between an actual drug action reported and this study (Table S1, Supporting Information). Although without guanine this may still be realized, a data for guanine would have made it more convincing.

**Interaction of Electrochemically Generated Reduction Products with Calf Thymus DNA.** A similar study as the one described above was performed maintaining calf thymus DNA in the immediate vicinity of electrochemically generated reduced species in aqueous solution at pH 7.4 using the same glassy carbon electrode maintained at the identified reduction potential of the compound. In experiments with calf thymus DNA, we subjected the system to slightly longer times than was used for electrochemical reduction of the compounds

to reduced species in case of nucleic acid bases, so that reduced products were produced in greater quantity and there occurred a detectable change in DNA, monitored by the fluorescence technique using EtBr.<sup>38–42</sup>

Figure 5 depicts plots showing fluorescence of calf thymus DNA with EtBr, after it was allowed to interact with reduced products generated electrochemically on each compound, in whose vicinity calf thymus DNA was maintained. In each experiment, mixtures of DNA and EtBr were excited at 510 nm and emission was measured at 600 nm.

Modification of calf thymus DNA was realized by plotting percentage of DNA remaining intact against time provided for the generation of electrochemically reduced species on each compound following maintenance of a glassy carbon electrode at the predetermined reduction potential of a compound in an aqueous solution at pH 7.4 (Figure 6). Both Figure 6 and

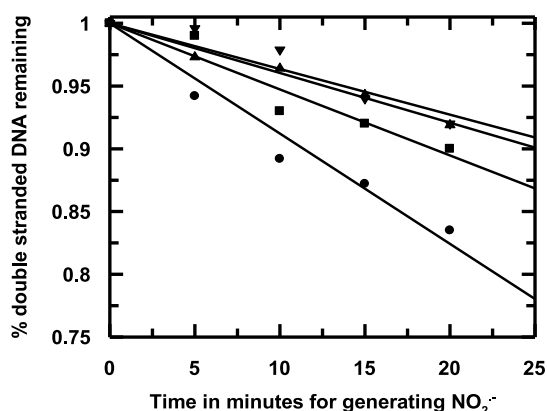


**Figure 6.** Degradation curves show modification of calf thymus DNA in the absence and presence of either tnz or (▲) its monomeric (■), dimeric (●) Cu(II) complexes;  $[tnz] = [Cu(tnz)_2Cl_2] = [Cu_2(OAc)_4(tnz)_2] = 1 \times 10^{-4} \text{ mol dm}^{-3}$ . (▼) indicates modification of calf thymus DNA in the absence of any compound when subjected to a constant potential of  $-0.700 \text{ V}$  for the same duration of time.

Table 2 indicate the damage caused to calf thymus DNA in the presence of the compounds used in the study. Considering  $I_0$  as the intensity of fluorescence of pure DNA treated with EtBr,  $I_{EtBr}$  as intensity of fluorescence for EtBr itself, and  $I_{expt}$  as the

intensity of fluorescence of a DNA sample subjected to conditions of the experiment and then treated with EtBr, the fraction of DNA remaining intact is obtained from

$$\text{fraction of DNA remaining} = \frac{(I_{\text{expt}} - I_{\text{EtBr}})}{(I_0 - I_{\text{EtBr}})}$$

**Inhibitory Action of Complexes on Biofilm Formation.** Determination of Minimum Bactericidal Concentration. The monomeric  $Cu^{II}$  complex showed the inhibition of biofilm formation for *S. aureus* and *P. aeruginosa* at concentrations of 12.5 and 20.25  $\mu\text{M}$ , respectively, while that for the dimeric complex was 40 and 45  $\mu\text{M}$ , respectively, suggesting that the monomeric complex showed better efficacy against biofilm formation by cells of *P. aeruginosa* and *S. aureus*. The minimum bactericidal concentrations of tnz for *S. aureus* and *P. aeruginosa* were 50 and 59.25  $\mu\text{M}$ , respectively. Although tnz is an established antibacterial drug,<sup>43,44</sup> very few literature show its antibiofilm properties.<sup>45,46</sup>

**Inhibition of Biofilm Formed by *P. aeruginosa* and *S. aureus*.** The monomeric complex of  $Cu^{II}$  inhibited biofilm formation due to *P. aeruginosa* by  $88.52 \pm 3.45\%$ , whereas the dimeric complex could decrease it by  $76.95 \pm 2.29\%$  (amoxicillin reduces biofilm formation by  $62.12 \pm 2.25\%$ ). For *S. aureus* decrease in biofilm formation due to the monomeric complex was by  $92.16 \pm 4.87\%$ , while for the dimeric complex, it was  $81.25 \pm 3.55$  (amoxicillin decreases it by  $72.56 \pm 1.29$ ) (monomer  $p < 0.01$ , dimer  $p < 0.05$ ) (Figure 7).

**Disintegration of Structural Component of EPS.** EPS matrix of a biofilm comprises a rich supply of nutrients in addition to lipid molecules, nucleic acids, proteins, extracellular DNA, quorum sensing (QS) signaling molecules and water. Hence, removal of biofilm involves strategies that target the EPS matrix leading to its disintegration via a decrease in the synthesis of biomolecules.

The monomeric complex inhibited carbohydrate content within the EPS of the biofilm formed due to *P. aeruginosa* by  $75.26 \pm 5.8\%$ , the dimeric complex by  $71.23 \pm 3.55\%$  and amoxicillin by  $61.78 \pm 2.47\%$ . In case of *S. aureus* for the monomeric complex, the decrease was by  $80.29 \pm 5.8\%$ , for the dimeric complex, by  $75.89 \pm 4.7\%$  and for amoxicillin, by  $69.56 \pm 3.25\%$  ( $p < 0.01$ ). It was further observed that the

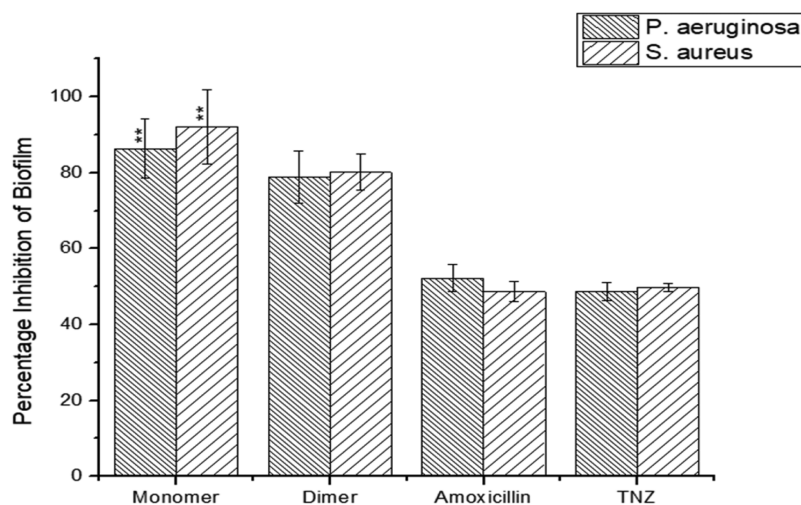


**Figure 7.** Maximum inhibition of biofilm formation due to *P. aeruginosa* and *S. aureus* was due to the monomeric complex ( $p < 0.01$ ).

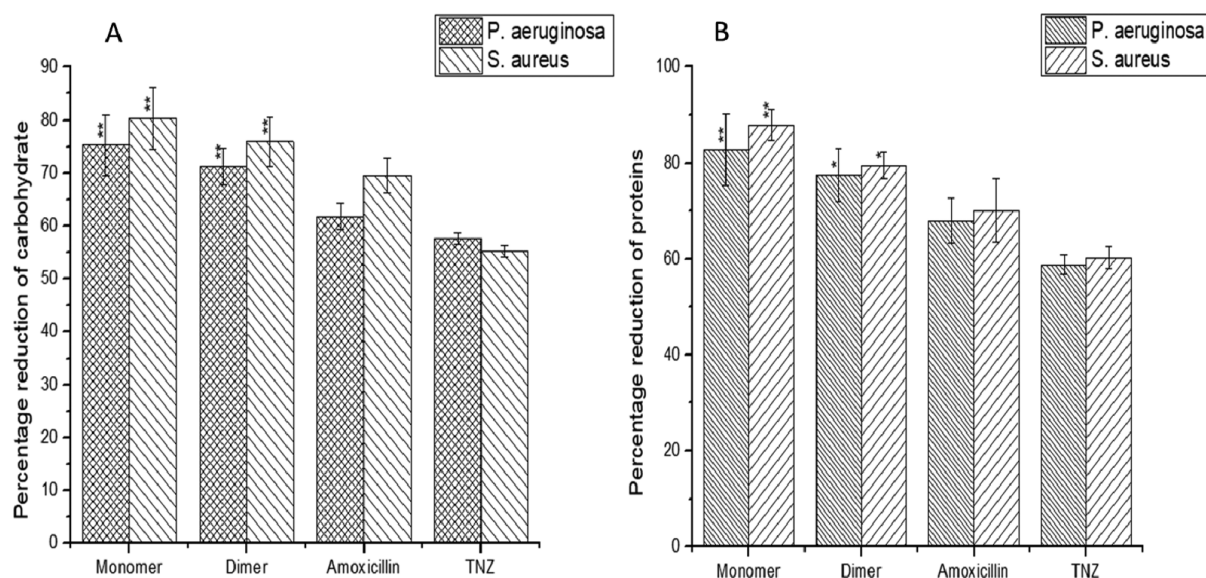


Figure 8. Reduction in carbohydrate (A) and protein (B) present within the EPS.

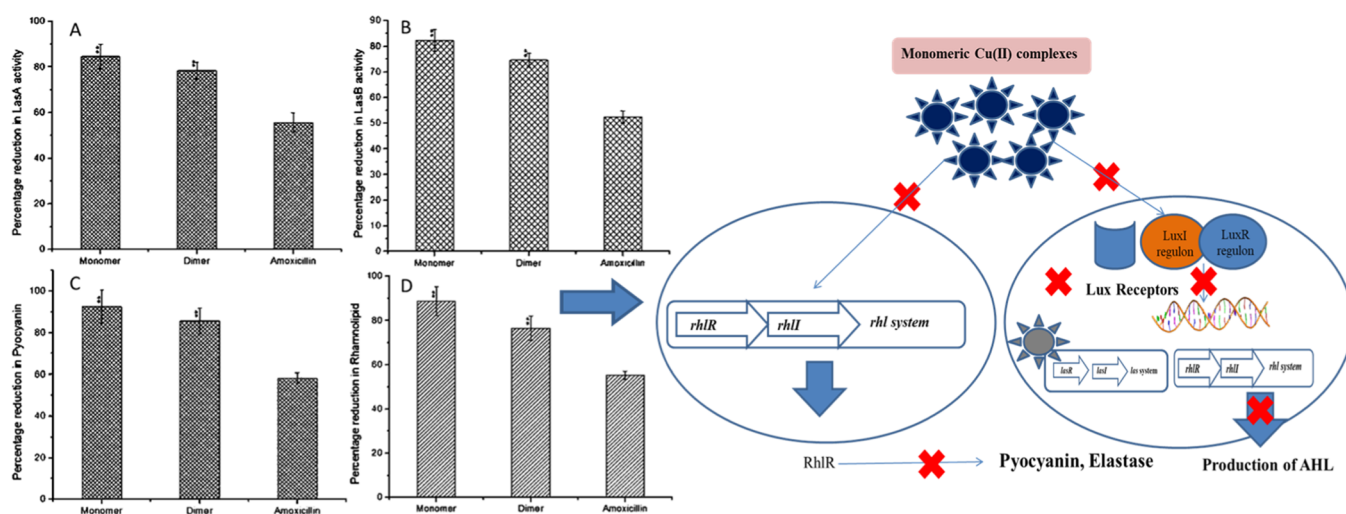


Figure 9. Inhibition of the QS signaling mechanism during biofilm formation.

monomeric complex was able to maximally reduce the protein content of EPS of *P. aeruginosa* and *S. aureus* by  $75.26 \pm 5.8$  and  $80.29 \pm 5.8\%$ , respectively ( $p < 0.01$ ), which was even higher than that achieved with the standard antibiotic amoxicillin (Figure 8).

**Downregulation of the QS Pathway during Biofilm Formation.** Antimicrobial potential of monomeric and dimeric complexes of  $\text{Cu}^{\text{II}}$  with tnz identifies them as important therapeutic agents. It was earlier observed that the monomeric complex plays a key role in controlling infections caused by microbes.<sup>21</sup> *P. aeruginosa* is known to have many virulence genes viz *LasI/Rhl* that are activated during the QS network leading to the expression of virulence factors such as elastase, rhamnolipid, and pyocyanin.<sup>47</sup> The amount of las A protease and las B elastase was monitored with or without  $\text{Cu}^{\text{II}}$  complexes (Figure 9). We observed that *las*-regulated virulence genes *las A* and *las B* were significantly downregulated to  $82.4 \pm 4.25\%$  in the presence of the monomeric complex (Figure 8 A,B) as compared to the dimeric one or even in comparison to amoxicillin suggesting that the monomeric complex has the ability to block the synthesis of signaling molecules responsible

for regulating biofilm formation by inhibiting *LasI/Rhl* I synthase.<sup>48</sup> A lack of production of virulence factor pyocyanin after treatment of *P. aeruginosa* with both complexes was observed with a maximum reduction of  $86.34 \pm 7.25\%$  in the presence of the monomeric complex. Thus experimental results show that the monomeric complex was able to bring about inhibition of QS maximally in *P. aeruginosa*.

## DISCUSSION

Maintenance of a glassy carbon electrode at the cathodic peak potential of a compound, in aqueous solution, is evidenced to bring about a “single-step four electron reduction” of 5-nitroimidazoles. As a result, species are expected to be sequentially generated within a small time scale. Hence, the damage caused to a target, that is, to nucleic acid bases or to calf thymus DNA, maintained in the immediate vicinity of the generation of reduced species may not be exclusively due to a particular species. While  $\text{RNO}_2^{\bullet-}$  could have a substantial role, other reduction products formed during the electrochemical reduction of the compounds would also generate species that could modify targets. Because formation of  $\text{RNO}_2^{\bullet-}$  is the first

## Scheme 1. Probable Mechanism for the Interaction of the Nitro-Radical Anion with Thymine

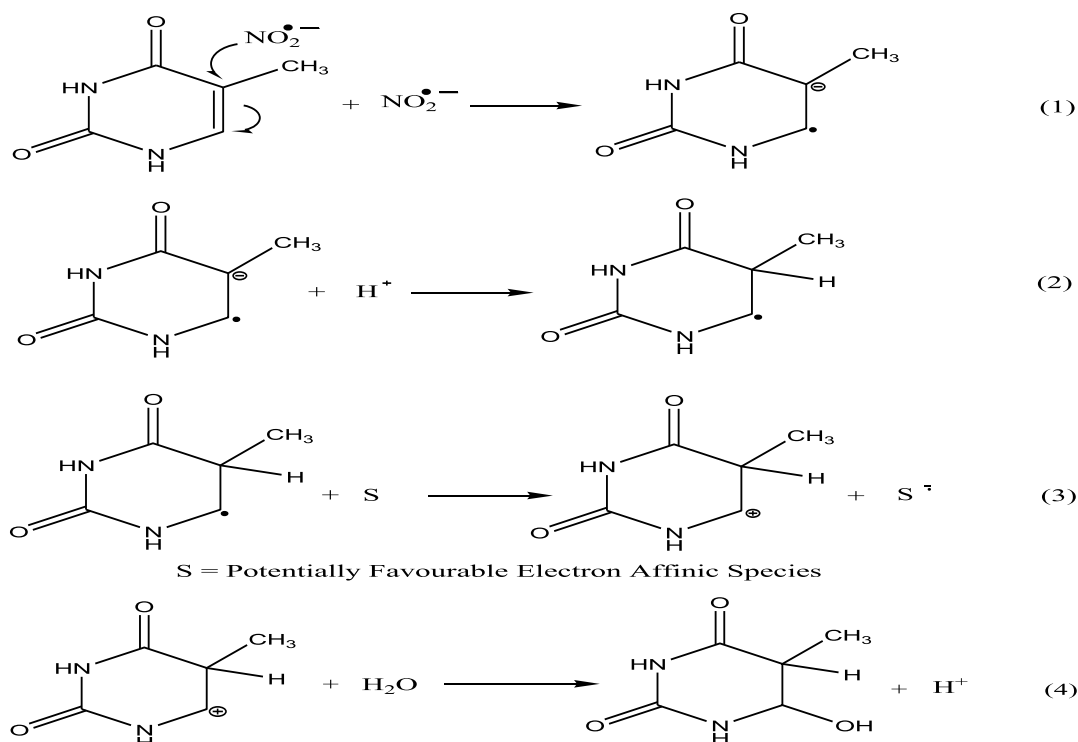


**Table 1. Enhancement Ratio for the Damage Caused to Thymine Following the Reduction of tnz and Its Cu(II) Complexes at Respective Reduction Potentials in Aqueous Solution**

sensitizer	loss of thymine from slope of degradation plot	enhancement ratio (for thymine)	loss of cytosine from slope of degradation plot	enhancement ratio (for cytosine)	loss of adenine from slope of degradation plot	enhancement ratio (for adenine)
tnz	0.73		0.51		0.61	
tnz	0.86	1.18	0.54	1.06	0.67	1.10
Cu–tnz <sup>monomer</sup>	1.43	1.96	0.65	1.27	2.11	3.46
Cu–tnz <sup>dimer</sup>	2.30	3.15	1.64	3.22	1.69	2.77

step of the reduction process and being a radical, it is likely to have a high probability to interact with a target before being reduced to its next state. If the rate of interaction of  $\text{RNO}_2^{\bullet-}$  either with a nucleic acid base or with calf thymus DNA is higher than its tendency to be reduced further, interaction with  $\text{RNO}_2^{\bullet-}$  would be predominant. Hence, while other reduction products of a complex or of tnz could well be involved in a modification of the target,  $\text{RNO}_2^{\bullet-}$  might have a substantial contribution to the damage detected (Scheme 1, shown with respect to thymine).<sup>27,35</sup> This study was actually performed to realize how different reduction products generated electrochemically either on tnz or on its complexes with Cu(II) interact with nucleic acid bases and with DNA to realize what would happen when they are present within cells and undergo enzymatic reduction. For several decades now, the reduction of nitroimidazoles is considered very crucial for cytotoxic action for which they are much sought after.<sup>1–3,5–14</sup>

Again, considering the variety of species that are formed in solution, there is a good possibility for the formation of  $\text{RNO}_2^{\bullet-}$  either directly or through comproportionation, when an  $-\text{NO}_2$  containing moiety (either on tnz or on a complex) interacts with another molecule that contains, say,  $-\text{NHOH}$ .<sup>19,35,36,49,50</sup> The possibility of disproportionation of  $\text{RNO}_2^{\bullet-}$ , known to depend on pH, on the solvent and also on the material of the electrode also exist.<sup>19,35,36,49,50</sup> Hence,

depending on different reduction products, that in turn depends on whether they were generated on tnz present alone or on tnz present as part of a complex, substrates (nucleic acid bases or calf thymus DNA) interacting with  $\text{RNO}_2^{\bullet-}$  become a high possibility. If the rate of depletion of  $\text{RNO}_2^{\bullet-}$  in solution either due to disproportionation or in some other pathway is less, there is a good possibility of it interacting with a target maintained in its immediate vicinity. If, however, it is otherwise, then the interaction due to  $\text{RNO}_2^{\bullet-}$  would not be dominant, that is, it would not be the major cause of transformations either on nucleic acid bases or on calf thymus DNA. However, given the experimental design, although disproportionation is a possibility, it would only occur if the concentration of the species formed in solution are higher than that in our experiments. Under the conditions of the experiment, concentrations of electrochemically reduced species formed on tnz or its complexes would never be very high in solution; in fact, immediately after their generation, they would see more of the nucleic acid bases than one of its own kind (target/compound: 10:1); hence, the scope of disproportionation of  $\text{RNO}_2^{\bullet-}$  would be small.<sup>19,35,36,49,50</sup> Although explained qualitatively,  $\text{RNO}_2^{\bullet-}$  could eventually become an important species among other reduced products generated either on free tnz or on tnz present as part of a Cu<sup>II</sup> complex that might interact with a target.

A comparison of the damage caused to nucleic acid bases (Table 1) or to calf thymus DNA (Table 2) reveals that the

**Table 2. Enhancement Ratio for the Damage Caused to Calf Thymus DNA Following the Reduction of tnz and Its Cu(II) Complexes at Their Respective Reduction Potentials in Aqueous Solution**

sensitizer	DNA double strand modification from slopes of degradation plots	enhancement <sup>ratio</sup> (for DNA)
	0.0036	
tnz	0.0040	1.10
Cu–tnz <sup>monomer</sup>	0.0053	1.45
Cu–tnz <sup>dimer</sup>	0.0088	2.40

dimeric complex is the most effective. As can be seen from the structures of the two complexes (Figure 1), both have two units of tnz in them. Moreover, because it has been shown earlier that complex formation of tnz by Cu<sup>II</sup> results in a decrease in nitro-radical anion formation;<sup>20,21</sup> hence, greater efficacy due to the dimeric complex and its difference with the monomeric one may not be due to the presence of tnz in the complexes. Rather, the dimeric complex having two Cu<sup>II</sup> centers, against one in the monomer, could serve as a possible reason for the difference in activity. A greater presence of Cu<sup>II</sup> in the dimer could be responsible for more interaction of the dimeric complex with thymine or cytosine or with calf thymus DNA via Cu<sup>II</sup> that could help in the modification of the target or simply enable the compound to engage more with the target. Either way, a certain amount of thymine or cytosine or a certain amount of calf thymus DNA would not be detected by HPLC as free thymine or free cytosine (Table 1) or as free calf thymus DNA in a fluorescence-based EtBr experiment (Table 2). In the case of adenine, however, the monomeric complex performs much better which could be due to the larger size of the dimeric complex and that adenine, being a purine-based nucleic acid base, is also large.

Quite interestingly, trends observed in Tables 1 and 2 are similar, indicating that DNA having a greater percentage of thymine, similar to that in calf thymus DNA (41.9 mol % G-C and 58.1 mol % A-T), should be susceptible to a greater attack by the Cu<sup>II</sup> complexes of tnz. Hence, a prior knowledge on the damaging ability of a compound on nucleic acid bases is extremely important because it helps one to use the correct compound in targeting a disease-causing microbe; at the same time, such prior knowledge also enables one to know the extent to which the compound could be harmful to the host, that is, whether it could affect the DNA of the host as well. Therefore, the findings of this study helps one to realize why tnz has been so successful against disease-causing microbes that have a high thymine content in their DNA (Table S1, Supporting Information).

In spite of decreased nitro-radical anion formation,<sup>20,21</sup> Cu<sup>II</sup> complexes of tnz were found to be better in performance on nucleic acid bases and calf thymus DNA than tnz. This is also very interesting when for the 5-nitroimidazole family of drugs, nitro-radical anion formation is considered important for drug action. Therefore, it seems that the efficacy of the complexes are not due to free radical formation involving redox pathways that involve tnz; rather, a better performance by complexes is due to certain attributes of complex formation, those that involve the Cu<sup>II</sup> center,<sup>41,42</sup> or due to interaction between the various constituents of DNA and the Cu<sup>II</sup> center that is able to

cause double strand modification which is also detected by the technique used (i.e., the decrease in DNA–EtBr fluorescence).<sup>38–42</sup> Therefore, results of experiments with calf thymus DNA indicate they are probably not a consequence of the free radical activity involving tnz, rather other factors, such as the presence of Cu<sup>II</sup> in the complex could well be involved.

To be sure about our model studies, an attempt was made to study the performance of the complexes, on their ability to prevent biofilm formation on *S. aureus* and *P. aeruginosa* that are responsible for causing nosocomial infections. Lower minimum bactericidal concentration (MBC) values for the monomeric and dimeric Cu<sup>II</sup> complexes compared to tnz suggests better efficacy due to the complexes in removing biofilm cells. The in-dwelling bacterial cells within the biofilm matrix have a continuous and rich supply of nutrients and water molecules, much needed for their survival under stressed conditions due to the extremes of temperature, pH, salt concentration, or the presence of antimicrobials. The biofilm matrix also consists of lipid molecules, nucleic acids, proteins, extracellular DNA, and QS signaling molecules needed of cell density-dependent intercellular communications that are required for the growth of the biofilm and its sustenance. It was found that Cu<sup>II</sup> complexes of tnz were able to bring about substantial changes in biofilm concentration both for *S. aureus* and *P. aeruginosa*; monomeric complex having a better efficacy against sessile colonies.

Biofilm-associated infections are found to occur via two mechanisms: (1) through biofilm formation by enhanced QS that occurs by the production of small signaling molecules capable of detecting the cell population density in the neighboring environment under stressed conditions and (2) by the spreading of microbial cells from the EPS matrix infecting newer places. From our study, we found that the monomeric complex has the ability to block the synthesis of signaling molecules responsible for regulating biofilm formation by inhibiting LasI/Rhl I synthase.<sup>48</sup> Thus, the monomeric complex has the potential of inhibiting the QS mechanism of *P. aeruginosa* by inhibiting QS-genes and blocking transcriptional regulatory proteins that inactivate LasR or RhlR systems.

While studying the interactions of tnz and its two complexes with nucleic acid bases and calf thymus DNA, it was revealed that the dimeric complex performs better, followed by the monomeric one and tnz. Therefore, it was expected that efficacy in prevention of biofilm formation would also follow the same trend. However, in case of biofilm-related experiments, we found that the monomeric complex was most efficacious to the pathogenic target, followed by the dimeric complex and tnz. Such an anomaly is not unexpected as nitro radical anions generated from tnz and its complexes vary widely. As observed in previous communications, complex formation is associated with quenching of nitro radical anion concentration.<sup>20,21</sup> We expect the monomeric complex to quench radical anion concentration in a manner just sufficient to eliminate the excess that would be responsible for toxic side effects, keeping the efficacious concentration of radical anions intact. This combined with improved binding with DNA over tnz is expected to give it the much superior boost for maximum efficacy. The dimeric complex, on the other hand, is expected to quench radical anion concentration more extensively due to the presence of two Cu<sup>II</sup> centers; hence, more of the efficacious portion of the nitro radical anion concentration is eliminated. Moreover, owing to a larger size, efficacy of the dimeric

complex through binding is probably compromised; reason why in our model studies also the dimeric complex performs better on pyrimidine-based nucleic acid bases cytosine and thymine but not on purine-based adenine. The dimeric complex was however found to be more efficacious than tnz owing to attributes of complex formation.

The concentrations of compounds varied from one another in biological studies on biofilm formation and the model studies because in the case of prevention or eradication of bacterial biofilm formation and growth, emphasis was given to the obtained minimum inhibitory concentration (MIC) and MBC values, respectively. Hence, while antibacterial and antibiofilm studies were performed keeping in mind MIC and MBC values on sessile *P. aeruginosa* (which for the monomeric Cu<sup>II</sup> complex was 20.25  $\mu\text{M}$  and for the dimeric complex, 45.0  $\mu\text{M}$ ), for the model studies, slightly higher concentrations were used because for the model studies, where the technique employed was electrochemical reduction, if sufficient material is not present, the species generated might not be adequate for interaction with nucleic acid bases or with DNA.

The expression of biofilm-forming bacterial genes is regulated by a cell-population density-dependent mechanism known as QS. Both Gram-negative and Gram-positive bacteria perform QS by the mechanism of small signal molecules that varies from Gram-negative to Gram-positive bacteria. *N*-Acyl homoserine lactone (AHL) molecules (autoinducer-1, AI-1) are widely detected in Gram-negative bacteria, while for Gram-positive bacteria mainly peptides [autoinducer peptides (AIP) or QS peptides] are used.<sup>49</sup> We also checked the expression of virulence factors such as pyocyanin production, elastase, las A protease, and las B elastase in *P. aeruginosa* (Gram-negative) in the presence of the monomeric form of the compound. This indicates the modulation and prevention of the biofilm forming a signaling network in the presence of antimicrobial agents. However, the expression of virulence factors in Gram-positive bacteria such as *S. aureus* is directly linked to alterations in expression profiles of peptides/proteins such as endotoxins, haemolysins, exotoxins, autoinducing peptide 2 (AIP 2), proteases, and so forth that were not monitored as a part of this study.<sup>50</sup>

Our main aim was to highlight antibiofilm properties of copper(II) complexes by the formation of electrochemically generated nitro radical anion triggering bacteria-mediated enzymatic reduction. For this purpose, we only showed alterations in QS mechanism in *P. aeruginosa*. Alteration in biofilm formation and growth is also affected in the presence of copper(II) complexes in *S. aureus* as realized from Figure 8 that clearly depicts the reduction of EPS components.

## CONCLUSIONS

Tnz is reported to bind to DNA while inside a cell initiating cytotoxic action on a pathogen by forming nitro radical anion, considered responsible for its efficacy. Excess production of such nitro radical anion is responsible for idiosyncratic side effects which metal complexes with reduced formation might control. Hence, both from model studies and from the prevention of biofilm formation, it may be said, what the complexes compromise in the free radical pathway, they make up through aspects such as better interaction with a target or due to the redox active Cu<sup>II</sup>/Cu<sup>I</sup> couple. Hence, Cu<sup>II</sup> complexes of tnz, on the one hand, by controlling the generation of RNO<sub>2</sub><sup>•-</sup>, might control neurotoxic side effects, and on the other hand, continue to be better cytotoxic agents

than parent 5-nitroimidazoles (here, tnz) when one actually might expect them to have compromised on efficacy. This was clearly realized with the help of model studies using thymine, cytosine, adenine, and calf thymus DNA as targets as well as through studies on the prevention of biofilm formation. Such electrochemically generated species using compounds under consideration mimics what happens when the compounds are actually reduced within cells, helping one to understand the mechanism by which compounds impart biological efficacy.

## EXPERIMENTAL SECTION

**Materials and Methods. Chemicals Used.** Tnz was purchased from Sigma-Aldrich and purified by re-crystallization from methanol. Copper(II) chloride (CuCl<sub>2</sub>·2H<sub>2</sub>O), copper(II) acetate [Cu(OAc)<sub>2</sub>·H<sub>2</sub>O], NaCl, NaNO<sub>3</sub>, trichloroacetic acid (TCA), glacial acetic acid, sodium dihydrogen phosphate, disodium hydrogen phosphate, anthrone as reagent, Folin-Ciocalteu as reagent, congo red, cetyltrimethylammonium bromide (CTAB), chitin flakes, Tris-HCl,  $\beta$ -mercaptoethanol, phenylmethylsulfonyl fluoride (PMSF), and KCl (all AR grade) were purchased from E. Merck, India. Thymine, cytosine, and adenine were purchased from TCI, Japan, and calf thymus DNA, crystal violet (CV), ethyl acetate, hydroxyl amine, NaOH, and ferric chloride were procured from Sisco Research Laboratories, India. Calf thymus DNA was dissolved in triple distilled water in the presence of 120 mM NaCl, 35 mM KCl, and 5 mM MgCl<sub>2</sub>. Its concentration was determined using a molar extinction coefficient of 6600 M<sup>-1</sup> cm<sup>-1</sup> at 260 nm. Absorbance of the DNA solution was also measured at 280 nm; A<sub>260</sub>/A<sub>280</sub> was determined. The value found in the range 1.8–1.9 was considered ready for use, not requiring further purification. Quality of calf thymus DNA was verified using circular dichroism (CD), recording its response at 260 nm on a CD spectropolarimeter (J815—JASCO, Japan). Aqueous solutions of all other substances were prepared in triple distilled water.

**Synthesis of [Cu<sup>II</sup>(tnz)<sub>2</sub>Cl<sub>2</sub>] and [Cu<sup>II</sup><sub>2</sub>(OAc)<sub>4</sub>(tnz)<sub>2</sub>].** A solution of tnz (0.494 g in 25 mL, 2.00 mmol) in methanol was gradually added with stirring to a solution of CuCl<sub>2</sub>·2H<sub>2</sub>O (0.17 g in 25 mL, 1.00 mmol) in methanol.<sup>21</sup> The mixture was warmed under reflux to ~60 °C for 6 h. A green crystalline monomeric compound was obtained after 10 days following slow evaporation of the solvent.<sup>21</sup> A solution of tnz (0.494 g in 25 mL, 2.00 mmol) in methanol was gradually added with stirring to a solution of Cu(II) acetate (0.400 g in 25 mL, 2.00 mmol) in mildly warm methanol.<sup>24</sup> The mixture was warmed under reflux to ~55 °C for 8 h. A dimeric Cu(II) complex of tnz was obtained after a week's time following slow evaporation of the solvent.<sup>24</sup> Both complexes were purified and crystallized.

**Electrochemical Measurements.** Electrochemical experiments were performed in an air-tight 50 mL electrochemical cell. Voltammograms were recorded on a Metrohm—Autolab PGSTAT 101 potentiostat. Analyses of data were done using the NOVA 1.10.1.9 program. A conventional three-electrode system, glassy carbon as the working electrode, platinum wire as the counter electrode, and Ag/AgCl, satd. KCl as the reference electrode were used. Solutions were degassed for ~30 min prior to an electrochemical experiment using high-purity argon. Reduction of the nitro group in both monomeric and dimeric Cu<sup>II</sup> complexes of tnz and on tnz itself were followed in aqueous, aqueous-dimethyl formamide (DMF), and pure DMF solvents using cyclic voltammetry. In the case

of pure DMF, the electrolyte was tetrabutyl ammonium bromide, while for aqueous solutions, it was KCl. In DMF, there is initially one-electron reduction to  $\text{NO}_2^{\bullet-}$  that subsequently undergoes three-electron reduction to  $-\text{NHOH}$ .<sup>35,36</sup> As the percentage of water increases, the clarity of two reduction peaks is lost, and in purely aqueous solution, a single-step four electron reduction occurs. Results were also analyzed by the Randles–Sevcik equation because this confirms that the process is diffusion controlled (eq 2), an important prerequisite for experiments performed in this study.<sup>35,51,52</sup>

$$i_{pc} = (2.69 \times 10^5) \cdot n^{3/2} \cdot D_0^{1/2} \cdot A \cdot C \cdot \nu^{1/2} \quad (2)$$

$i_{pc}$  refers to the current in amperes at the cathodic peak potential,  $n$  denotes the total number of electrons,  $D_0$  is the diffusion coefficient of species, and  $A$  refers to the area of electrode in  $\text{cm}^2$ ; surface area of the glassy carbon electrode used was  $0.1256 \text{ cm}^2$ .  $C$  refers to the concentration of compounds in  $\text{moles/cm}^3$  and  $\nu$ , the scan rate in  $\text{V s}^{-1}$ . Most of these parameters would have a role to play in the subsequent reduction of each compound performed in the presence of nucleic acid bases or calf thymus DNA.

**Interaction of Reduced Products of tnz,  $[\text{Cu}(\text{tnz})_2\text{Cl}_2]$ , and  $[\text{Cu}^{\text{II}}(\text{OAc})_4(\text{tnz})_2]$  with the Target.** The glassy carbon electrode maintained at a previously determined reduction potential of each compound helped to electrochemically generate different reduction products in aqueous solution that includes  $\text{RNO}_2^{\bullet-}$  under de-aerated (Ar saturated) conditions. Because in the immediate vicinity of such in situ generated reduction products, thymine or cytosine or adenine or calf thymus DNA were maintained (separately), and they got an opportunity to interact with the species generated.<sup>26,27,53</sup> Time for in situ electrochemical generation of reduced species either on the monomeric or dimeric complexes or on tnz was strictly maintained constant for a certain target so that results obtained for nucleic acid bases and calf thymus DNA, due to each compound used could be compared with regard to species generated in solution.<sup>54,55</sup> The generated species bring about a change on the target maintained in the immediate vicinity of their generation.<sup>53–55</sup> Using the same experimental setup in aqueous solution, reduction of tnz was carried out at  $-0.745 \text{ V}$  (pH 7.4), the monomeric complex at  $-0.700 \text{ V}$  (pH 7.4), and the dimeric complex at  $-0.710 \text{ V}$  (pH 7.4). The nucleic acid bases or calf thymus DNA were each investigated following interaction with reduced products formed either on tnz or on tnz present as a ligand in the complexes.<sup>26,27,53</sup> Concentrations of compounds used in the study were 1/10 that of the target (nucleic acid bases or calf thymus DNA). Control experiments were performed where aqueous solutions of nucleic acid bases or calf thymus DNA (without any compound) were subjected to a constant potential of  $-0.700 \text{ V}$  at pH 7.4 using the same glassy carbon electrode.<sup>26,27</sup>

The amount of nucleic acid bases remaining was determined using HPLC. A C-18 column was used as the stationary phase and 5% aqueous-methanol as the mobile phase.<sup>26,27</sup> Amount of calf thymus DNA remaining unaltered was determined by treating it with ethidium bromide (EtBr) and subsequently determining the fluorescence of the adduct on a RF-530 IPC Spectrofluorophotometer, Shimadzu, Japan.<sup>26,27</sup> Interaction of EtBr with DNA leads to an increase in fluorescence, a fact that was utilized in this case to determine the amount of DNA

remaining intact following interaction with electrochemically generated reduced species.<sup>38–42</sup>

**Determination of MIC and MBC.** MBC values of monomeric and dimeric complexes of  $\text{Cu}^{\text{II}}$  against *P. aeruginosa* ATCC and *S. aureus* ATCC were determined by micro-dilution techniques.<sup>56</sup> Bacterial cells were inoculated in microtiter plates at a concentration of  $10^6 \text{ CFU/mL}$  in a volume of 50 mL. Complexes of varying concentrations were added separately and incubated at  $37 \text{ }^\circ\text{C}$  for 24 h. Afterward, they were analyzed at 600 nm using a spectrophotometer. Antibacterial efficacy of monomeric and dimeric complexes was analyzed by determining the diameter of the zone of inhibition in millimeters. Sterilized discs of paper soaked in various concentrations of monomeric and dimeric complexes were placed on agar plates possessing *P. aeruginosa* and *S. aureus*, followed by the determination of clear zones of inhibition. Susceptibility of microbial strains to antimicrobial agents was determined by calculating the zone of inhibition as per recommendations of the National Committee for Clinical Laboratory Standards.<sup>57</sup>

#### Formation of *P. aeruginosa* and *S. aureus* Biofilm.

Formation of biofilm by *P. aeruginosa* and *S. aureus* was determined using 96 polystyrene well plates for a period of 72 h at  $37 \text{ }^\circ\text{C}$ , followed by washing with phosphate buffer and staining with 0.4% (v/v) CV, dissolved in glacial acetic acid 30% (v/v) for 10 min. It was then allowed to dry for 30–45 min, followed by rinsing with phosphate buffer. Subsequently, it was allowed to dry at room temperature for approximately an hour. A 33% (v/v) acetic acid solution was added and optical density (OD) was measured at 540 nm using a spectrophotometer.

**Assay of Antibiofilm Activity.** Rate of inhibition of biofilm formation achieved by the action of the monomeric and dimeric  $\text{Cu}^{\text{II}}$  complexes of tnz at MBC, incubated at  $37 \text{ }^\circ\text{C}$  for 72 h was detected by the CV assay.<sup>56,58</sup>

Percentage inhibition was measured with respect to untreated control using the formula mentioned in eq 3.

Percentage biofilm inhibition

$$= \frac{[(\text{OD of untreated control}) - (\text{OD of treated sample})]}{(\text{OD of untreated control})} \times 100 \quad (3)$$

Detection of QS in test *P. aeruginosa* and *S. aureus*

The supernatant of bacterial culture broth was filtered using a membrane filter having pore size  $0.2 \text{ }\mu\text{m}$ . Ethyl acetate was added to the filtrate with gentle shaking for 10 min to allow for phase separation.<sup>56,58</sup> The upper fraction of the mixture was mixed with 2 M hydroxyl amine and 3.5 M NaOH (1:1), followed by 10  $\mu\text{L}$  of alcoholic ferric chloride solution (ferric chloride in 95% 1:1 ethanol). Color of the solution was measured with a spectrophotometer at 520 nm.<sup>59</sup>

#### Quantification of Secondary Metabolite Pyocyanin Produced by *P. aeruginosa* during Biofilm Formation.

Quantification of pyocyanin<sup>60</sup> produced by *P. aeruginosa* upon incubation with MBC concentrations of monomeric and dimeric  $\text{Cu}^{\text{II}}$  complexes and amoxicillin (standard antibiotic) was done at  $37 \text{ }^\circ\text{C}$  for 48 h. The culture supernatant (5 mL) collected after centrifugation at 10,000 rpm for a period of 15 min<sup>61</sup> was added to 3 mL of chloroform, followed by re-extraction with 1 mL of 0.2 N HCl, resulting in a color change from orange to pink that was detected at 520 nm using a

spectrophotometer. This helped in determining the percentage reduction of pyocyanin.

**Determination of Elastase Activity.** Quantification of *las B* expression was done by determining the elastase activity. An aliquot of culture supernatant (100  $\mu\text{L}$ ) was added to 900  $\mu\text{L}$  of Elastin Congo red (ECR) and incubated at 37  $^{\circ}\text{C}$  for 3 h. Insoluble ECR was removed by centrifugation and absorbance was measured at 495 nm.<sup>62</sup>

**Determination of Rhamnolipid Production and Drop Collapse Assay.** The amount of rhamnolipid was estimated with CTAB-methylene blue plates in accordance with a method described earlier.<sup>63,64</sup> Plates were supplemented with 0.2% (w/v) CTAB, 0.0005% (w/v) methylene blue, and solidified with 1.5% (w/v) agar. An overnight grown liquid culture of *P. aeruginosa* was used and a spot was applied at the middle of the plate for swarming assays. To all plates, except control, monomeric, and dimeric,  $\text{Cu}^{\text{II}}$  complexes were added separately. Plates were incubated at 37  $^{\circ}\text{C}$  for 24 h, followed by incubation at room temperature for another 24 h. Production of rhamnolipid was estimated by measuring the dark blue halo surrounding the colony and quantification was done following a protocol described earlier.<sup>65</sup>

**Detection of Viability Count of the Sessile Group of Bacterial Cells.** The working strain grown on 0.1% chitin flakes (w/v) for 72 h was washed with 0.1% (w/v) normal saline to eliminate planktonic groups of cells. Following the treatment of sessile cells as control or with monomeric and dimeric  $\text{Cu}^{\text{II}}$  complexes, bacterial growth was determined at 590 nm using a spectrophotometer at varying intervals of time.<sup>66</sup>

**Determination of EPS Degradation on Being Challenged by Monomeric and Dimeric  $\text{Cu}^{\text{II}}$  Complexes.** Biofilms of the working strain were grown on chitin flakes 0.1% (w/v) separately in 100 mL of LB media and centrifuged at 12,000 rpm for 15 min at 4  $^{\circ}\text{C}$  to break the biofilm. 5 mL of PBS buffer was used to wash the pellets collected after centrifugation and mixed with 2.5 mL of 10 mM Tris-HCl (pH 7.8). After thorough cyclomixing, 20 mM  $\beta$ -mercaptoethanol and 1 mM PMSF were added. The cell suspension of bacterial culture was sonicated, followed by centrifugation (12,000 rpm, 30 min) at 4  $^{\circ}\text{C}$ , followed by the addition of 10% TCA in acetone.<sup>67</sup>

**Estimation of Carbohydrate and Protein Content in EPS when Challenged by Monomeric and Dimeric Complexes of  $\text{Cu}^{\text{II}}$ .** The carbohydrate present in EPS was quantified using the Anthrone method.<sup>68</sup> Protein present in EPS was quantified by the Lowry method.<sup>69</sup>

**Isolation and Estimation of DNA from Prokaryotic Cells.** To have a check on adverse effects related to the use of monomeric and dimeric  $\text{Cu}^{\text{II}}$  complexes on genomic DNA of bacterial strains, they were isolated using CTAB after treatment with monomeric and dimeric complexes for 2 h keeping the “control” untreated. Concentration of DNA was measured spectrophotometrically at 260 nm and quantified as in eq 4.

$$\begin{aligned} \text{Units}(\times) \text{mg mL}^{-1} \\ = 50 \times \text{OD at 260 nm} \times \text{dilution factor} \end{aligned} \quad (4)$$

## ■ ASSOCIATED CONTENT

### Supporting Information

The Supporting Information is available free of charge at <https://pubs.acs.org/doi/10.1021/acsomega.1c04822>.

HPLC chromatograms for  $10^{-3}$  M thymine, cytosine, and adenine, respectively, recorded at 254 nm to denote the region of elution of the three nucleic acid bases and activity of the drug Tindamax used to treat different types of disease-causing organisms along with the composition of A-T and G-C content of their DNA (PDF)

## ■ AUTHOR INFORMATION

### Corresponding Author

Saurabh Das – Department of Chemistry, Inorganic Chemistry Section, Jadavpur University, Kolkata 700 032, India; [orcid.org/0000-0002-0455-8760](https://orcid.org/0000-0002-0455-8760); Phone: +91 33 24572148; Email: [saurabh.das@jadavpuruniversity.in](mailto:saurabh.das@jadavpuruniversity.in), [dasrsv@yahoo.in](mailto:dasrsv@yahoo.in); Fax: +91 33 24146223

### Authors

Promita Nandy – Department of Chemistry, Inorganic Chemistry Section, Jadavpur University, Kolkata 700 032, India

Ramesh C. Santra – Department of Chemistry, Inorganic Chemistry Section, Jadavpur University, Kolkata 700 032, India

Dibyajit Lahiri – Department of Biotechnology, University of Engineering and Management, Kolkata 700 156, India

Moupriya Nag – Department of Biotechnology, University of Engineering and Management, Kolkata 700 156, India

Complete contact information is available at: <https://pubs.acs.org/10.1021/acsomega.1c04822>

### Author Contributions

The manuscript was written through contributions made by all authors. All authors have given their approval to the final version of the manuscript.

### Funding

Work in S.D.'s lab was supported by RUSA 2.0 Program of the Government of India operating at Jadavpur University in the scheme “Research Support to Faculty Members” in the Research Thrust Area: Research in Sustainable Development (Sanction Ref. no. R-11/438/19 dated 30.05.2019) and also by funds from UGC, New Delhi, received as part of the research on “Advanced Materials” related to UPE II at Jadavpur University, DST-PURSE and UGC-CAS programs of Government of India operating at Department of Chemistry, Jadavpur University. Work in M.N. and D.L.'s lab was supported by funds from University of Engineering & Management, Kolkata. P.N. was supported by a DST-INSPIRE Senior Research Fellowship of the Department of Science & Technology, New Delhi. Authors are grateful to Mr. Tanmoy Saha for his help in preparing certain representations in the manuscript.

### Notes

The authors declare no competing financial interest.

## ■ REFERENCES

- (1) Carlier, J. P.; Sellier, N.; Rager, M. N.; Reysset, G. Metabolism of a 5-nitroimidazole in susceptible and resistant isogenic strains of *Bacteroides fragilis*. *Antimicrob. Agents Chemother.* **1997**, *41*, 1495–1499.

- (2) Raether, W.; Hänel, H. Nitroheterocyclic drugs with broad spectrum activity. *Parasitol. Res.* **2003**, *90*, S19–S39.
- (3) Miyamoto, Y.; Kalisiak, J.; Korthals, K.; Lauwaet, T.; Cheung, D. Y.; Lozano, R.; Cobo, E. R.; Upcroft, P.; Upcroft, J. A.; Berg, D. E.; Gillin, F. D.; Fokin, V. V.; Sharpless, K. B.; Eckmann, L. Expanded therapeutic potential in activity space of next-generation 5-nitroimidazole antimicrobials with broad structural diversity. *Proc. Natl. Acad. Sci. U.S.A.* **2013**, *110*, 17564–17569.
- (4) Verderosa, A. D.; Totsika, M.; Fairfull-Smith, K. E. Bacterial Biofilm Eradication Agents: A Current Review. *Front. Chem.* **2019**, *7*, 824.
- (5) Ang, C. W.; Jarrad, A. M.; Cooper, M. A.; Blaskovich, M. A. T. Nitroimidazoles: Molecular fireworks that combat a broad spectrum of infectious diseases. *J. Med. Chem.* **2017**, *60*, 7636–7657.
- (6) Brown, J. M. The hypoxic cell: a target for selective cancer therapy—eighteenth Bruce F. Cain Memorial award lecture. *Cancer Res.* **1999**, *59*, 5863–5870.
- (7) Bonnet, M.; Hong, C. R.; Wong, W. W.; Liew, L. P.; Shome, A.; Wang, J.; Gu, Y.; Stevenson, R. J.; Qi, W.; Anderson, R. F.; Pruijn, F. B.; Wilson, W. R.; Jamieson, S. M. F.; Hicks, K. O.; Hay, M. P. Next-generation hypoxic cell radiosensitizers: Nitroimidazole alkylsulfonamides. *J. Med. Chem.* **2018**, *61*, 1241–1254.
- (8) Wardman, P. Nitroimidazoles as hypoxic cell radiosensitizers and hypoxia probes: misonidazole, myths and mistakes. *Br. J. Radiol.* **2019**, *92*, 20170915.
- (9) (a) Sood, S.; Kapil, A. An update on *Trichomonas vaginalis*. *Indian J. Sex. Transm. Dis.* **2008**, *29*, 7–14. (b) Puri, V. Metronidazole neurotoxicity. *Neurology* **2011**, *59*, 4–5.
- (10) Kato, H.; Sosa, H.; Mori, M.; Kaneko, T. Clinical Characteristics of Metronidazole-induced encephalopathy: A report of two cases and a review of 32 Japanese cases in the literature. *Kansenshogaku Zasshi* **2015**, *89*, 559–566.
- (11) Bakshi, J. S.; Ghiara, J. M.; Nanivadekar, A. S. How does tinidazole compare with metronidazole? A summary report of Indian trials in amoebiasis and giardiasis. *Drugs* **1978**, *15*, 33–42.
- (12) Crowell, A. L.; Sanders-Lewis, K. A.; Secor, W. E. In vitro metronidazole and tinidazole activities against metronidazole-resistant strains of *Trichomonas vaginalis*. *Antimicrob. Agents Chemother.* **2003**, *47*, 1407–1409.
- (13) Fung, H. B.; Doan, T.-L. Tinidazole: a nitroimidazole antiprotozoal agent. *Clin. Ther.* **2005**, *27*, 1859–1884.
- (14) Schwebke, J. R.; Desmond, R. A. A randomized trial of metronidazole in asymptomatic bacterial vaginosis to prevent the acquisition of sexually transmitted diseases. *Am. J. Obstet. Gynecol.* **2011**, *204*, 211.e1–211.e6.
- (15) Ebel, K.; Koehler, H.; Gamer, A. O.; Jäckh, R. Imidazole and Derivatives. In *Ullmann's Encyclopedia of Industrial Chemistry*; Wiley-VCH, 2002.
- (16) Cammarota, G.; Cannizzaro, O.; Cianci, R.; Armuzzi, A.; Gasbarrini, A.; Pastorelli, A.; Papa, A.; Gasbarrini, G. Six-day or seven-day regimens with ranitidine bismuth citrate plus high-dose clarithromycin and tinidazole are both effective against helicobacter pylori infection. *Dig. Dis. Sci.* **1999**, *44*, 2386–2389.
- (17) Plummer, E. L.; Vodstrcil, L. A.; Danielewski, J. A.; Murray, G. L.; Fairley, C. K.; Garland, S. M.; Hocking, J. S.; Tabrizi, S. N.; Bradshaw, C. S. Combined oral and topical antimicrobial therapy for male partners of women with bacterial vaginosis: Acceptability, tolerability and impact on the genital microbiota of couples—A pilot study. *PLoS One* **2018**, *13*, No. e0190199.
- (18) Edwards, D. I. Nitroimidazole drugs—action and resistance mechanisms. I. Mechanisms of action. *J. Antimicrob. Chemother.* **1993**, *31*, 9–20.
- (19) Armendáriz-Vidales, G.; Hernández-Muñoz, L. S.; González, F. J.; de Souza, A. A.; de Abreu, F. C.; Jardim, G. A. M.; da Silva, E. N.; Goulart, M. O. F.; Frontana, C. Nature of electrogenerated intermediates in nitro-substituted nor- $\beta$ -lapachones: The structure of radical species during successive electron transfer in multiredox centers. *J. Org. Chem.* **2014**, *79*, 5201–5208.
- (20) Santra, R. C.; Ganguly, D.; Singh, J.; Mukhopadhyay, K.; Das, S. A study on the formation of the nitro radical anion by ornidazole and its significant decrease in a structurally characterized binuclear Cu(II)-complex: impact in biology. *Dalton Trans.* **2015**, *44*, 1992–2000.
- (21) Santra, R. C.; Ganguly, D.; Jana, S.; Banyal, N.; Singh, J.; Saha, A.; Chattopadhyay, S.; Mukhopadhyay, K.; Das, S. Synthesizing a CuII complex of tinidazole to tune the generation of the nitro radical anion in order to strike a balance between efficacy and toxic side effects. *New J. Chem.* **2017**, *41*, 4879–4886.
- (22) Dan, M.; Wang, A. L.; Wang, C. C. Inhibition of pyruvate-ferredoxin oxidoreductase gene expression in *Giardia lamblia* by a virus-mediated hammerhead ribozyme. *Mol. Microbiol.* **2000**, *36*, 447–456.
- (23) Graves, K. J.; Novak, J.; Secor, W. E.; Kissinger, P. J.; Schwebke, J. R.; Muzny, C. A. A Systematic review of the literature on mechanisms of 5-nitroimidazole resistance in *trichomonas vaginalis*. *Parasitology* **2020**, *147*, 1383–1391.
- (24) Santra, R. C.; Sengupta, K.; Dey, R.; Shireen, T.; Das, P.; Guin, P. S.; Mukhopadhyay, K.; Das, S. X-ray crystal structure of a Cu(II) complex with the antiparasitic drug tinidazole, interaction with calf thymus DNA and evidence for antibacterial activity. *J. Coord. Chem.* **2014**, *67*, 265–285.
- (25) Nandy, P.; Singha, S.; Banyal, N.; Kumar, S.; Mukhopadhyay, K.; Das, S. A ZnII complex of ornidazole with decreased nitro radical anions that is still highly active on *Entamoeba histolytica*. *RSC Adv.* **2020**, *10*, 23286–23296.
- (26) Nandy, P.; Das, S. Interaction of electrochemically generated reduction products of ornidazole with nucleic acid bases and calf thymus DNA. *J. Indian Chem. Soc.* **2018**, *95*, 1009–1014.
- (27) Nandy, P.; Das, S. In situ reactivity of electrochemically generated nitro radical anion on ornidazole and its monomeric Cu(II) complex with nucleic acid bases and calf thymus DNA. *Inorg. Chim. Acta* **2020**, *501*, 119267.
- (28) Lund, H. Cathodic reduction of nitro and related compounds. In *Organic Electrochemistry*, 3rd ed.; Lund, H., Baizer, M. M., Eds.; M. Dekker Inc.: New York, 1990; p 411.
- (29) Costerton, J. W.; Stewart, P. S.; Greenberg, E. P. Bacterial biofilms: a common cause of persistent infections. *Science* **1999**, *284*, 1318–1322.
- (30) Khan, H. A.; Ahmad, A.; Mehboob, R. Nosocomial infections and their control strategies. *Asian Pac. J. Trop. Biomed.* **2015**, *5*, 509–514.
- (31) Potera, C. Forging a link between biofilms and disease. *Science* **1999**, *283*, 1837–1839.
- (32) Amorena, B.; Gracia, E.; Monzón, M.; Leiva, J.; Oteiza, C.; Pérez, M.; Alabart, J.-L.; Hernández-Yago, J. Antibiotic susceptibility assay for *Staphylococcus aureus* in biofilms developed in vitro. *J. Antimicrob. Chemother.* **1999**, *44*, 43–55.
- (33) Lahiri, D.; Dash, S.; Dutta, R.; Nag, M. Elucidating the effect of anti-biofilm activity of bioactive compounds extracted from plants. *J. Biosci.* **2019**, *44*, 52.
- (34) Stewart, P. S. Mechanisms of antibiotic resistance in bacterial biofilms. *Int. J. Med. Microbiol.* **2002**, *292*, 107–113.
- (35) Mandal, P. C. Reactions of the nitro radical anion of metronidazole in aqueous and mixed solvent: A cyclic voltammetric study. *J. Electroanal. Chem.* **2004**, *570*, 55–61.
- (36) Squella, J. A.; Gonzalez, P.; Bollo, S.; Núñez-Vergara, L. J. Electrochemical generation and interaction study of the nitro radical anion from nimesulide. *Pharm. Res.* **1999**, *16*, 161–164.
- (37) Das, S.; Saha, A.; Mandal, P. C. Radiosensitization of thymine by Fe(III)-1,2 dihydroxyanthraquinone complex in dilute aqueous solution. *J. Radioanal. Nucl. Chem.* **1995**, *196*, 57–63.
- (38) Morgan, A. R.; Lee, J. S.; Pulleyblank, D. E.; Murray, N. L.; Evans, D. H. Ethidium fluorescence assays. Part I. Physicochemical studies. *Nucleic Acids Res.* **1979**, *7*, 547–565.
- (39) Birnboim, H. C.; Jevcak, J. J. Fluorometric method for rapid detection of DNA strand breaks in human white blood cells produced by low doses of radiation. *Cancer Res.* **1981**, *41*, 1889–1892.

- (40) Prütz, W. A. Inhibition of DNA-ethidium bromide intercalation due to free radical attack upon DNA. I. Comparison of the effects of various radicals. *Radiat. Environ. Biophys.* **1984**, *23*, 1–6.
- (41) Das, S.; Saha, A.; Mandal, P. C. Radiation-induced double-strand modification in calf thymus DNA in the presence of 1, 2-dihydroxy-9,10-anthraquinone and its Cu(II) complex. *Environ. Health Perspect.* **1997**, *105*, 1459–1462.
- (42) Das, S.; Mandal, P. C. Anthracyclines as radiosensitizers: a Cu(II) complex of a simpler analogue modifies DNA in Chinese Hamster V79 cells under low-dose  $\gamma$  radiation. *J. Radioanal. Nucl. Chem.* **2014**, *299*, 1665–1670.
- (43) Nord, C. E. Microbiological properties of tinidazole: spectrum, activity and ecological considerations. *J. Antimicrob. Chemother.* **1982**, *10*, 35–42.
- (44) Nord, C. E.; Kager, L. Tinidazole — microbiology, pharmacology and efficacy in anaerobic infections. *Infection* **1983**, *11*, 54–60.
- (45) Jokipii, A. M. M.; Jokipii, L. Bactericidal activity of tinidazole. *Chemotherapy* **1977**, *23*, 25–31.
- (46) Machado, D.; Castro, J.; Palmeira-de-Oliveira, A.; Martinez-de-Oliveira, J.; Cerca, N. Bacterial vaginosis biofilms: Challenges to current therapies and emerging solutions. *Front. Microbiol.* **2016**, *6*, 1528.
- (47) Kostylev, M.; Kim, D. Y.; Smalley, N. E.; Salukhe, I.; Greenberg, E. P.; Dandekar, A. A. Evolution of the *Pseudomonas aeruginosa* quorum-sensing hierarchy. *Proc. Natl. Acad. Sci. U.S.A.* **2019**, *116*, 7027–7032.
- (48) Ahmed, S. A. K. S.; Rudden, M.; Smyth, T. J.; Dooley, J. S. G.; Marchant, R.; Banat, I. M. Natural quorum sensing inhibitors effectively downregulate gene expression of *Pseudomonas aeruginosa* virulence factors. *Appl. Microbiol. Biotechnol.* **2019**, *103*, 3521–3535.
- (49) Verbeke, F.; De Craemer, S.; Debunne, N.; Janssens, Y.; Wynendaele, E.; Van de Wiele, C.; De Spiegeleer, B. Peptides as quorum sensing molecules: Measurement techniques and obtained levels in vitro and in vivo. *Front. Neurosci.* **2017**, *11*, 183.
- (50) Kong, C.; Chee, C.-F.; Richter, K.; Thomas, N.; Abd. Rahman, N.; Nathan, S. Suppression of *Staphylococcus aureus* biofilm formation and virulence by a benzimidazole derivative, UM-C162. *Sci. Rep.* **2018**, *8*, 2758.
- (51) Bard, A. J.; Faulkner, L. R. *Electrochemical Methods Fundamental and Applications*; John Wiley & Sons, Inc.: New York, 2001.
- (52) Zanello, P. *Inorganic Electrochemistry: Theory, practice and application*; The Royal Society of Chemistry, 2003.
- (53) Núñez-Vergara, L. J.; García, F.; Domínguez, M. M.; de la Fuente, J.; Squella, J. A. In situ reactivity of the electrochemically generated nitro radical anion from nitrendipine with glutathione, adenine and uracil. *J. Electroanal. Chem.* **1995**, *381*, 215–219.
- (54) Saha, M.; Das, S. Free radical induced activity of an anthracycline analogue and its MnII complex on biological targets through in situ electrochemical generation of semiquinone. *Heliyon* **2021**, *7*, No. e07746.
- (55) Mandal, B.; Mondal, H. K.; Das, S. In situ reactivity of electrochemically generated semiquinone on Emodin and its CuII/MnII complexes with pyrimidine based nucleic acid bases and calf thymus DNA: Insight into free radical induced cytotoxicity of anthracyclines. *Biochem. Biophys. Res. Commun.* **2019**, *515*, 505–509.
- (56) Lahiri, D.; Nag, M.; Dutta, B.; Mukherjee, I.; Ghosh, S.; Dey, A.; Banerjee, R.; Ray, R. R. Catechin as the most efficient bioactive compound from *Azadirachta indica* with antibiofilm and anti-quorum sensing activities against dental biofilm: an In vitro and In silico study. *Appl. Biochem. Biotechnol.* **2021**, *193*, 1617–1630.
- (57) Balouiri, M.; Sadiki, M.; Ibsouda, S. K. Methods for in vitro evaluating antimicrobial activity: A review. *J. Pharm. Anal.* **2016**, *6*, 71–79.
- (58) Lahiri, D.; Nag, M.; Dutta, B.; Dash, S.; Ghosh, S.; Ray, R. R. Synergistic effect of quercetin with allicin from the ethanolic extract of *Allium cepa* as a potent anti-quorum sensing and anti-biofilm agent against oral biofilm. In *Advances in Bioprocess Engineering and Technology, Lecture Notes in Bioengineering*; Ramkrishna, D., Sengupta, S., Dey Bandyopadhyay, S., Ghosh, A., Eds.; Springer: Singapore, 2021; pp 69–81.
- (59) Taghadosi, R.; Shakibaie, M. R.; Masoumi, S. Biochemical detection of N-Acyl homoserine lactone from biofilm-forming uropathogenic *Escherichia coli* isolated from urinary tract infection samples. *Rep. Biochem. Mol. Biol.* **2015**, *3*, 56–61.
- (60) Essar, D. W.; Eberly, L.; Hadero, A.; Crawford, I. P. Identification and characterization of genes for a second anthranilate synthase in *Pseudomonas aeruginosa*: interchangeability of the two anthranilate synthases and evolutionary implications. *J. Bacteriol.* **1990**, *172*, 884.
- (61) Lee, J.-H.; Park, J.-H.; Cho, H. S.; Joo, S. W.; Cho, M. H.; Lee, J. Anti-biofilm activities of quercetin and tannic acid against *Staphylococcus aureus*. *J. Biofouling* **2013**, *29*, 491–499.
- (62) Rust, L.; Messing, C. R.; Iglewski, B. H. [44] Elastase assays. *Methods Enzymol.* **1994**, *235*, 554–562.
- (63) Siegmund, I.; Wagner, F. New method for detecting rhamnolipids excreted by *Pseudomonas* species during growth on mineral agar. *Biotechnol. Tech.* **1991**, *5*, 265–268.
- (64) Caiazza, N. C.; Shanks, R. M. Q.; O’Toole, G. A. Rhamnolipids modulate swarming motility patterns of *Pseudomonas aeruginosa*. *J. Bacteriol.* **2005**, *187*, 7351.
- (65) Murray, T. S.; Kazmierczak, B. I. *Pseudomonas aeruginosa* exhibits sliding motility in the absence of type IV pili and flagella. *J. Bacteriol.* **2020**, *190*, 2700.
- (66) Baishya, R.; Bhattacharya, A.; Mukherjee, M.; Lahiri, D.; Banerjee, S. Establishment of a simple reproducible model for antibiotic sensitivity pattern study of biofilm forming *Staphylococcus aureus*. *Mater. Today: Proc.* **2016**, *3*, 3461–3466.
- (67) Pereira, S.; Zille, A.; Micheletti, E.; Moradas-Ferreira, P.; De Philippis, R.; Tamagnini, P. Complexity of cyanobacterial exopolysaccharides: composition, structures, inducing factors and putative genes involved in their biosynthesis and assembly. *FEMS Microbiol. Rev.* **2009**, *33*, 917–941.
- (68) Morris, D. L. Quantitative determination of carbohydrates with Dreywood’s anthrone reagent. *Science* **1948**, *107*, 254–255.
- (69) Lowry, O.; Rosebrough, N.; Farr, A. L.; Randall, R. Protein measurement with the Folin phenol reagent. *J. Biol. Chem.* **1951**, *193*, 265–275.



# The importance of $pK_a$ in an analysis of the interaction of compounds with DNA



Mouli Saha<sup>1</sup>, Promita Nandy<sup>1</sup>, Mousumi Chakraborty, Piyal Das, Saurabh Das\*

Department of Chemistry, Jadavpur University, Kolkata 700 032, India

## HIGHLIGHTS

- Most of the compounds interacting with DNA exist in more than one form in solution.
- Most often this is a consequence of one or more proton dissociation equilibrium.
- The amount of the contributing forms present in solution keeps changing with pH.
- To know the correct amount of a form present appropriate  $pK_a$  must be used.
- Overall binding of a compound with DNA is a consequence of the contributions of different forms of it.

## GRAPHICAL ABSTRACT

Anthracycline analogues alizarin and purpurin were used to find how DNA influences determination of  $pK_a$ .  $pK_{a1}$  and  $pK_{a2}$  were different when evaluated in presence of DNA.  $pK_{a1}$  determined in presence of DNA was used to evaluate contributions of two forms of the molecules towards overall binding with calf thymus DNA. Revised calculations show contribution of the neutral form was different while that of the anionic form was same.

## ARTICLE INFO

### Keywords:

$pK_a$   
Alizarin  
Purpurin  
Contribution of species  
 $K^0$   
 $K^-$   
pH

## ABSTRACT

$pK_a$  of a compound is crucial for determining the contributions of different forms of it towards overall binding with DNA. Hence it is important to use correct  $pK_a$  values in DNA interaction studies. This study takes a look at the importance of  $pK_a$  values to realize binding of compounds with DNA. Since  $pK_a$  of a compound determined in the presence of DNA is quite different from that determined in its absence hence, presence of different forms of a compound during interaction with DNA is different from that realized if the determination of  $pK_a$  is done in normal aqueous solution in absence of DNA. Hence, calculations determining contributions of different forms of a compound interacting with DNA are affected accordingly. Two simple analogues of anthracyclines, alizarin and purpurin, were used to investigate the influence DNA has on  $pK_a$  values. Indeed, they were different in presence of DNA than when determined in normal aqueous solution.  $pK_{a1}$  for alizarin and purpurin determined in the absence and presence of calf thymus DNA were used in equations that determine contributions of two forms (neutral and anionic) towards overall binding with DNA. The study concludes that correct  $pK_a$  values, determined correctly i.e. under appropriate conditions, must be used for DNA binding experiments to evaluate contributions of individual forms.

## 1. Introduction

Studies on interaction of compounds with DNA are important for many reasons and there are lots of information in the literature as well [1–9]. They help us realize the utility of these interactions and their

relevance in different aspects of chemical biology [10–13]. Although lot is known on interaction of different compounds with DNA, it is still too early, even for experiments in vitro, to say that all interactions are characterized correctly. This is because there are too many factors involved in an interaction of a compound with DNA than we can possibly

\* Corresponding author.

E-mail address: [sdas@chemistry.jdvu.ac.in](mailto:sdas@chemistry.jdvu.ac.in) (S. Das).

<sup>1</sup> MS and PN have equal contribution.

imagine [6,10,12,14,16,17]. Things get even more complicated when the compound exists in more than one form in solution [18–23]. When that is the case, experimental values determined for overall binding constant are actually a consequence of the interaction of each individual form of the compound in solution [18–23]; each form interacting with DNA differently depending on its characteristic properties [16–18]. The amount of each form present during interaction with DNA is also crucial for a correct determination of binding parameters [18,20–23]. Since interaction of each form with DNA is different, it gets manifested in the overall binding constant, an experimentally determined parameter [18,20]. Hence, the contribution of different forms of a compound towards overall binding constant is important in understanding DNA interactions.

Reasons for the existence of a compound in more than one form are varied. It could be the consequence of a racemic mixture, or of *cis-trans* isomerism, or that the compound has one or more easily dissociable protons [18,20–22]. For a proton dependent equilibrium for example, the contributing forms of the compound change with changes in pH of the medium affecting binding parameters with DNA [20–23]. Most studies somehow fail to realize this. In fact, very few compounds exist exclusively in one form in solution; there is almost always another form present (however small it may be) that influences binding with DNA and hence determination of binding parameters.

DNA being a negative polymer, as a general rule, tendency of cationic species interacting with it is greater than species that are neutral which in turn is greater than species negatively charged [10,16–18]. A good deal of approximation has allowed most researchers to either knowingly or unknowingly report DNA binding data as if the compound exists in one form; not considering the fact there could be at least another form in solution under different experimental conditions like pH, ionic strength or temperature and that different structural forms interact differently with DNA [20–25]. In fact, some of the variations observed experimentally in the determination of overall binding constant of a compound with DNA under different conditions have sometimes been reported as “within experimental error” when these small differences were actually because different forms of the molecule were present in different amounts; their contribution to overall binding constant being different. For example, the titration of a compound at pH 6.8 and 7.5 would not be the same if it has a group present in it whose  $pK_a$  is 7.2. Species present in solution at the two pH would be completely different, having a huge impact on binding parameters. This is the case in cell biology processes which can therefore be explained [9–12]. Hence, there is a need to incorporate the aspect of contribution of different forms while considering data generated on DNA interaction to arrive at a realistic picture. As mentioned earlier, a vast majority of compounds studied for DNA binding exists in two or more forms in solution. The ones which do not apparently have a second form at a particular pH could dissociate under the influence of nucleic acids present in DNA as the compound tries to interact with it [26]. While some researchers have been careful to take a note of this, many neglected the fact there could be more than one form in solution whose interaction with DNA is different from the main species they were reporting [18–20,22,27].

Apart from the aspect mentioned above another reason for concern is the very determination of  $pK_a$  of a compound which is crucial for drug selection and optimization [28,29]. We usually determine  $pK_a$  in an aqueous solution at a low ionic strength of the medium and utilize it to understand its implications in different physicochemical experiments to realize its importance in physiological processes [30]. The question here is to what extent is this correct i.e. to use a  $pK_a$  determined in normal aqueous solution not containing DNA and to use it in a DNA binding analysis, the very experiment for which is performed at a reasonably high ionic strength [20,21,23]. Needless, to say this is one of many reasons why results for most compounds studied *in vitro* and *in vivo* differ in a big way. It is now known  $pK_a$  of a compound could be different in presence of DNA or more specifically in presence of nucleic

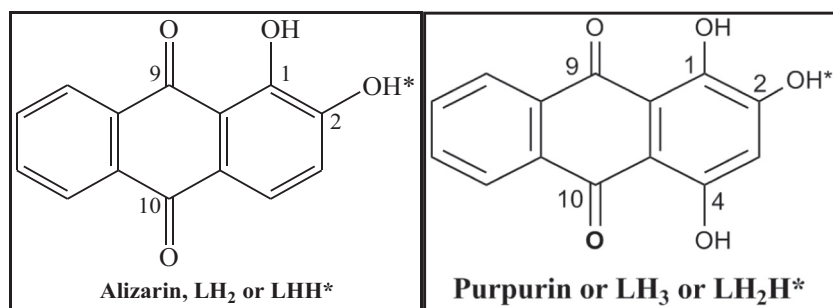
acid bases that make DNA [26]. In fact, DNA itself (i.e. nucleic acid bases that make it) undergoes significant changes owing to changes in the pH of the medium [26]. Protonation causes change in DNA conformation depending on the composition of nucleic acid bases present and the ionic strength of the medium [31,32]. For this reason, we decided to re-investigate some of our own DNA binding data where  $pK_a$  used to evaluate contributions of different forms of a compound binding with DNA was determined in normal aqueous solution [21].  $pK_a$  for the same dissociation was re-determined, this time in presence of different concentrations of calf thymus DNA and that was done in an ionic strength of the medium that is normally maintained for DNA titrations. Since different forms of the compound present in solution are a consequence of their proton dissociation equilibria, proper determination of  $pK_a$  becomes very essential.

When the  $pK_a$  of a compound falls in the physiological pH range in which most of our DNA titrations are performed its importance is even more. Any change in  $pK_a$  obviously affects the overall binding constant value since the contributing forms differ and hence their interaction with DNA [27,33]. Therefore, it is important to find out the reasons responsible for changes in  $pK_a$ . One important factor is the ionic strength of the medium but when ionic strength is kept constant it could vary depending on the amount of DNA present, with which it interacts [8,10,24–26,33]. Nucleic acid bases present in DNA influence proton-dissociation equilibria [26]. Moreover, when the pH of the medium is different it affects the three dimensional structure of DNA which in turn either exposes or withholds nucleic acid bases present in it in different ways that affect the manner in which they influence  $pK_a$  of the compound [26]. Only when  $pK_a$  value is either well below or well beyond the physiological pH range, a single form of a compound would exist or predominate [27]. As early as 1988, a report showed the base ellipticine ( $pK_a = 7.4$ ) binds calf thymus DNA at pH 5 when its cationic form, the ellipticinium cation predominates, while at pH 9 the neutral form is the principal species responsible for binding [34]. However, there are no reports to show what happens between pH 5 and pH 9 when both forms are simultaneously present in solution. Although an excellent piece of work, it does not consider the fact that at pH 5.0, apart from the cation there is ~0.40% of a neutral form and at pH 9.0, apart from ellipticine free base there would be ~2.45% of the cation in solution. This requires consideration for it affects overall binding constant values; hence values reported for the binding constant of the respective forms are not exclusively those claimed in the report. Although the situation is not that serious for the study mentioned above [34] because the presence of the minor form at any pH is really very small it could however altogether change binding constant values for many other compounds reported in the literature. In the example above, had titrations been done at four or five other pH values between pH 5.0 and pH 9.0 then with the help of appropriate equations and a proper use of  $pK_a$  contributions of the two forms could be obtained [18]. Using them, overall binding constant of ellipticine could then be known at any pH without having to perform a titration at that pH [18]. When  $pK_a$  of a compound lies in the physiological pH range as in the example above, a slight change due to interaction of the compound with nucleic acid bases could affect calculations. Therefore, the influence nucleic acid bases might have on a molecule chosen for DNA interaction needs proper investigation. In fact, if this is done, DNA binding parameters may be claimed to have been more rigorously determined. The present study makes an attempt to understand fluctuations in  $pK_a$  of alizarin and purpurin, simpler analogues of anthracycline anticancer agents, evaluated with the help of pH-metric titrations in presence of varying concentrations of calf thymus DNA against those determined in normal aqueous solution. When  $pK_a$  values determined in the presence of DNA were used in Eqs. (4) & (5) to determine contributions of each form to overall binding constant at physiological pH they gave different results from those determined earlier i.e. when  $pK_a$  values were determined in normal aqueous solution. The work allowed us to see manifestations small changes in  $pK_a$  has on contributions of different forms of a

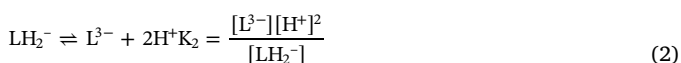
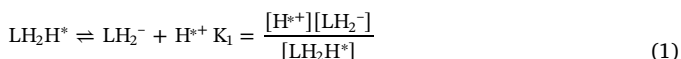
compound to its overall binding with DNA.

## 2. Experimental

Alizarin and purpurin (~96% pure) were purchased from Sigma-Aldrich and re-crystallized from an ethanol-water mixture. Since hydroxy-9,10-anthraquinones are photosensitive, compounds were carefully stored in the dark. Stock solutions in ethanol were  $\sim 10^{-4}$  M. HEPES buffer [4-(hydroxyethyl)-1-piperazine ethane sulphonic acid] was used. Sodium nitrate (AR) and sodium chloride (AR) were used to maintain ionic strength of the medium. Calf thymus DNA purchased from Sisco Research Laboratories, India was dissolved in triple distilled water using 120 mM NaCl, 35 mM KCl and 5 mM MgCl<sub>2</sub>. Concentration of DNA was determined from its absorbance at 260 and 280 nm respectively.  $A_{260}/A_{280}$  was calculated. The ratio obtained being in the range  $1.8 < A_{260}/A_{280} > 1.9$  indicate no further purification was required. The DNA was also characterized with the help of CD spectroscopy at 260 nm using a CD spectropolarimeter J815, JASCO. Concentration of DNA was determined in terms of nucleotide considering its molar extinction coefficient at 260 nm to be  $6600 \text{ M}^{-1} \text{ cm}^{-1}$ .



Proton dissociation constants of the compounds were determined with the help of pH-metric titrations in the presence of different concentrations of calf thymus DNA. 10% ethanol-90% aqueous solutions of compounds were used. The ionic strength of the medium was maintained at 0.12 M. pH was recorded with the help of a pH meter [Equiptronics, EQ-610, India]. Absorbance of alizarin recorded at 525 nm and purpurin at 513 nm were plotted against pH of the medium. Equilibrium showing dissociation of purpurin is provided in Eqs. (1) and (2) respectively. In case of alizarin,  $\text{LH}_2\text{H}^*$  would be  $\text{LHH}^*$  [20,30].



Eq. (3) yields values for  $\text{pK}_{a1}$  and  $\text{pK}_{a2}$  respectively [20,21,30,35]

$$A_{\text{obs}} = \frac{A_1}{(1 + 10^{\text{pH}-\text{pK}_{a1}} + 10^{\text{pH}-\text{pK}_{a2}})} + \frac{A_2}{(1 + 10^{\text{pK}_{a1}-\text{pH}} + 10^{\text{pH}-\text{pK}_{a2}})} + \frac{A_3}{(1 + 10^{\text{pK}_{a1}-\text{pH}} + 10^{\text{pK}_{a2}-\text{pH}})} \quad (3)$$

$A_1$ ,  $A_2$  and  $A_3$  refer to absorbance of the forms  $\text{LH}_2\text{H}^*$ ,  $\text{LH}_2^-$ ,  $\text{L}^{3-}$  respectively for purpurin and  $\text{LHH}^*$ ,  $\text{LH}^-$ ,  $\text{L}^{2-}$  respectively for alizarin [20,21,30].  $\text{pK}_{a1}$  and  $\text{pK}_{a2}$  are  $\text{pK}_a$  values for the dissociation of the two compounds in the presence of different concentrations of calf thymus DNA.

## 3. Results & discussion

The compounds were titrated very slowly using very dilute NaOH in the presence of different concentrations of calf thymus DNA at a constant ionic strength of the medium. Figs. 1 & 2(A and B) are typical plots for variation of absorbance of alizarin and purpurin with pH, recorded

at different concentrations of calf thymus DNA. Fitting the experimental data according to Eq. (3),  $\text{pK}_{a1}$  and  $\text{pK}_{a2}$  for alizarin and purpurin were determined. These were individually plotted against increased presence of calf thymus DNA for both compounds. It was observed that with an increase in concentration of calf thymus DNA,  $\text{pK}_{a1}$  of alizarin and purpurin decreased [Fig. 3] indicating constituent nucleic acid bases of DNA clearly affect the dissociation of phenolic –OH protons; the gradient of the plots were however different for the two compounds, which is expected. Since the second dissociation of alizarin [30], second and third dissociations of purpurin [36] occur well beyond physiological pH these were not included in the main text. The second and third dissociation of purpurin occur almost at the same time [21]; Fig. 1S [SI] is a plot of  $\text{pK}_{a2}$  of purpurin with increased concentrations of calf thymus DNA.

The interaction of purpurin with calf thymus DNA with regard to evaluation of the contribution of its neutral and anionic forms to overall binding constant under physiological conditions was revisited [21]. For alizarin, its interaction with calf thymus DNA with an emphasis on the contribution of its two forms was evaluated. Contributions of the neutral and anionic forms of the compounds towards their overall binding

constant with calf thymus DNA was determined by considering  $\text{pK}_{a1}$  once evaluated in normal aqueous solution and again in presence of a definite concentration of calf thymus DNA. For both compounds,  $\text{pK}_{a1}$  that was used in the calculations and determined in the presence of calf thymus DNA was chosen from Fig. 3A and B respectively (from best fit lines) by selecting a value intermediate between lowest and highest concentrations of DNA used in the plots. Values chosen for  $\text{pK}_{a1}$  were 5.94 for alizarin and 5.71 for purpurin. The corresponding values determined in normal aqueous solution was 6.2 for alizarin and 5.57 for purpurin.

Table 1 provides overall binding constant values of alizarin and purpurin determined at different pH at a constant ionic strength (with respect to 120 mM NaCl) of the medium. Considering overall binding constant values for the two compounds at different pH and using Eqs. (4) and (5), contributions of neutral ( $K^0$ ) and anionic ( $K^-$ ) forms of each compound to the overall binding constant with calf thymus DNA was evaluated.

$$K^*(1 + 10^{\text{pH}-\text{pK}}) = K^0 + K^- \times 10^{\text{pH}-\text{pK}} \quad (4)$$

$$\text{or } K^* = (K^0 + K^- \times 10^{\text{pH}-\text{pK}})/(1 + 10^{\text{pH}-\text{pK}}) \quad (5)$$

In Eqs. (4) & (5),  $K^*$  is the overall binding constant (determined experimentally) for the interaction of either alizarin or purpurin with calf thymus DNA.  $K^*$  is equal to  $\frac{[C_b]}{[C_f][\text{DNA}]}$ .  $K^*$  values of purpurin were taken from an earlier study [21] while that of alizarin was determined as a part of this study [Fig. 2S–Fig. 6S].  $K^0$  denotes the binding constant of the neutral form [ $K^0 = \frac{[C_b^0]}{[C_f^0][\text{DNA}]}$ ] and  $K^-$  that of the anionic form [ $K^- = \frac{[C_b^-]}{[C_f^-][\text{DNA}]}$ ] [18,21]. The total concentration of each compound was considered as  $C_0$  where  $C_0 = C_b + C_f$ .  $C_b$  denotes bound form and  $C_f$ , the free form of the two compounds interacting with calf thymus DNA.

Therefore, at any pH of the medium, during titration with calf

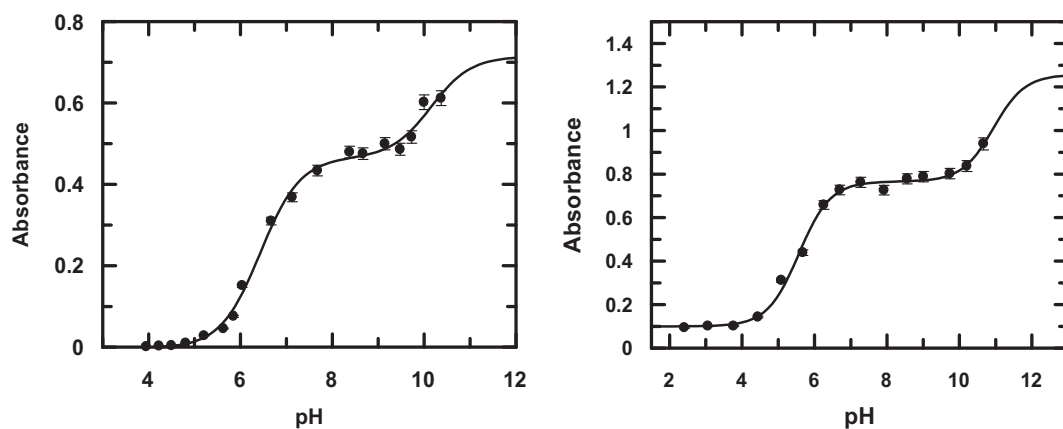


Fig. 1. pH-metric titration of alizarin as shown by a variation in absorbance at 525 nm in the presence of calf thymus DNA of concentrations (A) 62.7 μM and (B) 221.97 μM. [alizarin] = 100 μM; Temperature = 300 K.

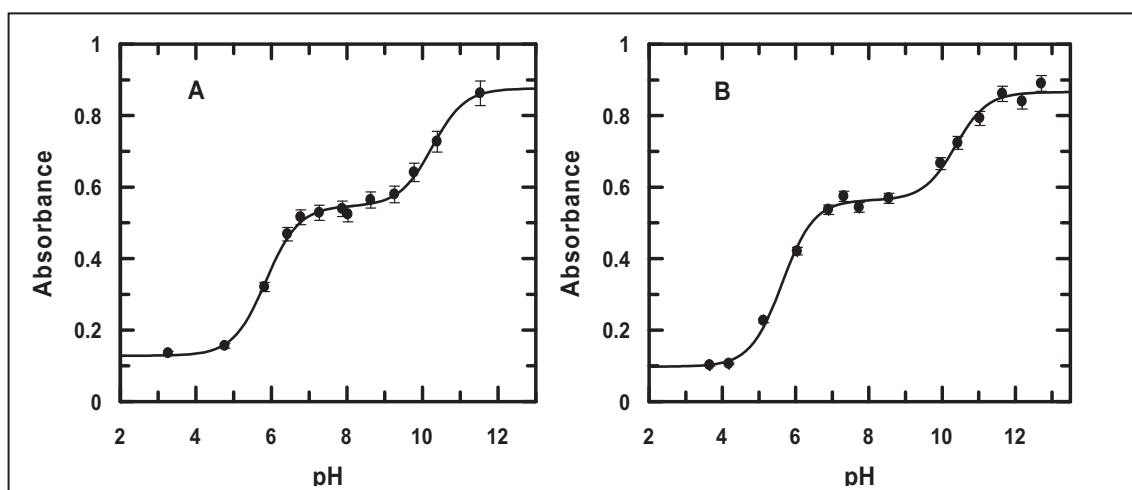


Fig. 2. pH-metric titration of purpurin as shown by a variation of absorbance at 513 nm in the presence of calf thymus DNA of concentrations (A) 66.88 μM and (B) 173.28 μM. [purpurin] = 100 μM; Temperature = 300 K.

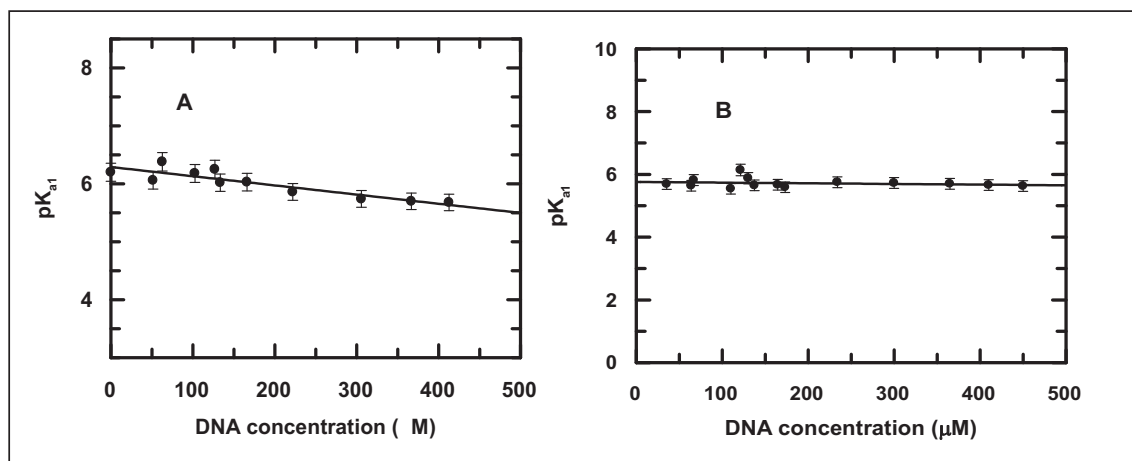


Fig. 3. A plot of  $pK_{a1}$  of (A) alizarin and (B) purpurin against increasing concentrations of calf thymus DNA. [Alizarin] = [Purpurin] = 100 μM; Temperature = 298 K.

thymus DNA both bound and free forms of the compounds would be present in solution. Of the bound form, a portion would bind to calf thymus DNA as neutral species while another portion would bind to it as anionic species. Similarly, the free form (not bound to DNA) would exist as neutral and anionic species. Hence, we may write

$$[C_b] = [C_b^0] + [C_b^-] \tag{6}$$

$$\text{and } [C_f] = [C_f^0] + [C_f^-] \tag{7}$$

A plot of  $K^*(1 + 10^{pH-pK})$  versus  $10^{pH-pK}$  (Eq. (4)) considering

**Table 1**

Overall binding constant values of alizarin and purpurin interacting with calf thymus DNA at different pH. Contributions of the neutral ( $K^0$ ) and anionic ( $K^-$ ) forms of each compound to their respective overall binding constants.

Compound	pH	Overall binding constant with calf thymus DNA ( $K^* \times 10^{-4}$ )	$pK_{a1}$ in the absence of DNA	$pK_{a1}$ in the presence of DNA	$K^0$ from Eq. (4) ( $K^0 \times 10^{-5}$ )	$K^0$ from Eq. (5) ( $K^0 \times 10^{-5}$ )	$K^-$ from Eq. (4) ( $K^- \times 10^{-4}$ )	$K^-$ from Eq. (5) ( $K^- \times 10^{-4}$ )
Alizarin	6.50	3.17	6.2		1.04	0.87	0.54	0.69
	6.70	2.80						
	7.02	1.91						
	7.40	1.04	5.94	1.68	1.31	0.56	0.75	
	7.65	1.05						
	7.97	0.67						
Purpurin	6.65	9.33	5.57		10.8	8.87	2.40	2.67
	6.88	6.45						
	7.16	4.84						
	7.40	4.51	5.71	8.0	6.68	2.39	2.65	
	7.88	2.95						
	8.35	2.56						

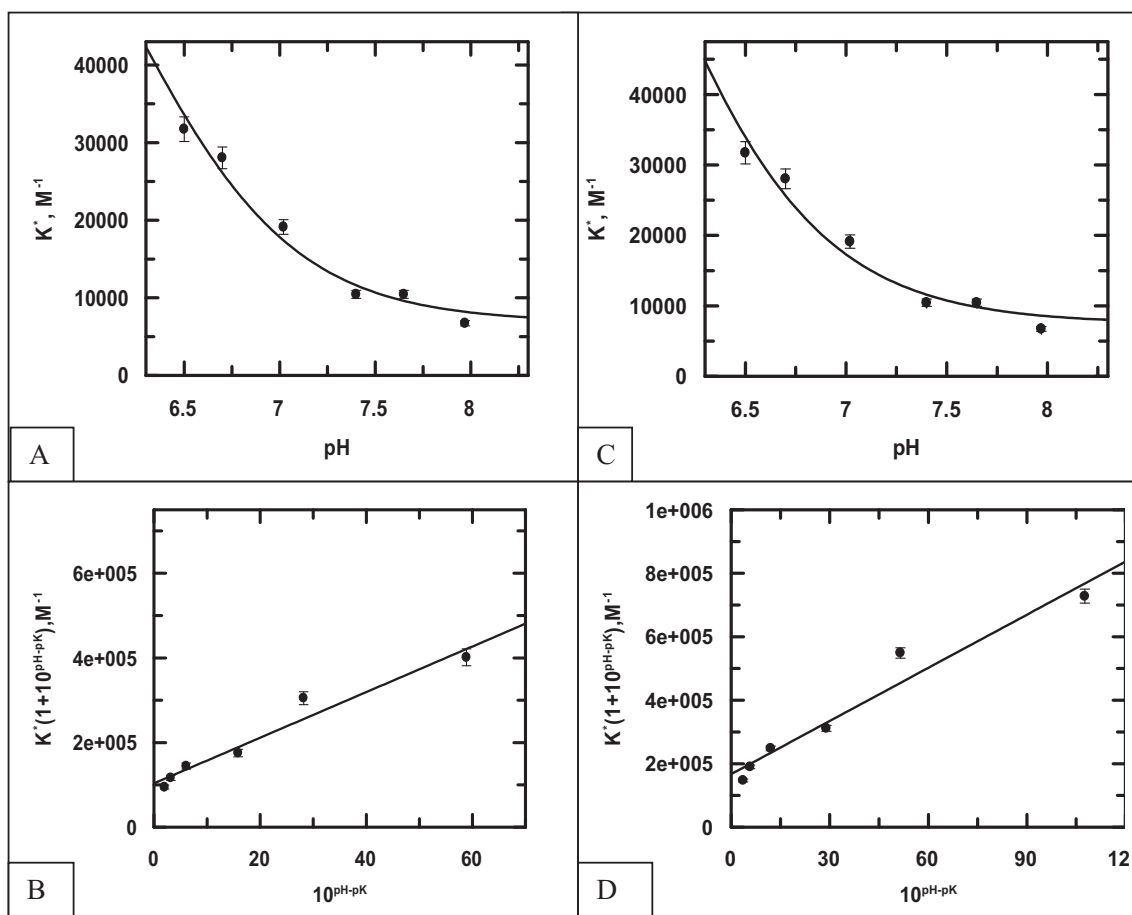


Fig. 4. (A) & (C) show overall binding constant ( $K^*$ ) for alizarin interacting with calf thymus DNA at different pH where the solid line is the fitted data obeying Eq. (5) considering  $pK_{a1} = 6.2$  (A) determined in normal aqueous solution in absence of DNA and  $pK_{a1} = 5.94$  (C) determined in presence of DNA. (B) and (D) are linear plots obtained by plotting  $K^*(1 + 10^{pH-pK})$  versus  $10^{pH-pK}$  where (B) uses  $pK_{a1}$  as 6.2 and (D) uses  $pK_{a1}$  as 5.94. They provide  $K^0$  and  $K^-$ , binding constants of neutral and anionic forms of alizarin from the intercept and slope respectively. [Alizarin] = 50  $\mu$ M; [NaCl] = 120 mM; [Tris buffer] = 30 mM; Temp. = 298 K.

different values of  $pK_{a1}$  for each compound (i.e. determined in the absence and presence of calf thymus DNA) generates a straight line (Fig. 4B & D, alizarin and Fig. 5B & D, purpurin) from where  $K^-$  was determined as the slope and  $K^0$  as the intercept (Table 1). Overall binding constant ( $K^*$ ) was also plotted against different pH for the two compounds. The data was fitted to Eq. (5) (Fig. 4A & C, alizarin and Fig. 5A & C, purpurin) and values for binding constants of the neutral and anionic species,  $K^0$  and  $K^-$  were evaluated. A comparison of the values obtained for  $K^0$  and  $K^-$  from Eqs. (4) & (5) for the two

compounds suggest they are close to each other. What was observed as a consequence of these calculations (Table 1) is that  $K^0$ , contribution of the neutral form to the overall binding constant ( $K^*$ ) showed a good variation corresponding to a change in  $pK_{a1}$  (i.e. determined in the absence and presence of DNA) while contribution of the anionic form ( $K^-$ ) remained practically the same.

In case of alizarin,  $K^0$  was slightly higher when  $pK_{a1}$  was considered to be 5.94 (determined in presence of DNA) than when it was 6.2 (determined in normal aqueous solution). In case of purpurin however,

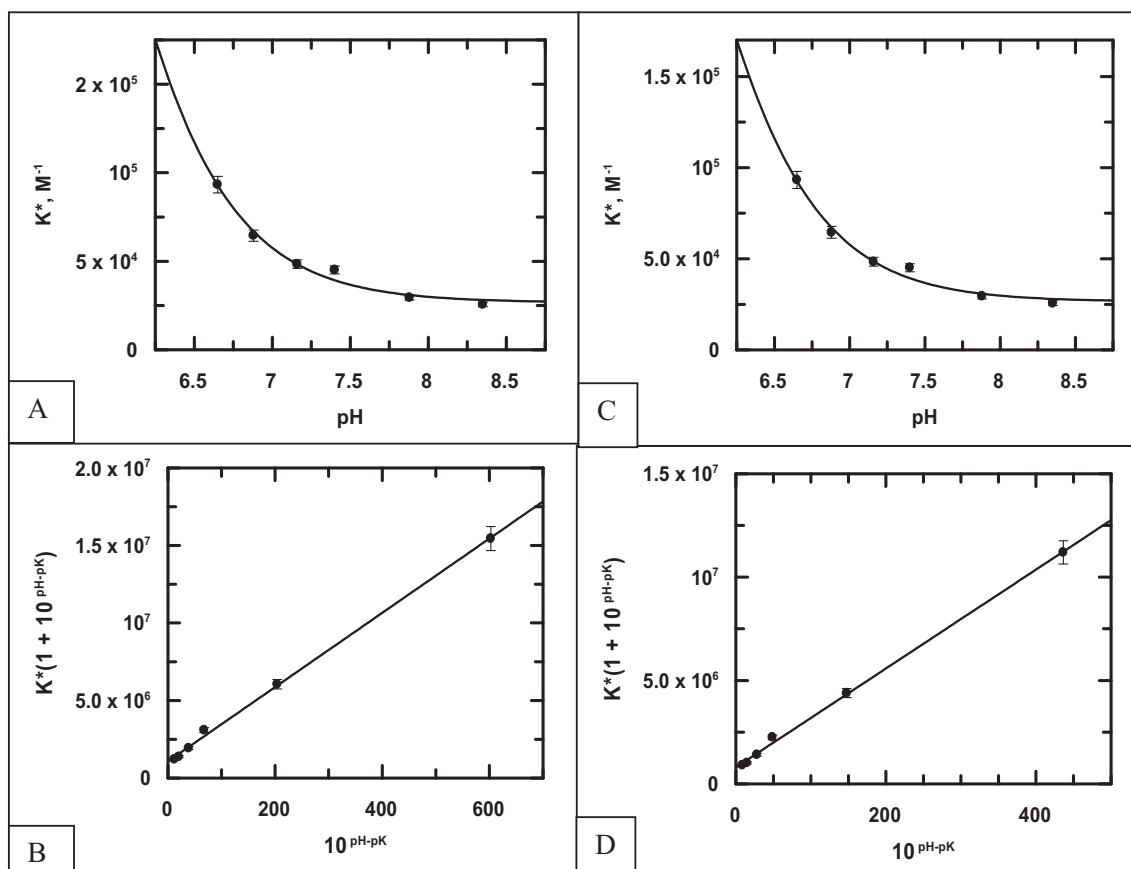


Fig. 5. (A) & (C) show overall binding constant ( $K^*$ ) for purpurin interacting with calf thymus DNA at different pH where the solid line is the fitted data obeying Eq. (5) considering  $pK_{a1} = 5.57$  (A) determined in normal aqueous solution in absence of DNA and  $pK_{a1} = 5.71$  (C) determined in presence of DNA. (B) and (D) are linear plots obtained by plotting  $K^*(1 + 10^{pH-pK_a})$  versus  $10^{pH-pK_a}$  where (B) uses  $pK_{a1}$  as 5.57 and (D) uses  $pK_{a1}$  as 5.71. They provide  $K^0$  and  $K^-$ , binding constants of the neutral and anionic forms of purpurin from the intercept and slope respectively. [Purpurin] = 75  $\mu M$ ; [NaCl] = 120 mM; [Tris buffer] = 30 mM; Temp. = 298 K.

$K^0$  was higher when  $pK_{a1}$  was 5.57 (determined in normal aqueous solution) than when it was 5.71 (determined in presence of DNA). It appears therefore that for alizarin contribution coming from the neutral form was greater when  $pK_{a1}$  used was determined in the presence of DNA while it was the reverse for purpurin; the value of  $K^-$  remained more or less the same, i.e. not showing much variation corresponding to a change in  $pK_{a1}$ .

Results clearly indicate that for both alizarin and purpurin, dissociation of phenolic  $-OH$  is influenced by the nucleic acid bases present in DNA. Therefore, such molecules that exist in two distinctly different forms at physiological pH, to correctly determine their contributions to the overall binding constant ( $K^*$ ) with DNA, it is essential that correct values of  $pK_a$  are used. A direct benefit of the study is that from a knowledge of  $K^0$  and  $K^-$  it would be possible to evaluate the overall binding constant of a molecule interacting with DNA at any pH without having to perform the experiment at that pH.

#### 4. Conclusion

The study helps us to realize that a proper determination of  $pK_a$  is essential for use in physicochemical experiments for determination of biophysical parameters. This was understood through this study using two hydroxy-9,10-anthraquinones, alizarin and purpurin. Evaluation of the contributions of the neutral and anionic forms of the molecules with the help of suitable equations, where  $pK_{a1}$  of the compounds have a decisive role, reveal contributions of different forms to the overall binding constants are actually different when the  $pK_a$  are different.

Therefore, if appropriate values of  $pK_a$  are not used, like that realized from this study, there is every possibility of either over emphasizing or under emphasizing the contribution of a certain form. The study emphasizes on the fact that there is a need to realize that most molecules interacting with DNA have more than one form in solution and that it must be considered for a correct analysis of any DNA interaction. This is also the reason why overall binding constants of a molecule change with a change in experimental (environmental) conditions having very high physiological significance. The study further revealed binding of purpurin to calf thymus DNA was higher than alizarin when the only difference between the two is an  $-OH$  group.

#### Acknowledgements

SD gratefully acknowledges financial support received from Department of Science & Technology, Govt. of West Bengal, India for the research project [794(Sanc.)1(10) ST/P/S&T/9G-23/2013]. MS expresses her gratitude to UGC, New Delhi for a Rajiv Gandhi National Fellowship. PN wish to thank the Department of Science & Technology, New Delhi for a DST-INSPIRE fellowship. SD is grateful to UGC, New Delhi for funds received as part of the research program on "Advanced Materials", as part of UPE II, under operation at Jadavpur University. He is grateful to DST-PURSE and UGC-CAS programs of the Government of India, operating at the Department of Chemistry, Jadavpur University for financial support. It needs mentioning here that the work was performed following a question by Dr. Sukanya Chakrabarti made at a seminar SD delivered at the Lady Brabourne College, Kolkata,

sometime in 2016, where he was asked whether it was correct to use  $pK_a$  values determined under normal conditions in aqueous solution for use in DNA binding analysis for evaluation of contribution of different forms of a compound binding to DNA. SD acknowledges the question once again.

## Appendix A. Supplementary data

Supplementary data to this article can be found online at <https://doi.org/10.1016/j.bpc.2018.02.001>.

## References

- [1] G.Y. Park, J.J. Wilson, Y. Song, S.J. Lippard, Phenanthriplatin, a monofunctional DNA-binding platinum anticancer drug candidate with unusual potency and cellular activity profile, *PNAS* 109 (2012) 11987–11992.
- [2] K. Cheung-Ong, G. Giaever, C. Nislow, DNA-damaging agents in cancer chemotherapy: serendipity and chemical biology, *Chem. Biol.* 20 (2013) 648–659.
- [3] S.S. David, E. Meggers, Inorganic chemical biology: from small metal complexes in biological systems to metalloproteins, *Curr. Opin. Chem. Biol.* 12 (2008) 194–196.
- [4] A. Abibi, E. Protozanova, V.V. Demidov, M.D. Frank-Kamenetskii, Specific versus nonspecific binding of cationic PNAs to duplex DNA, *Biophys. J.* 86 (2004) 3070–3078.
- [5] L.J. Boerner, J.M. Zaleski, Metal complex-DNA interactions: from transcription inhibition to photoactivated cleavage, *Curr. Opin. Chem. Biol.* 9 (2005) 135–144.
- [6] T. Fessl, F. Adamec, T. Polívka, S. Foldynová-Trantírková, F. Vácha, L. Trantírek, Towards characterization of DNA structure under physiological conditions in vivo at the single-molecule level using single-pair FRET, *Nucleic Acids Res.* 40 (2012) e121.
- [7] K.R. Fox, M.J. Waring, Investigations into the sequence-selective binding of mitramycin and related ligands to DNA, *Eur. J. Biochem.* 145 (1984) 579–586.
- [8] R.L. Jones, W.D. Wilson, Effect of ionic strength on the  $pK_a$  of ligands bound to DNA, *Biopolymers* 20 (1981) 141–154.
- [9] F. Barragán, P. López-Senín, L. Salassa, S. Betanzos-Lara, A. Habtemariam, V. Moreno, P.J. Sadler, V. Marchán, Photocontrolled DNA binding of a receptor-targeted organometallic ruthenium(II) complex, *J. Am. Chem. Soc.* 133 (2011) 14098–14108.
- [10] A. Paul, S. Bhattacharya, Chemistry and biology of DNA-binding small molecules, *Curr. Sci.* 102 (2012) 212–231.
- [11] R.E. Dickerson, H.R. Drew, B.N. Conner, M. Wing, A.V. Fratini, M.L. Kopka, The anatomy of A-, B-, and Z-DNA, *Science* 216 (1982) 475–485.
- [12] C.D. Mol, T. Izumi, S. Mitra, J.A. Tainer, DNA-bound structures and mutants reveal abasic DNA binding by APE1 DNA repair and coordination, *Nature* 403 (2000) 451–456.
- [13] A.D. Miroshnikova, A.A. Kuznetsova, N.A. Kuznetsov, O.S. Fedorova, Thermodynamics of damaged DNA binding and catalysis by human AP endonuclease 1, *Acta Nat.* 8 (2016) 103–110.
- [14] W. Engelen, B.M.G. Janssen, M. Merkkx, DNA-based control of protein activity, *Chem. Commun.* 52 (2016) 3598–3610.
- [15] M. Egli, DNA-cation interactions: quo vadis? *Chem. Biol.* 9 (2002) 277–286.
- [16] B.J. Pages, D.L. Ang, E.P. Wright, J.R. Aldrich-Wright, Metal complex interactions with DNA, *Dalton Trans.* 44 (2015) 3505–3526.
- [17] F. Frezard, A. Garnier-Suillerot, Comparison of the binding of anthracycline derivatives to purified DNA and to cell nuclei, *Biochim. Biophys. Acta* 1036 (1990) 121–127.
- [18] R. Comanici, B. Gabel, T. Gustavsson, D. Markovitsi, C. Cornaggia, S. Pommeret, C. Rusu, C. Kryschi, Femtosecond spectroscopic study of carminic acid–DNA interactions, *Chem. Phys.* 325 (2006) 509–518.
- [19] S. Mukherjee, P. Das, S. Das, Exploration of small hydroxy-9,10-anthraquinones as anthracycline analogues: physicochemical characteristics and DNA binding for comparison, *J. Phys. Org. Chem.* 25 (2012) 385–393.
- [20] P. Das, C.K. Jain, S.K. Dey, R. Saha, A.D. Chowdhury, S. Roychoudhury, S. Kumar, H.K. Majumder, S. Das, Synthesis, crystal structure, DNA interaction and in vitro anticancer activity of a Cu(II) complex of purpurin: dual poison for human DNA topoisomerase I and II, *RSC Adv.* 4 (2014) 59344–59357.
- [21] S. Mukherjee, P.K. Gopal, S. Paul, S. Das, Acetylation of 1,2,5,8-tetrahydroxy-9,10-anthraquinone improves binding to DNA and shows enhanced superoxide formation that explains better cytotoxicity on JURKAT T lymphocyte cells, *J. Anal. Oncol.* 3 (2014) 122–129.
- [22] P. Das, C.K. Jain, S. Roychoudhury, H.K. Majumder, S. Das, Design, synthesis and in vitro anticancer activity of a Cu(II) complex of carminic acid: a novel small molecule inhibitor of human DNA topoisomerase I and topoisomerase II, *ChemistrySelect* 1 (2016) 6623–6631.
- [23] B. Mandal, S. Singha, S.K. Dey, S. Mazumdar, T.K. Mondal, P. Karmakar, S. Kumar, S. Das, Synthesis, crystal structure from PXRD of a  $Mn^{II}$ (purp)<sub>2</sub> complex, interaction with DNA at different temperatures and pH and lack of stimulated ROS formation by the complex, *RSC Adv.* 6 (2016) 51520–51532.
- [24] B. Mandal, S. Singha, S.K. Dey, S. Mazumdar, S. Kumar, P. Karmakar, S. Das, Cu<sup>II</sup> complex of emodin with improved anticancer activity as demonstrated by its performance on HeLa and Hep G2 cells, *RSC Adv.* 7 (2017) 41403–41418.
- [25] A.B. Pradhan, L. Haque, S. Bhuiya, A. Ganguly, S. Das, Deciphering the positional influence of the hydroxyl group in the cinnamoyl part of 3-hydroxy flavonoids for structural modification and their interaction with the protonated and B form of calf thymus DNA using spectroscopic and molecular modeling studies, *J. Phys. Chem. B* 119 (2015) 6916–6929.
- [26] J. Markovits, C. Garbay-Jaureguiberry, B.P. Roques, J.B. Le Pecq, Acridine dimers: influence of the intercalating ring and of the linking-chain nature on the equilibrium and kinetic DNA-binding parameters, *Eur. J. Biochem.* 180 (1989) 359–366.
- [27] L. Di, E.H. Kerns, Application of pharmaceutical profiling assays for optimization of drug-like properties, *Curr. Opin. Discov. Devel.* 8 (2005) 495–504.
- [28] L. Di, E.H. Kerns, Profiling drug-like properties in discovery research, *Curr. Opin. Chem. Biol.* 7 (2003) 402–408.
- [29] S. Das, A. Saha, P.C. Mandal, Studies on the formation of Cu(II) and Ni(II) complexes of 1, 2-dihydroxy-9,10-anthraquinone and lack of stimulated superoxide formation by the complexes, *Talanta* 43 (1996) 95–102.
- [30] I.T. Suydam, S.D. Levandoski, S.A. Strobel, Catalytic importance of a protonated adenosine in the hairpin ribozyme active site, *Biochemistry* 49 (2010) 3723–3732.
- [31] S. Das, G.S. Kumar, M. Maiti, Conversions of the left-handed form and the protonated form of DNA back to the bound right-handed form by sanguinarine and ethidium: a comparative study, *Biophys. Chem.* 76 (1999) 199–218.
- [32] P. Das, D. Bhattacharya, P. Karmakar, S. Das, Influence of ionic strength on the interaction of THA and its Cu(II) complex with DNA helps to explain studies on various breast cancer cells, *RSC Adv.* 5 (2015) 73099–73111.
- [33] G. Dodin, M.-A. Schwaller, J. Aubard, C. Paoletti, Binding of ellipticine base and ellipticinium cation to calf-thymus DNA, *Eur. J. Biochem.* 176 (1988) 371–376.
- [34] P.S. Guin, S. Das, P.C. Mandal, Studies on the formation of a complex of Cu(II) with sodium 1,4-dihydroxy-9,10-anthraquinone-2-sulphonate – an analogue of the core unit of anthracycline anticancer drugs and its interaction with calf thymus DNA, *J. Inorg. Biochem.* 103 (2009) 1702–1710.
- [35] P. Das, P.S. Guin, P.C. Mandal, M. Paul, S. Paul, S. Das, Cyclic voltammetric studies of 1, 2, 4-trihydroxy-9,10-anthraquinone, its interaction with calf thymus DNA and anti-leukemic activity on MOLT-4 cell lines: a comparison with anthracycline anticancer drugs, *J. Phys. Org. Chem.* 24 (2011) 774–785.

# Utilization of Guanidine-Based Ancillary Ligands in Arene–Ruthenium Complexes for Selective Cytotoxicity

Jit Karmakar, Promita Nandy, Saurabh Das, Debalina Bhattacharya, Parimal Karmakar, and Samaresh Bhattacharya\*



Cite This: *ACS Omega* 2021, 6, 8226–8238



Read Online

ACCESS |



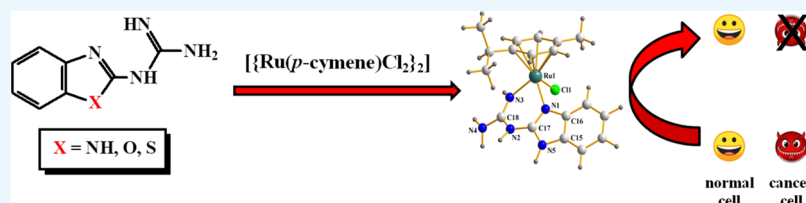
Metrics & More



Article Recommendations



Supporting Information



**ABSTRACT:** A family of three water-soluble half-sandwich arene–ruthenium complexes, depicted as  $C_1$ – $C_3$ , having the general formula  $[Ru(p\text{-cymene})(L)Cl]Cl$  has been synthesized, where L represents (1*H*-benzo[*d*]imidazol-2-yl)guanidine ( $L_1$ ) or (benzo[*d*]oxazol-2-yl)guanidine ( $L_2$ ) or (benzo[*d*]thiazol-2-yl)guanidine ( $L_3$ ). The crystal structure of complex  $C_3$  has been determined. The complexes show several absorption bands in the visible and ultraviolet regions, and they also show prominent emission in the visible region while excited near 400 nm. Studies on the interaction of ligands  $L_1$ – $L_3$  and complexes  $C_1$ – $C_3$  with calf thymus DNA reveal that the complexes are better DNA binders than the ligands, which is attributable to the imposed planarity of the ruthenium-bound guanidine-based ligand, enabling it to serve as a better intercalator. Molecular docking studies show that the complexes effectively bind with DNA through electrostatic and H-bonding interactions and partial intercalation of the guanidine-based ligands. Cytotoxicity studies carried out on two carcinoma cell lines (PC3 and A549) and on two non-cancer cell lines (BPH1 and WI-38) show a marked improvement in antitumor activity owing to complex formation, which is attributed to improvement in cellular uptake on complex formation. The  $C_1$  complex is found to exhibit the most prominent activity against the PC3 cell line. Inclusion of the guanidine-based ligands in the half-sandwich ruthenium–arene complexes is found to be effective for displaying selective cytotoxicity to cancer cells and also for convenient tracing of the complexes in cells due to their prominent emissive nature.

## 1. INTRODUCTION

Development of a new series of therapeutic agents and modification of any existing series are an essential and challenging aspect of research related to the treatment of cancer. Platinum metal-based species, especially coordination and organometallic complexes, are widely employed as chemotherapeutics in combating this dreadful disease.<sup>1</sup> However, relatively low selectivity and adverse side effects of majority of these species have led to new initiatives toward development of better chemotherapeutic agents, particularly of new platinum metal-based anticancer complexes with minimal side effects and high selectivity and cytotoxicity toward cancer cells.

Among the platinum metal-based species, ruthenium compounds have found a very special position owing to their prominent anticancer activities.<sup>2</sup> Ruthenium-based molecular species are found to be promising candidates for the development of novel anticancer agents, primarily as they can bind DNA in several possible modes, a property usually not found in platinum-based species. Hence, the ruthenium-based species also have the potential to treat platinum-resistant cancers. Among the different oxidation states of ruthenium, the

+2 state is most preferred for antitumor activity due to stability of the ruthenium(II) complexes in vitro. Proper choice of a ligand scaffold is crucial for inducing the desired DNA binding and antitumor activity in the ruthenium(II) complexes. In this context, half-sandwich ruthenium–arene complexes are particularly noteworthy.<sup>3,4</sup> The presence of the planar arene moiety primarily blocks one face of the complex and thus directs most of the reactivity toward the other side. Besides, *para*-cymene, a heavily used arene moiety, is known to cause distortion in DNA conformation that eventually leads to DNA damage.<sup>5</sup> In half-sandwich ruthenium–arene complexes, there is ample scope of varying the ligand/ligand combination to occupy the remaining three coordination sites on the metal center. In the present work, where our main objective was to develop a new family of half-sandwich ruthenium–arene

**Received:** December 24, 2020

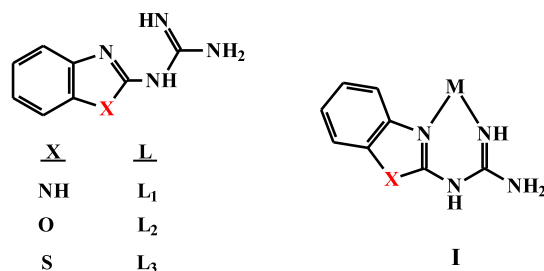
**Accepted:** March 11, 2021

**Published:** March 19, 2021



complexes for efficient DNA binding and anticancer activity, a group of three guanidine-based compounds was selected (Chart 1) as ancillary ligands. These ligands have several

Chart 1



important features, which are favorable for developing efficient DNA binding and anticancer agents. They have multiple N–H bonds, which are expected to favor solubility in water and binding with pyrimidine or purine bases via H-bonding and thus mislead the transcription process, resulting in DNA damage. In addition, the near-planar geometry of these ligands may enable them to function as intercalating moieties in the derived ruthenium complexes.<sup>3c,h,6</sup> The skeleton of the selected ligands has close resemblance with that of 4',6-diamidino-2-phenylindole (DAPI), a conjugated system that is known to efficiently stain DNA present in a cell,<sup>7</sup> which further encouraged us to use this group of ligands, with the hope that the mixed-ligand half-sandwich complexes derived from them may exhibit luminescence property and thus, they will be useful for measuring the capacity for cellular uptake and track a molecule within a cell. Among the three chosen ligands, synthesis of L<sub>1</sub> and L<sub>2</sub> and complexes of L<sub>1</sub> with few metals are known in the literature,<sup>8,9</sup> while L<sub>3</sub> is, to the best of our knowledge, new and coordination chemistry of L<sub>2</sub> and L<sub>3</sub> appears to remain unexplored. The L<sub>1</sub> ligand is known to coordinate metal centers as a bidentate N,N-donor, forming a stable six-membered chelate ring (I, X = NH),<sup>9</sup> and the L<sub>2</sub> and L<sub>3</sub> ligands are likely to display a similar mode of binding (I, X = O and S). As a source of ruthenium(II) and the arene moiety the dimeric [ $\{\text{Ru}(p\text{-cymene})\text{Cl}_2\}_2$ ] compound was utilized. Reaction of the selected guanidine-based ligands (L<sub>1</sub>–L<sub>3</sub>) with [ $\{\text{Ru}(p\text{-cymene})\text{Cl}_2\}_2$ ] indeed afforded half-sandwich ruthenium–arene complexes containing the ligands L<sub>1</sub>–L<sub>3</sub>. Herein, we describe the formation and characterization of these complexes, their DNA binding properties, and their cytotoxicity toward selected cancer cell lines.

## 2. EXPERIMENTAL SECTION

**2.1. Materials.** Ruthenium trichloride was purchased from Arora Matthey, Kolkata, India.  $\alpha$ -Phellandrene, [ $\text{Ru}(\text{bpy})_3$ ]( $\text{ClO}_4$ )<sub>2</sub>, and dicyandiamide were purchased from Sigma-Aldrich, USA. *o*-Phenylenediamine, 2-aminophenol, and 2-aminothiophenol were procured from Spectrochem, India. The guanidine-based ligands (L<sub>1</sub>–L<sub>3</sub>) were synthesized by reaction between *o*-phenylenediamine (or 2-aminophenol or 2-aminothiophenol) and dicyandiamide following a reported protocol.<sup>8</sup> [ $\{\text{Ru}(p\text{-cymene})\text{Cl}_2\}_2$ ] was synthesized by following a published procedure.<sup>10</sup> All other chemicals and solvents were reagent-grade commercial materials and were used as received.

**2.2. Physical Measurements.** Microanalyses (C, H, and N) were performed on a Heraeus Carlo Erba 1108 elemental analyzer. Magnetic susceptibilities were measured using a

Sherwood MK-1 balance. NMR spectra were recorded in CDCl<sub>3</sub> solution on Bruker Avance DPX 300 and 400 NMR spectrometers. IR spectra were obtained on a PerkinElmer Spectrum Two spectrometer with samples prepared as KBr pellets. Mass spectra were recorded with a Micromass LCT electrospray (Qtof Micro YA263) mass spectrometer. Electronic spectra were recorded on a PerkinElmer LAMBDA 25 spectrophotometer. Steady-state emission spectra were collected on a PerkinElmer LS 55 fluorescence spectrometer, and the quantum yields were determined by a relative method using [ $\text{Ru}(\text{bpy})_3$ ]<sup>2+</sup> as the standard. Solution electrical conductivities were measured using an Elico CM 180 conductivity meter with a solute concentration of ca. 10<sup>−3</sup> M. Geometry optimization by the density functional theory (DFT) method and electronic spectral analysis by TDDFT calculation were performed using the Gaussian 09 (B3LYP/SDD-6-31G) package.<sup>11</sup>

**2.3. X-ray Crystallography.** Single crystals of [ $\text{Ru}(p\text{-cymene})(\text{L}_3)\text{Cl}$ ] $\text{Cl}$  (C<sub>3</sub>) were grown by diffusion of diethyl ether vapor into a solution of the complex in acetonitrile. Selected crystal data and data collection parameters are given in Table 1. Data were collected on a Bruker SMART CCD

**Table 1. Crystal Data and Details of the Structure Determination for Complex C<sub>3</sub>**

empirical formula	C <sub>18</sub> H <sub>24</sub> Cl <sub>2</sub> N <sub>4</sub> ORuS
formula mass	516.45
crystal system	orthorhombic
space group	P2 <sub>1</sub> 2 <sub>1</sub> 2 <sub>1</sub>
<i>a</i> (Å)	7.5864(4)
<i>b</i> (Å)	12.9878(7)
<i>c</i> (Å)	21.6163(12)
<i>V</i> (Å <sup>3</sup> )	2129.9(2)
<i>Z</i>	4
<i>D</i> <sub>calcd</sub> (g/cm <sup>3</sup> )	1.611
<i>F</i> (000)	1048
crystal size (mm)	0.16 × 0.18 × 0.24
<i>T</i> (K)	296
$\mu$ (mm <sup>−1</sup> )	1.101
<i>R</i> <sub>1</sub> <sup>a</sup>	0.0452
<i>wR</i> <sub>2</sub> <sup>b</sup>	0.1175
GOF <sup>c</sup>	1.03

<sup>a</sup> $R_1 = \sum |F_o| - |F_c| / \sum |F_o|$ . <sup>b</sup> $wR_2 = [\sum [w(F_o^2 - F_c^2)^2] / \sum [w(F_o^2)^2]]^{1/2}$ . <sup>c</sup>GOF =  $[\sum [w(F_o^2 - F_c^2)^2] / (M - N)]^{1/2}$ , where *M* is the number of reflections and *N* is the number of parameters refined.

diffractometer using graphite monochromated Mo  $K\alpha$  radiation ( $\lambda = 0.71073$  Å) at 296 K. X-ray structure solution and refinement were done using the SHELX-97 package.<sup>12</sup> H atoms were added at calculated positions.

**2.4. Synthesis of Complexes.** The [ $\text{Ru}(p\text{-cymene})(\text{L})\text{Cl}$ ] $\text{Cl}$  complexes (C<sub>1</sub>–C<sub>3</sub>) were synthesized by following a general procedure as described below.

The guanidine-based ligand (L<sub>1</sub>–L<sub>3</sub>) (0.2 mmol) was dissolved in hot methanol (50 mL). To it was added a solution of [ $\{\text{Ru}(p\text{-cymene})\text{Cl}_2\}_2$ ] (50 mg, 0.08 mmol) in dichloromethane (10 mL). The resulting solution was heated at reflux for 4 h to generate a yellowish-orange solution. The solvent was evaporated to almost one-fourth of its initial volume, diethyl ether (50 mL) was added to it, and the mixture was kept in a freezer for 12 h. Orange crystalline solid was

separated, which was collected by filtration, washed with dichloromethane followed with diethyl ether, and dried in air.

**2.4.1. [Ru(*p*-cymene)(L<sub>1</sub>)Cl]Cl (C<sub>1</sub>).** Yield: 79%. Anal. Calcd for C<sub>18</sub>H<sub>23</sub>N<sub>5</sub>Cl<sub>2</sub>Ru: C, 44.90; H, 4.78; N, 14.55. Found: C, 45.02; H, 4.68; N, 14.42%. MS-ES<sup>+</sup> in CH<sub>3</sub>OH (*m/z*): 410.1216 [M - HCl-Cl]<sup>+</sup>. IR data/cm<sup>-1</sup>: 3367, 2969, 1673, 1611, 1581, 1462, 1268. <sup>1</sup>H NMR (DMSO-*d*<sub>6</sub>, 500 MHz): δ (ppm) 7.43 (br s, 1H, NH), 7.28 (m, 2H, ArH), 7.09 (m, 2H, ArH), 6.03 (d, 2H, ArH, <sup>3</sup>J<sub>HH</sub> = 5.6 Hz), 5.87 (d, 2H, ArH, <sup>3</sup>J<sub>HH</sub> = 5.5 Hz), 3.43 (m, 1H, CH), 2.49 (s, 3H, CH<sub>3</sub>), 1.01 (m, 6H, 2CH<sub>3</sub>). <sup>13</sup>C NMR (DMSO-*d*<sub>6</sub>, 400 MHz): δ (ppm) 158.6, 152.3, 129.2, 126.4, 122.0, 112.4, 111.5, 30.5, 24.3. Molar conductivity in methanol at 298 K [Λ<sub>M</sub>/S m<sup>2</sup> M<sup>-1</sup>]: 83.

**2.4.2. [Ru(*p*-cymene)(L<sub>2</sub>)Cl]Cl (C<sub>2</sub>).** Yield: 74%. Anal. Calcd for C<sub>18</sub>H<sub>22</sub>N<sub>4</sub>O<sub>1</sub>Cl<sub>2</sub>Ru: C, 44.81; H, 4.56; N, 11.61. Found: C, 44.50; H, 4.41; N, 11.91%. MS-ES<sup>+</sup> in CH<sub>3</sub>OH (*m/z*): 411.1928 [M - HCl-Cl]<sup>+</sup>. IR data/cm<sup>-1</sup>: 3392, 1690, 1620, 1562, 1457, 1324, 1243. <sup>1</sup>H NMR (DMSO-*d*<sub>6</sub>, 500 MHz): δ (ppm) 7.91 (br s, NH), 7.50 (d, 1H, ArH, <sup>3</sup>J<sub>HH</sub> = 8.0 Hz), 7.48 (d, 1H, ArH, <sup>3</sup>J<sub>HH</sub> = 8.0 Hz), 7.27 (m, 1H, ArH), 7.21 (m, 1H, ArH), 5.77 (d, 1H, ArH, <sup>3</sup>J<sub>HH</sub> = 6.0 Hz), 5.72 (d, 1H, ArH, <sup>3</sup>J<sub>HH</sub> = 5.5 Hz), 2.80 (m, 1H, CH), 2.50 (s, 3H, CH<sub>3</sub>), 1.17 (m, 6H, 2CH<sub>3</sub>). <sup>13</sup>C NMR (DMSO-*d*<sub>6</sub>, 400 MHz): δ (ppm) 158.1, 154.5, 135.5, 122.2, 116.0, 110.2, 106.3, 43.4, 35.6. Molar conductivity in methanol at 298 K [Λ<sub>M</sub>/S m<sup>2</sup> M<sup>-1</sup>]: 81.

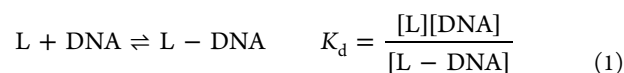
**2.4.3. [Ru(*p*-cymene)(L<sub>3</sub>)Cl]Cl (C<sub>3</sub>).** Yield: 81%. Anal. Calcd for C<sub>18</sub>H<sub>22</sub>N<sub>4</sub>S<sub>1</sub>Cl<sub>2</sub>Ru: C, 43.37; H, 4.41; N, 11.24. Found: C, 43.20; H, 4.43; N, 11.40%. MS-ES<sup>+</sup> in CH<sub>3</sub>OH (*m/z*): 427.0103 [M - HCl-Cl]<sup>+</sup>. IR data/cm<sup>-1</sup>: 3408, 3246, 2964, 2817, 1680, 1613, 1598, 1520, 1445, 1390, 1284, 1254, 1230. <sup>1</sup>H NMR (DMSO-*d*<sub>6</sub>, 400 MHz): δ (ppm) 7.25 (s, NH), 6.96 (d, 2H, ArH, <sup>3</sup>J<sub>HH</sub> = 8.5 Hz), 6.73 (d, 2H, ArH, <sup>3</sup>J<sub>HH</sub> = 8.5 Hz), 5.20 (br m, 2H, ArH), 4.96 (br m, 2H, ArH), 2.99 (m, 1H, CH), 1.59 (s, 3H, CH<sub>3</sub>), 1.40 (m, 6H, 2CH<sub>3</sub>). <sup>13</sup>C NMR (DMSO-*d*<sub>6</sub>, 500 MHz): δ (ppm) 160.1, 157.5, 152.0, 125.6, 120.0, 102.5, 30.7, 22.6. Molar conductivity in methanol at 298 K [Λ<sub>M</sub>/S m<sup>2</sup> M<sup>-1</sup>]: 85.

## 2.5. Biological Studies. 2.5.1. Interaction with CT-DNA.

Phosphate buffer was prepared using NaH<sub>2</sub>PO<sub>4</sub> and Na<sub>2</sub>HPO<sub>4</sub> using triple-distilled water. Sodium nitrate (AR) was used to maintain the ionic strength of the medium. Calf thymus DNA, purchased from Sisco Research Laboratories, India, was dissolved in triple-distilled water containing 120 mM NaCl, 35 mM KCl, and 5 mM CaCl<sub>2</sub>. Absorbance was recorded at 260 and 280 nm; A<sub>260</sub>/A<sub>280</sub> was determined. The ratio being between 1.8 and 1.9 suggests that the DNA was sufficiently free from protein. It was characterized by measuring its CD spectrum at 260 nm using a CD spectropolarimeter (J815, JASCO). Concentration was determined in terms of nucleotide, considering the molar extinction coefficient at 260 nm to be 6600 M<sup>-1</sup> cm<sup>-1</sup>.

50 μM L<sub>1</sub> (ligand) and 50 μM C<sub>1</sub> (complex) were titrated separately with calf thymus DNA at constant pH and ionic strength of the medium. For the interaction of L<sub>1</sub> followed by fluorescence spectroscopy, excitation was done at 295 nm and emission was recorded at 331 nm. For the complex, the excitation was done at 425 nm and emission was recorded at 496 nm. Ionic strength was maintained using NaCl and NaNO<sub>3</sub>. The interaction of the compounds with DNA during titration led to a decrease in fluorescence in the case of the ligand and to an increase in fluorescence for the complex at the respective wavelengths where they were followed. The

interaction of compounds with DNA could be realized with eq 1.<sup>13–18</sup>



L represents compounds and K<sub>d</sub> is the dissociation constant for the interaction whose reciprocal provides the apparent binding constant (K<sub>app</sub>). Equation 2 is obtained from eq 1 where the reciprocal of the change in absorbance was plotted against the reciprocal of (C<sub>D</sub> - C<sub>0</sub>).<sup>13–18</sup> C<sub>D</sub> refers to concentration of calf thymus DNA and C<sub>0</sub> refers to concentration of compounds. Using eq 2, ΔF<sub>max</sub> could be determined along with K<sub>app</sub> (1/K<sub>d</sub>) from the intercept and slope.<sup>13–18</sup>

$$\frac{1}{\Delta F} = \frac{1}{\Delta F_{\max}} + \frac{K_d}{\Delta F_{\max}(C_D - C_L)} \quad (2)$$

ΔF represents the change in fluorescence of the compounds interacting with the calf thymus DNA during titration, while ΔF<sub>max</sub> indicates the maximum possible change in fluorescence.

$$K_d = \frac{\left[ C_L - \left( \frac{\Delta F}{\Delta F_{\max}} \right) C_L \right] \left[ C_D - \left( \frac{\Delta F}{\Delta F_{\max}} \right) C_L \right]}{\left( \frac{\Delta F}{\Delta F_{\max}} \right) C_L} \quad (3)$$

$$C_L \left( \frac{\Delta F}{\Delta F_{\max}} \right)^2 - (C_L + C_D + K_d) \left( \frac{\Delta F}{\Delta F_{\max}} \right) + C_D = 0 \quad (4)$$

ΔF/ΔF<sub>max</sub> was plotted against C<sub>D</sub>. Equations 3 and 4 were used to fit the data to a non-linear square fit that provides another set of values for the apparent binding constant.<sup>13–18</sup>

Titration were also analyzed using a modified form of the Scatchard equation [eq 5].<sup>19</sup> The overall binding constant (K') and site size (n) were determined.

$$\frac{r}{C_f} = K'(n - r) \quad (5)$$

r denotes the ratio of the concentration of the compound bound to DNA to the total concentration of DNA present in the reaction mixture at any point of the titration (C<sub>b</sub>/C<sub>D</sub>); C<sub>b</sub> is the concentration of the bound compound, while C<sub>f</sub> is that of the free compound. "n" provides binding stoichiometry in terms of the bound compound per nucleotide, while "n<sub>b</sub>" being the reciprocal of "n" denotes binding site size in terms of the number of nucleotides bound to a compound. "n<sub>b</sub>" was obtained by plotting ΔF/ΔF<sub>max</sub> against C<sub>D</sub>/[compound]. K' may also be obtained by multiplying K<sub>app</sub> with "n<sub>b</sub>" and is compared with values obtained from a modified form of the Scatchard equation.

**2.5.2. Molecular Docking Studies.** Molecular docking studies on complexes C1–C<sub>3</sub> were performed using HEX 6.3 software to identify possible binding sites in biomolecules. The three guanidine-based ligands (L<sub>1</sub>–L<sub>3</sub>) were also docked using AutoDockTools 1.5.6 software. The coordinates of each ruthenium complex were taken from its optimized structure as a .mol file and converted to a .pdb format using PyMOL 2.4 software. The crystal structure of B-DNA (PDB ID: 1BNA) was retrieved from the Protein Data Bank (<http://www.rcsb.org/pdb>). Visualization of the docked systems was performed using BIOVIA Discovery Studio Visualizer (DSV) 2020 software. Default parameters were used for docking calculations with the correlation type shape only, FFT mode at the

3D level, and grid dimension of 0.6 with receptor range 180 and ligand range 180 with twist range 360 and distance range 40.

**2.5.3. Cell Culture.** PC3, BPH1, A549, and WI-38 lung fibroblast cells were cultured in RPMI or DMEM medium (GIBCO, Invitrogen, Carlsbad, CA, US) supplemented with 10% fetal bovine serum (GIBCO), 100 IU/mL penicillin, and 100  $\mu\text{g}/\text{mL}$  streptomycin at 37 °C in a humidified atmosphere containing 5%  $\text{CO}_2$  (Heraeus, Thermo Scientific, MA, USA). All cell lines were procured from the National Centre for Cell Science in Pune, India. Cells were seeded in 96 well plates for 24 h prior to treatment with compounds.

**2.5.4. MTT Assay.** The antiproliferative effect of three complexes and the guanidine-based ligands on four cell lines, PC3, BPH1, A549, and WI-38 was determined by the MTT assay. Cells were seeded at a density of  $1 \times 10^4$  cells per well in a 24-well plate. Next, the cells were exposed to the complex and its ligand at different concentrations for another 24 h. After incubation, cells were washed with  $1 \times$  PBS twice. Thereafter, they were treated with 0.5  $\text{mg mL}^{-1}$  MTT solution (SRL) and incubated for 3–4 h at 37 °C until an insoluble purple-colored formazan product developed. The resulting product was dissolved in MTT extraction buffer and the OD was measured at 570 nm using a microplate reader (Epoch). The percentage survival was calculated considering the untreated cells as 100%.

**2.5.5. Single-Cell Gel Electrophoresis/Comet Assay.** A comet assay was performed after treating the cells (PC3 and BPH1) with complex  $\text{C}_1$  for 24 h at the lower (20  $\mu\text{M}$ ) and higher (80  $\mu\text{M}$ ) concentrations of the  $\text{IC}_{50}$  dose of 39.5  $\mu\text{M}$  for PC3. Briefly,  $1 \times 10^5$  cells  $\text{mL}^{-1}$  were mixed with 0.7% LMPA and embedded onto frosted slides. The slides were then dipped in a lysis solution [2.5 M NaCl, 100 mM EDTA, 10 mM Tris-HCl (pH 10)] that contains freshly added 1% Triton-X 100 and 10% DMSO and incubated for 1 h at 4 °C and placed into a horizontal electrophoresis tank filled with freshly prepared buffer (1 mM EDTA, 300 mM NaOH). Next, electrophoresis was performed for 20 min at a fixed voltage of 25 V and 300 mA. After that, slides were washed with a neutralization buffer (0.4 M Tris-HCl, pH 7.5) followed by staining with 20  $\text{mg mL}^{-1}$  ethidium bromide (SRL, India) for 15 min. The slides were then washed three times with  $1 \times$  PBS and observed under a fluorescence microscope (model: Leica, Germany). Around 50 comets per slide were counted for both the cell lines. An extension of each comet was analyzed using a computerized image analysis system (Kometsoftware 5.5) that gave % of tail DNA.<sup>20</sup>

**2.5.6. DAPI Staining.** After exposure with complex  $\text{C}_1$  at lower and higher concentrations of the  $\text{IC}_{50}$  dose of PC3 (39.5  $\mu\text{M}$ ) for 24 h, both the cells (PC3 and BPH1) were washed several times with  $1 \times$  PBS and stained with 0.2  $\text{mg mL}^{-1}$  DAPI in Vecta shield (Vector Laboratories Inc.). The percentage of cells with ruptured and decondensed nuclei was counted under a fluorescence microscope (Leica) and photographs were taken at 40 $\times$  magnification.

**2.5.7. Measurement of Intracellular Reactive Oxygen Species.** The production of intracellular reactive oxygen species (ROS) was estimated using a fluorescent dye, DCFDA. Approximately,  $3 \times 10^5$  cells per well were seeded in 35 mm plates, and after 24 h of seeding, cells were incubated with 20  $\mu\text{M}$  DCFDA (Sigma) dye for 1 h at 37 °C under dark conditions followed by the treatment of complex  $\text{C}_1$  for 24 h, at the lower (20  $\mu\text{M}$ ) and higher (80  $\mu\text{M}$ ) concentrations of

the  $\text{IC}_{50}$  doses of PC3 (39.5  $\mu\text{M}$ ). Cells without the complex were used as control. Fluorescence intensity was measured in a fluorescence spectrophotometer (model Hitachi, USA) at excitation and emission wavelengths of 504 and 529 nm, respectively. To nullify the autofluorescence of the complex which may interfere with the DCFDA dye, a set of experiments without cells were performed simultaneously.

**2.5.8. Cellular Imaging Study.** Both the cell lines PC3 and BPH1 were seeded in a cover slip for overnight. Next day, cells were incubated with 3 mM complex  $\text{C}_1$  for 1 h in 37 °C in a  $\text{CO}_2$  incubator. After incubation, cells were washed several times with  $1 \times$  PBS under dark conditions. Cells were then stained with DAPI in Vecta shield and observed under a fluorescence microscope.

### 3. RESULTS AND DISCUSSION

**3.1. Synthesis and Characterization.** As delineated in the Introduction, the first task of the present study was to synthesize a group of arene–ruthenium complexes using the chosen guanidine-based ancillary ligands ( $\text{L}_1$ – $\text{L}_3$ ). Accordingly, reactions of these ligands ( $\text{L}_1$ – $\text{L}_3$ ) with  $[\{\text{Ru}(p\text{-cymene})\text{Cl}_2\}_2]$  were carried out in 5:1 methanol/dichloromethane, which furnished the desired complexes of type  $[\text{Ru}(p\text{-cymene})(\text{L})\text{Cl}]\text{Cl}$  in decent yields. The three complexes obtained with ligands  $\text{L}_1$ ,  $\text{L}_2$ , and  $\text{L}_3$  are depicted, respectively, as  $\text{C}_1$ ,  $\text{C}_2$ , and  $\text{C}_3$ . Preliminary characterization (microanalysis, mass, IR, and NMR) data of these complexes agreed well with their compositions. In order to ascertain the coordination mode of the guanidine-based ligands in these complexes, the crystal structure of  $\text{C}_3$  was determined by X-ray crystallography.<sup>21</sup> The structure is presented in Figure 1, and

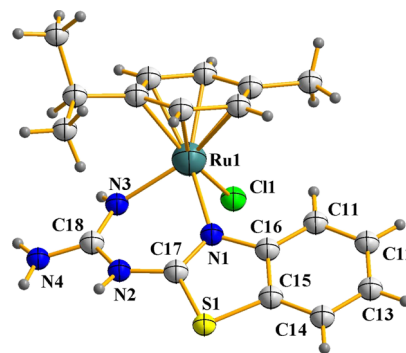


**Figure 1.** Crystal structure of the  $[\text{Ru}(p\text{-cymene})(\text{L}_3)\text{Cl}]^+$  complex.

some selected bond distances and angles are provided in Table 2. The structure reveals that the guanidine-based ligand ( $\text{L}_3$ ) is

**Table 2.** Selected Bond Distances and Bond Angles of Complex  $\text{C}_3$

Bond Distances (Å)			
Ru1–Cl1	2.4309(16)	N2–C18	1.377(8)
Ru1–N1	2.106(4)	N3–C18	1.308(8)
Ru1–N3	2.074(5)	N4–C18	1.340(9)
N1–C16	1.406(8)	S1–C15	1.734(7)
N1–C17	1.316(7)	S1–C17	1.739(6)
N2–C17	1.356(8)		
Bond Angles (deg)			
N1–Ru1–N3	82.83(19)	Cl1–Ru1–N1	86.13(16)
		Cl1–Ru1–N3	88.50(17)

coordinated to ruthenium as a neutral N,N-donor, forming a six-membered chelate ring (I, X = S and M = Ru) with a bite angle of  $\sim 83^\circ$ . The Ru(L<sub>3</sub>) fragment of the complex is found to be nearly planar, as envisaged. The *p*-cymene moiety is bound to ruthenium in the usual  $\pi$ -fashion, and a chloride ion has taken up the sixth coordination site on the metal center. Another isolated chloride ion was located outside the coordination sphere. The bond parameters around ruthenium and within the coordinated organic ligands are all found to be quite usual.<sup>3,9</sup> Based on the similarity of the synthetic method and properties (vide infra), the other two complexes (C<sub>1</sub> and C<sub>2</sub>) are assumed to have similar structures as C<sub>3</sub>.

**3.2. Spectral Studies.** Magnetic susceptibility measurements show that the C<sub>1</sub>–C<sub>3</sub> complexes are diamagnetic, which is consistent with the +2 oxidation state of ruthenium (low-spin  $d^6$   $S = 0$ ) in them. In the <sup>1</sup>H NMR spectra of the complexes, signals from both the coordinated *p*-cymene and guanidine-based ligand were expected, majority of which could be identified. For example, all the signals for the *p*-cymene ligand could be distinctly observed in all three complexes. Three signals from the alkyl groups are observed within 1.1–3.5 ppm and two signals from the aromatic fragment are observed within 5.2–5.8 ppm. From the guanidine-based ligands, the NH and NH<sub>2</sub> signals appeared within 6.5–8.2 ppm, while signals from the aromatic protons are observed around 7.5 ppm. In complex C<sub>1</sub>, a broad signal is observed at 10.50 ppm, which is absent in the spectra of the other two complexes, and hence, it is attributable to the benzimidazole-NH in metal-bound L<sub>1</sub>. <sup>13</sup>C NMR spectra of the complexes are also found to be consistent with their compositions. For the *p*-cymene ligand, three signals from the alkyl carbons are found below 40 ppm and four from the aromatic carbons appear within 70–90 ppm. For the guanidine-based ligands, two signals are observed above 150 ppm and signals from the phenyl ring are found within 110–130 ppm.

The mass spectra of complexes C<sub>1</sub>–C<sub>3</sub>, recorded in the positive ion mode, provide proof of coordination of the guanidine-based ligands. Each complex shows a peak at a  $m/z$  value that corresponds to the [Ru(*p*-cymene)(L-H)]<sup>+</sup> fragment, which is generated via loss of HCl from the cationic [Ru(*p*-cymene)(L)Cl]<sup>+</sup> unit. Associated with loss of the coordinated chloride ion, loss of proton is believed to take place from the central –NH– moiety of the guanidine-based ligand. This particular proton in such ligands is known to undergo facile dissociation.<sup>22</sup> Elimination of one equivalent HCl from compositionally similar arene–ruthenium complexes is precedent.<sup>22</sup> A similar mass spectral behavior of complexes C<sub>1</sub>–C<sub>3</sub> supports their similar composition and structure.

Infrared spectra of complexes C<sub>1</sub>–C<sub>3</sub>, recorded in the 450–4000 cm<sup>−1</sup> region, exhibit several bands. Upon comparison of the spectrum of each complex with that of the starting [{Ru(*p*-cymene)Cl<sub>2</sub>]<sub>2</sub>} complex reveals the presence of several new bands (near 3400, 3180, 1680, 1615, 1256, and 752 cm<sup>−1</sup>) in the spectra of the complexes, which are attributable to the coordinated guanidine-based ligand. Among these bands, the two near 3400 and 3180 cm<sup>−1</sup> are attributable to the –NH– and –NH<sub>2</sub> fragments, respectively. The NMR and IR data are therefore in good agreement with the composition of the complexes.

The C<sub>1</sub>–C<sub>3</sub> complexes are soluble in polar solvents, such as water, methanol, ethanol, dimethylformamide, and dimethylsulfoxide, producing yellow solutions. Electronic spectra of the complexes were recorded in methanol solutions. Spectral data

are presented in Table 3. Each complex shows four absorptions spanning the visible and ultraviolet regions. To have an insight

**Table 3. Electronic Absorption and Emission Spectral Data of the Complexes**

complex	absorption spectral data <sup>a</sup>		emission spectral data <sup>a</sup>	
	$\lambda_{\text{max}}$ nm ( $\epsilon$ , M <sup>−1</sup> cm <sup>−1</sup> )		$\lambda_{\text{F}}$ , nm [ $\Phi_{\text{F}} \times 10^{-3}$ ] <sup>c</sup>	life time ( $\tau$ )
C <sub>1</sub>	451 (400), 294 (5940), 237 <sup>b</sup> , 211 (21,970)		518 [8.6]	$\tau_1 = 0.26$ ns, $\tau_2 = 4.10$ ns
C <sub>2</sub>	449 (530), 282 (9190), 239 <sup>b</sup> , 209 (22,770)		558 [6.5]	$\tau_1 = 1.75$ ns
C <sub>3</sub>	429 (490), 289 (7780), 255 <sup>b</sup> , 220 (28,780)		486 [17.3]	$\tau_1 = 0.36$ ns, $\tau_2 = 5.02$ ns

<sup>a</sup>In methanol. <sup>b</sup>Shoulder. <sup>c</sup>Quantum yield was calculated with reference to [Ru(bpy)<sub>3</sub>]<sup>2+</sup> ( $\Phi_{\text{F}} = 0.09$ ).

into the nature of these absorptions, TDDFT calculations have been performed on the C<sub>1</sub>–C<sub>3</sub> complexes, using the Gaussian 09 package,<sup>11</sup> and the results are found to be similar for all the complexes. The DFT-optimized structures of the complexes are shown in Figure S1 (Supporting Information) and some computed bond parameters are listed in Table S1 (Supporting Information). The computed bond parameters in the DFT-optimized structure of C<sub>3</sub> are comparable with those found in its crystal structure. The main calculated transitions for the C<sub>1</sub>–C<sub>3</sub> complexes and compositions of the molecular orbitals associated with the transitions are presented in Tables S2–S7 (Supporting Information), and contour plots of selected molecular orbitals are shown in Figure S2 (Supporting Information). As the computed optical transitions and compositions of the participating orbitals are similar for all three complexes, the case of C<sub>1</sub> is described here as representative. Plots of experimental and theoretical spectra for C<sub>1</sub> are deposited in Figure S3 (Supporting Information). The close match between each set of experimental and theoretical spectra testifies validity of the optimized structures of the complexes, particularly of complexes C<sub>1</sub> and C<sub>2</sub>, for which crystal structures remained elusive. The lowest energy absorption at 451 nm is attributable primarily to a HOMO – 1 → LUMO transition, with much less HOMO – 3 → LUMO, HOMO – 2 → LUMO and HOMO → LUMO character. Additionally, based on the nature of the participating orbitals, the electronic excitation is best described as a MMCT transition mixed with some MLCT, LMCT, and LLCT character. The next absorption at 294 nm is mostly due to a HOMO – 1 → LUMO + 2 transition and assignable primarily to a MLCT transition with much less LLCT and ILCT character. The third absorption at 237 nm is largely due to a HOMO – 3 → LUMO + 2 transition and has a dominant MLCT character. The fourth absorption at 211 nm has a dominant HOMO – 3 → LUMO + 4 character and is assignable to a MLCT transition with some LLCT character.

Luminescence property of the complexes was examined in methanol solution. All three complexes were found to show prominent emission when excited near 400 nm (Table 3). It is interesting to note that the complexes absorb and emit in the visible region, a property much sought after in an antitumor agent for its easy identification in a biological matrix.

**3.3. DNA Binding Studies.** The interaction of the calf thymus DNA with complex C<sub>1</sub>, a representative of this family of complexes, was studied in detail to assess its potential as an antitumor agent. Initially, titration of the uncoordinated

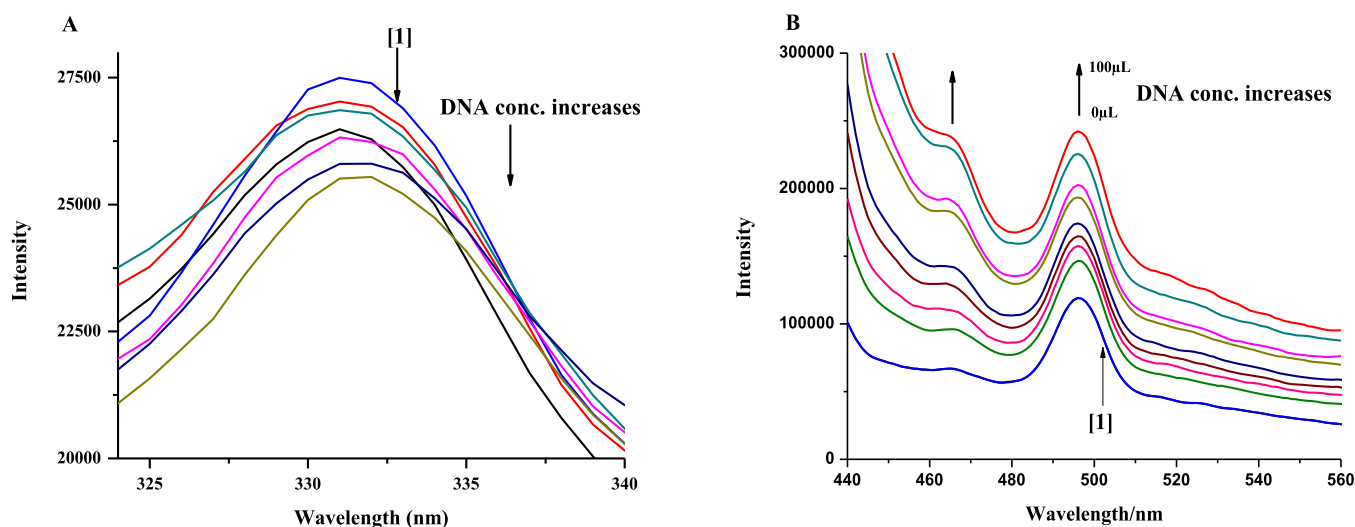


**Figure 2.** Fluorescence emission spectra of (A) 50  $\mu\text{M}$   $\text{L}_1$  and (B) 50  $\mu\text{M}$   $\text{C}_1$  in aqueous solution in the presence of 0.12 M NaCl and 30 mM Tris buffer (pH 7.4) in the absence (1) and presence of different concentrations of calf thymus DNA; temperature = 300 K.

**Table 4.** Binding Constant Values Obtained for the Interaction of Ligand  $\text{L}_1$  and Complex  $\text{C}_1$  with the Calf Thymus DNA that was Followed by Fluorescence Spectroscopy

compound	expt	$K_{\text{app}}$			site size $n_b$	$K^* = K_{\text{app}} \times n_b$			$K^*$ from Scatchard	$n_b$ from Scatchard as $n_b = (n^{-1})$
		from double-reciprocal plot (a)	from non-linear plot (b)	from double-reciprocal plot with $y$ -intercept = 1(c)		from double-reciprocal plot (a)	from non-linear plot (b)	from double-reciprocal plot with $y$ -intercept = 1(c)		
$\text{L}_1$	1	$2.80 \times 10^3$	$3.30 \times 10^3$	$1.60 \times 10^3$	8	$2.20 \times 10^4$	$2.60 \times 10^4$	$1.28 \times 10^4$	$1.86 \times 10^4$	8
	2	$2.20 \times 10^3$	$2.80 \times 10^3$	$2.20 \times 10^3$	9	$1.98 \times 10^4$	$2.50 \times 10^4$	$1.98 \times 10^4$	$3.60 \times 10^4$	7
$\text{C}_1$	1	$0.94 \times 10^4$	$0.80 \times 10^4$	$0.70 \times 10^4$	13	$1.20 \times 10^4$	$1.04 \times 10^4$	$0.91 \times 10^4$	$1.53 \times 10^4$	15
	2	$1.60 \times 10^3$	$1.04 \times 10^3$	$0.78 \times 10^3$	14	$2.20 \times 10^4$	$1.40 \times 10^4$	$1.09 \times 10^4$	$2.15 \times 10^4$	14

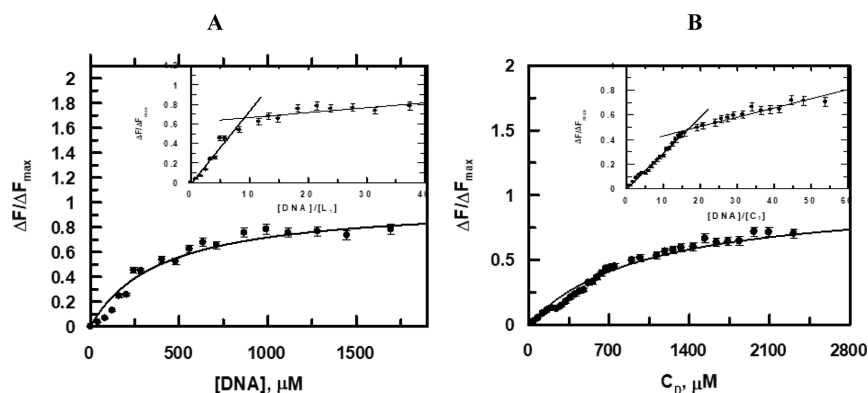


**Figure 3.** Binding isotherms for (A) ligand  $\text{L}_1$  and (B) complex  $\text{C}_1$  binding to the calf thymus DNA at pH  $\sim 7.4$  and an ionic strength of 0.12 M. Corresponding non-linear fits are shown for these titrations that evaluate  $K_{\text{app}}$ . Inset: plot of the normalized increase in fluorescence as a function of the ratio of the calf thymus DNA to (A) ligand  $\text{L}_1$  and (B) complex  $\text{C}_1$ .  $[\text{L}_1] = [\text{C}_1] = 50 \mu\text{M}$ , pH = 7.40,  $T = 300 \text{ K}$ .

guanidine-based ligand  $\text{L}_1$  was carried out with the calf thymus DNA. Figure 2A shows a typical plot of this titration at the ionic strength and pH mentioned. Figure 2B is a similar plot for a titration performed with complex  $\text{C}_1$ . The plots show that saturation is achieved in the binding of the compounds with DNA. Representative plots based on eq 2 are shown in Figure S4 (Supporting Information), from which the apparent binding constant ( $K_{\text{app}}$ ) was evaluated (Table 4).<sup>13–18</sup> Plots in Figure 3A,B were fitted by the non-linear square fit analysis that also helps to evaluate  $K_{\text{app}}$ . Different binding parameters are shown in Table 4. The inset of Figure 3A,B provides  $n_b$ , the number of nucleotides bound to each compound (Table 4).<sup>13–18</sup> It is

worth mentioning that the value for  $n_b$  obtained in the case of the complex binding to the calf thymus DNA was approximately 1.5 times greater than that obtained when the guanidine-based ligand  $\text{L}_1$  binds to the same DNA, suggesting that the complex engages more nucleic acid bases when it interacts with DNA, thus being able to bring about more distortion in DNA, an outcome of enforced planarity of the guanidine portion of the ligand following chelation to ruthenium (Table 4).<sup>15,16,18</sup>

Utilizing  $K_{\text{app}}$  and  $n_b$  from Table 4 and the relation  $K_{\text{app}} \times n_b = K^*$ , the overall binding constants could be evaluated for the uncoordinated guanidine-based ligand  $\text{L}_1$  and complex

$C_1$ .<sup>13–18</sup> Overall binding constants were also obtained from a modified version of the original Scatchard equation (eq 5),<sup>19</sup> and plots obeying this equation are shown in Figure S5 (Supporting Information). The overall binding constant values from the Scatchard equation were strikingly similar to those evaluated by multiplying  $K_{app}$  with  $n_b$  (eqs 2 and 4).

An interesting aspect regarding titration of the complex with the calf thymus DNA, followed by fluorescence spectroscopy, was that with an increase in the concentration of DNA (Figure 4), there was a gradual increase in fluorescence similar to that

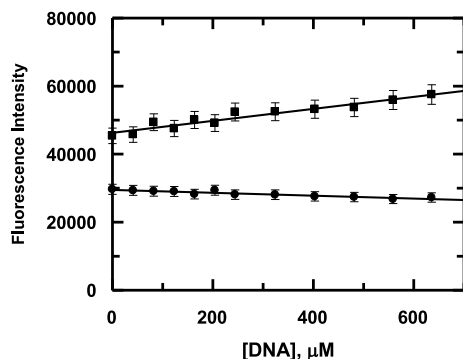


**Figure 4.** Gradual variation in fluorescence observed for the compounds as the calf thymus DNA was added during titration; (■) complex  $C_1$ , (●) ligand  $L_1$ . Ionic strength of medium = 0.12 M; pH  $\sim$  7.4;  $[L_1] = [C_1] = 50 \mu\text{M}$ ; temperature = 300 K.

observed for compounds including ethidium bromide that are known to intercalate DNA.<sup>23–26</sup> Hence, a logical conclusion is that the complex too is able to intercalate DNA, registering an increase in fluorescence. Such an increase in fluorescence upon interactions is an important attribute of the complex that may be utilized in a number of biological experiments to realize possible interactions of the compound with a biological target.

**3.4. Molecular Docking with DNA.** To elucidate the mode of interaction and binding affinity, docking studies were performed on B-DNA (PDB ID: 1BNA) in the presence of all the three complexes. The results show that the complexes interact with DNA quite similarly via the electrostatic mode. This is illustrated in Figure 5 for complex  $C_1$  and in Figures S6 and S7 (Supporting Information) for complexes  $C_2$  and  $C_3$ , respectively. In each case, the guanidine-based ligand is observed to form H-bonds with oxygen atoms of the phosphate backbone and also with the N3 atom of adenine of a single DNA strand. Additional H-bonding is observed in

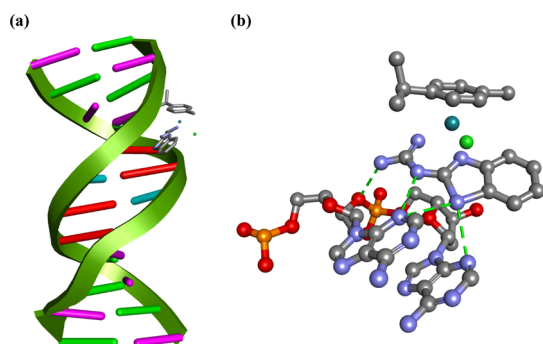


**Figure 5.** (a) Complex  $C_1$  interacted with the DNA strand and (b) core view of the interaction (ball and stick model).

complex  $C_1$  due to the presence of an NH fragment in  $L_1$  that is absent in  $L_2$  or  $L_3$ . The coordination-induced planarity of the guanidine-based ligands is found to favor strong H-bonding interactions, with better match of the complexes inside DNA strands allowing partial intercalation. Due to the combined effect of the van der Waals and H-bonding interactions, the complexes fit comfortably into the minor groove of the targeted DNA near the A–T rich regions.

Docking of the individual guanidine-based ligands with DNA has also been looked into. From the docked structures (Figure S8; Supporting Information), it is observed that the  $L_1$  ligand shows the highest binding affinity to DNA, which is attributable to additional H-bonding possible due to the presence of an NH fragment in  $L_1$ , instead of oxygen (in  $L_2$ ) or sulfur (in  $L_3$ ). The same trend is observed in the complexes, which is also manifested in the biological studies. It is interesting to note that while all the uncoordinated guanidine-based ligands preferred to approach the G–C base pairs, upon binding to the metal center, the A–T base pairs have become their preferred binding location. Planarity of the guanidine-based ligands in the complexes and the presence of the Ru-coordinated *p*-cymene probably have caused this observed variation in their binding preference.

**3.5. Cytotoxicity Studies.** Cisplatin shows a remarkable efficacy in treating prostate cancer and has been quite successfully and extensively used in the last few decades.<sup>27–29</sup>

However, as delineated in the Introduction, ruthenium-based molecular species, particularly the half-sandwich ruthenium–arene complexes, are also attracting attention owing to their demonstrated anticancer activities with minimal side effects. Encouraged by the prominent DNA binding properties of our three complexes ( $C_1$ ,  $C_2$ , and  $C_3$ ), we also determined the potency of these three complexes and cisplatin on the human prostate cancer cell line PC3 and the human benign prostate tumor cell line BPH1. Similarly, we have evaluated the toxic effect of these three complexes and cisplatin on the lung cancer cell line A549 and the normal lung fibroblast cell line WI-38. Cells were treated with three complexes ( $C_1$ ,  $C_2$ , and  $C_3$ ) in the concentration range of 0–100  $\mu\text{M}$  for 24 h, followed by MTT assay. The results are displayed in Figure 6. Complex  $C_1$  was found to be the most cytotoxic to PC3 cells ( $IC_{50} = 39.5 \pm 1.57 \mu\text{M}$ ) among the three complexes (Figure 6A). Complex  $C_1$  was found to be non-toxic to the human prostate benign tumor cell line BPH1 even after 24 h of treatment, which suggests no side effects of it on non-carcinoma cells in our body. In this context, it is worth mentioning that cisplatin shows comparable cytotoxicity toward both PC3 and BPH1 cell lines. In A549 and WI-38 cell lines,  $C_1$  shows moderate ( $IC_{50}$  values  $69.4 \pm 1.2$  and  $69.6 \pm 3.45$ ) and almost comparable cytotoxicity like cisplatin ( $IC_{50}$  values  $60.1 \pm 2.43$  and  $66.5 \pm 2.12$ ). Guanidine-based ligands ( $L_1$ ,  $L_2$ , and  $L_3$ ) have no cytotoxicity toward any type of cell lines, which signifies the effect of their coordination to ruthenium in antiproliferative activity. Figure 6B shows the % cell survival comparison between BPH1 and PC3 with  $C_1$  complex for 24 h. The  $IC_{50}$  doses for all the complexes and cisplatin are summarized in Table 5. Interestingly, it was observed that the complexes could not exert significant toxicity toward A549 and WI-38. Among the different cells we have tested, only PC3 is PTEN-negative. Thus, it is reasonable to state that cytotoxicity generated through the compounds is presumably governed by nonfunctional PTEN. Similar results are also found in the case

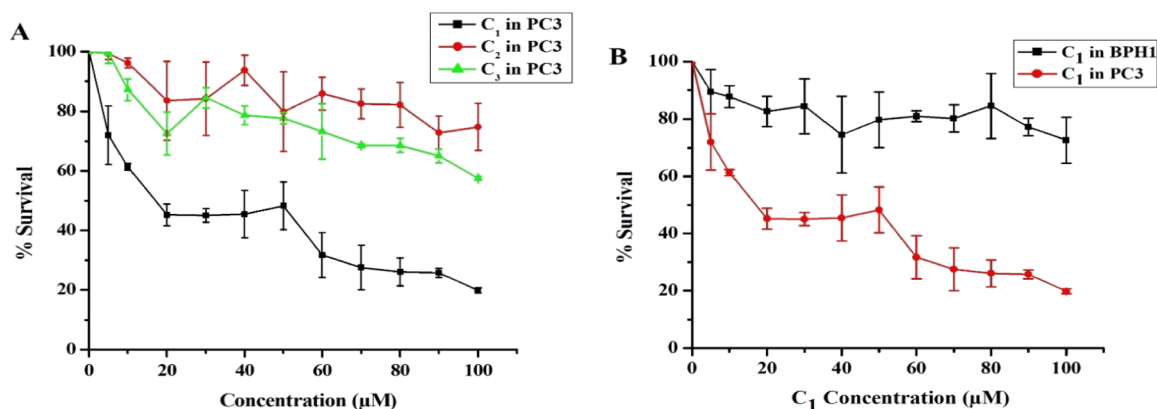


**Figure 6.** (A) MTT assay on the PC3 cell line after 24 h of treatment with three separate complexes  $C_1$ – $C_3$ . (B) MTT assay on PC3 and BPH1 cell lines after 24 h of treatment with the  $C_1$  complex. Data are presented as % survival relative to the untreated control. They are the mean  $\pm$  SD of three independent experiments.

**Table 5.** IC<sub>50</sub> Values of Ligands (L) and Complexes toward Different Cell Lines<sup>a</sup>

complex	PC3	BPH1	A549	WI-38	R <sub>1</sub> <sup>b</sup>	R <sub>2</sub> <sup>c</sup>
L <sub>1</sub>	121.0 $\pm$ 1.57	>500 $\pm$ 4.5	>200 $\pm$ 2.2	>500 $\pm$ 4.67	nd	nd
L <sub>2</sub>	168.8 $\pm$ 1.9	>500 $\pm$ 4.09	167.4 $\pm$ 1.77	>500 $\pm$ 5.03	nd	nd
L <sub>3</sub>	446.4 $\pm$ 1.05	>500 $\pm$ 2.32	>200 $\pm$ 1.86	>500 $\pm$ 4.41	nd	nd
C <sub>1</sub>	39.5 $\pm$ 1.57	263.0 $\pm$ 1.87	69.4 $\pm$ 1.2	69.6 $\pm$ 3.45	6.6	1.0
C <sub>2</sub>	267.3 $\pm$ 2.01	443.9 $\pm$ 1.04	168.6 $\pm$ 1.5	135.9 $\pm$ 3.21	1.6	0.8
C <sub>3</sub>	125.0 $\pm$ 1.43	175.2 $\pm$ 1.88	112.2 $\pm$ 1.9	135.7 $\pm$ 4.89	1.4	1.2
cisplatin	5.4 $\pm$ 1.93	8.0 $\pm$ 1.03	60.1 $\pm$ 2.43	66.5 $\pm$ 2.12	1.4	1.1

<sup>a</sup>The drug treatment period was 24 h. <sup>b</sup>R<sub>1</sub> = IC<sub>50</sub> ratio of BPH1 cells to PC3 cells. <sup>c</sup>R<sub>2</sub> = IC<sub>50</sub> ratio of WI-38 cells to A549 cells.

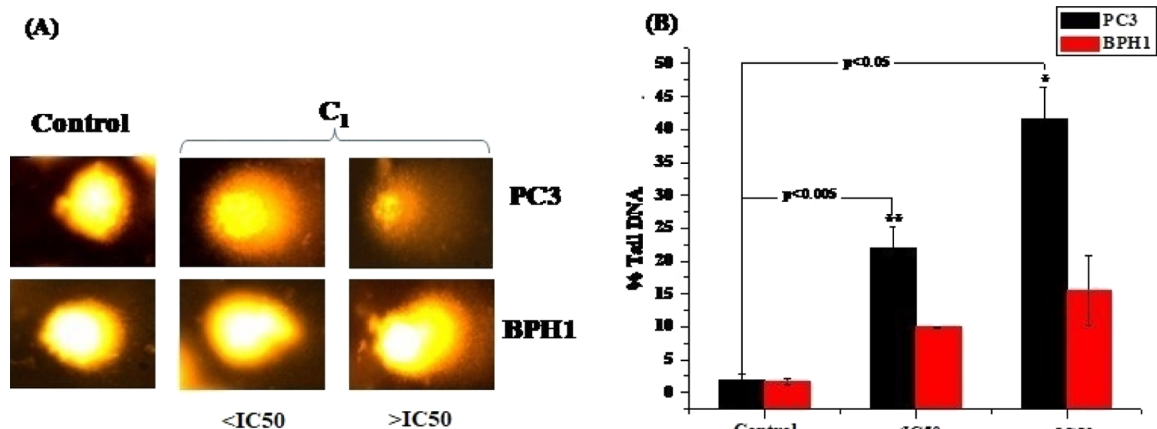


**Figure 7.** (A) Representative images of the comet assay of PC3 and BPH1 cell lines treated with the  $C_1$  complex with respect to the untreated control. (B) Histogram shows % of comet tail DNA for PC3 and BPH1 cells treated with the  $C_1$  complex for 24 h with respect to their untreated control at two different doses (<IC<sub>50</sub> and >IC<sub>50</sub> doses of PC3). Values are the mean  $\pm$  SD of three independent experiments. \* ( $p < 0.005$ ) and \*\* ( $p < 0.005$ ) denote the statistically significant difference compared to the untreated control.

of curcumin.<sup>30</sup> All the other biological studies were done on two cell lines, PC3 and BPH1, taking  $C_1$  as a model complex.

The cytotoxic effect of the  $C_1$  complex is most likely linked to the DNA-damaging effects of the compound, and hence, we performed comet assay, a very useful and sensitive experiment for elucidating single- or double-strand DNA damage caused by any exogenous or endogenous species.<sup>31</sup> A small amount of nucleides/cells is required to perform this experiment and the tail length is considered to represent the level of DNA damage.<sup>32</sup> As shown in Figure 7A, the  $C_1$  complex caused significantly ( $p < 0.05$ ) more DNA damage at a concentration <IC<sub>50</sub> or >IC<sub>50</sub> dose in the case of PC3. However, at the same

concentrations, no significant ( $p > 0.05$ ) DNA damage was observed when BPH1 is used. Consistent with these data, the percentage of tail DNA increased significantly ( $p < 0.05$ ) for  $C_1$  complex-treated PC3 cells after 24 h of treatment (Figure 7B).

Nuclear morphology and the nature of cell death were studied by DAPI staining. The fluorescence micrographs of DAPI-stained PC3 and BPH1 cell lines are shown in Figure 8A, and the percentage of apoptotic cells is presented graphically in Figure 8B. When PC3 cells were treated with the  $C_1$  complex at a concentration >IC<sub>50</sub> dose for 24 h, we

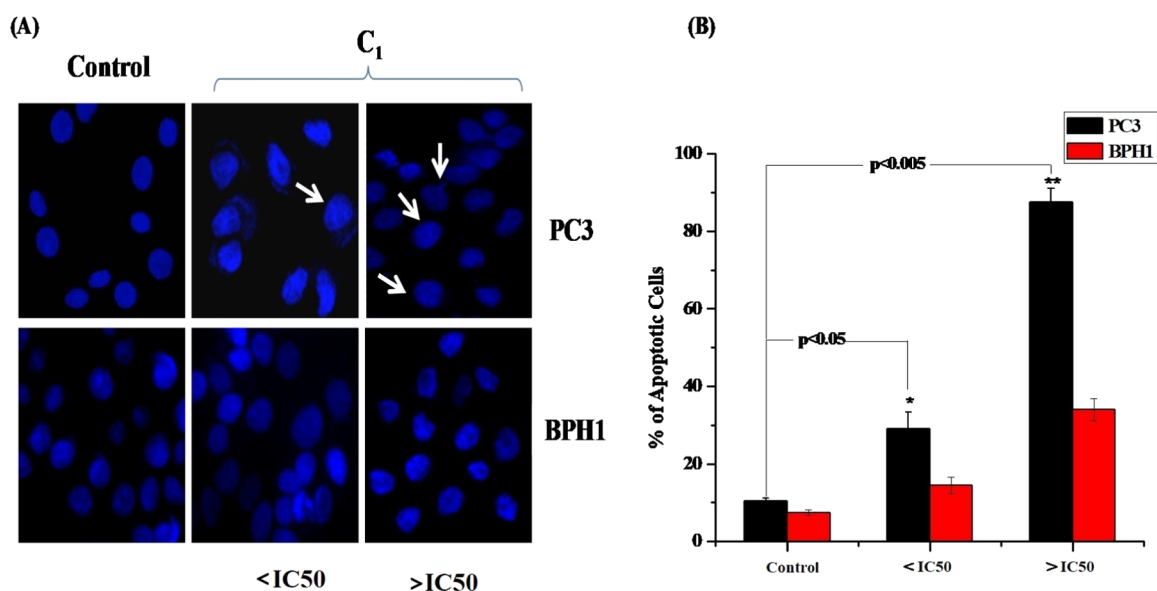


**Figure 8.** (A) Fluorescence micrographs of DAPI-stained PC3 and BPH1 cell lines under 40 $\times$  magnification. Both the cells are treated with the  $C_1$  complex for 24 h at two different doses (<math><IC\_{50}</math> and >math>>IC\_{50}</math> doses of PC3). The arrow represents the decondensed nucleus of the apoptotic cells. (B) % of apoptotic cells as determined by DAPI staining followed by fluorescence microscopic observations. Each value represents the mean  $\pm$  S.D. of three independent experiments. \* ( $p < 0.05$ ) and \*\* ( $p < 0.005$ ) denote the statistically significant difference compared to the untreated control.

found that 80–85% cells were apoptotic in nature, whereas for BPH1, the amount of apoptotic cells reduced to only 30–35%.

Ru(II)–arene complexes are well known to bring about cell damage via production of ROS within the cells.<sup>33</sup> It is interesting to note that among the other metals (such as Pt, Pd, and Au) used as therapeutics, only Ru shows higher antitumor activity mediated by an enhanced ROS production.<sup>34</sup> Apoptotic cell death and DNA damage are connected with ROS production, and we also estimated ROS production induced by the  $C_1$  complex in PC3 and BPH1, where we have used a fluorescent dye, DCFDA (2',7'-dichlorofluorescein diacetate), for indicating oxidative stress and hydroxyl and peroxy radical generation.<sup>35</sup> The ROS generation in PC3 and BPH1 cell lines after treating with the  $C_1$  complex for 24 h is shown in Figure 9. It was observed that PC3 cells exposed to

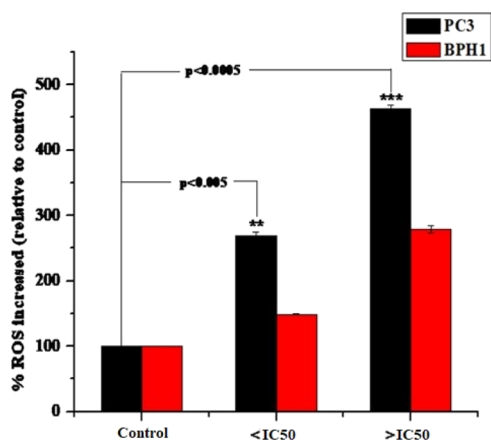


**Figure 9.** Intracellular ROS generation of PC3 and BPH1 cell lines treated with the  $C_1$  complex for 24 h at two different doses (<math><IC\_{50}</math> and >math>>IC\_{50}</math> doses of PC3). Data are presented as % increase in ROS relative to untreated controls. Values are the mean  $\pm$  SD of three independent experiments. \*\*\* ( $p < 0.0005$ ) and \*\* ( $p < 0.005$ ) denote the statistically significant difference compared to untreated controls.

the  $C_1$  complex produced a significantly high amount ( $p < 0.005$ ) of ROS, compared to BPH1 cells. The intracellular imaging behavior of the  $C_1$  complex was studied in both PC3 and BPH1 cell lines using fluorescence microscopy, and the results obtained are illustrated in Figure 10. After incubation with the  $C_1$  complex, BPH1 cells display no intracellular fluorescence. However, PC3 shows green fluorescence both in the cytoplasm and nuclei, suggesting that the  $C_1$  complex was distributed both in the cytosol and nucleus in the proliferating cancer cell line.

#### 4. CONCLUSIONS

The present study shows that the guanidine-based ligands (L) undergo facile reaction with  $[\{Ru(p\text{-cymene})Cl_2\}_2]$  to furnish cationic half-sandwich complexes of type  $[Ru(p\text{-cymene})(L)Cl]^+$ . This study also reveals that the complexes are better DNA binders than the corresponding uncoordinated guanidine-based ligands, and the observed enhancement in DNA binding is attributable to the imposed planarity of the guanidine-based ligand upon coordination to ruthenium that enabled it to serve as a better intercalator. Cytotoxicity studies also show a similar trend, the complexes being more cytotoxic than the uncoordinated guanidine-based ligands, presumably because complex formation leads to an improvement in cellular uptake that permits more molecules to enter cells, showing greater cytotoxicity. The other important aspect is that compared to cancer cells, the complexes were found to be significantly less toxic to normal cells, and this is most prominent in the  $C_1$  complex. This is probably due to the increased uptake of the complex molecules in cancer cells than normal cells, as the membrane transport system of cancer cells is more active than that of the normal cells or benign cells. Additionally, more uptake of complex molecules generates more reactive oxygen species that lead to more oxidative DNA damage as observed by the comet assay.<sup>36</sup> This study also demonstrates that inclusion of the guanidine-based ligands in the half-sandwich ruthenium–arene complexes, particularly in the  $C_1$  complex, has been useful for exhibition of remarkable

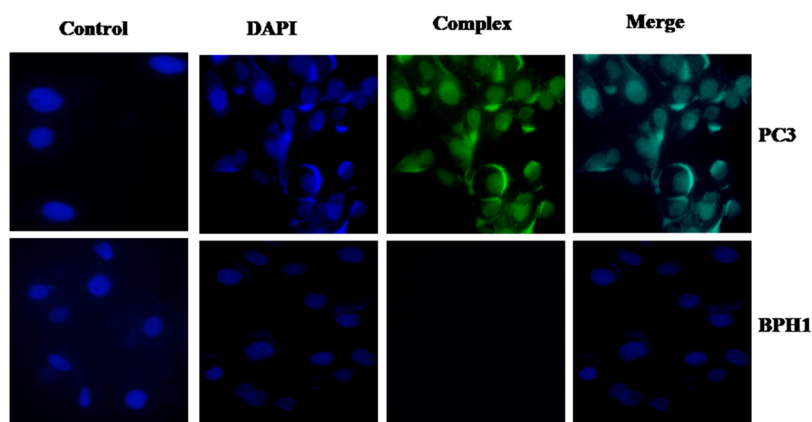


**Figure 10.** Cellular imaging of the  $C_1$  complex in both PC3 and BPH1 cell lines under a fluorescence microscope. DAPI and the  $C_1$  complex are visible as blue and green fluorescence, respectively. BPH1 cells display no intracellular fluorescence but PC3 shows green fluorescence both in the cytoplasm and nuclei.

antiproliferative activity against cancer cells with high selectivity and also for convenient tracing of the complexes in cells due to their prominent emissive nature. It is worth highlighting that such studies involving ligand modification at a single point (NH vs O vs S) are rare in the literature.<sup>37</sup>

## ■ ASSOCIATED CONTENT

### SI Supporting Information

The Supporting Information is available free of charge at <https://pubs.acs.org/doi/10.1021/acsomega.0c06265>.

DFT-optimized structures and computed bond parameters; data and figures related to TDDFT calculations; and figures and tables related to biological studies (PDF)

Crystallographic data (CIF)

### Accession Codes

CCDC 1955587 contains the supplementary crystallographic data for this paper.

## ■ AUTHOR INFORMATION

### Corresponding Author

Samaresh Bhattacharya – Department of Chemistry, Inorganic Chemistry Section, Jadavpur University, Kolkata 700 032, India; [orcid.org/0000-0002-6245-9752](https://orcid.org/0000-0002-6245-9752); Email: [samaresh\\_b@hotmail.com](mailto:samaresh_b@hotmail.com)

### Authors

Jit Karmakar – Department of Chemistry, Inorganic Chemistry Section, Jadavpur University, Kolkata 700 032, India

Promita Nandy – Department of Chemistry, Inorganic Chemistry Section, Jadavpur University, Kolkata 700 032, India

Saurabh Das – Department of Chemistry, Inorganic Chemistry Section, Jadavpur University, Kolkata 700 032, India; [orcid.org/0000-0002-0455-8760](https://orcid.org/0000-0002-0455-8760)

Debalina Bhattacharya – Department of Life Science and Biotechnology, Jadavpur University, Kolkata 700 032, India; Department of Microbiology, Maulana Azad College, Kolkata 700 013, India

Parimal Karmakar – Department of Life Science and Biotechnology, Jadavpur University, Kolkata 700 032, India

Complete contact information is available at:

<https://pubs.acs.org/10.1021/acsomega.0c06265>

## Notes

The authors declare no competing financial interest.

## ■ ACKNOWLEDGMENTS

Financial assistance received from the JU-RUSA 2.0 program (ref. no.: R-11/438/19 (S.D.); R-11/76/19 (P.K.); R-11/96/19 (S.B.)) is gratefully acknowledged. The UGC-CAS, DST-FIST, and DST-PURSE programs of the Department of Chemistry, Jadavpur University, are also gratefully acknowledged for providing financial and infrastructural supports. P.K. acknowledges financial support from DST-SERB (EMR/2016/001151), Government of India. J.K. thanks CSIR, New Delhi, for his fellowship (grant no.: 09/096(0842)/2015-EMR-I). D.B. thanks the National Postdoctoral Fellowship Program of DST, Government of India, for her fellowship (grant no.: PDF/2017/001334).

## ■ REFERENCES

- (1) (a) Soldevila-Barreda, J. J.; Metzler-Nolte, N. Intracellular Catalysis with Selected Metal Complexes and Metallic Nanoparticles: Advances toward the Development of Catalytic Metallotherapeutics. *Chem. Rev.* **2019**, *119*, 829–869. (b) Kenny, R. G.; Marmion, C. J. Toward Multi-Targeted Platinum and Ruthenium Drugs – A New Paradigm in Cancer Drug Treatment Regimens? *Chem. Rev.* **2019**, *119*, 1058–1137. (c) Thota, S.; Rodrigues, D. A.; Crans, D. C.; Barreiro, E. J. Ru(II) Compounds: Next-Generation Anticancer Metallotherapeutics? *J. Med. Chem.* **2018**, *61*, 5805–5821. (d) Meier-Menches, S. M.; Gerner, C.; Berger, W.; Hartinger, C. G.; Keppler, B. K. Structure-activity relationships for ruthenium and osmium anticancer agents – towards clinical development. *Chem. Soc. Rev.* **2018**, *47*, 909–928. (e) Zeng, L.; Gupta, P.; Chen, Y.; Wang, E.; Ji, L.; Chao, H.; Chen, Z.-S. The development of anticancer ruthenium(II) complexes: from single molecule compounds to nanomaterials. *Chem. Soc. Rev.* **2017**, *46*, 5771–5804. (f) Murray, B. S.; Babak, M. V.; Hartinger, C. G.; Dyson, P. J. The development of RAPTA compounds for the treatment of tumors. *Coord. Chem. Rev.* **2016**, *306*, 86–114. (g) Medici, S.; Peana, M.; Nurchi, V. M.; Lachowicz, J. I.; Crisponi, G.; Zoroddu, M. A. Noble metals in medicine: Latest advances. *Coord. Chem. Rev.* **2015**, *284*, 329–350. (h) Singh, A. K.; Pandey, D. S.; Xu, Q.; Braunstein, P. Recent advances in supramolecular and biological aspects of arene ruthenium(II) complexes. *Coord. Chem. Rev.* **2014**, *270–271*, 31–56. (i) Hartinger, C. G.; Metzler-Nolte, N.; Dyson, P. J. Challenges and Opportunities in the Development of Organometallic Anticancer Drugs. *Organometallics* **2012**, *31*, 5677–5685. (j) Gasser, G.; Ott, I.; Metzler-Nolte, N. Organometallic Anticancer Compounds. *J. Med. Chem.* **2011**, *54*, 3–25.

- (2) (a) Li, H.; Xie, C.; Lan, R.; Zha, S.; Chan, C.-F.; Wong, W.-Y.; Ho, K.-L.; Chan, B. D.; Luo, Y.; Zhang, J.-X.; Law, G.-L.; Tai, W. C. S.; Bünzli, J.-C. G.; Wong, K.-L. A Smart Europium-Ruthenium Complex as Anticancer Prodrug: Controllable Drug Release and Real-Time Monitoring under Different Light Excitations. *J. Med. Chem.* **2017**, *60*, 8923–8932. (b) Martínez, M. Á.; Carranza, M. P.; Massaguer, A.; Santos, L.; Organero, J. A.; Aliende, C.; de Llorens, R.; Ng-Choi, I.; Feliu, L.; Planas, M.; Rodríguez, A. M.; Manzano, B. R.; Espino, G.; Jalón, F. A. Synthesis and Biological Evaluation of Ru(II) and Pt(II) Complexes Bearing Carboxyl Groups as Potential Anticancer Targeted Drugs. *Inorg. Chem.* **2017**, *56*, 13679–13696. (c) Qu, F.; Park, S.; Martinez, K.; Gray, J. L.; Thowfeik, F. S.; Lundeen, J. A.; Kuhn, A. E.; Charboneau, D. J.; Gerlach, D. L.; Lockart, M. M.; Law, J. A.; Jernigan, K. L.; Chambers, N.; Zeller, M.; Piro, N. A.; Kassel, W. S.; Rthmehl, R. H.; Paul, J. J.; Merino, E. J.; Kim, Y.; Papish, E. T. Ruthenium Complexes are pH-Activated Metallo Prodrugs (pHAMPs) with Light-Triggered Selective Toxicity Toward Cancer Cells. *Inorg. Chem.* **2017**, *56*, 7519–7532. (d) Lenis-Rojas, O. A.; Roma-Rodrigues, C.; Fernandes, A. R.; Marques, F.; Pérez-Fernández, D.; Guerra-Varela, J.; Sánchez, L.; Vázquez-García, D.; López-Torres, M.; Fernández, A.; Fernández, J. J. Dinuclear RuII(bipy)2 Derivatives: Structural, Biological, and in vivo Zebrafish Toxicity Evaluation. *Inorg. Chem.* **2017**, *56*, 7127–7144. (e) Shen, J.; Kim, H.-C.; Wolfram, J.; Mu, C.; Zhang, W.; Liu, H.; Xie, Y.; Mai, J.; Zhang, H.; Li, Z.; Guevara, M.; Mao, Z.-W.; Shen, H. A Liposome Encapsulated Ruthenium Polypyridine Complex as a Theranostic Platform for Triple-Negative Breast Cancer. *Nano Lett.* **2017**, *17*, 2913–2920. (f) Heinemann, F.; Karges, J.; Gasser, G. Critical Overview of the Use of Ru(II) Polypyridyl Complexes as Photosensitizers in One-Photon and Two-Photon Photodynamic Therapy. *Acc. Chem. Res.* **2017**, *50*, 2727–2736.
- (3) (a) Jeyalakshmi, K.; Haribabu, J.; Balachandran, C.; Swaminathan, S.; Bhuvanesh, N. S. P.; Karvembu, R. Coordination Behavior of N,N',N''-Trisubstituted Guanidine Ligands in Their Ru-Arene Complexes: Synthetic, DNA/Protein Binding, and Cytotoxic Studies. *Organometallics* **2019**, *38*, 753–770. (b) Muralisankar, M.; Dheepika, R.; Haribabu, J.; Balachandran, C.; Aoki, S.; Bhuvanesh, N. S. P.; Nagarajan, S. Design, Synthesis, DNA/HSA Binding, and Cytotoxic Activity of Half-Sandwich Ru(II)-Arene Complexes Containing Triarylamine-Thiosemicarbazone Hybrids. *ACS Omega* **2019**, *4*, 11712–11723. (c) Sarkar, B.; Mondal, A.; Madaan, Y.; Roy, N.; Moorthy, A.; Kuo, Y.-C.; Paira, P. Luminescent anticancer ruthenium(II)-p-cymene complexes of extended imidazophenanthroline ligands: synthesis, structure, reactivity, biomolecular interactions and live cell imaging. *Dalton Trans.* **2019**, *48*, 12257–12271. (d) Yousuf, I.; Arjmand, F.; Tabassum, S.; Ahmad, M. Design and synthesis of a DNA intercalative half-sandwich organoruthenium(II)-chromone complex: cytotoxicity evaluation and topoisomerase  $\alpha$  inhibition assay. *New J. Chem.* **2019**, *43*, 5475–5487. (e) Lari, M.; Martínez-Alonso, M.; Busto, N.; Manzano, B. R.; Rodríguez, A. M.; Acuña, M. I.; Domínguez, F.; Albasanz, J. L.; Leal, J. M.; Espino, G.; García, B. Strong Influence of Ancillary Ligands Containing Benzothiazole or Benzimidazole Rings on Cytotoxicity and Photoactivation of Ru(II) Arene Complexes. *Inorg. Chem.* **2018**, *57*, 14322–14336. (f) Lenis-Rojas, O. A.; Robalo, M. P.; Tomaz, A. I.; Carvalho, A.; Fernandes, A. R.; Marques, F.; Folgueira, M.; Yáñez, J.; Vázquez-García, D.; López Torres, M.; Fernández, A.; Fernández, J. J. RuII(p-cymene) Compounds as Effective and Selective Anticancer Candidates with No Toxicity in Vivo. *Inorg. Chem.* **2018**, *57*, 13150–13166. (g) Li, J.; Tian, M.; Tian, Z.; Zhang, S.; Yan, C.; Shao, C.; Liu, Z. Half-Sandwich Iridium(III) and Ruthenium(II) Complexes Containing  $\beta$ P-Chelating Ligands: A New Class of Potent Anticancer Agents with Unusual Redox Features. *Inorg. Chem.* **2018**, *57*, 1705–1716. (h) Paitandi, R. P.; Sharma, V.; Singh, V. D.; Dwivedi, B. K.; Mobin, S. M.; Pandey, D. S. Pyrazole appended quinoline-BODIPY based arene ruthenium complexes: their anticancer activity and potential applications in cellular imaging. *Dalton Trans.* **2018**, *47*, 17500–17514. (i) Mandal, P.; Kundu, B. K.; Vyas, K.; Sabu, V.; Helen, A.; Dhankhar, S. S.; Nagaraja, C. M.; Bhattacharjee, D.; Bhabak, K. P.; Mukhopadhyay, S. Ruthenium(II) arene NSAID complexes: inhibition of cyclooxygenase and antiproliferative activity against cancer cell lines. *Dalton Trans.* **2018**, *47*, 517–527. (j) Gopalakrishnan, D.; Ganeshpandian, M.; Loganathan, R.; Bhuvanesh, N. S. P.; Sabina, X. J.; Karthikeyan, J. Water soluble Ru(II)-arene complexes of the antidiabetic drug metformin: DNA and protein binding, molecular docking, cytotoxicity and apoptosis-inducing activity. *RSC Adv.* **2017**, *7*, 37706–37719. (k) Jeyalakshmi, K.; Haribabu, J.; Balachandran, C.; Bhuvanesh, N. S. P.; Emi, N.; Karvembu, R. Synthesis of Ru(II)-benzene complexes containing aroylthiourea ligands, and their binding with biomolecules and in vitro cytotoxicity through apoptosis. *New J. Chem.* **2017**, *41*, 2672–2686. (l) Barragán, F.; López-Senín, P.; Salassa, L.; Betanzos-Lara, S.; Habtemariam, A.; Moreno, V.; Sadler, P. J.; Marchán, V. Photocontrolled DNA Binding of a Receptor-Targeted Organometallic Ruthenium(II) Complex. *J. Am. Chem. Soc.* **2011**, *133*, 14098.
- (4) (a) Ashraf, A.; Aman, F.; Movassaghi, S.; Zafar, A.; Kubanik, M.; Siddiqui, W. A.; Reynisson, J.; Söhnle, T.; Jamieson, S. M. F.; Hanif, M.; Hartinger, C. G. Structural Modifications of the Antiinflammatory Oxicam Scaffold and Preparation of Anticancer Organometallic Compounds. *Organometallics* **2019**, *38*, 361–374. (b) Swaminathan, S.; Haribabu, J.; Kalagatur, N. K.; Konakanchi, R.; Balakrishnan, N.; Bhuvanesh, N.; Karvembu, R. Synthesis and Anticancer Activity of [RuCl<sub>2</sub>( $\eta$ 6-arene)(aroylthiourea)] Complexes – High Activity against the Human Neuroblastoma (IMR-32) Cancer Cell Line. *ACS Omega* **2019**, *4*, 6245–6256. (c) Hager, L. A.; Mokesch, S.; Kieler, C.; Alonso-de Castro, S.; Baier, D.; Roller, A.; Kandlioller, W.; Keppler, B. K.; Berger, W.; Salassa, L.; Terenzi, A. Ruthenium-arene complexes bearing naphthyl-substituted 1,3-dioxindan-2-carboxamides ligands for G-quadruplex DNA recognition. *Dalton Trans.* **2019**, *48*, 12040–12049. (d) Sarkar, A.; Acharya, S.; Khushvant, K.; Purkait, K.; Mukherjee, A. Cytotoxic Ru<sup>II</sup>-p-cymene complexes of an anthraimidazoleione: halide dependent solution stability, reactivity and resistance to hypoxia deactivation. *Dalton Trans.* **2019**, *48*, 7187–7197. (e) Laurent, Q.; Batchelor, L. K.; Dyson, P. J. Applying a Trojan Horse Strategy to Ruthenium Complexes in the Pursuit of Novel Antibacterial Agents. *Organometallics* **2018**, *37*, 915–923. (f) Gatti, A.; Habtemariam, A.; Romero-Canelón, I.; Song, J.-I.; Heer, B.; Clarkon, G. J.; Rogolino, D.; Sadler, P. J.; Carcelli, M. Half-Sandwich Arene Ruthenium(II) and Osmium(II) Thiosemicarbazone Complexes: Solution Behavior and Antiproliferative Activity. *Organometallics* **2018**, *37*, 891–899. (g) Zhao, J.; Zhang, D.; Hua, W.; Li, W.; Xu, G.; Gou, S. Anticancer Activity of Bifunctional Organometallic Ru(II) Arene Complexes Containing a 7-Hydroxycoumarin Group. *Organometallics* **2018**, *37*, 441–447. (h) Mu, C.; Prosser, K. E.; Harrypsad, S.; MacNeil, G. A.; Panchmatia, R.; Thompson, J. R.; Sinha, S.; Warren, J. J.; Walsby, C. J. Activation by Oxidation: Ferrocene-Functionalized Ru(II)-Arene Complexes with Anticancer, Antibacterial, and Antioxidant Properties. *Inorg. Chem.* **2018**, *57*, 15247–15261. (i) Lenis-Rojas, O. A.; Robalo, M. P.; Tomaz, A. I.; Carvalho, A.; Fernandes, A. R.; Marques, F.; Folgueira, M.; Yáñez, J.; Vázquez-García, D.; López Torres, M.; Fernández, A.; Fernández, J. J. RuII(p-cymene) Compounds as Effective and Selective Anticancer Candidates with No Toxicity in vivo. *Inorg. Chem.* **2018**, *57*, 13150–13166. (j) Ma, L.; Lin, X.; Li, C.; Xu, Z.; Chan, C.-Y.; Tse, M.-K.; Shi, P.; Zhu, G. A Cancer Cell-Selective and Low-Toxic Bifunctional Heterodinuclear Pt(IV)-Ru(II) Anticancer Prodrug. *Inorg. Chem.* **2018**, *57*, 2917–2924. (k) Shanmugaraju, S.; la Cour Poulsen, B.; Arisa, T.; Umadevi, D.; Dalton, H. L.; Hawes, C. S.; Estalayo-Adrián, S.; Savyasachi, A. J.; Watson, G. W.; Williams, D. C.; Gunnlaugsson, T. Synthesis, structural characterization and antiproliferative activity of a new fluorescent 4-amino-1,8-naphthalimide Tröger's base-Ru(II)-curcumin organometallic conjugate. *Chem. Commun.* **2018**, *54*, 4120–4123. (l) Batchelor, L. K.; Păunescu, E.; Soudani, M.; Scopelliti, R.; Dyson, P. J. Influence of the Linker Length on the Cytotoxicity of Homodinuclear Ruthenium(II) and Gold(I) Complexes. *Inorg. Chem.* **2017**, *56*, 9617–9633. (m) Guerriero, A.; Oberhauser, W.; Riedel, T.; Peruzzini, M.; Dyson, P. J.; Gonsalvi, L. New Class of Half-Sandwich Ruthenium(II) Arene Complexes Bearing the Water-Soluble CAP

- Ligand as an *in vitro* Anticancer Agent. *Inorg. Chem.* **2017**, *56*, 5514–5518. (n) Mitra, R.; Samuelson, A. G. Mitigating UVA light induced reactivity of 6-thioguanine through formation of a Ru(II) half-sandwich complex. *RSC Adv.* **2014**, *4*, 24304–24306. Romero-Canelón, I.; Salassa, L.; Sadler, P. J. The Contrasting Activity of Iodido versus Chlorido Ruthenium and Osmium Arene Azo- and Imino-pyridine Anticancer Complexes: Control of Cell Selectivity, Cross-Resistance, p53 Dependence, and Apoptosis Pathway. *J. Med. Chem.* **2013**, *56*, 1291–1300. (p) Das, S.; Sinha, S.; Britto, R.; Somasundaram, K.; Samuelson, A. G. Cytotoxicity of half sandwich ruthenium(II) complexes with strong hydrogen bond acceptor ligands and their mechanism of action. *J. Inorg. Biochem.* **2010**, *104*, 93–104. (5) Novakova, O.; Chen, H.; Vrana, O.; Rodger, A.; Sadler, P. J.; Brabec, V. DNA Interactions of Monofunctional Organometallic Ruthenium(II) Antitumor Complexes in Cell-free Media. *Biochemistry* **2003**, *42*, 11544–11554. (6) (a) Arkin, M. R.; Jenkins, Y.; Murphy, C. J.; Turro, N. J.; Barton, J. K. Metallointercalators as Probes of the DNA  $\pi$ -way. *Mechanistic Bioinorganic Chemistry*; American Chemical Society, 1996; Chapter 17, pp 449–469. (b) Elmes, R. B. P.; Ryan, G. J.; Erby, M. L.; Frimannsson, D. O.; Kitchen, J. A.; Lawler, M.; Williams, D. C.; Quinn, S. J.; Gunnlaugsson, T. Synthesis, Characterization, and Biological Profiling of Ruthenium(II)-Based 4-Nitro- and 4-Amino-1,8-naphthalimide Conjugates. *Inorg. Chem.* **2020**, *59*, 10874–10893. (c) Zhang, S.-Q.; Meng, T.-T.; Li, J.; Hong, F.; Liu, J.; Wang, Y.; Gao, L.-H.; Zhao, H.; Wang, K.-Z. Near-IR/Visible-Emitting Thiophenyl-Based Ru(II) Complexes: Efficient Photodynamic Therapy, Cellular Uptake, and DNA Binding. *Inorg. Chem.* **2019**, *58*, 14244–14259. (d) Abreu, F. D.; Paulo, T. d. F.; Gehlen, M. H.; Ando, R. A.; Lopes, L. G. F.; Gondim, A. C. S.; Vasconcelos, M. A.; Teixeira, E. H.; Sousa, E. H. S.; de Carvalho, I. M. M. Aryl-Substituted Ruthenium(II) Complexes: A Strategy for Enhanced Photocleavage and Efficient DNA Binding. *Inorg. Chem.* **2017**, *56*, 9084–9096. (7) (a) Banerjee, D.; Pal, S. K. Excited-State Solvation and Proton Transfer Dynamics of DAPI in Biomimetics and Genomic DNA. *J. Phys. Chem. A* **2008**, *112*, 7314–7320. (b) Bourzac, K. M.; LaVine, L. J.; Rice, M. S. Analysis of DAPI and SYBR Green I as Alternatives to Ethidium Bromide for Nucleic Acid Staining in agarose Gel Electrophoresis. *J. Chem. Educ.* **2003**, *80*, 1292–1296. (c) Reha, D.; Kabelác, M.; Ryjáček, F.; Sponer, J.; Sponer, J. E.; Elstner, M.; Suhai, S.; Hobza, P. Intercalators. 1. Nature of Stacking Interactions between Intercalators (Ethidium, Daunomycin, Ellipticine, and 4',6-Diaminide-2-phenylindole) and DNA Base Pairs. *Ab Initio Quantum Chemical, Density Functional Theory, and Empirical Potential Study. J. Am. Chem. Soc.* **2002**, *124*, 3366. (d) Lan, T.; McLaughlin, L. W. The Energetic Contribution of a Bifurcated Hydrogen Bond to the Binding of DAPI to dA-dT Rich Sequences of DNA. *J. Am. Chem. Soc.* **2001**, *123*, 2064–2065. (e) Vlieghe, D.; Sponer, J.; Meervelt, L. V. Crystal Structure of d(GGCCAATTGG) Complexed with DAPI Reveals Novel Binding Mode. *Biochemistry* **1999**, *38*, 16443–16451. (f) Albert, F. G.; Eckdahl, T. T.; Fitzgerald, D. J.; Anderson, J. N. Heterogeneity in the Actions of Drugs That Bind in the DNA Minor Groove. *Biochemistry* **1999**, *38*, 10135–10146. (8) (a) Mohamed, S. K.; Soliman, A. M.; El-Remaly, M. A. A.; Abdel-Ghany, H. Eco Friendly Synthesis of Pyrimidine and Dihydropyrimidinone Derivatives under Solvent Free Condition and their Anti-microbial Activity. *Chem. Sci. J.* **2013**, *2013*, 1. (b) King, F. E.; Acheson, R. M.; Spensley, P. C. 275. Benzimidazole analogues of paludrine. *J. Chem. Soc.* **1948**, *17*, 1366–1371. (9) (a) Mukherjee, T.; Ganzmann, C.; Bhuvanesh, N.; Gladysz, J. A. Syntheses of Enantiopure Bifunctional 2-Guanidinobenzimidazole Cyclopentadienyl Ruthenium Complexes: Highly Enantioselective Organometallic Hydrogen Bond Donor Catalysts for Carbon-Carbon Bond Forming Reactions. *Organometallics* **2014**, *33*, 6723–6737. (b) Scherer, A.; Mukherjee, T.; Hampel, F.; Gladysz, J. A. Metal-Templated Hydrogen Bond Donors as “Organocatalysts” for Carbon-Carbon Bond Forming Reactions: Syntheses, Structures, and Reactivities of 2-Guanidinobenzimidazole Cyclopentadienyl Ruthenium Complexes. *Organometallics* **2014**, *33*, 6709–6722. (c) Sánchez-Guadarrama, O.; López-Sandoval, H.; Sánchez-Bartéz, F.; Gracia-Mora, I.; Höpfl, H.; Barba-Behrens, N. Cytotoxic activity, X-ray crystal structures and spectroscopic characterization of cobalt(II), copper(II) and zinc(II) coordination compounds with 2-substituted benzimidazoles. *J. Inorg. Biochem.* **2009**, *103*, 1204–1213. (d) Albada, G. A. v.; Turpeinen, U.; Reedijk, J. Two different isomers of tetrahedrally distorted square-planar Cu(II) triflate compounds with 2-guanidinobenzimidazole; synthesis, X-ray and spectroscopic characterization. *J. Mol. Struct.* **2006**, *789*, 182–186. (e) Zheng, L.; Zhang, J.; Yu, M.-M.; Ni, Z.-H.; Kou, H.-Z. Bis(2-guanidinobenzimidazole- $K^2$  N, N')copper(II) bis(dicyanamide). *Acta Crystallogr., Sect. E: Struct. Rep. Online* **2006**, *62*, m2470–m2472. (f) Arablo, N.; Torabi, S. A. A.; Morsali, A.; Skelton, B. W.; White, A. H. Cation Structures in Bis(2-Guanidino-benzimidazole)metal(II) Complexes: Crystal and Molecular Structure of the Copper(II) Perchlorate Adduct. *Aust. J. Chem.* **2003**, *56*, 945–947. (g) Cenicerós-Gómez, A. E.; Barba-Behrens, N.; Quiroz-Castro, M. E.; Bernès, S.; Nöth, H.; Castillo-Blum, S. E. Synthesis, X-ray and spectroscopic characterisation of chromium(III) coordination compounds with benzimidazolic ligands. *Polyhedron* **2000**, *19*, 1821–1827. (h) Cenicerós-Gómez, A. E.; Barba-Behrens, N.; Bernès, S.; Nöth, H.; Castillo-Blum, S. E. Synthesis, X-ray and NMR characterisation of cobalt(III) coordination compounds with 2-guanidinobenzimidazole. *Inorg. Chim. Acta* **2000**, *304*, 230–236. (i) Barba-Behrens, N.; Vázquez-Olmos, A.; Castillo-Blum, S. E.; Höjer, G.; Meza-Höjer, S.; Hernández, R. M.; de Jesús Rosales-Hoz, M.; Vicente, R.; Escuer, A. Coordination behaviour of 2-guanidinobenzimidazole towards cobalt(II), nickel(II), copper(II) and zinc(II). An experimental and theoretical study. *Transition Met. Chem.* **1996**, *21*, 31–37. (10) Bennett, M. A.; Huang, T. N.; Matheson, T. W.; Smith, A. K. *Inorg. Synth.* **1982**, *1*, 75. (11) Frisch, M. J.; Trucks, G. W.; Schlegel, H. B.; Scuseria, G. E.; Robb, M. A.; Cheeseman, J. R.; Scalmani, G.; Barone, V.; Mennucci, B.; Petersson, G. A.; Nakatsuji, H.; Caricato, M.; Li, X.; Hratchian, H. P.; Izmaylov, A. F.; Bloino, J.; Zheng, G.; Sonnenberg, J. L.; Hada, M.; Ehara, M.; Toyota, K.; Fukuda, R.; Hasegawa, J.; Ishida, M.; Nakajima, T.; Honda, Y.; Kitao, O.; Nakai, H.; Vreven, T.; Montgomery, J. A., Jr.; Peralta, J. E.; Ogliaro, F.; Bearpark, M.; Heyd, J. J.; Brothers, E.; Kudin, K. N.; Staroverov, V. N.; Kobayashi, R.; Normand, J.; Raghavachari, K.; Rendell, A.; Burant, J. C.; Iyengar, S. S.; Tomasi, J.; Cossi, M.; Rega, N.; Millam, J. M.; Klene, M.; Knox, J. E.; Cross, J. B.; Bakken, V.; Adamo, C.; Jaramillo, J.; Gomperts, R.; Stratmann, R. E.; Yazyev, O.; Austin, A. J.; Cammi, R.; Pomelli, C.; Ochterski, J. W.; Martin, R. L.; Morokuma, K.; Zakrzewski, V. G.; Voth, G. A.; Salvador, P.; Dannenberg, J. J.; Dapprich, S.; Daniels, A. D.; Farkas, Ö.; Foresman, J. B.; Ortiz, J. V.; Cioslowski, J.; Fox, D. J. *Gaussian 9*; Gaussian, Inc.: Wallingford CT, 2009. (12) Sheldrick, G. M. *SHELXS-97 and SHELXL-97, Fortran programs for crystal structure solution and refinement*; University of Göttingen: Göttingen, Germany, 1997. (b) Sheldrick, G. M. A short history of SHELX. *Acta Crystallogr., Sect. A: Found. Crystallogr.* **2008**, *64*, 112–122. (13) Das, S.; Dasgupta, D. Binding of (MTR)<sub>2</sub>Zn<sup>2+</sup> complex to chromatin: A comparison with (MTR)<sub>2</sub>Mg<sup>2+</sup> complex. *J. Inorg. Biochem.* **2005**, *99*, 707–715. (14) Roy, S.; Banerjee, R.; Sarkar, M. Direct binding of Cu(II)-complexes of oxamic NSAIDs with DNA backbone. *J. Inorg. Biochem.* **2006**, *100*, 1320–1331. (15) Guin, P. S.; Das, S.; Mandal, P. C. Studies on the formation of a complex of Cu(II) with sodium 1,4-dihydroxy-9,10-anthraquinone-2-sulphonate – An analogue of the core unit of anthracycline anticancer drugs and its interaction with calf thymus DNA. *J. Inorg. Biochem.* **2009**, *103*, 1702–1710. (16) Das, P.; Jain, C. K.; Dey, S. K.; Saha, R.; Chowdhury, A. D.; Roychoudhury, S.; Kumar, S.; Majumder, H. K.; Das, S. Synthesis, crystal structure, DNA interaction and *in vitro* anticancer activity of a Cu(II) complex of purpurin: dual poison for human DNA topoisomerase I and II. *RSC Adv.* **2014**, *4*, 59344–59357.

- (17) Das, P.; Jain, C. K.; Roychoudhury, S.; Majumder, H. K.; Das, S. Design, synthesis and *in vitro* anticancer activity of a Cu(II) complex of carminic acid: A novel small molecule inhibitor of human DNA topoisomerase I and topoisomerase II. *ChemistrySelect* **2016**, *1*, 6623–6631.
- (18) Mukherjee Chatterjee, S.; Jain, C. K.; Singha, S.; Das, P.; Roychoudhury, S.; Majumder, H. K.; Das, S. Activity of Co<sup>II</sup>–Quinalizarin: A novel analogue of anthracycline-based anticancer agents targets human DNA topoisomerase, whereas quinalizarin itself acts via formation of semiquinone on acute lymphoblastic leukemia MOLT-4 and HCT 116 cells. *ACS Omega* **2018**, *3*, 10255–10266.
- (19) Scatchard, G. The attractions of proteins for small molecules and ions. *Ann. N.Y. Acad. Sci.* **1949**, *51*, 660–672.
- (20) Singh, N. P.; McCoy, M. T.; Tice, R. R.; Schneider, E. L. A simple technique for quantitation of low levels of DNA damage in individual cells. *Exp. Cell Res.* **1988**, *175*, 184–191.
- (21) Attempts to grow single crystals of complexes C<sub>1</sub> and C<sub>2</sub> remained unsuccessful.
- (22) Nikolić, S.; Opsenica, D. M.; Filipović, V.; Dojčinović, B.; Arandelović, S.; Radulović, S.; Grgurić-Šipka, S. Strong *In Vitro* Cytotoxic Potential of New Ruthenium-Cymene Complexes. *Organometallics* **2015**, *34*, 3464–3473.
- (23) Morgan, A. R.; Pulleyblank, D. E. Native and denatured DNA, cross-linked and palindromic and circular covalently-closed DNA analyzed by a sensitive fluorimetric procedure. *Biochem. Biophys. Res. Commun.* **1974**, *61*, 396–403.
- (24) Birnboim, H. C.; Jevcak, J. J. Fluorometric method for rapid detection of DNA strand breaks in human white blood cells produced by low doses of radiation. *Cancer Res.* **1981**, *41*, 1889.
- (25) Das, S.; Saha, A.; Mandal, P. C. Radiation-induced double strand modification in calf thymus DNA in the presence of 1,2-dihydroxy-9,10-anthraquinone and its Cu(II) complex. *Environ. Health Perspect.* **1997**, *105*, 1459–1462.
- (26) Das, S.; Mandal, P. C. Anthracyclines as radiosensitizers: a Cu(II) complex of a simpler analogue modifies DNA in Chinese Hamster V79 cells under low-dose  $\gamma$  radiation. *J. Radioanal. Nucl. Chem.* **2014**, *299*, 1665–1670.
- (27) Tripathi, R.; Samadder, T.; Gupta, S.; Surolia, A.; Shaha, C. Anticancer activity of a combination of cisplatin and fisetin in embryonal carcinoma cells and xenograft tumors. *Mol. Cancer Ther.* **2011**, *10*, 255–268.
- (28) Dasari, S.; Bernard Tchounwou, P. Cisplatin in cancer therapy: molecular mechanisms of action. *Eur. J. Pharmacol.* **2014**, *740*, 364–378.
- (29) Gryparis, E. C.; Hatzia Apostolou, M.; Papadimitriou, E.; Avgoustakis, K. Anticancer activity of cisplatin-loaded PLGA-mPEG nanoparticles on LNCaP prostate cancer cells. *Eur. J. Pharm. Biopharm.* **2007**, *67*, 1–8.
- (30) Chen, L.; Li, W.; Wang, H.; Zhao, H.; Tang, J.; Wu, C.; Lu, L.; Liao, W.; Lu, X. Curcumin cytotoxicity is enhanced by PTEN disruption in colorectal cancer cells. *World J. Gastroenterol.* **2013**, *19*, 6814–6824.
- (31) Rodriguez, E.; Azevedo, R.; Fernandes, P.; Santos, C. a. Cr(VI) Induces DNA Damage, Cell Cycle Arrest and Polyploidization: A Flow Cytometric and Comet Assay Study in *Pisum sativum*. *Chem. Res. Toxicol.* **2011**, *24*, 1040–1047.
- (32) Stang, A.; Witte, I. Performance of the comet assay in a high-throughput version. *Mutat. Res., Genet. Toxicol. Environ. Mutagen.* **2009**, *675*, 5–10.
- (33) Dougan, S. J.; Habtemariam, A.; McHale, S. E.; Parsons, S.; Sadler, P. J. Catalytic organometallic anticancer complexes. *Proc. Natl. Acad. Sci. U.S.A.* **2008**, *105*, 11628–11633.
- (34) Molter, A.; Kathrein, S.; Kircher, B.; Mohr, F. Anti-tumour active gold(I), palladium(II) and ruthenium(III) complexes with thio- and selenoureato ligands: a comparative study. *Dalton Trans.* **2018**, *47*, 5055–5064.
- (35) Seršen, S.; Kljun, J.; Kryeziu, K.; Panchuk, R.; Alte, B.; Körner, W.; Heffeter, P.; Berger, W.; Turel, I. Structure-Related Mode-of-Action Differences of Anticancer Organoruthenium Complexes with  $\beta$ -Diketonates. *J. Med. Chem.* **2015**, *58*, 3984.
- (36) Tian, Z.; Li, J.; Zhang, S.; Xu, Z.; Yang, Y.; Kong, D.; Zhang, H.; Ge, X.; Zhang, J.; Liu, Z. Lysosome-Targeted Chemotherapeutics: Half-Sandwich Ruthenium(II) Complexes That Are Selectively Toxic to Cancer Cells. *Inorg. Chem.* **2018**, *57*, 10498–10502.
- (37) Ginzinger, W.; Mühlgassner, G.; Arion, V. B.; Jakupec, M. A.; Roller, A.; Galanski, M.; Reithofer, M.; Berger, W.; Keppler, B. K. A SAR Study of Novel Antiproliferative Ruthenium and Osmium Complexes with Quinoxalinone Ligands in Human Cancer Cell Lines. *J. Med. Chem.* **2012**, *55*, 3398–3413.